ISSN 0042-8469
e-ISSN 2217-4753
УДК 623 + 355/359

Вол. 73, бр. 3

2025

НАУЧНИ ЧАСОПИС МИНИСТАРСТВА ОДБРАНЕ И ВОЈСКЕ СРБИЈЕ

ВОЈНОТЕХНИЧКИ ГЛАСНИК

ВОЈНОТЕХНИЧКИ ГЛАСНИК

2025 3

втг.мо.упр.срб

www.vtg.mod.gov.rs

ВОЕННО-ТЕХНИЧЕСКИЙ ВЕСТНИК 2025 3

Том 73, № 3
2025

ISSN 0042-8469
e-ISSN 2217-4753
УДК 623 + 355/359

ВТВ

НАУЧНЫЙ ЖУРНАЛ МИНИСТЕРСТВА ОБОРОНЫ
И ВООРУЖЕННЫХ СИЛ РЕСПУБЛИКИ СЕРБИЯ

ВОЕННО-ТЕХНИЧЕСКИЙ ВЕСТНИК

втг.мо.упр.срб
www.vtg.mod.gov.rs

MILITARY TECHNICAL COURIER 2025 3

Vol. 73, Issue 3
2025

ISSN 0042-8469
e-ISSN 2217-4753
UDC 623 + 355/359

MTC

SCIENTIFIC JOURNAL OF THE MINISTRY OF DEFENCE AND THE SERBIAN ARMED FORCES

MILITARY TECHNICAL COURIER

втг.мо.упр.срб
www.vtg.mod.gov.rs

ISSN 0042-8469
e-ISSN 2217-4753
UDC 623 + 355/359

НАУЧНИ ЧАСОПИС МИНИСТАРСТВА ОДБРАНЕ И ВОЈСКЕ СРБИЈЕ

ВОЈНОТЕХНИЧКИ ГЛАСНИК

ВОЛУМЕН 73 • БРОЈ 3 • ЈУЛ – СЕПТЕМБАР 2025.

NAUČNI ČASOPIS MINISTARSTVA ODBRANE I VOJSKE SRBIJE

VOJNOTEHNIČKI GLASNIK

VOLUMEN 73 • BROJ 3 • JUL – SEPTEMBAR 2025.

втг.мо.упр.срб
www.vtg.mod.gov.rs
COBISS.SR-ID 4423938
DOI: 10.5937/VojnotehnickiGlasnik

ISSN 0042-8469
e-ISSN 2217-4753
UDC 623 + 355/359

НАУЧНЫЙ ЖУРНАЛ МИНИСТЕРСТВА ОБОРОНЫ И ВООРУЖЁННЫХ СИЛ РЕСПУБЛИКИ СЕРБИЯ

ВОЕННО-ТЕХНИЧЕСКИЙ ВЕСТНИК

ТОМ 73•НОМЕР ВЫПУСКА 3•ИЮЛЬ – СЕНТЯБРЬ 2025.

SCIENTIFIC JOURNAL OF THE MINISTRY OF DEFENCE AND SERBIAN ARMED FORCES

MILITARY TECHNICAL COURIER

VOLUME 73•ISSUE 3•JULY – SEPTEMBER 2025

втг.мо.упр.срб
www.vtg.mod.gov.rs
COBISS.SR-ID 4423938
DOI: 10.5937/VojnotehnickiGlasnik

ВЛАСНИЦИ:
Министарство одбране и Војска Србије
ИЗДАВАЧ:
Универзитет одбране у Београду, Војна академија

СОБСТВЕННИКИ: Министерство обороны и Вооружённые силы Республики Сербия
ИЗДАТЕЛЬСТВО: Университет обороны в г. Белград, Военная академия

OWNERS:
Ministry of Defence and Serbian Armed Forces
PUBLISHER:
University of Defence in Belgrade, Military Academy

С А Д Р Ж А Ј

ОРИГИНАЛНИ НАУЧНИ РАДОВИ

С О Д Е Р Ж А Н И Е

ОРИГИНАЛЬНЫЕ НАУЧНЫЕ СТАТЬИ

C O N T E N T S

ORIGINAL SCIENTIFIC PAPERS

ORIGINAL SCIENTIFIC PAPERS

On the sum of powers of vertex degrees of polycyclic graphs

Ivan Gutman

University of Kragujevac, Faculty of Science,
Kragujevac, Republic of Serbia,
e-mail: gutman@kg.ac.rs,
ORCID iD: https://orcid.org/0000-0001-9681-1550

https://doi.org/10.5937/vojtehg73-61342

FIELD: mathematics (mathematics subject classification: primary 05c07, secondary 05c09)
ARTICLE TYPE: original scientific paper

Abstract:

Introduction/purpose: The sum of powers of vertex degrees of graphs is much studied in the literature, but only for some fixed values of the power. General properties of these sums are studied to a much lesser extent. In this paper, we offer results along these lines.

Methods: Combinatorial graph theory is applied.

Results: A few lower bounds for the sum of powers of vertex degrees are established, applicable to all powers. Classes of polycyclic graphs with a minimum sum of powers of vertex degrees are characterized.

Conclusion: The paper contributes to the study of the sum of powers of vertex degrees of graphs.

Keywords: degree (of a vertex), sum of powers of vertex degrees of graphs, polycyclic graphs.

Introduction

In this paper, we consider simple graphs. Let G be such a graph, possessing n vertices and m edges. Throughout this paper, the parameters n and m are assumed to be constant. In order to avoid trivialities, we assume that the graphs considered are connected.

The cyclomatic number (or simply: the number of cycles) of a connected graph G is $c=m-n+1$ (Bondy & Murty, 1976). We say that a graph is polycyclic if it has two or more cycles (i.e., if $c \geq 2$).

The results reported in this paper extend and somewhat correct those from (Gutman, 2014). Therefore, we use the same notation as in (Gutman, 2014).

The degree of a vertex v of the graph G, denoted by deg(v), is the number of first neighbors of this vertex. In this paper, we will examine the sum

$$Z_p = Z_p(G) = \sum_v \deg(v)^p = \sum_{k \geq 1} k^p n_k \qquad (1)$$

where p is a positive integer, and where n_k denotes the number of vertices of the graph G whose degrees are equal to k. Recall that

$$\sum_{k \geq 1} n_k = n \ . \qquad (2)$$

For p=1, we have the well-known relation

$$\sum_v \deg(v) = \sum_{k \geq 1} k n_k = 2m \ . \qquad (3)$$

Let it be noted that formula (3) was discovered by Leonhard Euler in 1736, within his seminal work on the Königsberg bridge problem (Biggs et al, 1976).

The sum $Z_p(G)$ was separately investigated for a large number of particular values of the exponent p. Thus, $Z_2(G)$ is the much studied first Zagreb index (Gutman & Trinajstić, 1972, Nikolić et al, 2003); $Z_3(G)$ is the forgotted index, introduced in (Furtula & Gutman, 2015); $Z_4(G)$ has been named the Yemen index (Alameri et al, 2020); $Z_5(G)$, the so-called S-index, was investigated by (Nagarajan et al, 2021); the sums $Z_p(G)$ for p=6 and p=7 were studied by (Yousef et al, 2025) under the names G-index and P-index.

For the sake of completenesss, we mention here the inverse degree index $Z_{-1}(G)$ (Das et al, 2016) and the much studied zero-th order connectivity index $Z_{-1/2}(G)$ (Kier & Hall, 1976).

The results on the general properties of $Z_p(G)$, for arbitrary positive integer values of p, seem to be missing in the literature, with the exception of (Gutman, 2014). The present work is aimed at helping to fill in this gap.

A transformed version of Z_p

The dependence of $Z_p(G)$ on the degrees of the vertices of the graph G, based on Eq. (1) is simple, evident and straightforward. Therefore, in order to get a better insight into this dependence, we transform the sum $Z_p(G)$ by adding to it Eq. (2) multiplied by some constant α, and Eq. (3) multiplied by some constant β. By this we arrive at a transformed expression of the form

$$T_p(G) = Z_p(G) + \alpha n + 2\beta m \tag{4}$$

which in view of Eqs. (1), (2), and (3), yields

$$T_p(G) = \sum_{k \geq 1} \left(k^p + \alpha + \beta k \right) n_k = \sum_{k \geq 1} \Theta_p(k)\, n_k \,. \tag{5}$$

Via Eq. (5), we introduce the term

$$\Theta_p(k) = k^p + \alpha + \beta k \tag{6}$$

which is a polynomial of degree p, in the variable k.

It is purposeful to choose α=-γ and β=2γ, which results in the simplification

$$T_p(G) = Z_p(G) - 2\gamma(m - n) = Z_p(G) - 2\gamma(c - 1) \tag{7}$$

where c is the cyclomatic number, and

$$\Theta_p(k) = k^p - \gamma k + 2\gamma \,. \tag{8}$$

Throughout this paper, we assume that the parameter γ is positive valued. Then, from Eq. (7) we conclude the following:

In the case of trees (c=0), the terms we added to $Z_p(G)$ are necessarily positive valued. Therefore, whatever structural feature of G decreases/increases T_p(G), it will equially decrease/increase $Z_p(G)$, i.e., the proposed transformation is not applicable to trees.

The proposed transformation is also useless in the case of unicyclic graphs (c=1), since then T_p(G) and $Z_p(G)$ coincide.

Therefore, in what follows, we will only consider graphs whose cyclomatic number is greater than 1, that is, polycyclic graphs.

The parameter γ may be (reasonably) chosen to depend on p in many different ways. We first follow the model from (Gutman, 2014), and then offer a few more.

The first model: $\gamma = \lambda^p$

In (Gutman, 1914), the special case λ=3 was considered. Instead of it, here we report to have envisaged another such suitable option, $\lambda = 2\sqrt{2}$.

For $\lambda = 2\sqrt{2}$, Eq. (8) becomes

$$\Theta_p(k) = k^p - (2\sqrt{2})^p k + 2(2\sqrt{2})^p \,. \tag{9}$$

A simple calculation reveals the following:

For *p*=2, $\theta_p(k)=(k-4)^2$. Therefore, for all positive integer values of *k*, $\theta_2(k)$ is positive valued, except for *k*=4 when it is zero.

For *p*=3, by evaluating $\theta_2(1)$, $\theta_2(2)$, $\theta_2(3)$, $\theta_2(4)$ it becomes evidents that for all positive integer values of k, $\theta_2(k)>0$.

The same is found also for *p*=4 and for higher values of *p*.

This implies:

Theorem 1. Let *G* be a connected polycyclic graph with *n* vertices and *m* edges. Let among its vertices there are n_h vertices with degree *h* for some *h* different from 4. Then, for any value of the exponent *p*,

$$Z_p(G) \geq 2(2\sqrt{2})^p (m-n) - \Theta_p(h) n_h$$

where θ_p is the polynomial defined by Eq. (9).

Equality is attained only if *p*=2 and only if all the $n-n_h$ remaining vertices of *G* are of degree 4. This equality case pertains to a class of polycyclic (*n,m*) graphs with a fixed number of vertices of degree *h*. Their Z_2 values are minimal.

Proof. Rewriting Eqs. (5) and (7), we have

$$Z_p(G) = 2\gamma(m-n) - \sum_{k\geq 1} \Theta_p(k) n_k \,.$$

Above, we have shown that the terms $\theta_p(k)$ are always positive or zero. Therefore, by deleting the terms $\theta_p(k)n_k$ for all $k \neq h$, we obtain the inequality

$$Z_p(G) \geq 2\gamma(m-n) - \Theta_p(h) n_h \,.$$

Equality will happen if all the deleted terms were equal to zero. This requires that *p*=2 and k=4, i.e., that all the remaining vertices be of degree 4.

Thus, the graphs with a given number of vertices of degree *h* and all other vertices of degree 4 have the minimum Z_2 value.

As it was clarified above, consideration based on the transformation $Z_p \rightarrow T_p$ requires that the underlying graphs be polycyclic. $\blacksquare$

The analogous results for the choice λ=3 read as follows (the details are found in (Gutman, 1914)):

$\Theta_p(1)=1+3^p>0$ for any value of $p\geq 2$,

$\Theta_p(2)=2^p>0$ for any value of $p\geq 2$, and

$\Theta_p(3)=0$ for any value of $p\geq 2$.

For $p=2$, $\Theta_2(4)=-2$; for $p=3$, $\Theta_3(4)=10$; $\Theta_p(4)$ is positive valued also for $p>3$.

For $k\geq 5$, $\Theta_p(k)$ is positive valued for any $p\geq 2$.

This implies:

Theorem 2. Let *G* be a connected polycyclic graph with *n* vertices and *m* edges. Let among its vertices there are n_h vertices with degree *h* for some *h* different from 3. Then, for any value of the exponent $p\geq 3$,

$$Z_p(G) \geq 2\cdot 3^p(m-n) - \Theta_p(h)\,n_h$$

where θ_p is the polynomial defined by Eq. (10):

$$\Theta_p(k) = k^p - 3^p k + 2\cdot 3^p\,. \tag{10}$$

Equality is attained if and only if all the n-n_h remaining vertices of *G* are of degree 3. This equality case pertains to a class of polycyclic (*n,m*)-graphs with a fixed number of vertices of degree *h*. Their Z_p values are minimal for all $p\geq 3$.

Proof is analogous to the proof of Theorem 1, *mutatis mutandis*. $\blacksquare$

In Theorem 2, it is required that the exponent *p* be greater than 2. For the case $p=2$, from Eq. (10), we find that $\theta_2(4)=\theta_2(5)=-2$ and $\theta_2(6)=0$. Therefore, Theorem 2 cannot be extended to this case.

The second model: $\gamma = p^p$

Within this model,

$$\Theta_p(k) = k^p - p^p k + 2\cdot p^p\,. \tag{11}$$

For $p=2$, $\theta_2(k)=(k-2)^2+4$, which is positive valued for all *k*. Therefore, we may skip this case.

For $p=3$, we calculate that $\theta_3(1)=28$, $\theta_3(2)=8$, $\theta_3(3)=0$, $\theta_3(4)=202$, and all the folowing $\theta_3(k)$ values are evidently positive.

For $p=4$, we find that $\theta_4(1)$, $\theta_4(2)$, $\theta_4(4)$, $\theta_4(5)$, ... are positive, but $\theta_4(3)$ is negative.

For p=5, we find that $\theta_5(1)$, $\theta_5(2)$, $\theta_5(6)$, $\theta_5(7)$, ... are positive, whereas $\theta_5(3)$, $\theta_5(4)$ and $\theta_5(5)$ are negative. The same kind of anomaly exists also at p>6.

Thus, the model examined in this section can be used only at p=3, and we get:

Theorem 3. Let G be a connected polycyclic graph with n vertices and m edges. Let among its vertices there are n_h vertices with degree h for some h different from 3. Then, for $p=3$,

$$Z_p(G) \geq 2p^p(m-n) - \Theta_p(h)n_h$$

where θ_p is the polynomial defined by Eq. (11).

Equality is attained if and only if all the n-n_h remaining vertices of G are of degree 3. This equality case pertains to a class of polycyclic (n,m)-graphs with a fixed number of vertices of degree h. Their Z_3 values are minimal.

Note that the equality case in Theorem 3 (necessarily) agrees with that in Theorem 2.

The third model: $\gamma = \lambda p^p$

In the previous sections, we have seen that meaningful conclusions on the property of the sum of powers of vertex degrees can be deduced in the case when the polynomial $\theta_p(k)$ is zero for some particular value of p and k, whereas it is positive valued for all other choices of p and k. Therefore, in this section, we only focus on the condition $\theta_p(k)$=0 within our third model for the multiplier γ.

In this case, $\gamma=\lambda\, p^p$, and we get

$$\Theta_p(k) = k^p - \lambda p^p k + 2\lambda \cdot p^p \,. \tag{12}$$

Consider the functions $F_1(k) = k^p$ and $F_2(k) = -\lambda p^p k + 2\lambda \cdot p^p$. Noting that $F_1(0)$=0 and $F_2(0)=2\lambda p^p > 0$, and that F_1 is monotonically increasing whereas F_2 monotonically decreases, there must exist a point (not necessarily at an integer k) where they meet. If such a k is an integer, then $\theta_p(k)$, defined via Eq. (12), would become equal to zero. Then, the condition $\theta_p(k)$=0, for any chosen value of the exponent p, would determine a particular value of the parameter λ.

In what follows, we show how λ is determined when the condition $\theta_p(p)$=0 is imposed.

If $\theta_p(p)$=0, then by Eq. (12),

$$p^p - \lambda p^p \cdot p + 2\lambda \cdot p^p = 0 \,.$$

from which it immediately follows that $\lambda=1/(p-2)$. This result also indicated that the condition $\theta_p(p)=0$ is not applicable in the case $p=2$.

Additional examinations of our third model for γ, as well as of other possible models of this kind, is left for some later work. In any case, we believe that we clearly demonstrated that the paper (Gutman, 2014), recognized only the tip of an iceberg. It may be that here we did the same.

References

Alameri, A., Al-Naggar, N., Al-Rumaima, M. & Alsharafi, M. 2020. Y-Index of some graph operations. *International Journal of Appllied Engineering Research,* 15(2), pp.173-179. [online] https://www.ripublication.com/Volume/ijaerv15n2.htm [Accessed: 25 January 2025]

Biggs, N.L., Lloyd, E.K. & Wilson, R.J. 1976. *Graph Theory 1736 – 1936*. Oxford: Clarendon Press. ISBN 0-19-853916-9

Bondy, J.A. & Murty, U.S.R. 1976. *Graph Theory with Applications*. New York: Macmillan Press. ISBN: 0-444-19451-70.

Das, K.C., Xu, K. & Wnag, J. 2016. On inverse degree and topological indices of graphs. *Filomat*, 30, pp 2111-2120. [online] Available at: http://www.jstor.org/stable/24899231 [Accessed: 25 January 2025]

Furtula, B. & Gutman, I., 2015. A forgotten topological index. *Journal of Mathematical Chemistry*, 53, pp.1184-1190. Available at: https://doi.org/10.1007/s10910-015-0480-z

Gutman, I. 2014. An exceptional property of the first Zagreb index. *MATCH Communications in Mathematical in in Computer Chemistry,* 72, pp.733-740. [online] https://match.pmf.kg.ac.rs/electronic_versions/Match72/n3/match72n3_733-740.pdf [Accessed: 25 January 2025]

Gutman, I. & Trinajstić, N. 1972 Graph theory and molecular orbitals - Total π-electron energy of alternant hydrocarbons. *Chemical Physics Lettets*. 17, pp. 535-538. Available at: https://doi.org/10.1016/0009-2614(72)85099-1

Kier, L.B. & Hall, L.H. 1976. *Molecular Connectivity in Chemistry and Drug Research*. New York: Academic Press. ISBN: 0124065600

Nagarajan, S., Kayalvizhi, G. & Priyadharsini, G. 2021. S-index of different graph operations. *Asian Research Journal of Mathematics*, 17(12), pp.43--52. Available at: https://doi.org/10.9734/arjom/2021/v17i1230347

Nikolić, S., Kovačević, G., Miličević, A. & Trinajstić, N. 2003. The Zagreb indices 30 years after. *Croatica Chemica Acta.* 76, pp.113-124. [online] Available at: https: //hrcak.srce.hr/103086 [Accessed: 25 January 2025].

Yousef, W., Alameri, A., Alsharafi, M., Al-Naggar, N, & Al-Fuhaid, B. 2025. Topological and hyper topological coindices of benzenoid circumcoronene series. *Baghdad Science Journal*, 22(3). Available at: https://doi.org/10.21123/bsj.2024.10588

Sobre la suma de potencias de grados de vértices de grafos policíclicos

Ivan Gutman
Universidad de Kragujevac, Facultad de Ciencias, Kragujevac, República de Serbia,

CAMPO: matemáticas (clasificación de asignaturas de matemáticas: primaria 05c07, secundaria 05c09)
TIPO DE ARTÍCULO: artículo científico original

Resumen:

Introducción/propósito: La suma de potencias de los grados de los vértices de grafos se estudia ampliamente , pero solo para algunos valores fijos de la potencia. Las propiedades generales de estas sumas se estudian en mucha menor medida. En este artículo, presentamos resultados en este sentido.

Métodos: Se aplica la teoría de grafos combinatorios.

Resultados: Se establecen unos límites inferiores para la suma de potencias de grados de vértice, aplicables a todas las potencias. Se caracterizan las clases de grafos policíclicos con una suma mínima de potencias de grados de vértice.

Conclusión: El artículo contribuye al estudio de la suma de potencias de grados de vértices de grafos.

Palabras clave: grado (de un vértice), suma de potencias de grados de vértices de grafos, grafos policíclicos.

О сумме степеней вершин полициклических графов

Иван Гутман
Крагуевацкий университет, естественно-математический факультет,
г. Крагуевац, Республика Сербия

РУБРИКА ГРНТИ: 27.29.19 Краевые задачи и задачи на собственные значения для обыкновенных дифференциальных уравнений и систем уравнений
ВИД СТАТЬИ: оригинальная научная статья

Резюме:

Введение/цель: Несмотря на то что сумма степеней вершин графов широко изучена в литературе, многим значениям степени не уделено внимания. Общие свойства этих сумм *изучены в гораздо меньшей степени. В данной статье представлены новые результаты в этом направлении.*

Методы: В статье применена комбинаторная теория графов.

Результаты: Установлено несколько нижних границ для суммы степеней вершин, применимых ко всем степеням. Описаны классы графов с минимальной суммой степеней вершин.

Выводы: Результаты данной статьи вносят вклад в изучение суммы степеней вершин графов.

Ключевые слова: степень (вершины), сумма степеней вершин графов, полициклические графы.

О збиру потенцираних степена чворова полицикличних графова

Иван Гутман

Универзитет у Крагујевцу, Природно-математички факултет, Крагујевац, Република Србија

ОБЛАСТ: математика
КАТЕГОРИЈА (ТИП) ЧЛАНКА: оригинални научни рад

Сажетак:

Увод/циљ: Збир потенцираних степена чворова графа проучаван је у литератури само за одређене вредности потенције. Опште особине ових сума недовољно су истраживане, па се у овом раду наводе нови резултати истраживања.

Методе: Примењена је комбинаторна теорија графова.

Резултати: Добијено је неколико граница за збир потенцираних степена чворова, применљивих за све потенције. Карактерисане су класе графова са минималном сумом потенцираних степена.

Закључак: Рад доприноси проучавању збира потенцраних степена чворова графова.

Кључне речи: степен (чвора), збир потенцираних степена чворова графа, полициклични графови.

Paper received on: 07.09.2025.
Manuscript corrections submitted on: 26.09.2025.
Paper accepted for publishing on: 02.10.2025.

VOJNOTEHNIČKI GLASNIK / MILITARY TECHNICAL COURIER, 2025, Vol. 73, Issue 3

Some fixed point theorems via γ-ψ_S-contractions on S-metric spaces

Nihal Taş[a], *Elif* Kaplan [b]

[a] Balıkesir University, Department of Mathematics, 10145 Balıkesir, Türkiye;
e-mail: nihaltas@balikesir.edu.tr, **corresponding author**,
ORCID iD: https://orcid.org/0000-0002-4535-4019

[b] Ondokuz Mayis University, Department of Mathematics, 55200 Samsun, Türkiye,
e-mail: elifaydin@omu.edu.tr,
ORCID iD: https://orcid.org/0000-0002-7620-3387

doi https://doi.org/10.5937/vojtehg73-56176

FIELD: mathematics
ARTICLE TYPE: original scientific paper

Abstract:

Introduction: This paper focuses on extending the theory of fixed points in S-metric spaces by introducing new generalized contractive conditions. These developments aim to enrich the analytical tools available for studying such spaces.

Methods: A variety of fixed-point theorems is established by applying the newly defined contractive conditions. The methodology includes both standard and integral-type contractive mappings. Furthermore, a geometric approach is utilized to obtain novel fixed-circle theorems within the S-metric framework.

Results: Several fixed-point and fixed-circle theorems are proved under the proposed conditions. Illustrative examples are provided to validate the theoretical findings and demonstrate the applicability of the results.

Conclusion: The findings of this study not only broaden the scope of fixed-point theory in S-metric spaces but also offer potential implications for real-world applications. In particular, the results may contribute to developments in computational mathematics and the design of neural network activation functions.

Keywords: S-metric space, fixed-point theorem, generalized contraction, integral-type contraction, fixed-circle, geometric approach, activation function, neural networks.

Introduction and preliminaries

Fixed-point theory has far-reaching implications in mathematics and its applications to other disciplines. One of its most significant contributions is in the realm of dynamical systems, where it is used to analyze equilibrium points or steady states. For example, in economics, fixed points help to model market equilibria, where no participant has an incentive to change their strategy. In game theory, Nash equilibrium points are essentially fixed points of certain types of functions. Furthermore, in computational mathematics, algorithms such as those used in optimization or numerical methods often rely on fixed point results to guarantee convergence. The general idea that under certain conditions a system will reach a state of stability is a profound insight that has shaped much of theoretical and applied research.

Metric spaces are crucial for studying the topological properties of spaces, such as continuity, compactness, and convergence. They provide a framework for understanding distance-based relationships between objects in various fields, from analysis to geometric topology. For example, the concept of convergence in a metric space allows mathematicians to rigorously define limits and study the behavior of sequences and functions. Metric spaces are particularly important in functional analysis and measure theory, where the behavior of functions or sequences within these spaces is a key focus.

On the other hand, generalized metric spaces, including S-metric spaces (Sedghi et al, 2012), broaden the scope by allowing non-separable points, making them useful in settings like group theory or quotient spaces. S-metric spaces extend the traditional concept of metric spaces by incorporating a three-variable distance function, which enables more flexible modeling of geometric and topological structures. These spaces can model scenarios where traditional distance functions fail to capture equivalence relations or where the notion of “closeness” is not strict. In essence, generalized metric spaces offer a more flexible structure, which can be applied to various advanced topics in algebraic topology, category theory, and even computer science, especially in the study of data structures and approximation methods, for more details, see (Fetouci & Radenovic, 2009; Iqbal et al, 2024; Bimol et al, 2024).

Both metric and generalized metric spaces are foundational for many modern branches of mathematics, and their applications extend to fields such as signal processing, machine learning, network theory, and mathematical physics, underscoring their importance beyond theoretical investigations. These concepts help mathematicians and scientists model and understand complex phenomena in an increasingly interconnected world.

The paper by Özgür NY and Taş N., titled "Some Fixed-Circle Theorems on Metric Spaces", published in the Bulletin of the Malaysian Mathematical Sciences Society (Özgür & Taş, 2019a), explores important fixed-point results in the context of metric spaces, specifically focusing on "fixed-circle" theorems. In this study, the authors extend and generalize classical fixed point theorems by introducing new conditions under which fixed points can be guaranteed. Their work contributes to a deeper understanding of the structure of metric spaces and the behavior of certain types of mappings that preserve geometric properties, such as distance. These findings are significant for both theoretical and applied mathematics, as fixed point theorems play a crucial role in the areas such as dynamical systems, game theory, and optimization. By providing novel results in the realm of metric spaces, this research opens new pathways for investigating equilibrium solutions and offers tools for solving complex problems across various mathematical and interdisciplinary domains. The importance of this paper lies in its potential applications to both pure and applied fields, including analysis, topology, and computational mathematics.

By the above motivations, in this paper, we introduce some generalized contractive conditions on S-metric spaces. Using these new contractions, we prove some fixed-point theorem and integral type fixed-point theorems on S-metric spaces. Also, using the geometric approach, we obtain new fixed-circle results on S-metric spaces with necessary examples. Finally, in the conclusion section, we mention the importance of this paper with an example of activation functions.

The following is a definition of the concept of an S-metric space that was provided by Sedghi, Shobe, and Aliouche:

Definition 1. *(Sedghi et al, 2012) Let X be a nonempty set. An S-metric on X is a function $S : X \times X \times X \to [0, +\infty)$ that satisfies the following conditions for all $x, y, z, a \in X$:*

$(\boldsymbol{S}1)$ $S(x, y, z) = 0$ if and only if $x = y = z$,

$(\boldsymbol{S}2)$ $S(x, y, z) \leq S(x, x, a) + S(y, y, a) + S(z, z, a)$.

VOJNOTEHNIČKI GLASNIK / MILITARY TECHNICAL COURIER, 2025, Vol. 73, Issue 3

The pair (X,S) is called an S-metric space.

For an S-metric space, the symmetry condition can be considered as follows:

$$S(x,x,y) = S(y,y,x)$$

for all $x,y \in X$ (Sedghi et al, 2012).

Example 1. (Sedghi et al, 2012) Let $\mathbb{R}$ be the real line. Then

$$S(x,y,z) = |x-z| + |y-z|$$

for all $x,y,z \in \mathbb{R}$ is an S-metric on $\mathbb{R}$. This S-metric on $\mathbb{R}$ is called the usual S-metric.

Example 2. Let $X = \mathbb{R}$ and

$$S(x,y,z) = |y+z-2x| + |y-z|$$

for all $x,y,z \in X$. Then, (X,S) is an S-metric space (Sedghi et al, 2012). But this S-metric cannot be generated by any metric (Hieu et al, 2015) .

Example 3. (Özgür & Taş, 2017) Let $X = \mathbb{R}$ and define the function

$$S(x,y,z) = |x-z| + |x+z-2y|$$

for all $x,y,z \in X$. Then, (X,S) is an S-metric space. But this S-metric cannot be generated by any metric.

Definition 2. *(Sedghi et al, 2012) Let (X,S) be an S-metric space.*

1. A sequence $\{x_n\} \subset X$ converges to $x \in X$ if $S(x_n, x_{n,x}) \to 0$ as $n \to +\infty$.
2. A sequence $\{x_n\} \subset X$ is a Cauchy sequence if $S(x_n, x_n, x_m) \to 0$ as $n,m \to +\infty$.
3. The S-metric space (X,S) is complete if every Cauchy sequence is a convergent sequence.

Definition 3. *(Sedghi et al, 2014) Let $f : X \to Y$ be a map from an S-metric space X to an S-metric space. Then f is continuous at $x \in X$ if and only if $f(x_n) \to f(x)$ whenever $x_n \to x$.*

As demonstrated in (Hieu et al, 2015) and (Özgür & Taş, 2017), certain S-metrics cannot be derived from standard metrics. Consequently, investigating new fixed-point theorems within the context of S-metric spaces is essential.

A recent innovative approach to geometrically interpretations for fixed points, known as the fixed-circle problem (Özgür & Taş, 2019a), has emerged. The following concepts are now recalled, as they were defined in (Mlaiki et al, 2018), and (Özgür & Taş, 2019b).

Let (X, S) be an S-metric space and $T : X \to X$ a self-mapping. A circle $C^S_{x_0,r}$ and a disc $D^S_{x_0,r}$ are defined by

$$C^S_{x_0,r} = \{u \in X : S(u, u, x_0) = r\}$$

and

$$D^S_{x_0,r} = \{u \in X : S(u, u, x_0) \leq r\},$$

with the center $x_0 \in X$ and the radius $r > 0$.

If $Tx = x$ for all $x \in C^S_{x_0,r}$ (resp. $x \in D^S_{x_0,r}$) then the circle $C^S_{x_0,r}$ (resp. the disc $D^S_{x_0,r}$) is called the fixed circle (resp. fixed disc) of T.

For every function $\Psi : [0, +\infty) \to [0, +\infty)$, let ψ^n be the nth iterate of ψ. Then the following holds:

If Ψ is non-decreasing, then for each $t > 0$, $\lim_{n\to\infty} \psi^n(t) = 0$ implies $\Psi(t) < t$ (Raji et al, 2024).

In 2012, Samet et al. (Samet et al, 2012) introduced the class of α-admissible mappings.

Definition 4. *(Samet et al, 2012) Let X be a nonempty set, $T : X \to X$ and $\alpha : X \times X \to \mathbb{R}^+$, we say that T is an α-admissible mapping if*

$$x, y \in X, \alpha(x, y) \geq 1 \Longrightarrow \alpha(Tx, Ty) \geq 1.$$

Main results

In this section, we give some fixed-point theorems on S-metric spaces inspiring the approaches used in (Raji et al, 2024). Also, we present the integral versions of our obtained results using the technique given in (Branciari, 2002). As a geometric approach, we obtain new fixed-circle results on S-metric spaces.

DEFINITION 5. *Let (X,S) be an S-metric space and $f : X \to X$ be a self-mapping. f is called a γ-ψ_S-contractive mapping if there exist $\gamma : X \times X \times X \to [0,+\infty)$ and $\psi \in \Psi$ such that*

$$\gamma(x,x,y)\, S(fx,fx,fy) \leq \psi(\Delta(x,y)),$$

for all $x,y \in X$, where

$$\Delta(x,y) = \max \left\{ \begin{array}{c} S(x,x,y), S(x,x,fx), S(y,y,fy), \\ \frac{S(x,x,fx)S(y,y,fy)}{S(x,x,y)}, \\ \frac{S(x,x,fx)S(y,y,fy)}{S(x,x,y)+S(x,x,fy)+S(y,y,fx)}, \\ \frac{S(x,x,fx)S(x,x,fy)+S(y,y,fx)S(y,y,fy)}{S(y,y,fx)+S(x,x,fy)} \end{array} \right\}.$$

THEOREM 1. *Let (X,S) be a complete S-metric space and $f : X \to X$ be a γ-ψ_S-contractive mapping. If the following conditions are satisfied*:

(i) f is γ-admissible,

(ii) there exists $x_0 \in X$ such that $\gamma(x_0,x_0,fx_0) \geq 1$, and

(iii) f is continuous,
then there exists $a \in X$ such that $fa = a$.

Proof. By (ii), we say that there exists a point $x_0 \in X$ such that

$$\gamma(fx_0,fx_0,fx_0) \geq 1.$$

Let us define a sequence $\{x_n\}$ in X by $fx_n = x_{n+1}$ for all $n \geq 0$. If for some $n \geq 0$,

$$x_n = x_{n+1},$$

then

$$fx_n = x_{n+1} = x_n,$$

and so x_n is a fixed point of f. On the contrary, we suppose that

$$x_n \neq x_{n+1},$$

for all $n \geq 0$. Since f is γ-admissible, we get

$$\gamma(x_0,x_0,fx_0) = \gamma(x_0,x_0,x_1) \geq 1$$

$$\Longrightarrow \gamma(fx_0, fx_0, fx_1) = \gamma(x_1, x_1, x_2) \geq 1.$$

If we continue this process, we have

$$\gamma(x_n, x_n, x_{n+1}) \geq 1,$$

for all $n \geq 0$. Using the γ-ψ_S-contractive mapping definition, we have

$$\begin{aligned} S(x_{n+1}, x_{n+1}, x_n) &= S(fx_n, fx_n, fx_{n-1}) \\ &\leq \gamma(x_n, x_n, x_{n-1}) S(fx_n, fx_n, fx_{n-1}) \\ &\leq \psi(\Delta(x_n, x_{n-1})), \end{aligned} \tag{1}$$

for all $n \geq 1$, where

$$\Delta(x_n, x_{n-1}) =$$

$$= \max \left\{ \begin{array}{c} S(x_n, x_n, x_{n-1}), S(x_n, x_n, fx_n), S(x_{n-1}, x_{n-1}, fx_{n-1}), \\ \frac{S(x_n, x_n, fx_n) S(x_{n-1}, x_{n-1}, fx_{n-1})}{S(x_n, x_n, x_{n-1})}, \\ \frac{S(x_n, x_n, fx_n) S(x_{n-1}, x_{n-1}, fx_{n-1})}{S(x_n, x_n, x_{n-1}) + S(x_n, x_n, fx_{n-1}) + S(x_{n-1}, x_{n-1}, fx_n)}, \\ \frac{S(x_n, x_n, fx_n) S(x_n, x_n, fx_{n-1}) + S(x_{n-1}, x_{n-1}, fx_n) S(x_{n-1}, x_{n-1}, fx_{n-1})}{S(x_{n-1}, x_{n-1}, fx_n) + S(x_n, x_n, fx_{n-1})} \end{array} \right\}$$

$$\leq \max \left\{ \begin{array}{c} S(x_n, x_n, x_{n-1}), S(x_n, x_n, x_{n+1}), S(x_{n-1}, x_{n-1}, x_n), \\ S(x_n, x_n, x_{n+1}), S(x_n, x_n, x_{n+1}), S(x_{n-1}, x_{n-1}, x_n) \end{array} \right\}$$

$$= \max \{ S(x_n, x_n, x_{n-1}), S(x_n, x_n, x_{n+1}) \}.$$

By 1, we get

$$S(x_{n+1}, x_{n+1}, x_n) \leq \psi(\max \{ S(x_n, x_n, x_{n-1}), S(x_n, x_n, x_{n+1}) \}),$$

for all $n \geq 1$.

Case 1: Let $S(x_n, x_n, x_{n-1}) \leq S(x_n, x_n, x_{n+1})$. Then we get

$$S(x_{n+1}, x_{n+1}, x_n) \leq \psi(S(x_n, x_n, x_{n+1})) < S(x_n, x_n, x_{n+1}),$$

a contradiction.

Case 2: Let $S(x_n, x_n, x_{n+1}) \leq S(x_n, x_n, x_{n-1})$. Then we have

$$S(x_{n+1}, x_{n+1}, x_n) \leq \psi(S(x_n, x_n, x_{n-1})),$$

for all $n \geq 1$. Using the mathematical induction, if we continue this process, we obtain

$$S(x_{n+1}, x_{n+1}, x_n) \leq \psi^n(S(x_1, x_1, x_0)),$$

for all $n \geq 1$. Then, we get

$$S(x_n, x_n, x_{n+k}) \leq \sum_{p=n}^{n+k-1} 2\psi^p S(x_1, x_1, x_0), \tag{2}$$

for all $k \geq 1$. By 2, if we take $p \to +\infty$, we have

$$S(x_n, x_n, x_{n+k}) \to 0,$$

and so $\{x_n\}$ is Cauchy. Using the completeness hypothesis, there is $a \in X$ such that

$$\lim_{n\to+\infty} x_n = a.$$

By (iii), we have

$$fa = f\left(\lim_{n\to+\infty} x_n\right) = \lim_{n\to+\infty} fx_n = \lim_{n\to+\infty} x_{n+1} = a.$$

Therefore, a is a fixed point of f. □

Remark 1. Theorem 1 is an existence of a fixed point for the self-mapping f with the continuity hypothesis.

In the following existence theorem, we do not use the continuity hypothesis.

Theorem 2. *Let (X, S) be a complete S-metric space and $f : X \to X$ be a γ-ψ_S-contractive mapping. If the following conditions are satisfied*:

(i) f is γ-admissible,

(ii) there exists $x_0 \in X$ such that $\gamma(x_0, x_0, fx_0) \geq 1$, and

(iii) If $\{x_n\}$ is a sequence in X such that $\gamma(x_n, x_n, x_{n+1}) \geq 1$ for all n and $x_n \to x \in X$ as $n \to +\infty$, then there is a subsequence $\{x_{n_k}\}$ of $\{x_n\}$ such that $\gamma(x_{n_k}, x_{n_k}, x) \geq 1$ for all k,
then there is $a \in X$ such that $fa = a$.

Proof. Using the proof of Theorem 1, we can say that the sequence $\{x_n\}$ defined by

$$fx_n = x_{n+1},$$

for all $n \geq 0$, converges for some $a \in X$. By (iii), there is a subsequence $\{x_{n_k}\}$ of $\{x_n\}$ such that

$$\gamma\left(x_{n_k}, x_{n_k}, a\right) \geq 1,$$

for all k. Using the γ-ψ_S-contractive mapping hypothesis, we obtain

$$\begin{aligned} S\left(x_{n_k+1}, x_{n_k+1}, fa\right) &= S\left(fx_{n_k}, fx_{n_k}, fa\right) \\ &\leq \gamma\left(x_{n_k}, x_{n_k}, a\right) S\left(fx_{n_k}, fx_{n_k}, fa\right) \\ &\leq \psi\left(\Delta\left(x_{n_k}, a\right)\right), \end{aligned} \tag{3}$$

where

$$\Delta\left(x_{n_k}, a\right) = \max\left\{\begin{array}{c} S\left(x_{n_k}, x_{n_k}, a\right), S\left(x_{n_k}, x_{n_k}, x_{n_k+1}\right), S\left(a, a, fa\right), \\ \frac{S\left(x_{n_k}, x_{n_k}, x_{n_k+1}\right) S(a,a,fa)}{S\left(x_{n_k}, x_{n_k}, a\right)}, \\ \frac{S\left(x_{n_k}, x_{n_k}, x_{n_k+1}\right) S(a,a,fa)}{S\left(x_{n_k}, x_{n_k}, a\right) + S\left(x_{n_k}, x_{n_k}, fa\right) + S\left(a, a, x_{n_k+1}\right)}, \\ \frac{S\left(x_{n_k}, x_{n_k}, x_{n_k+1}\right) S\left(x_{n_k}, x_{n_k}, fa\right) + S\left(a, a, x_{n_k+1}\right) S(a,a,fa)}{S\left(a, a, x_{n_k+1}\right) + S\left(x_{n_k}, x_{n_k}, fa\right)} \end{array}\right\}.$$

Let us take $k \to \infty$, we have

$$\lim_{k \to +\infty} \Delta\left(x_{n_k}, a\right) = S\left(a, a, fa\right).$$

Now, we assume that $S\left(a, a, fa\right) > 0$. For large enough k, we have

$$\Delta\left(x_{n_k}, a\right) > 0$$

and

$$\psi\left(\Delta\left(x_{n_k}, a\right)\right) < \Delta\left(x_{n_k}, a\right).$$

By 1, we obtain

$$S\left(x_{n_{k+1}}, x_{n_{k+1}}, fa\right) < \Delta\left(x_{n_k}, a\right).$$

Let us take $k \to +\infty$, we get

$$S\left(a, a, fa\right) < S\left(a, a, fa\right),$$

a contradiction. It should be $S\left(a, a, fa\right) = 0$, that is, $fa = a$. Therefore, a is a fixed point of f. $\square$

Example 4. Let $X = \{(1,0), (0,1)\} \subset \mathbb{R}^2$ and define the S-metric as

$$S((x,y),(u,v),(a,b)) = |u-a| + |u+a-2x| + |v-b| + |u+b-2y|,$$

for all $(x,y),(u,v),(a,b) \in X$. Then, (X,S) is a complete S-metric space and the S-metric is not generated by any metric. Let us define the self-mapping $f : X \to X$ as

$$f(x,y) = (x,y),$$

for all $(x,y) \in X$. It is clear that f is continuous. Also, the following inequality is satisfied for any $\psi \in \Psi$,

$$\gamma((x,y),(x,y),(u,v))\, S(f(x,y), f(x,y), f(u,v)) \leq \psi(\Delta((x,y),(u,v))),$$

for all $(x,y),(u,v) \in X$, where

$$\gamma((x,y),(u,v),(a,b)) = \begin{cases} 1, & (x,y) = (u,v) = (a,b) \\ 0, & \text{otherwise} \end{cases}.$$

Then, f is a γ-ψ_S-contractive mapping. Also, f is γ-admissible. Indeed, for all $(x,y),(u,v),(a,b) \in X$, we get

$$\begin{aligned} \gamma((x,y),(u,v),(a,b)) &\geq 1 \\ &\implies (x,y) = (u,v) = (a,b) \\ &\implies f(x,y) = f(u,v) = f(a,b) \\ &\implies \gamma(f(x,y), f(u,v), f(a,b)) \geq 1. \end{aligned}$$

Also, for all $(x,y) \in X$, we have

$$\gamma((x,y),(u,v),(a,b)) \geq 1.$$

Hence, the conditions of Theorem 1 are satisfied. On the other hand, if $\{(x_n,y_n)\}$ is a sequence in X that converges to some point $(a,b) \in X$ with

$$\gamma((x_n,y_n),(x_n,y_n),(a,b)) \geq 1,$$

for all n, then by the definition of γ, we get

$$(x_n,y_n) = (a,b),$$

for all n, which implies that

$$\gamma((x_n,y_n),(x_n,y_n),(a,b)) = 1.$$

So, the conditions of Theorem 2 are satisfied. Consequently, f has two fixed points in X, that is, $Fix(f) = X$.

REMARK 2. From Example 4, it can be said that the fixed points of a given self-mapping which satisfies the conditions Theorem 1 (or Theorem 2) cannot be unique. For this reason, it is important to investigate the uniqueness conditions for the existence theorems. For this purpose, we consider the following condition:

(iv) There is $z \in X$ such that

$$\gamma(x, x, z) \geq 1 \text{ and } \gamma(y, y, z) \geq 1,$$

for all $x, y \in Fix(f)$.

THEOREM 3. *If we add the condition (iv) to the hypothesis of Theorem 1 (resp. Theorem 2), then a is a unique fixed point of f.*

Proof. Let b be another fixed point of f with $a \neq b$. By (iv), there exists $z \in X$ such that

$$\gamma(a, a, z) \geq 1 \text{ and } \gamma(b, b, z) \geq 1.$$

From the α-admissibility of f, we get

$$\gamma(a, a, f^n z) \geq 1 \text{ and } \gamma(b, b, f^n z) \geq 1,$$

for all n. Let us define the sequence $\{z_n\}$ in X by

$$fz_n = z_{n+1},$$

for all $n \geq 0$ and $z_0 = z$. Then, we have

$$\begin{array}{rcl} S(a, a, z_{n+1}) & = & S(fa, fa, fz_n) \\ & \leq & \gamma(a, a, z_n) S(fa, fa, fz_n) \\ & \leq & \psi(\Delta(a, z_n)), \end{array}$$

where

$$\Delta(a, z_n) = \max \left\{ \begin{array}{c} S(a, a, z_n), S(a, a, a), S(z_n, z_n, z_{n+1}), \\ \frac{S(a,a,a)S(z_n,z_n,z_{n+1})}{S(a,a,z_n)}, \\ \frac{S(a,a,a)S(z_n,z_n,z_{n+1})}{S(a,a,z_n)+S(a,a,z_{n+1})+S(z_n,z_n,a)}, \\ \frac{S(a,a,a)S(a,a,z_{n+1})+S(z_n,z_n,a)S(z_n,z_n,z_{n+1})}{S(z_n,z_n,a)+S(a,a,z_{n+1})} \end{array} \right\}$$

$$\leq \max\left\{S\left(a,a,z_n\right), S\left(a,a,z_{n+1}\right)\right\}.$$

Hence, using the monotone property of ψ, we obtain

$$S\left(a,a,z_{n+1}\right) \leq \psi\left(\max\left\{S\left(a,a,z_n\right), S\left(a,a,z_{n+1}\right)\right\}\right),$$

for all n. Without the generality, we assume that

$$S\left(a,a,z_n\right) > 0,$$

for all n.

Case 1: Let $\max\left\{S\left(a,a,z_n\right), S\left(a,a,z_{n+1}\right)\right\} = S\left(a,a,z_{n+1}\right)$. Then we have

$$S\left(a,a,z_{n+1}\right) \leq \psi\left(S\left(a,a,z_{n+1}\right)\right) < S\left(a,a,z_{n+1}\right),$$

a contradiction.

Case 2: $\max\left\{S\left(a,a,z_n\right), S\left(a,a,z_{n+1}\right)\right\} = S\left(a,a,z_n\right)$. Hence we get

$$S\left(a,a,z_n+1\right) \leq \psi\left(S\left(a,a,z_n\right)\right),$$

for all n. If we continue this process, then we have

$$S\left(a,a,z_n\right) \leq \psi^n\left(S\left(a,a,z_0\right)\right),$$

for all $n \geq 1$. Let us take $n \to +\infty$, we obtain

$$\lim_{n\to+\infty} S\left(a,a,z_n\right) = 0$$

and similarly,

$$\lim_{n\to+\infty} S\left(b,b,z_n\right) = 0$$

From the uniqueness of the limit point, we have

$$a = b.$$

Then a is the unique fixed point of f. □

EXAMPLE 5. Let $X=[0,1]$ and the S-metric be defined as

$$S(x,y,z)=|x-z|+|x+z-2y|,$$

for all $x,y,z\in X$ (Özgür & Taş, 2017). Then, the pair (X,S) is a complete S-metric space. Let us define the self-mapping $f:X\to X$ by

$$fx=\begin{cases}\frac{1}{8}, & x\in[0,1)\\ 0, & x=1\end{cases},$$

for all $x\in[0,1]$. It is clear that f is not a continuous function at the point $x_0=1$. Now we define the mapping $\gamma:X\times X\times X\to[0,+\infty)$ by

$$\gamma(x,y,z)=\begin{cases}1, & (x,y,z)\in\left(\left[0,\frac{1}{8}\right]\times\left[0,\frac{1}{8}\right]\times\left[\frac{1}{8},1\right]\right)\\ & \quad\cup\left(\left[\frac{1}{8},1\right]\times\left[\frac{1}{8},1\right]\times\left[0,\frac{1}{8}\right]\right)\\ 0, & \text{otherwise}\end{cases}$$

We show the validity of this example under the cases:

Case 1: f is a γ-ψ_S-contractive mapping with

$$\psi(t)=\frac{t}{4},$$

for all $t\geq 0$. If $x\in\left[0,\frac{1}{8}\right]$ and $z=1$, we have

$$\begin{aligned}\gamma(x,x,y)S(fx,fx,fy) &= S(fx,fx,fy)\\ &= 2|fx-fy|\\ &= 2\left|\frac{1}{8}-0\right|\\ &= \frac{1}{4}\\ &= \frac{1}{8}S(y,y,fy)\\ &\leq \psi(\Delta(x,y)).\end{aligned}$$

If $x=1$ and $y\in\left[0,\frac{1}{8}\right]$, we have

$$\begin{aligned}\gamma(x,x,y)S(fx,fx,fy) &= S(fx,fx,fy)\\ &= 2|fx-fy|\\ &= 2\left|0-\frac{1}{8}\right|\end{aligned}$$

$$\begin{aligned} &= \frac{1}{4} \\ &= \frac{1}{8} S(x,x,fx) \\ &\leq \psi(\Delta(x,y)). \end{aligned}$$

The other cases are clear.

Case2: f is γ-admissible. To show this, we assume that $(x,y,z) \in X \times X \times X$ such that

$$\gamma(x,y,z) \geq 1.$$

If $(x,y,z) \in \left[0, \frac{1}{8}\right] \times \left[0, \frac{1}{8}\right] \times \left[\frac{1}{8}, 1\right]$, then $(fx, fy, fz) \in \left[\frac{1}{8}, 1\right] \times \left[\frac{1}{8}, 1\right] \times \left[0, \frac{1}{8}\right]$ which implies

$$\gamma(fx, fy, fz) = 1.$$

If $(x,y,z) \in \left[\frac{1}{8}, 1\right] \times \left[\frac{1}{8}, 1\right] \times \left[0, \frac{1}{8}\right]$, then $(fx, fy, fz) \in \left[0, \frac{1}{8}\right] \times \left[0, \frac{1}{8}\right] \times \left[\frac{1}{8}, 1\right]$ which implies

$$\gamma(fx, fy, fz) = 1.$$

Consequently, f is γ-admissible.

Case 3: There is $x_0 \in X$ such that

$$\gamma(x_0, x_0, fx_0) \geq 1.$$

If we take $x_0 = 0$, then we have

$$\gamma(x_0, x_0, fx_0) = \gamma\left(0, 0, \frac{1}{8}\right) = 1.$$

Case 4: If $\{x_n\}$ is a sequence in X such that $\gamma(x_n, x_n, x_{n+1}) \geq 1$ for all n and $x_n \to x$ as $n \to +\infty$, then there is a subsequence $\{x_{n_k}\}$ of $\{x_n\}$ such that

$$\gamma(x_{n_k}, x_{n_k}, x) \geq 1,$$

for all k. By the definition of γ, we get

$$(x_n, x_n, x_{n+1}) \in \left(\left[0, \frac{1}{8}\right] \times \left[0, \frac{1}{8}\right] \times \left[\frac{1}{8}, 1\right]\right) \cup \left(\left[\frac{1}{8}, 1\right] \times \left[\frac{1}{8}, 1\right] \times \left[0, \frac{1}{8}\right]\right)$$

for all n.

Case 5: The uniqueness condition (iv) is satisfied. Let $(a,b) \in [0,1] \times [0,1]$. For $z = \frac{1}{8}$, we get

$$\gamma(a,a,z) = 1, \ \gamma(b,b,z) = 1.$$

Consequently, f has a unique fixed point $a = \frac{1}{8}$.

REMARK 3. If the S-metric is generated by any metric, then the notion of a γ-ψ_S-contractive mapping coincides with the notion of a generated α-ψ-contractive type mapping introduced in (Raji et al, 2024). Also, under this case, Theorem 1 (resp. Theorem 2, Theorem 3) coincides with Theorem 3.2 (resp. Theorem 3.3, Theorem 3.4) proven in (Raji et al, 2024).

If the b-metric d^S is generated by the S-metric, then we obtain the following definitions and corollaries.

DEFINITION 6. *Let (X, d^S) be a b-metric space and $f : X \to X$ be a self-mapping. f is called an α-ψ_b-contractive mapping if there are two functions $\alpha : X \times X \to [0, +\infty)$ and $\psi \in \Psi$ such that*

$$\alpha(x, y) d^S(fx, fy) \leq \psi(\Delta_b(x, y)),$$

for all $x, y \in X$, where

$$\Delta_b(x, y) = \max \left\{ \begin{array}{c} d^S(x, y), d^S(x, fx), d^S(y, fy), \\ \frac{d^S(x,fx) d^S(y,fy)}{d^S(x,y)}, \\ \frac{d^S(x,fx) d^S(y,fy)}{d^S(x,y) + d^S(x,fy) + d^S(y,fx)}, \\ \frac{d^S(x,fx) d^S(x,fy) + d^S(y,fx) d^S(y,fy)}{d^S(y,fx) + d^S(x,fy)} \end{array} \right\}.$$

THEOREM 4. *Let (X, d^S) be a complete b-metric space and $f : X \to X$ be an α-ψ_b-contractive mapping. If the following conditions are satisfied:*

(i) *f is α-admissible,*
(ii) *there exists $x_0 \in X$ such that $\alpha(x_0, fx_0) \geq 1, and$*
(iii) *f is continuous,*
then there exists $a \in X$ such that $fa = a$.

THEOREM 5. *Let (X, d^S) be a complete b-metric space and $f : X \to X$ be an α-ψ_b-contractive mapping. If the following conditions are satisfied:*
(i) *f is α-admissible,*
(ii) *there exists $x_0 \in$ X such that $\alpha(x_0, fx_0) \geq 1$, and*
(iii) *if $\{x_n\}$ is a sequence in Xsuch that $\alpha(x_n, x_{n+1}) \geq 1$ for all n and $x_n \to x \in$ X as n $\to \infty$,then there is a subsequence $\{x_{n_k}\}$ of $\{x_n\}$ such that $\alpha(x_{n_k}, x) \geq 1$ for all k, then there is a $\in$ X such that fa=a.*
(iv) *There is z $\in$ X such that $\alpha(x, z) \geq 1$ and $\alpha(y, z) \geq 1$, for all x,y $\in$ Fix(f).*

THEOREM 6. *If we add the condition (iv) to the hypothesis of Theorem 5 (resp. Theorem 6), then a is a unique fixed point of f.*

Some integral type fixed-point results on S-metric spaces

DEFINITION 7. *Let (X, S) be an S-metric space and $f : X \to X$ be a self-mapping. f is called an integral type γ-ψ_S-contractive mapping if there exist $\gamma : X \times X \to [0, +\infty)$ and $\psi \in \Psi$ such that*

$$\int_0^{\gamma(x,x,y)S(fx,fx,fy)} \varphi(t)\, dt \leq \int_0^{\psi(\Delta(x,y))} \varphi(t)\, dt,$$

for all $x, y \in X$, where $\varphi : [0, +\infty) \to [0, +\infty)$ is a Lebesque integrable mapping, which is summable, that is, with finite integral on each compact subset of $[0, +\infty)$, nonnegative and such that

$$\int_0^{\varepsilon} \varphi(t)\, dt > 0,$$

for each $\varepsilon > 0$.

REMARK 4. If we take $\varphi(t) = 1$ in Definition 7, then the notions of a γ-ψ_S-contractive mapping and an integral type γ-ψ_S-contractive mapping coincide.

THEOREM 7. *Let (X, S) be a complete S-metric space and $f : X \to X$ be an integral type γ-ψ_S-contractive mapping. If the following conditions are satisfied:*

(a) *f is γ-admissible,*

(b) *there exists $x_0 \in X$ such that $\gamma(x_0, x_0, fx_0) \geq 1, and$*

(c) *f is continuous,*

then there exists $a \in X$ such that $fa = a$.

Proof. By the similar arguments used in the proof of Theorem 1, this can be easily proved. □

REMARK 5. If we take $\varphi(t) = 1$ in Theorem 7, then Theorem 7 and Theorem 1 coincide.

THEOREM 8. *Let* (X, S) *be a complete* S*-metric space and* $f : X \to X$ *be an integral type* γ-ψ_S*-contractive mapping. If the following conditions are satisfied*:

(a) f *is* γ*-admissible,*
(b) *there exists* $x_0 \in X$ *such that* $\gamma(x_0, x_0, fx_0) \geq 1, and$
(c) *if* $\{x_n\}$ *is a sequence in* X *such that* $\gamma(x_n, x_n, x_{n+1}) \geq 1$ *for all* n *and* $x_n \to x \in X$ *as* $n \to \infty$*, then there is a subsequence* $\{x_{n_k}\}$ *of* $\{x_n\}$ *such that* $\gamma(x_{n_k}, x_{n_k}, x) \geq 1$ *for all* k,

then there is $a \in X$ *such that* $fa = a$.

Proof. By the similar arguments used in the proof of Theorem 2, this can be easily proved. □

REMARK 6. If we take $\varphi(t) = 1$ in Theorem 8, Theorem 8 and Theorem 2 coincide.

THEOREM 9. (d) *There is* $z \in X$ *such that*

$$\gamma(x, x, z) \geq 1 \text{ and } \gamma(y, y, z) \geq 1,$$

for all $x, y \in Fix(f)$.

THEOREM 10. *If we add the condition* (d) *to the conditions* (a)-(b)-(c) *given in Theorem* 8 (*resp. Theorem* 7)*, then* a *is a unique fixed point of* f.

REMARK 7.

(1) If we take $\varphi(t) = 1$ in Theorem 10, then Theorem 3 and Theorem 10 coincide.
(2) Theorem 7, Theorem 8 and Theorem 10 are integral type fixed point results and generalize Theorem 3.2, Theorem 3.3 and Theorem 3.5 proved in (Raji et al, 2024).
(3) The two examples given earlier provide integral type fixed-point theorems with $\varphi(t) = 1$.
(4) On b-metric spaces, the notion of an integral type α-ψ_b-contractive mapping can be defined and new integral type fixed point results can be proved as seen in the previous theorems.
(5) The results obtained in this article are new generalized fixed-point results for both S-metric spaces and b-metric spaces.

DEFINITION 8. *Let (X,S) be an S-metric space and $f : X \to X$ be a self-mapping. f is called a γ-ψ_S-f_{x_0}-contractive mapping if there exists $x_0 \in X$, $\gamma : X \times X \times X \to [1,+\infty)$ and $\psi \in \Psi$ such that*

$$S(fx,fx,x) > 0 \Rightarrow \gamma(x,x,x_0) S(fx,fx,x) \leq \psi(\Delta^*(x,x_0)),$$

for all $x \in X$, where

$$\Delta^*(x,y) = \max \left\{ \begin{array}{c} S(x,x,y), S(x,x,fx), S(y,y,fy), \\ \frac{S(x,x,fx)S(y,y,fy)}{S(x,x,y)+S(x,x,fy)+S(y,y,fx)}, \\ \frac{S(x,x,fx)S(x,x,fy)+S(y,y,fx)S(y,y,fy)}{S(y,y,fx)+S(x,x,fy)} \end{array} \right\}.$$

PROPOSITION 1. *If f is a γ-ψ_S-f_{x_0}-contractive mapping with $x_0 \in X$, then we have*

$$fx_0 = x_0.$$

Proof. On the contrary, we assume $fx_0 \neq x_0$, that is,

$$S(fx_0,fx_0,x_0) > 0.$$

Using the contraction hypothesis, we get

$$\gamma(x_0,x_0,x_0) S(fx_0,fx_0,x_0) \leq \psi(\Delta^*(x_0,x_0))$$

and

$$\begin{aligned} \Delta^*(x_0,x_0) &= \left\{ \begin{array}{c} S(x_0,x_0,x_0), S(x_0,x_0,fx_0), S(x_0,x_0,fx_0), \\ \frac{S(x_0,x_0,fx_0)S(x_0,x_0,fx_0)}{S(x_0,x_0,x_0)+S(x_0,x_0,fx_0)+S(x_0,x_0,fx_0)}, \\ \frac{S(x_0,x_0,fx_0)S(x_0,x_0,fx_0)+S(x_0,x_0,fx_0)S(x_0,x_0,fx_0)}{S(x_0,x_0,fx_0)+S(x_0,x_0,fx_0)} \end{array} \right\} \\ &= S(x_0,x_0,fx_0) \end{aligned}$$

Hence, using the symmetry property and the property of ψ, we have

$$\begin{aligned} \gamma(x_0,x_0,x_0) S(fx_0,fx_0,x_0) &\leq \psi(S(fx_0,fx_0,x_0)) \\ &< S(fx_0,fx_0,x_0), \end{aligned}$$

a contradiction. So, it should be

$$fx_0 = x_0.$$

$\square$

Taş, N. et al., Some fixed point theorems via γ-ψ_S-contractions on S-metric spaces, pp.736–762

THEOREM 11. *Let f be a γ-ψ_S-f_{x_0}-contractive mapping with $x_0 \in X$ and the number*

$$r = \inf \{S(fx, fx, x) : x \in X, x \neq fx\}. \tag{4}$$

If $fx \in C^S_{x_{0,r}}$ for each $x \in C^S_{x_{0,r}}$, then f fixes the circle $C^S_{x_{0,r}}$.

Proof. Let us consider the following cases:

Case 1: Let $r = 0$. Then, we get

$$C^S_{x_0,r} = \{x_0\}$$

and so by Proposition 1, we say that f fixes the circle $C^S_{x_0,r}$.

Case 2: Let $r > 0$ and $x \in C^S_{x_0,r}$ be any point such that

$$S(fx, fx, x) > 0.$$

Using the contraction hypothesis and $fx \in C^S_{x_0,r}$, we get

$$\gamma(x, x, x_0) S(fx, fx, x) \leq \psi(\Delta^*(x, x_0))$$

and

$$\begin{aligned} \Delta^*(x, x_0) &= \max \left\{ \begin{array}{c} S(x, x, x_0), S(x, x, fx), S(x_0, x_0, fx_0), \\ \frac{S(x,x,fx) S(x_0,x_0,fx_0)}{S(x,x,x_0)+S(x,x,fx_0)+S(x_0,x_0,fx)}, \\ \frac{S(x,x,fx)S(x,x,fx_0)+S(x_0,x_0,fx)S(x_0,x_0,fx_0)}{S(x_0,x_0,fx)+S(x,x,fx_0)} \end{array} \right\} \\ &= S(fx, fx, x). \end{aligned}$$

So, we obtain

$$\gamma(x, x, x_0) S(fx, fx, x) \leq \psi(S(fx, fx, x)) < S(fx, fx, x),$$

a contradiction and thus, it should be

$$S(fx, fx, x) = 0 \Longrightarrow fx = x.$$

Consequently, f fixes the circle $C^S_{x_0,r}$. □

COROLLARY 1. *Let f be a γ-ψ_S-f_{x_0}-contractive mapping with $x_0 \in X$ and r be defined as in 4. If $fx \in D^S_{x_0,r}$ for each $x \in D^S_{x_0,r}$, then f fixes the disc $D^S_{x_0,r}$.*

EXAMPLE 6. Let $X = \mathbb{R}$ be the S-metric space with the S-metric defined as

$$S(x, y, z) = |x - z| + |x + z - 2y|,$$

for all $x, y, z \in \mathbb{R}$ (Özgür & Taş, 2017). This S-metric is not generated by any metric. Let us define the mappings $f : X \to X$, $\gamma : X \times X \times X \to [1, +\infty)$ and $\psi : [0, +\infty) \to [0, +\infty)$ as, respectively,

$$fx = \begin{cases} 41, & x = 40 \\ 0, & x \in \mathbb{R} - \{0\} \end{cases},$$

$$\gamma(x, y, z) = 1$$

and

$$\psi(t) = \frac{t}{2}.$$

If we take $x_0 = 0$, then for $x = 40$, we get

$$\begin{aligned} \Delta^*(40, 0) &= \max \left\{ \begin{array}{c} S(40, 40, 0), S(40, 40, f40), S(0, 0, f0), \\ \frac{S(40,40,f40)S(0,0,f0)}{S(40,40,0)+S(40,40,f40)+S(0,0,f40)}, \\ \frac{S(40,40,f40)S(40,40,f0)+S(0,0,f40)S(0,0,f0)}{S(0,0,f40)+S(40,40,f0)} \end{array} \right\} \\ &= \max \left\{ 80, 2, 0, 0, \frac{160}{102} \right\} \\ &= 80 \end{aligned}$$

and

$$S(40, 40, f40) = S(40, 40, 41) = 2.$$

Then we have

$$\gamma(40, 40, f40)\, S(f40, f40, 40) = 2 \leq 40 = \frac{80}{2} = \psi(\Delta^*(40, 0)).$$

Consequently, f is a γ-ψ_S-f_{x_0}-contractive mapping with $x_0 = 0$. Also we have

$$r = 2$$

and so f fixes the circle $C^S_{0,2} = \{-1, 1\}$ and the disc $D^S_{0,2} = [-1, 1]$.

Since every S-metric generates a b-metric, then we get the following:

DEFINITION 9. *Let* $\left(X, d^S\right)$ *be a* b*-metric space and* $f : X \to X$ *be a self-mapping.* f *is called an* α-ψ_b-f_{x_0}*-contractive mapping if there exist* $x_0 \in X$, $\alpha : X \times X \to [1, +\infty)$ *and* $\psi \in \Psi$ *such that*

$$d^S\left(fx, x\right) > 0 \Longrightarrow \alpha\left(x, x_0\right) d^S\left(fx, x\right) \leq \psi\left(\Delta_b^*\left(x, x_0\right)\right),$$

for all $x \in X$, *where*

$$\Delta_b^*\left(x, y\right) = \max\left\{\begin{array}{c} d^S\left(x, y\right), d^S\left(x, fx\right), d^S\left(y, fy\right), \\ \frac{d^S(x,fx)d^S(y,fy)}{d^S(x,y)+d^S(x,fy)+d^S(y,fx)}, \\ \frac{d^S(x,fx)d^S(x,fy)+d^S(y,fx)d^S(y,fy)}{d^S(y,fx)+d^S(x,fy)} \end{array}\right\}.$$

PROPOSITION 2. *If* f *is an* α-ψ_b-f_{x_0}*-contractive mapping* $x_0 \in X$, *then we have* $fx_0 = x_0$.

THEOREM 12. *Let* f *be an* α-ψ_b-f_{x_0}*-contractive mapping with* $x_0 \in X$ *and the number*

$$r^* = \inf\left\{d^S\left(fx, x\right) : x \in X, x \neq fx\right\}. \tag{5}$$

If $fx \in C^b_{x_{0,r^*}}$ *for each* $x \in C^b_{x_{0,r^*}}$, *then* f *fixes the circle* $C^b_{x_{0,r^*}}$.

COROLLARY 2. *Let* f *be an* α-ψ_b-f_{x_0}*-contractive mapping with* $x_0 \in X$ *and* r^* *be defined as in 5. If* $fx \in D^b_{x_{0,r^*}}$ *for each* $x \in D^b_{x_{0,r^*}}$, *then* f *fixes the disc* $D^b_{x_{0,r^*}}$.

Using the integral type technique, we give the following.

DEFINITION 10. *Let* (X, S) *be an* S*-metric space and* $f : X \to X$ *be a self-mapping.* f *is called an integral type* α-ψ_b-f_{x_0}*-contractive mapping if there exist* $x_0 \in X, \gamma : X \times X \times X \to [1, +\infty)$ *and* $\psi \in \Psi$ *such that*

$$S\left(fx, fx, x\right) > 0 \Longrightarrow \int_0^{\gamma(x,x,x_0)S(fx,fx,x)} \varphi\left(t\right) dt \leq \int_0^{\psi(\Delta^*(x,x_0))} \varphi\left(t\right) dt,$$

for all $x \in X$.

REMARK 8. If we take $\varphi\left(t\right) = 1$ in Definition 10, then the notions of a γ-ψ_S-f_{x_0}-contractive mapping and an integral type γ-ψ_S-f_{x_0}-contractive mapping coincide.

PROPOSITION 3. *If* f *is an integral type* γ-ψ_S-f_{x_0}*-contractive mapping* $x_0 \in X$, *then we have* $fx_0 = x_0$.

Proof. By the similar arguments used in the proof of Proposition 1, this can be easily seen. □

THEOREM 13. *Let f be an integral type γ-ψ_S-f_{x_0}-contractive mapping $x_0 \in X$ and the number r be defined as in 4. If $fx \in C^S_{x_0,r}$ for each $x \in C^S_{x_0,r}$, then f fixes the circle $C^S_{x_0,r}$.*

Proof. By the similar arguments used in the proof of Theorem 11, this can be easily proved. □

COROLLARY 3. *Let f be an integral type γ-ψ_S-f_{x_0}-contractive mapping $x_0 \in X$ and the number r be defined as in 4. If $fx \in D^S_{x_0,r}$ for each $x \in D^S_{x_0,r}$, then f fixes the disc $D^S_{x_0,r}$.*

REMARK 9.

1. If we take $\varphi(t) = 1$, then Proposition 1 and Proposition 3 coincide.
2. If we take $\varphi(t) = 1$, then Theorem 11 and Theorem 13 coincide.
3. If we take $\varphi(t) = 1$, then Corollary 1 and Corollary 3 coincide.
4. On b-metric spaces, the notion of an integral type α-ψ_b-f_{x_0}-contractive mapping can be defined and some integral type fixed-circle results can be proved.

Conclusion

In this article, three different techniques used in fixed-point theory are used together. For this purpose, fixed-point theorems are obtained by using multiple new generalized contractive conditions on S-metric spaces, which are an example of generalized metric spaces. As an application of the obtained theorems, new results are obtained for the fixed-circle problem, which is a geometric generalization approach. On the other hand, another point that makes this study important is to further investigate the applications of the obtained fixed-circle results to activation functions. For example, we consider the Rectified linear unit (ReLU) activation function, (for more details, see (Nair & Hinton, 2010)), defined as

$$ReLU(x) = \begin{cases} 0, & x \leq 0 \\ x, & x > 0 \end{cases}$$

Let us take $X = \{-10\} \cup [0, +\infty)$ with the S-metric defined as in Example 3 and define the mappings $\gamma : X \times X \times X \to [1, +\infty)$ and $\psi : [0, +\infty) \to$

$[0, +\infty)$ as, respectively,

$$\gamma(x, y, z) = 1$$

and

$$\psi(t) = \frac{t}{2}.$$

If we take $x_0 = 20$, then for $x = -10$, we get

$$\Delta^*(-10, 20) = 60$$

and

$$S(-10, -10, ReLU(-10)) = 20.$$

Then we have

$$\begin{aligned}\gamma(-10, -10, 20)\, S(ReLU(-10), ReLU(-10), -10) &= 20 \leq 30 \\ &= \frac{60}{2} \\ &= \psi(\Delta^*(-10, 20)).\end{aligned}$$

Hence, ReLU is a γ-ψ_S-f_{x_0}-contractive mapping $x_0 = 20$. Also, we have

$$r = 20$$

and so ReLU fixes the circle $C^S_{20,20} = \{10, 30\}$ and the disc $D^S_{20,20} = [10, 30]$.

References

Bimol, T., Priyobarta, N., Rohen, Y., & Singh, KA. 2024. Fixed points for S-contractions of type E on S-metric spaces. *Nonlinear Functional Analysis and Applications*, 29(3), pp.635-648. Available at: https://doi.org/10.22771/nfaa.2024.29.03.02

Branciari, A. 2002. A fixed point theorem for mappings satisfying a general contractive condition of integral type. *International Journal of Mathematics and Mathematical Sciences*, 29 (9), pp.531-536. Available at: https://onlinelibrary.wiley.com/doi/pdf/10.1155/S0161171202007524

Fetouci, N., & Radenovic, S. 2009. Some remarks and corrections of recent results from the framework of S-metric spaces. *Journal of Siberian Federal University. Mathematics & Physics*, 2(3), pp.258-270.

Hieu, N T., Ly, NT. & Dung, NV. 2015. A generalization of Ciric quasi-contractions for maps on S-metric spaces. *Thai Journal of Mathematics*, 13 (2), pp.369-380. Available at: https://thaijmath2.in.cmu.ac.th/index.php/thaijmath/article/view/515

Iqbal, M., Batool, A., Hussain, A., & Alsulami, H. 2024. Fuzzy Fixed Point Theorems in S-Metric Spaces: Applications to Navigation and Control Systems. *Axioms*, 13(9), pp.650. Available at: https://doi.org/10.3390/axioms13090650

Mlaiki, N., Çelik, U., Taş, N., Özgür, NY. & Mukheimer, A. 2018. Wardowski type contractions and the fixed-circle problem on S-metric spaces. *Journal of Mathematics*, 9. Available at: https://doi.org/10.1155/2018/9127486

Nair, V. & Hinton, GE. 2010. Rectified linear units improve restricted boltzmann machines, In *27th International Conference on Machine Learning, ICML'10*, Haifa, Israel on June 21-24, 2010, pp.807-814. ISBN: 978-1-60558-907-7

Özgür, NY. & Taş, N. 2017. Some new contractive mappings on S-metric spaces and their relationships with the mapping (S25). *Mathematical Sciences*, 11(1), pp.7-16. Available at: https://doi.org/10.1007/s40096-016-0199-4

Özgür, NY. & Taş, N. 2019. Some fixed-circle theorems on metric spaces. *Bulletin of the Malaysian Mathematical Sciences Society* , 42(4), pp.1433-1449. Available at: https://doi.org/10.1007/s40840-017-0555-z

Özgür, NY. & Taş, N. 2019. Fixed-circle problem on S-metric spaces with a geometric viewpoint. *Facta Universitatis, Series: Mathematics and Informatics* , 34(3), pp. 459-472. Available at: https://doi.org/10.22190/FUMI1903459O

Raji, M., Rajpoot, AK., Al-omeri, WF., Rathour, L., Mishra, LN. & Mishra, VN. 2024. Generalized α-ψ contractive type mappings and related fixed point theorems with applications. *Tuijin Jishu/Journal of Propulsion Technology*, 45(10), pp.5235-5246. Available at: https://www.propulsiontechjournal.com/index.php/journal/article/view/5543/3766

Samet, B., Vetro, C., Vetro, P. 2012. Fixed point theorem for contractive type mappings. *Nonlinear Analysis: Theory, Methods & Applications*, 75, pp.2154-2165. Available at: https://doi.org/10.1016/j.na.2011.10.014

Sedghi, S., Shobe, N. & Aliouche, A. 2012. A generalization of fixed point theorems in S-metric spaces. *Matematički Vesnik*, 64(3), pp.258-266. Available at: https://www.emis.de/journals/MV/123/mv12309.pdf

Sedghi, S., & Van Dung, N. 2014. Fixed point theorems on S-metric spaces. *Matematički Vesnik*, 255, pp.113-124. Available at: https://www.emis.de/journals/MV/141/mv14112.pdf

---

Algunos teoremas de punto fijo mediante contracciones γ-ψ_S-en espacios S-métricos

Nihal Taş [a], *Elif* Kaplan [b]

[a] Universidad de Balıkesir, Departamento de Matemáticas, 10145 Balıkesir, Turquiae **autor de correspondencia**

[b] Universidad Ondokuz Mayis, Departamento de Matemáticas, 55200 Samsun, Turquia

CAMPO: ej. matemáticas
TIPO DE ARTÍCULO: artículo científico original

Resumen

Introducción: Este artículo se centra en la extensión de la teoría de puntos fijos en espacios S-métricos mediante la introducción de nuevas condiciones contractivas generalizadas. Estos desarrollos buscan enriquecer las herramientas analíticas disponibles para el estudio de dichos espacios

Métodos: Se establecen diversos teoremas de punto fijo mediante la aplicación de las condiciones contractivas recientemente definidas. La metodología incluye aplicaciones contractivas tanto estándar como integrales. Además, se utiliza un enfoque geométrico para obtener nuevos teoremas de círculo fijo dentro del marco de la métrica S.

Resultados: Se demuestran varios teoremas de punto fijo y círculo fijo en las condiciones propuestas. Se proporcionan ejemplos ilustrativos para validar los hallazgos teóricos y demostrar su aplicabilidad.

Conclusión: Los hallazgos de este estudio no solo amplían el alcance de la teoría de punto fijo en espacios S-métricos, sino que también ofrecen posibles implicaciones para aplicaciones prácticas. En particular, los resultados podrían contribuir al desarrollo de las matemáticas computacionales y al diseño de funciones de activación de redes neuronales.

Palabras claves: espacio S-métrico, teorema del punto fijo, contracción generalizada, contracción de tipo integral, círculo fijo, enfoque geométrico, función de activación, redes neuronales.

Некоторые теоремы о неподвижной точке γ-ψ_S-сжатия на S-метрическом пространстве

Нихал Тас [а], *Элиф* Каплан [б]

[а] Балыкесирский университет, математический факультет, 10145 Балыкесир, Турецкая Республика, **корреспондент**

[б] Университет «19 мая» математический факультет, 55200, Самсун, Турецкая Республика

РУБРИКА ГРНТИ: 27.47.19 27.47.19 Исследование операций;
ВИД СТАТЬИ: оригинальная научная статья

Резюме:

Введение: Данная статья посвящена расширению теории неподвижных точек в S-метрических пространствах путем введения новых обобщенных условий сжатия. Исследование направлено на улучшение аналитических инструментов, доступных в изучении подобных пространств

Методы: Установлен ряд теорем о неподвижных точках с применением условий. Методология включает как стандартные, так и инте- гральные принципы сжимающих отображений. Помимо того, используется геометрический подход для получения новых теорем о неподвижных точках в S метрическом пространстве.

Результаты: Доказаны некоторые теоремы о непо- движных точках и неподвижных окружностях. предложен- ных условиях. Приведены наглядные примеры для подтверждения теоретических выводов и демонстрации применимости результатов.

Заключение: Результаты данного исследования не только расширяют область применения теории неподвижной точки в S-метрических пространствах, но и могут быть использованы в прикладных приложениях. В частности, результаты могут способствовать развитию вычислительной математики и разработке функций активации нейронных сетей. В частности, они могут способствовать развитию вычислительной математики и проектирова- нию функций активации в нейронных сетях.

Ключевые слова: S-метрическое пространство, теорема о неподвижной точке, обобщенное сжатиеённая , сжатие интегрального типа, неподвижная окружность, геометрический подход, функция активации, нейронные сети.

Неке теореме о непокретној тачки преко γ-ψ_S контракција на С-метричким просторима

Нихал Таш [а], *Елиф* Каплан [б]

[а] Универзитет Баликесир, Одсек за математику. 10145 Баликесир, Турска, **аутор за преписку**

[б] Универзитет Ондокуз Мајис, Одсек за математику, 55200, Самсун, Турска

ОБЛАСТ: математика

КАТЕГОРИЈА (ТИП) ЧЛАНКА: оригинални научни рад

Сажетак:

Увод: Тежиште овог рада је на проширењ теорије непокретних тачака у С-метричке просторе увођењем новеих генерализованеих контрактивнеих условеа. Циљ овог проширивања јесте да се обогате аналитички алати доступни за проучавање оваквих простора.

Методе: Различите теореме о непокретној тачки успостављене су коришћењем новодефинисаних контрактивних услова. Методологија обухвата стандардна пресликавања, као и пресликавања интегралног типа контракције Такође, користи се и геометријски приступ дакако би се добиле нове теореме о непокретној тачцки унутар С-метричког простора.

Резултати: Доказано је неколико теорема о непокретним тачкама и непокретним круговима под предложеним условима. Наведени примери илуструју теоријске налазе и показују примењљивост резултата.

Закључак: Резултати овог рада не само да проширују домен теорије непокретних тачака на С-метричке просторе већ, и нуде потенцијалне импликације за примену у стварности. Такође, могу да допринесу развоју у областима рачунарске математике и пројектовања активационих функција неуронских мрежа.

Кључне речи: С-метрички простор, теорема о непокретној тачки, генерализована контракција, контракција интегралног типа, непокретни круг, геометријски приступ, активациона функција, неуронске мреже.

Paper received on: 20.01.2025.
Manuscript corrections submitted on: 10.03.2025.
Paper accepted for publishing on: 11.03.2025.

Periodic semi-linear functional differential inclusion system with state-dependent delays

Khelifa Daoudi[a], *Mohamed* Belaidi[b]

[a] University Center of Nour Bachir El-Bayadh, El-Bayadh, Algeria, Institute of Sciences, El-Bayadh, Algeria +
Université de Sidi Bel-Abbes, Laboratoire de Mathématiques, Algeria, Sidi Bel-Abbes, Algeria,
e-mail: khelifa.daoudi@gmail.com, k.daoudi@cu-elbayadh.dz,
corresponding author,
ORCID iD: https://orcid.org/0000-0002-5444-1181

[b] University Center of Nour Bachir El-Bayadh, El-Bayadh, Algeria, Institute of Sciences, El-Bayadh, Algeria
e-mail: m.belaidi@cu-elbayadh.dz,
ORCID iD: https://orcid.org/0000-0001-8543-6927

https://doi.org/10.5937/vojtehg73-52847

FIELD: mathematics
ARTICLE TYPE: original scientific paper

Abstract:

Introduction/Purpose: The study addressed the existence and uniqueness of mild solutions for a class of periodic semi-linear functional differential inclusion systems with state-dependent delays. Such systems are of growing interest due to their wide range of applications in control theory, biological systems, and engineering models involving time delays and uncertainties.

Methods: The investigation was conducted within the framework of Banach spaces. The Perov fixed point theorem, known for its effectiveness in handling systems with multiple components, was applied to establish the existence of mild solutions. The analytical approach incorporated techniques suitable for differential inclusions and operator theory, particularly focusing on systems influenced by state-dependent delays.

Results: Several results were obtained concerning the existence and uniqueness of mild solutions for the considered system. The application of the Perov fixed point theorem allowed the derivation of sufficient conditions under which such solutions exist. Furthermore, the periodic nature of the system was accounted for, ensuring the solutions adhered to the prescribed temporal structure.

Conclusions: The findings confirmed that under specific assumptions, the system admits at least one mild solution. The results contributed to the theoretical foundation of functional differential inclusions with delays. Researchers were encouraged to further explore these outcomes and to *develop computational and numerical methods for approximating the theoretical solutions, thereby extending the applicability of the current research.*

Key words: mild solutions, state-dependent delays, Banach spaces, multivalued maps, fixed points, functional differential inclusions, semi-linear systems

Introduction

Functional differential equations and inclusions play a crucial role in various fields such as biology, physics, and engineering, and have attracted significant attention in recent years.To navigate the extensive literature on functional differential equations, valuable resources include books by Hale (1977), Hale and Lunel (2013), Kolmanovskii & Myshkis, (1999), along with the references contained therein.

Over the past decades, researchers have conducted extensive investigations into the existence and uniqueness of solutions for semi-linear functional differential equations and inclusions. Various types of solutions, including mild, strong, classical, almost periodic, and almost automorphic solutions, have been explored using methodologies such as semigroup theory, fixed point arguments, degree theory, and measures of non-compactness. Noteworthy contributions to this body of work can be found in books by (Ahmed, 1991, Kolmanovskii et al, 1999 & Wu 1996), and the related references such as the articles by (Daoudi et al, 2018; Mohamed & Tayeb, 2019).

In this paper, we consider a system with state-dependent delays of the following form:

$$\begin{cases} x'^{(t)} - A_1 x(t) \in F_1\left(t\,, x\big(t-\mathcal{T}_1(t,x_t)\big), y\big(t-\mathcal{T}_2(t,y_t)\big)\right), t \in J := [0,b] \\ y'(t) - A_2 y(t) \in F_2\left(t, x\big(t-\mathcal{T}_1(t,x_t)\big), y\big(t-\mathcal{T}_2(t,y_t)\big)\right), t \in J := [0,b] \\ x(t) = \varphi_1(t), t \in [-r,0] \qquad\qquad (\mathbf{1}) \\ y(t) = \varphi_2(t), \qquad t \in [-r,0] \\ \qquad x(0) = x(b) \; and \;\; y(0) = y(b) \end{cases}$$

where the operators $\mathrm{A_i}, \mathrm{i} = 1; 2$ are the infinitesimal generator of a $\mathrm{C_0}$-semigroup $\mathrm{T_i(t)_{t\geq 0}}$ on a Banach space E. b; r are real numbers with

b, r>0 .

$\mathrm{F_1}, \mathrm{F_2} : \mathrm{J} \times \mathrm{E} \times \mathrm{E} \to \mathcal{P}(\mathrm{E})$ are multifunctions, and

$\mathcal{T}_\mathrm{i} : [0, \mathrm{b}] \times \mathrm{C}([-\mathrm{r}, 0], \mathrm{E}) \to [0, \mathrm{r}], \mathrm{i} = 1; 2$ are the given continuous functions.

For any function x defined on $[-r;\ b]$ and any $t \in J$, we denote by x_t the element of $C([-r;\ 0], E)$ defined by

$$x_t(\theta) = x(t+\theta), \theta \in [-r, 0].$$

Here, $x_t(\cdot)$ represents the history of the state from the time $t-r$, up to the present time t.

Throughout this paper, the operators $A_i,\ i = 1, 2$ are the infinitesimal generator of a C_0 –semigroup $T_i(t)_{t\geq 0}$ and there exists $M > 0$ such that

$$\|T(t)\| \leq M \text{ for all } t \in J.$$

$C([-r, b], E)$ is the Banach space of all continuous functions from $[-r;\ b]$ into E with the norm

$$\|x\|_\infty = \sup_{\theta\in[-r,0]} \sup_{t\in[0,b]} \|x(t+\theta)\|.$$

Set $C_r := C([-r, 0], E)$ and $C := C([-r, b], E)$.

This paper is organized as follows: Section 2 briefy recalls some basic definitions and preliminary facts which will be used throughout the following sections.

Section 3 proves the existence of set solutions for a functional differential inclusions system with state-dependent delays with periodic conditions.

Preliminaries

In this section, we introduce notations, definitions, and preliminary facts which are used throughout this paper.

Definition (2.1) (Daoudi, 2018): A square matrix of real numbers is said to converge to zero if and only if its spectral radius $\rho(M)$ is strictly less than 1. In other words, this means that all the eigenvalues of M are in the open unit disc $\text{i.e}|\lambda| < 1$; for every $\lambda \in \mathbb{C}$ with $\det(M - \lambda I) = 0$, where I denote the unit matrix of $M_{n\times n}(\mathbb{R})$.

Multi-valued analysis

Let (X, d)be a metric space and Y be a subset of X: Denote by

• $\mathcal{P}(X) = \{Y \subset X : Y \neq \emptyset\}$.

• $\mathcal{P}_p(X) = \{Y \in \mathcal{P}(X) : Y$ has the property "p"$\}$ where p could be: cl =closed,

b=bounded, cp =compact, cv =convex, etc. Thus,

•$\mathcal{P}_{cl}(X) = \{Y \in \mathcal{P}(X) : Y\ closed\}$

• $\mathcal{P}_b(X) = \{Y \in \mathcal{P}(X) : Y\ bounded\}$.

•$\mathcal{P}_{cp}(X) = \{Y \in \mathcal{P}(X) : Y \text{ compact}\}$.

• $\mathcal{P}_{cv}(X) = \{Y \in \mathcal{P}(X): Y\ convex\}$where X is a Banach space.
• $\mathcal{P}_{cv,cp}(X) = \mathcal{P}_{cv}(X) \cap \mathcal{P}_{cp}(X)$.

Let $(\mathrm{X}, \mathrm{d}_*)$ be a metric space. Denote by $\mathrm{H}_{\mathrm{d}_*}$the Hausdorff pseudo-metric distance on $\mathrm{P(X)}$ defined as

$$H_{d_*}: \mathcal{P}(X) \times \mathcal{P}(X) \to \mathbb{R}_+ \cup \{\infty\}, H_{d_*}(A, B) = max\left\{\sup_{a\in A} d_*(a, B), \sup_{b\in B} d_*(A, b),\right\}.$$

where $\mathrm{d}_*(A, b) = \inf_{a\in A} d_*(a, b\ )$ and $d_*(a, B) = \inf_{b\in B} d_*(a, b)$. Then $(\mathcal{P}_{b,cl}(X), H_{d_*})$ is a metric space and $(\mathcal{P}_{\mathrm{cl}}(\mathrm{X}), \mathrm{H}_{\mathrm{d}_*})$ is a generalized metric space. In particular, $\mathrm{H}_{\mathrm{d}_*}$ satisfies the triangle inequality.

Consider the generalized Hausdorff pseudo-metric distance
$\mathrm{H}_{\mathrm{d}}: \mathcal{P}(\mathrm{X}) \times \mathcal{P}(\mathrm{X}) \to \mathbb{R}_+^{\mathrm{n}} \cup \{\infty\}$
defined by

$$H_d(A, B) \coloneqq \begin{pmatrix} H_{d_1}(A, B) \\ \cdots \\ H_{d_n}(A, B) \end{pmatrix}.$$

Definition 2.2 (Daoudi, 2018): Let (X, d) be a generalized metric space, and let $N: X \to \mathcal{P}_{cl}(X)$ be a multivalued operator. The operator N is said to be contractive if there exists a matrix $\mathrm{M} \in \mathcal{M}_{n\times n}(\mathbb{R}_+)$ such that
$M^k \to 0\ as\ k\ \to \infty$
and
$H_d\big(N(u), N(v)\big) \leq\ Md(u, v), \qquad for\ all\ u, v\ \in\ X.$

Let (X, d) and (Y, ρ) be two metric spaces and $\mathrm{F}: \mathrm{X} \to \mathcal{P}(\mathrm{Y}\ )$ be a multi-valued mapping. Then F is said to be *lower semi-continuous* $(\mathrm{l.s.c.})$ if the inverse image of V by F

$$F^{-1}(V\ ) = \{x \in X: F(x) \cap V\ \neq \emptyset\}$$

is open for any open set V in Y . Equivalently, F is l.s.c. if the core of V by F

$$F^{+1}(V\ ) = \{x \in X: F(x) \subset V\ \}$$

is closed for any closed set V in Y .

Likewise, the map F is called upper semi-continuous$(\mathrm{u.s.c.})$ on X if for each $x_0 \in\ \mathrm{X}$ the set $\mathrm{F}(x_0)$ is a nonempty, closed subset of X, and if for each open set N of Y containing $\mathrm{F}(\mathrm{x}_0)$, there exists an open neighborhood M of x_0 such that $\mathrm{F(M)} \subseteq \mathrm{Y}$. That is, if the set $\mathrm{F}^{-1}(\mathrm{V}\ )$ is closed for any closed set V in Y. Equivalently, F is $\mathrm{u.s.c.}$ if the set $\mathrm{F}^{+1}(\mathrm{V}\ )$is open for any open set V in Y .

The mapping F is said to be completely continuous if it is $\mathrm{u.s.c.}$ and, for every bounded subset $\mathrm{A} \subseteq \mathrm{X}$, $\mathrm{F(A)}$ is relatively compact, i.e., there exists a relatively compact set $\mathrm{K} = \mathrm{K(A)} \subset \mathrm{X}$ such that

$$F(A) = \bigcup \{F(x) : x \in A\} \subset K.$$

Also, F is compact if $\mathrm{F(X)}$ is relatively compact, and it is called locally compact if for each $x \in \mathrm{X}$, there exists an open set U containing x such that $\mathrm{F(U)}$ is relatively compact.

We denote the graph of F to be the set

$Graph(F) = \{(x, y) \in X \times Y, y \in F(x)\}$, and we recall the following facts.

Definition 2.3 (Daoudi, 2018): A multivalued map $F: [a, b] \to \mathcal{P}(Y)$ is said to be measurable if for every open $U \subset Y$; the set

$\mathrm{F}_{+}^{-1}(\mathrm{U}) = \{x \in \mathrm{Y}: \mathrm{F}(x) \subset \mathrm{U}\}$ is Lebesgue measurable.

Definition 2.4 (Djebali et al, 2010): A multi-map F is called a Carathéodory function if

(a) the multi-map $t \to F(t, x)$ is measurable for each $x \in \mathrm{X}$;

(b) for a.e. $\mathrm{t} \in \mathrm{J}$, the map $x \to \mathrm{F}(\mathrm{t}, x)$ is upper semi-continuous.

Furthermore, F is L^1-Carathéodory if it is further locally integrably bounded, i.e., for each positive r, there exists $\mathrm{h_r} \in \mathrm{L}^1(\mathrm{J}, \mathbb{R}^+)$ such that

$\|(\mathrm{t}, x)\|_{\mathcal{P}} \leq \mathrm{h_r}(\mathrm{t}), \quad \text{for a.e. } \mathrm{t} \in \mathrm{J} \text{ and all } |x| \leq \mathrm{r}.$

Lemma 2.5 (Hale, 1977) : The multivalued map $F: [a, b] \to P_{cl}(Y)$ is measurable if and only if for each $x \in \mathrm{Y}$, the function $\zeta: [a, b] \to [0, +\infty)$ defined by

$\zeta(t) = dist(x, F(t)) = inf\{\|x - y\| : y \in F(t)\}, t \in [a, b]$, *is* Lebesgue measurable.

The following two lemmas are needed. The first one is the celebrated Kuratowski-Ryll-Nardzewski selection theorem.

Lemma 2.6 (Daoudi, 2018): Let Y be a separable metric space and $F: [a, b] \to \mathcal{P}(Y)$ a measurable multi-valued map with nonempty closed values. Then F has a measurable selection.

Lemma 2.7 (Daoudi, 2018): Let I be a compact interval and E be a Banach space. Let F be an L^1-Carathéodory multi-valued map with $\mathrm{S_{F,y}} \neq \emptyset$, and let Γ be a linear continuous mapping from $\mathrm{L}^1(\mathrm{I}, \mathrm{E})$ to $\mathrm{C(I, E)}$. Then, the operator

$$\Gamma o S_F: C(I, E) \to \mathcal{P}_{cp,c}(E), \qquad y \to (\Gamma o S_F)(y) = \Gamma(S_{F,y}),$$

is a closed graph operator in $\mathrm{C(I, E)} \times \mathrm{C(I, E)}$, where $\mathrm{S_{F,y}}$ is known as the selectors set from F and given by

$$f \in S_{F,y} = \{ f \in L^1(I, E): f(t) \in F(t, y(t)) \; for \; a.e. t \in I\}.$$

Lemma 2.8 (Daoudi, 2018): Let I be a compact interval and E be a Banach space. Let F be an L^1-Carathéodory multi-valued map with $\mathrm{S}_{\mathrm{F,y}} \neq \emptyset$, and let Γ be a linear continuous mapping from $\mathrm{L}^1(\mathrm{I,E})$ to $\mathrm{C}(\mathrm{I,E})$. Then, the operator

$$\Gamma o S_F: C(I,E) \to \mathcal{P}_{cp,c}(E), y \to (\Gamma o S_F)(y) = \Gamma\left(S_{F,y}\right),$$

is a closed graph operator in $\mathrm{C}(\mathrm{I,E}) \times \mathrm{C}(\mathrm{I,E})$, where $\mathrm{S}_{\mathrm{F,y}}$ is known as the selectors set from F and given by

$$f \in S_{F,y} = \left\{f \in L^1(I,E): f(t) \in F\big(t,y(t)\big)\, for\ a.e.t \in I\right\}.$$

Lemma 2.9 (Aubin & Frankowska, 1990): If $G: X \to \mathcal{P}_{cp}$is $\mathrm{u.s.c}$, then for any $\lim\limits_{\mathrm{x}\to\mathrm{x}_0} \sup \mathrm{G}(x) = \mathrm{G}(x_0)$.

Lemma 2.10 (Aubin & Frankowska, 1990): Let $(k_n)_{n\in\mathbb{N}} \subset k \subset X$ be a sequence of subsets where K is compact in the separable Banach space X. Then

$$\overline{\mathrm{co}}\left(\lim_{\mathrm{n}\to\infty} \sup \mathrm{k_n}\right) = \bigcap_{\mathrm{N}>0} \overline{\mathrm{co}}\left(\bigcup_{\mathrm{n}\geq\mathrm{N}} \mathrm{k_n}\right),$$

where $\overline{\mathrm{co}}\mathrm{A}$ refers to the closure of the convex hull of A.

Lemma 2.11 (Aubin & Frankowska, 1990): Every semi-compact sequence $L^1([0;\ b],E)$ is weakly compact in $L^1([0;\ b],;E)$.

Lemma 2.12 (Djebali et al 2010): Let E be a normed space and $x_{kk\in\mathbb{N}} \subset E$ be a sequence weakly converging to a limit $x \in E.$ Then there exists a sequence of convex combinations $\mathrm{y_m} = \sum_{\mathrm{k}=1}^{\mathrm{k}=\mathrm{m}} \alpha_{\mathrm{mk}} x_{\mathrm{k}}$ with $\alpha_{\mathrm{mk}} > 0$ for $\mathrm{k} = 1,2,\dots,\mathrm{m}$ and $\mathrm{y_m} = \sum_{\mathrm{k}=1}^{\mathrm{k}=\mathrm{m}} \alpha_{\mathrm{mk}} = 1$, which converges strongly to x.

Theorem 2.13 (Sinacer et al, 2016): Let (X; d) be a complete generalized metric space and $\mathrm{F}: \mathrm{X} \to \mathcal{P}_{\mathrm{cl,b}}(\mathrm{X})$ a contractive multivalued operator with the Lipschitz matrix M. Then N has a unique fixed point.

Theorem 2.14 (Wu, 1996): Let $(\mathrm{X,d})$ be a complete generalized metric space and $\mathrm{F}: \mathrm{X} \to \mathcal{P}_{\mathrm{cl}}(\mathrm{X})$ be a multivalued map. Assume that there exist $A, B, C \in \mathcal{M}_{n\times n}(\mathbb{R}_+)$ such that

$$H_d\big(F(x),F(y)\big) \leq Ad(x,y) + Bd\big(y,F(x)\big) + Cd\big(x,F(x)\big),$$

where $\mathrm{A} + \mathrm{C}$ converge to zero. Then there exists $\mathrm{x} \in \mathrm{X}$ such that $x \in \mathrm{F}(\mathrm{x})$.

Existence results

In this section, we assume that 1∈ ρ(T(b)) and give our main existence and uniqueness result for problem (1). Before starting and proving this result, we give the definition of its mild solution.

Definition 3.1 See details in (Djebali et al 2010).

A function $(x, y) \in C \times C$ is said to be a mild solution of problem (1) if $x(t) = \varphi_1(t),\ y(t) = \varphi_2(t), t \in [-r, 0]$ and if there exists $v_1, v_2 \in L^1(J, E)$ such that

$$v_i \in F_i\left(t, x\left(t - \tau_1(t, x_t)\right), y\left(t - \tau_2(t, y_t)\right)\right) \text{ a.e. on J such that}$$

$$x(t) = T_1(t)(I - T_1(b))^{-1} \int_0^b T_1(b - s) v_1(s)\, ds + \int_0^t T_1(t - s)\, v_1 ds,$$

$$y(t) = T_2(t)(I - T_2(b))^{-1} \int_0^b T_2(b - s) v_2(s)\, ds + \int_0^t T_2(t - s)\, v_2 ds,$$

$$x_0 = x_b \text{ and } y_0 = y_b.$$

Assume that the following conditions:

(G_1) $F_i : J \times E \times E \to P_{cp,cv}(E); t \mapsto F_i(t, u, v);\ i = 1,2$ are measurable for each $t \in J$ and $u, v \in C$.

(G_2) There exist functions $l_i, \overline{l_i} \in L^1(J, \mathbb{R}) \to \mathbb{R}_+, i = 1,2$ such that $H_d\left(F_i(t, u, v) - F_i(t, \tilde{u}, \tilde{v})\right) \le l_i(t)\|u - \tilde{u}\| + \overline{l_\iota}(t)\|v - \tilde{v}\|$ for every $t \in J, u, \tilde{u}, v, \tilde{v} \in E$ and

$H_d\left(0, F_i(t, 0,0)\right) \le l_i(t), for\ all\ a.e.\, t \in J\ and\ i = 1,2.$

(G_3) There exists a constant $\rho_i \ge 0, i = 1;\ 2$ such that

$$\|\tau_i(t, u) - \tau_i(t, \tilde{u})\|) \le \rho_i \|u - \tilde{u}\|$$

for all $u;\ \tilde{u} \in E$ and $t \in J$.

(G_4) There exists a constant $k_i \ge 0, i = 1;\ 2$ such that

$H_d(F_i(t;\ u(s_1);\ v(s_1)) - F_i(t;\ u(s_2);\ v(s_1)) \le k_1|s_1 - s_2| + k_2|s_1 - s_2|,$ for every $t \in J,\ s_1;\ s_2 \in [-r;\ b]$ and $u;\ v \in E$.

Theorem (3.2): Assume that (G_1) , (G_2) , (G_3) and (G_4) are satisfied and the matrix

$$\overline{M} = \left(\frac{M^2}{\|I - T(b)\|_\infty} + M\right)\begin{pmatrix} k_1\rho_1 + \|l_1\|_{L^1} & \bar{k}_1\rho_2 + \left\|\bar{l}_1\right\|_{L^1} \\ k_2\rho_1 + \|l_2\|_{L^1} & \bar{k}_2\rho_2 + \left\|\bar{l}_2\right\|_{L^1} \end{pmatrix}$$

converges to zero; then problem (1) has a unique mild solution.

Proof: Consider the operator $N: C \times C \rightarrow P(C \times C)$ defined for $(x, y) \in C \times C$ by

$$N(x;\ y) = \left\{ (h_1, h_2) \in C \times C : \begin{pmatrix} h_1(t) \\ h_2(t) \end{pmatrix} = \begin{pmatrix} T_1(t)\big(I - T_1(b)\big)^{-1} \int_0^b T_1(b-s) v_1(s) ds \\ + \int_0^t T_1(t-s) v_1(s) ds \\ T_2(t)\big(I - T_2(b)\big)^{-1} \int_0^b T_2(b-s) v_2(s) ds \\ + \int_0^t T_2(t-s) v_2(s) ds \end{pmatrix}, for\ t \in [0, b] \right\}$$

and $h_1(t) = \varphi_1(t);\ h_2(t) = \varphi_2(t)$ for $t \in [-r;\ 0]$, where

$$v_i \in S_{F_i, x, y} = \Big\{ f \in L^1(J, E) : f(t) \in F_i\Big(t, x\big(t - \tau_1(t, x_t)\big), y\big(t - \tau_2(t, y_t)\big)\Big), a.e.\ t \in J \Big\}.$$

Clearly, the fixed points of the operator N are the solutions of problem (1). Let

$$N_1(x,y)=\left\{h_1\in C: h_1(t)=\left\{\begin{matrix} T_1(t)\big(I-T_1(b)\big)^{-1}\int_0^b T_1(b-s)v_1(s)ds \\ +\int_0^t T_1(t-s)v_1(s)ds\,,\ \ t\in J:=[0,b]\end{matrix}\right\}\right.$$

and

$$\mathrm{N}_2(x,y)=\left\{h_2\in C: h_2(t)=\left\{\begin{matrix} T_2(t)\big(I-T_2(b)\big)^{-1}\int_0^b T_2(b-s)v_2(s)ds \\ +\int_0^t T_2(t-s)v_2(s)ds\,,\ \ t\in J:=[0,b]\end{matrix}\right\}\right..$$

Hence,

$$N(x,y)=\big(N_1(x,y),N_2(x,y)\big)\ \ for\ every\ \ (x,y)\in C\times C.$$

Since for each $(x,\mathrm{y})\in \mathrm{C}\times\mathrm{C}$, the nonlinearity $\mathrm{F_i}$ takes convex values, the selection set $\mathrm{S_{F_i,x,y}}$ is convex, then N has convex values. We show that N satisfies the assumptions of Theorem 2.13.

Let $(\mathrm{x},\mathrm{y}),(\tilde{\mathrm{x}},\tilde{\mathrm{y}})\in \mathrm{C}^2\times\mathrm{C}^2$and $(\mathrm{h}_1,\mathrm{h}_2)\in\mathrm{N}(\mathrm{x},\mathrm{y})$. Then there exists $\mathrm{v_i}\in \mathrm{F_i}\Big(\mathrm{t},\mathrm{x}\big(\mathrm{t}-\tau_1(\mathrm{t},\mathrm{x_t})\big),\mathrm{y}\big(\mathrm{t}-\tau_2(\mathrm{t},\mathrm{y_t})\big)\Big)$, $\mathrm{i}=1{,}2$ such that

$$\begin{pmatrix}h_1(t)\\ h_2(t)\end{pmatrix}=\begin{pmatrix} T_1(t)\big(I-T_1(b)\big)^{-1}\int_0^b T_1(b-s)v_1(s)ds \\ +\int_0^t T_1(t-s)v_1(s)ds \\ T_2(t)\big(I-T_2(b)\big)^{-1}\int_0^b T_2(b-s)v_2(s)ds \\ +\int_0^t T_2(t-s)v_2(s)ds\end{pmatrix},for\ t\in[0,b]$$

(G_2) implies that

$$\begin{aligned}&H_{d_1}\big(F_1(t,x\big(t-\tau_1(t,x_t)\big),y(t-\tau_2(t,y_t)))\\ &\qquad-F_1(t,\tilde{x}\big(t-\tau_1(t,\tilde{x}_t)\big),\tilde{y}(t-\tau_2(t,\tilde{y}_t)))\big)\le\\ &H_{d_1}\big(F_1(t,x\big(t-\tau_1(t,x_t)\big),y(t-\tau_2(t,y_t)))\\ &\qquad-F_1(t,\tilde{x}\big(t-\tau_1(t,\tilde{x}_t)\big),\tilde{y}(t-\tau_2(t,\tilde{y}_t)))\big)+\\ &H_{d_1}\big(F_1(t,\tilde{x}\big(t-\tau_1(t,x_t)\big),\tilde{y}(t-\tau_2(t,y_t)))\\ &\qquad-F_1(t,\tilde{x}\big(t-\tau_1(t,\tilde{x}_t)\big),\tilde{y}(t-\tau_2(t,\tilde{y}_t)))\big)\le\\ &l_1(t)\big(\big\|x\big(t-\tau_1(t,x_t)\big)-\tilde{x}\big(t-\tau_1(t,\tilde{x}_t)\big)\big\|+k_1\|\tau_1(t,x_t)-\tau_1(t,x_t)\|\big)+\end{aligned}$$

$$\bar{l}_1(t)(\|y(t-\tau_2(t,y_t)) - \tilde{y}(t-\tau_2(t,y_t))\| + \bar{k}_1\|\tau_2(t,y_t) - \tau_2(t,\tilde{y}_t)\|) \leq$$
$$l_1(t)(\|x(t-\tau_1(t,xx_t)) - \tilde{x}(t-\tau_1(t,x_t))\| + k_1\rho_1\|x_t - \tilde{x}_t\|) +$$
$$\bar{l}_1(t)(\|y(t-\tau_2(t,y_t)) - \tilde{y}(t-\tau_2(t,y_t))\| + \bar{k}_1\rho_2\|y_t - \tilde{y}_t\|), \qquad t \in J$$

and

$$H_{d_2}(F_1(t,x(t-\tau_1(t,x_t)), y(t-\tau_2(t,y_t))) - F_1(t,\tilde{x}(t-\tau_1(t,\tilde{x}_t)), \tilde{y}(t-\tau_2(t,\tilde{y}_t)))) \leq$$
$$H_{d_2}(F_1(t,x(t-\tau_1(t,x_t)), y(t-\tau_2(t,y_t))) - F_1(t,\tilde{x}(t-\tau_1(t,x_t)), \tilde{y}(t-\tau_2(t,y_t)))) +$$
$$H_{d_2}(F_1(t,\tilde{x}(t-\tau_1(t,x_t)), \tilde{y}(t-\tau_2(t,y_t))) - F_1(t,\tilde{x}(t-\tau_1(t,\tilde{x}_t)), \tilde{y}(t-\tau_2(t,\tilde{y}_t)))) \leq$$
$$l_2(t)(\|x_t(t-\tau_1(t,x_t)) - \tilde{x}_t(t-\tau_1(t,x_t))\| + k_1\|\tau_1(t,x_t) - \tau_1(t,\tilde{x}_t)\|) +$$
$$\bar{l}_2(t)(\|y(t-\tau_2(t,y_t)) - \tilde{y}(t-\tau_2(t,y_t))\| + \bar{k}_1\|\tau_2(t,y_t) - \tau_2(t,\tilde{y}_t)\|) \leq$$
$$l_2(t)(\|x(t-\tau_1(t,x_t)) - \tilde{x}(t-\tau_1(t,x_t))\| + k_1\rho_1\|x_t - \tilde{x}\|) +$$
$$\bar{l}_2(t)(\|y(t-\tau_2(t,y_t)) - \tilde{y}(t-\tau_2(t,y_t))\| + \bar{k}_1\rho_2\|y_t - \tilde{y}\|), t \in J.$$

Hence, there is some

$$(w,\tilde{w}) \in F_1(t,x(t-\tau_1(t,x_t)), y(t-\tau_2(t,y_t))) \times F_2(t,x(t-\tau_1(t,x_t)), y(t-\tau_2(t,y_t)))$$

such that for each $t \in J$

$$\|v_1(t) - \overline{w}\| \leq l_1(t)(\|x(t-\tau_1(t,x_t)) - \tilde{x}(t-\tau_1(t,x_t))\| + k_1\rho_1\|x_t - \tilde{x}\|) + \bar{l}_1(t)(\|y(t-\tau_2(t,y_t)) - \tilde{y}(t-\tau_2(t,y_t))\| + \bar{k}_1\rho_2\|y_t - \tilde{y}_t\|)$$

and

$$\|v_2(t) - \overline{w}\| \leq l_2(t)\|x(t-\tau_1(t,x_t)) - \tilde{x}(t-\tau_1(t,x_t))\| + k_1\rho_1\|x_t - \tilde{x}_t\| + \bar{l}_2(t)\|y(t-\tau_2(t,y_t)) - \tilde{y}(t-\tau_2(t,y_t))\| + \bar{k}_1\rho_2\|y_t - \tilde{y}_t\|).$$

Consider the multi-valued maps $U_i: J \to \mathbb{R}, i = 1;\ 2$ defined by

$$U_1(t) = \{f \in F_1(t,x(t-\tau_1(t,x_t)), y(t-\tau_2(t,y_t))):$$
$$\|v_1(t) - w\| \leq l_1(t)\|x(t-\tau_1(t,x_t)) - \tilde{x}(t-\tau_1(t,x_t))\| + k_1\rho_1\|x_t - x_t\| + \bar{l}_1(t)\|y(t-\tau_2(t,y_t)) - \tilde{y}(t-\tau_2(t,y_t))\| + \bar{k}_1\rho_2\|y_t - \tilde{y}_t\|)$$

and

$$U_2(t) = \{f \in F_2(t,x(t-\tau_1(t,x_t)), y(t-\tau_2(t,y_t))):$$
$$\|v_2(t) - w\| \leq l_2(t)\|x(t-\tau_1(t,x_t)) - \tilde{x}(t-\tau_1(t,x_t))\| + k_1\rho_1\|x_t - \tilde{x}_t\|$$

$$+\bar{l}_2(t)\big\|y\big(t-\tau_2(t,y_t)\big)-\tilde{y}\big(t-\tau_2(t,y_t)\big)\big\|+\bar{k}_1\rho_2\|y_t-\tilde{y}_t\|\big).$$

Then $U_i(t)$ is a nonempty set and Theorem III,4.1 in (Daoudi, 2018) tells us that U_i is measurable. Moreover, the multi-valued intersection operator $V_i(\cdot)=U_i(\cdot)\cap F_i\Big(\cdot,x\big(\cdot-\tau_1(\cdot,x)\big),y\big(\cdot-\tau_2(\cdot,y)\big)\Big)$ is measurable. Therefore, by Lemma 2.6, there exists a function $t\to\bar{v}_i$, which is a measurable selection for V_i, that is

$\tilde{v}_i\in F_i\Big(t,x\big(t-\tau_1(t,x_t)\big),y\big(t-\tau_2(t,y_t)\big)\Big)$ and

$$\|v_1(t)-\tilde{v}_1(t)\|\le l_1(t)\big\|x\big(t-\tau_1(t,x_t)\big)-\tilde{x}\big(t-\tau_1(t,x_t)\big)\big\|+k_1\rho_1\|x_t-\tilde{x}_t\|$$
$$+\bar{l}_1(t)\big\|y\big(t-\tau_2(t,y_t)\big)-\tilde{y}\big(t-\tau_2(t,y_t)\big)\big\|+\bar{k}_1\rho_2\|y_t-\tilde{y}_t\|\big)$$

and

$$\|v_2(t)-\tilde{v}_2(t)\|\le l_2(t)\big\|x\big(t-\tau_1(t,x_t)\big)-\tilde{x}\big(t-\tau_1(t,x)\big)\big\|+k_1\rho_1\|x_t-\tilde{x}_t\|$$
$$+\bar{l}_2(t)\big\|y\big(t-\tau_2(t,y_t)\big)-\tilde{y}\big(t-\tau_2(t,y_t)\big)\big\|+\bar{k}_1\rho_2\|y_t-\tilde{y}_t\|\big).$$

Define $\tilde{h}_1,\tilde{h}_2$ by

$$\tilde{h}_1(t)=T_1(t)\big(I-T_1(b)\big)^{-1}\int_0^b T_1(b-s)v_1(s)ds+\int_0^t T_1(t-s)v_1(s)ds,t\in J$$

and

$$\tilde{h}_2(t)=T_2(t)\big(I-T_2(b)\big)^{-1}\int_0^b T_2(b-s)v_2(s)ds+\int_0^t T_2(t-s)v_2(s)ds\,,t\in J.$$

Then for $t\in J$, there is

$$\big\|h_1(t)-\tilde{h}_1(t)\big\|$$
$$\le\frac{M^2}{\|I-T(b)\|}\bigg(\int_0^b l_1(s)\big\|x\big(s-\tau_1(s,x_s)\big)-\tilde{x}\big(s-\tau_1(s,x_s)\big)\big\|$$
$$+k_1\rho_1\|x_s-\tilde{x}_s\|+\bar{l}_1(s)\big\|y\big(s-\tau_1(s,y_s)\big)-\tilde{y}\big(s-\tau_2(s,y_s)\big)\big\|$$
$$+\bar{k}_1\rho_2\|y_s-\tilde{y}_s\|\big)\,ds$$

$$+M\left(\int_0^t l_1(s)\big\|x\big(s-\tau_1(s,x_s)\big)-\tilde{x}\big(s-\tau_1(s,x_s)\big)\big\|+k_1\rho_1\|x_s-\tilde{x}_s\|+\bar{l}_1(s)\big\|y\big(s-\tau_2(s,y_s)\big)-\tilde{y}\big(s-\tau_2(s,y_s)\big)\big\|+\bar{k}_1\rho_2\|y_s-\tilde{y}_s\|\right)ds$$

$$\leq\left(\frac{M^2}{\|1-T(b)\|}+M\right)\left(\int_0^b l_1(s)\|x(s-\tau_1(s,x_s))-\tilde{x}(s-\tau_1(s,x_s))\|\right.$$
$$+k_1\rho_1\|x_s-\tilde{x}_s\|+\bar{l}_1(s)\|y(s-\tau_2(s,y_s))-\tilde{y}(s-\tau_2(s,y_s))\|$$
$$\left.+\bar{k}_1\rho_2\|y_s-\tilde{y}_s\|)ds\right)$$
$$\leq\left(\frac{M^2}{\|1-T(b)\|}+M\right)\left(k_1\rho_1+\|l_1\|_{L^1},\bar{k}_1\rho_2+\|\bar{l}_1\|_{L^1}\right)(\|x-\tilde{x}\|_\infty,\|y-\tilde{y}\|_\infty).$$

Thus,

$$\|h_1-\tilde{h}_1\|_\infty\leq\left(\frac{M^2}{\|1-T(b)\|}+M\right)\left(k_1\rho_1+\|l_1\|_{L^1},\bar{k}_1\rho_2\right.$$
$$\left.+\|\bar{l}_1\|_{L^1}\right)(\|x-\tilde{x}\|_\infty,\|y-\tilde{y}\|_\infty).$$

By an analogous relation, one finally arrives at the estimate

$$H_{d_1}(N_1(x,y),N_1(\tilde{x},\tilde{y}))$$
$$\leq\left(\frac{M^2}{\|1-T(b)\|}+M\right)\left(k_1\rho_1+\|l_1\|_{L^1},\bar{k}_1\rho_2+\|\bar{l}_1\|_{L^1}\right)(\|x-x\|_\infty,\|y-\tilde{y}\|_\infty).$$

Similarly, there is

$$H_{d_2}(N_2(x,y),N_2(\tilde{x},\tilde{y}))$$
$$\leq\left(\frac{M^2}{\|1-T(b)\|}+M\right)\left(k_2\rho_1+\|l_2\|_{L^1},\bar{k}_2\rho_2\right.$$
$$\left.+\|\bar{l}_2\|_{L^2}\right)(\|x-\tilde{x}\|_\infty,\|y-\tilde{y}\|_\infty)$$

Therefore,

$$H_d(N(x,y),N(\tilde{x},\tilde{y}))\leq\overline{M}\begin{pmatrix}\|x-\tilde{x}\|_\infty\\\|y-\tilde{y}\|_\infty\end{pmatrix},for\ all(x,y),(\tilde{x},\tilde{y})\in C^2\times C^2.$$

Thus, by Theorem 2.13, the operator N has a unique fixed point which is a unique mild solution to problem (1).

Conclusion

This paper, using the recent Perov fixed point theorem technique on a Banach space, presents an existence result for a mild solution to a semi-linear operator system of periodic functional differential inclusions.

Researchers are encouraged to explore these findings further and develop computational and numerical methods to approximate the results, providing an alternative approach to advancing the current study.

References

Ahmed, N.U. 1991. *Semigroup Theory with Applications to Systems and Control*, Pitman Research Notes in Mathematics Series, ISBN-10: 0582065992.

Aubin, J.P. & Frankowska, H. 1990. *Set-Valued Analysis*, Birkhäuser, Boston ISBN: 978-0-8176-4847-3.

Daoudi, K. 2018. *Contribution aux équations et inclusions différentielles à retard dépendant de l´etat*, PhD thesis. Djillali Liabes University (in French).

Daoudi, K., Henderson J. & Ouahab, A. 2018. Existence and uniqueness of solutions for some neutral differential equations with state-dependent delays. *Communications in Applied Analysis*, 22(3), pp.333-351. Available at: https://scholar.google.com/citations?view_op=view_citation&hl=ar&user=zSKiQwIAAAAJ&citation_for_view=zSKiQwIAAAAJ:u-x6o8ySG0sC

Djebali, S., Gorniewicz L. & Ouahab, A. 2010. First-order periodic impulsive semilinear differential inclusions: Existence and structure of solution sets. *Mathematical and Computer Modelling*, *52*(5-6), pp.683-714. Available at: https://www.sciencedirect.com/science/article/pii/S0895717710002062

Hale, J. K. 1977. *Theory of Functional Differential Equations*. Springer-Verlag, New York. ISBN -13: 978-1-4612-9894-6.

Hale, J. K. & Lunel, S.M.V. 2013. *Introduction to Functional -Differential Equations*, Applied Mathematical Sciences, Springer Science & Business Media, LLC. ISBN 978-1-4612-8741-4.

Kolmanovskii, V. & Myshkis, A. 1999. *Introduction to the Theory and Applications of Functional-Differential Equations.* Springer Science & Business Media, B.V. ISBN: 978-90-481-5148-6.

Mohamed, F. & Tayeb, B. 2019. Random semilinear system of differential equations with state-dependent delay. *Advances in the Theory of Nonlinear Analysis and its Applications*, 3(1), pp.1-10. Available at: https://doi.org/10.31197/atnaa.468807

Sinacer, M.L., Nieto, J.J. & Ouahab, A., 2016. Random fixed point theorem in generalized Banach space and applications. *Random Operators and Stochastic Equations*, *24*(2), pp.93-112. Available at: https://www.degruyterbrill.com/document/doi/10.1515/rose-2016-0007/html

Wu, J. 1996. *Theory and Applications of Partial Functional Differential Equations*, Springer-Verlag, New York. ISBN-13: 978-1-4612-8479-6.

Sistema de inclusión diferencial funcional semilineal periódico con retardos dependientes del estado

Khelifa Daoudi[a], **autor de correspondencia,** *Mohamed* Belaidi[a]

[a] Centro Universitario de Nour Bachir El-Bayadh, El-Bayadh, Argelia, Instituto de Ciencias, El-Bayadh, Argelia

[b] Université de Sidi Bel-Abbes, Laboratoire de Mathématiques, Argelia, Sidi Bel-Abbes, Argelia

CAMPO: Matemáticas
TIPO DE ARTÍCULO: artículo científico original

Resumen:

Introducción/objetivo: El estudio abordó la existencia y singularidad de soluciones suaves para una clase de sistemas de inclusión diferenciales funcionales semilineales periódicos con retardos dependientes del estado. Estos sistemas son de creciente interés debido a su amplia gama de aplicaciones en teoría de control, sistemas biológicos y modelos de ingeniería que involucran retrasos de tiempo e incertidumbres.
Métodos: La investigación se realizó en el marco de los espacios de Banach. Se aplicó el teorema del punto fijo de Perov, conocido por su eficacia en el manejo de sistemas con múltiples componentes, para establecer la existencia de soluciones suaves. El enfoque analítico incorporó técnicas adecuadas para inclusiones diferenciales y teoría de operadores, con especial atención a sistemas influenciados por retardos dependientes del estado.
Resultados: Se obtuvieron varios resultados relativos a la existencia y unicidad de soluciones suaves para el sistema considerado. La aplicación del teorema del punto fijo de Perov permitió derivar las condiciones suficientes para la existencia de dichas soluciones. Además, se tuvo en cuenta la naturaleza periódica del sistema, asegurando que las soluciones se ajustaran a la estructura temporal prescrita.
Conclusión: Los hallazgos confirmaron que, bajo supuestos específicos, el sistema admite al menos una solución moderada. Los resultados contribuyeron a la fundamentación teórica de las inclusiones diferenciales funcionales con retardos. Se alentó a los investigadores a explorar más a fondo estos resultados y a desarrollar métodos computacionales y numéricos para aproximar las soluciones teóricas, ampliando así la aplicabilidad de la investigación actual.

Palabras claves: soluciones suaves, retardos dependientes del estado, espacios de Banach, aplicaciones multivaluadas, puntos fijos, inclusiones diferenciales funcionales, sistemas semilineales

Периодическая полулинейная функционально-дифференциальная система включения с зависящими от состояния задержками

Халифа Даудия[аб], **корреспондент,** *Мохамед* Белаиди[а]
[а] Университетский центр Нур-Башир-Эль-Баяд, Эль-Баяд, Алжир, Научный институт, Эль-Баяд, Алжир
[б] Университет Сиди-Бель-Аббеса, Математическая лаборатория, Алжир, Сиди-Бель-Аббес, Алжир,

РУБРИКА ГРНТИ: 27.01.00 Общие вопросы математики
ВИД СТАТЬИ: оригинальная научная статья

Резюме:

Введение/цель: В данном исследовании рассматривались существование и уникальность мягких решений для класса периодических полулинейных систем функционально-дифференциального включения с задержками, зависящими от состояния. Такие системы вызывают большой интерес из-за их широкого спектра применения в теории управления, биологических системах и инженерных моделях, связанных с временными задержками и неопределенностями.

Методы: *Исследование проводилось в рамках банахового пространства. Теорема Перова о неподвижной точке, отличающаяся эффективностью в работе с многокомпонентными системами, была применена для выявления слабых решений. Аналитический подход включал методы, подходящие для дифференциальных включений и теории операторов, с особым упором на системы, подверженным задержкам, зависящим от состояния.*

Результаты: В ходе исследования было получено несколько результатов, касающихся существования и уникальности слабых решений по анализируемой системе. Применение теоремы Перова о неподвижной точке помогло выявить условия, при которых такие решения могут использоваться. Помимо того, был учтен периодический характер системы, что гарантировало соответствие решений предписанной временной структуре.

Выводы: Результаты подтвердили, что при определенных обстоятельствах система допускает хотя бы одно мягкое решение. Результаты способствовали теоретическому обоснованию функционально-дифференциальных включений с задержками. Исследователям было предложено продолжить изучение полученных результатов и разработать численные методы для аппроксимации теоретических решений, тем самым расширив применимость данного исследования.

Ключевые слова: мягкие решения, зависящие от состояния задержки, банахово пространство, многозначные отображения, неподвижные точки, функционально-дифференциальные включения, полулинейные системы.

Периодични семилинеарни функционални систем инклузије са кашњењима зависним од стања

Калифа Дауди[а,б], ***аутор за преписку,*** *Мохамед* Белаиди[а]

[а] Универзитетски центар Ноур Бачир Ел-Бајад
Институт наука, Ел-Бајад, Алжир, +

[б] Лабораторија за математику, Универзитет Сиди Бел-Абес,
Сиди Бел-Абес, Алжир,

ОБЛАСТ: математика
КАТЕГОРИЈА (ТИП) ЧЛАНКА: оригинални научни рад

Сажетак:

Увод/Циљ: У овој студији обрађује се постојање и јединственост слабих решења за класу периодичних семилинеарних функционалних диференцијалних система инклузије са кашњењима зависним од стања. Све је веће интересовање за ове системе због њиховог широког спектра примене у теорији управљања, биолошким системима, као и инжењерским моделима који укључују временска кашњења и неизвесности.

Методе: Истраживање је спроведено унутар Банахових простора. Теорема о фиксној тачки Перова, позната по својој ефикасности при раду са вишекомпонентним системима, примењена је како би се утврдило постојање слабих решења. Аналитички приступ укључивао је технике погодне за диференцијалне инклузије и теорију оператора, с посебним фокусом на системе под утицајем кашњења зависних од стања.

Резултати: Добијено је неколико резултата који се односе на постојање и јединственост слабих решења за разматрани систем. Примена теореме о фиксној тачки Перова омогућила је извођење довољних услова под којима таква решења постоје. Штавише, узета је у обзир периодична природа система, што је обезбедило да се решења придржавају прописане временске структуре.

Закључак: Налази су потврдили да, под специфичним претпоставкама, систем дозвољава најмање једно слабо решење. Резултати су допринели теоријској основи функционалних диференцијалних инклузија са кашњењима. Истраживачи се подстичу да даље испитују ова решења и да развијају рачунарске и нумеричке методе за апроксимацију теоријских решења, што би омогућило ширу примену овог истраживања.

Кључне речи: слаба решења, кашњења зависна од стања, Банахови простори, вишевредносне мапе, непомичне тачке, функционалне диференцијалне инклузије, семилинеарни системи

Paper received on: 19.08.2024.
Manuscript corrections submitted on:23.03.2025.
Paper accepted for publishing on: 29.04.2025.

A novel intuitionistic fuzzy FMEA framework with Dombi aggregation for service quality in industry 4.0: application in higher education

Biplab Biswas[a], *Sanjib* Biswas[b]

[a] ICFAI University, Ranchi, Jharkhand, Republic of India + Amity University, Amity Business School, Kolkata, West Bengal, Republic of India,
e-mail: biplabdimat@gmail.com,
ORCiD: https://orcid.org/0000-0001-5869-4998

[b] Amity University, Amity Business School, Kolkata, Republic of India,
e-mail: sanjibbiswas1981@gmail.com, **corresponding author**,
ORCiD: https://orcid.org/0000-0002-9243-2403

doi https://doi.org/10.5937/vojtehg73-55682

FIELD: mathematics, decision science
ARTICLE TYPE: original scientific paper

Abstract:

Introduction/purpose: Higher educational service quality (HSQ) is one of the prominent areas redefined in I4, imposing many challenges on higher educational institutions (HEIs). In this context, the present work aims to fulfill two objectives: a) to develop a novel risk assessment framework for failure mode and effect analysis (FMEA) using the intuitionistic fuzzy set (IFS) and b) to assess potential risk factors or failures faced by HEIs in delivering superior HSQ in Industry 4.0 (I4).

Methods: The present work uses a multi-criteria decision-making (MCDM) model, such as comparisons between ranked criteria (COBRAC), with IFS-based Dombi aggregation for group decision making to develop a novel extension of the FMEA framework. The present work proposes an innovative approach by incorporating an additional dimension in the classical FMEA model such as intractability. The failure modes (FMs) are identified from the viewpoint of the HSQ attributes. Subsequently, the present work examines the validity of the outcome by comparing several MCDM models and sensitivity analysis.

Results: Based on the opinions of 23 experts, the current work reveals the dominance of risk factors such as ethical concerns (FM-9), infrastructural constraints (FM-2), and shortage of funds (FM-6).

Conclusion: The paper highlights the need to build a holistic ecosystem with available resources. The ongoing study provides several novelties, such as an extension of FMEA with an additional dimension and IFS-Dombi *aggregation, using the COBRAC model for FMEA, and an innovative approach to risk assessment for HSQ, which are helpful for decision makers and researchers.*

Key words: service quality, higher educational institutions, FMEA, intuitionistic fuzzy set, COBRAC, Dombi aggregation.

Introduction

The higher education system (HES) is pivotal in ensuring economic growth, fostering sustainable development, developing and nurturing talents for future potential, and building an innovative ecosystem while integrating society, business, and government. A well-developed and executed HES promotes innovation and technical progress, sustaining economic prosperity. It advances social fairness, enabling more seamless transfers within the job market. Higher education investments favourably correlate with economic growth, particularly in human capital development (Chaabouni & Mbarek, 2023). After the beginning of Industry 4.0 in 2011, the HES and higher educational institutions (HEIs) have witnessed phenomenal technological growth in Industry 4.0 (I4). The recent pandemic has pronounced the power of digital technologies in higher education. Digital technologies like smart classrooms, augmented and virtual reality, the Internet of Things (IoT), cloud-based interactivity and computing, cutting-edge computing tools and techniques, digital twins, chatbots, and blockchains have redefined HSQ offered by the HES in I4. The changes are reflected in the curriculum transformation (emphasizing technical, cognitive, and problem-solving skills, entrepreneurial mindset and adaptive thinking for career development, and ethical concerns), innovative teaching-learning environment (using flipped classrooms, AR/VR-based interactions, use of avatars and simulations, emphasis on experiential learning, personalized and blended learning and content delivery), student engagement, stakeholder connect, administrative process, and collaborative research and partnerships (Jamaludin et al, 2020; Moraes et al, 2023; Dempere et al, 2023; Alenezi, 2023; Biswas et al, 2023; Wang et al, 2023).

While technological progress has offered several opportunities for HEIs, the HES has also been exposed to many unprecedented challenges or potential risk factors. The risks stem from the factors such as digital inclusion, accessibility and implementation of technological advancements, competency building for faculty members and students, and re-alignment of the existing HES and teaching-learning processes in the realm of technological progress while maintaining diversity and ethics to satisfy the needs of stakeholders (Majid et al, 2022). The digital revolution of higher education encounters obstacles in equipping educators with essential digital competencies for effective teaching. Assessing digital competencies is essential for successful digital learning programs, and inadequate training may impede these advantages (Akhmetshin et al, 2020; Chaabouni & Mbarek, 2023). Given the opportunities and challenges posited by technological advancements for HEIs, the present age invokes adaptability to the evolving demands of students and other stakeholders, including corporate bodies, efficient technology utilization, and prioritization of quality and accessibility (Liu & Shi, 2023; Abulibdeh et al, 2024). Digital transformation in higher education emphasizes tailored learning environments, improving engagement and motivation, and aligning with the connectivism theory to ensure sustainability and academic achievement and address different student requirements (Shenkoya & Kim, 2023; Leow et al, 2023). HEIs must bring about a cultural shift within and around the HES to overcome the challenges and risk factors for developing a conducive and adaptable innovative ecosystem to ride on technological growth (Alenezi & Akour, 2023). The myriad of contributions toward unlocking the potential and challenges for HEIs in I4 necessitates the development of a comprehensive risk assessment framework for evaluating possible failure modes or risk factors. The existing literature does not reveal plentiful contributions using a multidimensional risk assessment framework for unearthing criticalities of the risk factors. The aforesaid gap in the literature motivates us to be committed to this work.

The current work utilizes a widely used risk assessment framework such as failure mode and effects analysis (FMEA). The classical FMEA framework embodies priority scores of the risk factors based on three dimensions such as severity (S) (signifying the extent to which the concerned risk factor is affecting the system), occurrence (O) (indicating the likelihood of occurrence of the corresponding risk factor), and detectability (D) (reflects the extent to which the system can identify the corresponding risk factor). The overall priority of the risk factor is determined by a risk priority number (RPN) ($RPN = S \times O \times D$) (Bowles & Peláez, 1995).

FMEA has been widely applied by scholars in various risk assessment problems, *see,* e.g., (Peddi et al, 2023; Sun et al, 2023; Resende et al, 2024). The existing literature shows several applications of FMEA in higher education, *see,* e.g., (Lin & Lo, 2024; Nasrallah et al, 2023). Nevertheless, FMEA has enormous potential for applications in higher education to evaluate risk priority in various processes, including HSQ (Zulfiqar et al, 2024). Some contributions used FMEA vis-à-vis HSQ (Anastasiadou & Zirinoglou, 2020). However, the applications of FMEA for figuring out service quality risks for higher education in I4 are limited, almost rare. This has motivated us to utilize FMEA to evaluate the priorities of the failure modes (FM) of HSQ. Further, we learn some limitations of the classical FMEA model from scholars (Salah et al, 2023; Liu et al, 2024; Sumrit & Keeratibhubordee, 2025). The classical FMEA model suffers from limitations such as the following ones: a) Conventional FMEA model cannot capture the impreciseness of information and subjective bias; b) In the conventional FMEA model, there is no prioritization of individual dimensions. Further, there is no room for assigning relative importance to the risk factors from the perspective of the context of the problem. As a result, on many occasions, there may be multiple FMs having the same RPN value; c) There are no options to assign weights to decision makers (based on their expertise or experience, etc.) in traditional FMEA; and d) The calculation of the RPN is relatively simple, which often dilutes the outcome.

Given these limitations, numerous contributions have modified classical FMEA using uncertainty-based modelling (Yu et al, 2023; Sun et al, 2023). This paper uses IFS-based analysis to capture uncertainty and subjective bias for carrying out FMEA. Some studies incorporated additional dimensions in the conventional FMEA model. For instance, Salah et al. (2023) used an additional criterion, such as the dependency of the risk factors on each other. Besides dependency, the aforesaid work also applied the Pareto principle to classify the risk factors. The work of Sumrit & Keeratibhubordee (2025) proposes three additional dimensions: cost of FM, complexity of resolution, and impact on business. However, none of the previous extensions of FMEA have precisely considered a crucial aspect called the manageability of risk. It is important to determine the mitigation plan for managing the risks effectively. Given volatility, uncertainty, complexity, and ambiguity (VUCA) prevailing over the external environment, the identified risks' manageability helps decision makers prepare contingency and preventive action plans. The proposed FMEA approach of this study is thus an action plan driven approach with wide practical applications. In this work, we fill the stated gap in the literature by providing an innovative approach of carrying out FMEA. Hence, the current study sets the following research objectives:

- *RO 1*. To develop a multi-perspective framework for evaluating the priorities of the risk factors or failure modes of higher education service quality in Industry 4.0.

- *RO2.* To modify the conventional FMEA framework and extend it using subjective information under uncertainty.

To widen the applicability of classical fuzzy sets (CFSs) (Zadeh, 1965), the concept of IFSs was proposed to capture the vagueness through two types of membership functions such as the membership (μ) and the non-membership (ϑ), subject to their interrelationship determined by the inequality μ + ϑ ≤1 (Atanassov, 1986). Table 1 provides a summary of some of the advancements of CFSs. Table 1 shows that the IFS provides more pragmatic analysis under uncertainty than the CFS, yet it is simple to apply and conceptualize.

Table 1 – Evolution of fuzzy sets and its advancements

Type of Fuzzy Sets	Concept	Remarks	Reference
CFSs	Consider only $\mu \in [0,1]$	Limited but straightforward to consider the imprecision	Zadeh (1965)
Type 2 Fuzzy Sets	Fuzziness of the membership degree	Can handle a higher level of uncertainty, but complex in calculation, and consider a single membership	Zadeh (1975a)
Interval-Valued Fuzzy Sets	Membership degree is expressed in terms of the interval	A better representation than CFSs but limited to a single membership interval	Zadeh (1975b)
IFSs	Consider both $\mu, \vartheta \in [0,1]$ such that $\mu + \vartheta \leq 1$	Simple to understand and a better representation of imprecision. However, they are constrained by the cases where $\mu + \vartheta > 1$	Atanassov (1986)
Hesitant Fuzzy Sets	Existence of multiple membership degrees	Able to deal with indeterminacy but computationally complex for large datasets	Torra (2010)
Spherical Fuzzy Sets	Consider the neutral membership degree such that $\mu^2 + \eta^2 + \vartheta^2 \leq 1$.	A generalization of PyFS with the degree of neutrality. They are limited to spherical constraint and complex	Gündoğdu & Kahraman (2019)
p, q-Quasirung Orthopair Fuzzy Sets	Consider both $\mu, \vartheta \in [0,1]$ such that $\mu^p + \vartheta^q \leq 1; p, q \geq 1$	Further generalization of qROFSs but suffer from complexity in parameter selection	Seikh & Mandal (2022)

The remainder of this manuscript is organized in the following manner. The subsequent section (Section 2) revisits recent studies published in related fields. Section 3 exhibits the preliminary concepts of the IFS. Section 4 outlines the steps of the research methodology. Section 5 records significant findings. Section 6 discusses the findings and outlines research implications. In the end, Section 7 provides the concluding remarks and highlights future scopes.

Underpinning of related work

This section revisits the existing literature to provide a theoretical foundation for the current study.

Theoretical underpinning: Service quality models

The SERVQUAL model defines service quality (SQ) as a measure to close the gap between expected and experienced service levels. The classical SERVQUAL framework has five underlying dimensions: reliability, tangibles, responsiveness, assurance, and empathy. HEIs have adopted the SERVQUAL model to define HSQ. According to the SERVQUAL model used in the HES, HSQ is measured by the effectiveness in teaching and learning, faculty and student quality, and facilitating conditions to support students. Many HEIs have used the SERVQUAL model to define measurable performance attributes while upholding the reliability and trust of service delivery, ultimately leading to stakeholder satisfaction and organizational excellence (Oliso et al, 2024; Fuchs & Fangpong, 2021; Abbas, 2020). For the enduring performance and competitiveness of HEIs to achieve sustainable growth, the nexus between service quality, satisfaction, and loyalty is essential (Nguyen et al, 2024).

Nevertheless, several scholars highlighted the pressing need to revise the conventional SERVQUAL model while being adopted in the HES. Researchers devised an alternative framework, such as the HEdPERF (Higher Education PERFormance) model (Abdullah, 2005). This model evaluates service quality in higher education through five dimensions: academic and non-academic components, reputation, access, and program-related difficulties. It assesses instructional quality, extracurricular attributes, prestige, accessibility, and course pertinence to ensure an exceptional educational experience (Feifei et al, 2022).

The SQM-HEI approach, created by Indian academics, emphasizes the assessment of service quality in higher education, incorporating instructional methods, environmental modifications, and disciplinary measures to improve educational quality in the nation (Khan et al, 2022; Subandi & Hamid, 2021). Research indicates a favorable correlation between transformative service quality and satisfaction in higher education. The technical dimension of service quality, incredibly transformational service quality, profoundly influences student satisfaction. Students' mental goodness shapes their emotional response toward their university, and they anticipate equitable treatment. Functional service quality significantly influences the perceived value more than the technical component (Teeroovengadum et al, 2019).

The theoretical contributions reveal that HSQ depends on several attributes. Some of the crucial attributes are outlined below.

- The evolving and contemporary curriculum is a pivotal attribute in enhancing HSQ. It is the cornerstone for skill development, enhancing students' employability, promoting analytical reasoning, innovative concepts, efficient decision making, and adaptability to evolving educational requirements.
- Knowledge discovery and dissemination play crucial roles in HSQ. They indicate the development of requisite competencies and skills, fostering research, innovation, curriculum development, and stakeholder engagement.
- Innovative teaching-learning environment: This is required to foster experiential learning, linking theoretical knowledge to practical application, and equipping students for employment.
- Physical and technological infrastructure: This attribute entails the resources supporting interdisciplinary programs, experiential learning, and entrepreneurial programs, innovative teaching and learning through flipped classrooms, online platforms, innovative delivery, and simulations to provide students with a comprehensive, personalized and immersive learning experience while enhancing student satisfaction and upholding institutional prestige.
- Support services: Refer to the availability of responsive, empathetic, and accessible administrative and academic support to cater to the needs of diverse student categories while offering necessary guidance and counseling.
- Organizational culture is about shared values and ethics and promoting community impact. An open culture, led by good governance, promotes student development, equity, and adaptability.

Challenges of HEIs in the digital age

This section summarizes some related past studies discussing challenges or potential risk factors for HEIs to deliver superior HSQ in I4. The challenges are discussed in various contexts, and scholars have adopted different methodologies, as recorded in Table 2.

Table 2 – Summary of some research contributions discussing challenges for HEIs

Author(s)	Context	Theory	Key challenges	Methodology
Benavides et al, 2020	Digital technology applications in higher education	NA	Curriculum upgradation and flexibility, lack of innovation, knowledge and competencies, organizational change	Qualitative: a review of the literature
Bonfield et al, 2020	Application of I4 technologies in HEIs across different countries	NA	Shortage of skills, creation of a memorable student experience, security and privacy, innovative teaching methods	Qualitative – scenario analysis and case studies
Mahyoob, 2020	Challenges faced by learners attending e-learning programs in the context of COVID-19	Activity theory	Inefficiency in technology use, language issues	Descriptive analysis of the responses received from 148 students
Fahim et al, 2021	Enrolment in MBA programs offered by HEIs	NA	Poor employability, lack of entrepreneurial programs, cost, long payback period, poor ROI	Subjective information-based grey incidence analysis
Žalėnienė & Pereira, 2021	Sustainability in higher education	NA	Sustainability-focused curriculum development and organizational culture, community connect	Qualitative-discussions and perspectives
Wang et al, 2023	HEIs in I4	NA	Upgradation and development of contemporary curriculum, integration of digital technologies, adoption of advanced computing such as cloud computing	Subjective and objective information-based application of the q Rung Orthopair fuzzy MEREC-SWARA-CoCoSo framework

Author(s)	Context	Theory	Key challenges	Methodology
Rasul et al, 2023	Use of generative AI (ChatGPT) in higher education	Constructivist theory of learning	Maintenance of ethics and equity, academic integrity, information distortion, lack of skills, evaluation of learning outcome	Qualitative: a review of the literature and conceptual framework
Chan & Hu, 2023	Students' perception of the use of generative AI in higher education	NA	Ethics and privacy issues, lack of competencies, diluted human values, improper policy	Mixed method: empirical analysis of 339 responses from Hong Kong using descriptive and thematic analysis
Abulibdeh et al, 2024	Digital technologies for sustainable development	NA	Shortage of IT and analytical skills, curriculum update, shortage of infrastructure, and industry connect	Qualitative: a review of the literature
Li, 2024	Role of higher education in developing workforce for manufacturing	NA	Skill development	Qualitative: a review of the literature and conceptual framework
This paper	HSQ of Indian HEIs in I4	Mixed theory	Ethical concerns, infrastructural constraints, shortage of funds	Modified FMEA framework with the IFS-Dombi aggregation-based COBRAC method

Failure Modes and Effect Analysis framework for risk assessment

The FMEA framework is a widely used model for evaluating risk factors. Its applications are found in various domains such as engineering, technology, basic science, social science, and management. Scholars have modified and extended the FMEA model using uncertainty measures, MCDM models, and machine learning methods. Table 3 provides a summary of some of the recent contributions.

Table 3 – Summary of research contributions applying FMEA

Author(s)	Application area	Dimen sions	Information type	Approach
Sun et al, 2023	Lead-acid battery manufacturing process	S, O, D	Subjective	FMEA using regret theory and ORESTE
Ervural & Ayaz, 2023	Manufacturing	S, O, D	Objective	FMEA using modified CRITIC and Alternative by Alternative Comparison (ABAC)
Park et al, 2023	Cybersecurity	S, O, D	Subjective	FMEA using a rule-based Bayesian network (RBN)
Ceylan et al, 2023	Maritime logistics	S, O, D	Objective and subjective	Classical FMEA
Liu et al, 2023a	Aircraft power system	S, O, D	Subjective	FMEA using the unbalanced hesitant fuzzy linguistic term sets and experts' weighting
Peddi et al, 2023	Food waste management in the supply chain	S, O, D	Subjective	Dynamic prediction of RPN values using deep neural network (machine learning) based FMEA
Liu et al, 2023b	Social network analysis	S, O, D	Subjective	Probabilistic double hierarchy linguistic term sets and WASPAS method and weight determination
Yu et al, 2023	Maritime logistics (submarine pipeline failures)	S, O, D	Subjective	Interval-valued intuitionistic fuzzy rough number and modified TODIM and PROMETHEE-II methods
Xue et al, 2024	Identification of barriers to electric vehicles	S, O, D	Subjective	FMEA using interval-valued intuitionistic fuzzy sets, grey relational analysis, and expert weighting

Author(s)	Application area	Dimensions	Information type	Approach
Sumrit & Keeratibhuborde e, 2025	Sustainable supply chain management	S, O, D + cost, complexity, and impact on business	Objective and subjective	FMEA with MCDM models such as LOPCOW, AHP, and ARAS
Nasrallah et al, 2023	Safety risk measures in laboratories	S, O, D	Objective	Classical FMEA
This paper	Higher education service quality in I4	S, O, D + **Intractability (new dimension)**	Subjective	FMEA with intuitionistic fuzzy sets and the Dombi aggregation-based COBRAC method and experts' weighting

MCDM methods for criteria weighting

The field of MCDM methods for determining criteria weights using subjective opinions has been rapidly expanded over the last few decades. The Analytic Hierarchy Process (AHP) method is one of the widely used approaches. However, AHP suffers from more pairwise comparisons and demonstrates inconsistencies in decision making while considering more criteria and respondents. Scholars (Keršuliene et al, 2010) gradually developed a SWARA method that requires only (n-1) pairwise comparisons. However, this method requires sorting the criteria at the beginning and considerably depends on the values assigned to the criteria. Rezaei (2015) introduced BWM to solve the issue of cognitive burden. BWM sets the references at the beginning by identifying the best and worst criteria. BWM requires much fewer pairwise comparisons (2n-3) than AHP, can deal with an extensive criteria set, and provides a consistency checking. Pamucar et al. (2019) developed the FUCOM method to reduce pairwise comparisons while checking for consistency. FUCOM requires only (n-1) number of global pairwise comparisons.

Related work on the applications of Dombi aggregation

Several researchers have applied Dombi aggregation to MCDM-related problems using imprecise information. Seikh and Chatterjee (2024) developed a confidence level based IFS Dombi aggregation for e-learning website selection. Zhang & Ye (2024) introduced single-valued neutrosophic fuzzy trigonometric Dombi aggregation operators for vaccine selection. Ali & Yang (2024) defined circular qROFS based Dombi aggregation operators for MCDM applications. Liu et al. (2024) devised complex Pythagorean fuzzy Dombi aggregation for green supply chain management applications. Recently, Khan et al. (2025) applied intuitionistic fuzzy rough set and Dombi aggregation to solar cell selection problem.

Research gaps and motivations of the present study

The following research gaps, revealed from Table 1, can be noticed. First, studies using theoretical lenses are not plentiful. Second, except for a few studies, most past contributions used conceptual and review papers to address the application and challenges of digital technologies in higher education. Third, there is a lack of focus on HSQ in I4.

It can be noticed (Table 2) that most contributions are made in manufacturing, logistics, supply chain management, and engineering problems. However, FMEA has also been used in several problems concerning the HES. It is evident that FMEA has not been applied extensively concerning HSQ in I4. Several studies have used subjective information-based analysis, many of which have used MCDM models. A few studies have put forth extended FMEA models, but none have considered manageability.

Some studies incorporated additional dimensions in the conventional FMEA model. For instance, Salah et al. (2023) used an additional criterion such as the dependency of risk factors on each other. Besides dependency, the aforesaid work also applied the Pareto principle to classify risk factors. The work of Sumrit and Keeratibhubordee (2025) proposes three additional dimensions: cost of FM, complexity of resolution, and impact on business. However, none of these extensions have precisely considered a crucial aspect called the manageability of risk, which is very important to know for mitigation.

Scholars have felt the importance of Dombi aggregation in solving complex real-life problems with MCDM applications. However, we could not trace any application of Dombi aggregation with FMEA to discover the key risk factors of HSQ. The application of Dombi aggregation in higher education is scant. Because of its usefulness, Dombi aggregation effectively decides the key risk factors. Furthermore, the use of IFSs reduces the computational complexity.

Contributions of the present study

In summary, the present work offers several contributions to the growing strand of literature, as outlined below.

1) The present work is the first contribution that provides a novel modification of the existing FMEA framework with an additional dimension known as Intractability (I).
2) A novel IFS and Dombi aggregation-based modified FMEA is proposed that uses the robust algorithm of COBRAC to determine the relative importance of FMs from the perspective of higher education and compute the scores of the FMs under each dimension of FMEA. COBRAC has an inherent advantage in examining deviations from consistency. Further, the COBRAC method uses fewer local pairwise comparisons, reducing computational complexity. Thus, the COBRAC method provides a more reliable approach to determining the risk appraisal score (RAS). Further, IFS and Dombi aggregation helps capture the respondents' impreciseness and subjective bias simply and flexibly.
3) The use of Dombi aggregation provides several advantages (Dombi, 1982; Xu & Yager, 2006): a) it provides a flexible aggregation by tuning the parameter (β) to capture optimism, neutrality, and pessimism; b) it helps to aggregate the effect values when criteria are not additive in nature, rather following a nonlinear relationship; c) depending on the parameter values, Dombi aggregation stands as a generalization of the simple arithmetic, geometric or harmonic means; d) it provides a better discrimination of the alternatives or criteria when the performance or effect values are subtle, i.e., very close to each other; and e) it also enables the examination of the sensitivity of the outcome concerning the variations in the external conditions. In this problem, we decide the RAS depending on the aggregated result of four risk dimensions. The experts who rated the risk factors have different risk perceptions - aggressive, conservative, and neutral. Hence, a small imprecision in the subjective opinion-based prioritization of the risk factors may result in an amplified error in the RAS. Therefore, the IFS with Dombi aggregation provides a reliable risk assessment framework for complex real-life problems.
4) An innovative approach using the conceptual approach of a simple additive weighting (SAW) method to determine the RAS using the relative importance of FMs and their positions based on FMEA

dimensions such as S, O, D, and I. In effect, a scientific basis is provided to arrive at the RAS other than a simple multiplication of the dimensions of FMEA.

5) It is also evident that the application of FMEA in HSQ literature is minimal, almost negligible. Hence, the present paper demonstrates an efficient approach to determining the RAS of various risk factors of HSQ in I4.
6) Four-dimensional modified FMEA with IFS and Dombi aggregation is apparently the first application for assessing the RAS of the FMs to ensure HSQ in I4. The existing literature shows past contributions related to various barriers or challenges to the HEIs' adoption of digital technologies in I4. However, there is a scantiness of contributions weighing the risk factors based on their likelihood of happening, consequence, detectability, and manageability. This paper fulfills the gap in the literature on HSQ concerning the effect of advanced digital technologies.
7) It demonstrates the sensitivity analysis and reliability assessment of the FMEA framework with an additional dimension and IFS-based appraisal.

Preliminary concepts

The present module discusses some preliminary definitions and rules for operating with IFSs. Past studies (Atanassov, 1986; Hong & Choi,2000; Xu & Yager, 2006; Xu, 2007) have given the basic definitions and operations below.

Definition 1.

Let Ω be the universe of discourse containing the IFS, defined as

$$\Upsilon = \left\{ \left\langle y, \mu(y), \vartheta(y) \right\rangle \middle| y \in \Omega \right\}$$

where $\mu(y), \vartheta(y)$ are defining the degree of membership and non-membership of the elements y such that

$$0 \le \mu(y) + \vartheta(y) \le 1 \quad for\ all\ y \in \Omega \to [0,1]$$

The degree of indeterminacy is derived from the definition of the IFS as

$$\zeta(y) = 1 - \mu(y) - \vartheta(y) \,. \tag{1}$$

In line with the definition of the IFS, an intuitionistic fuzzy number (IFN) can be expressed as $\gamma = (\mu, \vartheta)$ such that $\mu \in [0,1]; \vartheta \in [0,1]; \mu + \vartheta \le 1$.

Definition 2.

Let $\gamma = (\mu, \vartheta), \gamma_1 = (\mu_1, \vartheta_1)$ and $\gamma_2 = (\mu_2, \vartheta_2)$ be three IFNs. Here are the following definitions for operations on IFNs.

$$\gamma_1 \oplus \gamma_2 = (\mu_1 + \mu_2 - \mu_1\mu_2, \vartheta_1\vartheta_2)$$

$$\gamma_1 \otimes \gamma_2 = (\mu_1\mu_2, \vartheta_1 + \vartheta_2 - \vartheta_1\vartheta_2)$$

$$a\gamma = (1-(1-\mu)^a, \vartheta^a); a > 0 \text{ is any scalar quantity}$$

$$\gamma^a = (\mu^a, 1-(1-\vartheta)^a); a > 0$$

$$\gamma^c = (\vartheta, \mu)$$

Definition 3.

The following definition is used to determine the score value of an IFN.

$$\wp = Score(\gamma) = \mu - \vartheta; \wp \in [-1,1] \tag{2}$$

The accuracy value of an IFN is obtained as

$$\lambda = accuracy(\gamma) = (\mu + \vartheta); \lambda \in [0,1] \tag{3}$$

The following comparison rules are used to compare two IFNs.

If $\wp_1 > \wp_2$ then $\gamma_1 \succ \gamma_2$ otherwise

If $\wp_1 < \wp_2$ then $\gamma_1 < \gamma_2$ else

If $\wp_1 = \wp_2$ then if $\lambda_1 < \lambda_2$ then $\gamma_1 < \gamma_2$

Proceeding further, the scholars (Deb et al, 2022, 2023) came up with a new definition of the score function below.

$$\wp^* = \frac{1}{2}(1 + \mu - \vartheta) \tag{4}$$

Definition 4.

Dombi aggregation

The Dombi t-norm and t-conorm (Dombi, 1982) for any two real numbers R_1 and R_2 with the parameter value $\beta \geq 1;\ (R_1, R_2) \in [0,1] \times [0,1]$ can be expressed as

$$\mathrm{T}_{norm}(R_1, R_2) = \frac{1}{1 + \left\{ \left(\frac{1-R_1}{R_1} \right)^{\beta} + \left(\frac{1-R_2}{R_2} \right)^{\beta} \right\}^{\frac{1}{\beta}}} \tag{5}$$

$$T_{co-norm}(R_1,R_2) = 1 - \frac{1}{1+\left\{\left(\frac{R_1}{1-R_1}\right)^{\beta} + \left(\frac{R_2}{1-R_2}\right)^{\beta}\right\}^{\frac{1}{\beta}}} \tag{6}$$

Given a series of IFNs $\gamma_i = (\mu_i, \vartheta_i);\ (i = 1, 2...n)$ having weights $w_i\ (w_i > 0;\ \sum_{i=1}^{n} w_i = 1)$, the intuitionistic fuzzy Dombi weighted geometric aggregation (IFDWGA) is defined by scholars (Seikh & Mandal, 2021) as

$$IFDWGA(\gamma_1,\gamma_2,\gamma_3,....\gamma_n) = \overset{n}{\underset{i=1}{\otimes}}(\gamma_i)^{w_i}$$

$$= \left(\begin{array}{l} \dfrac{1}{1+\left\{\sum_{i=1}^{n} w_i \left(\frac{1-\mu_i}{\mu_i}\right)^{\beta}\right\}^{\frac{1}{\beta}}}, \\ 1 - \dfrac{1}{1+\left\{\sum_{i=1}^{n} w_i \left(\frac{\vartheta_i}{1-\vartheta_i}\right)^{\beta}\right\}^{\frac{1}{\beta}}} \end{array} \right) \tag{7}$$

Materials and methods

In this section, the research methodology is briefly outlined.

Description of the failure modes

The present study identifies nine FMs, as described below in Table 4.

Table 4 – Failure modes or risk factors for delivering HSQ in I4

S/L	Failure mode	Description
FM-1	Lack of information about digital technologies	It describes the stakeholders' unfamiliarity and lack of knowledge (students, parents, and staff) about digital technologies and their usage.
FM -2	Infrastructural constraints	It indicates inadequate digital infrastructure, including tools, internet connectivity, and resources. It also includes good administrative support services.

S/L	Failure mode	Description
FM-3	Potential skill gap	It indicates a lack of expertise among instructors and students in using advanced digital technologies, a lack of training programs and development initiatives, and a lack of connection among industry, R&D, society, and HEIs. It also entails inadequate knowledge capital and intellectual outputs.
FM-4	Cultural inertia	It describes the cultural barriers and resistance to adopting new technologies and modes of operation, such as flipped classrooms, hybrid modes, self-paced personalized learning, immersive experiential learning, fear of becoming outdated, and a lack of room for innovation. It also showcases the absence of supportive leadership.
FM-5	Difficulty in matching diverse student needs	It entails difficulty offering personalized learning experiences to students with diverse socio-demographic backgrounds and ineffective academic advising, career counseling, and mental health services. This is a critical issue, especially for students from rural and less tech-savvy backgrounds. In effect, student engagement becomes a challenge.
FM-6	Shortage of funds	It indicates the inadequacy of fund support for adopting advanced technologies, building supportive infrastructure, providing experiential learning, connecting with the community, and instilling training and development programs to bridge the skill gaps.
FM-7	Interoperability risk	It is important to compare a new technology system with the existing one before adopting it. The advanced technologies of I4 and new systems like flipped classrooms, experiential learning, and gaming require seamless integration with the existing process.
FM-8	Inability to scale up	This indicates the limited access of all departments in HEIs or all regional units to advanced technologies and processes. Further, implementing a new system on a massive scale within a short period poses a significant operational challenge.
FM-9	Ethical concerns	This includes security and privacy issues, data mismanagement, gender disparity, lack of equity, and regulatory and compliance issues.

Data collection

Twenty-three experts participated in this study's survey. These experts have substantial experience in higher education management and recruitment. Their profiles are summarized in Table 5.

An online questionnaire (using the identified FMs) was prepared and circulated to the experts. Informal discussions were also held with them while finalizing the FMs. The rating scales in linguistic terms and their corresponding IFNs are given in Table 6. Weights were also assigned to the experts based on their experience. Table 7 gives the linguistic scale to rate the experts.

Table 5 – Profile of the experts

Role	Number	Qualification	Number
Faculty member	13	Ph.D./ post-doctorate	11
Academic administrator	7	Master degree	11
Industry Practitioners/Entrepreneurs	3	Graduation	1
Total	23	Total	23
Background	Number	Experience	Number
Management/ Social Science	8	More than 25 years	7
Basic Science/ Technology	7	20 to 25 years	8
Arts/Humanities	3	15 to 20 years	4
Commerce	5	10 to 15 years	4
Total	23	Total	23

Table 6 – Linguistic rating scale and the IFNs
(to rate the FMs on the dimensions S, O, D, and I)

Linguistic scale	Code	μ	ϑ
Very High	5	0.9	0.1
High	4	0.7	0.3
Medium	3	0.5	0.5
Low	2	0.3	0.7
Very Low	1	0.1	0.9

Table 7 – Linguistic rating scale and the IFNs (to rate the experts)

		IFN	
Linguistic scale	Code	μ	ϑ
Very experienced	4	0.85	0.1
Experienced	3	0.6	0.35
Medium	2	0.35	0.6
Less experienced	1	0.1	0.85

Modified FMEA framework with the IFS and Dombi aggregation

The steps of the modified FMEA framework with the IFS and Dombi aggregation are below.

Step 1. Figure out the FMs

The FMs are identified based on a literature review and experts' opinions (Table 4). Suppose fm_j denotes the j^{th} FM.

Step 2. Selection of experts and finding out their weights

Suppose there are $i = 1, 2, ..., k$ experts. Then, the weight of the i^{th} expert is calculated by using Eq. 8 (Tooranloo & sadat Ayatollah, 2016)

$$\omega_k = \frac{\left(\mu_k + \zeta_k\left(\frac{\mu_k}{\mu_k + \vartheta_k}\right)\right)}{\sum_{i=1}^{k}\left(\mu_i + \zeta_i\left(\frac{\mu_i}{\mu_i + \vartheta_i}\right)\right)} \tag{8}$$

Step 3. Rating of each FM by the experts based on each of the dimensions of the modified FMEA model, such as S, O, D and I.

Let

$\varphi_{ij(S)} = \left(\mu_{ij(S)}, \vartheta_{ij(S)}\right), \varphi_{ij(O)} = \left(\mu_{ij(O)}, \vartheta_{ij(O)}\right), \varphi_{ij(D)} = \left(\mu_{ij(D)}, \vartheta_{ij(D)}\right) \, and \; \varphi_{ij(I)} = \left(\mu_{ij(I)}, \vartheta_{ij(I)}\right)$ be the ratings (expressed in terms of IFNs corresponding to the linguistic scale selected for rating) of j^{th} FM, given by the i^{th} expert based on the dimensions of the modified FMEA model, such as S, O, D, and I, respectively.

Step 4. For each of the dimensions of the modified FMEA (M-FMEA) model, aggregate expert responses by using Dombi aggregation (Eq. 7).

The aggregated ratings of the FMs for all dimensions of M-FMEA are given by $\varphi_{j(S)} = \left(\mu_{j(S)}, \vartheta_{j(S)}\right), \varphi_{j(O)} = \left(\mu_{j(O)}, \vartheta_{j(O)}\right), \varphi_{j(D)} = \left(\mu_{j(D)}, \vartheta_{j(D)}\right) \, and \; \varphi_{j(I)} = \left(\mu_{j(I)}, \vartheta_{j(I)}\right)$ respectively. For instance,

$$\varphi_{j(S)} = \left(\mu_{j(S)}, \vartheta_{j(S)}\right) = IFDWGA(\varphi_{1j(S)}, \varphi_{2j(S)}, ..., \varphi_{kj(S)})$$

$$= \left(\begin{array}{c} \dfrac{1}{1+\left\{\sum_{i=1}^{k}\omega_i\left(\dfrac{1-\mu_{ij(S)}}{\mu_{ij(S)}}\right)^{\beta}\right\}^{\frac{1}{\beta}}}, \\ 1-\dfrac{1}{1+\left\{\sum_{i=1}^{k}\omega_i\left(\dfrac{\vartheta_{ij(S)}}{1-\vartheta_{ij(S)}}\right)^{\beta}\right\}^{\frac{1}{\beta}}} \end{array} \right) \quad (9)$$

where $\omega_i > 0; \sum_{i=1}^{k}\omega_i = 1$ is the weight assigned to the i^{th} expert (see Eq. 8) and β is the parameter of Dombi aggregation. In a similar way, all other aggregations are calculated.

For example, $\varphi_{j(O)} = \left(\mu_{j(O)}, \vartheta_{j(O)}\right), \varphi_{j(D)} = \left(\mu_{j(D)}, \vartheta_{j(D)}\right)$ *and* $\varphi_{j(I)} = \left(\mu_{j(I)}, \vartheta_{j(I)}\right)$

Step 5. Obtain the score values of the aggregated ratings.

The score values are obtained using Eq. 4 for all aggregated ratings. For example, the score value of $\varphi_{j(S)} = \left(\mu_{j(S)}, \vartheta_{j(S)}\right)$ is obtained as

$$\wp^*_{j(S)} = \frac{1}{2}(1+\mu_{j(S)} - \vartheta_{j(S)}) \quad (10)$$

In a similar way, $\wp^*_{j(O)}, \wp^*_{j(D)}$ *and* $\wp^*_{j(I)}$ are derived.

Step 6. Use the computed score values for ranking, pairwise comparison, and calculation of FMs' risk scores for each dimension of M-FMEA separately. For this purpose, the procedural steps of the COBRAC method (see Section 4.4) are followed. Let $\phi_{j(S)}, \phi_{j(O)}, \phi_{j(D)}$ *and* $\phi_{j(I)}$ denote the risk scores of j^{th} FM on the dimensions of M-FMEA.

Step 7. Obtain the priority weights of the FNs based on their importance to HEIs.

The experts use the linguistic scales and the corresponding IFNs in Table 5 to rate the FNs. Let, w_j be the priority weight of j^{th} FM. The priority weight is obtained by executing the process described in steps 2 to 5.

Step 8. Find out the weighted risk scores of the FNs for each dimension of M-FMEA separately. This can be obtained by multiplying the risk score with the priority weight. For example, the weighted risk score of j^{th} FM for the dimension S is found as

$$\psi_{j(S)} = w_j \times \phi_{j(S)} \tag{11}$$

In a similar way, the weighted risk scores for all other dimensions of M-FMEA, i.e., $\psi_{j(O)}, \psi_{j(D)}$ *and* $\psi_{j(I)}$ are found.

Step 9. Obtain the final risk appraisal scores (RASs) of the FMs.

The simple additive weighting (SAW) method (MacCrimmon, 1968) is followed to calculate the RAS. Accordingly, the RAS of j^{th} FM is calculated using Eq. 12, as follows:

$$\alpha_j = \psi_{j(S)} + \psi_{j(O)} + \psi_{j(D)} + \psi_{j(I)} \tag{12}$$

The higher the RAS, the more significant the corresponding FM.

Conventional COBRAC method

The Comparisons Between Ranked Criteria (COBRAC) method is developed to derive criteria weights based on localized pairwise comparison and minimization of deviation from the consistency level. COBRAC offers several benefits to analysts, providing: a) a lesser number of local comparisons helping to reduce subjective bias and produce reliable decision making; b) a large scale for local comparisons to decision makers; c) a built-in mechanism to examine consistency in decision making; and d) a reliable and consistent calculation for varying the size of attributes or criteria sets. COBRAC has started garnering attention from researchers in various applications (Biswas et al, 2024; Demir & Moslem, 2024).

The procedural steps of the conventional COBRAC method are described below.

Step 1. Ranking of the criteria

Assuming that $C_j (j \in [1,n])$ is the most influential or important criterion as compared with other criteria from the set, the preferential order is obtained as $C_{j(1)} > C_{j(2)} > ...... > C_{j(t)}$ where $t \in [1,m]$ Indicates the corresponding rank. This selection can be based on experts' opinions on a pre-defined linguistic scale or their performance score values.

Step 2. Pairwise comparison of the criteria

COBRAC works on the philosophy of local pairwise comparisons. After a pairwise comparison of the criteria, each pair of criteria is assigned a value. $\xi_{j-1,j} \in [0,1]$. For instance, $\xi_{1,2}$ is the assigned value to the first and second-ranked criteria, and $\xi_{n-1,n}$ is the assigned value for the pairwise comparison between the next to the last and the last ranked criterion. The result of the local pairwise comparison is expressed as a percentage contribution of the corresponding criteria in the interval [0,1]. For example, if $C_{j-1} > C_j$ with an assigned value $\xi_{j-1,j} = 0.60$, then it implies that C_{j-1} holds 60% of the interval [0,1], while the contribution of C_j is 40%. In the next step, a transitive relationship is formulated to obtain the global significance of the criteria.

Step 3. Obtain the weights of the criteria

The COBRAC method performs a total of $(n-1)$ number of pairwise comparisons for the n criteria. The relationships can be expressed as

$$\begin{aligned} & w_1 : w_2 = \xi_{1,2} : (1-\xi_{1,2}); \\ & w_2 : w_3 = \xi_{2,3} : (1-\xi_{2,3}); \\ & \ldots\ldots\ldots \quad \ldots\ldots\ldots\ldots\ldots\ldots \\ & w_{n-1} : w_n = \xi_{n-1,n} : (1-\xi_{n-1,n}) \end{aligned} \tag{13}$$

Consistency in decision making can be achieved by meeting the transitivity condition.

$$\frac{w_{n-1}}{w_n} - \frac{\xi_{n-1,n}}{(1-\xi_{n-1,n})} = 0 \tag{14}$$

In reality, the objective is set to minimize the deviations from the consistency, i.e., $\left| \frac{\omega_{m-1}}{\omega_m} - \frac{\xi_{m-1,m}}{(1-\xi_{m-1,m})} \right| \leq 0; j = 1,2...m$

To achieve the aforementioned objective, the following model is formulated.

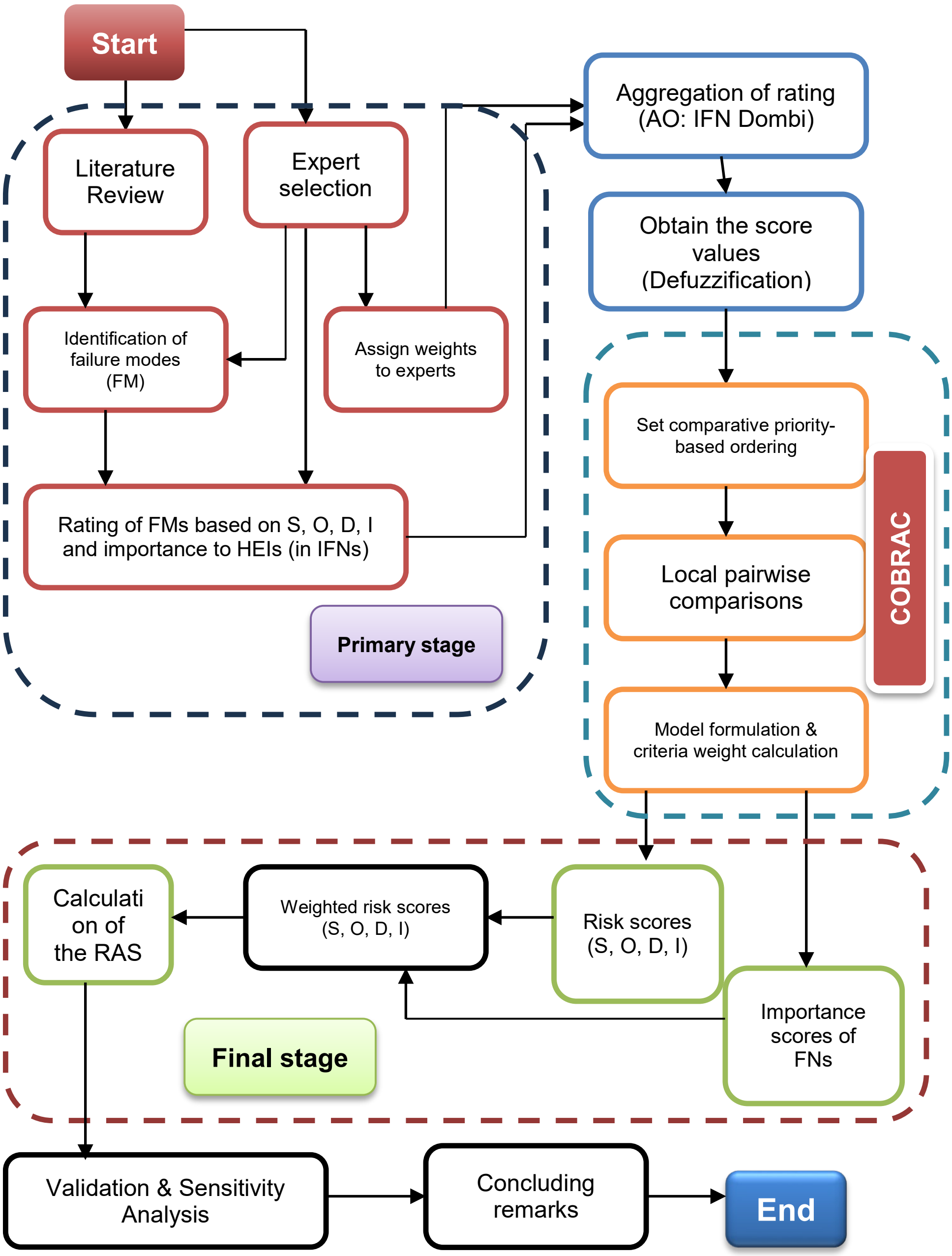

Figure 1 – Flowchart of the research methodology

$$\min \max_j \left\{ \left| \frac{w_{n-1}}{w_n} - \frac{\xi_{n-1,n}}{(1-\xi_{n-1,n})} \right| \right\}$$

$$s.t.$$

$$\sum_{j=1}^{n} w_j = 1; w_j \geq 0 \ \forall j \tag{15}$$

The above model (Expression 15) is converted into a final model, from which the criteria weights are obtained.

$$Min\ \chi$$

$$s.t.$$

$$\left| \frac{w_{n-1}}{w_n} - \frac{\xi_{n-1,n}}{(1-\xi_{n-1,n})} \right| \leq \chi, \forall j$$

$$\sum_{j=1}^{n} w_j = 1; w_j \geq 0 \forall j \tag{16}$$

The steps of the research methodology are depicted in Figure 1.

Findings

This section demonstrates the step-by-step findings. Nine FMs (mentioned in Table 3) are involved in this work, and 23 experts participated in the study. Hence, there are j = 9 and k = 23. The experts are rated in linguistic terms (Table 7) according to their experience. Then, the experts' weights are found using Eq. 8. Table 5 outlines the experts' profiles, and Table 8 summarizes the calculation of their weights.

Table 8 – Calculation of the weights of the experts

Expert	Rating	μ	ϑ	ω	Expert	Rating	μ	ϑ	ω
R1	4	0.85	0.10	0.0677	R13	4	0.85	0.10	0.0677
R2	1	0.10	0.85	0.0080	R14	3	0.60	0.35	0.0478
R3	3	0.60	0.35	0.0478	R15	4	0.85	0.10	0.0677
R4	4	0.85	0.10	0.0677	R16	3	0.60	0.35	0.0478
R5	2	0.35	0.60	0.0279	R17	2	0.35	0.60	0.0279
R6	3	0.60	0.35	0.0478	R18	3	0.60	0.35	0.0478

Expert	Rating	μ	ϑ	ω	Expert	Rating	μ	ϑ	ω
R7	3	0.60	0.35	0.0478	R19	1	0.10	0.85	0.0080
R8	2	0.35	0.60	0.0279	R20	4	0.85	0.10	0.0677
R9	4	0.85	0.10	0.0677	R21	1	0.10	0.85	0.0080
R10	3	0.60	0.35	0.0478	R22	3	0.60	0.35	0.0478
R11	2	0.35	0.60	0.0279	R23	4	0.85	0.10	0.0677
R12	1	0.10	0.85	0.0080					

As a demonstration, the weight of the fifth expert is calculated as

$$\omega_5 = \frac{\left(\mu_5 + \zeta_5\left(\frac{\mu_5}{\mu_5 + \vartheta_5}\right)\right)}{\sum_{i=1}^{23}\left(\mu_i + \zeta_i\left(\frac{\mu_i}{\mu_i + \vartheta_i}\right)\right)} = \frac{\left(\mu_5 + \zeta_5\left(\frac{\mu_5}{\mu_5 + \vartheta_5}\right)\right)}{\left(\mu_1 + \zeta_1\left(\frac{\mu_1}{\mu_1 + \vartheta_1}\right)\right) + \left(\mu_2 + \zeta_2\left(\frac{\mu_2}{\mu_2 + \vartheta_2}\right)\right) + \ldots + \left(\mu_{23} + \zeta_{23}\left(\frac{\mu_{23}}{\mu_{23} + \vartheta_{23}}\right)\right)}$$

$$= \frac{\left(0.35 + 0.05\left(\frac{0.35}{0.35 + 0.6}\right)\right)}{\left(0.85 + 0.05\left(\frac{0.85}{0.85 + 0.1}\right)\right) + \left(0.1 + 0.05\left(\frac{0.1}{0.1 + 0.85}\right)\right) + \ldots + \left(0.85 + 0.05\left(\frac{0.85}{0.85 + 0.1}\right)\right)} = 0.0279$$

The experts rate various FMs based on their severity (S), occurrence (O), detectability (D), and intractability (I) using the linguistics scales provided in Table 6. For instance, experts' responses to rate various FMs based on severity are shown in Table 9. Table 6 is then used to find the corresponding IFNs for the linguistic ratings. The ratings of FMs for other dimensions (i.e., occurrence, detectability, and intractability) are shown in Tables A1 to A3 (Appendix A). Tables A5 to A8 exhibit the corresponding IFNs. Then proceed to step 4. The IFDWGA operator (Eq. 7) aggregates individual ratings of various FMs. For example, the aggregation of individual ratings for the fifth FN (indicating its severity) can be demonstrated by applying Eq. 9.

$$\varphi_{5(S)} = \left(\mu_{5(S)}, \vartheta_{5(S)}\right) = IFDWGA(\varphi_{(1)5(S)}, \varphi_{(2)5(S)}, ..., \varphi_{(23)5(S)})$$

$$= \left(\begin{array}{c} \dfrac{1}{1+\left\{\sum_{i=1}^{23}\omega_i\left(\dfrac{1-\mu_{i5(S)}}{\mu_{i5(S)}}\right)^{\beta}\right\}^{\frac{1}{\beta}}}, \\ 1-\dfrac{1}{1+\left\{\sum_{i=1}^{k}\omega_i\left(\dfrac{\vartheta_{i5(S)}}{1-\vartheta_{i5(S)}}\right)^{\beta}\right\}^{\frac{1}{\beta}}} \end{array} \right)$$

By setting $\beta = 1$ (initial case), one gets $\varphi_{5(S)} = \left(0.7046, \quad 0.2954\right)$

The aggregated values for all other FNs are similarly obtained according to their severity. It may be noted that all these aggregated results are IFNs. Next, Eq. 10 is applied to get the score values (i.e., defuzzified values) of these aggregated IFNs. For instance, the score value of $\varphi_{5(S)}$ is obtained as $\wp^{*}_{5(S)} = \frac{1}{2}(1+\mu_{5(S)} - \vartheta_{5(S)}) = \frac{1+0.7046-0.2954}{2} = 0.7046$

Table 9 – Rating of the FNs by the experts (Dimension: severity)

Respondent	FM1	FM2	FM3	FM4	FM5	FM6	FM7	FM8	FM9
R1	4	4	4	4	4	4	4	4	4
R2	1	4	5	3	5	4	4	5	5
R3	3	3	3	3	5	3	4	3	4
R4	5	4	4	2	4	4	3	3	2
R5	4	5	4	4	4	3	4	4	4
R6	4	5	4	2	3	5	5	5	2
R7	3	4	4	4	3	4	3	2	4
R8	2	3	4	3	2	5	4	3	4
R9	3	4	4	4	4	3	3	4	4
R10	4	3	3	4	3	4	3	4	4
R11	4	5	5	4	5	4	5	5	4
R12	1	4	4	2	3	4	3	4	3
R13	2	2	3	3	4	5	5	5	5
R14	4	4	5	2	4	3	4	4	5

Respondent	FM1	FM2	FM3	FM4	FM5	FM6	FM7	FM8	FM9
R15	2	3	3	3	3	3	3	3	3
R16	4	5	3	2	3	5	5	4	5
R17	5	5	5	5	5	5	5	5	5
R18	1	5	2	1	2	5	2	4	1
R19	3	4	4	3	4	3	3	4	4
R20	5	4	5	3	3	5	4	4	4
R21	2	3	3	3	3	5	4	4	3
R22	2	4	3	3	4	5	3	2	5
R23	2	5	4	4	3	4	4	2	4

Table 10 – Dombi aggregation (β = 1) and the calculated score values (Dimension: severity)

Failure mode	μ	ϑ	Score
FM1	0.7148	0.2852	0.7148
FM2	0.7961	0.2039	0.7961
FM3	0.7495	0.2505	0.7495
FM4	0.6045	0.3955	0.6045
FM5	0.7046	0.2954	0.7046
FM6	0.8208	0.1792	0.8208
FM7	0.7630	0.2370	0.7630
FM8	0.7459	0.2541	0.7459
FM9	0.7798	0.2202	0.7798

The aforementioned defuzzified score values are used as inputs to the procedural steps of the COBRAC method for determining the risk scores of the FNs based on their severity. The use of the COBRAC method is justified for two reasons: the consistency in decision making is thus examined and, in some instances, two FNs may obtain the same defuzzified score values making them inseparable. Following the steps mentioned in Section 4.4, one derives the risk scores of the FNs based on their severity (Table 11). The final model to derive the risk scores is given below.

$$
\begin{aligned}
& Min\ \chi \\
& s.t. \\
& \left|\frac{w_6}{w_2}-1.0310\right| \leq \chi, \left|\frac{w_2}{w_9}-1.0208\right| \leq \chi, \left|\frac{w_9}{w_7}-1.0221\right| \leq \chi, \left|\frac{w_7}{w_3}-1.0181\right| \leq \chi, \\
& \left|\frac{w_3}{w_8}-1.0047\right| \leq \chi, \left|\frac{w_8}{w_1}-1.0436\right| \leq \chi, \left|\frac{w_1}{w_5}-1.0144\right| \leq \chi, \left|\frac{w_5}{w_4}-1.1657\right| \leq \chi \\
& \sum_{j=1}^{9} w_j = 1; w_j \geq 0 \forall j
\end{aligned} \tag{17}
$$

Table 11 – Calculation of the risk scores using the COBRAC method (Dimension: severity)

Failure mode	Score	ξ	1-ξ	ξ/(1-ξ)	w
FM6	0.8208	0.5076	0.4924	1.0310	0.1229
FM2	0.7961	0.5052	0.4948	1.0208	0.1192
FM9	0.7798	0.5055	0.4945	1.0221	0.1168
FM7	0.7630	0.5045	0.4955	1.0181	0.1142
FM3	0.7495	0.5012	0.4988	1.0047	0.1122
FM8	0.7459	0.5107	0.4893	1.0436	0.1117
FM1	0.7148	0.5036	0.4964	1.0144	0.1070
FM5	0.7046	0.5383	0.4617	1.1657	0.1055
FM4	0.6045				0.0905
	χ	0.00000		Sum	1.0000

Similarly, one calculates the risk scores of the FNs based on occurrence, detectability, and intractability (see Tables 12 to 14). Lingo (version 20) was used for solving Eq. 17. The sample code is given in Appendix A.

Table 12 – Calculation of the risk scores using the COBRAC method (Dimension: occurrence)

Failure mode	Score	ξ	1-ξ	ξ/(1-ξ)	w
FM2	0.8101	0.5136	0.4864	1.0559	0.1252
FM6	0.7672	0.5035	0.4965	1.0139	0.1186
FM9	0.7566	0.5071	0.4929	1.0289	0.1170
FM1	0.7354	0.5059	0.4941	1.0238	0.1137

Failure mode	Score	ξ	1-ξ	ξ/(1-ξ)	w
FM8	0.7183	0.5010	0.4990	1.0042	0.1111
FM7	0.7154	0.5102	0.4898	1.0416	0.1106
FM3	0.6868	0.5117	0.4883	1.0481	0.1062
FM4	0.6553	0.5125	0.4875	1.0511	0.1013
FM5	0.6234				0.0964
	χ	0.00000		Sum	1.0000

Table 13 – Calculation of the risk scores using the COBRAC method (Dimension: detectability)

Failure mode	Score	ξ	1-ξ	ξ/(1-ξ)	w
FM9	0.7394	0.5370	0.4630	1.1600	0.1389
FM7	0.6374	0.5037	0.4963	1.0150	0.1198
FM4	0.6280	0.5130	0.4870	1.0533	0.1180
FM5	0.5962	0.5094	0.4906	1.0384	0.1120
FM6	0.5742	0.5119	0.4881	1.0486	0.1079
FM1	0.5476	0.5015	0.4985	1.0058	0.1029
FM3	0.5444	0.5055	0.4945	1.0224	0.1023
FM8	0.5325	0.5049	0.4951	1.0198	0.1001
FM2	0.5221				0.0981
	χ	0.00000		Sum	1.0000

Table 14 – Calculation of the risk scores using the COBRAC method (Dimension: Intractability)

Failure mode	Score	ξ	1-ξ	ξ/(1-ξ)	w
FM6	0.7748	0.5089	0.4911	1.0363	0.1275
FM9	0.7477	0.5019	0.4981	1.0075	0.1231
FM2	0.7421	0.5062	0.4938	1.0252	0.1222
FM4	0.7238	0.5129	0.4871	1.0530	0.1192
FM7	0.6874	0.5217	0.4783	1.0909	0.1132
FM5	0.6301	0.5017	0.4983	1.0069	0.1037
FM8	0.6258	0.5110	0.4890	1.0451	0.1030
FM3	0.5988	0.5237	0.4763	1.0997	0.0986
FM1	0.5445				0.0896
	χ	0.00000		Sum	1.0000

Next, the priority weights of the FNs are calculated based on their importance to HEIs. The rating of the FNs in the linguistic scales and the corresponding IFNs are given in Tables A4 and A9 (Appendix A). The same process is followed as in finding out the risk scores. Table 15 shows the calculated priority weight values of the FNs. It may be noted that in all these calculations (of risk scores and priority weights), the deviations from consistency (χ) are almost negligible (≈ 0.0000). It reflects the robustness of the calculation.

Table 15 – Calculation of the priority weights of the FNs using the COBRAC method

Failure mode	Score	ξ	1-ξ	ξ/(1-ξ)	w
FM2	0.8426	0.5121	0.4879	1.0496	0.1282
FM6	0.8028	0.5012	0.4988	1.0048	0.1222
FM9	0.7990	0.5151	0.4849	1.0624	0.1216
FM1	0.7520	0.5074	0.4926	1.0302	0.1144
FM3	0.7299	0.5135	0.4865	1.0553	0.1111
FM7	0.6917	0.5035	0.4965	1.0142	0.1053
FM5	0.6820	0.5005	0.4995	1.0022	0.1038
FM8	0.6805	0.5355	0.4645	1.1530	0.1036
FM4	0.5902				0.0898
	χ	0.00000		Sum	1.0000

Eq. 11 is subsequently used to obtain the weighted risk scores of the FNs for each dimension of M-FMEA, i.e., severity, occurrence, detectability, and intractability. Then, Eq. 12 is used to compute the RASs of all FNs and to rank them (Table 16).

Table 16 – Calculation of the RASs of the FNs (M-FMEA)

		Weighted risk scores					
Failure Modes	Priority weights of failure modes	S	O	D	I	RAS	Rank
FM-1	0.1144	0.1070	0.1137	0.1029	0.0896	0.0473	5
FM-2	0.1282	0.1192	0.1252	0.0981	0.1222	0.0596	2
FM-3	0.1111	0.1122	0.1062	0.1023	0.0986	0.0466	6
FM-4	0.0898	0.0905	0.1013	0.1180	0.1192	0.0385	9
FM-5	0.1038	0.1055	0.0964	0.1120	0.1037	0.0433	8

Failure Modes	Priority weights of failure modes	S	O	D	I	RAS	Rank
FM-6	0.1222	0.1229	0.1186	0.1079	0.1275	0.0583	3
FM-7	0.1053	0.1142	0.1106	0.1198	0.1132	0.0482	4
FM-8	0.1036	0.1117	0.1111	0.1001	0.1030	0.0441	7
FM-9	0.1216	0.1168	0.1170	0.1389	0.1231	0.0603	1

Validation

A two-stage validation is performed in this paper.

First, the FMs are ranked based on their weighted risk scores related to the dimensions of M-FMEA. The FM with the highest weighted risk score is ranked first. Then, the rank index method (RIM) (Yang et al, 2019) is used to obtain the rank frequency numbers and the final rank index values. The alternative with the lowest rank index value is ranked first. Next, both ranking orders (the one obtained with M-FMEA and the other obtained with RIM) are compared, followed by the Spearman's rank correlation test. The value of the Spearman's rank correlation coefficient is obtained using Eq. 18.

$$\rho = 1 - \frac{6\sum d_i^2}{n(n^2-1)} \quad (18)$$

d_i is the difference in the ranks between the constituent elements of the i^{th} pair and n is the number of elements.

The value of $\rho = 0.9167$ is obtained. This is significant at the 0.05 level (two-tailed), which confirms a significantly positive association or consistency between M-FMEA and RIM.

The existing literature shows the comparison of several MCDM models to ascertain the reliability of a specific method (Biswas & Pamucar, 2021; Pamucar et al, 2023). The FMs are ranked based on the RASs for each such case. Then, the study examines the correlation of the rankings (obtained using alternative methods) with the original results obtained using the COBRAC method. The Spearman's rank correlation test is performed to examine the correlation (Table 17).

Table 17 – Comparison of the MCDM models for the ranking of the FNs (M-FMEA)

Method		COBRAC	LBWA	PIPRECIA-S	FUCOM
LBWA	Spearman's rho	0.933 ***	—		
	p-value	< .001	—		
PIPRECIA-S	Spearman's rho	0.904 ***	0.979 ***	—	
	p-value	< .001	< .001	—	
FUCOM	Spearman's rho	0.983 ***	0.917 **	0.887 **	—
	p-value	< .001	0.001	0.001	—

* p < .05, ** p < .01, *** p < .001

The MCDM models maintain a very high and significant correlation with the COBRAC method, suggesting its reliability.

Sensitivity analysis

MCDM models are susceptible to various external conditions that influence the outcome of data analysis. The selection of methodological steps, model formulation, normalization schemes, the interplay between alternatives and criteria, the size of the alternatives and criteria sets, and aggregation approaches often make MCDM results sensitive to external variations. Therefore, the stability of the outcome is a crucial aspect of its reliability (Puška et al, 2023). Sensitivity analysis is performed to examine the stability of the outcome. The study varies the parameter values in Dombi aggregation (Görçün et al, 2023). Eight experimental cases are generated and the FNs are ranked under each such case (Table 18). The result of the sensitivity analysis is plotted in Figure 2. It is visible that the top five and bottom-most positions remain unaltered despite changes in the value. It indicates the stable ordering of the superior and inferior options. It can be noticed that for high values of β (focusing more on the membership aspect), the sub-optimum alternative FM-5 shows an improvement in its risk scores (a jump of two positions), while FM-3 and FM-8 exhibit one-step inferiority. Hence, it may be contended that this paper's model shows considerable stability.

Table 18 – Ranking of the FNs (M-FMEA) under various experimental cases

Failure Mode	Initial	Case 1	Case 2	Case 3	Case 4	Case 5	Case 6	Case 7	Case 8
	β = 1	β = 2	β = 3	β = 5	β = 7	β = 9	β = 20	β = 30	β = 50
FM1	5	5	5	5	5	5	5	5	5
FM2	2	2	2	2	2	2	2	2	2
FM3	6	6	6	6	6	6	7	7	7
FM4	9	9	9	9	9	9	9	9	9
FM5	8	8	8	8	8	8	6	6	6
FM6	3	3	3	3	3	3	3	3	3
FM7	4	4	4	4	4	4	4	4	4
FM8	7	7	7	7	7	7	8	8	8
FM9	1	1	1	1	1	1	1	1	1

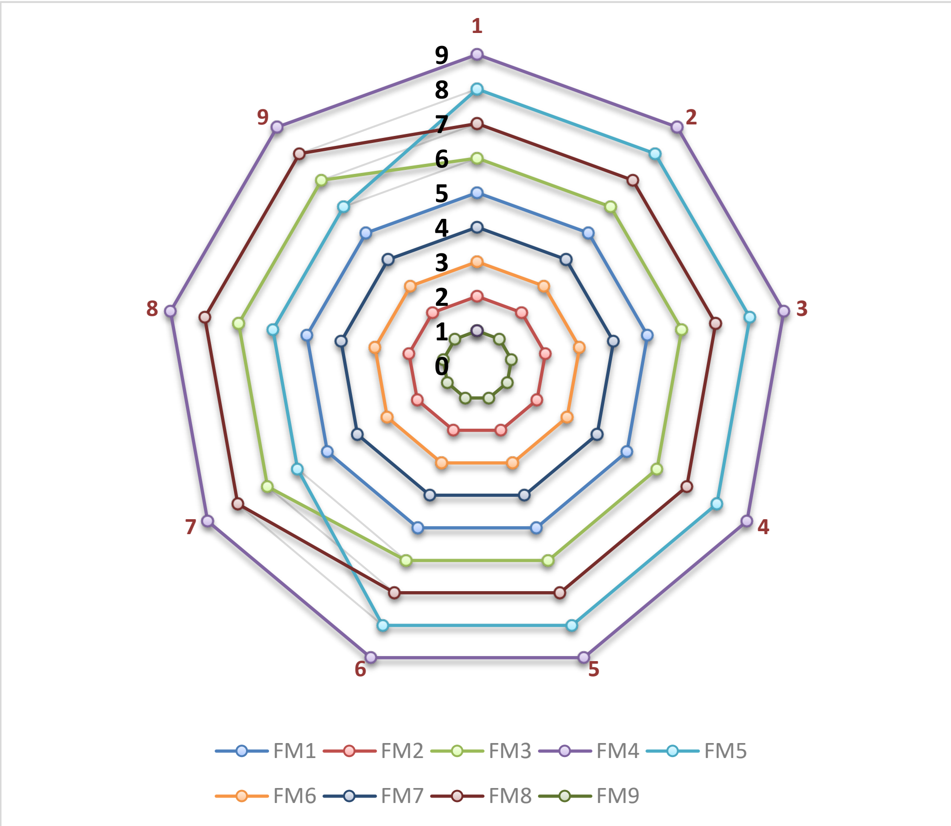

Figure 2 – Result of the sensitivity analysis

Discussion

The paper introduces a new methodology for assessing the risk factors associated with HSQ in I4. It proposes a new M-FMEA model that utilizes IFS and Dombi aggregation to fill the gaps in the literature on risk assessment frameworks and measurement of HSQ. The newly added feature (intractability) evinces the manageability of risks while providing practical insights for HEIs. From the result analysis, it is noticed that ethical concerns (FM-9), infrastructural constraints (FM-2), and shortage of funds (FM-6) are positioned as the top three FMs. More advanced technologies are invading all spheres of higher education, and ethical conduct breaches have risen. For instance, the recent development of generative AI has a double-edged effect on HSQ for good and evil intentions. Cybersecurity and privacy are of great concern today and are often affected implicitly. Moreover, scholars have been emphasizing the dark side of technology in terms of its effect on mental health and social misconduct. The breach of ethical conduct is, in fact, a silent enemy that can make or break HEIs.

Although there is a proliferation of data and rapid technological developments, many HEIs cannot leverage them because of inadequate infrastructure and resources. The availability of adequate infrastructure is a key cornerstone of the successful use of advanced technologies to deliver superior HSQ. In I4, internet connectivity and digital tools are essential to providing fast, timely, and personalized services. The traditional HES needs to undergo a massive transformation, which requires a lot of initial capital expenditure. Moreover, HEIs need to be prepared for offsetting technological obsolescence. In order to make use of digital technologies, HEIs need to create awareness and educate their stakeholders at all corners. A conducive ecosystem must connect all stakeholders, including alumni and corporates. For this, visionary and vigilant governance is of paramount importance. HEIs must prioritize the implementation of rigorous data governance frameworks and cultivate an egalitarian digital ecosystem to prevent these threats. However, the elevation of the level of HSQ requires a seamless transition, during which the compatibility of the new and existing systems stands out as a crucial success factor.

The proposed method shows high reliability, resulting in a) almost no deviation from consistency, b) a highly significant correlation with other MCDM models, and c) a high amount of internal stability. The modified FMEA approach has several advantages. First of all, this model considers the manageability aspect, which helps analysts understand the risks from the perspective of mitigation. Also, the proposed framework uses IFS-based analysis which enables to capture the subjectivity in a simple manner. Further, the use of Dombi aggregation allows decision makers to flexibly select the parameter values to examine the model sensitivity. In addition, the present model assigns weights to experts (based on their expertise/experience), which enables to consider their opinions comprehensively. Then, the developed model uses the COBRAC method to calculate the risk scores of FNs on each of the dimensions (S, O, D and I). In effect, an inherent consistency checking is built into the process for each such calculation. Hence, the calculation is examined for its robustness. The same is examined when one calculates the importance of FNs from the perspective of HEIs. Finally, in this model, the final RAS considers the dimensions like S, O, D, and I, and the priorities of FNs to HEIs. Therefore, the modified FMEA model provides a comprehensive prioritization of FNs.

The focal point of the developed FMEA framework is the use of the COBRAC method that requires only the $(n-1)$ number of local pairwise comparisons, contrast to its counterparts like BWM ($2n-3$) and AHP ($n(n-1)/2$). In this study, the number of risk factors is $n=9$. The COBRAC method (8) clearly has an advantage over BWM (15) and AHP (36). The contemporary methods like FUCOM, LBWA and SWARA also require the $(n-1)$ number of comparisons. However, FUCOM works with a globalized comparison. The LBWA method sometimes suffers from the issue of the criteria's level-wise inseparability, resulting in a high elasticity coefficient value. The SWARA method often suffers from judgmental errors.

However, the current model showcases foreseeable limitations, one of them being a slight limitation in selecting the membership and non-membership grades from a wider perspective because of linear inequality. Also, it does not consider the degree of indeterminacy. These limitations could be avoided by using other variants of fuzzy sets like p, q – Quasirung Orthopair fuzzy sets, picture fuzzy sets, and spherical fuzzy sets. Another drawback is that this framework considers a single aggregation operator and suffers from generalizability. It may be an interesting study to use multiple aggregation methods such as Dombi-Bonferroni (DOBI) that also considers the risk attitude of decision makers. Finally, the present model does not separately calculate the weights of the risk dimensions since we use priority to business as a multiplier for each of them. Nevertheless, in some cases, multiplier values and risk scores on the dimensions of the modified FMEA may be equal, resulting in possible inseparability of FNs.

The results of this study possess considerable social consequences, especially in improving equity and accessibility in higher education. By emphasizing infrastructural enhancements and tackling ethical issues like data privacy and digital ethics, HEIs may cultivate inclusive educational settings. The focus on customizing solutions for varied student requirements, particularly for individuals from minority or rural backgrounds, reduces systemic inequalities. Furthermore, the framework facilitates the identification of practical measures to establish a resilient and adaptive higher education ecosystem, crucial for cultivating socially responsible graduates prepared to succeed in a digitally driven environment.

From a managerial viewpoint, the present study demonstrates a systematic framework for resource allocation and risk management in higher education institutions. It integrates intractability to prioritize investments in feasible domains, maximizing resource allocation. The COBRAC-based ranking ensures a consistent risk assessment, facilitating strategic planning and operational efficacy. The framework incorporates modern digital technologies while adhering to ethical and legal requirements, enabling higher education institutions to be competitive in Industry 4.0. Ethical concerns, such as security, privacy, and compliance, are identified as the primary risk factor. Institutions must prioritize data governance rules and create an egalitarian digital ecosystem. Infrastructural limitations, such as inadequate digital resources and connectivity, highlight the need for scalable and sustainable infrastructure.

Conclusion

The present work demonstrates the use of a novel FMEA framework with uncertainty measures for risk appraisal. This paper considers HSQ as a problem statement. The attributes of HSQ in I4 are figured out through literature review and theoretical underpinning. Subsequently, potential risk factors or FMs have been identified. This work has formulated a focus group of 23 experts to confirm and prioritize the identified FMs according to their severity, occurrence, detectability, and a new dimension called intractability. The modified FMEA used IFSs to capture subjective bias involved in group decision making. Dombi aggregation is used to aggregate experts' responses, which provides notable flexibility to decision makers when examining the model sensitivity. The COBRAC method has been used to ascertain the least deviation from consistency, ensuring the robustness of the model. The results indicate that the essential risk factors, including ethical issues, infrastructural limitations, and financial deficiencies, profoundly affect the provision of quality education in the digital era.

Nevertheless, the current study offers several scopes for further research. First, the present work has not used any causal analysis to delve into the interrelationship among various risk factors and their effects on the performance of HEIs. Second, technological capability and intention to use have not been studied distinctly. In future work, the effect of technology adaptation as a mediator can be analysed. Third, the perspectives of various stakeholders have not been precisely considered regarding their expectations of the services rendered to them. Future studies may try to figure out the additional attributes of HSQ and incorporate these aspects into the FMEA framework to update FMs. Fourth, future studies may further augment the dimensions of M-FMEA by adding dimensions like complexity and opportunity cost. Fifth, the proposed M-FMEA framework may be applied to other various complex problems. Sixth, the IFS has a limitation in selecting membership and non-membership grades. Future studies may overcome these issues using q Rung Orthopair or p, q – Quasirung Orthopair fuzzy sets. Rough sets or intuitionistic fuzzy rough sets may also be explored for granular analysis. Seventh, the present work is also constrained by the limited sample size, which may be overcome by conducting analysis on a large scale.

References

Abbas, J. 2020. Service quality in higher education institutions: qualitative evidence from the students' perspectives using Maslow hierarchy of needs. *International Journal of Quality and Service Sciences*, 12(3), pp.371-384. Available at: https://doi.org/10.1108/ijqss-02-2020-0016

Abdullah, F. 2005. HEdPERF versus SERVPERF: The quest for ideal measuring instrument of service quality in higher education sector. *Quality Assurance in Education,* 13(4), pp.305-328. Available at: https://doi.org/10.1108/09684880510626584

Abulibdeh, A., Zaidan, E. & Abulibdeh, R. 2024. Navigating the confluence of artificial intelligence and education for sustainable development in the era of industry 4.0: Challenges, opportunities, and ethical dimensions. *Journal of Cleaner Production*, 437, p.140527. Available at: https://doi.org/10.1016/j.jclepro.2023.140527

Akhmetshin, E.M., Barmuta, K., Vasilev, V.L., Okagbue, H.I. & Ijezie, O.A. 2020. Principal directions of digital transformation of higher education system in sustainable education. *E3S Web of Conferences*, 208, p.09042. Available at: https://doi.org/10.1051/e3sconf/202020809042

Alenezi, M. 2023. Digital learning and digital institution in higher education. *Education Sciences*, 13(1), p.88. Available at: https://doi.org/10.3390/educsci13010088

Alenezi, M. & Akour, M. 2023. Digital transformation blueprint in higher education: A case study of PSU. *Sustainability*, 15(10), p.8204. Available at: https://doi.org/10.3390/su15108204

Ali, Z. & Yang, M.S. 2024. On circular q-rung orthopair fuzzy sets with Dombi aggregation operators and application to symmetry analysis in artificial intelligence. *Symmetry*, 16(3), p.260. Available at: https://doi.org/10.3390/sym16030260

Anastasiadou, S. & Zirinoglou, P. 2020. Failure modes and effects analysis (FMEA) application in Greek tertiary education. In: *ICERI2020 Proceedings*, pp.7767-7772. IATED. Available at: https://doi.org/10.21125/iceri.2020.1695

Atanassov, K.T. 1986. Intuitionistic fuzzy sets. *Fuzzy Sets and Systems*, 20(1), pp.87-96. Available at: https://doi.org/10.1016/S0165-0114(86)80034-3

Benavides, L.M.C., Tamayo Arias, J.A., Arango Serna, M.D., Branch Bedoya, J.W. & Burgos, D. 2020. Digital transformation in higher education institutions: A systematic literature review. *Sensors*, 20(11), p.3291. Available at: https://doi.org/10.3390/s20113291

Biswas, S., Pamucar, D., Raj, A. & Kar, S. 2023. A proposed q-rung orthopair fuzzy-based decision support system for comparing marketing automation modules for higher education admission. In: *Computational Intelligence for Engineering and Management Applications: Select Proceedings of CIEMA 2022*, pp.885-912. Singapore: Springer Nature Singapore. Available at: https://doi.org/10.1007/978-981-19-8493-8_66

Biswas, S., Pamucar, D. & Simic, V. 2024. Technology adaptation in sugarcane supply chain based on a novel p, q quasirung orthopair fuzzy decision-making framework. *Scientific Reports*, 14(1), p.26486. Available at: https://doi.org/10.1038/s41598-024-75528-5

Biswas, S. & Pamučar, D.S. 2021. Combinative distance-based assessment (CODAS) framework using logarithmic normalization for multi-criteria decision making. *Serbian Journal of Management*, 16(2), pp.321-340. Available at: https://doi.org/10.5937/sjm16-27758

Bonfield, C.A., Salter, M., Longmuir, A., Benson, M. & Adachi, C. 2020. Transformation or evolution?: Education 4.0, teaching and learning in the digital age. *Higher Education Pedagogies*, 5(1), pp.223-246. Available at: https://doi.org/10.1080/23752696.2020.1816847

Bowles, J.B. & Peláez, C.E. 1995. Fuzzy logic prioritization of failures in a system failure mode, effects and criticality analysis. *Reliability Engineering & System Safety*, 50(2), pp.203-213. Available at: https://doi.org/10.1016/0951-8320(95)00068-D

Ceylan, B.O., Akyar, D.A. & Celik, M.S. 2023. A novel FMEA approach for risk assessment of air pollution from ships. *Marine Policy*, 150, p.105536. Available at: https://doi.org/10.1016/j.marpol.2023.105536

Chaabouni, S. & Mbarek, M.B. 2023. What will be the impact of the COVID-19 pandemic on the human capital and economic growth? Evidence from Eurozone. *Journal of the Knowledge Economy*, 15(1), pp.2482-2498. Available at: https://doi.org/10.1007/s13132-023-01328-3

Chan, C.K.Y. & Hu, W. 2023. Students' voices on generative AI: Perceptions, benefits, and challenges in higher education. *International Journal of Educational Technology in Higher Education*, 20(1), p.43. Available at: https://doi.org/10.1186/s41239-023-00411-8

Deb, P.P., Bhattacharya, D., Chatterjee, I., Chatterjee, P. & Zavadskas, E.K. 2023. An intuitionistic fuzzy consensus WASPAS method for assessment of open-source software learning management systems. *Informatica*, 34(3), pp.529-556. Available at: https://doi.org/10.15388/23-INFOR523

Deb, P.P., Bhattacharya, D., Chatterjee, I., Saha, A., Mishra, A.R. & Ahammad, S.H. 2022. A decision-making model with intuitionistic fuzzy information for selection of enterprise resource planning systems. *IEEE Transactions on Engineering Management*, 71, pp.4820-4834. Available at: https://doi.org/10.1109/TEM.2022.3215608

Demir, A.T. & Moslem, S. 2024. A novel fuzzy multi-criteria decision-making for enhancing the management of medical waste generated during the coronavirus pandemic. *Engineering Applications of Artificial Intelligence*, 133, p.108465. Available at: https://doi.org/10.1016/j.engappai.2024.108465

Dempere, J., Modugu, K., Hesham, A. & Ramasamy, L.K. 2023. The impact of ChatGPT on higher education. In: *Frontiers in Education*, 8, p.1206936. Frontiers Media SA. Available at: https://doi.org/10.3389/feduc.2023.1206936

Dombi, J. 1982. A general class of fuzzy operators, the DeMorgan class of fuzzy operators and fuzziness measures induced by fuzzy operators. *Fuzzy Sets and Systems*, 8(2), pp.149-163.Available at: https://doi.org/10.1016/0165-0114(82)90005-7

Ervural, B. & Ayaz, H.I. 2023. A fully data-driven FMEA framework for risk assessment on manufacturing processes using a hybrid approach. *Engineering Failure Analysis*, 152, p.107525. Available at: https://doi.org/10.1016/j.engfailanal.2023.107525

Fahim, A., Addae, B.A., Ofosu-Adarkwa, J., Qingmei, T. & Bhatti, U.A. 2021. Industry 4.0 and higher education: An evaluation of barriers affecting master's in business administration enrolments using a grey incidence analysis. *IEEE Access*, 9, pp.76991-77008. Available at: https://doi.org/10.1109/ACCESS.2021.3082144

Feifei, L., Kian, M.W. & Adaikalam, J. 2022. A review on service quality dimensions in higher education sector and research prospects after COVID-19 pandemic. *International Journal of Academic Research in Business and Social Sciences*, 12(1), pp.328-337. Available at: http://dx.doi.org/10.6007/IJARBSS/v12-i1/12052

Fuchs, K. & Fangpong, K. 2021. Using the SERVQUAL framework to examine the service quality in higher education in Thailand. *Education Quarterly*

Reviews, 4(2), pp.363-370. Available at: https://doi.org/10.31014/aior.1993.04.02.286

Görçün, Ö.F., Pamucar, D. & Biswas, S. 2023. The blockchain technology selection in the logistics industry using a novel MCDM framework based on Fermatean fuzzy sets and Dombi aggregation. *Information Sciences*, 635, pp.345-374. Available at: https://doi.org/10.1016/j.ins.2023.03.113

Gündoğdu, F.K. & Kahraman, C. 2019. Spherical fuzzy sets and spherical fuzzy TOPSIS method. *Journal of Intelligent & Fuzzy Systems*, 36(1), pp.337-352. Available at: https://doi.org/10.3233/JIFS-181401

Hong, D.H. & Choi, C.H. 2000. Multicriteria fuzzy decision-making problems based on vague set theory. *Fuzzy Sets and Systems*, 114, pp.103-113. Available at: https://doi.org/10.1016/S0165-0114(98)00271-1

Jamaludin, R., McKay, E. & Ledger, S. 2020. Are we ready for Education 4.0 within ASEAN higher education institutions? Thriving for knowledge, industry and humanity in a dynamic higher education ecosystem? *Journal of Applied Research in Higher Education*, 12(5), pp.1161-1173. Available at: https://doi.org/10.1108/JARHE-06-2019-0144

Keršuliene, V., Zavadskas, E.K. & Turskis, Z. 2010. Selection of rational dispute resolution method by applying new step-wise weight assessment ratio analysis (SWARA). *Journal of Business Economics and Management*, 11(2), pp.243-258. Available at: https://doi.org/10.3846/jbem.2010.12

Khan, S., Zaman, S.I. & Rais, M. 2022. Measuring student satisfaction through overall quality at business schools: A structural equation modeling: Student satisfaction and quality of education. *South Asian Journal of Social Review*, 1(2), pp.34-55. Available at: https://doi.org/10.57044/sajsr.2022.1.2.2210

Khan, M.R., Ullah, K., Khan, Q. & Pamucar, D. 2025. Intuitionistic fuzzy Dombi aggregation information involving lower and upper approximations. *Computational and Applied Mathematics*, 44(1), pp.1-45. Available at: https://doi.org/10.1007/s40314-024-03044-3

Leow, A., Billett, S. & Le, A.H. 2023. Towards a continuing education and training ecosystem: A case study of Singapore. *International Journal of Training Research*, 21(3), pp.226-242. Available at: https://doi.org/10.1080/14480220.2023.2203944

Li, L. 2024. Reskilling and upskilling the future-ready workforce for industry 4.0 and beyond. *Information Systems Frontiers*, 26, pp.1697-1712. Available at: https://doi.org/10.1007/s10796-022-10308-y

Lin, S.W. & Lo, H.W. 2024. An FMEA model for risk assessment of university sustainability: Using a combined ITARA with TOPSIS-AL approach based neutrosophic sets. *Annals of Operations Research*, 342, pp.2119-2145. Available at: https://doi.org/10.1007/s10479-023-05250-4

Liu, Y. & Shi, Y. 2023. Digital transformation of college teacher education from the perspective of behaviorist psychology: Initiatives, effectiveness and pitfalls. *Applied Mathematics and Nonlinear Sciences*, 9(1). Available at: https://doi.org/10.2478/amns.2023.2.01598

Liu, P., Wu, Y., Li, Y. & Wu, X. 2024. An improved FMEA method based on the expert trust network for maritime transportation risk management. *Expert Systems with Applications*, 238, p.121705. Available at: https://doi.org/10.1016/j.eswa.2023.121705

Liu, P., Ali, Z. & Ding, J. 2024. Power Dombi aggregation operators for complex Pythagorean fuzzy sets and their applications in green supply chain management. *International Journal of Fuzzy Systems*, 26(5), pp.1618-1633. Available at: https://doi.org/10.1007/s40815-024-01691-6

Liu, Z., Zhao, Y. & Liu, P. 2023a. An integrated FMEA framework considering expert reliability for classification and its application in aircraft power supply system. *Engineering Applications of Artificial Intelligence*, 123, p.106319. Available at: https://doi.org/10.1016/j.engappai.2023.106319

Liu, P., Shen, M. & Geng, Y. 2023b. Risk assessment based on failure mode and effects analysis (FMEA) and WASPAS methods under probabilistic double hierarchy linguistic term sets. *Computers & Industrial Engineering*, 186, p.109758. Available at: https://doi.org/10.1016/j.cie.2023.109758

Mahyoob, M. 2020. Challenges of e-learning during the COVID-19 pandemic experienced by EFL learners. *Arab World English Journal (AWEJ)*, 11(4), pp.351-362. Available at: https://dx.doi.org/10.24093/awej/vol11no4.23

Majid, M., Habib, S., Javed, A.R., Rizwan, M., Srivastava, G., Gadekallu, T.R. & Lin, J.C.W. 2022. Applications of wireless sensor networks and internet of things frameworks in the industry revolution 4.0: A systematic literature review. *Sensors*, 22(6), p.2087. Available at: https://doi.org/10.3390/s22062087

MacCrimmon, K.R. 1968. Decision making among multiple-attribute alternatives: A survey and consolidated approach. *Rand Corp Santa Monica Ca*. Available at: https://www.rand.org/pubs/research_memoranda/RM4823.html

Moraes, E.B., Kipper, L.M., Hackenhaar Kellermann, A.C., Austria, L., Leivas, P., Moraes, J.A.R. & Witczak, M. 2023. Integration of Industry 4.0 technologies with Education 4.0: Advantages for improvements in learning. *Interactive Technology and Smart Education*, 20(2), pp.271-287. Available at: https://doi.org/10.1108/ITSE-11-2021-0201

Nasrallah, I., Sabbah, I., Haddad, C., Ismaiil, L., Kotaich, J., Salameh, P. ... & Bawab, W. 2023. Evaluating the academic scientific laboratories' safety by applying failure mode and effect analysis (FMEA) at the public university in Lebanon. *Heliyon*, 9(12), p.e21145. Available at: https://doi.org/10.1016/j.heliyon.2023.e21145

Nguyen, H.V., Vu, T.D., Saleem, M. & Yaseen, A. 2024. The influence of service quality on student satisfaction and student loyalty in Vietnam: The moderating role of the university image. *Journal of Trade Science*, 12(1), pp.37-59. Available at: https://doi.org/10.1108/jts-12-2023-0032

Oliso, Z.Z., Alemu, D.D. & Jansen, J.D. 2024. The impact of educational service quality on student academic performance in Ethiopian public universities: A mediating role of students' satisfaction. *Journal of International Education in Business*, 17(2), pp.340-370. Available at: https://doi.org/10.1108/jieb-07-2023-0042

Pamucar, D., Torkayesh, A. E., & Biswas, S. 2023. Supplier selection in healthcare supply chain management during the COVID-19 pandemic: a novel fuzzy rough decision-making approach. *Annals of Operations Research*, 328(1), 977-1019. Available at: https://doi.org/10.1007/s10479-022-04529-2

Pamucar, D., Stević, Ž., & Sremac, S. 2019. A new model for determining weight coefficients of criteria in MCDM models: Full Consistency Method (FUCOM). *Symmetry*, 11(2), 271. Available at: https://doi.org/10.3390/sym11020271

Park, C., Kontovas, C., Yang, Z., & Chang, C. H. 2023. A BN driven FMEA approach to assess maritime cybersecurity risks. *Ocean & Coastal Management*, 235, 106480. https://doi.org/10.1016/j.ocecoaman.2023.106480

Peddi, S., Lanka, K., & Gopal, P. R. C. 2023. Modified FMEA using machine learning for food supply chain. *Materials Today: Proceedings*. Available at: https://doi.org/10.1016/j.matpr.2023.04.353

Puška, A., Štilić, A., Nedeljković, M., Božanić, D., & Biswas, S. 2023. Integrating fuzzy rough sets with LMAW and MABAC for green supplier selection in agribusiness. *Axioms*, 12(8), 746. Available at: https://doi.org/10.3390/axioms12080746

Rasul, T., Nair, S., Kalendra, D., Robin, M., de Oliveira Santini, F., Ladeira, W. J., Sun, M., Day, I., Rather, R. A. & Heathcote, L. 2023. The role of ChatGPT in higher education: Benefits, challenges, and future research directions. *Journal of Applied Learning and Teaching*, 6(1), 41-56. Available at: https://doi.org/10.37074/jalt.2023.6.1.29

Resende, B. A. D., Dedini, F. G., Eckert, J. J., Sigahi, T. F., Pinto, J. D. S., & Anholon, R. 2024. Proposal of a facilitating methodology for fuzzy FMEA implementation with application in process risk analysis in the aeronautical sector. *International Journal of Quality & Reliability Management,* 41(4), 1063-1088. Available at: https://doi.org/10.1108/IJQRM-07-2023-0237

Rezaei, J. 2015. Best-worst multi-criteria decision-making method. *Omega*, *53*, 49-57. Available at: https://doi.org/10.1016/j.omega.2014.11.009

Salah, B., Alnahhal, M., & Ali, M. 2023. Risk prioritization using a modified FMEA analysis in industry 4.0. *Journal of Engineering Research*, 11(4), 460-468. Available at: https://doi.org/10.1016/j.jer.2023.07.001

Seikh, M. R., & Mandal, U. 2021. Intuitionistic fuzzy Dombi aggregation operators and their application to multiple attribute decision-making. *Granular Computing*, 6, 473-488. https://doi.org/10.1007/s41066-019-00209-y

Seikh, M. R., & Chatterjee, P. 2024. Evaluation and selection of E-learning websites using intuitionistic fuzzy confidence level based Dombi aggregation operators with unknown weight information. *Applied Soft Computing*, *163*, 111850. Available at: https://doi.org/10.1016/j.asoc.2023.111850

Seikh, M. R., & Mandal, U. 2022. Multiple attribute group decision making based on quasirung orthopair fuzzy sets: Application to electric vehicle charging station site selection problem. *Engineering Applications of Artificial Intelligence*, 115, 105299. Available at: https://doi.org/10.1016/j.engappai.2022.105299

Shenkoya, T., & Kim, E. 2023. Sustainability in Higher Education: Digital Transformation of the Fourth Industrial Revolution and Its Impact on Open Knowledge. *Sustainability*, 15(3), 2473. Available at: https://doi.org/10.3390/su15032473

Subandi, S., & Hamid, M. S. 2021. Student satisfaction, loyalty, and motivation as observed from the service quality. *Journal of Management and Islamic Finance*, 1(1), 136-153. Available at: https://doi.org/10.22515/jmif.v1i1.3552

Sumrit, D., & Keeratibhubordee, J. 2025. Risk Assessment Framework for Reverse Logistics in Waste Plastic Recycle Industry: A Hybrid Approach Incorporating FMEA Decision Model with AHP-LOPCOW-ARAS Under Trapezoidal Fuzzy Set. *Decision Making: Applications in Management and Engineering,* 8(1), 42-81. Available at: https://doi.org/10.31181/dmame812025984

Sun, J., Liu, Y., Xu, J., Wang, N., & Zhu, F. 2023. A probabilistic uncertain linguistic FMEA model based on the extended ORESTE and regret theory. *Computers & Industrial Engineering*, 180, 109251. Available at: https://doi.org/10.1016/j.cie.2023.109251

Teeroovengadum, V., Nunkoo, R., Gronroos, C., Kamalanabhan, T. J., & Seebaluck, A. K. 2019. Higher education service quality, student satisfaction and loyalty: Validating the HESQUAL scale and testing an improved structural model. *Quality assurance in education*, 27(4), 427-445. Available at: https://doi.org/10.1108/QAE-01-2019-0003

Tooranloo, H. S., & sadat Ayatollah, A. 2016. A model for failure mode and effects analysis based on intuitionistic fuzzy approach. *Applied soft computing*, 49, 238-247. Available at: http://doi.org/10.1016/j.asoc.2016.07.047

Torra, V. 2010. Hesitant fuzzy sets. *International Journal of Intelligent Systems*, 25(6), 529–539. Available at: https://doi.org/10.1002/int.20418

Wang, K., Li, B., Tian, T., Zakuan, N., & Rani, P. 2023. Evaluate the drivers for digital transformation in higher education institutions in the era of industry 4.0 based on decision-making method. *Journal of Innovation & Knowledge*, 8(3), 100364. Available at: https://doi.org/10.1016/j.jik.2023.100364

Xu, Z. & Yager, R.R. 2006. Some geometric aggregation operators based on intuitionistic fuzzy sets. *International Journal of General Systems*, 35(4), pp.417-433. Available at: https://doi.org/10.1080/03081070600574353

Xu, Z.S. 2007. Models for multiple attribute decision making with intuitionistic fuzzy information. *International Journal of Uncertainty, Fuzziness and Knowledge-Based Systems*, 15(3), pp.285-297. https://doi.org/10.1142/S0218488507004686

Xue, Y., Zhang, J., Zhang, Y. & Yu, X. 2024. Barrier assessment of EV business model innovation in China: An MCDM-based FMEA. *Transportation Research Part D: Transport and Environment*, 136, p.104404. Available at: https://doi.org/10.1016/j.trd.2024.104404

Yang, W.C., Chon, S.H., Choe, C.M. & Un-Ha, K. 2019. Materials selection method combined with different MADM methods. *Journal of Artificial Intelligence*, 1(2), pp.89-99. Available at: https://doi.org/10.32604/jai.2019.07885

Yu, Y., Yang, J. & Wu, S. 2023. A novel FMEA approach for submarine pipeline risk analysis based on IVIFRN and ExpTODIM-PROMETHEE-II. *Applied Soft Computing*, 136, p.110065. Available at: https://doi.org/10.1016/j.asoc.2023.110065

Zadeh, L.A. 1965. Fuzzy sets. *Information and Control*, 8(3), pp.338-353. Available at: https://doi.org/10.1016/S0019-9958(65)90241-X

Žalėnienė, I. & Pereira, P. 2021. Higher education for sustainability: A global perspective. *Geography and Sustainability*, 2(2), pp.99-106. Available at: https://doi.org/10.1016/j.geosus.2021.05.001

Zadeh, L.A. 1975a. The concept of a linguistic variable and its application to approximate reasoning. *Information Sciences*, 8(3), pp.199–249. Available at: https://doi.org/10.1016/0020-0255(75)90036-5

Zadeh, L.A. 1975b. The concept of a linguistic variable and its application to approximate reasoning—III. *Information Sciences*, 9(1), pp.43–80. Available at: https://doi.org/10.1016/0020-0255(75)90017-1

Zhang, R. & Ye, J. 2024. Multiple attribute decision making technique using single-valued neutrosophic trigonometric Dombi aggregation operators. *Soft Computing*, 28(5), pp.4217-4234. Available at: https://doi.org/10.1007/s00500-023-09440-x

Zulfiqar, M., Bhat, S., Sony, M., Salentijn, W., Swarnakar, V., Antony, J., Cudney, E.A., Furterer, S., McDermott, O., Jayaraman, R. & Foster, M. 2024. Unveiling the potential of FMEA in higher education: Pathway to improved risk management and quality. *The TQM Journal*. Available at: https://doi.org/10.1108/TQM-01-2024-0017

Un nuevo marco intuicionista de FMEA difuso con agregación Dombi para la calidad del servicio en la industria 4.0: aplicación en la educación superior

Biplab Biswas[ab], *Sanjib Biswas*[b], **autor de correspondencia**

[a] *Universidad ICFAI, Ranchi, Jharkhand, India*

[b] *Universidad Amity, Escuela de Negocios Amity, Calcuta, Bengala Occidental, India*

CAMPO: matemáticas, ciencias de la decisión
TIPO DE ARTÍCULO: artículo científico original

Resumen:

Introducción/objetivo: La calidad de los servicios de educación superior (CSS) es una de las áreas destacadas que se han redefinido en la I4, lo que plantea numerosos desafíos a las instituciones de educación superior (IES). En este contexto, el presente trabajo busca cumplir dos objetivos: a) desarrollar un nuevo marco de evaluación de riesgos para el análisis modal de fallos y efectos (AMEF) mediante el conjunto difuso intuicionista (IFS) y b) evaluar los posibles factores de riesgo o fallos que enfrentan las IES al ofrecer una CSS superior en la Industria 4.0 (I4).

Métodos: El presente trabajo utiliza un modelo de toma de decisiones multicriterio (MCDM), como la comparación entre criterios jerarquizados (COBRAC), con agregación Dombi basada en IFS para la toma de decisiones grupales, con el fin de desarrollar una nueva extensión del marco AMFE. El presente trabajo propone un enfoque innovador al incorporar una dimensión adicional al modelo AMFE clásico, como la intratabilidad. Los modos de fallo (MF) se identifican desde la perspectiva de los atributos HSQ. Posteriormente, se examina la validez de los resultados mediante la comparación de varios modelos MCDM y un análisis de sensibilidad.

Resultados: Basado en las opiniones de 23 expertos, el trabajo actual revela el predominio de factores de riesgo como preocupaciones éticas (FM-9), limitaciones de infraestructura (FM-2) y escasez de fondos (FM-6).

Conclusión:. El artículo destaca la necesidad de construir un ecosistema holístico con los recursos disponibles. El estudio en curso aporta varias novedades, como una extensión del AMFE con una dimensión adicional y la agregación IFS-Dombi, utilizando el modelo COBRAC para AMFE, y un enfoque innovador para la evaluación de riesgos en HSQ, que resultan útiles para los responsables de la toma de decisiones y los investigadores.

Palabras claves: *calidad del servicio, instituciones de educación superior, FMEA, conjunto difuso intuicionista, COBRAC, agregación Dombi.*

Новая интуиционистская нечеткая модель FMEA с агрегацией Dombi для повышения качества услуг в эпоху четвертой промышленной революции: применение в высшем образовании

Биплаб Бишвас[аб], *Санджив Бишвас*[б], **корреспондент**
[а] *Университет ICFAI, Ранчи, Джаркханд, Республика Индия*
[б] *Университет Эмити, Бизнес-школа Эмити, Калькутта, Западная Бенгалия, Республика Индия*

РУБРИКА ГРНТИ: 27.47.00 Математическая кибернетика,
27.47.19 Исследование операций,
28.17.31 Моделирование процессов управления
ВИД СТАТЬИ: оригинальная научная статья

Резюме:

Введение/цель: Качество услуг высшего образования (КВО) является одной из важнейших областей, пересмотренных в условиях четвертой промышленной революции, которая ставит перед высшими учебными заведениями множество задач. В этом контексте данная статья направлена на достижение двух целей: а) разработать новую систему оценки рисков для анализа режимов и последствий сбоев (FMEA) с использованием интуиционистских нечетких множеств (ИНМ); б) оценить потенциальные факторы *риска или сбоев, с которыми сталкиваются вузы при обеспечении высокого качества КВО в условиях четвертой промышленной революции (I4).*

Методы: В статье используется многокритериальная модель принятия решений (МКМПР), основанная на сравнении ранжированных критериев (COBRAC), с агрегацией Dombi на основе IFS группового принятия решений для разработки нового расширения системы FMEA. В данной статье предлагается инновационный подход, заключающийся во внедрении дополнительного измерения отказоустойчивости в классическую модель FMEA. Виды отказов (FM) определяются с точки зрения атрибутов КВО. В заключении статьи проведена валидация достоверности полученных результатов путем сравнения нескольких моделей МКМПР и анализа чувствительности.

Результаты: На основании мнения 23 экспертов выявлены доминирующие факторы риска: этические вопросы (FM-9), инфраструктурные ограничения (FM-2) и нехватка средств (FM-6).

Вывод: В статье подчеркивается необходимость создания целостной экосистемы с использованием имеющихся ресурсов. Данное исследование содержит несколько новшеств, таких как расширение FMEA за счет дополнительного измерения и агрегации IFS-Dombi с использованием модели COBRAC для FMEA, а также инновационный подход к оценке рисков КВО, которые будут полезными для лиц, принимающих решения, и исследователей.

Ключевые слова: качество услуг, высшие учебные заведения, FMEA, интуиционистское нечеткое множество, COBRAC, агрегация Домби.

Нови интуистички расплинути ФМЕА оквир са Домби агрегацијом за квалитет услуге у индустрији 4.0 – примена у високом образовању

Биплаб Бишвас[аб], *Санџив* Бишвас[б], **аутор за преписку**

[а] Универзитет ИЦФАИ, Ранчи, Џарканд, Република Индија

[б] Универзитет Амити, Пословна школа Амити, Калкута, Западни Бенгал, Република Индија

ОБЛАСТ: математика, операциона истраживања
КАТЕГОРИЈА (ТИП) ЧЛАНКА: оригинални научни рад

Сажетак:

Увод/циљ: Једна од важних области које се преиспитују у четвртој индустријској револуцији јесте квалитет услуга високог образовања (HSQ), што представља изазов за високошколске установе. У том контексту, овај рад има двоструки циљ: да развије *нови оквир за процену ризика за анализу начина и ефеката отказа (FMEA) помоћу интуитивног фази скупа (IFS), као и да процени потенцијалне факторе ризика или отказа са којима се високошколске установе суочавају при пружању високог квалитета у четвртој индустријској револуцији (I4).*

Методе: У раду је коришћен модел вишекритеријумског одлучивања (MCDM) као што је поређење рангираних критеријума (COBRAC) са Домби агрегацијом заснованом на интуитивном фази скупу за групно одлучивање ради развијања нове екстензије методе FMEA. Предложен је иновативни приступ који укључује тешкоћу контролисања као додатни критеријум у класични модел FMEA. Начини отказа (FM) идентификују се са становишта атрибута HSQ. Такође, испитана је валидност исхода поређењем неколико модела MCDM и анализе осетљивости.

Резултати:На основу мишљења 23 експерта, у раду се утврђују доминантни фактори ризика, као што су етичка питања (FM-9), инфраструктурна ограничења (FM-2) и недостатак финансијских средстава (FM-6).

Закључак: У раду се наглашава потреба за креирањем холистичког екосистема са расположивим средствима. Студија у развоју предлаже неколико новина корисних за доносиоце одлука и истраживаче, као што су проширивање методе FMEA додатним критеријумом и Домби агрегацијом на основу интуитивног фази скупа, коришћење модела COBRAC за FMEA, као и иновативни приступ процени ризика за HSQ.

Кључне речи: квалитет услуге, високошколске установе, FMEA, интуитивни фази скуп, COBRAC, Домби агрегација

Paper received on: 25.12.2024.
Manuscript corrections submitted on: 11.01.2025.
Paper accepted for publishing on: 11.03.2025.

Optimization of the short-range surface-to-air artillery-missile system design process using the hybridized triangular IT2FS-DEMATEL-MABAC approach

Ivan B. Petrović[a], *Milan* D. Petrović[b]

University of Defence, Military Academy, Belgrade, Republic of Serbia

[a] e-mail: ivanpetrovic1977@gmail.com, **corresponding author**,
ORCID iD: https://orcid.org/0000-0001-7372-637X

[b] e-mail: milan07501@gmail.com,
ORCID iD: https://orcid.org/0009-0003-0328-3456

doi https://doi.org/10.5937/vojtehg73-57246

FIELD: aplied mathematics, operational research, military sciences
ARTICLE TYPE:original scientific paper

Abstract:

Introduction/purpose: The possibility of optimizing a short-range surface-to-air artillery- missile (short-range SAAM) system design process by applying the hybridized multi-criteria decision-making (integration of DEMATEL and MABAC methods) approach in the triangular interval type 2 fuzzy environments is shown in the paper. By analyzing the content of the literature, the tactical-technical requirements and sub-requirements were selected. Furthermore, the weights of these requirements and sub-requirements are determined. After that, a multi-criteria decision-making (MCDM) model was created for the evaluation of different initial projects of designing a short-range SAAM, which was also tested in this paper.

Methods: The proposed approach that combine the DEMATEL and MABAC methods have been modified by triangular interval type 2 fuzzy sets (IT2FSs). The triangular IT2F-DEMATEL method was applied to determine the weights of the requirements and sub-requirements, while the triangular IT2FS -MABAC method was applied to evaluate the alternatives – initial project designs of a short-range SAAM.

Results: Integrating the multiple triangular IT2FS-MCDM approach into a unique model that can be applied in the process of defining the optimal initial design project of a short-range SAAM.

Conclusion: The paper contributes to military science in making decisions related to the design of a short-range SAAM.

Keywords: DEMATEL, MABAC, Triangular Interval Type 2 Fuzzy Sets, Short-Range Surface-to-Air Artillery-Missile System.

ACKNOWLEDGMENT: This paper was written as a part of the scientific research project funded by the Ministry of Defence, Republic of Serbia: ŠNO/DH/1/24-26.

Introduction

This paper will rely on the state's ability to design and mostly produce new air defense weapons in its limited qualitative and quantitative capabilities (in terms of population, size of territory, development of the military-industrial complex, GDP, geopolitical influence, etc.). An example of the development of a short-range air defense missile system is given in the paper. This case is possible only in conditions of exponential development of the military-industrial complex and the transfer of technology and knowledge (Petrović & Petrović, 2024). As an initial step in the design of a new, technologically advanced, short-range air defense missile system, the formation of a certain number of tactical and technical requirements and sub-requirements is imposed, which the weapon must meet in order to oppose modern threats from the air space. An example of the evaluation of these requirements is given in order to determine their importance in the formation of requirements and sub-requirements of each requirement for the design of a modern short-range SAAM (Petrović & Petrović, 2024). The research aims to optimize the design process of a short-range SAAM using a hybrid MCDM approach. The specific objective is aimed at improving the accuracy of the decision-making process, handling uncertainty, and optimizing the selection of tactical-technical requirements. Namely, the process of forming requirements for military technical-technological solutions is currently based on normative-legal documents that do not take into account precise scientific validation. The current process is based on a detailed content analysis, a large database of processed data, but scientific methodology is not used when drawing conclusions. Bearing in mind that military organizations are used in partially controlled conditions (in a combat environment they depend on the enemy and other components of the operational environment), it is clear that the selection of requirements for the selection of weapon systems takes place in conditions of uncertainty (military decision making is realized in partially determined and indeterminate conditions). Bearing this in mind, the aforementioned military decision making can be improved by applying fuzzy theory, in this case IT2FSs. Also, decision making in military processes aims to create optimal conditions for the implementation of the decision, based on the proposals of experts from several fields (as is the case when defining the initial requirements for designing a weapon system). This results in the need to improve the decision-making process in order to optimize the decision, which results in the application of MCDM methods.

By analyzing the literature, it was concluded that there are scientific articles that researched this problem or similar research problems. There are also studies relating to the development of the technology of individual elements of weapons systems including anti-aircraft missile systems (Cheng & Mon, 1994; Ding et al, 2018; Jiang et al, 2011). Particularly interesting is the work that deals with the formation of initial requirements for designing a fighter aircraft based on overall evaluation criteria by Mavris & DeLaurentis (1995). The optimization of equipping with a missile system for combat operations using multi-criteria decision-making methods was also investigated in some scientific papers (Tešić & Božanić, 2023; Karadayi et al, 2019; Dağıstanlı, 2025; Dağdeviren et al, 2009). Based on the aforementioned papers, initial tactical and technical requirements were formed in this research, with the help of a group of experts who evaluated them for the needs of optimizing the design of a new short-range air defense missile system. The formed requirements are as follows: spatial capabilities (R1), fire capabilities (R2), time capabilities (R3), forces protection capability (R4), and accessibility and technological reliability (R5) (Petrović & Petrović, 2024). These requirements are further classified into sub-requirements. The spatial capabilities (R1) can be classified into: ability to detect targets (R11), size of the destruction zone of aerodynamic and ballistic targets (R12), RCS of the detected target (R13). The fire capabilities (R2) can be classified into: probability of target destruction (R21), mathematical expectation of the number of destroyed targets (R22), channel by target (R23), channel by missile (R24), and system armament (R25). The time capabilities (R3) can be classified into: fire maneuver (R31), movement maneuver (32), firing cycle (R33), ability to provide ordnance and anti-aircraft rockets (R34), and reaction time (R35). The forces protection capability (R4) can be classified into: frequency agility of autonomous radars (R41), pulse repetition frequency (R42), autonomy in operation of combat platforms (R43), ability of passive sensors (R44), combined guidance (R45), and the ability to protect against continuous interference (JATDS) (R46). The accessibility and technological reliability (R5) can be classified into: investment costs (R51), operating costs (R52), possibility of an "offset" component production (R53), possibility of installation of components of domestic production (R54), and possibility of linking with the existing surface to air assets (R55). The sub-requirements investment costs (R51) and the operating costs (R52) are the cost sub-requirements. Other sub-requirements are benefit sub-requirements. The research is conducted by using multi-criteria decision-making methods (MCDM). The types of MCDM methods used in the research are multiple-attribute decision-making (MADM) methods. MADM involves the selection of the "best" alternative from the pre-specified alternatives described in terms of multiple attributes (Zavadskas et al, 2014; Sabaei et al, 2015). These methods enable the prioritization of a discrete - finite number of requirements and sub-requirements and attributes in hierarchically structured qualitative - quantitative ambiguous (imperfect) problems (Petrović & Milenković, 2024). Bearing in mind that in the work it is necessary to prioritize the final number of requirements and sub-requirements, as well as the ranking of the final number of the alternatives – initial project documentation, the application of hybridized MADM methods is completely approved. For the purpose of determining the mutual influence between the requirements and the sub-requirements, the Decision - Making Trial and Evaluation Laboratory (DEMATEL) method was applied in the paper. The evaluation of the project documentation was performed using the Multi-Attributive Border Approximation area Comparison (MABAC) method. The justification for applying the hybridized DEMATEL-MABAC approach is based on the following facts. Using the DEMATEL method, it is possible to investigate the mutual influence of the requirements and the sub-requirements for choosing the optimal offer for designing a SAAM. Bearing in mind that all the capabilities of a weapon system depend on the mutual influence of its tactical-technical characteristics, as well as on the influence of other factors of the operational environment during combat operations, the application of the DEMATEL method fully ensures the prioritization of the requirements and sub-requirements of the weapon system, such as a SAAM. The MABAC method ensures optimal ranking of the project documentation from a pre-defined number of bidders. Also, this method provides an assessment of the distance of the quantitatively expressed characteristics (requirements and sub-requirements) of the offered project documentation from the boundary approximate areas, which, in addition to the numerical results, enables the visualization of the obtained results. Also, the MABAC method provides a solution to problems where there is a conflict between criteria - requirements, which is also the case when designing a SAAM (for example, increasing the number of target aircraft affects the reduction of the protection of forces from the enemy action). All this results in the DEMATEL-MABAC approach being completely complementary to the research problem.

The research algorithm is shown in Figure 1.

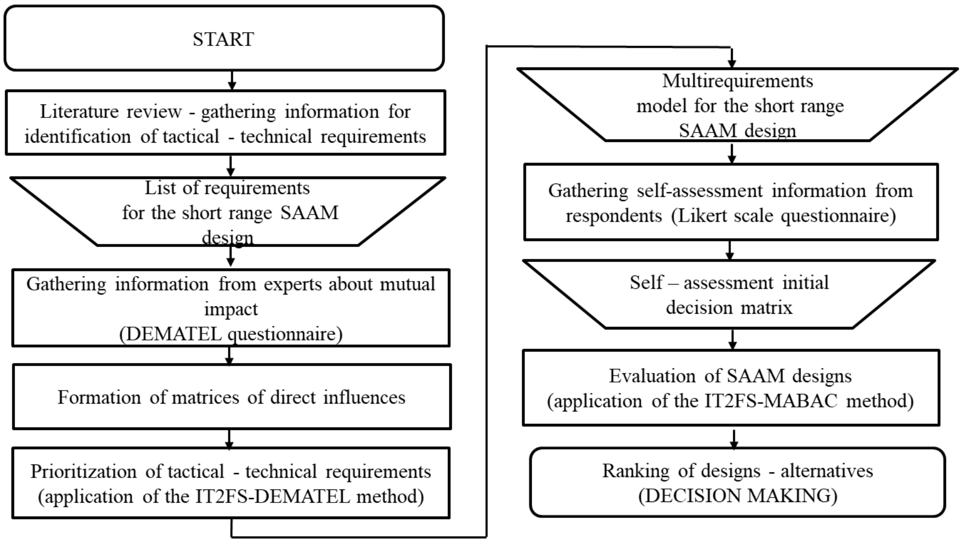

Figure 1 – Algorithm of the research

Background of the methodology

Bearing in mind that type 1 fuzzy sets are not appropriate to model words, T2FSs are developed. This type of fuzzy sets is an extension of type 1 fuzzy sets, and they ensure the use of a linguistic variable in the conditions of linguistic uncertainty (Kahraman et al, 2014). Type-1 fuzzy sets have been applied successfully in many areas including modeling, control, and data mining (Huang et al, 2014). Other types of fuzzy numbers have been developed in fuzzy theory. For example, unlike type 1 fuzzy sets, intuitionistic fuzzy sets take into account more uncertainties in the form of the membership function (membership degree, non-membership degree, and hesitation degree, Deng et al, 2016). However, neither type-1 fuzzy sets nor intuitionistic fuzzy sets represent the optimal choice when making decisions in conditions of uncertainty characterized by the ambiguity of the collected linguistic data. A Type-2 Fuzzy Set (T2FS) is characterized by membership functions, i.e., the membership values for each element of this set. The membership value of a T2FS is a fuzzy set in [0,1], not a crisp number (Huang et al, 2014). The T2FS can express more fuzzy semantics of humans' thoughts, and recently it has attracted the researchers' attention. It has been widely developed and successfully used in many practical real-world applications and many areas, including signal processing, human silhouette extraction, diet application, and pattern recognition design (Huang et al, 2014). Bearing in mind the aforementioned, the use of T2FSs when solving the problem of evaluating the project documentation for designing the short-range SAAM is fully justified. The data, collected for the research purpose, and referring to the determination of the importance of requirements and sub-requirements for the creation of the model, as well as for the evaluation of the initial project documentation, are ambiguous and of a qualitative type. Also, these data reflect the subjective assessment of a small number of respondents. The foregoing implies that decision making takes place in conditions of uncertainty and multi-knowledge, which is the reason why the triangular interval type 2 fuzzy sets (IT2FSs) were applied in the paper. IT2FSs are widely used in solving optimization issues in various fields. For example, Hsien-De Huang et al. (2014) proposed a novel soft-computing mechanism based on the ontology model for malware behavioral analysis by using IT2FSs. Liu et al. (2024) used IT2FSs for the control design of uncertain dynamical systems to relax this limitation of conventional T1FS-based control design. Tekeli et al. (2024) conducted a numerical performance analysis of tank coatings in chemical tankers to contribute to the decision-making process of shipowners and safety professionals by IT2FSs. This type of fuzzy sets ensures the unambiguity of the answers obtained from a small number of corespondents in conditions of uncertainty and increases the reliability of the obtained results. Namely, in contrast to a type-1 fuzzy set, which has the membership grade as a crisp number, an IT2FS has membership functions which are also fuzzy numbers. Whilst type-1 fuzzy sets have membership functions which are two-dimensional, type-2 fuzzy sets are three-dimensional (Baratimehr et al, 2023; Kiracı & Akan, 2020; Uçal Sari et al, 2013). The third dimension provides additional degrees of freedom for possibility in models of uncertainty (Uçal Sari et al, 2013).

The form of the triangular ITFS is (Kahraman et al, 2014):

$$\tilde{\tilde{A}}_i = \left(\tilde{A}_i^U, \tilde{A}_i^L\right) = \left(a_{i1}^U, a_{i2}^U, a_{i3}^U; H\left(\tilde{A}_i^U\right)\right), \left(a_{i1}^L, a_{i2}^L, a_{i3}^L; H\left(\tilde{A}_i^L\right)\right) \tag{1}$$

where:

$H\left(\tilde{A}_i^U\right)$ is the membership value of the element a_{i2}^U in the upper triangular function of the membership, and $H\left(\tilde{A}_i^L\right)$ is the membership value of the element a_{i2}^L in the lower triangular function of the membership, $H\left(\tilde{A}_i^U\right) \in [0,1], H\left(\tilde{A}_i\right) \in [0,1], 1 \le i \le n$ (Kiracı & Akan, 2020; Baykasoğlu & Gölcük, 2017; Petrović & Petrović, 2024).

For two triangular IT2FSs:

$$\tilde{\tilde{A}}_1 = \left(\tilde{A}_1^U, \tilde{A}_1^L\right) = \left(a_{11}^U, a_{12}^U, a_{13}^U; H\left(\tilde{A}_1^U\right)\right), \left(a_{11}^L, a_{12}^L, a_{13}^L; H\left(\tilde{A}_1^L\right)\right)$$

$$\tilde{\tilde{A}}_2 = \left(\tilde{A}_2^U, \tilde{A}_2^L\right) = \left(a_{21}^U, a_{22}^U, a_{23}^U; H\left(\tilde{A}_2^U\right)\right), \left(a_{21}^L, a_{22}^L, a_{23}^L; H\left(\tilde{A}_2^L\right)\right)$$

Their elementary operations are respectively given as follows (Kiracı & Akan, 2020; Kahraman et al, 2014):

$$\tilde{\tilde{A}}_1 \oplus \tilde{\tilde{A}}_2 = \left[a_{11}^U + a_{21}^U, a_{12}^U + a_{22}^U, a_{13}^U + a_{23}^U; \min\left(H\left(\tilde{A}_1^U\right)\right), \min\left(H\left(\tilde{A}_2^U\right)\right)\right], \left[a_{11}^L + a_{21}^L, a_{12}^L + a_{22}^L, a_{13}^L + a_{23}^L; \min\left(H\left(\tilde{A}_1^L\right)\right), \min\left(H\left(\tilde{A}_2^L\right)\right)\right] \quad (2)$$

$$\tilde{\tilde{A}}_1 - \tilde{\tilde{A}}_2 = \left[a_{11}^U - a_{23}^U, a_{12}^U - a_{22}^U, a_{13}^U - a_{21}^U; \min\left(H\left(\tilde{A}_1^U\right), H\left(\tilde{A}_2^U\right)\right)\right], \left[a_{11}^L - a_{23}^L, a_{12}^L - a_{22}^L, a_{13}^L - a_{21}^L; \min\left(H\left(\tilde{A}_1^L\right), H\left(\tilde{A}_2^L\right)\right)\right] \quad (3)$$

$$\tilde{\tilde{A}}_1 \otimes \tilde{\tilde{A}}_2 = \left[a_{11}^U \times a_{21}^U, a_{12}^U \times a_{22}^U, a_{13}^U \times a_{23}^U; \min\left(H\left(\tilde{A}_1^U\right)\right), \min\left(H\left(\tilde{A}_2^U\right)\right)\right], \left[a_{11}^L \times a_{21}^L, a_{12}^L \times a_{22}^L, a_{13}^L \times a_{23}^L; \min\left(H\left(\tilde{A}_1^L\right)\right), \min\left(H\left(\tilde{A}_2^L\right)\right)\right] \quad (4)$$

$$\frac{\tilde{\tilde{A}}_1}{\tilde{\tilde{A}}_2} = \left[\frac{a_{11}^U}{a_{23}^U}, \frac{a_{12}^U}{a_{22}^U}, \frac{a_{13}^U}{a_{21}^U}; \min\left(H\left(\tilde{A}_1^U\right), H\left(\tilde{A}_2^U\right)\right)\right], \left[\frac{a_{11}^L}{a_{23}^L}, \frac{a_{12}^L}{a_{22}^L}, \frac{a_{13}^L}{a_{21}^L}; \min\left(H\left(\tilde{A}_1^L\right), H\left(\tilde{A}_2^L\right)\right)\right] \quad (5)$$

$$k \otimes \tilde{\tilde{A}}_i = k \otimes \left(\tilde{A}_i^U, \tilde{A}_i^L\right) = \left(k \times a_{i1}^U, k \times a_{i2}^U, k \times a_{i3}^U; H\left(\tilde{A}_i^U\right)\right), \left(k \times a_{i1}^L, k \times a_{i2}^L, k \times a_{i3}^L; H\left(\tilde{A}_i^L\right)\right) \quad (6)$$

$$\frac{\tilde{\tilde{A}}_i}{k} = \left[\frac{a_{i1}^U}{k}, \frac{a_{i2}^U}{k}, \frac{a_{i3}^U}{k}; H\left(\tilde{A}_i^U\right)\right], \left[\frac{a_{i1}^L}{k}, \frac{a_{i2}^L}{k}, \frac{a_{i3}^L}{k}; H\left(\tilde{A}_i^L\right)\right] \quad (7)$$

k is a scalar.

$$\frac{1}{\tilde{\tilde{A}}_i} = \left[\frac{1}{a_{i3}^U}, \frac{1}{a_{i2}^U}, \frac{1}{a_{i1}^U}; H\left(\tilde{A}_i^U\right)\right], \left[\frac{1}{a_{i3}^L}, \frac{1}{a_{i2}^L}, \frac{1}{a_{i1}^L}; H\left(\tilde{A}_i^L\right)\right] \quad (8)$$

$$\sqrt[m]{\tilde{\tilde{A}}_i} = \left[\left(\sqrt[m]{a_{i1}^U}, \sqrt[m]{a_{i2}^U}, \sqrt[m]{a_{i3}^U}; H\left(\tilde{A}_i^U\right)\right), \left(\sqrt[m]{a_{i1}^L}, \sqrt[m]{a_{i2}^L}, \sqrt[m]{a_{i3}^L}; H\left(\tilde{A}_i^L\right)\right)\right] \quad (9)$$

The ranking value of the triangular IT2FS $\tilde{\tilde{A}}_i$ can be calculated as follows (Kiracı & Akan, 2020; Baykasoğlu & Gölcük, 2017; Petrović & Petrović, 2024):

$$Rank\left(\tilde{\tilde{A}}_i\right)=M_1\left(\tilde{A}_i^U\right)+M_1\left(\tilde{A}_i^L\right)+M_2\left(\tilde{A}_i^U\right)+M_2\left(\tilde{A}_i^L\right)-\frac{1}{3}$$
$$\left(S_1\left(\tilde{A}_i^U\right)+S_1\left(\tilde{A}_i^L\right)+S_2\left(\tilde{A}_i^U\right)+S_2\left(\tilde{A}_i^L\right)+S_3\left(\tilde{A}_i^U\right)+S_3\left(\tilde{A}_i^L\right)\right)+H\left(\tilde{A}_i^U\right)+H\left(\tilde{A}_i^L\right) \quad (10)$$

$$M_p\left(\tilde{A}_i^j\right)=\left(a_{ip}^j+a_{i(p+1)}^j\right)\Big/2 \;, 1\le p\le 2 \quad (11)$$

$S_p\left(\tilde{A}_i^j\right)$ - the standard deviation of the elements a_{ip}^j and $a_{i(p+1)}^j$:

$$S_p\left(\tilde{A}_i^j\right)=\sqrt{\frac{1}{2}\sum_{k=p}^{p+1}\left(a_{ik}^j-\frac{1}{2}\sum_{k=p}^{p+1}a_{ik}^j\right)^2} \;, 1\le p\le 2 \quad (12)$$

$S_3\left(\tilde{A}_i^j\right)$ - the standard deviation of the elements a_{ip}^j, $1\le p\le 3$:

$$S_3\left(\tilde{A}_i^j\right)=\sqrt{\frac{1}{3}\sum_{k=1}^{3}\left(a_{ik}^j-\frac{1}{3}\sum_{k=1}^{3}a_{ik}^j\right)^2} \quad (13)$$

The formula for the defuzzification of the triangular IT2FS $\tilde{\tilde{A}}_i$ is (Kahraman et al, 2014):

$$DTriT\tilde{\tilde{A}}_i=\frac{1}{2}\begin{Bmatrix}\left[\left(a_{i3}^U-a_{i1}^U\right)+\left(a_{i2}^U-a_{i1}^U\right)\right]/3+a_{i1}^U+\\ H(\tilde{A}_i^L)\times\left[\left[\left(a_{i3}^L-a_{i1}^L\right)+\left(a_{i2}^L-a_{i1}^L\right)\right]/3+a_{i1}^L\right]\end{Bmatrix} \quad (14)$$

Interval type-2 fuzzy sets-DEMATEL method

The weights of the requirements and the sub-requirements of each requirement were calculated by using the triangular IT2FS-DEMATEL method. This method is based on the determination of direct and indirect influences between each criterion on each criterion (Lee et al, 2013; Kahraman et al, 2014). It was developed with the aim of studying groups with complex and connected relationships. This method was chosen for the prioritization of criteria because it analyzes structures with complex causal relationships between their elements in partially determined or non-deterministic organizational systems and processes (Petrović &

Milenković, 2024; Shieh & Wu, 2016). It should be noted that there are limitations when using the hybridized MCDM approach when using the DEMATEL method, as has been written about by a number of authors (Demir, 2025; Kolour et al, 2025). The procedure of the triangular IT2FS-DEMATEL method is as follows (Baykasoğlu & Gölcük, 2017; Petrović & Petrović, 2024):

1) The average IT2FS matrix of the influence between the tactical - technical requirements was obtained as follows:

$$\tilde{\tilde{D}} = \left[\tilde{\tilde{D}}_{ij}\right]_{n\times n} = \left[\frac{\tilde{\tilde{D}}_{ij}^{(1)} \oplus \tilde{\tilde{D}}_{ij}^{(2)} \oplus \ldots \oplus \tilde{\tilde{D}}_{ij}^{(k)}}{k}\right]_{n\times n} \qquad (15)$$

$\tilde{\tilde{D}}^{(k)} = \left[\tilde{\tilde{D}}_{ij}^{(k)}\right]_{n\times n}$ - individual IT2FS matrix of the influence between the requirements of the k-th expert (after the transformation of linguistic variables in the IT2FS),

k - number of experts,

n - number of requirements.

$\tilde{\tilde{D}}_{ij} = \left(\tilde{D}_{ij}^{U}, \tilde{D}_{ij}^{L}\right) = \left(d_{ij1}^{U}, d_{ij2}^{U}, d_{ij3}^{U}; H\left(\tilde{D}_{ij}^{U}\right)\right), \left(d_{ij1}^{L}, d_{ij2}^{L}, d_{ij3}^{L}; H\left(\tilde{D}_{ij}^{L}\right)\right)$ is the triangular IT2FS element of the non-negative average IT2FS matrix of the influence between tactical - technical requirements.

If $s = 1 \Big/ \max\left(\max_{1\le i\le n} \sum_{j=1}^{n} d_{ij3}^{U}, \max_{1\le j\le n} \sum_{i=1}^{n} d_{ij3}^{U}\right)$, the normalized direct-relation matrix is:

$$\tilde{\tilde{X}} = \left[\tilde{\tilde{x}}_{ij}\right]_{n\times n},$$

$\tilde{\tilde{x}}_{ij} = \left(\tilde{x}_{ij}^{U}, \tilde{x}_{ij}^{L}\right) = \left(x_{ij1}^{U}, x_{ij2}^{U}, x_{ij3}^{U}; H\left(\tilde{x}_{ij}^{U}\right)\right), \left(x_{ij1}^{L}, x_{ij2}^{L}, x_{ij3}^{L}; H\left(\tilde{x}_{ij}^{L}\right)\right)$ is the triangular IT2FS element of the normalized direct-relation matrix.

$$\tilde{\tilde{x}}_{ij} = s \otimes \tilde{\tilde{D}}_{ij}$$

$$H\left(\tilde{x}_{ij}^{U}\right) = H\left(\tilde{D}_{ij}^{U}\right), H\left(\tilde{x}_{ij}^{L}\right) = H\left(\tilde{D}_{ij}^{L}\right), i = 1,\ldots n, j = 1,2,\ldots,n \qquad (16)$$

2) The total relation matrix is:

$\tilde{\tilde{T}} = \left[\tilde{\tilde{t}}_{ij}\right]_{n\times n}, \tilde{\tilde{t}}_{ij} = \left(\tilde{t}_{ij}^{U}, \tilde{t}_{ij}^{L}\right) = \left(t_{ij1}^{U}, t_{ij2}^{U}, t_{ij3}^{U}; H\left(\tilde{t}_{ij}^{U}\right)\right), \left(t_{ij1}^{L}, t_{ij2}^{L}, t_{ij3}^{L}; H\left(\tilde{t}_{ij}^{L}\right)\right)$ - The IT2FS element of the total relation matrix, where:

$$t_{ij1}^{U} = x_{ij1}^{U} \times (i_{ij1}^{U} - x_{ij1}^{U})^{-1}, ..., t_{ij3}^{U} = x_{ij3}^{U} \times (i_{ij3}^{U} - x_{ij3}^{U})^{-1},$$
$$t_{ij1}^{L} = x_{ij1}^{L} \times (i_{ij1}^{L} - x_{ij1}^{L})^{-1}, ..., t_{ij3}^{L} = x_{ij3}^{L} \times (i_{ij3}^{L} - x_{ij3}^{L})^{-1},$$
$$H\left(\tilde{t}_{ij}^{U}\right) = H\left(\tilde{x}_{ij}^{U}\right), H\left(\tilde{t}_{ij}^{L}\right) = H\left(\tilde{x}_{ij}^{L}\right), i = 1,...n, j = 1,2,...,n \quad (17)$$

$\tilde{\tilde{I}} = \left[\tilde{\tilde{i}}_{ij}\right]_{n\times n}, \tilde{\tilde{i}}_{ij} = \left(i_{ij1}^{U}, i_{ij2}^{U}, i_{ij3}^{U}; H\left(\tilde{x}_{ij}^{U}\right)\right), \left(i_{ij1}^{L}, i_{ij2}^{L}, i_{ij3}^{L}; H\left(\tilde{x}_{ij}^{L}\right)\right)$ - is the triangular IT2FS identity square matrix with the elements on the main diagonal:

$$\tilde{\tilde{i}}_{ij} = \left(1,1,1; H\left(\tilde{x}_{ij}^{U}\right)\right), \left(1,1,1; H\left(\tilde{x}_{ij}^{L}\right)\right), 1 \le i \le n, 1 \le j \le n, i = j,$$

Other elements are:

$$\tilde{\tilde{i}}_{ij} = \left(0,0,0; H\left(\tilde{x}_{ij}^{U}\right)\right), \left(0,0,0; H\left(\tilde{x}_{ij}^{L}\right)\right), 1 \le i \le n, 1 \le j \le n, i \ne j$$

3) Using formula 10, the defuzzification of the elements of the triangular IT2FS total relation matrix elements $DTriT\tilde{\tilde{T}} = T = \left[t_{ij}\right]_{n\times n}$ was obtained. From the defuzzificated total relation matrix, the sum of the rows $D_i, i = 1,2,...,n$ (efect each requirements on other requirements) and the sum of the columns $R_j, j = 1,2,...,n$ (cause relationship – influence other requirements on each requirement) were calculated as follows (Baykasoğlu & Gölcük, 2017; Petrović & Petrović, 2024):

$$D_i = \sum_{j=1}^{n} t_{ij}^{def} \quad (19)$$

$$R_j = \sum_{i=1}^{n} t_{ij}^{def} \quad (20)$$

4) The requirements' weights of importance are :

$$impw_i = \sqrt{(D_i + R_i)^2 + (D_i - R_i)^2} \quad (21)$$

5) The normalized requirements' weights of importance are:
6) $impW_i = \dfrac{impw_i}{\sum_{i=1}^{n} impw_i}$, $i = 1,...,n$ - number of requirements(22)

The same procedure was used to evaluate all sub-requirements of each requirement. After normalization, the sum of weights for all sub-requirements of each i - requirement is:

$W_i = \sum_{r=1}^{m} w_r^i$, $r = 1,\ldots,m$ - the number of the sub-requirements of the i - requirement, respectively, sum of all sub-requirements, is:

$$\sum_{r=1}^{m}\sum_{i=1}^{n} w_r^i = 1 \tag{23}$$

Where w_r^i represents the weights of the r sub-requirements of the i - requirement.

Interval type-2 fuzzy sets-MABAC method

One of the MADM methods that provides a solution to a wide range of problems is the MABAC method developed by Pamučar & Ćirović (2015). The application of the MABAC method ensures evaluation and selection of the most appropriate alternative among a set of pre-specified alternatives. By applying the MABAC method with simplier computation steps, the most suitable solution is determined based on the comparison of the distance of each observed alternative from the boundary approximate areas - BAA (Pamučar & Ćirović, 2015). Furthermore, this method ensures solving the MADM problem with the properties of attributes that can be in conflict. Also, it allows selection and ranking of alternatives using linguistic variables for forming the initial decision matrix (Torkayesh et al, 2023). There are also limitations related to the application of MABAC as described by Mehdiabadi et al. (2025) and Yalçın et al. (2025). For model testing, the integrated IT2FS-MABAC approach was applied. This approach provides valid results in the conditions of high level of uncertainty, which is the situation with the initial projects of designing combat systems.

The procedure of the IT2FS-MABAC method is as follows (Pamučar & Ćirović, 2015; Torkayesh et al, 2023):

1) In the first step, from the data about the sub-requirements and the alternatives (project designs of the short-range artillery-missile air defense system) the initial decision matrix is formed by applying formulas 2 and 7.

$$\tilde{\tilde{F}} = \left[\tilde{\tilde{f}}_{ij} \right]_{n \times n} \cong \left[\tilde{\tilde{f}}_{ij}^{(1)} \oplus \tilde{\tilde{f}}_{ij}^{(2)} \oplus \ldots \oplus \tilde{\tilde{f}}_{ij}^{(k)} \right]_{n \times m}$$

$$\tilde{\tilde{F}} = \left[\tilde{\tilde{f}}_{ij} \right]_{n \times m}, 1 \le i \le n, 1 \le j \le m$$

$$\tilde{\tilde{f}}_{ij} = \left(\tilde{f}_{ij}^{U}, \tilde{f}_{ij}^{L} \right) = \left(f_{ij1}^{U}, f_{ij2}^{U}, f_{ij3}^{U}; H\left(\tilde{f}_{ij}^{U} \right) \right), \left(f_{ij1}^{L}, f_{ij2}^{L}, f_{ij3}^{L}; H\left(\tilde{f}_{ij}^{L} \right) \right)$$

- The IT2FS element of the initial decision matrix,
n - number of sub-requirements,
m - number of alternatives – number of offers for designing a short-range artillery-missile air defense system,
k - number of experts who evaluate the submitted documentation for each element of the initial decision matrix (the summary initial decision matrix is calculated from the individual initial decision matrices that were formed on the basis of expert evaluation - for each expert individually).

2) The normalized IT2FS decision matrix is calculated as follows:

$$\tilde{\tilde{R}} = \left[\tilde{\tilde{r}}_{ij} \right]_{n \times m}, \tilde{\tilde{r}}_{ij} = \left(\tilde{r}_{ij}^{U}, \tilde{r}_{ij}^{L} \right) = \left(r_{ij1}^{U}, r_{ij2}^{U}, r_{ij3}^{U}; H\left(\tilde{r}_{ij}^{U} \right) \right), \left(r_{ij1}^{L}, r_{ij2}^{L}, r_{ij3}^{L}; H\left(\tilde{r}_{ij}^{L} \right) \right)$$

- The IT2FS element of the normalized decision matrix, where:

a) For the sub-requirements of the benefit type:

$$\tilde{\tilde{r}}_{ij} = \begin{bmatrix} \left(\dfrac{f_{ij1}^{U} - f_{j}^{U-}}{f_{j}^{U+} - f_{j}^{U-}}, \dfrac{f_{ij2}^{U} - f_{j}^{U-}}{f_{j}^{U+} - f_{j}^{U-}}, \dfrac{f_{ij3}^{U} - f_{j}^{U-}}{f_{j}^{U+} - f_{j}^{U-}}; H\left(\tilde{r}_{ij}^{U} \right) \right), \\ \left(\dfrac{f_{ij1}^{L} - f_{j}^{U-}}{f_{j}^{U+} - f_{j}^{U-}}, \dfrac{f_{ij2}^{L} - f_{j}^{U-}}{f_{j}^{U+} - f_{j}^{U-}}, \dfrac{f_{ij3}^{L} - f_{j}^{U-}}{f_{j}^{U+} - f_{j}^{U-}}; H\left(\tilde{r}_{ij}^{L} \right) \right) \end{bmatrix}, \tag{24}$$

b) For the sub-requirements of the cost type:

$$\tilde{\tilde{r}}_{ij} = \begin{bmatrix} \left(\dfrac{f_{j}^{U+} - f_{ij3}^{U}}{f_{j}^{U+} - f_{j}^{U-}}, \dfrac{f_{j}^{U+} - f_{ij2}^{U}}{f_{j}^{U+} - f_{j}^{U-}}, \dfrac{f_{j}^{U+} - f_{ij1}^{U}}{f_{j}^{U+} - f_{j}^{U-}}; H\left(\tilde{r}_{ij}^{U} \right) \right), \\ \left(\dfrac{f_{j}^{U+} - f_{ij3}^{L}}{f_{j}^{U+} - f_{j}^{U-}}, \dfrac{f_{j}^{U+} - f_{ij2}^{L}}{f_{j}^{U+} - f_{j}^{U-}}, \dfrac{f_{j}^{U+} - f_{ij1}^{L}}{f_{j}^{U+} - f_{j}^{U-}}; H\left(\tilde{r}_{ij}^{L} \right) \right) \end{bmatrix}, \tag{25}$$

where:

$$f_j^{U+} = \max\left(j \le 1 \le m(f_{ij3}^U)\right),$$
$$f_j^{U-} = \min\left(j \le 1 \le m(f_{ij1}^U)\right),$$
$$H\left(\tilde{r}_{ij}^U\right) = H\left(\tilde{f}_{ij}^U\right),$$
$$H\left(\tilde{r}_{ij}^L\right) = H\left(\tilde{f}_{ij}^L\right),$$

3) In the next step, the weighted decision matrix is constructed:

$\tilde{\tilde{V}} = \left[\tilde{\tilde{v}}_{ij}\right]_{n\times m}, \tilde{\tilde{v}}_{ij} = \left(\tilde{v}_{ij}^U, \tilde{v}_{ij}^L\right) = \left(v_{ij1}^U, v_{ij2}^U, v_{ij3}^U; H\left(\tilde{v}_{ij}^U\right)\right), \left(v_{ij1}^L, v_{ij2}^L, v_{ij3}^L; H\left(\tilde{v}_{ij}^L\right)\right)$ -The triangular IT2FS element of the weighted decision matrix, where:

$\tilde{\tilde{v}}_{ij} = W_i \otimes \left(\tilde{\tilde{r}}_{ij} \oplus \tilde{\tilde{1}}\right)$, or (according to formulas 2 and 6):

$$\tilde{\tilde{v}}_{ij} = \left(W_i \times (r_{ij1}^U + 1), W_i \times (r_{ij2}^U + 1), W_i \times (r_{ij3}^U + 1); H\left(\tilde{v}_{ij}^U\right)\right),$$
$$\left(W_i \times (r_{ij1}^L + 1), W_i \times (r_{ij2}^L + 1), W_i \times (r_{ij3}^L + 1); H\left(\tilde{v}_{ij}^L\right)\right)$$
$$H\left(\tilde{v}_{ij}^U\right) = H\left(\tilde{r}_{ij}^U\right),$$
$$H\left(\tilde{v}_{ij}^L\right) = H\left(\tilde{r}_{ij}^L\right), \tag{26}$$

4) Using formulas 4 and 9, the border approximation area (BAA) is calculated as follows (for each sub-requirement):

$$\tilde{\tilde{G}} = \left[\tilde{\tilde{g}}_i\right]_{n\times 1}, \tilde{\tilde{g}}_i = \sqrt[m]{\tilde{\tilde{v}}_{i1} \otimes \tilde{\tilde{v}}_{i2} \otimes \ldots \otimes \tilde{\tilde{v}}_{im}}, 1 \le i \le n \tag{27}$$

5) The distance matrix from the BAA is calculated as follows:

$$\tilde{\tilde{Q}} = \left[\tilde{\tilde{q}}_{ij}\right]_{n\times m} = \left[\tilde{\tilde{v}}_{ij} - \tilde{\tilde{g}}_i\right]_{n\times m} \tag{28}$$

6) By summing the elements of the matrix $\tilde{\tilde{Q}}$ for each alternative (for all values of n) the final values of the requirement functions of the alternative (the closeness coefficient $\tilde{\tilde{S}}_j$ to the BAA for each alternative) are obtained:

$$\tilde{\tilde{S}}_j = \tilde{\tilde{q}}_{1j} \oplus \tilde{\tilde{q}}_{2j} \oplus \ldots \oplus \tilde{\tilde{q}}_{nj}, j = 1, \ldots, m \tag{29}$$

7) Ranking values S_j are calculated by formulas 10-13:

$$S_j = Rank\left(\tilde{\tilde{S}}_j\right), j = 1,...,m$$

8) Finally, the alternatives are ranked. The optimal alternative is the one that has the largest value of S .

Results

The requirements' weights (R1-R5) were calculated by using the triangular IT2FS-DEMATEL method. There is no influence of the requirement in itself. The values of influence expressed by linguistic variables and IT2FS are shown in Table 1.

Table 1 – DEMATEL Causal influence linguistic variables

Linguistic variable of influence	Triangular IT2FS
No (N)	((0,0,0;1),(0,0,0;0.8))
Low (L)	((0,0.2,0.4;1),(0,0.1,0.3;0.8))
Medium (M)	((0.2,0.4,0.6;1),(0.1,0.3,0.5;0.8))
High (H)	((0.4,0.6,0.8;1),(0.3,0.5,0.7;0.8))
Very high (VH)	((0.6,0.8,1;1),(0.5,0.7,0.9;0.8))

Firstly, by using DEMATEL causal influence linguistic variables of pairwise comparisons between requirements, the mutual influence between the requirements was determined by four experts individually (Table 2), and transformed into the triangular IT2FS (based on Table 1).

The average IT2FS matrix of the influence between the requirements $\tilde{\tilde{D}}$ was obtained by using formula 11 (Table 3).

Table 2 – Answers of experts in linguistic variables - matrix of mutual influence (Petrović & Petrović, 2024)

R	R1	R2	R3	R4	R5
R1	N	3L+M	2L+2M	H+3VH	H+3VH
R2	3L+M	N	2M+2H	4VH	H+3VH
R3	3L+M	3L+M	N	H+3VH	2H+2VH
R4	L+M+2H	2M+2H	2H+2VH	N	4VH
R5	L+3M	3M+H	2M+2VH	4VH	N

Table 3 – Average IT2FS matrix of influence (Petrović & Petrović, 2024)

R	R1	R2	R3	R4	R5
R1	0,0,0; 0,0,0	0.05,0.25,0.45; 0.03,0.15,0.35	0.1,0.3,0.5; 0.05,0.2,0.4	0.55,0.75,0.95; 0.45,0.65,0.85	0.55,0.75,0.95; 0.45,0.65,0.85
R2	0.05,0.25,0.45; 0.03,0.15,0.35	0,0,0; 0,0,0	0.3,0.5,0.7; 0.2,0.4,0.6	0.6,0.8,1; 0.5,0.7,0.9	0.55,0.75,0.95; 0.45,0.65,0.85
R3	0.05,0.25,0.45; 0.03,0.15,0.35	0.05,0.25,0.45; 0.03,0.15,0.35	0,0,0; 0,0,0	0.55,0.75,0.95; 0.45,0.65,0.85	0.5,0.7,0.9; 0.4,0.6,0.8
R4	0.25,0.45,0.65; 0.18,0.35,0.55	0.2,0.4,0.6; 0.3,0.5,0.7	0.5,0.7,0.9; 0.4,0.6,0.8	0,0,0; 0,0,0	0.6,0.8,1; 0.5,0.7,0.9
R5	0.13,0.35,0.55; 0.08,0.25,0.45	0.25,0.45,0.65; 0.15,0.35,0.55	0.4,0.6,0.8; 0.3,0.5,0.7	0.6,0.8,1; 0.5,0.7,0.9	0,0,0; 0,0,0
$H\left(\tilde{D}_{ij}^{U}\right)=1, H\left(\tilde{D}_{ij}^{L}\right)=0.8, i=1,\ldots,5; j=1,\ldots,5$					

The normalized direct-relation matrix $\tilde{\tilde{X}}$ and the total relation matrix $\tilde{\tilde{T}}$ were obtained using formulas 12-13. The defuzzificated total relation matrix was obtained using formula 10, and the sum of rows and the sum of columns of the total relation matrix were calculated using formulas 14 and 15. The weights of importance of the requirements were calculated using formulas 16-17, respectively (Table 4) (Petrović & Petrović, 2024).

Table 4 – Defuzzificated total relation matrix and requirements'weights (Petrović & Petrović, 2024)

R	R1	R2	R3	R4	R5	D_i	R_j	w_i	W_i
R1	0	0.017	0.024	0.074	0.073	0.188	0.084	0.292	0.143
R2	0.017	0	0.042	0.087	0.078	0.223	0.100	0.342	0.168
R3	0.015	0.016	0	0.073	0.066	0.171	0.180	0.350	0.172
R4	0.030	0.036	0.064	0	0.087	0.217	0.318	0.549	0.270
R5	0.022	0.031	0.051	0.085	0	0.189	0.304	0.502	0.247

The weights of the sub-requirements, shown in Table 5 and Figure 2, were determined in the same way.

Table 5 – Total relation matrix and sub-requirements' weights

R		D_r^i	R_r^i	$impw_r^i$	$impW_r^i$	w_r^i
R1	R11	0.294	0.245	0.734	0.306	0.044
	R12	0.323	0.375	0.835	0.348	0.050
	R13	0.351	0.338	0.830	0.346	0.049
R2	R21	0.224	0.214	0.662	0.212	0.036
	R22	0.157	0.211	0.607	0.194	0.033
	R23	0.274	0.224	0.706	0.226	0.038
	R24	0.124	0.097	0.470	0.150	0.025
	R25	0.214	0.254	0.684	0.219	0.037
R3	R31	0.122	0.134	0.506	0.162	0.028
	R32	0.217	0.202	0.647	0.208	0.036
	R33	0.214	0.243	0.676	0.217	0.037
	R34	0.199	0.175	0.611	0.196	0.034
	R35	0.243	0.217	0.678	0.217	0.037
R4	R41	0.045	0.053	0.313	0.095	0.026
	R42	0.055	0.071	0.355	0.108	0.029
	R43	0.317	0.285	0.776	0.236	0.064
	R44	0.194	0.212	0.637	0.194	0.052
	R45	0.185	0.174	0.599	0.182	0.049
	R46	0.194	0.173	0.606	0.184	0.050
R5	R51	0.371	0.285	0.810	0.262	0.065
	R52	0.199	0.203	0.634	0.205	0.051
	R53	0.092	0.147	0.489	0.158	0.039
	R54	0.103	0.135	0.488	0.158	0.039
	R55	0.234	0.219	0.673	0.218	0.054

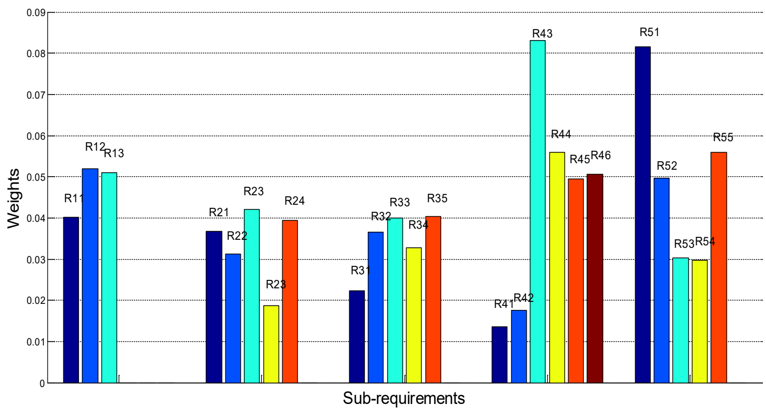

Figure 2 – Weights of importance of the sub-requirements

The initial estimations were transformed into the triangular IT2FS based on the equivalence shown in Table 6.

Table 6 – MABAC linguistic and triangular IT2FS variables for the rating of alternatives

Linguistic variable of influence	Triangular IT2FS
Very poor (VP)	((0,0,0;1),(0,0,0;0.8))
Poor (P)	((0,0.2,0.4;1),(0,0.1,0.3;0.8))
Medium (M)	((0.2,0.4,0.6;1),(0.1,0.3,0.5;0.8))
Good (G)	((0.4,0.6,0.8;1),(0.3,0.5,0.7;0.8))
Very good (VG)	((0.6,0.8,1;1),(0.5,0.7,0.9;0.8))

After the calculated weights of the sub-requirements and the formed model for ranking and the delivery of the bidder's initial project documentation (five bids) in accordance with the established requirements, the model was tested. Model testing was performed using the triangular IT2FS-MABAC method. This method was applied due to the fact that the offers are of a descriptive-qualitative nature, which is why the triangular IT2FS was applied in order to eliminate ambiguity in the project documentation offers. Hypothetically, the project teams submitted the initial project documentation, and the experts completed the initial assessment for each submitted offer. For each sub-requirement, experts for the selection of the short-range SAAM individually perform a qualitative assessment in the form of the following linguistic variables: very poor (VP), poor (P), medium (M), good (G), and very good (VG). Linguistic variables were adapted based on the Likert scale of ranking. The obtained estimates are grouped in Table 7.

Table 7 – Initial decision matrix (linguistic variables)

Criteria/Alt.		A1	A2	A3	A4	A5
R1	R11	3G+2VG	3M+2VG	5VG	5VG	VG+4G
	R12	2G+3VG	4G+VG	G+4VG	4VG+G	VG+4M
	R13	4G+VG	3G+2M	4VG+G	4VG+G	G+4M
R2	R21	2G+3VG	5M	3M+2G	M+4G	3M+2G
	R22	G+4VG	2M+3P	VP+4P	5VP	2M+3G
	R23	G+4VG	2M+3G	M+4G	5VP	3M+2G
	R24	4M+P	VP+2P+2M	M+4G	M+4P	4VP+P
	R25	2G+3M	3M+2G	VG+4G	M+4P	4P+M
R3	R31	3VG+2G	3G+2M	3G+3VG	G+4VG	G+4VG
	R32	2VG+3G	VG+4G	5VG	G+4G	5VG
	R33	M+4G	2M+P+2VP	G+4G	5VG	M+4P
	R34	2VG+3G	G+4M	5VG	5VG	M+4P
	R35	5G	2VG+3G	5G	2M+3G	G+4M
R4	R41	4G+M	2G+2M+P	4G+1VG	G+4M	5G
	R42	3M+2P	M+4G	M+4P	M+4P	5M
	R43	4M+G	5VG	4VG+G	3G+2VG	2M+3G
	R44	3M+2G	G+4M	3G+2M	G+4VG	5VG
	R45	P+4M	M+4P	3G+2M	G+4VG	G+4VG
	R46	5VG	G+4M	G+4G	5M	G+4VG
R5	R51	3G+2M	4VG+G	M+4P	5G	2M+3P
	R52	VG+4G	M+4P	G+4VG	G+4VG	G+4M
	R53	VG+4G	5VG	G+4VG	G+4VG	VG+4G
	R54	2G+2M+VG	G+4M	M+4G	G+4VG	G+4M
	R55	G+4VG	M+3G+VG	2G+3VG	G+4VG	G+4M

After the linguistic variables were transformed into the triangular IT2FS, the summary initial decision matrix was calculated. After that, the normalized triangular IT2FS decision matrix was calculated by formulas 24-25. The weighted IT2FS decision matrix was calculated by using formula 26. The border approximation area (BAA), the distance matrix from the BAA, was calculated respectively by using formulas 27 and 28.

The criterion functions for all alternatives - bids $\tilde{\tilde{S}}_j$ were calculated by using formula 29. The ranking values S_j were calculated by using formulas 10-13. Based on the obtained results, the project documentation was ranked. The obtained results are shown in Tables 8-9.

Table 8 – Summary IT2FS initial decision matrix $\tilde{\tilde{F}}$

Criteria/Alt.		A1	A2	A3	A4	A5
R1	R11	2.4,3.4,4.4; 1.9,2.9,3.9	1.8,2.8,3.8; 1.3,2.3,3.3	3,4,5; 2.5,3.5,4.5	3,4,5; 2.5,3.5,4.5	2.2,3.2,4.2; 1.7,2.7,3.7
	R12	2.6,3.6,4.6; 2.1,3.1,4.1	2.2,3.2,4.2; 1.7,2.7,3.7	2.8,3.8,4.8; 2.3,3.3,4.3	2.8,3.8,4.8; 2.3,3.3,4.3	1.4,2.4,3.4; 0.9,1.9,2.9
	R13	2.2,3.2,4.2; 1.7,2.7,3.7	1.6,2.6,3.6; 1.1,2.1,3.1	2.8,3.8,4.8; 2.3,3.3,4.3	2.8,3.8,4.8; 2.3,3.3,4.3	1.2,2.2,3.2; 0.7,1.7,2.7
R2	R21	2.6,3.6,4.6; 2.1,3.1,4.1	1,2,3; 0.5,1.5,2.5	1.4,2.4,3.4; 0.9,1.9,2.9	1.8,2.8,3.8; 1.3,2.3,3.3	1.4,2.4,3.4; 0.9,1.9,2.9
	R22	2.8,3.8,4.8; 2.3,3.3,4.3	0.4,1.4,2.4; 0.2,0.9,1.9	0,0.8,1.6; 0,0.4,1.2	0,0,0; 0,0,0	1.6,2.6,3.6; 1.1,2.1,3.1
	R23	2.8,3.8,4.8; 2.3,3.3,4.3	1.6,2.6,3.6; 1.1,2.1,3.1	1.8,2.8,3.8; 1.3,2.3,3.3	0,0,0; 0,0,0	1.4,2.4,3.4; 0.9,1.9,2.9
	R24	0.8,1.8,2.8; 0.4,1.3,2.3	0.4,1.2,2; 0.2,0.8,1.6	1.8,2.8,3.8; 1.3,2.3,3.3	0.2,1.2,2.2; 0.1,0.7,1.7	0,0.2,0.4; 0,0.1,0.3
	R25	1.4,2.4,3.4; 0.9,1.9,2.9	1.4,2.4,3.4; 0.9,1.9,2.9	2.2,3.2,4.2; 1.7,2.7,3.7	0.2,1.2,2.2; 0.1,0.7,1.7	0.2,1.2,2.2; 0.1,0.7,1.7
R3	R31	2.6,3.6,4.6; 2.1,3.1,4.1	1.6,2.6,3.6; 1.1,2.1,3.1	2.4,3.4,4.4; 1.9,2.9,3.9	2.8,3.8,4.8; 2.3,3.3,4.3	2.8,3.8,4.8; 2.3,3.3,4.3
	R32	2.4,3.4,4.4; 1.9,2.9,3.9	2.2,3.2,4.2; 1.7,2.7,3.7	3,4,5; 2.5,3.5,4.5	2,3,4; 1.5,2.5,3.5	3,4,5; 2.5,3.5,4.5
	R33	1.8,2.8,3.8; 1.3,2.3,3.3	0.4,1,1.6; 0.2,0.7,1.3	2,3,4; 1.5,2.53.5	3,4,5; 2.5,3.5,4.5	0.2,1.2,2.2; 0.1,0.7,1.7
	R34	2.4,3.4,4.4; 1.9,2.9,3.9	1.2,2.2,3.2; 0.7,1.7,2.7	3,4,5; 2.5,3.5,4.5	3,4,5; 2.5,3.5,4.5	0.2,1.2,2.2; 0.1,0.7,1.7
	R35	2,3,4; 1.5,2.5,3.5	2.4,3.4,4.4; 1.9,2.9,3.9	2,3,4; 1.5,2.5,3.5	1.6,2.6,3.6; 1.1,2.1,3.1	1.2,2.2,3.2; 0.7,1.7,2.7
R4	R41	1.8,2.8,3.8; 1.3,2.3,3.3	1.2,2.2,3.2; 0.8,1.7,2.7	2.2,3.2,4.2; 1.7,2.7,3.7	1.2,2.2,3.2; 0.7,1.7,2.7	2,3,4; 1.5,2.5,3.5
	R42	0.6,1.6,2.6; 0.3,1.1,2.1	1.8,2.8,3.8; 1.3,2.3,3.3	0.21.2,2.2; 0.1,0.7,1.7	0.2,1.2,2.2; 0.1,0.7,1.7	1,2,3; 0.5,1.5,2.5
	R43	1.2,2.2,3.2; 0.7,1.7,2.7	3,4,5; 2.5,3.5,4.5	2.83.8,4.8; 2.3,3.3,4.3	2.4,3.4,4.4; 1.9,2.9,3.9	1.6,2.6,3.6; 1.1,2.1,3.1

Criteria/Alt.		A1	A2	A3	A4	A5
R4	R44	1.4,2.4,3.4; 0.9,1.9,2.9	1.2,2.2,3.2; 0.7,1.7,2.7	1.6,2.6,3.6; 1.1,2.1,3.1	2.8,3.8,4.8; 2.3,3.3,4.3	3,4,5; 2.5,3.5,4.5
	R45	0.8,1.8,2.8; 0.4,1.3,2.3	0.2,1.2,2.2; 0.1,0.7,1.7	1.6,2.6,3.6; 1.1,2.1,3.1	2.8,3.8,4.8; 2.3,3.3,4.3	2.8,3.8,4.8; 2.3,3.3,4.3
	R46	3,4,5; 2.5,3.5,4.5	1.2,2.2,3.2; 0.7,1.7,2.7	2,3,4; 1.5,2.5,3.5	1,2,3; 0.5,1.5,2.5	2.8,3.8,4.8; 2.3,3.3,4.3
R5	R51	1.6,2.6,3.6; 1.1,2.1,3.1	2.8,3.8,4.8; 2.3,3.3,4.3	0.2,1.2,2.2; 0.1,0.7,1.7	2,3,4; 1.5,2.5,3.5	0.4,1.4,2.4; 0.2,0.91.9
	R52	2.2,3.2,4.2; 1.7,2.7,3.7	0.2,1.2,2.2; 0.1,0.7,1.7	2.8,3.8,4.8; 2.3,3.3,4.3	2.8,3.8,4.8; 2.3,3.3,4.3	1.2,2.2,3.2; 0.7,1.7,2.7
	R53	2.2,3.24.2; 1.7,2.7,3.7	3,4,5; 2.5,3.5,4.5	2.8,3.8,4.8; 2.3,3.3,4.3	2.8,3.8,4.8; 2.3,3.3,4.3	2.2,3.2,4.2; 1.7,2.7,3.7
	R54	1.8,2.8,3.8; 1.3,2.3,3.3	1.2,2.2,3.2; 0.7,1.7,2.7	1.8,2.8,3.8; 1.3,2.3,3.3	2.8,3.8,4.8; 2.3,3.3,4.3	1.2,2.2,3.2; 0.7,1.7,2.7
	R55	2.8,3.8,4.8; 2.3,3.3,4.3	2,3,4; 1.5,2.5,3.5	2.6,3.6,4.6; 2.1,3.1,4.1	2.8,3.8,4.8; 2.3,3.3,4.3	1.2,2.2,3.2; 0.7,1.7,2.7
$H\left(\tilde{f}_{ij}^{U}\right)=1, H\left(\tilde{f}_{ij}^{L}\right)=0.8, i=1,...,24; j=1,...,5$						

Table 9 – IT2FS and 'crisp' values of the closeness coefficient to the BAA and the rank of the alternatives

Candidates	$\tilde{\tilde{S}}_j$	$Rank\left(\tilde{\tilde{S}}_j\right)$	Ranking
A1	(0.035,0.039,0.044;1), (0.027,0.037,0.044;0.8)	1.943248956	2
A2	(-0.057,-0.057,-0.056;1), (-0.056,-0.057,-0.059;0.8)	1.570539829	5
A3	(0.085,0.088,0.091;1), (0.081,0.086,0.086;0.8)	2.141097582	1
A4	(0.030,0.019,0.010;1), (0.036,0.024,0.017;0.8)	1.877131511	3
A5	(-0.025,-0.026,-0.026;1), (-0.023,-0.026,-0.028;0.8)	1.694628858	4

A sensitivity analysis was done through changes in the weights of requests. The sensitivity analysis was carried out through 20 scenarios (Table 10). In each scenario, the weights of all sub-requirements within one requirement are increased (reduced) by 20%, and 40%, respectively. The weights of the other requirements and sub-requirements are increased (decreased) so that the sum of the criteria values is 1.

Table 10 – Sensitivity analysis of the results

$R_1 = R_{1old} \times 1.2$	$R_1 = R_{1old} \times 1.4$	$R_1 = R_{1old} \times 0.8$	$R_1 = R_{1old} \times 0.6$
$A3 > A1 > A4 > A5 > A2$	$A1 > A3 > A4 > A2 > A5$	$A3 > A1 > A4 > A5 > A2$	$A3 > A1 > A4 > A2 > A5$
$R_2 = R_{2old} \times 1.2$	$R_2 = R_{2old} \times 1.4$	$R_2 = R_{2old} \times 0.8$	$R_2 = R_{2old} \times 0.6$
$A3 > A1 > A4 > A5 > A2$	$A1 > A3 > A4 > A5 > A2$	$A3 > A1 > A4 > A5 > A2$	$A1 > A3 > A5 > A4 > A2$
$R_3 = R_{3old} \times 1.2$	$R_3 = R_{3old} \times 1.4$	$R_3 = R_{3old} \times 0.8$	$R_3 = R_{3old} \times 0.6$
$A3 > A1 > A4 > A5 > A2$	$A3 > A1 > A4 > A2 > A5$	$A3 > A1 > A5 > A4 > A2$	$A3 > A1 > A4 > A5 > A2$
$R_4 = R_{4old} \times 1.2$	$R_4 = R_{4old} \times 1.4$	$R_4 = R_{4old} \times 0.8$	$R_4 = R_{4old} \times 0.6$
$A3 > A1 > A5 > A4 > A2$	$A3 > A1 > A4 > A5 > A2$	$A3 > A1 > A5 > A4 > A2$	$A3 > A4 > A1 > A5 > A2$
$R_5 = R_{5old} \times 1.2$	$R_5 = R_{5old} \times 1.4$	$R_5 = R_{5old} \times 0.8$	$R_5 = R_{5old} \times 0.6$
$A1 > A3 > A5 > A4 > A2$	$A3 > A1 > A5 > A4 > A2$	$A3 > A1 > A4 > A5 > A2$	$A3 > A4 > A1 > A5 > A2$

The results in the table show that the ranking of the alternatives changed through 11 scenarios. In other scenarios, the ranking of the alternatives did not change. The correlation of the results was tested using Kendall’s coefficient of concordance W. This coefficient represents a measure of the agreement between several judges (in this case 20 scenarios) who have rank ordered a set of entities (in this case five alternatives) (Field, 2005). The value of Kendall's coefficient of concordance for all 20 scenarios and 5 variables is 0.8635. The value of the coefficient of 0.8635 is extremely significant for a significance of 0.05. Thus, it can be concluded that there is a very high correlation (closeness) of ranks through the scenarios and that the results obtained using the hybridized fuzzy-DEMATEL-MABAC approach are credible.

Discussion

Based on the obtained results (Tables 3 – 4), it can be concluded that the requirement related to the ability to protect forces has the greatest weight (Petrović & Petrović, 2024). The next requirement in order of importance is the ability to protect forces, followed by: time capabilities, spatial capabilities and fire capabilities which represent the requirement that has the least weight - the least importance (Petrović & Petrović, 2024). It is obvious that, according to the experts, the most important ability to protect forces and force`s survival (R4) is the most important requirement when using a modern weapon system. In order to carry out a combat mission, it is necessary to ensure the survival of the forces. Bearing in mind the modest GDP and the limited capabilities of the military industry, the experts believe that when designing new weapons, the cost of the technological process, as well as the cost of use and maintenance, are very significant - requirement (R5). The importance of the time capabilities of (R3) is reflected in the modern conditions of Air Force and Air Defence warfare, which affect the need for high maneuverability of units with the ability to repel mass air strikes. The importance of the other two requirements, R1 and R2, is a bit lower than that of the others, but despite that their influence on the design of a new air defense missile system is extremely large.

The obtained results for the sub-requirements (Table 5 and Figure 2) indicate that the experts single out two sub-requirements during evaluation, while they evaluate the others almost equally. Sub-requirement R43 (autonomy in operation of combat platforms) - 0.064 and R52 (investment costs) have significantly greater importance than the others. This is justified by the fact that the SAAM for anti-aircraft operations, following the tendencies of the complexity of modern conflicts, must be able to react completely independently and in a timely manner to threats in the airspace. An extreme importance of operational autonomy is evident on the example of missile systems of older technological generations, composed of several subsystems. In the event that any of these subsystems is damaged or destroyed by enemy action, the system's operation would not be possible. It is also understandable that the price of the investment is of great importance, regarding that a complex asset like that is viewed as a long-term investment in the defense system. The experts placed slightly less importance on sub-requirements R44 (ability of passive sensors) -0.052 and R55 (possibility of linking with the existing surface to air assets) - 0.054 and R52 (operating costs) - 0.051 and R12 (size of the destruction zone of aerodynamic and ballistic targets) - 0.050. This is a consequence of the fact that there is a constant tendency to passivate the operation of the system, which reduces the total radiation time and thus enables safer work in terms of observation, detection and tracking of targets in the airspace. Also, the possibility of linking with the existing surface to air assets increases overall compatibility and excludes additional costs of procurement and training of staff. Also, SAAMs often require constant maintenance, training, and logistical support. High operating costs can strain a nation's budget, especially if these systems need to be kept at a high state of readiness at all times. Ensuring that operating costs are manageable helps maintain a sustainable defense posture over the long term. The destruction zone's size is crucial for air defense, directly affecting interception effectiveness. A larger zone increases the chances of neutralizing aerodynamic and ballistic threats by providing more engagement opportunities. It accommodates evasive maneuvers, enables simultaneous target management, and improves tracking of stealth aircraft or decoys. A broader zone also enhances adaptability to various attacks, ensures comprehensive coverage, and strengthens system integration. Ultimately, it optimizes resources and boosts overall defense reliability and success.

According to the experts, the least important sub-requirements are R24 (channel by missile) - 0.025, R41 (frequency agility of autonomous radars) - 0.026, R31 (fire maneuver) - 0.028, and R42 (pulse repetition frequency) - 0.029. Although rated much lower, sub-requirement R41 (frequency agility of autonomous radars) should not be forgotten because the ability of radars to work at different frequencies is crucial for the effectiveness of the SAAM because it increases their ability to detect and track different targets. Lower frequencies extend the detection range, aiding in spotting large objects such as aircraft. Higher frequencies improve resolution, enabling precise tracking of small or fast-moving targets such as missiles or drones. Low-frequency radars perform better in poor weather, while high frequencies are more vulnerable to interference. Multi-frequency radars resist countermeasures, enhancing reliability in combat. Higher frequencies also enable faster tracking of threats like incoming missiles. Overall, operating across different frequencies maximizes detection, resolution, and defense resilience. The weights of other sub-requirements are approximate. Based on the obtained data, it can be concluded that the ability to protect forces has the greatest importance. This is understandable because in combat operations, the human resource is the most important resource. Protecting forces in combat is crucial for maintaining capability and minimizing losses, ensuring operational continuity. It also boosts morale, which is a key to long-term success. Reducing manpower losses lowers training costs and shortens the time needed to regain readiness. Ultimately, sustained force protection increases the chances of success in combat. After the analysis of the obtained results of the weights of certain requirements and sub-requirements, a model was created for evaluating the initial project documentation of the respective bidders (project teams) for the design of the short-range SAAM. In the next step, the mentioned MCDM model was tested. It was assumed that five bidders applied for the competition and that they submitted the basis of the project proposal based on the created model. The obtained results are shown in Table 9. Based on the obtained results, it can be concluded that the offer number 3 is the best, while the offer of the project team number 2 is the worst. It can also be seen from the results that the MCDM model is successful and that there is a clear numerical difference between the bidders (alternatives) that ensures their ranking. In this way, by applying the IT2FS-COPRAS method, the MCDM model was successfully tested and it was shown that it works.

Conclusion

The paper shows the possibility of applying the IT2FS-DEMATEL-MABAC approach for the purpose of forming a model with which it is possible to evaluate the initial project documentation for designing the short-range SAAM. The IT2FS-DEMATEL approach was applied for the evaluation of requirements and sub-requirements and the formation of a model for the evaluation of the INITIAL project documentation. The IT2FS-MABAC approach was applied to test the model based on the estimated data for five providers of the initial project documentation. The application of the IT2FS was conditioned by the need to eliminate ambiguity in the obtained results. Based on the results obtained in the research, it can be concluded that this approach when defining the basic conditions - requirements that are necessary for the assessment of the initial project documentation for designing a short-range SAAM can have its scientifically based application.

There are numerous practical possibilities of applying the results of this research. Namely, in the future, based on the obtained results, it is possible to form a unique model with the help of which it is possible to design the production of SAAMs or similar combat systems. Also, this model can serve as a basis for choosing the optimal weapon system when equipping armed forces. Also, this model can serve as a basis for the modernization of certain weapon systems based on the estimated requirements for modernization. The MCDM decision-making model can also have a comprehensive practical application during the optimization of the decision-making process when solving other numerous problems in military units.

In the following research, it is necessary to consider the operationalization of tactical-technical requirements in order to create a wider scope of conditions that determine the ability of the project contractor to design a short-range SAAM in accordance with real current and future needs. Also, it is possible to improve the model through the application of other MCDM approaches that will include other MADM methods in different fuzzy theory conditions.

References

Baratimehr, K., Moosavi, M.R. & Tahayori, H. 2023. Measures for evaluating IT2FSs constructed from data intervals. *Applied Soft Computing*, 136, 110084. Available at: https://doi.org/10.1016/j.asoc.2023.110084

Baykasoğlu, A. & Gölcük, İ. 2017. Development of an interval type-2 fuzzy sets based hierarchical MADM model by combining DEMATEL and TOPSIS. *Expert Systems with Applications*, 70, pp. 37-51. Available at: https://doi.org/10.1016/j.eswa.2016.11.001

Cheng, C.H. & Mon, D.L. 1994. Evaluating weapon system by analytical hierarchy process based on fuzzy scales. *Fuzzy sets and systems*, 63(1), pp. 1-10. Available at: https://doi.org/10.1016/0165-0114(94)90140-6

Dağdeviren, M., Yavuz, S. & Kılınç, N. 2009. Weapon selection using the AHP and TOPSIS methods under fuzzy environment. *Expert systems with applications*, 36(4), pp. 8143-8151. Available at: https://doi.org/10.1016/j.eswa.2008.10.016

Dağıstanlı, H.A. 2025. Weapon System Selection for Capability-Based Defense Planning using Lanchester Models integrated with Fuzzy MCDM in Computer Assisted Military Experiment. *Knowledge and Decision Systems with Applications*, 1, pp. 11-23. Available at: https://doi.org/10.59543/kadsa.v1i.13601

Demir, G. 2025. Strategic Assessment of IoT Technologies in Healthcare: Grey MCDM Approach. *Spectrum of Decision Making and Applications*, 2 (1), pp. 376-389. Available at: https://doi.org/10.31181/sdmap21202528

Deng, H., Sun, X., Liu, M., Ye, C. & Zhou, X. 2016. Image enhancement based on intuitionistic fuzzy sets theory. *IET Image Processing*, 10 (10), pp. 701-709. Available at: https://doi.org/10.1049/iet-ipr.2016.0035

Ding, J., Si, G., Ma, J., Wang, Y. & Wang, Z. 2018. Mission evaluation: expert evaluation system for large-scale combat tasks of the weapon system of systems. *Science China Information Sciences*, 61, pp. 1-19. Available at: https://doi.org/10.1007/s11432-016-9071-5

Field A.P. 2005. Kendall's Coefficient of Concordance. In: Everitt, B.S. & Howell, D.C. (Eds.) Encyclopedia of Statistics in Behavioral Science, 2, pp.1010-1011. New York: Wiley [online]. Available at: https://discoveringstatistics.com/repository/kendall's_coefficient_of_concordance_ebs.pdf [Acessed: 23 March 2025]. ISBN: 978-0-470-86080-9

Huang, H. D., Lee, C. S., Wang, M. H. & Kao, H. Y. 2014. IT2FS-based ontology with soft-computing mechanism for malware behavior analysis. *Soft Computing*, *18*, pp. 267-284. Available at: https://doi.org/10.1007/s00500-013-1056-0

Jiang, J., Li, X., Zhou, Z. J., Xu, D. L. & Chen, Y. W. 2011. Weapon system capability assessment under uncertainty based on the evidential reasoning approach. *Expert Systems with Applications*, 38(11), 13773-13784. Available at: https://doi.org/10.1016/j.eswa.2011.04.179

Kahraman, C., Öztayşi, B., Sarı, İ. U. & Turanoğlu, E. 2014. Fuzzy analytic hierarchy process with interval type-2 fuzzy sets. *Knowledge-Based Systems*, 59, pp. 48-57. Available at: http://dx.doi.org/10.1016/j.knosys.2014.02.001

Karadayi, M.A., Ekinci, Y. & Tozan, H. 2019. A Fuzzy MCDM Framework for Weapon Systems Selection. In Tozan H. & Karatas M. (Eds.) *Operations Research for Military Organizations*, pp. 185-204. IGI Global Scientific Publishing. Avaliable at: https://doi.org/10.4018/978-1-5225-5513-1.ch009

Kiracı, K. & Akan, E. 2020. Aircraft selection by applying AHP and TOPSIS in interval type-2 fuzzy sets. Journal of Air Transport Management, 89, pp. 1-16. Available at: https://doi.org/10.1016/j.jairtraman.2020.101924

Kolour, H. R., Momayezi, V. & Momayezi, F. 2025. Enhancing Supplier Selection in Public Manufacturing: A Hybrid Multi-Criteria Decision-Making Approach. Spectrum of Decision Making and Applications, 3 (1), pp. 1-20. Available at: https://doi.org/10.31181/sdmap31202629

Lee, H. S., Tzeng, G. H., Yeih, W., Wang, Y. J. & Yang, S. C. 2013. Revised DEMATEL: resolving the infeasibility of DEMATEL. *Applied Mathematical Modelling*, 37(10-11), pp. 6746-6757. Available at: https://doi.org/10.1016/j.apm.2013.01.016

Liu, Y., Yin, H., Xia, B., Yu, D. & Chen, Y. H. 2024. Interval type-2 fuzzy set-theoretic control design for uncertain dynamical systems. *International Journal of Fuzzy Systems*, 26(3), pp. 1069-1087. Available at: https://doi.org/10.1007/s40815-023-01654-3

Mavris, D. & DeLaurentis, D.1995. An integrated approach to military aircraft selection and concept evaluation. In:the 1st AIAA Aircraft Engineering Technology, and Operations Congress, Los Angeles, CA, pp.1-11. September 19-21. Available at: https://doi.org/10.2514/6.1995-3921

Mehdiabadi, A., Sadeghi, A., Yazdi, A. K. & Tan, Y. 2025. Sustainability service chain capabilities in the oil and gas industry: a fuzzy hybrid approach swara-mabac. *Spectrum of Operational Research*, 2 (1), pp. 92-112. Available at: https://doi.org/10.31181/sor21202512

Pamučar, D. & Ćirović, G. 2015. The selection of transport and handling resources in logistics centers using Multi-Attributive Border Approximation area Comparison (MABAC). *Expert systems with applications*, 42(6), pp. 3016-3028. Available at: https://doi.org/10.1016/j.eswa.2014.11.057

Petrović, I. & Milenković, M. 2024. Improvement of the operations planning process using a hybridized fuzzy-multi-criteria decision-making approach. *Vojnotehnički glasnik/Military Technical Courier*, 72(3), pp. 1093-1119. Available at: https://doi.org/10.5937/vojtehg72-51473

Petrović, M. & Petrović, I. 2024. Optimization of the design of combat systems on the example of a short - range artillery-missile air defense system using the IT2FS-DEMATEL method. In:*SYM-OP-IS 2024: 51th International Symposium on Operational Research*, Tara, pp.433-438. September16-19. 2024. Available at: https://symopis2024.ftn.uns.ac.rs/wp-content/uploads/2024/11/SYM-OP-IS-2024_PROCEEDINGS_final.pdf

Sabaei, D., Erkoyuncu, J. & Roy, R. 2015. A Review of Multi-criteria Decision Making Methods for Enhanced Maintenance Delivery. *Procedia CIRP*, 37, pp.30-35. Available at: https://doi.org/10.1016/j.procir.2015.08.086

Shieh, J. I., & Wu, H. H. 2016. Measures of consistency for DEMATEL method. *Communications in Statistics-Simulation and Computation*, 45(3), pp. 781-790. Available at: https://doi.org/10.1080/03610918.2013.875564

Tekeli, M. M., Bal Besikci, E., Gul, M., Akyuz, E., & Arslan, O. 2024. Application of IT2Fs-AHP and TOPSIS modeling for performance analysis of tank coatings in chemical tankers. *Proceedings of the Institution of Mechanical Engineers, Part M: Journal of Engineering for the Maritime Environment*, 238 (3), pp. 622-632. Available at: https://doi.org/10.1177/14750902231194703

Tešić, T. & Božanić, D. 2023. Optimizing Military Decision-Making: Application of the FUCOM– EWAA–COPRAS-G MCDM Model. Acadlore *Transactions on Applied Mathematics and Statistics*, 1(3), pp.148-160. Available at: https://doi.org/10.56578/atams010303

Torkayesh, A. E., Tirkolaee, E. B., Bahrini, A., Pamucar, D., & Khakbaz, A. 2023. *A systematic literature review of MABAC method and applications: An outlook for sustainability and circularity. Informatica*, 34(2), pp. 415-448. Available at: https://doi.org/10.15388/23-INFOR511

Uçal Sary, I., Öztayşi, B., & Kahraman, C. 2013. Fuzzy analytic hierarchy process using type-2 fuzzy sets: An application to warehouse location selection. Multicriteria decision aid and artificial intelligence: Links, theory and applications, pp. 285-308. Available at: https://doi.org/10.1002/9781118522516.ch12

Yalçın, G. C., Kara, K., & Özyürek, H. 2025. Evaluating Financial Performance of Companies in the Borsa Istanbul Sustainability Index Using the CRITIC-MABAC Method. Spectrum of Operational Research, 2 (1), pp. 323-346. Available at: https://doi.org/10.31181/sor21202530

Zavadskas, E.K., Turskis, Z. & Kildienė, S. 2014. State of art surveys of overviews on MCDM/MADM methods. *Technological and Economic Development of Economy*, 20(1), pp.165-179. Available at: https://doi.org/10.3846/20294913.2014.892037

Optimización del proceso de diseño de sistemas de misiles de artillería tierra-aire de corto alcance utilizando el enfoque triangular híbrido IT2FS-DEMATEL-MABAC

Ivan B. Petrović, **autor de correspondencia**, *Milan* D. Petrović

Universidad de Defensa de Belgrado, Academia Militar, Belgrado, República de Serbia

CAMPO: matemáticas aplicadas, operational research, ciencias militares
TIPO DE ARTÍCULO: artículo científico original

Resumen:

Introducción/objetivo: La posibilidad de optimizar el proceso de diseño de un sistema de artillería-misil tierra-aire de corto alcance (SAAM de corto alcance) mediante la aplicación del enfoque híbrido de toma de decisiones multicriterio (integración de los métodos DEMATEL y MABAC) en entornos difusos de intervalo triangular tipo 2, se muestra en este artículo. Mediante el análisis del contenido de la literatura, se seleccionaron los requisitos y subrequisitos táctico-técnicos. Además, se determinaron los pesos de estos requisitos y subrequisitos. Posteriormente, se creó un modelo de toma de decisiones multicriterio (MCDM) para la evaluación de diferentes proyectos iniciales de diseño de un SAAM de corto alcance, que también se probó en este artículo.

Métodos: El enfoque propuesto, que combina los métodos DEMATEL y MABAC, se modificó mediante conjuntos difusos de intervalo triangular tipo 2 (IT2FS). El método triangular IT2F-DEMATEL se aplicó para determinar los pesos de los requisitos y subrequisitos, mientras que el método triangular IT2FS-MABAC se aplicó para evaluar las alternativas (diseños iniciales del proyecto de un SAAM de corto alcance).

Resultados: Integración del enfoque triangular múltiple IT2FS-MCDM en un modelo único que se puede aplicar en el proceso de definición del proyecto de diseño inicial óptimo de un SAAM de corto alcance.

Conclusión: El artículo contribuye a la ciencia militar en la toma de decisiones relacionadas con el diseño de un SAAM de corto alcance.

Palabras claves: DEMATEL, MABAC, conjuntos difusos de intervalo triangular tipo 2, sistema de artillería y misiles tierra-aire de corto alcance.

Оптимизация процесса проектирования зенитно-ракетного комплекса малой дальности с использованием гибридного треугольного подхода IT2FS-DEMATEL-MABAC

Иван Б. Петрович, **корреспондент**, *Милан* Д. Петрович

Университет обороны в Белграде, Военная академия,
г. Белград, Республика Сербия

РУБРИКА ГРНТИ: 27.47.19 Исследование операций,
28.17.31 Моделирование процессов управления
ВИД СТАТЬИ: оригинальная научная статья

Резюме:

Введение/цель: В данной статье представлены возможности оптимизации процесса проектирования зенитно-ракетного комплекса малой дальности с помощью гибридного многокритериального подхода к принятию решений (интеграция методов DEMATEL и MABAC) в нечеткой среде с треугольным *интервалом второго типа. Контент-анализ использовался для выбора тактических и технических требований и задач. В статье расставлены приоритеты требований, определены их весовые коэффициенты, а также разработана многокритериальная модель принятия решений (МКМПР) для оценки первоначальных проектов зенитно-ракетного комплекса противовоздушной обороны малой дальности. В статье также представлены результаты тестирования данной модели.*

Методы: Предложенный подход, сочетающий методы DEMATEL и MABAC, модифицирован с помощью нечетких множеств с треугольным интервалом второго типа (IT2FS). Треугольный метод IT2F-DEMATEL был применен для определения весовых коэффициентов требований и задач, а треугольный метод IT2FS-MABAC был применен для оценки альтернатив первоначальных проектных решений зенитно-ракетного комплекса малой дальности.

Результаты: Интеграция множественного треугольного подхода IT2FS-MCDM в единую модель, которая может применяться в процессе определения оптимального первоначального проекта зенитно-ракетного комплекса малой дальности.

Вывод: Данная статья вносит вклад в развитие военной науки в области принятия решений, связанных с разработкой зенитно-ракетного комплекса малой дальности.

Ключевые слова: DEMATEL, MABAC, нечеткие множества с треугольным интервалом второго типа, зенитно-ракетный комплекс малой дальности.

Оптимизација процеса дизајнирања артиљеријско-ракетног система за противваздухопловна дејства применом хибридног троугластог приступа ИТ2ФС-ДЕМАТЕЛ-МАБАК

Иван Б. Петровић, **аутор за преписку**, *Милан* Д. Петровић
Универзитет одбране у Београду, Војна академија

ОБЛАСТ: примењена математика, операциона истраживања, војне науке
КАТЕГОРИЈА (ТИП) ЧЛАНКА: оригинални научни рад

Сажетак:

Увод/циљ: У раду је приказана могућност оптимизације процеса дизајнирања артиљеријско-ракетног система за противваздухопловна дејства малог домета применом хибридног вишекритеријумског (интеграцијом метода ДЕМАТЕЛ и МАБАК) приступа у одлучивању у троугластом интервалном фази окружењу типа 2. Анализом садржаја извршена је селекција *тактичко-техничких захтева и подзахтева. Такође, обављена је приоритетизација захтева, одређене су релативне тежине захтева и подзахтева и креиран вишекритеријумски модел одлучивања (ВКО модел) за евалуацију почетних пројеката дизајнирања артиљеријско-ракетног система за противваздухопловна дејства малог домета. Извршено је и тестирање модела.*

Методе: Предложен модел ВКО комбинује методе ДЕМАТЕЛ и МАБАК модифковане помоћу троугластих интервалних фази скупова типа 2 (ИТ2ФС). Троугласти метод ИТ2ФС-ДЕМАТЕЛ примењен је за одређивање тежине захтева и подзахтева, док је троугласта метода ИТ2ФС-МАБАК примењена за евалуацију алтернатива – почетне пројектне документације за дизајнирање артиљеријско- ракетног система за противваздухопловна дејства малог домета.

Резултати: Интегрисање вишеструког ВКО приступа заснованог на троугластим ИТ2ФС у јединствени модел може се применити у процесу дефинисања оптималне почетне пројектне документације за дизајнирање артиљеријско-ракетног система за противваздухопловна дејства малог домета.

Закључак: Рад доприноси војној науци приликом доношења одлука у процесу дизајнирања артиљеријско-ракетног система за противваздухопловна дејства малог домета.

Кључне речи: ДЕМАТЕЛ, МАБАК, троугласти интервални фази скупови типа 2, артиљеријско-ракетни систем малог домета.

Paper received on: 04.03.2025.
Manuscript corrections submitted on:20.03.2025.
Paper accepted for publishing on: 08.04.2025.

Selection of an airsoft rifle for urban combat using the hybrid multi-criteria decision-making model Borda-AHP-SAW and Entropy-CRITIC-FanMa-SAW

Aleksandar R. Aleksić[a], *Miša* D. Živković[b], *Damir* M. Projović[c], *Milorad* M. Petronijević[d], *Darko* I. Božanić[e]

[a] University of Defense in Belgrade, Military Academy, Department of Tactics with Weapon Systems, Belgrade, Republic of Serbia,
e-mail: aleksic.aleksandar1004@gmail.com
ORCID iD: https://orcid.org/0000-0003-1103-8410

[b] University of Defense in Belgrade, Military Academy, Department of Tactics with Weapon Systems, Belgrade, Republic of Serbia,
e-mail: zivkovic.misa@yahoo.com
ORCID iD: https://orcid.org/0009-0007-1918-4259

[c] University of Defense in Belgrade, Military Academy, Department of Command and Leadership, Belgrade, Republic of Serbia,
e-mail: Damirpro@yahoo.com
ORCID iD: https://orcid.org/0000-0002-6285-3485

[d] University of Defense in Belgrade, Military Academy, Department of Tactics with Weapon Systems, Belgrade, Republic of Serbia,
e-mail: petronijevicm@hotmail.rs
ORCID iD: https://orcid.org/0009-0003-0018-1729

[e] University of Defense in Belgrade, Military Academy, Department of Tactics with Weapon Systems, Belgrade, Republic of Serbia,
e-mail: dbozanic@yahoo.com
ORCID iD: https://orcid.org/0000-0002-9657-0889

doi https://doi.org/10.5937/vojtehg73-57771

FIELD: applied mathematics, mechanical engineering, military sciences (tactics with weapons systems)
ARTICLE TYPE: original scientific paper

Summary:

Introduction/purpose: The paper presents the application of multi-criteria decision-making methods in order to select an airsoft replica of an automatic rifle for practicing tactical actions in urban combat. First, experts ranked the criteria according to which alternatives would be selected. By applying the Borda and AHP methods, the weighting coefficients of the criteria were determined, and then the most favorable alternative was selected by applying the SAW method. The selection procedure was repeated when the selection was made without experts, but the weighting coefficients of the criteria were determined by the objective Entropy, CRITIC, and FanMa methods and a comparative analysis of the results was performed. The aim of the paper is to select the most effective airsoft rifle for professional and civilian use for practicing tactical actions and actions in urban combat by combining multi-criteria decision-making methods. Minimal resource consumption is always the starting point today, while ensuring the most efficient way to practice tactical actions that are as close as possible to real conditions.

Methods: For the first time, the method of determining the weighting coefficients of criteria using multidisciplinary methods of multi-criteria decision making on a specific problem in the field of tactics with weapons systems was shown with expert opinion, and then the results were compared when experts were not engaged. The experts in the field of Tactics and Weapons from the Military Academy first selected and ranked seven criteria. Then, their opinions were refined using the Borda method, and the results were entered into the AHP method to select the weighting coefficients of the criteria. Finally, the most favorable alternative was selected based on the SAW method. Since the above procedure for determining the weighting coefficients of the criteria was calculated for the first time by engaging experts in this way, the procedure for selecting the most favorable alternative was repeated without engaging experts, but the weights of the criteria were determined using objective methods and the results were compared through comparative analysis. The alternatives are five airsoft rifles with a hopup chamber, some of which are used at the Military Academy and in special army units for training in various combat-tactical actions, while in civilian life they are used by airsoft weapon enthusiasts.

Results: The most affordable airsoft rifle was chosen to provide minimum resource consumption with maximum performance and bring the greatest possible realism to combat situations when practicing tactical actions in urban environment.

Conclusion: The solution, with a comparative analysis of the results obtained in two ways, takes into account the simultaneous optimization of seven criteria which differ slightly, in order to select the most effective airsoft rifle for practicing tactical procedures in order to provide conditions that are closest to real combat situations at short distances.

Key words: airsoft rifle, selection, Borda, AHP, SAW, Entropy, CRITIC, FanMa method.

Introduction

With the advent of airsoft guns with adjustable hopup chambers that improve the flight characteristics of their projectiles, many "games" have replaced paintball weapons with the newly appeared ones. Paintball weapons rarely found their place in defense system units, except for some countries (Константинов & Шохирев, 2023), while the emergence of airsoft weapons has almost supplanted the use of classic weapons in military units (Lee et al, 2023) and police units (Martinez, 2008) for practicing certain tactical actions and playing out different situations in urban environments through different concepts (Dustin & Firmansyah, 2023; Putra et al, 2024; Lisboa & de Moraes, 2025), in closed spaces, underground installations, etc. In appearance, airsoft replicas are identical to classic weapons, and only good experts in weapons, at a closer distance of a few meters, can notice the differences, which is the goal of manufacturers of this type of weapon, regardless of the country of production (Menet & Szarucki, 2020).

There are many works in the literature on the selection of military equipment or fighters using multi-criteria decision making, for example, for: choosing an assault rifle, Radovanović et al, (2024); weapon selection, Dağdeviren et al, (2009); fighter optimal, Suo et al, (2025); framework for armed unmanned aerial vehicles, Keleş (2024); evaluating military tanks, Genc (2015); a multi-criteria decision-making approach for equipment evaluation, Guan et al, (2024); selection of vehicles, Araujo et al, (2023); selection of fighter aircraft, Rajurkar et al, (2023); optimising assault boat selection for military operations, Tešić et al, (2023a); weapon system selection, Dağıstanlı, (2025); and pontoon bridge selection, Tešić et al, (2023b). An analysis of domestic literature does not reveal many works on the topic of airsoft weapons, while in foreign literature there are studies not only about this type of weapon but also about injuries caused by it (Endo et al, 2001; Strong & Coady 2014; Pratama & Aryanto, 2024). The advantages of airsoft over paintball for civilian use and classic weapons for defensive use are many. Unlike with classic weapons, the shot is almost silent and can be used near settlements, while the use of maneuver ammunition for practicing tactical actions is generally prohibited near settlements and even in military and police facilities. The noise level generated by shooting airsoft weapons indoors is negligible and protects the hearing, unlike when firing a maneuver bullet. Maintaining airsoft weapons after using pellets is much simpler compared to using a dummy bullet with classic weapons and paint with paintball. There is less mass of ammunition and less environmental pollution from pellets compared to the combustion products of gunpowder and metal (mainly brass or copper) shells that are not removed after use, as well as paint from using paintball ammunition. Pellets are cheaper than dummy bullets and paintball ammunition and cause less damage to the walls of buildings and surrounding areas. Among the disadvantages, it can be noted that wearing glasses, a mask and gloves is mandatory, i.e. every part of the body must be covered and the player must be dressed in several layers regardless of the weather conditions - a pellet hit in the body through clothing if an individual is lightly dressed is extremely painful, depending on the characteristics of the weapon. For civilian use, the key difference between paintball and airsoft weapons is that airsoft weapon users must be morally responsible and admit to being hit by a pellet instead of suffer pain and immorally continue playing, while a paintball hit with colored ammunition is easily noticeable. While taking these features into consideration in a wide range of airsoft weapon manufacturers, it is necessary to choose the most favorable one for a particular situation in which it is intended to be used.

The aim of this research is to find the most optimal solution from the five airsoft rifles offered, taking into account the specifics of the scientific field of Military Sciences - Tactics with Weapon Systems, by applying the multi-criteria optimization method. The solution is based on the sublimation of the opinions of the Military Academy experts in this field, who use this type of weapon in the training of cadets. They do not know multi-criteria decision-making methods, since these experts are not expected to be knowledgeable about multi-criteria decision making. The proposed methodology was introduced with the idea of bringing decision making down to the lowest infantry level in the army, down to the department commander, with the aim of accepting and using it in various situations of decision making at the lowest level, not only in the selection of equipment. Based on the criteria defined by the experts, the alternatives were selected. After that, the criteria were ranked using the Borda method and the weighting coefficients of the criteria were determined using the AHP method. This method was chosen to avoid matrix inconsistency when comparing criteria in pairs and because the experts were not familiar with multi-criteria decision-making methods. Then, the ranking of the alternatives was carried out using the SAW method and the most optimal alternative was selected. Instead of the Borda method, any other method of counting ranks could have been used. The SAW method was chosen as the oldest and simplest method for ranking alternatives, while the use of other methods is a suggestion for future research. The applied method of determining the weighting coefficients of the criteria was determined in the above manner for the first time in a paper and requires verification. It was carried out by determining the weighting coefficients of the criteria using three objective methods: Entropy, CRITIC, and FanMa, included in the SAW method, and then a comparative analysis of the results was performed using Spearman's rank correlation coefficient.

Problem description

Simulators, airsoft weapons and the use of drones will play an enviable role in the training of military and police units in the future, as well as in many other areas of life and work. Jokić et al, (2025) describe the development of a decision support system in the process of training soldiers. Airsoft weapons are a simulator of classic weapons that can be owned by every citizen of the Republic of Serbia over the age of sixteen. Airsoft weapons are constantly developing, reaching initial bullet speeds that are similar to those of a classic pistol, which requires stricter legal regulations. These velocities of 6 mm bullets were provided by the development of a hopup chamber that can be easily adjusted by the user depending on the external temperature and the age of the replica, and high-quality electric motors located in the rifle handle. The hopup chamber ensures the movement of the bullet along an inverted parabola at distances of up to 100 m. Aiming is done based on muscle memory and by observing the course of the ball trajectory, and of course, mechanical or various optical sights can be used for certain distances, depending on the chamber settings. Durable and quickly rechargeable lithium-polymer Li-Po batteries, which are additional equipment, ensure long-term operation of the device in extreme conditions, while charging takes about ten minutes. All these are data - criteria that are difficult to obtain by the manufacturer, but can only be demonstrated based on experience and prolonged use of the rifle.

In order for the research to be conducted properly, it is necessary to implement each step and phase with sufficient attention so that the results are valid - Figure 1.

Available criteria from manufacturers include mass, price, length of the replica and the barrel, power of the replica, initial bullet velocity, magazine capacity and battery capacity, etc. These known and available criteria were taken into consideration for the research along with the opinion of experts in the field of tactics with weapon systems.

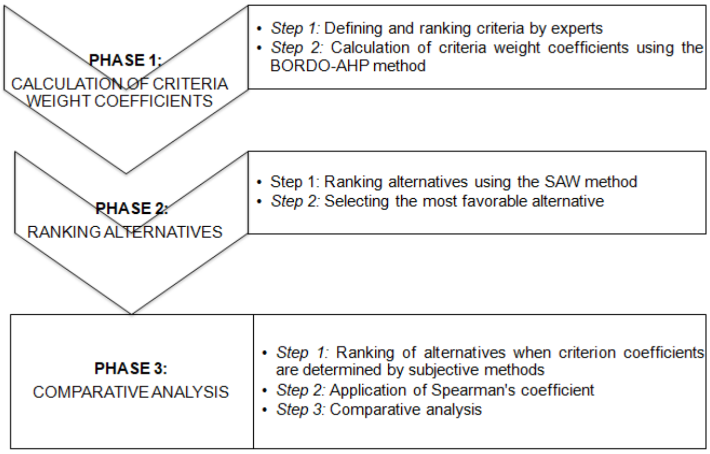

Figure 1- Phases and steps of the research

Hybrid multi-criteria decision-making models have already been applied in the field of military sciences, namely: Radovanović et al, (2023) DIBR-FUCOM-LMAW-Bonferroni-grey-EDAS model; Markatos & Pantelakis, (2023) holistic approach based on multi-criteria decision making for aircraft evaluation and comparison; Jokic et al, (2024) selection of calibers for weapons in the Serbian Army; Tešić et al, (2024) improvement of multi-criteria decision making using fuzzy logic; Ayvaz et al, (2024) integrated Fine-Kinney risk assessment model using Fermatean fuzzy AHP-WASPAS for occupational hazards in the aquaculture sector; Božanić et al, (2024) Fuzzy DIBR II-MABAC model for flood prevention; and Kress & MacKayetc (2025) Lanchester-type models for attritional warfare balance military casualties in two opposing forces.

Description of the methods used

The work will use the Borda group multi-criteria decision-making method, the AHP and SAW individual multi-criteria decision-making methods and the Entropy, CRITIC, and FanMa methods. The most sensitive part of the model is the definition of the weighting coefficients of the criteria, which is performed using the AHP method. There are a number of methods for defining the weighting coefficients of the criteria, which have certain advantages compared to the AHP method. Although the AHP method is one of the older methods of multi-criteria decision making, it has certain qualities that recommend it over others. The large number of criteria comparisons that exist in the AHP method, on the one hand, represents more laborious work for experts and analysts who process information, but on the other hand, it provides rich information from the comparison of criteria in pairs. In general, newer methods (such as BWM, LBWA, FUCOM, DIBR, and DIBR II) have a much smaller number of mutual comparisons of criteria, but they do not perform all mutual comparisons of criteria, but only a part. Considering that information is drawn from a smaller number of comparisons than when applying the AHP, it is also clear that the possibility of error in defining the weighting coefficients of the criteria in newer methods is much higher compared to the one involving the AHP. The mentioned, newer methods have defined techniques for checking consistency. That check is performed on the segment of pairwise comparisons, unlike with the AHP method where the consistency check is comprehensive.

Description of the Borda method of group reading

The Borda method is one of the oldest methods of group decision making, developed by the Frenchman Borda in 1781. It was widely used in the process of voting for the election of deputies in many countries of the world (Costa, 2017; Barberà et al, 2023; Saari, 2023). It can be used in its original form (Ilmiyah et al, 2023), and there are a number of modifications (Lin & Lin, 2023; Jones & Wilson, 2024; Biswas et al, 2025b). The basis of the method is to choose the alternative that in most cases was the first or tended to be the first one.

A matrix is formed in accordance with the rank of all decision makers, where the first column shows the rank of alternatives and the first row shows decision makers (Çalikoğlu & Łuczak, 2024). The second matrix is formed where the decision makers are in the left-wing column of the alternatives and in the first row, and the cells - fields of the matrix are filled by assigning the value 0 to the last ranked alternative for each decision maker, the second ranked alternative from the back the value 1 and the best placed alternative An the value n - 1. Finally, the vector W is obtained in the new right column where the values by rows are summarized. The best placed alternative - the most acceptable alternative is the one that has the highest value of the vector W.

Description of the AHP method

The Analytical Hierarchy Process method was developed by Thomas Saaty (1980). The method has undergone a large number of modifications, but in some cases it is still used in its original form both in individual and group decision making, Tešić et al, (2024), and is used in a large number of different decision-making cases. One of the most recent comprehensive surveys on recent modified and hybrid approaches to the AHP method can be read in Ashour & Mahdiyar (2024). Here, a modification will be presented for the first time, where instead of the classic Saaty scale, a scale derived from the Borda method is used.

A matrix with n rows and columns of criteria is formed and filled first along the unit diagonal because the criterion is compared with itself and then the newly introduced scale is used while respecting the filling below the diagonal based on the formula:

$$a_{ij} = 1 / a_{ji} \tag{1}$$

The value above the diagonal is filled while the opposite cell is the reciprocal of the filled value, otherwise the matrix will not be consistent. There are many works on modifications and scales of the AHP method, one of which is (Shageev, 2022). When filling the matrix from the upper side of the diagonal, the following should be observed - the value of the normalized initial vector from the Borda method is subtracted - from the criterion vector in the row, subtract the criterion vector in the column. In the case of a negative value, enter the reciprocal of the positive value using the formula:

$$- a_{ij} = 1 / a_{ij} \tag{2}$$

The next step is to sum the column values. A new matrix of n*n criteria is formed, the cells of which are filled as the quotient of the cell of the previous matrix with the divisor of the sum by type of the previous matrix. Finally, the columns are summed and the obtained values represent the weight coefficients of the criteria and their sum must be 1.

The next step is to calculate the consistency ratio of the CR matrix, which must be less than 0.1.

$$CR = CI / RI \tag{3}$$

where CI is the consistency index

$$CI = (\lambda max - n) / (n-1) \tag{4}$$

and RI is a random index according to Saaty and depends on the number of criteria and is taken from the table (in this case it is 4 criteria, i.e., 0.9); λmax is its own value which is calculated in accordance with the formula for each criterion

$$\lambda max = (Aw^*w) / w^*w \tag{5}$$

A is the criteria comparison matrix.

Table 1 – Random index by Saati

n	3	4	5	6	7	8	9	10
RI	0.58	0.9	1.12	1.24	1.32	1.41	1.45	1.49

The matrix is multiplied by the vector by multiplying W by each row-row cell and summing the products. If the consistency ratio (CR) is greater than 0.1, the criteria matrix is inconsistent and it is necessary to check the comparisons or change the method. The closer CR is to 0, the more consistent the matrix is, and one goes to the initial - main matrix.

Then the weighted sum is calculated for all alternatives, by multiplying the matrix by W. This is done by writing W below the alternatives and adding the product of the cells of the matrix and the vector W. In this way, the cells of the alternatives are joined. Again, the number of columns is 1. By comparing the numbers, the most favorable alternative is reached. The higher the value, the more acceptable the alternative.

The AHP method for ranking most often uses the Saaty scale. The scale used in the paper differs from the Saaty scale in that it is derived from counting the ranks of criteria ranked by experts. Therefore, the scale may have a larger or smaller interval than the Saaty scale, depending on the ranking of the criteria by experts and the number of experts. If all experts rate a criterion as the least important, the scale will have a large range. If all experts rate one criterion as the most important, the Borda method is unusable because the value of one criterion cannot be 0, nor can two criteria have the same rank. In these cases, the presented method is unusable. In order for the scale to start from 1, all criteria are divided by the weight of the criterion that is best ranked by experts. So the ratio of the best ranked criterion to the worst ranked criterion can vary within the limits of maximum d*c-1 where d is the number of experts and c is the number of criteria.

Description of the SAW method

Simple Additive Weighting is one of the oldest and simplest methods for ranking alternatives (Churchman & Ackoff, 1954). Many modern methods have found their footing in it, and the results obtained are approximately the same. It is used in both natural and social sciences in hybridization with another method to determine the weights of criteria. In scientific papers it has been compared with other methods or used independently (Lubis et al, 2021; Ciardiello & Genovese, 2023; Stević et al, 2024; Wang et al, 2024; Susilo & Wahyuni, 2024; Briscilla & Sundarrajan, 2024; Eti & Yüksel, 2024).

It is easy to use and in the first step gives the researcher the freedom to use any formula for normalizing the initial decision matrix. In this case, vector normalization was used according to the formulas for:

a) benefit criteria

$$n_{ij} = \frac{f_{ij}}{\sqrt{\sum_{i=1}^{m} f_{ij}^2}} \tag{6}$$

b) cost criteria

$$n_{ij} = 1 - \frac{f_{ij}}{\sqrt{\sum_{i=1}^{m} f_{ij}^2}} \tag{7}$$

where: f_{ij} – cell of the initial decision matrix; n_{ij} – normalized matrix cell; m – number of alternatives; j – number of criteria.

The next step is to weight the normalized matrix by multiplying each cell with a weighting coefficient for that criterion obtained by some other method.

$$o_{ij} = n_{ij} * w_i \tag{8}$$

Finally, in the third step, the cells are summed by type and the total weight value for each alternative is obtained. The sum of all alternative weights is 1. The most optimal alternative is the alternative with the highest sum value.

Description of the Entropy, CRITIC, and FanMa method

When the weighting coefficients of the criteria are determined based on the objective methods: Entropy (Srđević et al, 2003), CRITIC (Diakoulaki et al, 1995), and FanMa method (Srđević, 2005).

Entropy is a method that has been used in various forms since ancient times in natural sciences (Jaynes, 1982; Sakata & Sato, 1990). Since the beginning of this century, it has also appeared in many works in social sciences (Abbas, 2003, 2006; Sun et al, 2023; Basilio et al, 2023; Shanmugapriya et al, 2024; Ali et al, 2024). In social sciences, it is used to determine the weights of criteria in combination with other methods when ranking alternatives (Kizielewicz & Sałabun, 2025). It is based on the use of the natural logarithm ln. The calculation is the same for benefit and cost criteria (Žižović & Albijanić, 2025). The initial matrix has numerical values where the rows represent alternatives and the columns represent criteria (Biswas et al, 2025a). First, the decision matrix is normalized by filling the cells of the normalized matrix by dividing the cell of the initial matrix by the sum of the cells of the matrix by the columns-criteria. The next step is to calculate the entropy of the coefficient according to the formula:

$$e_j = -k\sum_{i=1}^{n} r_{ij} \ln r_{ij} \tag{9}$$

where: e_j – entropy of the criterion coefficient, κ – coefficient obtained as the reciprocal of the natural logarithm of the number of alternatives, in this case ln 5; r_{ij} – normalized matrix cell, and n – number of alternatives. In the next step, the degree of divergence of the criteria is calculated by subtracting e_j. from 1. Finally, the divergence is normalized by dividing the divergence of one criterion by the sum of the divergences of all criteria, thus obtaining w_i. the weighting coefficient of the criterion.

CRITIC is also a method by which the weighting coefficients of criteria can be determined objectively based on mathematical calculations. It appears in works of domestic and foreign authors (Diakoulaki et al, 1995; Zhong et al, 2023; Krishnan, 2024; Kim et al, 2024). Unlike the previous method, when normalizing the matrix, it is necessary to pay attention to benefit and cost criteria (Mallick et al, 2023; Yalçın et al, 2025). For benefit criteria, it is calculated by subtracting the minimum value of the column for that criterion from the matrix cell and dividing it by the difference between the maximum and minimum values (Basuri et al, 2025). While for cost criteria, the value of the cell of the initial matrix is subtracted from the maximum value per column and the value is divided by the difference between the maximum and minimum values per column - criterion. Then, the standard deviation of the coefficients per column is calculated. The next step is to form a matrix of linear correlation coefficients, where each coefficient is compared with each other, where the value 1 is obtained along the diagonals of the matrix, and below and above the diagonal are the same values and they can be negative. The next matrix is formed by subtracting the value of the cell of the previous matrix from the number 1, thus avoiding negative cell values. Then the column values are summed and the sum is multiplied by the linear correlation coefficient. Finally, the criterion weighting coefficient value is obtained when the previous sum value is divided by the column sum for all coefficients.

The FanMa method is an objective method for determining the weight coefficients of criteria based on mathematical calculations. Although the calculations are simpler, it is less commonly used than the previous two methods (Krstic et al, 2015; Petrovic et al, 2024). As with the previously described method, matrix normalization is performed, for benefit criteria it is calculated by subtracting the minimum column value for that criterion from the matrix cell and dividing it by the difference between the maximum and minimum column values, and for cost criteria the value of the initial matrix cell is subtracted from the maximum value per column and the value is divided by the difference between the maximum and minimum values per column – criterion. Then the weighting coefficient is calculated by the formula:

$$w_j^* = \frac{1}{\left[\sum_{i=1}^{n}\left(x_j^* - x_{ij}\right)^2\right]\left[\sum_{j=1}^{m}\frac{1}{\sum_{i=1}^{n}\left(x_j^* - x_{ij}\right)^2}\right]} \tag{10}$$

where x^*_j is the maximum criteria value per column and the sum is always 1, x_{ij} represents the coefficient values for each alternative, and j is the number of criteria.

Description of the criteria and the alternatives

The seven numerical criteria (three of which are cost and four are benefit, based on which the alternatives will be ranked) are as follows:

- C1 - length of the rifle barrel in **mm;**
- C2 - length of the rifle in the combat position in **mm;**
- C3 - initial velocity of the bullet expressed in **m/s;**
- C4 - price in **eur**;
- C5 - rifle power depending on the hopup chamber in **J**;
- C6 - frame capacity in pieces of bullets (**pcs**), and
- К7 - mass in **kg**.

The five alternatives that were selected according to the available criteria proposed by experts are given in Figure 2.

The use of classic weapon maneuver ammunition in urban combat does not have the target impact effect, and, since the sound created by firing a maneuver bullet requires the use of earmuffs, they jeopardize the ability to maintain communication and, consequently, command. The reality of the situation refers to the elimination of soldiers from combat, which would be done in a real situation by a live ammunition hit. On the other hand, when an airsoft rifle projectile with criteria aggregated and ranked by experts (3- initial bullet velocity; 2- barrel length that provides the previous one; 6- frame capacity that does not require constant replacement during use) hits another soldier, the pain will force him to admit that he has been hit and force him to abandon the fight, i.e. he will be thrown out of the fight.

Figure 2: Five airsoft guns as alternatives

Prices of alternatives vary from seller to seller. In this paper, prices are taken from the same domestic website in Serbia and converted into euros, to avoid discrepancies between the price of the replica and the data.

Table 2 – Criteria values for alternatives

Alternatives/ C		C1	C2	C3	C4	C5	C6	C7
A1	BT5 A5	229	735	100	221	1	200	1.9
A2	SLV36	247	500	100	213	1	470	2.85
A3	M15A4	372	850	95	195	0.9	300	2.15
A4	SA M7 W	445	870	95	255	0.9	600	2.98
A5	Cyma 077	455	940	120	340	1.7	600	3.42

Other criteria are also publicly available from manufacturers and sellers themselves and everything except the power of the replica can be checked by the user after purchase. Of course, they are dependent on each other, so the power of the replica affects the range of the bullet. All automatic rifles use the same 6 mm diameter bullet, weighing 2 g, the so-called twenty, which can be of different colors and is mostly white, so this information is not taken as a criterion.

Ranking results

The criteria available for airsoft weapons were ranked by the experts from the Military Academy, professors who teach cadets specified types of weapons, and operators who have maintained rifles for a longer period. They develop tactical and technical requirements and make proposals to the Military Academy on weapon purchase; this work will be one of the guidelines for the procurement of the next range of rifles. In order to verify the results of the experts, objective methods were also used, and two of the three give identical results as the ranking by the experts.

First, five experts in the field of Military Sciences from the Military Academy ranked the seven criteria as given in Table 3.

Table 3 – Ranking of the alternatives according to the time criterion

Rang	E1	E2	E3	E4	E5
1	C5	C1	C5	C4	C5
2	C1	C4	C1	C1	C4
3	C7	C7	C6	C7	C1
4	C4	C5	C7	C5	C7
5	C6	C2	C4	C6	C6
6	C3	C3	C3	C2	C3
7	C2	C6	C2	C3	C2

To determine the scale for the AHP method using the Borda method, the expert ratings were entered into a table, summed by type, and all cells divided by 9, as this was the lowest weight, as shown in the table. A problem for the above implementation may arise if two criterion weights are equally important. In that case, use another method of determining criterion weights.

Table 4 – Determining the weight coefficient by the Borda method

C / E	E1	E2	E3	E4	E5	WB	RANG	WB/5
C1	1	0	1	1	2	5	7	1
C2	6	4	6	5	6	27	1	5.4
C3	5	5	5	6	5	26	2	5.2
C4	3	1	4	0	1	9	5	1.8
C5	0	3	0	3	0	6	6	1.2
C6	4	6	2	4	4	20	3	4
C7	2	2	3	2	3	12	4	2.4

In the event that all experts have selected one criterion as the most important or that two criteria are of the same rank, the proposed method is unusable and then it is preferable to use the classical AHP method with the Saaty scale or some of the other subjective methods for selecting criterion coefficients such as BVM, LBVA, FUCOM and DIBR I and II which have fewer steps compared to the AHP.

These results were used for the scale used in the AHP method in accordance with 1 and 2 and the following criteria comparison table was obtained.

Table 5 – Initial matrix of the criteria rankings

C	C1	C2	C3	C4	C5	C6	C7
C1	1	0.2273	0.2381	1.25	5	0.3333	0.7143
C2	4.4	1	0.2	3.6	4.2	1.4	3
C3	4.2	5	1	3.4	4	1.2	2.8
C4	0.8	0.2778	0.2941	1	0.6	0.4545	1.6667
C5	0.2	0.2381	0.2500	1.6667	1	0.3571	0.8333
C6	3	0.7143	0.8333	0.6	2.8	1	1.6
C7	1.4	0.3333	0.3571	0.6	1.2	0.625	1

Based on the normalization of the previous matrix and further summarization by types, the weighting coefficients of the criteria in Table 4 were obtained.

Table 6 – Ranking of the alternatives according to the criterion weight

w1	w2	w3	w4	w5	w6	w7
0.0948	0.2178	0.3136	0.0749	0.0645	0.1538	0.0806

Now it is necessary to check the consistency of the matrix and the consistency ratio CR (3, 4, 5). It can be concluded that CR=0.095, which is less than 0.1, meaning the matrix is consistent, and the coefficients are then ranked using the same procedure.

When the weighting coefficients of the criteria from Table 6 and the data from Table 2 are entered into the SAW method, by applying formulas 6, 7 and 8, the following rank is obtained.

Table 7 – Final ranking of the alternatives with the SAW method

A1	0.4070	5.
A2	0.4350	2.
A3	0.4112	4.
A4	0.4266	3.
A5	0.4401	1.

Therefore, the best ranked alternative is A5. In order to check the procedure and for small deviations in the weights on the basis of which the alternatives are ranked, it is necessary to perform a sensitivity analysis or some other method. Here, the alternatives will be ranked using the same method when the criteria are determined on the basis of subjective methods.

The best ranked alternative is the most expensive, if the price is considered. Since the material base is always the desired minimized criterion (Karel & Plašil, 2024), if this criterion were reduced and its reduction distributed to the other criteria, there would be no change in the rankings. Considering the qualities and advantages of the other criteria that are important for close urban combat, despite the highest price, this alternative was selected as the most favorable.

Comparative analysis

The weighting coefficients of the criteria were determined by simple counting - using the Borda group decision-making method that uses an ordinal scale. Since the experts were not required to do so, and therefore the relationship between the two criteria was not taken into account, the question arises whether the method is valid and verification is necessary. In order to verify the reliability of the procedure for determining the weighting coefficients of the criteria using the Borda and AHP methods, an analysis was performed based on a comparison of the ranks of alternatives when objective methods for determining the weights of the criteria were applied.

When the data from Table 2 are included in the three objective methods (Entropy, CRITIC and FanMa) for calculating the criterion coefficients, they amount to

Table 7 – Rank and size of the criteria with the objective methods

Method / C	C1	C2	C3	C4	C5	C6	C7
Entropy	0.1799 2	0.0983 5	0.0185 7	0.0968 6	0.1590 3	0.3434 1	0.1040 4
CRITIC	0.1559 2	0.1371 5	0.1251 7	0.1529 3	0.1279 6	0.1408 4	0.1602 1
FanMa	0.1505 4	0.2325 1	0.0910 6	0.1072 5	0.0845 7	0.1790 2	0.1553 3

If the ranking of criteria and their weighting coefficients for both the hybrid Borda-AHP method and the objective methods are presented graphically, it looks like this:

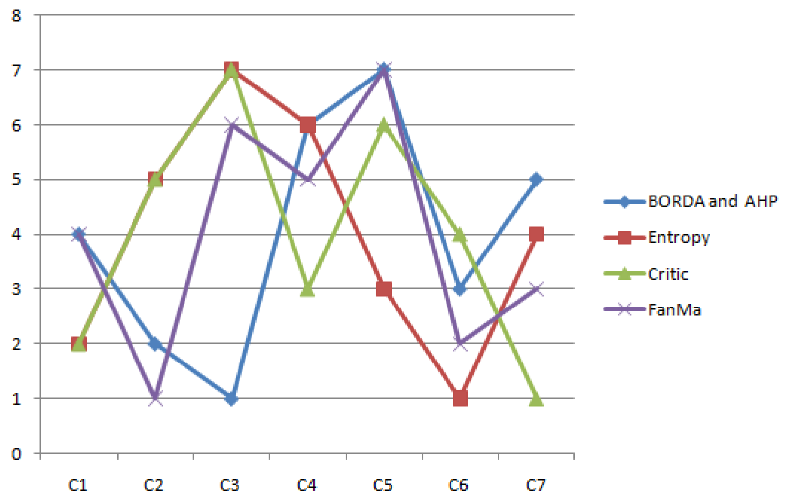

Figure 3: Graphical ranking of the criteria

The graph shows that the importance of the criteria varies from method to method. The C3 criterion, which represents the initial velocity of the projectile and is directly related to the C5, is the most important for experts, while subjective methods see it as the least important. The situation is similar with the C6, which represents the capacity of the frame, so the experts put it in third place because it can be replaced with a frame of a different capacity, while mathematical objective methods do not see this and Entropy puts it in first place. The C7 is also interesting, changing places from first to fifth depending on the method of determination. Then experts placed it in the fifth place, although it is important how much weight soldiers will carry with them, and yet airsoft rifles are lighter than real combat weapons.

If the coefficients obtained by the objective methods are entered into the SAW method, the following ranks with their weights are obtained.

Table 8 – Rank and weights of the alternative choices when the coefficient weights are calculated using different methods

A/Method	Borda/AHP		Entropy		CRITIC		FanMa	
A1	0.4070	5	0.33602	5	0.45501	5	0.4790	5
A2	0.4350	2	0.37974	3	0.47196	3	0.5065	1
A3	0.4112	4	0.36069	4	0.46689	4	0.4896	4
A4	0.4266	3	0.40394	2	0.47467	2	0.5045	3
A5	0.4401	1	0.41707	1	0.48193	1	0.5054	2

Table 8 shows that the last ranked alternative A1 and the second to the last ranked alternative A3 are the same in all four cases. The alternative A5 is in the first place three times, while when the weighting coefficients of the criteria are selected using the FanMa method, it is in the second place. It is also observed in the FanMa method that the difference in weight between the first alternative and the second one is small, only 0.009. The A2 can be said to be a critical alternative for some reason because it changes ranks from method to method, from the first to the third, so it is necessary to deal with it more in a deeper sensitivity analysis, e.g. by reducing the most significant criterion or the least significant one at the expense of the others, which is a suggestion for future research. It is probably because of these deviations that it is used less in works. This is shown graphically in Figure 4.

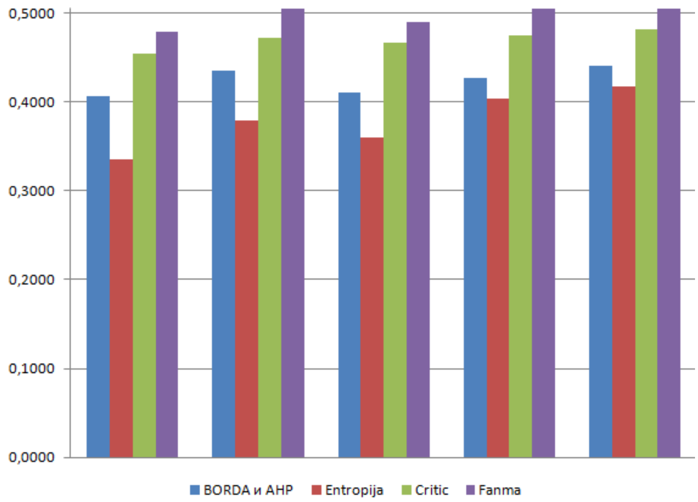

Figure 4: Graphical representation of the rank of the alternatives when coefficient weights are determined by different methods

Spearman's rank correlation coefficient is very useful for analyzing the obtained ranks (Wardany & Zahedi, 2024). If Spearman's rank correlation coefficient is used, it is calculated using the formula:

$$S = 1 - \frac{6\sum_{i=1}^{n} D_i^2}{n(n^2-1)} \qquad (11).$$

where D is the difference in ranks and n is the number of sample members.

If the starting point is the ranks obtained by the SAV method, it looks like this:

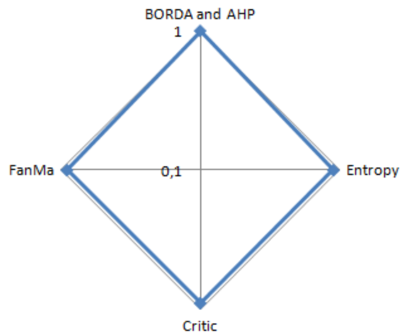

Figure 5: Spearman's rank correlation coefficient of the alternatives

Spearman's coefficient shows (1; 0.9; 0.9; 0.9) a very high correlation between the ranks of the alternatives, although the A2 shows a deviation of two ranks. Since in three out of four cases the A5 is the first-ranked alternative, it is also the best solution for purchasing an airsoft rifle for urban combat and practicing close-range combat actions.

Conclusion

Based on previous research in the field of multi-criteria decision making in the field of military sciences, one of hybrid decision-making models is presented and a new methodology for calculating the weighting coefficients of criteria is proposed. Based on the experts' proposals, the criteria were selected, and based on them, alternatives were found. By applying the hybrid model of three multi-criteria decision-making methods, the weighting coefficients of the criteria were first determined using the Borda-AHP model, then five alternatives were ranked using the SAW method, and the most favorable one was selected. Based on the analysis of the factual situation, airsoft rifles are already in use in military units for these purposes. The proposed model is in accordance with the opinion of the five experts who teach Tactics with Weapon Systems at the Military Academy. The proposed method for ranking and selecting airsoft weapons will serve experts in purchasing a new quantity of rifles for the needs of the Military Academy. It can also be used by other structures for the acquisition of other types of equipment, subject to restrictions. The rifle selected in this way with the above criteria is best for close distances in urban combat as well as for combat in underground installations, which are topics studied at the third and fourth year of the Infantry Module. The rifle can also be used for various demonstrations of close urban combat implemented by special army units and the Military Academy. The rifle selected in this way with the most significant weighting coefficient and initial bullet velocity has the appropriate accuracy of hitting the target at longer distances and over 50 m; it is more effective compared to other rifles and can be used at longer distances.

The presented method of selecting weighting coefficients, which is an innovation in multi-criteria decision making, has yielded results in this case. A problem may arise if two criteria in the Borda method have the same rank, and it is necessary to further improve it and adapt it to the specific situation. A comparative analysis has shown that the proposed model for determining the weighting coefficients of criteria is valid and one of the ways of determining the weights of criteria is given when experts are not familiar with the methods of multi-criteria decision making, which is also a contribution to the methodology of multi-criteria decision making. Also, the weights of criteria that vary depending on the method of determination did not greatly affect the rank of alternatives. The presented model can be further improved by examining and checking the ranking through other methods for ranking criteria and alternatives. It can also be checked and compared using the Saaty scale. A more detailed sensitivity analysis can be performed by gradually reducing the number of criteria or eliminating a criterion. The presented method of determining the weights of criteria based on a simple ranking of them by experts, which was applied for the first time, showed satisfactory results in sensitivity analysis. It is necessary to further develop and upgrade it and examine its application in combination with other methods. Based on the research, it can be concluded that the existing method of defining the weighting coefficients of criteria is very simple to calculate, especially with a large number of criteria and does not require knowledge of multi-criteria decision-making methods by experts. It can also be undoubtedly concluded that the aforementioned methodology can be used in other situations when choosing new weapons and military equipment.

References

Abbas, A. E. 2003. Entropy methods for univariate distributions in decision analysis. In AIP Conference Proceedings (Vol. 659, No. 1, pp. 339-349). *American Institute of Physics*. Available at: https://doi.org/10.1063/1.1570551

Abbas, A. E. 2006. Entropy methods for joint distributions in decision analysis. *IEEE Transactions on Engineering Management*, 53(1), 146-159. Available at: https://doi.org/10.1109/TEM.2005.861803

Ali, S. I., Lalji, S. M., Haider, S. A., Haneef, J., Husain, N., Yahya, A., ... & Arfeen, Z. A. 2024. Risk prioritization in a core preparation experiment using fuzzy

VIKOR integrated with Shannon entropy method. *Ain Shams Engineering Journal*, 15(2), 102421. Available at: https://doi.org/10.1016/j.asej.2023.102421

Araujo, J. V. G. A., Moreira, M. Â. L., Gomes, C. F. S., dos Santos, M., de Araújo Costa, I. P., de Pina Corriça, J. V., ... & de Moura Pereira, D. A. 2023. Selection of a vehicle for Brazilian Navy using the multi-criteria method to support decision-making TOPSIS-M. *Procedia Computer Science*, 221, 261-268. Available at: https://doi.org/10.1016/j.procs.2023.07.036

Ashour, M., & Mahdiyar, A. 2024. A comprehensive state-of-the-art survey on the recent modified and hybrid analytic hierarchy process approaches. *Applied Soft Computing*, 150, 111014. Available at: https://doi.org/10.1016/j.asoc.2023.111014

Ayvaz, B., Tatar, V., Sağır, Z., & Pamucar, D. 2024. An integrated Fine-Kinney risk assessment model utilizing Fermatean fuzzy AHP-WASPAS for occupational hazards in the aquaculture sector. *Process Safety and Environmental Protection*, 186, 232-251. Available at: https://doi.org/10.1016/j.psep.2024.04.025

Barberà, S., Bossert, W. & Moreno-Ternero, J.D. 2023. Wine rankings and the Borda method. *Journal of Wine Economics*, 18(2), pp.122-138. Available at: https://doi.org/10.1017/jwe.2023.7

Basilio, M. P., Pereira, V., & Yigit, F. 2023. New hybrid EC-promethee method with multiple iterations of random weight ranges: applied to the choice of policing strategies. *Mathematics*, 11(21), 4432. Available at: https://doi.org/10.3390/math11214432

Basuri, T., Gazi, K. H., Bhaduri, P., Das, S. G., & Mondal, S. P. 2025. Decision-analytics-based Sustainable Location Problem - Neutrosophic CRITIC-COPRAS Assessment Model. *Management Science Advances*, 2(1), 19-58. Available at: https://doi.org/10.31181/msa2120257

Biswas, A., Gazi, K. H., Bhaduri, P., & Mondal, S. P. 2025a. Site Selection for Girls Hostel in a University Campus by MCDM based Strategy. *Spectrum of Decision Making and Applications*, 2(1), 68-93. Available at: https://doi.org/10.31181/sdmap21202511

Biswas, S., Biswas, B., & Mitra, K. 2025b. A Novel Group Decision Making Model to Compare Online Shopping Platforms. *Spectrum of Decision Making and Applications*, 2(1), 1-27. Available at: https://doi.org/10.31181/sdmap2120259

Božanić, D., Borota, M., Štilić, A., Puška, A., & Milić, A. 2024. Fuzzy DIBR II-MABAC model for flood prevention: A case study of the river Veliki Rzav. *Journal of Decision Analytics and Intelligent Computing*, 4(1), 285-298. Available at: https://doi.org/10.31181/jdaic10031122024b

Briscilla, S. J., & Sundarrajan, R. 2024. A Multi-Criteria Decision Making for Employee Selection Using SAW and Profile Matching. *Journal of Advanced Computational Intelligence and Intelligent Informatics*, 28(5), 1117-1125. Available at: https://doi.org/10.20965/jaciii.2024.p1117

Çalikoğlu, C., & Łuczak, A. 2024. Multidimensional assessment of SDI and HDI using TOPSIS and bilinear ordering. *International Journal of Economic*

Sciences, 13(2), 116-128. Available at: https://doi.org/10.52950/ES.2024.13.2.007

Ciardiello, F., & Genovese, A. 2023. A comparison between TOPSIS and SAW methods. *Annals of Operations Research*, 325(2), 967-994. Available at: https://doi.org/10.1007/s10479-023-05339-w

Costa, H.G. 2017. AHP-De Borda: a hybrid multicriteria ranking method. *Brazilian Journal of Operations & Production Management*, 14(3), pp.281-287. Available at: https://doi.org/10.14488/BJOPM.2017.v14.n3.a1

Churchman, C.W., and R.L. Ackoff. 1954. An approximate measure of value. *Journal of Operations Research Society of America*, 2(1), 172–187. Available at: https://doi.org/10.1287/opre.2.2.172

Dağdeviren, M., Yavuz, S., & Kılınç, N. 2009. Weapon selection using the AHP and TOPSIS methods under fuzzy environment. *Expert systems with applications*, 36(4), 8143-8151. Available at: https://doi.org/10.1016/j.eswa.2008.10.016

Dağıstanlı, H. A. 2025. Weapon System Selection for Capability-Based Defense Planning using Lanchester Models integrated with Fuzzy MCDM in Computer Assisted Military Experiment. *Knowledge and Decision Systems with Applications*, 1, 11-23. Available at: https://doi.org/10.59543/kadsa.v1i.13601

Diakoulaki, D., Mavrotas, G., & Papayannakis, L. 1995. Determining objective weights in multiple criteria problems: The critic method. *Computers & Operations Research*, 22(7), 763-770. Available at: https://doi.org/10.1016/0305-0548(94)00059-H

Dustin, B., & Firmansyah, H. 2023. Analisis Keberadaan Senjata Airsoft Gun dalam Peraturan Perundang-Undangan Negara Republik Indonesia. *Syntax Literate; Jurnal Ilmiah Indonesia*, *8*(11), 6347-6360. Available at: https://doi.org/10.36418/syntax-literate.v8i11.13738

Endo, S., Ishida, N., & Yamaguchi, T. 2001. Tear in the trabecular meshwork caused by an airsoft gun. *American journal of ophthalmology*, *131*(5), 656-657. Available at: https://doi.org/10.1016/S0002-9394(00)00877-1

Eti, S., & Yüksel, S. 2024. Integrating pythagorean fuzzy SAW and entropy in decision-making for legal effectiveness in renewable energy projects: Legal effectiveness in renewable energy projects. *Computer and Decision Making: An International Journal*, 1, 13-22. Available at: https://doi.org/10.59543/comdem.v1i.10043

Genc, T. 2015. Application of ELECTRE III and PROMETHEE II in evaluating the military tanks. *International Journal of Procurement Management*, 8(4), 457-475. Available at: https://doi.org/10.1504/IJPM.2015.070743

Guan, J., Liu, J., Chen, H., & Bi, W. 2024. A Multi-Criteria Decision-Making Approach for Equipment Evaluation Based on Cloud Model and VIKOR Method. *International Journal of Advanced Computer Science & Applications*, 15(7). Available at: https://doi.org/10.14569/IJACSA.2024.01507127

Ilmiyah, N.F., Al Hasani, S.Z.N. & Renaningtyas, D. 2023. Combination of saw-topsis and borda count methods in sequencing potential convalescent plasma donors. *Barekeng: Jurnal Ilmu Matematika dan Terapan*, 17(3), pp.1521-1532. Available at: https://doi.org/10.30598/barekengvol17iss3pp1521-1532

Jaynes, E. T. (1982). On the rationale of maximum-entropy methods. *Proceedings of the IEEE,* 70(9), 939-952. Available at: https://doi.org/10.1109/PROC.1982.12425

Jokić, Ž., Radovanović, S., Petrović, A., & Delibašić, B. 2025. Razvoj sistema za podršku odlučivanju u procesu obuke vojnika. *InfoM*, 24(79/80), 14-21. Available at: https://rfos.fon.bg.ac.rs/handle/123456789/2940 [Accessed: 10 April 2025]

Jokic, Z., Delibasic, B., & Randjelovic, A. 2024. Selection of Rifle Caliber in Rearming Process of the Serbian Army. Management: *Journal of Sustainable Business and Management Solutions in Emerging Economies*, 29(1), 41-52. Available at: https://doi.org/10.7595/management.fon.2021.0011

Jones, M.A. & Wilson, J. 2024. The Colley Method is an Extension of the Borda Count. *Mathematics Magazine*, 97(2), pp.140-150. Available at: https://doi.org/10.1080/0025570X.2024.2312781

Karel, T., & Plašil, M. 2024. Application of hierarchical Bayesian models for modeling economic costs in the implementation of new diagnostic tests. *International journal of economic sciences*, 13(2), 20-37. Available at: https://doi.org/10.52950/ES.2024.13.2.002

Keleş, N. 2024. A comparative evaluation of multi-criteria decision-making framework for armed unmanned aerial vehicle. *International Journal of Intelligent Unmanned Systems*, 12(4), 433-453. Available at: https://doi.org/10.1108/IJIUS-03-2023-0026

Kim, H. C., Son, W. J., Lee, J. S., & Cho, I. S. 2024. Identification of maritime areas with high vessel traffic based on polygon shape similarity. *IEEE Access*. Available at: https://doi.org/10.1109/ACCESS.2024.3422398

Kizielewicz, B., & Sałabun, W. 2024. SITW Method: A New Approach to Re-identifying Multi-criteria Weights in Complex Decision Analysis. *Spectrum of Mechanical Engineering and Operational Research,* 1(1), 215-226. Available at: https://doi.org/10.31181/smeor11202419

Константинов, В. Н., & Шохирев, В. В. 2023. Использование пейнтбольного и страйкбольного оружия для повышения стрелковой подготовленности обучающихся. *Полицейская деятельность*, (5), 76-88. Available at: https://doi.org/10.7256/2454-0692.2023.5.43904

Kress, M., & MacKay, N. 2025. Modeling Civilian and Militant Casualties in Asymmetric Wars: The Case of Gaza 2024. *Spectrum of Operational Research*, 2(1), 259-267. Available at: https://doi.org/10.31181/sor21202518

Krishnan, A. R. 2024. Research trends in criteria importance through intercriteria correlation (CRITIC) method: a visual analysis of bibliographic data using the Tableau software. *Information Discovery and Delivery*. Available at: https://doi.org/10.1108/IDD-02-2024-0030

Krstic, B., Petrovic, J., & Stanišić, T. 2015. Analysis of key indicators of economic dimensions of spas'sustainable development in Serbia as tourism destinations. Ekonomika, *Journal for Economic Theory and Practice and Social Issues*, 61(3), 61-71. Available at: https://doi.org/10.22004/ag.econ.212937

Lee, C. I., Kim, D. S., Kang, M. G., & Park, S. H. 2023. A Study on the Effectness of Military Training with Air soft Gun. *The Journal of the Convergence on Culture Technology*, 9(6), 807-812. Available at: https://doi.org/10.17703/JCCT.2023.9.6.807

Lin, H. & Lin, D. 2023. Evaluation of Online Learners' Learning Performance Based on Fuzzy Borda Method. *International Journal of Emerging Technologies in Learning*, 18(14), pp.244-255. Available at: https://doi.org/10.3991/ijet.v18i14.40397

Lisboa, R. M., & de Moraes, T. F. B. 2025. "Airsoft": Proposta de implementação como modalidade de treinamento na pmto. *Revista Foco*, *18*(1), e7601-e7601. Available at: https://doi.org/10.54751/revistafoco.v18n1-110

Lubis, A. H., Khairina, N., & Riandra, M. F. 2021. Comparison between Multiple Attribute Decision Making Methods through Objective Weighting Method in Determining Best Employee. *International Journal of Innovative Research in Computer Science & Technology (IJIRCST)* Available at: https://doi.org/10.55524/ijircst.2023.11.2.10

Mallick, R., Pramanik, S., & Giri, B. 2023. Neutrosophic MAGDM Based on CRITIC-EDAS Strategy Using Geometric Aggregation Operator. *Yugoslav Journal of Operations Research*, 33(4), 683-698. Available at: https://doi.org/10.2298/YJOR221017016M

Markatos, D. N., & Pantelakis, S. G. 2023. Implementation of a holistic MCDM-based approach to assess and compare aircraft, under the prism of sustainable aviation. *Aerospace*, 10(3), 240. Available at: https://doi.org/10.3390/aerospace10030240

Martinez, L. E. 2008. Force-on-Force Police Training Using Airsoft: A Manual for the Law Enforcement Trainer on the Use of Airsoft Non-Lethal Technology. *Outskirts Press*. Available at: https://books.google.rs/books?hl=sr&lr=&id=_XuQxMqKM_cC&oi=fnd&pg=PA2&dq=Martinez,+L.+E.+(2008).+Force-on-Force+Police+Training+Using+Airsoft:+A+Manual+for+the+Law+Enforcement+Trainer+on+the+Use+of+Airsoft+Non-Lethal+Technology.+Outskirts+Press.+ISBN:+978-1-4327-2684-3&ots=MBV4S-S9je&sig=uKC8K9-8vVA8IOAREAVsfBSiMXQ&redir_esc=y#v=onepage&q&f=false ISBN: 978-1-4327-2684-3 [Accessed: 10 April 2025]

Menet, G., & Szarucki, M. 2020. Impact of value co-creation on international customer satisfaction in the airsoft industry: does country of origin matter?. *Journal of Risk and Financial Management*, 13(10), 223. Available at: https://doi.org/10.3390/jrfm13100223

Petrovic, N., Jovanovic, V., Markovic, S., Marinkovic, D., & Petrovic, M. 2024. Multicriteria sustainability assessment of transport modes: A European Union case study for 2020. *Journal of green economy and low-carbon development*, 3(1), 36-44. Available at: https://doi.org/10.56578/jgelcd030104

Pratama, B., & Aryanto, J. 2024. Optimalisasi Pengelolaan Data Member Club Airsoft Gun sebagai Strategi Transformasi Digital untuk Memfasilitasi Hobi Masyarakat. *Decode: Jurnal Pendidikan Teknologi Informasi*, *4*(3), 1166-1179. Available at: https://doi.org/10.51454/decode.v4i3.857

Putra, R. I. P., Azizah, S. A. S., & Poedjioetami, E. P. E. 2024. Penerapan Konsep Dinamis pada Bentuk Bangunan Real Airsoft Gun Games. *Tekstur (Jurnal Arsitektur)*, 5(2), 191-200. Available at: https://doi.org/10.31284/j.tekstur.2024.v5i2.5244

Radovanović, M., Božanić, D., Tešić, D., Puška, A., Hezam, I., & Jana, C. 2023. Application of hybrid DIBR-FUCOM-LMAW-Bonferroni-grey-EDAS model in multicriteria decision-making. *Facta Universitatis, Series: Mechanical Engineering*, 21(3), 387-403. Available at: https://doi.org/10.22190/FUME230824036R

Radovanović, M., Petrovski, A., Cirkin, E., Behlić, A., Jokić, Željko, Chemezov, D., Hashimov, E. G., Bouraima, M. B., & Jana, C. 2024. Application of the new hybrid model LMAW-G-EDAS multi-criteria decision-making when choosing an assault rifle for the needs of the army. *Journal of decision analytics and intelligent computing*, 4(1), 16-31. Available at: https://doi.org/10.31181/jdaic10021012024r

Rajurkar, K. S., Khade, S. P., Sawant, O. M., Dobe, M. P., & Kamble, A. G. 2023. Selection of fighter aircraft by using multi attributes decision making methods. *International Journal of Process Management and Benchmarking*, 14(4), 460-477. Available at: https://doi.org/10.1504/IJPMB.2023.132217

Saaty, T. L. 1980. The analytic hierarchy process. *McGraw Hill*, New York, Available at: https://d1wqtxts1xzle7.cloudfront.net/51627807/saaty-libre.pdf?1486172407=&response-content-disposition=inline%3B+filename%3DSaaty.pdf&Expires=1756729784&Signature=LmJmvBJ8bVBalour9n5NDHXvSj-RmTFsN06T-BFnJxD-oN7-ghOdoAbOtx3hSbUenYF1de2eIq~tApin3qHJa4nFI3UzwmcezGvfK9SR45ezyHYbl5gTtXbKwNs9u96yulunPEH90UxMQrR1NPXVlq9025ReP3Q6fPvOly3Grz9m1qFt9xdtD6R2McfNEqvU~mSnzQGHXzzECzwaFddfiFF2h6WV0NjqFoe71s6FSTSo5e7O05dODU70mzQ-C8BItEGsJe0aZVTtVSTlVtirwfXgRUjQVoqjur8w~9alcTyP58HkEttTczGeo-KuIyWtMHUCLGJzSLXQu-~J4gfDSQ__&Key-Pair-Id=APKAJLOHF5GGSLRBV4ZA [Accessed: 11 April 2025]

Saari, D.G. 2023. Selecting a voting method: the case for the Borda count. *Constitutional Political Economy*, 34(3), pp.357-366. Available at: https://doi.org/10.1007/s10602-022-09380-y

Sakata, M., & Sato, M. 1990. Accurate structure analysis by the maximum-entropy method. *Foundations of Crystallography*, 46(4), 263-270. Available at: https://doi.org/10.1107/S0108767389012377

Shageev, D. A. 2022. Search for a measurement standard in the modifications of the first generation AHP for the method of effective projects selection and other fields of science. *Воронежского Государственного Университета Инженерных Технологий Вестник ВГУИТ 2022*, Том. 84, №, 388. Available at: https://doi.org/10.20914/2310-1202-2022-1-388-409

Shanmugapriya, P., Selvakumari, K., & Kavitha, S. 2024. Entropy Method of Multi-Attribute Decision-Making Problems. In E3S Web of Conferences (Vol. 491, p. 02001). *EDP Sciences*. Available at: https://doi.org/10.1051/e3sconf/202449102001

Srđević, B. 2005. Nepristrasna ocena značaja kriterijuma u višekriterijumskoj optimizaciji. *Vodoprivreda*, Available at: https://www.vodoprivreda.net/wp-content/uploads/2014/08/neprostrasna.pdf (in Serbian). ISBN 0350-0519 [Accessed: 15 March 2025]

Srđević B, Medeiros Y, Faria A, & Schaer M. 2003. Objective Evaluation of Performance Criteria for a Reservoir System. *Vodoprivreda*, 35(3-4), 163-176. Available at: https://www.vodoprivreda.net/objektivno-vrednovanje-kriterijuma-performanse-sistema-akumulacija/ (in Serbian). ISBN 0350-0519 [Accessed: 10 April 2025]

Stević, Ž., Baydaş, M., Kavacık, M., Ayhan, E., & Marinković, D. 2024. Selection of data conversion technique via sensitivity-performance matching: Ranking of small e-vans with probid method. *Facta Universitatis, Series: Mechanical Engineering*, 22(4), 643-671. Available at: https://doi.org/10.22190/FUME240305023S

Strong, B., & Coady, M. 2014. Penetrating facial injury with an "Airsoft" pellet: a case report. *British journal of oral and maxillofacial surgery*, *52*(9), e129-e131. Available at: https://doi.org/10.1016/j.bjoms.2014.05.007

Sun, Q., Wu, J., Chiclana, F., Wang, S., Herrera-Viedma, E., & Yager, R. R. 2023. An approach to prevent weight manipulation by minimum adjustment and maximum entropy method in social network group decision making. *Artificial Intelligence Review*, 56(7), 7315-7346. Available at: https://doi.org/10.1007/s10462-022-10361-8

Suo, M., Xing, J., Ma, K., Xiao, D., & Song, D. 2025. Fighter optimal selection based on sequential multi-criteria decision-making with uncertainty measurement. *The Aeronautical Journal*, 1-23. Available at: https://doi.org/10.1017/aer.2024.125

Susilo, J., & Wahyuni, E. G. 2024. Comparison of SAW and TOPSIS Methods in Decision Support Systems for Contraceptive Selection. International *Journal Software Engineering and Computer Science (IJSECS)*, 4(2), 792-807. Available at: https://doi.org/10.35870/ijsecs.v4i2.2815

Tešić, D., Božanić, D. & Khalilzadeh, M. 2024. Enhancing Multi-Criteria Decision-Making with Fuzzy Logic: An Advanced Defining Interrelationships Between Ranked II Method Incorporating Triangular Fuzzy Numbers. *Journal of Intelligent Management Decision*, 3(1), pp.56-67. Available at: https://doi.org/10.56578/jimd030105

Tešić, D., Božanić, D., & Milić, A. 2023a. A multi-criteria decision-making model for pontoon bridge selection: An application of the DIBR II-NWBM-FF

MAIRCA approach. *Journal of Engineering Management and Systems Engineering*, 2(4), 212-223. Available at: https://doi.org/10.56578/jemse020403

Tešić, D., Božanić, D., Radovanović, M., & Petrovski, A. 2023b. Optimising assault boat selection for military operations: An application of the DIBR II-BM-CoCoSo MCDM model. *J. Intell. Manag. Decis*, 2(4), 160-171. Available at: https://doi.org/10.56578/jimd020401

Wang, J., Setiawansyah, S., & Rahmanto, Y. 2024. Decision Support System for Choosing the Best Shipping Service for E-Commerce Using the SAW and CRITIC Methods. *Jurnal Ilmiah Informatika dan Ilmu Komputer (JIMA-ILKOM)*, 3(2), 101-109. Available at: https://doi.org/10.58602/jima-ilkom.v3i2.32

Wardany, R., & Zahedi, 2024. A Study Comparative of PSI, PSI-TOPSIS, and PSI-MABAC Methods in Analyzing the Financial Performance of State-Owned Enterprises Companies Listed on the Indonesia Stock Exchange. *Yugoslav Journal Of Operations Research,* Online first. Available at: https://doi.org/10.2298/YJOR240115017W

Yalçın, G. C., Kara, K., & Özyürek, H. 2025. Evaluating Financial Performance of Companies in the Borsa Istanbul Sustainability Index Using the CRITIC-MABAC Method. *Spectrum of Operational Research*, 2(1), 323-346. Available at: https://doi.org/10.31181/sor21202530

Zhong, S., Chen, Y., & Miao, Y. 2023. Using improved CRITIC method to evaluate thermal coal suppliers. *Scientific reports*, 13(1), 195. Available at: https://doi.org/10.1038/s41598-023-27495-6

Žižović, M., & Albijanić, M. 2025. An Implementation of the Entropy Method for Determining Weighing Coefficients in a Multicriteria Optimization of Public Procurements. *Spectrum of Engineering and Management Sciences*, 3(1), 28-44. Available at: https://doi.org/10.31181/sems31202528z

Selección de un rifle airsoft para combate urbano utilizando el modelo híbrido de toma de decisiones multicriterio Borda-AHP-SAW y Entropy-CRITIC-FanMa-SAW

Aleksandar R. Aleksić, **autor de correspondencia**, *Miša* D. Živković, *Damir* M. Projović, *Milorad* M. Petronijević, *Darko* I. Božanić

Universidad de Defensa de Belgrado, Academia Militar Departamento de Tácticas con Sistemas de Armas, Belgrado, República de Serbia,
Universidad de Defensa de Belgrado, Academia Militar, Departamento de Comando y Liderazgo, Belgrado, República de Serbia,

CAMPO: matemáticas aplicadas, ingeniería mecánica, ciencias militares (tácticas con sistemas de armas)
TIPO DE ARTÍCULO: artículo científico original

Resumen:

Introducción/objetivo: El artículo presenta la aplicación de métodos de toma de decisiones multicriterio para seleccionar una réplica airsoft de un rifle automático para la práctica de acciones tácticas en combate urbano. Primero, expertos clasificaron los criterios según los cuales se seleccionarían las alternativas. Mediante los métodos Borda y AHP, se determinaron los coeficientes de ponderación de los criterios, y posteriormente se seleccionó la alternativa más favorable mediante el método SAW. El procedimiento de selección se repitió cuando la selección se realizó sin expertos, pero los coeficientes de ponderación de los criterios se determinaron mediante los métodos de Entropía Objetiva, CRITIC y FanMa, y se realizó un análisis comparativo de los resultados. El objetivo del artículo es seleccionar el rifle airsoft más efectivo para uso profesional y civil para la práctica de acciones tácticas en combate urbano mediante la combinación de métodos de toma de decisiones multicriterio. El consumo mínimo de recursos es siempre el punto de partida, garantizando al mismo tiempo la forma más eficiente de practicar acciones tácticas lo más cercanas posible a las condiciones reales.

Métodos: Por primera vez, se presentó el método para determinar los coeficientes de ponderación de criterios mediante métodos multidisciplinarios de toma de decisiones multicriterio sobre un problema específico en el campo de las tácticas con sistemas de armas, con la opinión de expertos. Posteriormente, se compararon los resultados sin la participación de expertos. Los expertos en Tácticas y Armas de la Academia Militar seleccionaron y clasificaron siete criterios. Posteriormente, sus opiniones se refinaron mediante el método Borda y los resultados se incorporaron al método AHP para seleccionar los coeficientes de ponderación de los criterios. Finalmente, se seleccionó la alternativa más favorable con base en el método SAW. Dado que el procedimiento descrito para determinar los coeficientes de ponderación de los criterios se calculó por primera vez con la participación de expertos, se repitió el procedimiento para seleccionar la alternativa más favorable sin la participación de expertos, pero se determinaron los pesos de los criterios mediante métodos objetivos y se compararon los resultados mediante análisis comparativo. Las alternativas son cinco rifles de airsoft con recámara hop-up, algunos de los cuales se utilizan en la Academia Militar y en unidades especiales del ejército para entrenamiento en diversas acciones tácticas de combate, mientras que en la vida civil son utilizados por entusiastas de las armas airsoft.

Resultados: Se eligió el rifle airsoft más asequible para ofrecer un consumo mínimo de recursos con el máximo rendimiento y aportar el mayor realismo posible a las situaciones de combate al practicar acciones tácticas en el entorno urbano.

Conclusión: La solución, con un análisis comparativo de los resultados obtenidos de dos maneras, considera la optimización simultánea de siete criterios ligeramente diferentes para seleccionar el rifle airsoft más eficaz para la práctica de procedimientos tácticos, con el fin de proporcionar condiciones lo más cercanas posible a las situaciones reales de combate a corta distancia.

Palabras claves: rifle airsoft, selección, Borda, AHP, SAW, entropía, CRITIC, método FanMa.

Выбор страйкбольной винтовки для боев в городских условиях с использованием гибридной многокритериальной модели принятия решений BORDA-AHP-SAW и ENTROPY-CRITIC-FANMA-SAW

Александар Р. Алексич, **корреспондент**, *Миша* Д. Живкович, *Дамир* М. Пройович, *Милорад* М. Петрониевич, *Дарко* И. Божанич

Университет обороны в Белграде, Военная академия, кафедра тактики и вооружения, г. Белград, Республика Сербия,

РУБРИКА ГРНТИ: 27.47.19 Исследование операций,
28.17.31 Моделирование процессов управления
ВИД СТАТЬИ: оригинальная научная статья

Резюме:

Введение/цель: В данной статье представлено применение методов многокритериального принятия решений при выборе страйкбольной копии автоматической винтовки для отработки тактических приемов в городских условиях. Сначала экспертами было произведено ранжирование критериев, на основании которых в дальнейшем будет сделан выбор подходящего варианта. Применяя методы BORDA и AHP, были определены весовые коэффициенты критериев, а затем с помощью метода SAW был выбран лучший вариант. Процедура отбора была повторена, когда отбор проводился без участия экспертов. В этом случае весовые коэффициенты критериев были определены с помощью объективных методов Entropy-CRITIC-FanMa, а затем проведен сравнительный анализ результатов. Цель статьи заключается в выборе наиболее эффективной страйкбольной винтовки для служебного и гражданского использования в отработке тактических приемов в городских условиях путем сочетания методов принятия многокритериальных решений. В современном мире отправной точкой является минимальное потребление ресурсов, но при этом обязательно должна быть обеспечена наиболее эффективная отработка тактических приемов в условиях, приближенных к реальным.

Методы: Сначала был применен экспертный метод определения весовых коэффициентов критериев с использованием междисциплинарных методов многокритериального принятия решений по конкретной проблеме в области военной тактики. В случае, когда эксперты не привлекались, был проведен сравнительный анализ результатов. Эксперты в области тактики и вооружения из Военной академии сначала выбрали и ранжировали семь критериев. Затем их мнения были подтверждены с помощью метода BORDA, после чего результаты были введены в метод AHP для выбора весовых коэффициентов критериев. В конце на основании метода SAW был выбран лучший вариант. Поскольку описанная выше процедура определения весовых коэффициентов критериев впервые была рассчитана экспертами таким образом, процедура выбора лучшего варианта была повторена без привлечения экспертов, но веса критериев были определены с использованием объективных методов, а результаты сопоставлены с помощью сравнительного анализа. Альтернативными вариантами были пять страйкбольных винтовок с патронником hop-up, некоторые из которых используются в Военной академии и в специальных военных подразделениях при обучении военно-тактической подготовке и просто любителями страйкбольного оружия.

Результаты Выбор подходящей страйкбольной винтовки был сделан с учетом минимального расхода ресурсов и максимальной эффективности отработки тактических приемов в условиях, приближенных к реальным.

Вывод: Решение, основанное на сравнительном анализе результатов, полученных двумя способами, учитывает одновременную оптимизацию семи критериев, которые незначительно отличаются друг от друга, с целью выбора наиболее эффективной страйкбольной винтовки для отработки тактических приемов на ближних дистанциях в условиях, приближенных к реальным.

Ключевые слова: страйкбольная винтовка, выбор, методы BORDA, AHP, SAW, Entropy, CRITIC, FanMa.

Избор airsoft пушке за урбану борбу применом хибридног модела вишекритеријумског одлучивања BORDA-AHP-SAW и Entropy-Critic-FanMa-SAW

Александар Р. Алексић, **аутор за преписку**, *Миша* Д. Живковић, *Дамир* М. Пројовић, *Милорад* М. Петронијевић, *Дарко* И. Божанић

Универзитет одбране у Београду, Војна академија,
Катедра тактике са системима наоружања, Београд, Република Србија

ОБЛАСТ: примењена математика, машинство, војне науке
(тактика са системима наоружања)
КАТЕГОРИЈА (ТИП) ЧЛАНКА: оригинални научни рад

Сажетак:

Увод/циљ: У раду је представљен начин примене метода вишекритеријумског одлучивања ради одабира airsoft реплике аутоматске пушке за увежбавање тактичких поступака у борби у урбаној средини. Најпре су експерти извршили рангирање критеријума по којима ће се вршити избор алтернативе. Применом метода BORDA и AHP одређени су тежишни коефицијенти критеријума, а затим је најповољнија алтернатива одабрана применом метода SAW. Поступак одабира у којем експерти не учествују је поновљен , па су тежишни коефицијенти критеријума одређени објективним методама Entropy-CRITIC-FanMa *и извршена је компаративна анализа резултата. Циљ рада јесте да се комбинацијом метода вишекритеријумског одлучивања одабере најефикаснија airsoft пушка за професионалну и цивилну употребу за увежбавање тактичких радњи и поступака у борби у урбаној средини. Минималан утрошак ресурса увек је полазна основа, уз обезбеђење што ефикаснијег начина увежбавања тактичких радњи које су приближне стварним условима.*

Методе: По први пут је приказан експертски начин одређивања тежишних коефицијената критеријума употребом мултидисциплинарних метода вишекритеријумског одлучивања на конкретном проблему из области тактике са системима наоружања, а затим су, у одсуству експерата, резултати упоређени.Експерти из области тактике и наоружања са Војне академије најпре су одабрали и рангирали седам критеријума, а затим су њихова мишљења сублимирана уз помоћ метода BORDA, и резултати унесени у метод AHP ради избора тежишних коефицијената критеријума. На крају је, на основу метода SAW , извршен избор најповољније алтернативе. Пошто је наведени поступак одређивања тежишних коефицијената критеријума по први пут прорачунат ангажовањем експерата на овај начин, поступак одабира најповољније алтернативе је поновљен без ангажовања експерата, а тежине критеријума одређене су објективним методама, па су резултати упоређени компаративном анализом. Алтернативу представља пет airsoft пушака са hopup комором, од којих се неке користе на Војној академији и у специјалним јединицама Војске за увежбавање различитих борбено-тактичких радњи, а користе их и цивили, љубитељи airsoft наоружања.

Резултат: Избор најповољније airsoft пушке, која ће обезбедити минималан утрошак ресурса и најповољније перформансе у условома најприближнијим борбеној ситуацији при увежбавању тактичких радњи у урбаној средини.

Закључак: Решење уз компаративну анализу резултата добијених на два начина узима у обзир истовремену оптимизацију седам критеријума, који се незнатно разликују, ради одабира најефикасније airsft пушке за увежбавање тактичких поступака ради обезбеђења услова најприближнијих реалној борбеној ситуацији на кратким дистанцама.

Кључне речи: airsoft пушка, одабир, BORDA, AHP, SAW, Entropy, CRITIC, метод FanMa.

Paper received on: 25.03.2025.
Manuscript corrections submitted on: 01.04.2025.
Paper accepted for publishing on: 29.04.2025.

A multi-criteria decision-making approach for wheelchair selection using intuitionistic fuzzy TOPSIS

Prasant Ranjan Dhal[a], *Bibhuti* Bhusan Choudhury[b], *Sushil* Kumar Sahoo[c], *Dragan* Pamucar[d], *Vladimir* Simic[e]

[a] Indira Gandhi Institute of Technology (BPUT, Rourkela), Department of Mechanical Engineering, Sarang, Dhenkanal, Odisha, India, e-mail: prdhal@gmail.com, ORCID ID: https://orcid.org/0000-0002-7402-2187

[b] Indira Gandhi Institute of Technology (BPUT, Rourkela), Department of Mechanical Engineering, Sarang, Dhenkanal, Odisha, India, e-mail: bbcigit@gmail.com, ORCID ID: https://orcid.org/0000-0002-2990-3911

[c] Indira Gandhi Institute of Technology (BPUT, Rourkela), Department of Mechanical Engineering, Sarang, Dhenkanal, Odisha, India, e-mail: sushilkumar00026@gmail.com, **corresponding author,** ORCID ID: https://orcid.org/0000-0002-8551-7353

[d] University of Belgrade, Department of Operations Research and Statistics, Faculty of Organizational Sciences, Belgrade, Serbia + Faculty of Engineering, Dogus University, Umraniye, Istanbul, Türkiye, e-mail: dragan.pamucar@fon.bg.ac.rs, ORCID ID: https://orcid.org/0000-0001-8522-1942,

[e] University of Belgrade, Faculty of Transport and Traffic Engineering, Vojvode Stepe 305, Belgrade, Serbia + Department of Computer Science and Engineering, College of Informatics, Korea University, Seoul 02841, Republic of Korea , e-mail: vsima@sf.bg.ac.rs, ORCID ID: https://orcid.org/0000-0001-5709-3744

doi https://doi.org/10.5937/vojtehg73-56837

FIELD: decision sciences, mechanical engineering
ARTICLE TYPE: original scientific paper

Abstract:

Introduction/purpose: Selecting an appropriate wheelchair is vital for ensuring mobility, comfort, and independence for individuals with disabilities. The primary objective is to assist in identifying the optimal wheelchair by considering a range of user-centric criteria and mitigating decision-making ambiguities.

Methods: The proposed framework leverages intuitionistic fuzzy sets to account for the hesitancy and imprecision often present in decision making.

ACKNOWLEDGEMENT: We want to express our sincere gratitude to everyone who made this research project possible. We also want to express our gratitude to our academic advisors for all of their support and assistance.

Criteria weights and alternative evaluations were determined with expert input. Sensitivity analysis was conducted to ensure the robustness and reliability of the ranking process. A case study was performed to validate the effectiveness of the methodology and to illustrate its practical application.

Results: The study demonstrated that AI-powered wheelchairs (APWs) outperformed other wheelchair options based on the selected criteria and sub-criteria.

Conclusion: The findings highlight the utility of the intuitionistic fuzzy TOPSIS approach in facilitating well-informed wheelchair selection decisions. This method benefits end users, caregivers, and medical professionals by addressing the complexities of subjective and uncertain decision making, ultimately leading to more inclusive and reliable outcomes. The framework proves to be an effective tool for improving the decision-making process in wheelchair selection.

Keywords: wheelchair selection, intuitionistic fuzzy, triangular fuzzy, TOPSIS, sensitivity analysis.

Introduction

Wheelchair selection is a pivotal decision for stakeholders, including users, caregivers, healthcare professionals, and manufacturers, as it profoundly influences the user's quality of life. A wheelchair is not merely a mobility device but a critical enabler of independence, comfort, and inclusion. Choosing the right wheelchair ensures users can move freely and participate actively in social, professional, and personal activities, thereby fostering autonomy and reducing dependence on others. Griggs (2024) emphasizes that when choosing a wheelchair, the user's comfort and health are among the most important factors. An ill-fitting wheelchair can lead to physical discomfort, pressure sores, and long-term musculoskeletal issues. Properly designed and selected wheelchairs promote optimal posture, reduce the risk of secondary health complications, and enhance overall well-being. For individuals with specific medical conditions or disabilities, the wheelchair must meet unique ergonomic and functional requirements to support their physical needs effectively by Kargi et al. (2023).

Rotschedl et al. (2024) highlight that economic factors significantly influence the decision-making process. Wheelchairs come in various designs and price ranges, and selecting an appropriate model ensures cost-effectiveness. Stakeholders must balance the user's specific requirements with budgetary constraints to maximize utility and longevity while avoiding overspending on unnecessary features. Furthermore, a suitable wheelchair contributes to accessibility and inclusivity by enabling users to navigate diverse environments seamlessly. Sahoo and Choudhury (2024) suggest that incorporating advanced features such as adjustable seats, lightweight frames, and smart technology can greatly enhance the user experience. For stakeholders, a thoughtful selection process is not just about mobility but about empowering users to lead fulfilling, independent lives while ensuring physical and emotional well-being.

Selecting an ideal wheelchair—manual (MW), electric (EW), or AI-powered (APW)—requires evaluating diverse criteria to address user-specific needs and circumstances. Manual wheelchairs suit those with sufficient upper body strength, while electric and AI-powered models cater for individuals needing greater assistance or advanced features like automated navigation. Factors such as cost, maintenance, terrain compatibility, and comfort are critical for ensuring usability and long-term satisfaction. Verma et al. (2024) explain that by evaluating these factors, stakeholders can align the wheelchair features with the user's physical condition, environment, and lifestyle, thereby improving mobility and independence. Wheelchair selection is widely recognized as a multi-criteria decision-making challenge. Recent research emphasizes the effectiveness of MCDM methods, particularly intuitionistic fuzzy techniques, in addressing uncertainties inherent in the decision-making process.

Most past studies on wheelchair selection used classical fuzzy numbers, such as fuzzy AHP. However, Sahoo and Choudhury (2021) argue that intuitionistic fuzzy numbers can provide better results. Introduced by Atanassov and Atanassov (1999), the intuitionistic fuzzy set (IFS) theory extends classical fuzzy sets, providing greater flexibility for handling imprecise situations. Imran et al. (2024) and Sarfraz (2024) have extensively used IFS to provide more reliable solutions when making decisions in challenging situations. Considering the issues discussed and insights from the reviewed literature, limited studies have integrated MCDM with IFS for wheelchair selection. For an actual-world wheelchair selection scenario, this study suggests an MCDM framework based on the intuitionistic fuzzy TOPSIS approach. TOPSIS assesses both positive-ideal and negative-ideal solutions and is renowned for its transparency and ease of use. Combining TOPSIS with IFS enhances decision making by addressing uncertainty and vagueness effectively, providing a robust and user-centric approach to wheelchair selection.

This paper is organized as follows. A thorough assessment of literature is provided first, followed by a description of the conceptual foundation of the suggested approach and the research methodology. The case study, implementation, comparison with triangular fuzzy TOPSIS, and sensitivity assessment of the suggested intuitionistic fuzzy TOPSIS approach are then discussed with research findings, implications, and managerial insights. Finally, the study is concluded with a conclusion and suggestions for future research directions.

Literature review

Wheelchair selection criteria and sub-criteria

For people with mobility problems, choosing an appropriate wheelchair is crucial. Zhang et al. (2024) emphasize in their study the importance of evaluating wheelchairs using multiple criteria due to significant differences in their features, designs, and capacities. By taking into account a number of variables that impact user experience, comfort, and general functionality, an MCDM approach offers an organized method for evaluating alternative wheelchair solutions. This approach enables users and healthcare professionals to make well-informed decisions based on specific needs and preferences. Below is a detailed explanation of the key criteria and sub-criteria to consider when selecting a wheelchair:

- *User's physical condition (C-1)*

Fasipe et al. (2024) assess this criterion based on the user's physical health, limitations, and needs. Different users have varying levels of strength, mobility, and coordination. The wheelchair must cater for the user's specific condition (e.g., paralysis, arthritis, or general weakness), ensuring that it provides the necessary support and ease of movement. It encompasses various factors such as strength and endurance (SC-1) which refers to the user's physical ability to propel or control the wheelchair over extended periods. By ensuring that the wheelchair offers appropriate alignment and comfort, posture support (SC-2) lowers the possibility of strain or pain. To guarantee that the wheelchair can securely carry the user's weight without sacrificing functionality or safety, weight capacity (SC-3) is crucial. For users with restricted mobility, range of motion (SC-4) is crucial because it guarantees that the wheelchair can adapt to their motions and make the required modifications to enhance comfort and usability. When combined, these sub-criteria guarantee that the wheelchair is customized to meet the individual physical requirements of the user.

- *Comfort (C-2)*

Mohebbi et al. (2024) highlight that comfort plays a vital role in influencing long-term wheelchair use. It includes various factors such as seat cushioning (SC-5) which plays a vital role in reducing pressure points and preventing discomfort or sores, ensuring a more comfortable sitting experience. Back support (SC-6) is equally important, providing the necessary lumbar or full-back support to maintain proper posture and alleviate back pain during extended use. Adjustability (SC-7) allows the user to customize the wheelchair to their specific needs, such as adjusting the seat depth or backrest angle for enhanced comfort. Ergonomics (SC-8) focuses on the overall design of the wheelchair, ensuring that it conforms to the user's body to reduce strain and improve ease of use.

- Ease of use (C-3)

The term "ease of use" describes how easy and straightforward it is for the user to operate the wheelchair, as by Kulich et al. (2024). It encompasses various factors such as maneuverability (SC-9) which focuses on how easily the wheelchair can be controlled and moved, especially in tight or crowded spaces. A wheelchair with an easy-to-use control interface simplicity (SC-10) ensures that users can quickly master the controls, whether they are manual or powered, without extensive training. Caregiver involvement (SC-11) highlights how accessible and manageable the wheelchair is for caregivers who assist the user, making tasks like pushing or adjusting settings easier. Last but not least, a low user learning curve (SC-12) guarantees that new users can quickly become accustomed to the wheelchair's functionality, reducing frustration and promoting independence.

- *Control interface (C-4)*

The control interface refers to the system that allows the user to operate the wheelchair, according to Kocejko et al. (2024). It encompasses various controls such as joystick control (SC-13), which is one of the most common options, providing intuitive, precise movement control for users, especially in powered wheelchairs. Voice or gesture control (SC-14) represents advanced technology, allowing users to control the wheelchair with spoken commands or hand movements, enhancing accessibility for individuals with limited dexterity. Manual control options (SC-15) ensure that users who prefer or need manual operation have simple, effective mechanisms to propel or steer the wheelchair. Lastly, a caregiver assist mode (SC-16) allows caregivers to control the wheelchair remotely, providing extra support when necessary.

- *Customization (C-5)*

Nace et al. (2023) define customization as the ability to adjust the wheelchair to meet the user's specific needs or preferences. It encompasses various elements such as adjustable footrests (SC-17) which enable users to modify the position of the footrests for optimal comfort and posture, reducing pressure on the legs and feet. Adjustable armrests (SC-18) provide flexibility in supporting the arms, ensuring comfort for users of varying heights and arm lengths. The seat size and configuration (SC-19) is another key factor, as it ensures the wheelchair fits the user's body dimensions, promoting comfort and preventing issues like pressure sores. Finally, accessory options (SC-20), such as cushions, trays, or cup holders, offer additional customization to enhance functionality and comfort, allowing users to adapt the wheelchair to their lifestyle.

- *Mobility & maneuverability (C-6)*

Mobility and maneuverability focus on the wheelchair's ability to navigate various environments, see de Vries et al. (2023). It encompasses various factors such as turning radius (SC-21) which refers to the wheelchair's ability to navigate tight spaces, which is especially important for users in confined areas like hallways or small rooms. Indoor and outdoor usability (SC-22) ensures that the wheelchair can function effectively in both settings, providing the necessary adaptability to various environments. Terrain compatibility (SC-23) is important for users who need to navigate different surfaces such as grass, gravel, or rough pavement. Finally, stability on uneven surfaces (SC-24) ensures that the wheelchair remains steady and safe, even on terrains like slopes or bumpy sidewalks. Together, these factors ensure that the wheelchair offers reliable and smooth mobility in a variety of settings.

- *Battery life/power supply (C-7)*

Nagde and Dhobe (2021) emphasize that battery life and power supply are crucial for powered wheelchairs to ensure continuous use throughout the day. It encompasses various factors such as battery capacity (SC-25) which refers to the total energy stored in the battery, which influences how long the wheelchair can operate before needing a recharge. Charging time (SC-26) measures how long it takes to fully charge the battery, with faster charging times enhancing convenience for users who require quick turnarounds. Wheelchair users who must travel long distances should be aware of the range per charge (SC-27), which shows how far the wheelchair can go on a single charge. Lastly, power durability (SC-28) assesses the battery's long-term performance and ability to retain charge over time, ensuring reliable use without frequent battery replacements. Together, these factors ensure that the wheelchair provides sufficient power for daily activities and extended use.

- *Durability (C-8)*

Kim et al. (2024) describe durability as the wheelchair's ability to endure extended use and environmental conditions without failing. A durable wheelchair is made from high-quality materials that resist wear and tear, offering a long lifespan even under frequent use. Durability is especially important for users who rely on their wheelchair daily and in a variety of environments. It encompasses various factors such as frame strength (SC-29) which is essential for supporting the user's weight and providing structural integrity, preventing damage under stress. Wheel durability (SC-30) is equally important, as it ensures the wheels can handle regular use on various surfaces without wearing down prematurely. Long-term reliability (SC-31) refers to the wheelchair's ability to perform consistently over time, with minimum maintenance or repairs needed. Finally, resistance to wear and tear (SC-32) ensures that materials and components resist degradation from daily use, maintaining the wheelchair's function and appearance for an extended period. Together, these factors provide a reliable and long-lasting wheelchair solution.

- *Cost (C-9)*

Cost is a critical factor for most individuals and organizations when selecting a wheelchair, as by Rivas et al. (2024). It encompasses various factors such as initial purchase cost (SC-33) which refers to the upfront price of the wheelchair, which can vary depending on its features and functionality. Maintenance expenses (SC-34) involve the ongoing costs associated with repairs, part replacements, and servicing to keep the wheelchair in optimal condition. Insurance coverage (SC-35) plays a role in reducing out-of-pocket costs by covering a portion of the wheelchair's purchase or maintenance. Lastly, warranty (SC-36) provides peace of mind by ensuring that the wheelchair is protected against defects or malfunctions for a certain period, reducing potential unexpected costs. Together, these factors help balance affordability with quality and long-term investment.

- *Safety features (C-10)*

Sahoo and Choudhury (2024) stress that safety features are vital for preventing accidents and ensuring the user's well-being. They argue that a wheelchair must offer a safe riding experience, particularly when navigating ramps or slopes. It encompasses various factors such as an anti-tip mechanism (SC-37), which helps prevent the wheelchair from tipping over, especially when navigating slopes or uneven surfaces. Seat belts and harnesses (SC-38) provide additional support and security for users, reducing the risk of falls or injury during movement. Braking systems (SC-39) are vital for controlling the wheelchair's movement, ensuring it remains stationary when needed, and preventing unintentional rolling. Lastly, collision detection (SC-40) technology can alert the user to obstacles or prevent collisions by automatically stopping or adjusting the wheelchair's movement. These safety features collectively enhance stability and minimize the risk of accidents during daily use.

- *Technology integration (C-11)*

Zhang et al. (2024) highlight that modern wheelchairs integrate advanced technology such as automated braking, tilt and recline mechanisms, GPS tracking, and mobile device connectivity for remote control. It encompasses various factors such as GPS navigation (SC-41), which allows users to navigate unfamiliar environments with ease, providing directions and real-time location tracking for greater independence. Sensor integration (SC-42) includes features like proximity sensors or obstacle detection, improving safety by alerting users to potential hazards or automatically adjusting the wheelchair's movement. Software updates (SC-43) ensure that the wheelchair's system remains up-to-date with new features, performance improvements, and bug fixes. Lastly, smartphone compatibility (SC-44) enables users to control or monitor their wheelchair via a mobile app, offering added convenience and customization options. These technological advancements make the wheelchair more adaptive, responsive, and efficient in meeting the user's needs.

Each of these criteria and sub-criteria plays a vital role in ensuring the selected wheelchair meets the user's needs, providing a comprehensive solution for mobility, comfort, safety, and independence. A more informed and efficient decision process might result from consumers prioritizing these aspects according to their own needs and preferences by employing an MCDM strategy.

Wheelchair selection methods

A variety of models have been created to identify the ideal wheelchair, each incorporating diverse methodologies. Since wheelchair selection necessitates balancing several conflicting objectives and criteria under unknown circumstances, MCDM techniques are frequently employed.

Mao et al. (2024) highlighted that most wheelchair selection models have integrated fuzzy concepts into traditional MCDM methods due to the capability of fuzzy-based approaches to manage uncertainty and imprecision in human judgment. Unni et al. (2024) point out that, while extensive research has integrated the traditional fuzzy set theory (FST) with various MCDM methods, less attention has been given to intuitionistic fuzzy sets (IFSs). Kousar and Kausar (2025) and Dağıstanlı (2024) explain that, unlike traditional fuzzy sets, an IFS enhances the concept of fuzzy sets and is better suited for practical applications. An IFS is more flexible in complex decision-making situations since it is defined by a membership function, a non-membership function, and a hesitation degree (hesitation margin).

Saqlain and Saeed (2024) argue that, unlike traditional fuzzy sets, which rely solely on a membership function, IFSs offer a more precise representation of the fuzzy nature of data. The hesitation degree in IFSs effectively manages ambiguity and uncertainty regarding membership and non-participation in a set. Decision -makers (DMs) especially benefit from this hesitation characteristic. The fuzzy set theory has been effectively applied to wheelchair selection in a number of research studies. An overview of the strategies and tactics used in wheelchair selection is given in Table 1, with an emphasis on user-centered and sustainable criteria.

Our study differentiates itself from prior research studies in several key aspects:

i. To our knowledge, the application of IFS-TOPSIS in wheelchair selection remains underexplored, with limited real-world implementations. Görçün et al. (2024) and Sampathkumar (2024) have combined MCDM with IFSs to select assistive devices in their studies; these approaches tend to rely on empirical data rather than on real-world case studies. This paper presents a case study focused on wheelchair selection for individuals with mobility challenges.

ii. The criteria and sub-criteria were carefully chosen through an extensive review of the literature and then further validated with input from decision-makers. This process ensures a more practical and precise approach by bridging theoretical and real-world perspectives.

iii. On a theoretical level, by adding a component-wise matrix multiplication operator to aggregate the weights of the criterion and sub-criteria, the suggested approach improves upon the IFS-TOPSIS architecture. The idea improves the precision and dependability of the decision-making process when choosing the best wheelchair.

Research design

The methodology framework

The framework designed for selecting wheelchairs using the intuitionistic fuzzy TOPSIS method is presented in Figure 1.

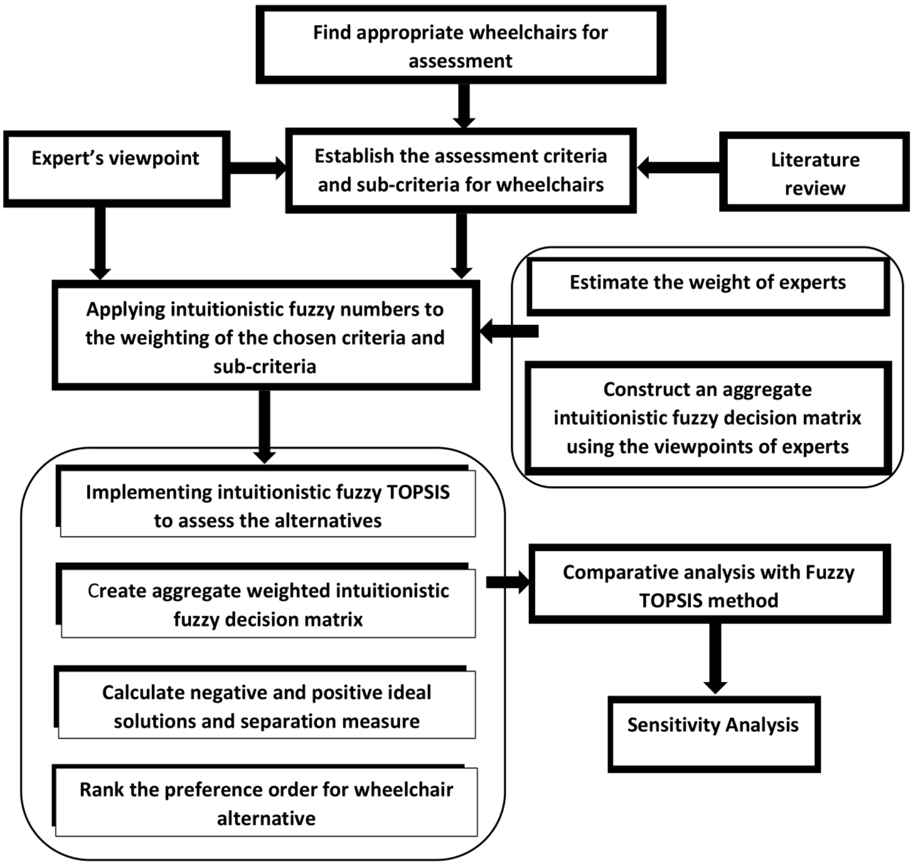

Figure 1 - Proposed wheelchair selection framework

The proposed wheelchair selection framework involves identifying suitable wheelchairs, gathering expert opinions, establishing criteria, and applying intuitionistic fuzzy TOPSIS for evaluation, with a comparison to fuzzy TOPSIS. A comparative analysis and sensitivity analysis ensure the robustness and reliability of rankings, making the framework effective for informed wheelchair selection decisions with the following steps:

Step 1 focuses on compiling different types of wheelchair models for evaluation.

Step 2 emphasizes defining the selection criteria and their associated sub-criteria. These are categorized under three main dimensions: performance, usability, and cost. The criteria were determined through an extensive literature review and validated by experts in assistive technology using the Nominal Group Technique (NGT). NGT ensures that the selection process is inclusive and unbiased by encouraging equal participation from all group members, thus eliminating dominant opinions and fostering a balanced evaluation.

Step 3 involves assigning weights to the criteria and sub-criteria. To accommodate for ambiguities and subjective variances, decision-makers (DMs) express their opinions using intuitionistic fuzzy numbers. These weights are essential for the evaluation stage and show how important each criterion is in relation to the others.

Step 4 entails evaluating the shortlisted wheelchairs using the intuitionistic fuzzy-TOPSIS method. After generating a weighted decision matrix, the best solutions and separation metrics are determined in order to rank and compare the options with fuzzy TOPSIS method. This guarantees a thorough and impartial selection procedure.

This framework offers a systematic and reliable approach to wheelchair selection, integrating expert input and robust decision-making tools.

Intuitionistic fuzzy sets

In order to overcome difficulties in human decision making, Zadeh (1978) created the idea of the fuzzy set theory. Subsequently, Atanassov and Atanassov (1999) created intuitionistic fuzzy sets (IFSs) which are used extensively in domains such as evaluation functions, preference relations, medical diagnosis, logic programming, and decision making. An overview of IFSs is given in this section.

An IFS can be defined by considering W as an IFS within a finite set D. The definition of an IFS W is expressed in Eq. (1):

$$W = \{d, \mu_w(d), \vartheta_w(d) | d \in D\} \qquad (1)$$

where $\mu_w(d): D \to [0,1]$ is a membership function and $\vartheta_w(d): D \to [0,1]$ is a non-membership function, in which $0 \leq \mu_w(d) + \vartheta_w(d) \leq 1$.

An IFS includes a third parameter called the hesitation degree. Let π_w(d) represent the hesitation degree regarding whether d belongs to W or not. The hesitation degree π_w(d) is expressed in Eq. (2):

$$\pi_w(d) = 1 - \mu_w(d) - \vartheta_w(d) \qquad (2)$$

where for every $d \in D$: $0 \leq \pi_w(d) \leq 1$.

When W(d) has a low value, there is greater confidence in the information about d. Conversely, a high value of W(d) indicates greater uncertainty regarding d. The multiplication operator for IFSs, as shown in Eq. (3), applies to two IFSs, W and X, within the set D.

$$W \times X = \{\mu_w(d).\mu_x(d), \vartheta_w(d) + \vartheta_x(d) - \vartheta_w(d).\vartheta_x(d) | d \in D\} \qquad (3)$$

Element-wise matrix multiplication is determined as shown in Eq. (4) and it applies to two IFSs, W and X, within the set D.

$$W * X = |[\min\{\mu_w(d), \mu_x(d)\}], [\max\{\vartheta_w(d), \vartheta_x(d)\}]| \qquad (4)$$

Intuitionistic fuzzy TOPSIS

The TOPSIS method is a commonly used methodology that was first presented by Hwang and Yoon in 1981. An alternative that is closest to the positive-ideal solution is considered the best option by Shih et al. (2022). TOPSIS is preferred over AHP and PROMETHEE for its computational efficiency and straightforward ranking based on proximity to ideal solutions. Unlike AHP, which requires pairwise comparisons, and PROMETHEE, which involves preference functions, TOPSIS efficiently handles multiple criteria without extensive complexity.

Fuzzy numbers are frequently used in practical applications to handle the subjective judgments and inherent uncertainties in practical applications decision making. A more complex framework is offered by intuitionistic fuzzy sets (IFSs) which better capture decision-makers' acceptance, rejection, and hesitation levels, as by Naveed and Ali (2025). As suggested by Rouyendegh (2015), this section describes an intuitionistic fuzzy TOPSIS model for assessing options based on a variety of criteria. In this study, intuitionistic fuzzy TOPSIS (IF-TOPSIS) enhances traditional TOPSIS by incorporating IFNs, capturing acceptance, rejection, and hesitation levels. This improves expert judgment representation, making the approach more robust for complex decision-making environments.

Let the set of wheelchair alternatives be $W_A=\{W_{A1},W_{A2},\ldots,W_{Am}\}$, the set of criteria $W_C=\{W_{C1},W_{C2},\ldots,W_{Cn}\}$, and the set of experts $E=\{E_1,E_2,\ldots,E_k\}$. The ranking process follows a structured seven-step algorithm:

Step 1: Estimate the relative importance weights of the experts.

A group of E experts assigns relevance using linguistic terms represented as intuitionistic fuzzy numerals. Let the intuitionistic fuzzy number for the n_{th} expert be denoted as $E_k = [\mu_n, v_n, \pi_n]$, where μ_n, v_n, and π_n represent membership, non-membership, and hesitation degrees, respectively. The weight of the n_{th} expert can then be determined using Eq. (5).

$$\lambda_n = \left[\frac{\mu_n + \pi_n\left(\frac{\mu_n}{\mu_n + \vartheta_n}\right)}{\sum_{n=1}^{E}\left[\mu_n + \pi_n\left(\frac{\mu_n}{\mu_n + \vartheta_n}\right)\right]}\right] \tag{5}$$

where $\sum_{n=1}^{E} \lambda_n = 1$.

Step 2: Evaluate the criterion's weight based on the opinions of experts.

Eq. (6) is used to calculate the weight of the criteria based on the linguistic terms in Table 1.

$$\begin{aligned} w_j = {} & IFWA_\lambda(w_j^1, w_j^2, \dots w_j^E) \\ & = \lambda_1 w_j^1 \oplus \lambda_2 w_j^2 \oplus, \dots, \oplus \lambda_n w_j^E \\ & = \left[1 - \prod_{E=1}^{n}(1-\mu_{ij}^E)^{\lambda_E},\ \prod_{E=1}^{n}(\vartheta_{ij}^E)^{\lambda_E},\ \prod_{E=1}^{n}(1-\mu_{ij}^E)^{\lambda_E} \right. \\ & \quad \left. - \prod_{E=1}^{n}(1-\vartheta_{ij}^E)^{\lambda_E}\right] \end{aligned} \tag{6}$$

Step 3: Establish the intuitionistic fuzzy decision matrix (IFDM).

The weights of the potential alternate wheelchair are estimated using the numerical equivalents of the verbal terms mentioned in Table 2. Using the intuitionistic fuzzy weighted averaging (IFWA) operator, the weights of the decision-makers are integrated to produce the aggregated intuitionistic fuzzy decision matrix (AIFDM), by Panda and Pal (2015). Using Eq. (7), the AIFDM model is produced by integrating the many perspectives of a group of decision-makers into a single, coherent perspective.

$R^{(E)} = (r_{ij}^1)_{m*n}$ is the AIFDM of each expert.

$\lambda = \{\lambda_1, \lambda_2, \lambda_3, \dots\dots, \lambda_E\}$ is the weight of the expert.

$R = (r_{ij})_{m'*n'}$

$$\begin{aligned} r_{ij} = {} & IFWA_\lambda(r_{ij}^1, r_{ij}^2, \dots r_{ij}^E) \\ & = \lambda_1 r_{ij}^1 \oplus \lambda_2 r_{ij}^2 \oplus, \dots, \oplus \lambda_n r_{ij}^E \end{aligned}$$

$$= \left[1 - \prod_{E=1}^{n}\left(1-\mu_{ij}^{E}\right)^{\lambda_E}, \ \prod_{E=1}^{n}\left(\vartheta_{ij}^{E}\right)^{\lambda_E}, \ \prod_{E=1}^{n}\left(1-\mu_{ij}^{E}\right)^{\lambda_E} - \prod_{E=1}^{n}\left(1-\vartheta_{ij}^{E}\right)^{\lambda_E}\right] \quad (7)$$

Table 1 - Linguistic terms for experts, criteria and sub-criteria

Linguistic terms	IFNs
Very Important (VI)	[0.90, 0.05, 0.05]
Important (I)	[0.70, 0.25, 0.05]
Medium (M)	[0.50, 0.40, 0.10]
Unimportant (U)	[0.30, 0.65, 0.05]
Very unimportant (VU)	[0.05, 0.90, 0.05]

Table 2 - Linguistic terms for ranking possible alternatives of wheelchairs

Linguistic terms	IFNs
Extremely high (EH)	[1.00, 0.00, 0.00]
Very high (VH)	[0.90, 0.05, 0.05]
High (H)	[0.70, 0.25, 0.05]
Medium high (MH)	[0.60, 0.35, 0.05]
Medium (M)	[0.50, 0.45, 0.05]
Medium low (ML)	[0.40, 0.55, 0.05]
Low (L)	[0.30, 0.65, 0.05]
Very low (VL)	[0.10, 0.85, 0.05]
Extremely low (EL)	[0.00, 1.00, 0.05]

Step 4: The S matrix computation.

This step involves determining the criteria weights (W) in respect to the IFD matrix (R) using Eq. (8).

$$S = R \otimes W = \left(\mu'_{ij}, \vartheta'_{ij}\right) = \left\{\langle x, \mu_{ij} \times \mu_{ij}, \left(\vartheta_{ij} + \vartheta_j\right) - \left(\vartheta_{ij} \times \vartheta_j\right)\rangle\right\} \quad (8)$$

Step 5: Compute the IF ideal positive and negative outcomes.

The benefit criterion is represented by J_1, and the cost criterion is indicated by J_2. The IF positive-ideal outcome is represented by A^+, whereas the IF negative-ideal outcome is represented by A^-. The following formula is used to obtain these outcomes, A^+ and A^-, using Eq. (9).

$$A^+ = \left(r_1'^+, r_2'^+, \dots, r_n'^+\right), r_j'^+ = \left(\mu_j'^+, \vartheta_j'^+, \pi_j'^+\right), j = 1,2,\dots,n$$

$$A^- = \left(r_1'^-, r_2'^-, \dots, r_n'^-\right), r_j'^- = \left(\mu_j'^-, \vartheta_j'^-, \pi_j'^-\right), j = 1,2,\dots,n \quad (9)$$

where

$\mu_j'^{+} = \{(max_i(\mu_{ij}')j\epsilon J_1), (min_i(\mu_{ij}')j\epsilon J_2)\}$,

$\vartheta_j'^{+} = \{(min_i(\vartheta_{ij}')j\epsilon J_1), (max_i(\vartheta_{ij}')j\epsilon J_2)\}$,

$\pi_j'^{+} = \{(1 - max_i(\mu_{ij}') - min_i(\vartheta_{ij}')j\epsilon J_1), (1 - min_i(\mu_{ij}') - max_i(\vartheta_{ij}')j\epsilon J_2)\}$,

$\mu_j'^{-} = \{(min_i(\mu_{ij}')j\epsilon J_1), (max_i(\mu_{ij}')j\epsilon J_2)\}$,

$\vartheta_j'^{-} = \{(max_i(\vartheta_{ij}')j\epsilon J_1), (min_i(\vartheta_{ij}')j\epsilon J_2)\}$,

$\pi_j'^{-} = \{(1 - min_i(\mu_{ij}') - max_i(\vartheta_{ij}')j\epsilon J_1), (1 - max_i(\mu_{ij}') - min_i(\vartheta_{ij}')j\epsilon J_2)\}$.

Step 6: Estimate the separation measures between different possible wheelchairs.

Ashraf et al. (2021) explain that various distance metrics are used to assess the separation between alternatives in an IFS. These metrics include normalized versions of the Euclidean and Hamming distances as well as their generalizations. The separation measurements for each option are calculated after a particular distance measure has been chosen. These metrics express how far an option is from the negative ideal solution (S_i^+) and the positive ideal solution (S_i^-) using Eq. (10).

$$S_i^+ = \sqrt{\frac{1}{2n}\sum_{j=1}^{n}\left[\left(\mu_{ij}' - \mu_j'^{*}\right)^2 + \left(\vartheta_{ij}' - \vartheta_j'^{*}\right)^2 + \left(\pi_{ij}' - \pi_j'^{*}\right)^2\right]}$$

$$S_i^- = \sqrt{\frac{1}{2n}\sum_{j=1}^{n}\left[\left(\mu_{ij}' - \mu_j'^{-}\right)^2 + \left(\vartheta_{ij}' - \vartheta_j'^{-}\right)^2 + \left(\pi_{ij}' - \pi_j'^{-}\right)^2\right]} \quad (10)$$

Step 7: Estimate the final ranking of different possible wheelchairs.

The following Eq. (11) is the expression for the relative closeness coefficient of an alternative, A_i, with respect to the intuitionistic fuzzy positive ideal solution, A^+:

$$C_i^* = \frac{S_i^-}{S_i^+ + S_i^-}, and\ 0 \le C_i^* \le 1 \quad (11)$$

The preference ranking is then calculated by sorting the C_i^* values in the descending order. Higher values indicate better success. The alternative's performance within the sector is reflected in the C_i value.

Triangular fuzzy TOPSIS

Jana et al. (2024) validate and confirm the outcomes of the intuitionistic fuzzy TOPSIS technique by applying the fuzzy TOPSIS method with triangular fuzzy integers in this section. The process consists of the following steps:

Step 1: Specify the criteria and sub-criteria weights.

Triangular fuzzy numbers are used to assess each criterion and sub-criterion's relevance.

Step 2: Aggregate the weights of the sub-criteria and criteria.

Taking $\overline{X_E} = (p_{iE}, q_{iE}, r_{iE})$ is a triangular fuzzy number indicated by the weight of the wheelchair criteria $\overline{X_E}$ determined by the expert E, and $\overline{Y_E} = \left(p_{jE}, q_{jE}, r_{jE}\right)$ is also a triangular fuzzy number indicated by the weight of the wheelchair sub-criteria $\overline{Y_E}$ of criteria $\overline{X_E}$ calculated by the Eth expert. The aggregate weight (AW_E) of the Eth criteria and its respective sub-criteria can be estimated using Eq. (12) [9].

$$AW_E = (\alpha, \beta, \gamma) \tag{12}$$

where

$\alpha = min\left(p_{iE}, p_{jE}\right),$

$\beta = \sqrt[E]{\prod_{E=1}^{n} q_{ik}, q_{jk}}$ and

$\alpha = max\left(r_{iE}, r_{jE}\right).$

Step 3: Integrate the expert's views.

Using the same procedure described in Step 2, the combined weights of the criterion and sub-criteria from each expert are combined in this phase.

Step 4: Normalize the aggregated decision matrix.

A linear scale transformation is used to normalize the fuzzy decision matrix $(\overline{FB})$. The following Eq. (13) is used for the normalization procedure.

$$\overline{FB} = \left[fb_{ij}\right]_{m\times n}$$

$$fb_{ij} = \left(\frac{p_{ij}}{q_j^+}, \frac{q_{ij}}{q_j^+}, \frac{r_{ij}}{q_j^+}\right) \text{ for the benefit criteria}$$

$$fb_{ij} = \left(\frac{p_j^-}{p_{ij}}, \frac{p_j^-}{q_{ij}}, \frac{p_j^-}{r_{ij}}\right) \text{ for the cost criteria} \tag{13}$$

Step 5: Develop a fuzzy aggregated fuzzy decision matrix.

Let a_{ij} represent the rate of the given aggregated weights of the criterion and sub-criteria (determined in Step 3); the aggregated fuzzy decision matrix of the options $\overline{AFB}$ can be constructed using Eq.(14).

$$\overline{AFB} = \begin{bmatrix} a_{11}\ a_{12}\ a_{1j}\ a_{1m} \\ a_{i1}\ a_{i2}\ a_{ij}\ a_{im} \\ a_{n1}\ a_{n2}\ a_{nj}\ a_{nm} \end{bmatrix} \quad (14)$$

Step 6: Normalize the aggregate fuzzy decision matrix of the alternatives.

Using the same equations as in Step 4, the aggregated fuzzy decision matrix is normalized in Step 5.

Step 7: Establish the weighted normalized decision matrix (WN) by multiplying the weights of the aggregated criteria's normalized elements by the aggregated fuzzy decision matrix $\overline{AFB}$ by the sub-criteria using Eq. (15).

$$WN = a_{ij} \times \overline{AFB} \quad (15)$$

Step 8: Identify the fuzzy positive ideal solution and the fuzzy negative ideal solution.

The fuzzy positive ideal solution (I^+) and the fuzzy negative ideal solution (I^-) are calculated using Eq. (16).

$$I^+ = \{\theta_1^+, \theta_j^+, \dots., \theta_m^+\}$$
$$I^- = \{\theta_1^-, \theta_j^-, \dots., \theta_m^-\} \quad (16)$$

where $\theta_j^+ = (1,1,1)$ and $\theta_j^- = (0,0,0)$.

Step 9: Compute each alternative's distance from the fuzzy positive and negative ideal solutions.

Let (S_i^+) and (S_i^-) denote the distances of each alternative wheelchair from $\theta_j^+$and θ_j^-, respectively, and calculated using Eq. (17).

$$S_i^+ = \sum_{j=1}^{n} d_v\left(\theta_{ij}, \theta_j^+\right)$$
$$S_i^- = \sum_{j=1}^{n} d_v\left(\theta_{ij}, \theta_j^-\right) \quad (17)$$

where dv (.,.) uses the vertex method to display the distance between two fuzzy numbers. When triangular fuzzy numbers are involved, it can be computed using Eq. (18) as follows:

$$S(x,y) = \sqrt{\frac{1}{3}\left[\left(p_x - p_y\right)^2 + \left(q_x - q_y\right)^2 + \left(r_x - r_y\right)^2\right]} \quad (18)$$

Step-10: Ranking of the wheelchair alternatives.

The alternatives are ranked in the descending order of the closeness coefficient C_i^*.

Numerical example

The proposed case study

For those with physical limitations, mobility solutions are crucial, and wheelchairs continue to be a vital tool for enhancing their quality of life. Depending on the demands of the user, different wheelchair types—such as manual (MW), electric (EW), or AI-powered (APW) wheelchairs—offer unique benefits and drawbacks. The Educational Institute (EI) tries to develop a wheelchair prototype and aims to choose the best wheelchair type for its customers by balancing cost, usefulness, and user-specific needs.

The EI wants to enhance its wheelchair prototype by switching to contemporary, eco-friendly, and effective wheelchair solutions in light of growing awareness of user-centered design and wheelchair technological breakthroughs. The Institute is dedicated to meeting various demands of its users while ensuring that its services are in line with the WHO standards for assistive technology. In order to do this, the EI started a methodical assessment to determine which wheelchair type would work best for various user groups.

Three wheelchair models were selected for further evaluation. Manual wheelchairs are affordable, lightweight, and appropriate for people with strong upper bodies. Electric wheelchairs are battery-powered devices with sophisticated functions which are ideal for anyone with poor physical strength or movement. AI-powered wheelchairs are designed for people with severe mobility issues or cognitive impairments. These wheelchairs have voice control, intelligent navigation, and obstacle avoidance features. An in-depth comprehension of user profiles, environmental factors, and financial limitations was necessary for the evaluation.

To evaluate the choices, a team of three experts—robotic engineers, biomedical engineers, and occupational therapists—was selected for their expertise in wheelchair technology, human mobility, and user-centered design. This multidisciplinary team ensures a balanced evaluation by integrating technical innovation, medical considerations, and practical usability. While a larger panel could provide broader insights, three experts were deemed sufficient for an initial assessment, ensuring efficiency without compromising decision quality. In order to identify the most qualified wheelchair, the following process was taken into consideration.

Establishing the criteria and sub- criteria for choosing a qualified wheelchair

These criteria and their sub-criteria were chosen based on the literature research, and they were then validated and modified in response to DMs' feedback, as indicated in Table 3.

Table 3 - Identified criteria and sub- criteria

Dimension	**Criteria**	**Sub-criteria**
User-centric factors	User’s physical condition (C-1)	Strength and endurance (SC-1)
		Posture support (SC-2)
		Weight capacity (SC-3)
		Range of motion (SC-4)
	Comfort (C-2)	Seat cushioning (SC-5)
		Back support (SC-6)
		Adjustability (SC-7)
		Ergonomics (SC-8)
	Ease of use (C-3)	Maneuverability (SC-9)
		Control interface simplicity (SC-10)
		Caregiver involvement (SC-11)
		User learning curve (SC-12)
	Control interface (C-4)	Joystick control (SC-13)
		Voice or gesture control (SC-14)
		Manual control options (SC-15)
		Caregiver assist mode (SC-16)
	Customization (C-5)	Adjustable footrests (SC-17)
		Adjustable armrests (SC-18)
		Seat size and configuration (SC-19)
		Accessory options (SC-20)
Performance & durability	Mobility & maneuverability (C-6)	Turning radius (SC-21)
		Indoor and outdoor usability (SC-22)
		Terrain compatibility (SC-23)
		Stability on uneven surfaces (SC-24)

VOJNOTEHNIČKI GLASNIK / MILITARY TECHNICAL COURIER, 2025, Vol. 73, Issue 3

Dimension	Criteria	Sub-criteria
	Battery life/power supply (C-7)	Battery capacity (SC-25)
		Charging time (SC-26)
		Range per charge (SC-27)
		Power durability (SC-28)
	Durability (C-8)	Frame strength (SC-29)
		Wheel durability (SC-30)
		Long-term reliability (SC-31)
		Resistance to wear and tear (SC-32)
Cost, safety & technology	Cost (C-9)	Initial purchase cost (SC-33)
		Maintenance expenses (SC-34)
		Insurance coverage (SC-35)
		Warranty (SC-36)
	Safety features (C-10)	Anti-tip mechanism (SC-37)
		Seat belts and harnesses (SC-38)
		Braking systems (SC-39)
		Collision detection (SC-40)
	Technology integration (C-11)	GPS navigation (SC-41)
		Sensor integration (SC-42)
		Software updates (SC-43)
		Smartphone compatibility (SC-44)

Selection of wheelchairs using intuitionistic fuzzy TOPSIS and its results

The linguistic terms from Table 1 were used to estimate the criteria and the experts. The significance of each expert in the group decision-making process is seen in Table 4. Furthermore, the significance of the criteria and sub-criteria was evaluated using the linguistic phrases listed in Table 1. Using Eq. (5), the expert weights were determined.

Table 4 - Significance of professionals and their weights

	E1	E2	E3
Linguistic terms	Very Important	Important	Very Important
Weights	0.36	0.28	0.36

Table 5 - Ratings of the alternatives, ratings of the alternatives based on IFNs, AIFD matrix

Criteria	Types	Ratings			Ratings based on IFNs			AIFD matrix
		E-1	E-2	E-3	E-1	E-2	E-3	
C1	MW	L	ML	VL	[0.30, 0.65]	[0.40, 0.55]	[0.10, 0.85]	[0.266, 0.683, 0.051]
	EW	M	MH	ML	[0.50, 0.45]	[0.60, 0.35]	[0.40, 0.55]	[0.498, 0.451, 0.051]
	APW	H	VH	MH	[0.70, 0.25]	[0.90, 0.05]	[0.60, 0.35]	[0.755, 0.180, 0.065]
C2	MW	ML	L	M	[0.40, 0.55]	[0.30, 0.65]	[0.50, 0.45]	[0.413, 0.536, 0.050]
	EW	M	MH	H	[0.50, 0.45]	[0.60, 0.35]	[0.70, 0.25]	[0.609, 0.339, 0.051]
	APW	H	EH	VH	[0.70, 0.25]	[1.00, 0.00]	[0.90, 0.05]	[1.000, 0.000, 0.000]
C3	MW	L	ML	VL	[0.30, 0.65]	[0.40, 0.55]	[0.10, 0.85]	[0.266, 0.683, 0.051]
	EW	M	MH	MH	[0.50, 0.45]	[0.60, 0.35]	[0.60, 0.35]	[0.539, 0.383, 0.078]
	APW	EH	VH	EH	[1.00, 0.00]	[0.90, 0.05]	[1.00, 0.00]	[1.000, 0.000, 0.000]
C4	MW	EL	EL	EL	[0.00, 1.00]	[0.00, 1.00]	[0.00, 1.00]	[0.000, 1.000, 0.000]
	EW	ML	M	M	[0.40, 0.55]	[0.50, 0.45]	[0.50, 0.45]	[0.466, 0.484, 0.050]
	APW	VH	EH	VH	[0.90, 0.05]	[1.00, 0.00]	[0.90, 0.05]	[1.000, 0.000, 0.000]
C5	MW	EL	VL	EL	[0.00, 1.00]	[0.10, 0.85]	[0.00, 1.00]	[0.029, 0.956, 0.015]
	EW	M	MH	M	[0.50, 0.45]	[0.60, 0.35]	[0.50, 0.45]	[0.530, 0.419, 0.050]
	APW	H	EH	VH	[0.70, 0.25]	[1.00, 0.00]	[0.90, 0.05]	[0.781, 0.000, 0.219]
C6	MW	VL	EL	VL	[0.10, 0.85]	[0.00, 1.00]	[0.10, 0.85]	[0.073, 0.890, 0.037]
	EW	H	H	VH	[0.70, 0.25]	[0.70, 0.25]	[0.90, 0.05]	[0.798, 0.140, 0.062]
	APW	H	VH	EH	[0.70, 0.25]	[0.90, 0.05]	[1.00, 0.00]	[1.000, 0.000, 0.000]
C7	MW	EL	EL	EL	[0.00, 1.00]	[0.00, 1.00]	[0.00, 1.00]	[0.000, 1.000, 0.000]
	EW	M	M	ML	[0.50, 0.45]	[0.50, 0.45]	[0.40, 0.55]	[0.466, 0.484, 0.050]
	APW	VH	H	H	[0.90, 0.05]	[0.70, 0.25]	[0.70, 0.25]	[0.798, 0.140, 0.062]
C8	MW	MH	M	MH	[0.60, 0.35]	[0.50, 0.45]	[0.60, 0.35]	[0.574, 0.376, 0.050]
	EW	MH	MH	H	[0.60, 0.35]	[0.60, 0.35]	[0.70, 0.25]	[0.639, 0.310, 0.051]
	APW	MH	H	VH	[0.60, 0.35]	[0.70, 0.25]	[0.90, 0.05]	[0.776, 0.158, 0.066]
C9	MW	EL	VL	L	[0.00, 1.00]	[0.10, 0.85]	[0.30, 0.65]	[0.146, 0.818, 0.036]
	EW	H	MH	MH	[0.70, 0.25]	[0.60, 0.35]	[0.60, 0.35]	[0.639, 0.310, 0.051]
	APW	EH	VH	EH	[1.00, 0.00]	[0.90, 0.05]	[1.00, 0.00]	[1.000, 0.000, 0.000]
C10	MW	L	VL	VL	[0.30, 0.65]	[0.10, 0.85]	[0.10, 0.85]	[0.178, 0.772, 0.050]
	EW	H	MH	MH	[0.70, 0.25]	[0.60, 0.35]	[0.60, 0.35]	[0.639, 0.310, 0.051]
	APW	EH	EH	VH	[1.00, 0.00]	[1.00, 0.00]	[0.90, 0.05]	[1.000, 0.000, 0.000]
C11	MW	VL	L	VL	[0.10, 0.85]	[0.30, 0.65]	[0.10, 0.85]	[0.161, 0.788, 0.050]
	EW	M	M	ML	[0.50, 0.45]	[0.50, 0.45]	[0.40, 0.55]	[0.466, 0.484, 0.050]
	APW	MH	H	MH	[0.60, 0.35]	[0.70, 0.25]	[0.60, 0.35]	[0.631, 0.319, 0.051]

Table 2 lists the linguistic terms that were used to rank the wheelchair alternatives. Table 5 summarizes the expert's ratings for the three wheelchair options: manual, electric, and AI-powered and also displays the IFNs that were created from these ratings. By integrating the views of the experts, the AIFD matrix (Eq. (7)) was produced as shown in Table 5.The significance of the wheelchair selection criteria and sub-criteria, as stated in linguistic terms, is shown in Tables 6 and 7. Subsequently, these linguistic terms were transformed into IFNs which are also displayed in Table 7. To calculate the weight of each criterion, the opinions of the decision-makers were compiled using Eq. (5.) The ultimate weight of the combined criterion and sub-criteria, as well as their final combined importance, are displayed in Table 8.

Table 6 - Ratings of the criteria

Criteria	Ratings of the criteria		
	E-1	E-2	E-3
C1	I	M	I
C2	M	I	I
C3	I	VI	I
C4	I	I	M
C5	M	I	M
C6	VI	I	VI
C7	I	M	I
C8	M	I	VI
C9	VI	VI	I
C10	I	VI	I
C11	I	M	VI

Table 7 - Ratings of the sub-criteria, and ratings of the sub-criteria based on IFNs

Sub-criteria	Ratings			Ratings of the sub-criteria based on IFNs		
	E-1	E-2	E- 3	E-1	E-2	E-3
SC-1	M	U	M	(0.50, 0.40)	(0.30, 0.65)	(0.50, 0.40)
SC-2	I	M	VI	(0.70, 0.25)	(0.50, 0.40)	(0.90, 0.05)
SC-3	I	M	I	(0.70, 0.25)	(0.50, 0.40)	(0.70, 0.25)
SC-4	I	I	VI	(0.70, 0.25)	(0.70, 0.25)	(0.90, 0.05)
SC-5	I	VI	I	(0.70, 0.25)	(0.90, 0.05)	(0.70, 0.25)
SC-6	M	VI	M	(0.50, 0.40)	(0.90, 0.05)	(0.50, 0.40)
SC-7	M	I	I	(0.50, 0.40)	(0.70, 0.25)	(0.70, 0.25)
SC-8	I	I	M	(0.70, 0.25)	(0.70, 0.25)	(0.50, 0.40)
SC-9	VI	VI	I	(0.90, 0.05)	(0.90, 0.05)	(0.70, 0.25)
SC-10	I	VI	M	(0.70, 0.25)	(0.90, 0.05)	(0.50, 0.40)
SC-11	U	VU	U	(0.30, 0.65)	(0.05, 0.90)	(0.30, 0.65)
SC-12	M	M	I	(0.50, 0.40)	(0.50, 0.40)	(0.70, 0.25)
SC-13	I	M	M	(0.70, 0.25)	(0.50, 0.40)	(0.50, 0.40)
SC-14	VI	VI	I	(0.90, 0.05)	(0.90, 0.05)	(0.70, 0.25)
SC-15	M	U	U	(0.50, 0.40)	(0.30, 0.65)	(0.30, 0.65)
SC-16	M	U	M	(0.50, 0.40)	(0.30, 0.65)	(0.50, 0.40)
SC-17	I	VI	I	(0.70, 0.25)	(0.90, 0.05)	(0.70, 0.25)
SC-18	VI	I	VI	(0.90, 0.05)	(0.70, 0.25)	(0.90, 0.05)
SC-19	VI	I	VI	(0.90, 0.05)	(0.70, 0.25)	(0.90, 0.05)
SC-20	VI	I	VI	(0.90, 0.05)	(0.70, 0.25)	(0.90, 0.05)
SC-21	I	M	I	(0.70, 0.25)	(0.50, 0.40)	(0.70, 0.25)

Sub-criteria	E-1	E-2	E- 3	E-1	E-2	E-3
SC-22	I	VI	VI	(0.70, 0.25)	(0.90, 0.05)	(0.90, 0.05)
SC-23	VI	VI	VI	(0.90, 0.05)	(0.90, 0.05)	(0.90, 0.05)
SC-24	VI	VI	VI	(0.90, 0.05)	(0.90, 0.05)	(0.90, 0.05)
SC-25	I	VI	I	(0.70, 0.25)	(0.90, 0.05)	(0.70, 0.25)
SC-26	M	I	M	(0.50, 0.40)	(0.70, 0.25)	(0.50, 0.40)
SC-27	VI	VI	I	(0.90, 0.05)	(0.90, 0.05)	(0.70, 0.25)
SC-28	I	I	I	(0.70, 0.25)	(0.70, 0.25)	(0.70, 0.25)
SC-29	VI	I	VI	(0.90, 0.05)	(0.70, 0.25)	(0.90, 0.05)
SC-30	M	M	I	(0.50, 0.40)	(0.50, 0.40)	(0.70, 0.25)
SC-31	I	I	M	(0.70, 0.25)	(0.70, 0.25)	(0.50, 0.40)
SC-32	U	I	M	(0.30, 0.65)	(0.70, 0.25)	(0.50, 0.40)
SC-33	VI	VI	I	(0.90, 0.05)	(0.90, 0.05)	(0.70, 0.25)
SC-34	U	M	VU	(0.30, 0.65)	(0.50, 0.40)	(0.05, 0.90)
SC-35	VI	M	VU	(0.90, 0.05)	(0.50, 0.40)	(0.05, 0.90)
SC-36	I	M	I	(0.70, 0.25)	(0.50, 0.40)	(0.70, 0.25)
SC-37	I	VI	VI	(0.70, 0.25)	(0.90, 0.05)	(0.90, 0.05)
SC-38	VI	M	I	(0.90, 0.05)	(0.50, 0.40)	(0.70, 0.25)
SC-39	VI	VI	VI	(0.90, 0.05)	(0.90, 0.05)	(0.90, 0.05)
SC-40	VI	I	VI	(0.90, 0.05)	(0.70, 0.25)	(0.90, 0.05)
SC-41	I	I	I	(0.70, 0.25)	(0.70, 0.25)	(0.70, 0.25)
SC-42	I	I	M	(0.70, 0.25)	(0.70, 0.25)	(0.50, 0.40)
SC-43	VI	M	I	(0.90, 0.05)	(0.50, 0.40)	(0.70, 0.25)
SC-44	VI	M	I	(0.90, 0.05)	(0.50, 0.40)	(0.70, 0.25)

Table 8 - Final aggregated significance of the criteria and the sub-criteria

Combined	E-1	E-2	E-3	Final weight aggregated criteria and sub-criteria
C-1	(0.50, 0.40)	(0.30, 0.65)	(0.50, 0.40)	(0.451, 0.458, 0.091)
C-2	(0.50, 0.40)	(0.70, 0.25)	(0.50, 0.40)	(0.567, 0.351, 0.083)
C-3	(0.30, 0.65)	(0.05, 0.90)	(0.30, 0.65)	(0.238, 0.712, 0.050)
C-4	(0.50, 0.40)	(0.30, 0.65)	(0.30, 0.65)	(0.380, 0.546, 0.074)
C-5	(0.70, 0.25)	(0.70, 0.25)	(0.70, 0.25)	(0.700, 0.250, 0.050)
C-6	(0.70, 0.25)	(0.50, 0.40)	(0.70, 0.25)	(0.654, 0.285, 0.061)
C-7	(0.50, 0.40)	(0.70, 0.25)	(0.50, 0.40)	(0.567, 0.351 0.083)
C-8	(0.30, 0.65)	(0.50, 0.40)	(0.50, 0.40)	(0.436, 0.476, 0.088)
C-9	(0.30, 0.65)	(0.50, 0.40)	(0.05, 0.90)	(0.289, 0.638, 0.073)
C-10	(0.70, 0.25)	(0.50, 0.40)	(0.70, 0.25)	(0.654, 0.285,0.061)
C-11	(0.70, 0.25)	(0.50, 0.40)	(0.50, 0.40)	(0.584, 0.338, 0.078)

For the wheelchair selection C-1, C-2, C-3, C-4, C-5, C-6, C-7, C-8, C-10, and C-11 are the benefit criteria where C-9 is the cost criteria. The IF positive-ideal solution (A^+) and the IF negative-ideal solution (A^-) for the wheelchair selection were determined using Eqs. (8) and (9) as its results are shown in Table 9.

Table 9 - Intuitionistic fuzzy positive and negative ideal solutions

	A^+	A^-
C-1	(0.341, 0.556, 0.104)	(0.120, 0.828, 0.052)
C-2	(0.567,0.351, 0.082)	(0.234, 0.699, 0.067)
C-3	(0.238, 0.712, 0.050)	(0.063, 0.909, 0.028)
C-4	(0.380, 0.546, 0.074)	(0.000, 1.000, 0.000)
C-5	(0.547, 0.250, 0.203)	(0.020, 0.967, 0.013)
C-6	(0.654, 0.285, 0.061)	(0.048, 0.921, 0.031)
C-7	(0.452, 0.442, 0.106)	(0.000, 1.000, 0.000)
C-8	(0.338, 0.559, 0.103)	(0.279, 0.638, 0.083)
C-9	(0.042, 0.934, 0.024)	(0.289, 0.638, 0.073)
C-10	(0.654, 0.285, 0.061)	(0.116, 0.837, 0.047)
C-11	(0.369, 0.549, 0.082)	(0.094, 0.860, 0.046)

The normalized Euclidean distance was used to determine the positive (S^+) and negative (S^-) separation measures for each wheelchair alternative, and the results are shown in Table10 using Eq. (10). The relative closeness coefficients C_i^* were initially computed in order to rank the wheelchair options using Eq. (11). After that, the options were arranged in accordance with their C_i^* values in the descending order.

The wheelchair types in this case study were ranked as follows: AI-Powered >Electric > Manual. As a result, the electric AI-powered wheelchair was chosen as the best choice out of the available options.

Table 10 - Separation measures and the relative closeness coefficient for each wheelchair alternative

Wheelchair	S^+	S^-	C_i^*	Rank
MW	0.410	0.083	0.169	3rd
EW	0.179	0.256	0.589	2nd
APW	0.083	0.409	0.832	1st

Selection of the wheelchair using fuzzy TOPSIS

The weights assigned to the criteria and sub-criteria were determined in order to begin the evaluation procedure. The linguistic terms listed in Table 11 were used to do this. The same table shows the TFNs that were used to quantify these linguistic phrases. TFNs, which offer a range of values to better capture the subjective assessments of experts, are frequently used to manage uncertainty and imprecision in decision-making processes.

Table 11 - Linguistic terms for the criteria and sub-criteria

Linguistic terms	TFNs
Very important (VI)	(0.75, 0.90, 1.00)
Important (I)	(0.60, 0.75, 0.90)
Medium (M)	(0.30, 0.45, 0.60)
Unimportant (U)	(0.15, 0.30, 0.45)
Very unimportant (VU)	(0.00, 0.15, 0.30)

As shown in Tables 12 and 13, the experts first used linguistic terms to represent the priority levels of the criterion and the sub-criteria. The experts' qualitative inputs are compiled in these tables which also represent their opinions on the relative importance of each criterion and sub-criterion.

Table 12 - Linguistic terms and TFNs for the criteria

Criteria	Linguistic terms			TFNs for the criteria		
	E-1	E-2	E-3	E-1	E-2	E-3
C1	I	M	I	(0.60, 0.75, 0.90)	(0.30, 0.45, 0.60)	(0.60, 0.75, 0.90)
C2	M	I	I	(0.30, 0.45, 0.60)	(0.60, 0.75, 0.90)	(0.60, 0.75, 0.90)
C3	I	VI	I	(0.60, 0.75, 0.90)	(0.75, 0.90, 1.00)	(0.60, 0.75, 0.90)
C4	I	I	M	(0.60, 0.75, 0.90)	(0.60, 0.75, 0.90)	(0.30, 0.45, 0.60)
C5	M	I	M	(0.30, 0.45, 0.60)	(0.60, 0.75, 0.90)	(0.30, 0.45, 0.60)
C6	VI	I	VI	(0.75, 0.90, 1.00)	(0.60, 0.75, 0.90)	(0.75, 0.90, 1.00)
C7	I	M	I	(0.60, 0.75, 0.90)	(0.30, 0.45, 0.60)	(0.60, 0.75, 0.90)
C8	M	I	VI	(0.30, 0.45, 0.60)	(0.60, 0.75, 0.90)	(0.75, 0.90, 1.00)
C9	VI	VI	I	(0.75, 0.90, 1.00)	(0.75, 0.90, 1.00)	(0.60, 0.75, 0.90)
C10	I	VI	I	(0.60, 0.75, 0.90)	(0.75, 0.90, 1.00)	(0.60, 0.75, 0.90)
C11	I	M	VI	(0.60, 0.75, 0.90)	(0.30, 0.45, 0.60)	(0.75, 0.90, 1.00)

Table 13 - Linguistic terms and TFNs for the sub-criteria

Sub-criteria	Linguistic terms			TFNs for the sub-criteria		
	E-1	E-2	E-3	Expert 1	Expert 2	Expert 3
SC-1	M	U	M	(0.30, 0.45, 0.60)	(0.15, 0.30, 0.45)	(0.30, 0.45, 0.60)
SC-2	I	M	VI	(0.60, 0.75, 0.90)	(0.30, 0.45, 0.60)	(0.75, 0.90, 1.00)
SC-3	I	M	I	(0.60, 0.75, 0.90)	(0.30, 0.45, 0.60)	(0.60, 0.75, 0.90)
SC-4	I	I	VI	(0.60, 0.75, 0.90)	(0.60, 0.75, 0.90)	(0.75, 0.90, 1.00)
SC-5	I	VI	I	(0.60, 0.75, 0.90)	(0.75, 0.90, 1.00)	(0.60, 0.75, 0.90)
SC-6	M	VI	M	(0.30, 0.45, 0.60)	(0.75, 0.90, 1.00)	(0.30, 0.45, 0.60)
SC-7	M	I	I	(0.30, 0.45, 0.60)	(0.60, 0.75, 0.90)	(0.60, 0.75, 0.90)
SC-8	I	I	M	(0.60, 0.75, 0.90)	(0.60, 0.75, 0.90)	(0.30, 0.45, 0.60)
SC-9	VI	VI	I	(0.75, 0.90, 1.00)	(0.75, 0.90, 1.00)	(0.60, 0.75, 0.90)
SC-10	I	VI	M	(0.60, 0.75, 0.90)	(0.75, 0.90, 1.00)	(0.30, 0.45, 0.60)
SC-11	U	VU	U	(0.15, 0.30, 0.45)	(0.00, 0.15, 0.30)	(0.15, 0.30, 0.45)
SC-12	M	M	I	(0.30, 0.45, 0.60)	(0.30, 0.45, 0.60)	(0.60, 0.75, 0.90)
SC-13	I	M	M	(0.60, 0.75, 0.90)	(0.30, 0.45, 0.60)	(0.30, 0.45, 0.60)
SC-14	VI	VI	I	(0.75, 0.90, 1.00)	(0.75, 0.90, 1.00)	(0.60, 0.75, 0.90)
SC-15	M	U	U	(0.30, 0.45, 0.60)	(0.15, 0.30, 0.45)	(0.15, 0.30, 0.45)
SC-16	M	U	M	(0.30, 0.45, 0.60)	(0.15, 0.30, 0.45)	(0.30, 0.45, 0.60)
SC-17	I	VI	I	(0.60, 0.75, 0.90)	(0.75, 0.90, 1.00)	(0.60, 0.75, 0.90)
SC-18	VI	I	VI	(0.75, 0.90, 1.00)	(0.60, 0.75, 0.90)	(0.75, 0.90, 1.00)
SC-19	VI	I	VI	(0.75, 0.90, 1.00)	(0.60, 0.75, 0.90)	(0.75, 0.90, 1.00)
SC-20	VI	I	VI	(0.75, 0.90, 1.00)	(0.60, 0.75, 0.90)	(0.75, 0.90, 1.00)
SC-21	I	M	I	(0.60, 0.75, 0.90)	(0.30, 0.45, 0.60)	(0.60, 0.75, 0.90)
SC-22	I	VI	VI	(0.60, 0.75, 0.90)	(0.75, 0.90, 1.00)	(0.75, 0.90, 1.00)
SC-23	VI	VI	VI	(0.75, 0.90, 1.00)	(0.75, 0.90, 1.00)	(0.75, 0.90, 1.00)
SC-24	VI	VI	VI	(0.75, 0.90, 1.00)	(0.75, 0.90, 1.00)	(0.75, 0.90, 1.00)
SC-25	I	VI	I	(0.60, 0.75, 0.90)	(0.75, 0.90, 1.00)	(0.60, 0.75, 0.90)
SC-26	M	I	M	(0.30, 0.45, 0.60)	(0.60, 0.75, 0.90)	(0.30, 0.45, 0.60)
SC-27	VI	VI	I	(0.75, 0.90, 1.00)	(0.75, 0.90, 1.00)	(0.60, 0.75, 0.90)
SC-28	I	I	I	(0.60, 0.75, 0.90)	(0.60, 0.75, 0.90)	(0.60, 0.75, 0.90)
SC-29	VI	I	VI	(0.75, 0.90, 1.00)	(0.60, 0.75, 0.90)	(0.75, 0.90, 1.00)
SC-30	M	M	I	(0.30, 0.45, 0.60)	(0.30, 0.45, 0.60)	(0.60, 0.75, 0.90)
SC-31	I	I	M	(0.60, 0.75, 0.90)	(0.60, 0.75, 0.90)	(0.30, 0.45, 0.60)
SC-32	U	I	M	(0.15, 0.30, 0.45)	(0.60, 0.75, 0.90)	(0.30, 0.45, 0.60)
SC-33	VI	VI	I	(0.75, 0.90, 1.00)	(0.75, 0.90, 1.00)	(0.60, 0.75, 0.90)
SC-34	U	M	VU	(0.15, 0.30, 0.45)	(0.30, 0.45, 0.60)	(0.00, 0.15, 0.30)
SC-35	VI	M	VU	(0.75, 0.90, 1.00)	(0.30, 0.45, 0.60)	(0.00, 0.15, 0.30)
SC-36	I	M	I	(0.60, 0.75, 0.90)	(0.30, 0.45, 0.60)	(0.60, 0.75, 0.90)
SC-37	I	VI	VI	(0.60, 0.75, 0.90)	(0.75, 0.90, 1.00)	(0.75, 0.90, 1.00)

Sub-criteria	E-1	E-2	E-3	Expert 1	Expert 2	Expert 3
SC-38	VI	M	I	(0.75, 0.90, 1.00)	(0.30, 0.45, 0.60)	(0.60, 0.75, 0.90)
SC-39	VI	VI	VI	(0.75, 0.90, 1.00)	(0.75, 0.90, 1.00)	(0.75, 0.90, 1.00)
SC-40	VI	I	VI	(0.75, 0.90, 1.00)	(0.60, 0.75, 0.90)	(0.75, 0.90, 1.00)
SC-41	I	I	I	(0.60, 0.75, 0.90)	(0.60, 0.75, 0.90)	(0.60, 0.75, 0.90)
SC-42	I	I	M	(0.60, 0.75, 0.90)	(0.60, 0.75, 0.90)	(0.30, 0.45, 0.60)
SC-43	VI	M	I	(0.75, 0.90, 1.00)	(0.30, 0.45, 0.60)	(0.60, 0.75, 0.90)
SC-44	VI	M	I	(0.75, 0.90, 1.00)	(0.30, 0.45, 0.60)	(0.60, 0.75, 0.90)

Further, the ratings of the combined criteria and sub-criteria (CCS) based on the triangular fuzzy numbers and the aggregated decision using Eq. (12) are shown in Table 14. This table provides a thorough assessment of the options in accordance with the predetermined criteria and sub-criteria by synthesizing the data acquired in the previous steps.

Table 14 - Aggregated decision matrix of the experts

CCS	Expert 1	Expert 2	Expert 3	Aggre. decision
CCS 1	(0.30, 0.68, 0.90)	(0.15, 0.46, 0.90)	(0.30, 0.73, 1.00)	(0.15, 0.61, 1.00)
CCS 2	(0.30, 0.55, 0.90)	(0.60, 0.80, 1.00)	(0.30, 0.61, 0.90)	(0.30, 0.64, 1.00)
CCS 3	(0.15, 0.58, 1.00)	(0.00, 0.58,1.00)	(0.15, 0.56, 0.90)	(0.00, 0.57, 1.00)
CCS 4	(0.30, 0.63, 1.00)	(0.15, 0.49, 1.00)	(0.15, 0.46, 0.90)	(0.15, 0.52, 1.00)
CCS 5	(0.30, 0.76, 1.00)	(0.60, 0.78, 1.00)	(0.30, 0.76, 1.00)	(0.30, 0.77, 1.00)
CCS 6	(0.60, 0.84, 1.00)	(0.30, 0.76, 1.00)	(0.60, 0.87, 1.00)	(0.30, 0.82, 1.00)
CCS 7	(0.30, 0.70, 1.00)	(0.30, 0.73, 1.00)	(0.30, 0.68, 0.90)	(0.30, 0.70, 1.00)
CCS 8	(0.15, 0.53, 1.00)	(0.30, 0.68, 0.90)	(0.30, 0.66, 1.00)	(0.15, 0.62, 1.00)
CCS 9	(0.15, 0.70, 1.00)	(0.30, 0.59, 1.00)	(0.00, 0.39, 0.90)	(0.00, 0.54, 1.00)
CCS 10	(0.60, 0.84, 1.00)	(0.30, 0.76, 1.00)	(0.60, 0.84, 1.00)	(0.30, 0.81, 1.00)
CCS 11	(0.60, 0.81, 1.00)	(0.30, 0.55, 0.90)	(0.30, 0.70, 1.00)	(0.30, 0.68, 1.00)

The fuzzy TOPSIS methodology's Step 4 equations are used to calculate the normalized values of the created decision matrix. Table 15 presents the normalized results. The language terms used to rate the alternatives are also shown in Table 16.

Table 15 - Normalized aggregated score of the experts

Criteria	Normalized score		
C1	0.15	0.61	1.00
C2	0.30	0.64	1.00

Criteria	Normalized score		
C3	0.00	0.57	1.00
C4	0.15	0.52	1.00
C5	0.30	0.77	1.00
C6	0.30	0.82	1.00
C7	0.30	0.70	1.00
C8	0.15	0.62	1.00
C9	0.00	0.00	0.00
C10	0.30	0.81	1.00
C11	0.30	0.68	1.00

Table 16 – Ranking of the alternatives in linguistic terms

Linguistic terms	TFNs
Extremely high (EH)	[0.80, 0.90, 1.00]
Very high (VH)	[0.70, 0.80, 0.90]
High (H)	[0.60, 0.70, 0.80]
Medium high (MH)	[0.50, 0.60, 0.70]
Medium (M)	[0.40, 0.50, 0.60]
Medium low (ML)	[0.30, 0.40, 0.50]
Low (L)	[0.20, 0.30, 0.40]
Very low (VL)	[0.10, 0.20, 0.30]
Extremely low (EL)	[0.00, 0.10, 0.20]

Table 17 summarizes the evaluations given to the three wheelchairs by the experts based on the language terms included in Table 16. To account for the subjectivity and inherent ambiguity of the assessments, these ratings are then converted into triangular fuzzy numbers. Table 17 provides the options' comprehensive fuzzy representations, allowing for additional investigation.

The fuzzy aggregated decision matrix based on the collective views of the experts is displayed in Table 18. Tables 19 and 20 display the normalized version and the related weighted normalized fuzzy aggregated decision matrix, respectively. The calculations used adhere to the same methodology described in Eq. (12) which is used for the aggregation of the criterion and the sub-criteria.

For each aggregated criterion and sub-criterion, the ratings of each alternative were then calculated in relation to the fuzzy positive ideal solution (I^+) and the fuzzy negative ideal solution (I^-). The proximity of each alternative to the ideal and non-ideal solutions is measured by these computations. Tables 21 and 22 provide an evaluation of the outcomes of these calculations.

Table 17 - Rating and TFNs of the alternatives

Criteria	Types	Linguistic terms E-1	E-2	E-3	TFNs for the alternatives E-1	E-2	E-3
C1	MW	L	ML	VL	[0.20, 0.30, 0.40]	[0.30, 0.40, 0.50]	[0.10, 0.20, 0.30]
	EW	M	MH	ML	[0.40, 0.50, 0.60]	[0.50, 0.60, 0.70]	[0.30, 0.40, 0.50]
	APW	H	VH	MH	[0.60, 0.70, 0.80]	[0.70, 0.80, 0.90]	[0.50, 0.60, 0.70]
C2	MW	ML	L	M	[0.30, 0.40, 0.50]	[0.20, 0.30, 0.40]	[0.40, 0.50, 0.60]
	EW	M	MH	H	[0.40, 0.50, 0.60]	[0.50, 0.60, 0.70]	[0.60, 0.70, 0.80]
	APW	H	EH	VH	[0.60, 0.70, 0.80]	[0.80, 0.90, 1.00]	[0.70, 0.80, 0.90]
C3	MW	L	ML	VL	[0.20, 0.30, 0.40]	[0.30, 0.40, 0.50]	[0.10, 0.20, 0.30]
	EW	M	MH	MH	[0.40, 0.50, 0.60]	[0.50, 0.60, 0.70]	[0.50, 0.60, 0.70]
	APW	EH	VH	EH	[0.80, 0.90, 1.00]	[0.70, 0.80, 0.90]	[0.80, 0.90, 1.00]
C4	MW	EL	EL	EL	[0.00, 0.10, 0.20]	[0.00, 0.10, 0.20]	[0.00, 0.10, 0.20]
	EW	ML	M	M	[0.30, 0.40, 0.50]	[0.40, 0.50, 0.60]	[0.40, 0.50, 0.60]
	APW	VH	EH	VH	[0.70, 0.80, 0.90]	[0.80, 0.90, 1.00]	[0.70, 0.80, 0.90]
C5	MW	EL	VL	EL	[0.00, 0.10, 0.20]	[0.10, 0.20, 0.30]	[0.00, 0.10, 0.20]
	EW	M	MH	M	[0.40, 0.50, 0.60]	[0.50, 0.60, 0.70]	[0.40, 0.50, 0.60]
	APW	H	EH	VH	[0.60, 0.70, 0.80]	[0.80, 0.90, 1.00]	[0.70, 0.80, 0.90]
C6	MW	VL	EL	VL	[0.10, 0.20, 0.30]	[0.00, 0.10, 0.20]	[0.10, 0.20, 0.30]
	EW	H	H	VH	[0.60, 0.70, 0.80]	[0.60, 0.70, 0.80]	[0.70, 0.80, 0.90]
	APW	H	VH	EH	[0.60, 0.70, 0.80]	[0.70, 0.80, 0.90]	[0.80, 0.90, 1.00]
C7	MW	EL	EL	EL	[0.00, 0.10, 0.20]	[0.00, 0.10, 0.20]	[0.00, 0.10, 0.20]
	EW	M	M	ML	[0.40, 0.50, 0.60]	[0.40, 0.50, 0.60]	[0.30, 0.40, 0.50]
	APW	VH	H	H	[0.70, 0.80, 0.90]	[0.60, 0.70, 0.80]	[0.60, 0.70, 0.80]
C8	MW	MH	M	MH	[0.50, 0.60, 0.70]	[0.40, 0.50, 0.60]	[0.50, 0.60, 0.70]
	EW	MH	MH	H	[0.50, 0.60, 0.70]	[0.50, 0.60, 0.70]	[0.60, 0.70, 0.80]
	APW	MH	H	VH	[0.50, 0.60, 0.70]	[0.60, 0.70, 0.80]	[0.70, 0.80, 0.90]
C9	MW	EL	VL	L	[0.00, 0.10, 0.20]	[0.10, 0.20, 0.30]	[0.20, 0.30, 0.40]
	EW	H	MH	MH	[0.60, 0.70, 0.80]	[0.50, 0.60, 0.70]	[0.50, 0.60, 0.70]
	APW	EH	VH	EH	[0.80, 0.90, 1.00]	[0.70, 0.80, 0.90]	[0.80, 0.90, 1.00]
C10	MW	L	VL	VL	[0.20, 0.30, 0.40]	[0.10, 0.20, 0.30]	[0.10, 0.20, 0.30]
	EW	H	MH	MH	[0.60, 0.70, 0.80]	[0.50, 0.60, 0.70]	[0.50, 0.60, 0.70]
	APW	EH	EH	VH	[0.80, 0.90, 1.00]	[0.80, 0.90, 1.00]	[0.70, 0.80, 0.90]
C11	MW	VL	L	VL	[0.10, 0.20, 0.30]	[0.20, 0.30, 0.40]	[0.10, 0.20, 0.30]
	EW	M	M	ML	[0.40, 0.50, 0.60]	[0.40, 0.50, 0.60]	[0.30, 0.40, 0.50]
	APW	MH	H	MH	[0.50, 0.60, 0.70]	[0.60, 0.70, 0.80]	[0.50, 0.60, 0.70]

Table 18 - Experts' fuzzy aggregated assessment matrix for each choice

Criteria	MW	EW	APW
AC1	[0.10, 0.29, 0.50]	[0.30, 0.49, 0.70]	[0.50, 0.69, 0.90]
AC2	[0.20, 0.39, 0.60]	[0.40, 0.59, 0.80]	[0.60, 0.80, 1.00]
AC3	[0.10, 0.29, 0.50]	[0.40, 0.56, 0.70]	[0.70, 0.86, 1.00]
AC4	[0.00, 0.10, 0.20]	[0.30, 0.46, 0.60]	[0.70, 0.83, 1.00]
AC5	[0.00, 0.13, 0.30]	[0.40, 0.53, 0.70]	[0.60, 0.78, 1.00]
AC6	[0.00, 0.16, 0.30]	[0.60, 0.73, 0.90]	[0.60, 0.80, 1.00]
AC7	[0.00, 0.10, 0.20]	[0.30, 0.46, 0.60]	[0.60, 0.73, 0.90]
AC8	[0.40, 0.56, 0.70]	[0.50, 0.63, 0.80]	[0.50, 0.69, 0.90]
AC9	[0.00, 0.18, 0.40]	[0.50, 0.63, 0.80]	[0.70, 0.86, 1.00]
AC10	[0.10, 0.23, 0.40]	[0.50, 0.66, 0.80]	[0.70, 0.86, 1.00]
AC11	[0.10, 0.23, 0.40]	[0.30, 0.46, 0.60]	[0.50, 0.63, 0.80]

Table 19 - Experts' normalized fuzzy aggregated assessment matrix for each choice

Criteria	MW	EW	APW
AC1	[0.10, 0.29, 0.50]	[0.30, 0.49, 0.70]	[0.50, 0.69, 0.90]
AC2	[0.20, 0.39, 0.60]	[0.40, 0.59, 0.80]	[0.60, 0.80, 1.00]
AC3	[0.10, 0.29, 0.50]	[0.40, 0.56, 0.70]	[0.70, 0.86, 1.00]
AC4	[0.00, 0.10, 0.20]	[0.30, 0.46, 0.60]	[0.70, 0.83, 1.00]
AC5	[0.00, 0.13, 0.30]	[0.40, 0.53, 0.70]	[0.60, 0.78, 1.00]
AC6	[0.00, 0.16, 0.30]	[0.60, 0.73, 0.90]	[0.60, 0.80, 1.00]
AC7	[0.00, 0.10, 0.20]	[0.30, 0.46, 0.60]	[0.60, 0.73, 0.90]
AC8	[0.40, 0.56, 0.70]	[0.50, 0.63, 0.80]	[0.50, 0.69, 0.90]
AC9	[0.00, 0.00, 0.00]	[0.00, 0.00, 0.00]	[0.00, 0.00, 0.00]
AC10	[0.10, 0.23, 0.40]	[0.50, 0.66, 0.80]	[0.70, 0.86, 1.00]
AC11	[0.10, 0.23, 0.40]	[0.30, 0.46, 0.60]	[0.50, 0.63, 0.80]

Table 20 - Experts' weighted normalized fuzzy aggregated assessment matrix for each choice

Criteria	MW	EW	APW
AC1	[0.015, 0.177, 0.500]	[0.045, 0.299, 0.700]	[0.075, 0.421, 0.900]
AC2	[0.060, 0.249, 0.600]	[0.120, 0.377, 0.800]	[0.180, 0.512, 1.000]
AC3	[0.000, 0.165, 0.500]	[0.000, 0.319, 0.700]	[0.000, 0.490, 1.000]
AC4	[0.000, 0.052, 0.200]	[0.045, 0.239, 0.600]	[0.105, 0.432, 1.000]
AC5	[0.000, 0.100, 0.300]	[0.120, 0.408, 0.700]	[0.180, 0.600, 1.000]
AC6	[0.000, 0.131, 0.300]	[0.180, 0.598, 0.900]	[0.018, 0.656, 1.000]

Criteria	MW	EW	APW
AC7	[0.000, 0.070, 0.200]	[0.090, 0.322, 0.060]	[0.180, 0.511, 0.900]
AC8	[0.060, 0.347, 0.700]	[0.075, 0.390, 0.800]	[0.075, 0.428, 0.900]
AC9	[0.000, 0.000, 0.000]	[0.000, 0.000, 0.000]	[0.000, 0.000, 0.000]
AC10	[0.030, 0.186, 0.400]	[0.150, 0.535, 0.800]	[0.210, 0.696, 1.000]
AC11	[0.030, 0.156, 0.400]	[0.090, 0.313, 0.600]	[0.150, 0.428, 0.800]

Table 21 – Rating the distances between every choice and the fuzzy positive ideal solution I^+

Criteria	MW	EW	APW
AC1	0.795	0.706	0.633
AC2	0.732	0.633	0.551
AC3	0.806	0.720	0.648
AC4	0.920	0.742	0.612
AC5	0.876	0.636	0.527
AC6	0.865	0.530	0.601
AC7	0.914	0.851	0.554
AC8	0.683	0.650	0.631
AC9	1.000	1.000	1.000
AC10	0.809	0.571	0.489
AC11	0.819	0.698	0.603
SI^+	9.219	7.737	6.847

Table 22 - Rating the distances between each choice and the fuzzy negative ideal solution I^-

Criteria	MW	EW	APW
AC1	0.306	0.440	0.575
AC2	0.377	0.515	0.657
AC3	0.304	0.444	0.643
AC4	0.119	0.374	0.632
AC5	0.183	0.473	0.681
AC6	0.189	0.632	0.691
AC7	0.122	0.196	0.606
AC8	0.452	0.516	0.577
AC9	0.000	0.000	0.000
AC10	0.255	0.562	0.714
AC11	0.248	0.394	0.531
SI^-	2.556	4.547	6.307

Table 23 - Each wheelchair ranking, separation metrics, and relative closeness coefficient

Alternatives	SI^+	SI^-	Ci*	Rank
MW	9.219	2.556	0.217	3rd
EW	7.737	4.547	0.370	2nd
APW	6.847	6.307	0.479	1st

The three options were ordered in descending order of the relative proximity coefficients (Ci*), which were computed in order to rate the different options. According to the fuzzy TOPSIS analysis results in Table 30, APW > EW > MW is the ranking. As a result, APW was determined to be the wheelchair option that was the most preferred.

Sensitivity analysis

A sensitivity analysis that looked at how different factors affected the ranking of the wheelchairs is presented in this section. Three different circumstances were examined in the analysis, each concentrating on a different set of criteria. A thorough summary of these situations is given in Table 24 which also highlights the variables assessed in each scenario. In order to rank the alternatives, the analysis additionally analyzes the results of the intuitionistic fuzzy TOPSIS and fuzzy TOPSIS methodologies; the results are shown in Table 24.

Table 24 - Sensitivity analysis results for multiple circumstances

Circumstance	Decision criteria	Experts	Wheelchair ranking	
			Intuitionistic fuzzy TOPSIS	Triangular fuzzy TOPSIS
Current circumstance	C-1, C-2, C-3, C-4, C-5, C-6, C-7, C-8, C-9, C-10, C-11	E1, E2, E3	APW > EW > MW	APW > EW > MW
Circumstance 1	C-1, C-2, C-3, C-4, C-5 (User-centric factors)	E1, E2, E3	APW > EW > MW	APW > EW > MW
Circumstance 2	C-6, C-7, C-8 (Performance & durability)	E1, E2, E3	APW > EW > MW	APW > EW > MW
Circumstance 3	C-9, C-10, C-11 (Cost, safety & technology)	E1, E2, E3	APW > EW > MW	APW > EW > MW

Figures 2 and 3 provide a visual representation of the sensitivity analysis findings. These numbers show how well the two approaches perform in comparison under various conditions. In contrast to the conventional fuzzy TOPSIS approach, the intuitionistic fuzzy TOPSIS method exhibits an equivalent sensitivity to scenario modifications, as illustrated. The intuitionistic fuzzy TOPSIS method's increased sensitivity is especially useful in situations where criteria are very subjective and need intricate assessments. The intuitionistic fuzzy TOPSIS approach gives decision-makers a more thorough and reliable way to distinguish between options when criteria are qualitative in nature, including user-centric factors, performance & durability, and cost, safety & technology for nuanced decision making. This feature promotes more educated wheelchair selection decisions and improves the dependability of the rating process. Overall, the findings highlight how crucial it is to use cutting-edge techniques like intuitionistic fuzzy TOPSIS when dealing with situations involving subjective criteria since they provide more accuracy and flexibility in supplier evaluation for the selection of sustainable wheelchairs.

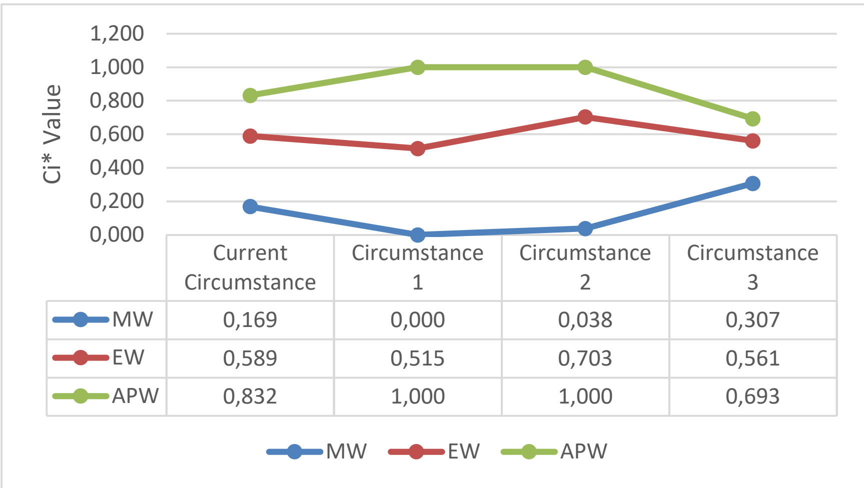

Figure 2 - Intuitionistic fuzzy TOPSIS approach sensitivity analysis results

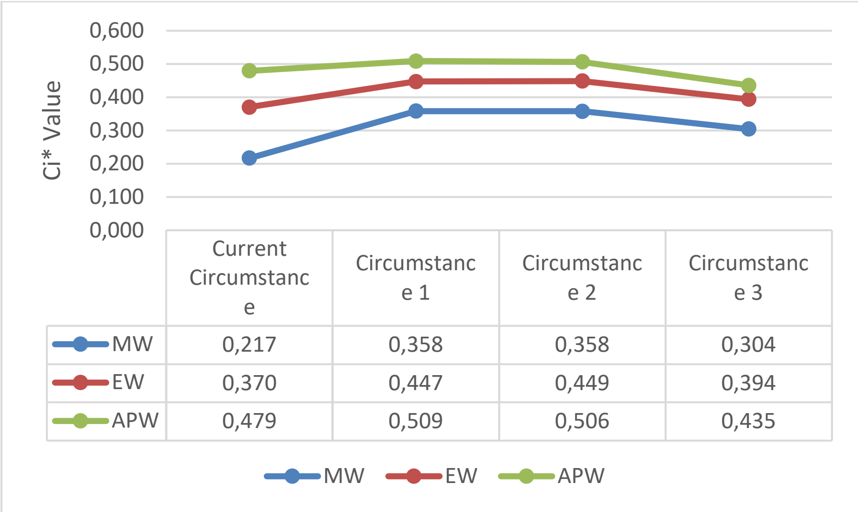

Figure 3 - Triangular fuzzy TOPSIS approach sensitivity analysis results

Discussion

Research findings

The MCDM method based on intuitionistic fuzzy TOPSIS is introduced in this study, adding to the body of knowledge on wheelchair selection. The approach successfully tackles the subjectivity and ambiguity of wheelchair evaluation. A thorough sensitivity analysis was conducted, contrasting the results of intuitionistic fuzzy TOPSIS with those of conventional fuzzy TOPSIS, in order to verify its robustness.

The sensitivity analysis for wheelchair selection was performed across three distinct circumstances to evaluate how varying decision criteria influence the rankings generated by the intuitionistic fuzzy TOPSIS and triangular fuzzy TOPSIS methods. The "Current circumstance" considered all decision criteria (C-1 to C-11) and expert opinions (E1, E2, E3), with both methods yielding the same ranking: APW > EW > MW. In "Circumstance 1," which focused on user-centric factors (C-1 to C-5), the rankings remained unchanged across both methods, highlighting the consistency of the alternatives under user-specific priorities. Similarly, "Circumstance 2," emphasizing performance and durability (C-6 to C-8), and "Circumstance 3," addressing cost, safety, and technology (C-9 to C-11), also produced identical rankings across both methods: APW > EW > MW. This consistency across all circumstances indicates that both methods are robust under varying criteria; however, intuitionistic fuzzy TOPSIS is better equipped to detect subtle variations and differences in certain subjective scenarios, as it incorporates a higher degree of sensitivity and adaptability. This capability makes intuitionistic fuzzy TOPSIS particularly advantageous when dealing with highly subjective and nuanced decision-making contexts.

The selected wheelchair alternatives differ significantly in functionality, making their ranking relatively intuitive, even for non-experts. However, this example serves as an illustration to demonstrate the applicability of intuitionistic fuzzy TOPSIS and to highlight the importance of various criteria in the selection process. The true value of this approach lies in its ability to handle complex decision-making scenarios where differences are less obvious. Intuitionistic fuzzy TOPSIS enhances sensitivity and adaptability, making it particularly useful for nuanced and highly subjective decision-making contexts.

Research implications

This method is unique in that it uses intuitionistic fuzzy numbers in conjunction with the TOPSIS method to solve imprecise decision making. With an emphasis on wheelchair selection, it assesses the aspects related to cost, safety, and technology, as well as user-centric factors including performance and durability. The study helps stakeholders grasp the fundamentals of a thorough wheelchair assessment for improved decision making by rating and choosing the best choices based on these criteria.

Real-world applications and managerial perspectives

The application of Intuitionistic Fuzzy TOPSIS and Triangular Fuzzy TOPSIS in wheelchair selection provides significant managerial insights by emphasizing the effectiveness of APW over EW and MW. Both methods address uncertainties and subjective judgments in evaluating user-centric factors, performance & durability, and cost, safety & technology dimensions. The consistent superiority of APW highlights its ability to prioritize criteria effectively, leading to accurate and user-aligned decisions. While APW may suggest options with higher initial costs, these selections typically offer better durability, safety, and user satisfaction, reducing long-term expenses. These approaches empower managers to make holistic, data-driven, and sustainable decisions, balancing economic, functional, and technological priorities.

Conclusion and future work

Adopting sustainable and user-centric techniques is essential when choosing wheelchairs in order to satisfy a variety of needs while taking durability and long-term cost effectiveness into consideration. The intricacy and subjectivity of decision making make it difficult to choose the best wheelchair model based on predetermined criteria. Using an intuitionistic fuzzy TOPSIS approach, this paper proposes a useful decision-making framework to investigate the wheelchair choosing process. The most pertinent criteria and sub-criteria across the user-centric factors, performance & durability, and cost, safety & technology aspects were found by a thorough literature research. The collective views of experts led to the finalization of these criteria. The suggested approach takes subjective assessments and uncertainties into consideration when ranking and choosing the best wheelchair model. A comparison with the fuzzy TOPSIS method under three distinct scenarios was carried out to verify the robustness of the strategy and show the model's sensitivity and dependability.

Although practitioners in other contexts would need to reinterpret the criteria and ratings based on expert judgments to meet their particular needs, the system can be modified for new fields. Because of its adaptability, the framework can be used in a variety of industries while still being accurate and relevant. This study's absence of interdependencies between the criterion and the sub-criteria, which could affect results, is a limitation. In order to account for these interdependencies and further improve the selection process, future research could address this by including approaches like the Analytic Hierarchy Process.

References

Ashraf, Z., Khan, M.S., Tiwari, A. and Danish Lohani, Q.M., 2021. Difference sequence-based distance measure for intuitionistic fuzzy sets and its application in decision making process. *Soft Computing*, *25*(14), pp.9139-9161. Available at: https://doi.org/10.1007/s00500-021-05875-2

Atanassov, K.T. and Atanassov, K.T., 1999. *Intuitionistic fuzzy sets* (pp. 1-137). Physica-Verlag HD. Available at: https://doi.org/10.1007/978-3-7908-1870-3_1

Dağıstanlı, H.A., 2024. An interval-valued intuitionistic fuzzy VIKOR approach for R&D project selection in defense industry investment decisions. *Journal of Soft Computing and Decision Analytics*, *2*(1), pp.1-13. Available at: https://doi.org/10.31181/jscda21202428 de Vries, W.H., van der Slikke, R.M., van Dijk, M.P. and Arnet, U., 2023. Real-life wheelchair mobility metrics from IMUs. *Sensors*, *23*(16), p.7174. Available at: https://doi.org/10.3390/s23167174

Fasipe, G., Goršič, M., Rahman, M.H. and Rammer, J., 2024. Community mobility and participation assessment of manual wheelchair users: a review of current techniques and challenges. *Frontiers in human neuroscience*, *17*, p.1331395. Available at: https://doi.org/10.3389/fnhum.2023.1331395

Görçün, Ö.F., Ulutaş, A., Topal, A. and Ecer, F., 2024. Telescopic forklift selection through a novel interval-valued Fermatean fuzzy PIPRECIA–WISP approach. *Expert Systems with Applications*, *255*, p.124674. Available at: https://doi.org/10.1016/j.eswa.2024.124674

Griggs, K.E., 2025. Wheelchair satisfaction and recommended improvements of manual wheelchairs in the UK. *Disability and Rehabilitation: Assistive Technology*, *20*(1), pp.163-170. Available at: https://doi.org/10.1080/17483107.2024.2359473

Hwang, C.L. and Yoon, K., 1981. Methods for multiple attribute decision making. *Multiple attribute decision making: methods and applications a state-of-the-art survey*, pp.58-191. Available at: https://doi.org/10.1007/978-3-642-48318-9_3

Imran, R., Ullah, K., Ali, Z. and Akram, M., 2024. A multi-criteria group decision-making approach for robot selection using interval-valued intuitionistic fuzzy information and aczel-alsina bonferroni means. *Spectrum of Decision Making and Applications*, *1*(1), pp.1-32. Available at: https://doi.org/10.31181/sdmap1120241

Jana, C., Simic, V., Pal, M., Sarkar, B. and Pamucar, D., 2024. Hybrid multi-criteria decision-making method with a bipolar fuzzy approach and its applications to economic condition analysis. *Engineering Applications of Artificial Intelligence*, *132*, p.107837. Available at: https://doi.org/10.1016/j.engappai.2023.107837

Kargi, B., Coccia, M. and Uçkaç, B.C., 2023. Findings from the first wave of covid-19 on the different impacts of lockdown on public health and economic growth. *International Journal of Economic Sciences*, *12*(2), pp.21-39. Available at: https://doi.org/10.52950/ES.2023.12.2.002

Kim, J.H., Kim, Y.R., Han, M.H., Han, S., Jeon, E.H., Hwang, E.Y., Yang, J.W., Lee, S.Y. and Lee, G., 2024. A study on the formative usability testing for modular powered wheelchair. *Disability and Rehabilitation: Assistive Technology*, pp.1-9. Available at: https://doi.org/10.1080/17483107.2024.2372310

Kocejko, T., Matuszkiewicz, N., Durawa, P., Madajczak, A. and Kwiatkowski, J., 2024. How integration of a brain-machine interface and obstacle detection system can improve wheelchair control via movement imagery. *Sensors*, *24*(3), p.918. Available at: https://doi.org/10.3390/s24030918

Kousar, S. and Kausar, N., 2025. Multi-Criteria Decision-Making for Sustainable Agritourism: An Integrated Fuzzy-Rough Approach. *Spectrum of Operational Research*, *2*(1), pp.134-150. Available at: https://doi.org/10.31181/sor21202515

Kulich, H.R., Bass, S.R. and Koontz, A.M., 2024. Rehabilitation professional and user evaluation of an integrated push-pull lever drive system for wheelchair mobility. *Assistive Technology*, *36*(5), pp.329-337. Available at: https://doi.org/10.1080/10400435.2020.1836068

Mao, Q., Gao, Y. and Fan, J., 2024. An investment decision framework for offshore CCUS project under interval-valued fermatean fuzzy environment. *Environmental Technology*, pp.1-26. Available at: https://doi.org/10.1080/09593330.2024.2376291

Mohebbi, V., Dianat, I. and Castellucci, H.I., 2024. Psychometric properties of the Iranian version of the wheelchair seating discomfort assessment tool (WcS-DAT)–section II: a revised two-dimensional structure of comfort and discomfort to improve inclusive design practice. *Disability and Rehabilitation: Assistive Technology*, *19*(4), pp.1351-1357. Available at: https://doi.org/10.1080/17483107.2023.2176556

Nace, S., Tiernan, J., Ní Annaidh, A. and Holland, D., 2023. Development and evaluation of a facile mesh-to-surface tool for customised wheelchair cushions. *3D Printing in Medicine*, *9*(1), p.3. Available at: https://doi.org/10.1186/s41205-022-00165-5

Nagde, K.R. and Dhoble, S.J., 2021. Li-S ion batteries: A substitute for Li-ion storage batteries. In *Energy Materials* (pp. 335-371). Elsevier. Available at: https://doi.org/10.1016/B978-0-12-823710-6.00008-X

Naveed, H. and Ali, S., 2025. Addressing decision-making challenges: similarity measures for interval-valued intuitionistic fuzzy hypersoft sets. *Decision Making Advances*, *3*(1), pp.175-184. Available at: https://doi.org/10.31181/dma31202566

Panda, A. and Pal, M., 2015. A study on pentagonal fuzzy number and its corresponding matrices. *Pacific Science Review B: Humanities and Social Sciences*, *1*(3), pp.131-139. Available at: https://doi.org/10.1016/j.psrb.2016.08.001

Rivas, F., Sierra, J.E. and Cámara, J.M., 2024. Architectural Proposal for Low-Cost Brain–Computer Interfaces with ROS Systems for the Control of Robotic Arms in Autonomous Wheelchairs. *Electronics*, *13*(6), p.1013. Available at: https://doi.org/10.3390/electronics13061013

Rotschedl, J., Neugebauer, J., Vokoun, M. and Barák, V., 2024. Neuroeconomics-a review of the influence of neurotransmitters on the behaviour and decision-making of individuals in economic matters. *International Journal of Economic Sciences*, *13*(2), pp.129-149. Available at: https://doi.org/10.52950/ES.2024.13.2.008

Rouyendegh, B.D., 2015. Developing an integrated ANP and intuitionistic fuzzy TOPSIS model for supplier selection. *Journal of Testing and Evaluation*, *43*(3), pp.664-672. Available at: https://doi.org/10.1520/JTE20130114

Sahoo, S.K. and Choudhury, B.B., 2021. A Fuzzy AHP Approach to Evaluate the Strategic Design Criteria of a Smart Robotic Powered Wheelchair Prototype. In *Intelligent Systems: Proceedings of ICMIB 2020* (pp. 451-464). Singapore: Springer Singapore. Available at: https://doi.org/10.1007/978-981-33-6081-5_40

Sahoo, S.K. and Choudhury, B.B., 2024. An Integrated MCDM Framework for Optimizing Rotary Actuator Selection in Smart Robotic Power Wheelchair Prototypes. *Jordan Journal of Mechanical & Industrial Engineering*, *18*(3). Available at: https://doi.org/10.59038/jjmie/170419

Sampathkumar, S., Augustin, F., Narayanamoorthy, S., Ahmadian, A., Ferrara, M. and Kang, D., 2024. Centroid and Graded Mean Ranking Methods for Intuitionistic Trapezoidal Dense Fuzzy Set to Solve MCDM Problems of Robot Selection. *International Journal of Fuzzy Systems*, pp.1-24. Available at: https://doi.org/10.1007/s40815-023-01647-2

Saqlain, M. and Saeed, M., 2024. From ambiguity to clarity: unraveling the power of similarity measures in multi-polar interval-valued intuitionistic fuzzy soft sets. *Decision Making Advances*, *2*(1), pp.48-59. Available at: https://doi.org/10.31181/dma21202421

Sarfraz, M., 2024. Application of Interval-valued T-spherical Fuzzy Dombi Hamy Mean Operators in the antiviral mask selection against COVID-19. *Journal of Decision Analytics and Intelligent Computing*, *4*(1), pp.67-98. Available at: https://doi.org/10.31181/jdaic10030042024s

Shih, H.S. and Olson, D.L., 2022. *TOPSIS and its extensions: A distance-based MCDM approach* (Vol. 447, pp. 1-215). Springer. Available at: https://doi.org/10.1007/978-3-031-09577-1

Unni, A., John, S.J. and Baiju, T., 2024. Circular Intuitionistic Fuzzy Soft Set Theoretic Approach to Decision Making Problems. *IEEE Access*. Available at: https://doi.org/10.1109/ACCESS.2024.3472215

Verma, A., Shrivastava, S. and Ramkumar, J., 2024. Mapping wheelchair functions and their associated functional elements for stair climbing accessibility: a systematic review. *Disability and Rehabilitation: Assistive Technology*, *19*(1), pp.200-221. Available at: https://doi.org/10.1080/17483107.2022.2075476

Zadeh, L.A., 1978. Fuzzy sets as a basis for a theory of possibility. *Fuzzy sets and systems*, *1*(1), pp.3-28. Available at: https://doi.org/10.1016/0165-0114(78)90029-5

Zhang, Z., Xu, P., Wu, C. and Yu, H., 2024. Smart nursing wheelchairs: A new trend in assisted care and the future of multifunctional integration. *Biomimetics*, *9*(8), p.492. Available at: https://doi.org/10.3390/biomimetics9080492

Un enfoque de toma de decisiones de múltiples criterios para la selección de sillas de ruedas utilizando topsis difuso intuicionista

Prasant Ranjan Dhal[a], *Bibhuti* Bhusan Choudhury[a], *Sushil* Kumar Sahoo[a], **autor de correspondencia**, *Dragan* Pamucar[b], *Vladimir* Simic[c]

[a] Instituto de Tecnología Indira Gandhi (BPUT, Rourkela), Departamento de Ingeniería Mecánica, Sarang, Dhenkanal, Odisha, India,

[b] Universidad de Belgrado, Departamento de Investigación Operativa y Estadística, Facultad de Ciencias Organizacionales, Belgrado, Serbia + Facultad de Ciencia y Tecnología, Universidad de Corea, Departamento de

Ciencias Matemáticas Aplicadas, Sejong, República de Corea
[c] Universidad de Belgrado, Facultad de Ingeniería de Transporte y Tráfico, Vojvode Stepe 305, Belgrado, Serbia,

CAMPO: ciencias de la decisión, ingeniería mecánica
TIPO DE ARTÍCULO: artículo científico original

Resumen:

Introducción/objetivo: Seleccionar una silla de ruedas adecuada es vital para garantizar la movilidad, la comodidad y la independencia de las personas con discapacidad. El objetivo principal es ayudar a identificar la silla de ruedas óptima considerando diversos criterios centrados en el usuario y minimizando las ambigüedades en la toma de decisiones.
Métodos: El marco propuesto aprovecha conjuntos difusos intuicionistas para abordar la indecisión y la imprecisión que suelen presentarse en la toma de decisiones. La ponderación de los criterios y las evaluaciones de alternativas se determinaron con la participación de expertos. Se realizó un análisis de sensibilidad para garantizar la robustez y fiabilidad del proceso de clasificación. Se realizó un estudio de caso para validar la eficacia de la metodología e ilustrar su aplicación práctica.
Resultados: El estudio demostró que las sillas de ruedas impulsadas por IA (APW) superaron a otras opciones de sillas de ruedas según los criterios y subcriterios seleccionados.
Conclusión: Los hallazgos resaltan la utilidad del enfoque intuicionista difuso TOPSIS para facilitar la toma de decisiones bien informadas en la selección de sillas de ruedas. Este método beneficia a usuarios finales, cuidadores y profesionales médicos al abordar las complejidades de la toma de decisiones subjetiva e incierta, lo que en última instancia conduce a resultados más inclusivos y confiables. El marco demuestra ser una herramienta eficaz para mejorar el proceso de toma de decisiones en la selección de sillas de ruedas.

Palabras claves: selección de silla de ruedas, difuso intuicionista, difuso triangular, TOPSIS, análisis de sensibilidad.

Многокритериальный подход к принятию решений при выборе инвалидной коляски с использованием интуиционистского нечеткого topsis метода

Прасант Ранджан Дхал[а], *Бибути* Бусан Чоудури[а], *Сушил* Кумар Саху[а], **корреспондент**, *Драган* Памучар[б], *Владимир* Симич[в]

[а] Технологический институт имени Индиры Ганди (BPUT, Руркела), факультет машиностроения, Саранг, Дхенканал, Одиша, Республика Индия
[б] Белградский университет, факультет организационных наук, кафедра операционных исследований и статистики, Белград, Республика Сербия

+ Корейский университет, колледж науки и технологий, факультет прикладных наук, кафедра математических наук, Седжон, Республика Корея

[в] Белградский университет, факультет транспорта и организации движения, ул. Воеводы Степы, д.305, г. Белград, Республика Сербия

РУБРИКА ГРНТИ: 73.47.12 Организация управления и автоматизированные системы управления транспортом,

ВИД СТАТЬИ: оригинальная научная статья

Резюме:

Введение/цель: Выбор подходящей инвалидной коляски имеет жизненно важное значение для обеспечения мобильности, комфорта и независимости людей с ограниченными возможностями. Основная цель статьи – помочь в выборе наиболее подходящей инвалидной коляски, принимая во внимание ряд критериев, ориентированных на пользователя, и сводя к минимуму неопределенность при принятии решений.

Методы: В предлагаемой структуре используется интуиционистские нечеткие множества, объясняющие неопределенность и неточность часто присутствующих в процессе принятия решений. Веса критериев и оценки альтернатив были утверждены экспертами. Для обеспечения надежности и устойчивости процесса ранжирования применялся анализ чувствительности. Для подтверждения эффективности методологии и иллюстрации ее практического применения было проведено тематическое исследование.

Результаты: Исследование показало, что инвалидные коляски с искусственным интеллектом (APW) превосходят другие варианты инвалидных колясок по выбранным критериям и подкритериям.

Вывод: Результаты показывают, что подход интуиционистских нечетких множеств TOPSIS облегчает процесс принятия решений при выборе инвалидной коляски, основанный на обширной информации. Этот метод приносит пользу конечным пользователям, лицам, осуществляющим уход, и медицинским работникам, поскольку устраняет сложности субъективного и неопределенного процесса принятия решений, что в конечном итоге приводит к более надежным и всеобъемлющим результатам. Доказано, что данная система является эффективным инструментом для оптимизации процесса принятия решений при выборе инвалидной коляски.

Ключевые слова: выбор инвалидной коляски, интуиционистское нечеткое множество, треугольная нечеткое множество, TOPSIS, анализ чувствительности.

Вишекритеријумски приступ одлучивању при избору инвалидских колица помоћу интуитивне фази TOPSIS методе

Прасант Ранџан Дала[а], *Бибути* Бусан Чоудхурја [а], *Сушил* Кумар Саху[а], **аутор за преписку**, *Драган* Памучар[б], *Владимир* Симић[в]

[а] Технолошки институт Индире Ганди (BPUT, Роуркела), Одсек за машинство, Саранг, Дхенканал, Одиша, Индија

[б] Универзитет у Београду, Факултет организационих наука, Катедра за операциона истраживања и статистику, Београд, Србија + Колеџ за науку и технологију, Корејски универзитет, Одсек за примењене математичке науке, Сеџонг, Република Кореја

[в] Универзитет у Београду, Саобраћајни факултет, Београд, Србија

ОБЛАСТ: операциона истраживања, механика

КАТЕГОРИЈА (ТИП) ЧЛАНКА: оригинални научни рад

Сажетак:

Увод/циљ: Избор одговарајућих инвалидских колица од суштинске је важности за обезбеђивање мобилности, удобности и независности особа са инвалидитетом. Примарни циљ рада је да помогне да тај избор буденајпогоднији узимајући у обзир низ критеријума који се односе на корисника и да се притом неизвесност при одлучивању сведе на што мању меру.

Методе: Предложени оквир примењује интуитивне фази скупове да би објаснио неодлучност и непрецизност честе при одлучивању. Тежине критеријума и процене алтернатива одређене су уз помоћ експерата. Примењена је анализа осетљивости како би се обезбедила робустност и поузданост процеса рангирања. Урађена је студија случаја која потврђује ефикасност методологије и илуструје њену практичну примену.

Резултати: Студија је показала да су се инвалидска колица на погон помоћу вештачке интелигенције показала бољим од осталих опција на основу изабраних критеријума и поткритеријума.

Закључак: Налази показују да је интуитивни фази TOPSIS приступ користан при одлучивању на основу обиља информација при избору инвалидских колица. Крајњи корисници, неговатељи и медицински радници имају користи од ове методе која се бави сложеношћу субјективног и неизвесног одлучивања, што у крајњој линији води ка инклузивнијим и поузданијим резултатима. Овај оквир се показао као ефикасно средство за побољшање процеса одлучивања при избору инвалидских колица.

Кључне речи: избор инвалидских колица, интуитивни фази, троугласти фази, TOPSIS, анализа осетљивости

Paper received on:17.02.2025.
Manuscript corrections submitted on:23.03.2025.
Paper accepted for publishing on: 25.03.2025.

Using the finite element method for developing a new model predicting the burst pressure of straight defects in corroded pipes repaired with bonded composite wraps

Aicha Metehri[a], *Belaïd* Mechab[b], *Bel Abbes Bachir* Bouadjra[c]

University of Sidi Bel Abbès, Faculty of Technology, Mechanical Engineering Department, Laboratory of Physical Mechanics of Materials, Sidi Bel Abbès, People's Democratic Republic of Algeria.

[a] e-mail: ametehri@yahoo.com, **corresponding author**, ORCID iD: https://orcid.org/0009-0002-2221-6833

[b] e-mail: bmechab@yahoo.fr, ORCID iD: https://orcid.org/0009-0000-7483-5527

[c] e-mail: bachirbou@yahoo.fr, ORCID iD: https://orcid.org/0000-0002-1925-7194

https://doi.org/10.5937/vojtehg73-56344

FIELD: Computer sciences, mechanical engineering, materials

ARTICLE TYPE: original scientific paper

Abstract:

Introduction/purpose: This work aims to create a novel model that predicts the burst pressure of straight flaws under internal pressure in corroded pipes that have been repaired with bonded composite wraps.

Methods: Geometrical aspects affected the repair performances. The composite patch behaviour strongly depends on several parameters such as pipe size, defect size, composite ply number, ply orientation, composite properties, and adhesive thickness. The effects of all these parameters on the repair efficiency were analyzed.

Results: The obtained results showed that the composite wrap reduces the stress concentration caused by the corrosion defect, which improves the long-term durability of pipes.

Conclusion: The comparison between the new analytically developed model and the finite element (FE) calculations showed good agreement for the repaired corroded pipe.

Keywords: corrosion, uniform pressure, analytical model, pipe, bonded composite repairs

Introduction

Composites are materials of two or more distinct components, offering superior properties to individual materials. However, if a composite has defects, its rigidity decreases (Metehri et al, 2009; 2019; 2024a; Nadia et al, 2024).

Surface flaws are believed to be most common in pipe systems and pressure containers (Mechab et al, 2011; 2014; 2018). A surface fracture is often overlooked during the inspection of a structural component (Mechab et al, 2020). Deterministic approaches are commonly employed in fracture mechanics to evaluate components with suspected or confirmed flaws. These approaches depend on precise hypotheses about the condition of the fault, the material's strength and durability, and the applied force (Fezazi et al, 2021).

Pipe corrosion is a common problem that can lead to leaks and failures. Causes include water or gas quality, temperature, internal pressure, manufacturing defects, etc. Regarding the research method, many researchers have studied the behaviours of composite-repaired corroded pipelines employing field experiments, theoretical deductions, and numerical simulations (Metehri et al, 2024b; 2024c; Alabtah et al, 2021; Kong et al, 2022).

Bonded composite repairs of the structure have become a helpful piping life extension solution over the last two decades (Benyahia et al, 2014; Ibrahim et al, 2018). These repairs provide an efficient method for restoring the ultimate load capability of the structure (Madjdoub et al, 2019). The durability and reliability of structures repaired with composite patches depend mainly on the mechanical and thermal behaviour of the adhesive layer. These are the essential points for studying the causes of failure and the degradation of the entire repair (Lim et al, 2019; Singh et al, 2021).

Glass fibre hoop-reinforced composite systems have proven to be an effective and successful approach for repairing onshore pipelines that have suffered from corrosion and mechanical damage, mainly when the primary stress factor is internal pressure (Chandra Khan et al, 2017). Extending these repair methods to offshore pipelines, such as risers, necessitates a comprehensive understanding of intricate combined load profiles, including substantial tension overlay (De Barros et al, 2018).

Repair methods utilizing glass fiber reinforced materials are employed to restore corroded or damaged pipelines. In this approach, the affected section is strengthened by applying a composite wrap, typically made of glass/epoxy or carbon/epoxy, around the transmission pipelines (Da

Costa-Mattos et al, 2009; Budhe et al, 2017; Alexander et al, 2014). The ability of these Glass fibre-reinforced materials to resist corrosion, their relatively high strength-to-weight ratio, load-bearing capacity, and stiffness makes them an excellent choice for rehabilitating corroded steel pipelines and other mechanical structures. The composite overwrap can ensure an optimal level of pressure-bearing capacity and structural integrity in cases of partial corrosion or partial wall loss defects. However, they may be less effective in preventing leaks in localized through-thickness corrosion defects (Budhe et al, 2020).

Few models in the literature forecast burst pressure in repaired pipes, so we conducted this study to create an analytical model that makes this prediction possible and aids in composite wrap repair design. A finite element analysis presented in this work also describes the impacts of different parameters influencing the repair performances of corroded pipes. The constructed analytical model included each of these parameters.

Geometrical model

In this study, it is supposed that there exists a corrosion defect of a rectangular shape in the central outer wall of a pipeline. The dimensions of the defect are: length (L=300 mm), width (l=200 mm) and defect ratio of the defect depth on the pipe thickness (r=d/t =0.1, 0.2, 0.3, 0.4 and 0.5 mm). The outside diameter of the pipe Dext is 600 mm, Dint represents the inside diameter (Dint = 580 mm), and "t" designates the pipe thickness (t = 10mm); the length of the pipe is 2500mm. The pipeline is subjected to an internal uniform pressure of P=8.42 MPa. Figure 1 illustrates the geometric characteristics of the pipe.

The pipe is made of APC X65 steel, and the corrosion defect is repaired using a glass/epoxy composite wrap with two layers of 0.5 mm thickness for each layer. The ply orientation in the composite is [55/-55]. The composite wrap is bidirectional. We chose to adopt the [55/-55] fiber orientations in the wrapping composite, as this configuration promotes better shear stress absorption which can be significant when repairing pipes exposed to internal pressures. These orientations allow the composite to better withstand the pressure forces exerted on the corroded pipe during its operation, which is crucial for ensuring the repair's effectiveness. Furthermore, the [55/-55] orientations provide increased flexibility, enabling them to more easily conform to the shape of the pipe and ensure optimal adhesion to the corroded surface. This is particularly important for preventing delamination or failure of the repair.

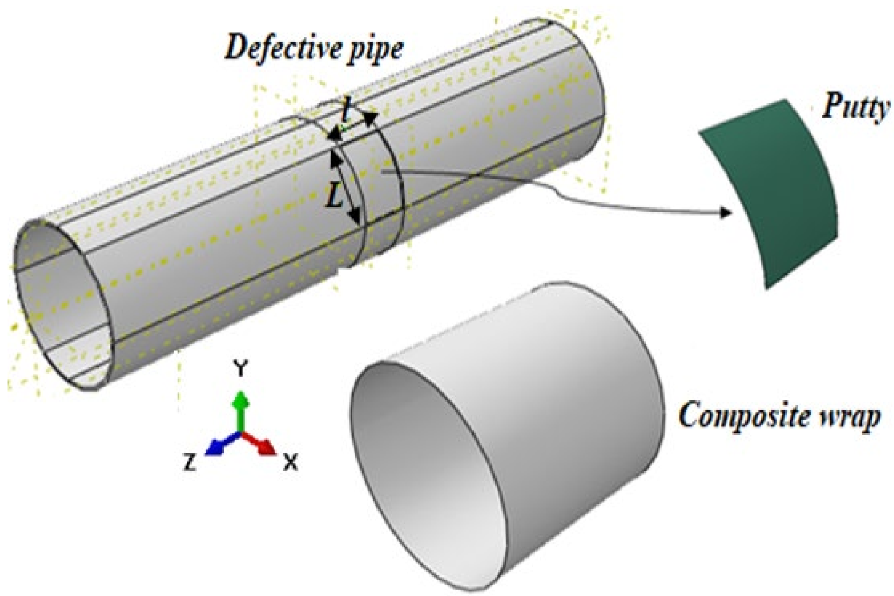

Figure 1 – Corroded pipe repaired with a composite patch wrap and putty

Table 1 – Mechanical properties of different materials used in this study

	Materials				
	Steel X65 (Fatoba & Akid, 2014)	Glass/epoxy (Campilho et al, 2011)	Carbone/ Epoxy (Arroussi et al, 2023)	Araldite 2015 Adhesive (Arroussi et al, 2023)	Putty: Resin Epoxy
E1 (GPa)	211	50	112	1.85	35.9
E2 (GPa)		14.5	8.20		
E3 (GPa)		14.5	8.20		
υ12	0.3	0.33	0.3	0.33	0.389
υ13		0.33	0.3		
υ23		0.33	0.3		
G12 (GPa)		2.56	4.5		
G13 (GPa)		2.56	4.5		
G23 (GPa)		2.24	4.5		
σ_{uits} (MPa)	500				
σ_e (MPa)	380				
n	0.127				

The corrosion defect is then cleaned, and a layer of epoxy putty is applied to fill the cavity with a thickness of 0.5 mm. The adhesive used for bonding the pipe to the composite wrap is the Araldite 2015 Epoxy with a thickness of ta= 0.3 mm.

Table 1 shows the elastic properties of the pipe, the patch, and the adhesive. Pipe steel is supposed to have an elastic-plastic behaviour.

Initial conditions and limitations

The extremities of the pipe were constrained (all displacements and rotations were blocked), i.e., U1 = U2 = U3 = 0, UR1 = UR2 = UR3 = 0) to ensure the proper execution of the calculation. Furthermore, the length of the section was chosen so that this indentation does not affect the stress calculations in the corroded and repaired areas. The pipe is subjected to a constant internal pressure of 8.42 MPa, applied uniformly, without considering other real-world specific effects. (The boundary conditions are presented in Figure 2).

In Abaqus software, the contact between the three components in an assembly (pipe, putty, and composite wrap) can be defined by assigning suitable interaction properties (normal and tangential) to the surface-to-surface contacts.

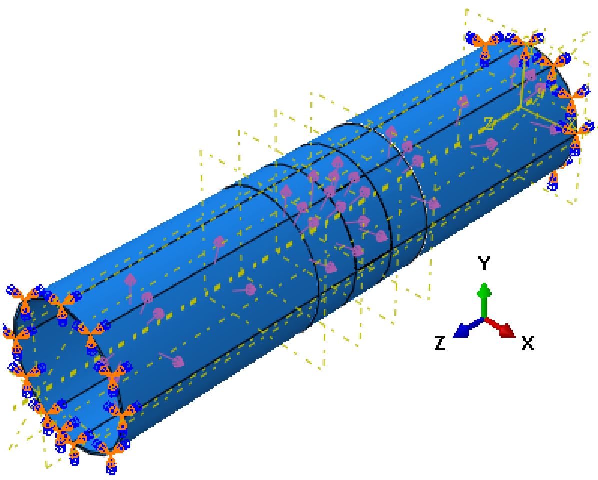

Figure 2 – Boundary condition of the corroded pipe

Metehri, A. et al., Using the finite element method for developing a new model predicting the burst pressure of straight defects in corroded pipes repaired with bonded composite wraps, pp.931-954

FEM model and convergence analysis

The Abaqus calculation code (Dassault Systems, The 3D EXPERIENCE platform, 2014) was used to calculate the stresses in the corroded and repaired pipe. The finite element model was divided into three subsections: the repaired pipe, the epoxy putty, and the composite wrap. The pipe is modelled with different elements along the thickness direction: one layer for the pipe, one layer for the repair putty, and two layers for the composite wrap.

Changing the density of the mesh elements stabilized the equivalent stress value in the repaired pipe (see Figure 3).

Table 2 – Numbers of the nodes and the mesh elements

Model	Number of nodes	Number of elements
Pipe with a rectangular defect	61248	40475
Repaired pipe with a composite patch wrap	67030	45788

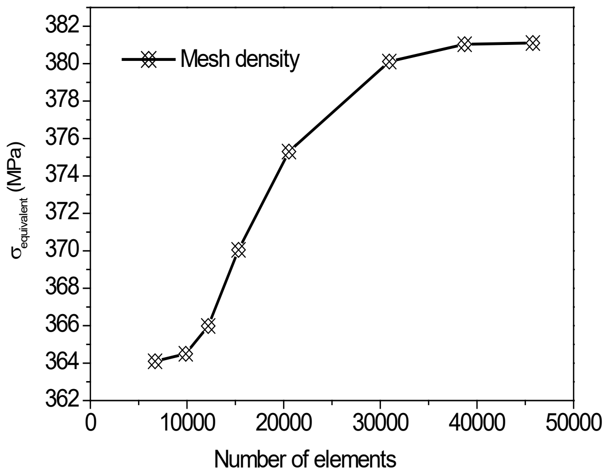

Figure 3 – Variation of von Mises stress in the corroded pipe repaired with composite material as a function of mesh density

Several computational runs with mesh density optimization were used to obtain reliable results and good convergence (see Figure 3). To assess the impact of the number of nodes on stress variation, the type of structural hexahedral linear element was fixed, and an attempt was made to increase the number of nodes to refine the model progressively. Figure 3 illustrates the mesh of the repaired pipe based on the number of nodes.

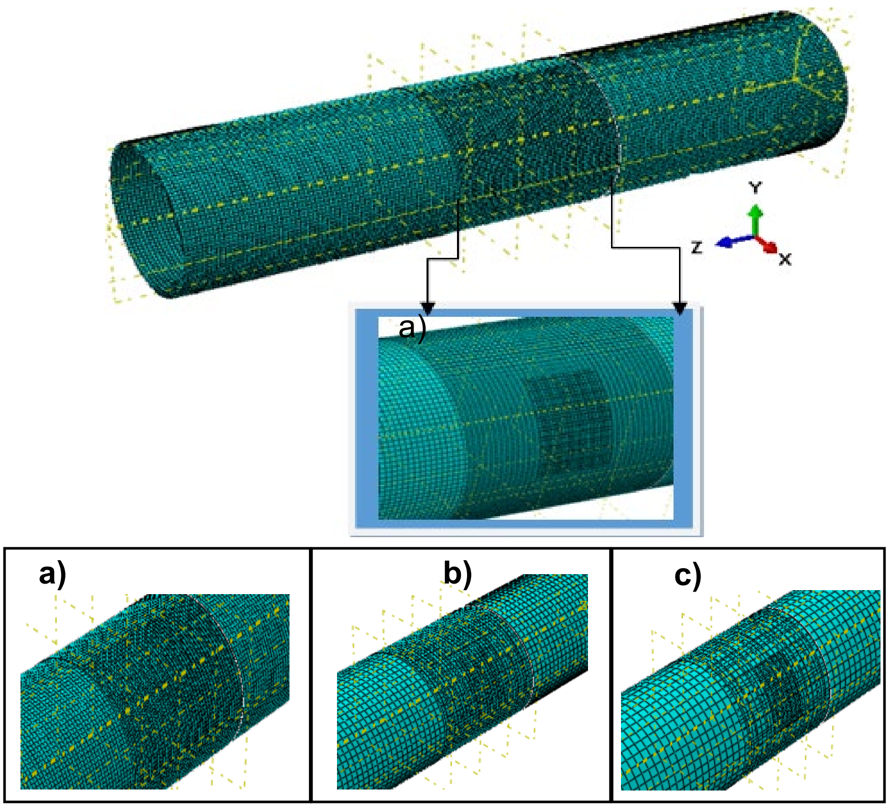

Figure 4 – Detailed mesh used for a numerical model of the defective pipe with composite repair: a) refined mesh, b) medium mesh, and c) non-refined mesh.

The type of element chosen must correspond to the topological shape of the model structure. The element types depend on the three-dimensional shapes, such as tetrahedra, wedges, and hexahedra.

In previous studies (Medjdoub et al, 2018) on the behaviour of repaired pipelines, C3D8R mesh elements were tested and they provided reliable results.

However, the element type was not altered in this work, as the C3D8R element is the most efficient in most numerical analyses; therefore, this element type was selected at the outset of the analysis.

In terms of the mesh type, we opted for the elements (C3D8R) which have been frequently used in the modelling of such structures, along with

5040 linear quadrilateral elements of type S4R for the envelope and 40748 linear hexahedral elements of type C3D8R for the pipe and the putty. Refining the mesh at a defect level is also important to better determine the value of the equivalent and circumferential stresses. The general configuration is based on a regular mesh, which is kept constant for all the analyses carried out in this study to avoid any influence of the mesh on the results. The total number of the nodes and the pipe elements is demonstrated in Table 2. Figure 4 illustrates the structure of the mesh employed for this calculation.

The mesh models shown in Figures 4a, b, and c were generated by adjusting the element density for each material until a mesh size was achieved. This ensured a regular and refined mesh, particularly at the defect level, where corrosion necessitates a refined mesh with a minimum element size.

Finite element results

Comparison between repaired and non-repaired pipes

A comparative study analyzed the stress distribution between an unrepaired corroded pipe and a corroded pipe repaired with a glass/epoxy wrap consisting of two composite layers [55/-55]. The internal uniform pressure applied was 8.42 MPa. The circumferential stress distributions are shown in Figure 5. This Figure shows that the composite wrap's presence considerably reduces the pipe's equivalent stresses, particularly in the corroded region. The presence of the composite shell increases the lifespan of the corroded pipe.

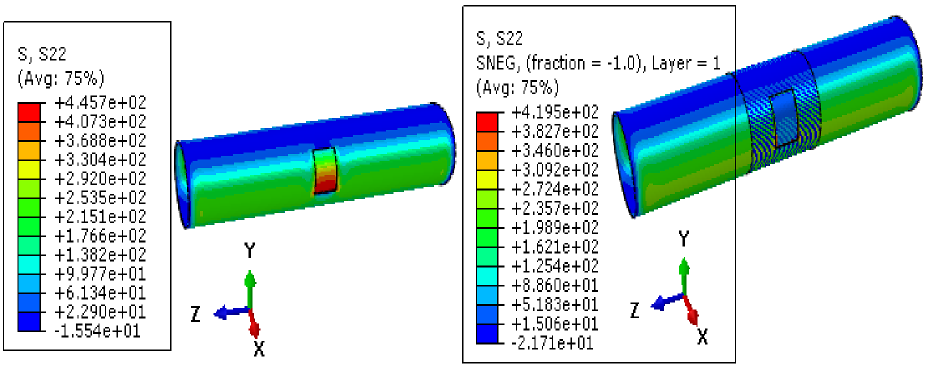

Figure 5 – Contour of circumferential stress with a rectangular centred defect, a) pipe without repaired, b) repaired pipe, under internal pressure. (d/t=0.5)

The stress reduction can be seen more clearly in Figure 6, which shows the maximum stresses for a repaired pipe and an unrepaired pipe as a function of the d/t ratio. From this Figure, it can be seen that the increase in the d/t ratio leads to an increase in the maximum stresses of about 160 MPa from 0.1 to 0.5 for both repaired and unrepaired pipes. However, according to Figure 6, it can be seen that the reduction of the circumferential stress by the composite wrap is constant regardless of the values of the d/t ratio. This means that the rate of stress transfer from the corroded pipe to the composite repair through the adhesive layer is independent of the d/t ratio.

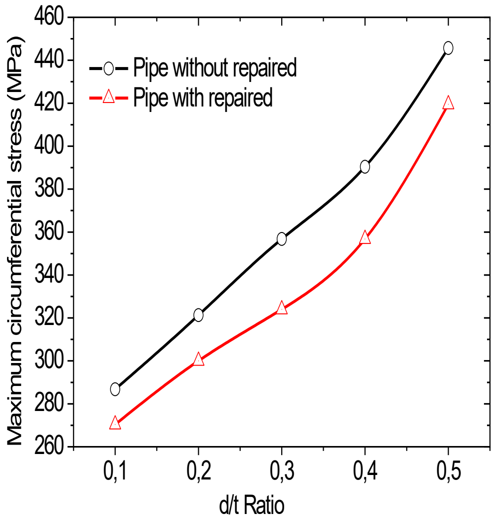

Figure 6 –Variation of the maximum circumferential stress with the repaired pipe and the non- repaired pipe in accordance with the d/t ratio

Effects of the geometrical parameters on the repair performances

Pipe size effect

This part presents the influence of the d/t ratio on the maximum value of the circumferential stress. The study was carried out on a pipe repaired with a composite wrap in glass/epoxy with the ply orientation of [55/-55]; each ply is 0.5 mm thick. The internal uniform pressure of P= 8.42 MPa was applied.

Figure 7 presents the variation of the maximum circumferential stress in the repaired pipe as a function of the d/t ratio for different pipe diameters (400, 500, and 600 mm). From this Figure, it can be noted that the maximum stresses are higher for higher pipe diameters regardless of the d/t ratio. This shows that repair efficiency will be reduced as the pipe diameter increases. This behaviour is due to the fact that the load transfer from the pipe to the composite wrap will be less significant as the pipe diameter increases. It is, therefore, easier to repair a smaller pipe. However, this disadvantage can be overcome by increasing the thickness of the composite by increasing the number of plies, which will result in a higher stress transfer to the composite wrap. Thus, the effectiveness of the repair will be improved.

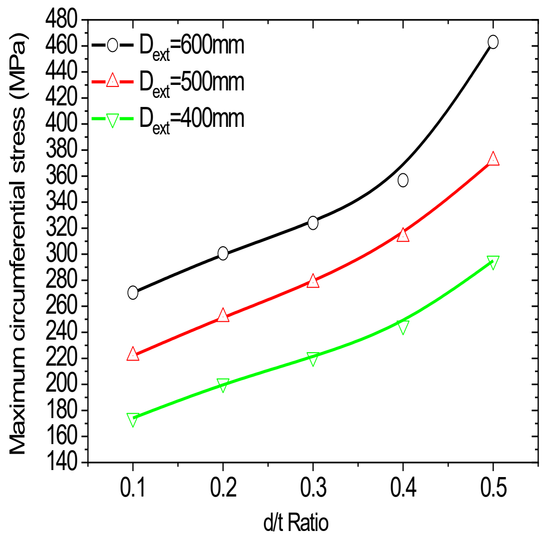

Figure 7 – Variation of the maximum circumferential stress in the repaired pipe as a function of the d/t ratio and the exterior radius

Effect of the defect length

This part of the study focuses on analyzing the effect of defect length on the level of the circumferential stresses in the repaired pipe. For this reason, the defect lengths were L1=500mm, L2=350mm, and L3=110mm. Figure 8 presents the variation of the maximum stress in the repaired pipe as a function of the ratio (d/t) of different defect lengths (L).

This Figure shows that defect length considerably determines the level of circumferential stresses. The repair efficiency is closely related to defect length. For more significant defects, the stress level will be higher and significant even after repair. However, many authors have investigated the effect of defect length (Al-Amin & Zhou, 2013; Hocine et al, 2024; Netto et al, 2007). We can solve this problem by increasing the composite thickness, which will improve the repair effectiveness.

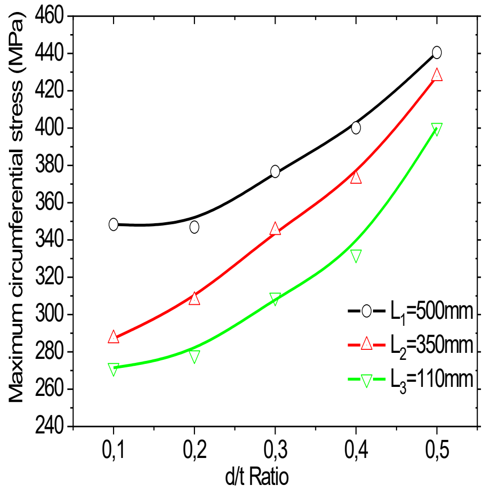

Figure 8 – Variation of the maximum circumferential stress in the repaired pipe as a function of the d/t ratio of different defect lengths

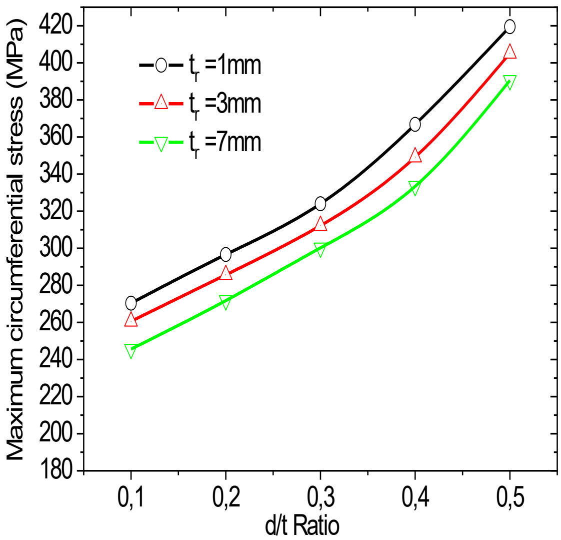

Figure 9 – Maximum circumferential stress variation in accordance with the composite patch thickness

Effect of the composite wrap thickness

To analyze the effects of the composite envelope thickness on the repair effectiveness, we considered three thicknesses of the repair composite: tr =1, 3, and 7 mm (as shown in Figure 9). It can be seen from this last Figure that increasing the thickness of the composite gives a considerable reduction in the maximum stress in the repaired pipe, which allows us to assert that increasing the number of layers of the repair composite improves the repair effectiveness and thus increases the longevity of the pipe. However, we recommend optimizing this thickness to avoid high repair costs, as costly repair may be less cost-effective than replacing the corroded part of the pipe.

Effect of the material properties of the composite wrap

The choice of the composite wrap type is of paramount importance when reinforcing pipelines. Several types of reinforcement are available, the most effective choices being glass/epoxy and carbon/epoxy. These types of composite wraps have demonstrated superior performance by improving mechanical properties.

Table 1 presents the elastic properties of carbon and epoxy compared to those of glass and epoxy.

Figure 10 presents the variation of the maximum circumferential of the repaired corroded pipe with both composites (glass/epoxy and carbon/epoxy). A comparison between the two patches, glass/epoxy and carbon/epoxy, reveals that the glass/epoxy patches offer superior performance in corroded pipeline repair. The stress in the corroded pipe is lower when it is repaired with glass/epoxy than when it is repaired with carbon epoxy, particularly for a lower ratio (d/t). For higher values of the d/t ratio, the two composites give the same circumferential stress. We conclude that the choice of the composite type significantly impacts the repair efficiency. It is recommended for corroded pipes under internal pressure to use glass/epoxy because of its relatively low cost and best efficiency.

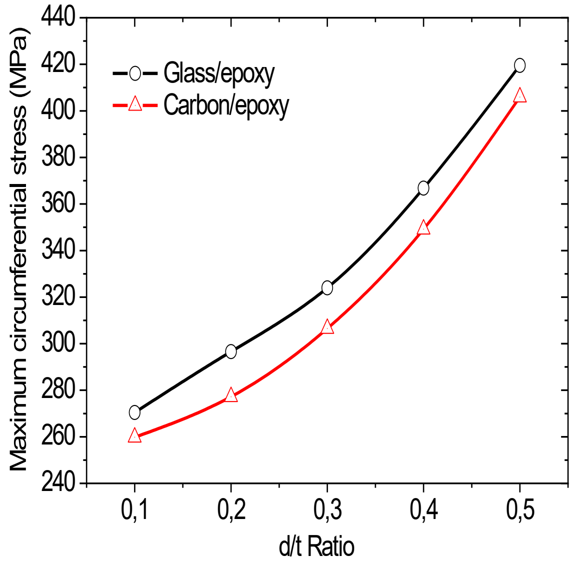

Figure 10 – Variation of the maximum circumferential stress of a repaired pipe in accordance with the composite wrap type

Several studies have been conducted to assess the mechanical properties in order to select the proper material for repairing the damaged cavity of a damaged pipeline (Lim et al, 2019; Da Costa Mattos et al, 2009; Djahida et al, 2021; Zecheru et al, 2018; Duell et al, 2008).

Effect of the adhesive thickness

The adhesive layer plays an important role in the repair of corroded pipes. The thickness and mechanical properties of the adhesive are essential in the load transfer between the corroded pipe and the composite wrap. Figure 11 presents the variation of the repaired pipe's maximum von Mises stress in accordance with the adhesive thickness. From Figure 11, it can be seen that increasing the adhesive thickness leads to a decrease in the equivalent stresses of the corroded pipe. This increase indicates that a moderately thin adhesive (t_a=0.4mm) facilitates better load transfers from the defect to the composite patch. It can be seen that the adhesive thickness influences the equivalent stresses. The minimum value of the equivalent stress is recorded in the interval of (0.3-0.4 mm) for the adhesive thickness; for the adhesive thicknesses higher than 0.4 mm, the stresses increase considerably, and the repair efficiency will be reduced. We recommend using the optimum value of the adhesive thickness (t_a=0.3mm) to repair corroded pipelines.

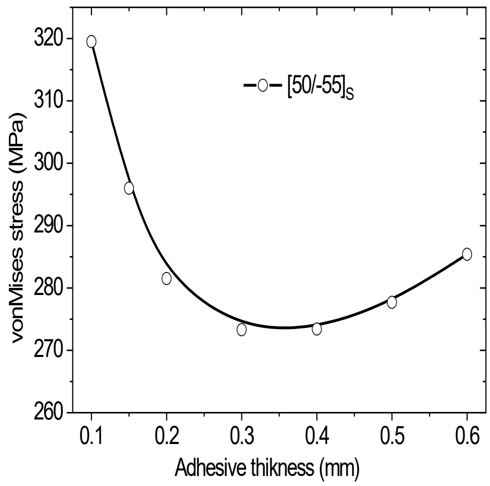

Figure 11 – Variation of the repaired pipe's maximum von Mises stress as a function of the adhesive thickness

Analytical model of the burst pressure of a repaired pipe

Finite element analysis has shown that several parameters influence the burst pressure of a corroded steel pipe repaired with a composite wrap. These parameters include the geometric properties of the pipe, the corrosion defect and the repair composite, the elastic properties of the composite, and the internal pressure applied to the pipe. We have combined all these parameters into an analytical model estimating the burst pressure of the repaired pipe. This model, developed for the first time, can be used to design the composite wrap repair. This model is written in the form:

$$P_b = \frac{2t\,\sigma_{uts}}{(D-t)\,H} \quad .\text{For} \quad 1{,}345 \le \frac{L}{\sqrt{Dt}} \le 6{,}455 \quad ,0.1 \le \frac{d}{t} \le 0.5 \tag{1}$$

$$H = \zeta.\xi.\chi.f\left(\frac{L}{\sqrt{D.t}},\frac{d}{t}\right) \tag{2}$$

$$\zeta = \left(\frac{E_1}{G_{12}}\right).\left(\frac{E_2}{E_3}\right).\left(\frac{G_{13}}{G_{23}}\right) \tag{3}$$

$$\xi = \left(\frac{t}{t_r}\right) \tag{4}$$

$$\chi = \left(\frac{E_a}{E_p}\right) \cdot \left(\frac{\upsilon_a}{\upsilon_p}\right) \tag{5}$$

$$f\left(\frac{L}{\sqrt{D.t}}, \frac{d}{t}\right) = A_0 + A1\left(\frac{L}{\sqrt{D.t}}\right) + A2\left(\frac{L}{\sqrt{D.t}}\right)^2 \tag{6}$$

$$\begin{aligned} A_0 &= -13{,}13312\left(\frac{d}{t}\right)^2 + 11{,}17065\left(\frac{d}{t}\right) + 1{,}93764 \\ A_1 &= 5{,}05975\left(\frac{d}{t}\right)^2 - 3{,}2674\left(\frac{d}{t}\right) + 0{,}36372 \\ A_2 &= -0{,}60838\left(\frac{d}{t}\right)^2 + 0{,}40765\left(\frac{d}{t}\right) - 0{,}0331 \end{aligned} \tag{7}$$

This model is one of a few ones in the literature to predict the burst pressure of a corroded pipe repaired with a composite wrap. Comparing its results with those obtained by finite element analysis shows an excellent agreement (see Figure 12). Indeed, the relative difference between the burst pressure estimated by the model and that calculated by finite elements does not exceed 0.1 %.

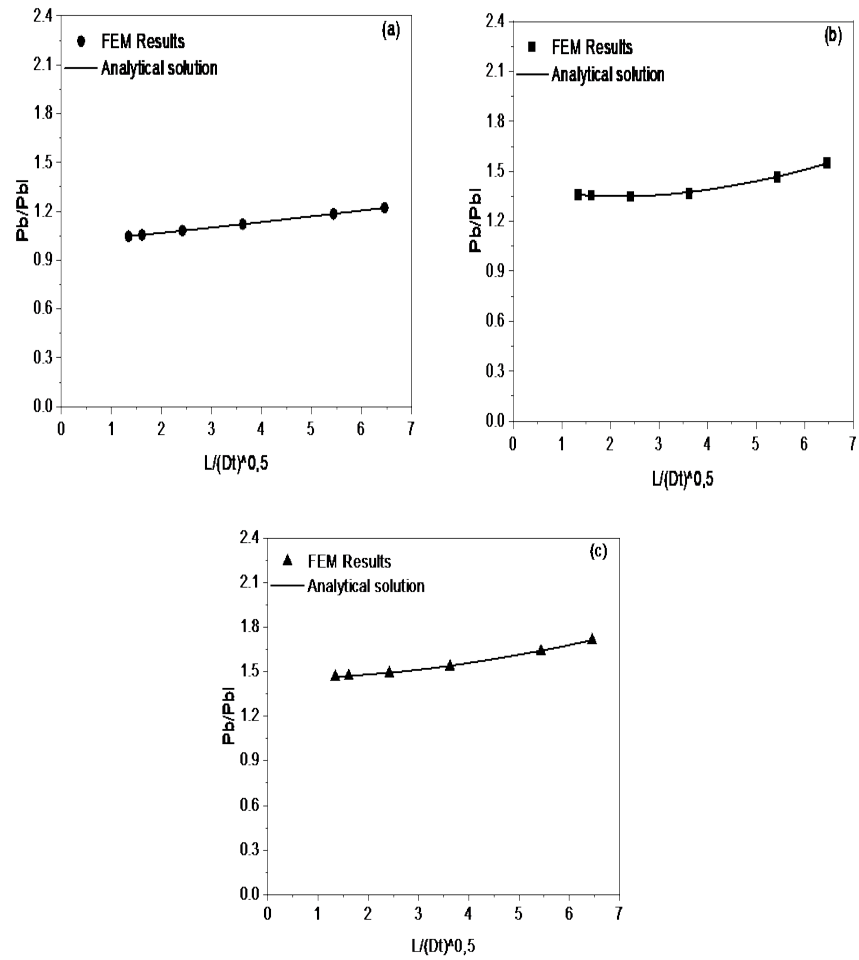

Figure 12 – Burst pressure of the corroded pipe vs L/ (Dt) 0.5

Conclusion

This work develops a new predictive model for calculating the burst pressure of straight defects subjected to internal pressure in corroded pipes that have been repaired with bonded composite coverings. Various criteria are examined, including pipe dimensions, defect size, number of composite plies, ply orientation, composite material characteristics, and adhesive thickness. The following conclusions can be made:

- ✓ The increase in the (d/t) ratio leads to an increase in the maximum stresses for both repaired and unrepaired pipes.

- ✓ As the pipe diameter increases, the load transfer from the pipe to the composite wrap becomes less significant, making repairs easier for smaller pipes. However, this limitation can be mitigated by increasing the composite thickness with additional plies, which improves stress transfer to the composite wrap. As a result, the effectiveness of the repair is enhanced.
- ✓ The defect length plays a crucial role in determining the level of circumferential stresses and directly affects the repair efficiency. For larger defects, stress levels remain high even after the repair. However, increasing the composite thickness helps distribute the stresses more effectively, thereby improving the overall effectiveness of the repair.
- ✓ Increasing the thickness of the composite significantly reduces the maximum stress in the repaired pipe. This demonstrates that adding more layers of the composite improves the repair effectiveness and extends the pipe's service life.
- ✓ Glass/epoxy offers better performance in terms of strength and flexibility, making it more effective in restoring the integrity of damaged pipes. This combination proves to be more advantageous for ensuring durable and reliable repair.
- ✓ It has been determined that the adhesive thickness should be 0.3 mm to ensure optimum adhesion between the composite layer and the thick pipe. This precise value guarantees an effective repair by maintaining a strong and uniform interface between the different layers of the repair system.
- ✓ The present model exhibits excellent agreement with finite element results in predicting the burst pressure of a corroded pipe repaired with a composite wrap, with the relative difference not exceeding 0.1%.

Nomenclature

FEM:	Finite element method
σ_{eq}:	Maximum von-Mises equivalent stress
S_{22}:	Circumferential (Hoop) stress
σ_{uits}:	Ultimate stress
σ_e :	Yield stress
a:	Pipe length
A_0, A_1 and A_2:	Integration functions
d:	Defect depth
N_{ext}:	Pipe external diameter

Metehri, A. et al., Using the finite element method for developing a new model predicting the burst pressure of straight defects in corroded pipes repaired with bonded composite wraps, pp.931-954

D_{int}:	Pipe internal diameter
E_1 :	Young's modulus in the X direction (GPa)
E_2 :	Young's modulus in the Y direction (GPa)
E_3 :	Young's modulus in the Z direction (GPa)
Ea :	Young's modulus of adhesive
E_P :	Young's modulus of steel
G_{12} :	Shear modulus in the X-Y plan (GPa)
G_{13} :	Shear modulus in the X-Z plan (GPa)
G_{23} :	Shear modulus in the Y-Z plan (GPa)
l :	Defect width
L_1, L_2, L_3 :	Defect length
n:	Work hardening coefficient
LPC:	Line pipe corrosion model
P:	Internal pressure
P_b :	Burst pressure
r=d/t:	Geometrical ratio of the defect
t :	Pipe thickness
T_a:	Adhesive thickness
T_r:	Patch thickness
ζ :	Properties ratio of the composite
η :	Function depending on the ratio of the defect
ν_{12} :	Poisson's ratio in the X-Y plan
ν_{13} :	Poisson's ratio in the X-Z plan
ν_{23} :	Poisson's ratio in the Y-Z plan
ξ:	Thickness ratio
χ :	Properties ratio of steel and adhesive

References

Hocine, A., Achira, F.S.K., Habbar, G., Levent, A., Medjdoub, S.M., Maizia, A., Dhaou, M.H. & Bezazi, A. 2024. Structural integrity assessment of corroded pipelines repaired with composite materials – Literature review. *International Journal of Pressure Vessels and Piping*, 210, p.105253. Available at: https://doi.org/10.1016/J.Ijpvp.2024.105253

Alabtah, F.G., Mahdi, E. & Eliyan, F.F. 2021.The use of fiber reinforced polymeric composites in pipelines: A review. *Composite Structures*, 276, p.114595. Available at: https://doi.org/10.1016/j.compstruct.2021.114595

Al-Amin, M. & Zhou, W. 2013. Evaluating the system reliability of corroding pipelines based on inspection data. *Structure and Infrastructure Engineering*, 10(9), pp.1161–1175. Available at: https://doi.org/10.1080/15732479.2013.793725

Alexander, C., Vyvial, B. & Wilson, F. 2014. Pipeline repair of corrosion and dents: comparing composite repairs and steel sleeves, In: *10th International pipeline conference*, Alberta. Available at: https://doi.org/10.1115/IPC2014-33410

Benyahia F, Albedah A. & Bachir Bouiadjra. B. 2014. Stress Intensity Factor for Repaired Circumferential Cracks in Pipe With Bonded Composite Wrap. *Journal of Pressure Vessel Technology*. 136(4), p.041201. Available at: https://doi.org/10.1115/1.4026022

Budhe, S., Banea, M.D. & de Barros, S. 2020. Analysis of Failure Pressure of Defective Pipes Repaired with Composite Systems Considering the Plastic Deformation of Pipe. *Journal of the Institution of Engineers (India) Series C*, 101, pp.929-936. Available at: https://doi.org/10.1007/s40032-020-00612-4

Budhe, S., Banea, M.D., Rohem, N.R.F., Sampaio, E.M. & de Barros, S. 2017. Failure pressure analysis of composite repair system for wall loss defect of metallic pipelines. *Composite Structure*., 176, pp.1013-1019. Available at: https://doi.org/10.1016/j.compstruct.2017.06.044

Campilho. R.D.S.G., Pinto, A.M.G., Banea, M.D., Silva R.F. & da Silva L.F.M. 2011. Strength Improvement of Adhesively-Bonded Joints Using a Reverse-Bent Geometry. *Journal of Adhesion Science and Technology* 25, pp.2351–2368. Available at: https://doi.org/10.1163/016942411x580081

Arroussi, C., Belalia, A. & Meliani, M. H. 2023. Effects of composite and metallic patch on the limit load of pressurized steel pipes elbow with internal defects under opening bending moment. *Structural Monitoring and Maintenance*, 10(3), pp.221–242. Available at: https://doi.org/10.12989/smm.2023.10.3.221

Da Costa-Mattos, H.S., Reis, J.M.L., Sampaio, R.F. & Perrut, V.A. 2009. An alternative methodology to repair localized corrosion damage in metallic pipelines with epoxy resins. *Materials and Design*, 30, pp 3581–3591. Available at: https://doi.org/10.1016/j.matdes.2009.02.026

De Barros, S., Budhe, S., Banea, M.D., Rohem, N.R.F., Sampaio, E.M., Perrut, V.A. & Lana, L.D.M. 2018. An assessment of composite repair system in the offshore platform for corroded circumferential welds in super duplex steel pipe. *Frattura ed Integrità Strutturale* (Fracture and Structural Integrity), 44, pp. 151–160. Available at: https://doi.org/10.3221/IGF-ESIS.44.12

Djahida, D., Tewfik, G., Witek, M. & Abdelghani, M. 2021. Analytical Model and Numerical Analysis of Composite Wrap System Applied to Steel Pipeline. *Materials* 14, p.6393. Available at: https://doi.org/10.3390/Ma14216393

Duell, J.M., Wilson, J.M. & Kessler, M.R. 2008. Analysis of a carbon composite overwrap pipeline repair system. *International Journal of Pressure Vessels and Piping*, Volume 858(11), pp.782-788. Available at: https://doi.org/10.1016/J.Ijpvp.2008.08.001

Fezazi, A.I., Mechab. B., Mokadem, S. & Serier B. 2021. Numerical prediction of the ductile damage for axial cracks in pipe under internal pressure. *Frattura ed Integrità Strutturale*, *15*(58), pp.231-241; Available at: https://doi.org/10.3221/IGF-ESIS.58.17

Dassault Systems, The 3D EXPERIENCE platform. 2014. Simulia: Abaqus Finite Element Analysis for Mechanical Engineering and Civil Engineering [online].

Available at: https://www.3ds.com/products/simulia/abaqus [Accessed: 19 March 2025].

Ibrahim N.C., Boualem, S. & Belaïd, M. 2018. Analysis of the crack-crack interaction effect initiated in aeronautical structures and repaired by composite patch. *Fracture and Structural Integrity*, *12*(46), pp.140-149. Available at: https://doi.org/10.3221/IGF-ESIS.46.14

Kong, D., Li, C., Huang, X., Xin, M. & Xian, G. 2022. Mechanical analysis and parameter design of CFRP-Wrapped defected steel pipe.*International. Journal of Pressure Vessels and Piping*, 197, p.104653. Available at: https://doi.org/10.1016/J.Ijpvp.2022.104653

Lim, K.S., Azraai, S.N.A., &Yahaya, N. 2019. Behaviour of steel pipelines with composite repairs analyzed using experimental and numerical approaches. *Thin Wall Structure*, 139, pp.321-333. Available at: https://doi.org/10.1016/j.tws.2019.03.023

Mechab, B., Serier, B., Kaddouri,.K. & Bouiadjra. B.B. 2014. Probabilistic elastic-plastic analysis of cracked pipes subjected to internal pressure load, *Nuclear Engineering and Design*, 275, pp.281–286. Available at: https://doi.org/10.1016/j.nucengdes.2014.05.008

Mechab, B., Salem, M., Malika, M. & Boualem, S. 2020. Probabilistic elastic-plastic fracture mechanics analysis of propagation of cracks in pipes under internal pressure. *Frattura ed Integrità Strutturale*, 54, pp.202-210. Available at: https://doi.org/10.3221/IGF-ESIS.54.15

Mechab, B., Chioukh, N., Mechab, B. & Serier B. 2018. Probabilistic Fracture Mechanics for Analysis of Longitudinal Cracks in Pipes Under Internal Pressure. *Journal of Failure Analysis and Prevention,* 18(6), pp.1643–1651. Available at: https://doi.org/10.1007/S11668-018-0564-8

Mechab, B., Serier, B., Bouiadjra, B.B., Kaddouri, K. & Feaugas, X. 2011. Linear and nonlinear analyses for semi-elliptical surface cracks in pipes under bending, *International Journal of Pressure Vessels and Piping*, 88(1), pp.57–63. Available at: https://doi.org/10.1016/j.ijpvp.2010.11.001

Medjdoub, S.M., Bouiadjra, B.B. & Abdelkader, M. 2018. Effect of the geometrical parameters on the efficiency of bonded composite wrap for repairing cracked pipes. *Strength, Fracture and Complexity, 11*(4), pp.309-317. Available at: https://doi.org/10.3233/SFC-180232

Metehri, A., Kouider, M., Belaïd M., Mohammed M. & Ilias M.A.G., 2024a. Tensile examination of progressive damage and failure in porous ceramic composite material using the XFEM technique. *Vojnotehnički glasnik/Military Technical Courier*, 72(3), pp.1188-1213. Available at: https://doi.org/10.5937/vojtehg72-50091

Metehri, A., Serier, B., Belhouari, M. & Mecirdi, M.A. 2009. Numerical analysis of the residual stresses in polymer matrix composites. *Materials & Design*, 30(7), pp.2332–2338. Available at: https://doi.org/10.1016/j.matdes.2008.11.009

Metehri, A., Belaïd, M. & Abbès B.B.B. 2024b. A new investigation used to predict the burst pressure in straight corroded pipes under internal pressure.

Vojnotehnički glasnik/Military Technical Courier, 72(4), pp.1747-1771. Available at: https://doi.org/10.5937/vojtehg72-50357

Metehri, A., Belaïd M. & Abbès, B.B.B. 2024c. Modeling with prediction of burst pressure of elliptical corroded pipeline. *Xi'an Shiyou Daxue Xuebao (Ziran Kexue Ban)/ Journal of Xi'an Shiyou University, Natural Sciences Edition,* 67(11), pp.86-96. Available at: https://doi.org/10.5281/zenodo.14195656

Metehri, A., Kouider, M. & Lousdad, A. 2019. Effect of crack position and size of particle on SIF in SiC particles reinforced Al composite. *Frattura ed Integrità Strutturale*, 13(48), pp.152-160. Available at: https://doi.org/10.3221/IGF-ESIS.48.18

Nadia, B., Belaïd, M., Malika, M., Aicha, M., Mokadem, S. & Abbès B.B.B. 2024. Analytical and numerical methods for estimating the probability of interlaminar fracture in Mode I of composite structures under the peel test. *Vojnotehnički glasnik/Military Technical Courier*, 72(4) pp.1601-1622. Available at: https://doi.org/10.5937/vojtehg72-49978

Netto, T.A., Ferraz, U.S. & Botto, A. 2007. On the effect of corrosion defects on the collapse pressure of pipelines. *International Journal of Solids and Structures,* 44(22-23), pp.7597–7614, Available at: https://doi.org/10.1016/j.ijsolstr.2007.04.028

Fatoba, O. & Akid, R. 2014. Low Cycle Fatigue Behaviour of API 5L X65 Pipeline Steel at Room Temperature. *Procedia Engineering*, 74, pp.279-286. Available at: https://doi.org/10.1016/J.Proeng.2014.06.263

Salem, M., Mechab, B., Berrahou, M., Bachir Bouiadjra, B. & Serier, B. 2019. Failure Analyses of Propagation of Cracks in Repaired Pipe Under Internal Pressure. *Journal of Failure Analysis and Prevention*, 19(1), pp.212–218. Available at: https://doi.org/10.1007/s11668-019-00592-3

Singh, D.K., Villamayor, A. & Hazra, A. 2021. Numerical and experimental analysis of loctite adhesive composite wrapping on EN 10028 steel pipes. *Materials Today: Proceedings,* 44(6), pp.4158-4165. Available at: https://doi.org/10.1016/j.matpr.2020.10.525

Chandra Khan, V., Balaganesan, G., Kumar Pradhan, A. & Sivakumar, M. S. 2017. Nanofillers Reinforced Polymer Composites Wrap to Repair Corroded Steel Pipe Lines. *Journal of Pressure Vessel Technology*, 139(4) p.041411. Available at: https://doi.org/10.1115/1.4036534

Zecheru, G., Dumitrescu, A., Diniţă, A. & Yukhymets, P. 2018. Design of Composite Repair Systems. *Engineering Materials*, pp.269–285. Available at: https://doi.org/10.1007/978-3-319-56579-8_17

Utilización del método de elementos finitos para el desarrollo de un nuevo modelo que predice la presión de ruptura de defectos rectos en tuberías corroídas reparadas con envolturas compuestas adheridas

Aicha Metehri, **autor de correspondencia**, *Belaïd* Mechab, *Bel Abbes Bachir* Bouadjra

Universidad de Sidi Bel Abbès, Facultad de Tecnología, Departamento de Ingeniería Mecánica, Laboratorio de Mecánica Física de Materiales, Sidi Bel Abbès, República Argelina Democrática y Popular.

CAMPO: Informática, ingeniería mecánica, materiales
TIPO DE ARTÍCULO: artículo científico original

Resumen:

Introducción/objetivo: Este trabajo tiene como objetivo crear un nuevo modelo que prediga la presión de ruptura de fallas rectas bajo presión interna en tuberías corroídas que han sido reparadas con envolturas compuestas.

Métodos: Los aspectos geométricos influyeron en el rendimiento de la reparación. El comportamiento del parche compuesto depende en gran medida de varios parámetros, como el tamaño de la tubería, el tamaño del defecto, el número de capas del compuesto, la orientación de las capas, las propiedades del compuesto y el espesor del adhesivo. Se analizaron los efectos de todos estos parámetros en la eficiencia de la reparación.

Resultados: Los resultados obtenidos mostraron que la envoltura compuesta reduce la concentración de tensiones causada por el defecto de corrosión, lo que mejora la durabilidad a largo plazo de las tuberías.

Conclusión: La comparación entre el nuevo modelo desarrollado analíticamente y los cálculos de elementos finitos (EF) mostraron una buena concordancia para la tubería corroída reparada.

Palabras claves: corrosión, presión uniforme, modelo analítico, tuberías, reparaciones con compuestos adheridos

---

Использование метода конечных элементов в разработке новой модели, прогнозирующей давление разрыва прямого дефекта в корродированной трубе, отремонтированной с помощью клеевой композитной заплаты

Айша Матери, **коррепондент,** Белаид Мечаб,

Бель-Аббес Башир Буаджра

Университет Сиди-Бель-Аббес, технологический факультет,
отделение машиностроения,
лаборатория физической механики материалов,
Сиди-Бель-Аббес, Алжирская Народная Демократическая Республика.

РУБРИКА ГРНТИ: 23.25 Информационные системы с базами знаний,
30.15.35 Теория механизмов и машин,
81.09.00 Материаловедение
ВИД СТАТЬИ: оригинальная научная статья

Резюме:

Введение/цель: Цель данной статьи заключается в создании новой модели, прогнозирующей давление разрыва прямых дефектов вследствие внутреннего давления в корродированных трубах, отремонтированных с помощью композитной заплаты.

Методы: Геометрические характеристики влияют на эффективность ремонта. Поведение композитной заплаты сильно зависит от нескольких параметров таких как размер трубы, размер дефекта, количество слоев композита, ориентация слоев, свойства композита и толщина клея. В статье проведен анализ влияния всех этих параметров на эффективность ремонта.

Результаты: Полученные результаты показали, что композитная заплата снижает концентрацию напряжения, вызванного коррозионным дефектом, что повышает долговечность трубы.

Выводы: Сравнение новой аналитически разработанной модели с расчетами методом конечных элементов (FE) показало положительное совпадение касательно отремонтированных корродированных труб.

Ключевые слова: коррозия; равномерное давление; аналитическая модель; труба; ремонт композитных материалов на клеевом соединении.

Коришћење методе крајњих елемената ради развијања новог модела за предвиђање притиска пуцања праволинијског дефекта у кородираним цевима поправљеним лепљењом композитном закрпом

Ајша Метехри, **аутор за преписку,** *Белаид* Мехаб*, Бел Абес Бахир* Буаџра

Универзитет Сиди Бел Абеса, Технолошки факултет,
Одељење за машинство,
Лабораторија физичке механике материјала,
Сиди Бел Абес, Народна Демократска Република Алжир

ОБЛАСТ: рачунарске науке, механика, материјали
КАТЕГОРИЈА (ТИП) ЧЛАНКА: оригинални научни рад

Сажетак:

Увод/циљ: Циљ овог рада јесте креирање новог модела за предвиђање притиска пуцања праволинијских дефеката услед унутрашњег притиска у кородираним цевима поправљеним лепљеном композитном закрпом.

Методе: Геометријске карактеристике утичу на перформансе поправке. Понашање композитне закрпе у великој мери зависи од неколико параметара, као што су величина цеви, величина дефекта, број слојева композита, оријентација слојева, својства композита и дебљина лепка. Анализиран је утицај свих наведених параметара на ефикасност поправке.

Резултати: Добијени резултати су показали да је композитна облога смањила концентрацију напона проузрокованог дефектом услед корозије, чиме се побољшава дугорочна издржљивост цеви.

Закључак: Поређење новог, аналитички развијеног модела и прорачуна методом коначних елемената (FE) показало је добро слагање код поправљених кородираних цеви.

Кључне речи: корозија, равномерни притисак, аналитички модел, цев, поправке лепљење композита.

Paper received on: 28.01.2025.
Manuscript corrections submitted on: 13.03.2025.
Paper accepted for publishing on: 25.03.2025.

Analysis of the application of vibration diagnostics and thermography methods for an early detection of defects in an industrial mixer-gearbox system – a case study

Borivoj Z. Novaković[a], *Luka* Djordjević[b], *Damir* Jerković[c], *Mihalj Bakator*[d]

[a] University of Novi Sad, Technical Faculty "Mihajlo Pupin", Zrenjanin, Republic of Serbia
e-mail: borivoj.novakovic@tfzr.rs
ORCID ID: https://orcid.org/0000-0003-2816-3584

[b] University of Novi Sad, Technical Faculty "Mihajlo Pupin", Zrenjanin, Republic of Serbia
e-mail: luka.djordjevic@tfzr.rs
ORCID iD: https://orcid.org/0000-0003-4578-9060

[c] University of Defence, Military Academy, Belgrade, Republic of Serbia
e-mail: damir.jerkovic@va.mod.gov.rs
ORCID ID: https://orcid.org/0000-0001-5182-7057

[d] University of Novi Sad, Technical Faculty "Mihajlo Pupin", Zrenjanin, Republic of Serbia
e-mail: mihalj.bakator@tfzr.rs
ORCID ID: https://orcid.org/0000-0001-8540-2460

doi https://doi.org/10.5937/vojtehg73-55834

FIELD: mechanical engineering
ARTICLE TYPE: original scientific paper

Abstract:

Introduction/purpose: Bearings constitute essential components without which the functioning of systems subject to significant loads would be inconceivable. The bearing installation process in rotational systems diligently influences their longevity, reliability, and efficiency. Accurate and meticulous bearing installation is of paramount importance to ensure optimal operational performance of rotational systems. A proper bearing assembly assists in the even distribution of loads, reduction of friction, and minimization of wear. Additionally, appropriately mounted bearings decrease the risk of vibrations, noise, and potential system failures. Therefore, the bearing installation process represents a crucial step in maintaining the reliable and efficient operation of rotational systems, thereby extending their operational lifespan and reducing the need for repairs.

Methods: The methodology employed in this study combines vibrodiagnostic analysis of an industrial mixer equipped with a planetary *gearbox and the concurrent application of thermographic techniques. This integrated approach provides a comprehensive understanding of the system's condition and helps identify potential sources of heating within both the gearbox and the mixer. Vibrodiagnostic examinations encompassed the analysis of vibrations generated by the planetary gearbox during its operation, coupled with the interpretative scrutiny of results aimed at detecting possible imbalances, damage, or irregularities within the mechanical system. On the other hand, the application of thermography contributed to generating a visual representation of temperature distributions at critical points of the gearbox, facilitating the identification of thermal anomalies. The integration of these methods enables a holistic scientific approach to the analysis of the planetary gearbox system, allowing for detailed diagnostics and an understanding of the root causes of potential operational issues in the gearbox.*

Results: The meticulous interpretation of the acquired data facilitated the identification of potential causes of thermal loading in the planetary gearbox, providing a comprehensive insight into the mechanical and thermal facets of the entire system. The integration of vibrodiagnostic and thermograpfic methods constitutes a pivotal component of a holistic analytical approach, crucial for an exhaustive understanding of the performance and overall condition of the planetary gearbox and the industrial mixer. The obtained results serve as the foundation for the development of precise diagnostic procedures, laying the groundwork for the implementation of pertinent improvements or maintenance strategies within the system. This, in turn, holds the potential to optimize the operational performance of the planetary gearbox and extend its operational lifespan.

Conclusion: The applied methodology, based on vibrodiagnostic analyses and thermographic techniques, has provided a comprehensive insight into the condition of both the planetary gearbox and the industrial mixer containing it, with all analyses described in the text conducted on each component within the mixer system. The detailed interpretation of data has enabled the identification of potential causes of gearbox heating, offering a deeper understanding of the mechanical and thermal aspects of the system. In this manner, the efficiency of maintaining the examined system can be enhanced.

Key words: planetary gearbox, industrial mixer, vibrodiagnostic, thermograpfic, analysis, bearing, reliability, maintenance.

Introduction

Planetary gearboxes have a wide range of applications, starting from the automotive industry, extending through the aerospace industry, and reaching heavy metal industries (Guo & Parker, 2011; McNames, 2002). This type of gearbox is primarily utilized in harsh working conditions, which significantly affects the lifespan of the system and its components. Such conditions directly contribute to damage within the system, most commonly resulting from material fatigue (Cheng et al., 2012). The foundation of a reliable and high-quality operation of any technical system lies in the design of its transmission system, aiming to ensure optimal energy efficiency and proper lubrication. This approach helps to maintain system performance and prolong the lifespan of its components (Zhang, 2013). Bearings, as fundamental components of any gearbox, endure significant loads during operation and are therefore prone to frequent potential failures, as described in the paper (Lu et al., 2020). Testing the operational integrity of planetary gearboxes can involve various diagnostic methods. In the study by (Lei et al., 2013), an adaptive resonance method is described for diagnosing planetary gearbox faults. Planetary gearboxes are frequently subjected to dynamic loads, as outlined in the paper (Batinic, 2013), which can lead to elevated vibrations within the gearbox. Modern diagnostic methods for assessing the condition of planetary gearboxes are integral to implementing higher-quality maintenance practices, with some primary diagnostics described in studies (Chatterjee & Dethlefs, 2021; Lei et al., 2010). Vibration diagnostics is a crucial method for monitoring and diagnosing the condition of rotating equipment, such as pumps, compressors, turbines, gears, and other machinery systems in industrial and engineering facilities. Since rotating equipment is continuously subjected to mechanical loads and dynamic stresses, timely detection of irregularities and the early stages of damage is essential for ensuring the reliability and longevity of these systems.

Vibration diagnostics methodologies include signal analysis in both the frequency and time domains, with advanced techniques increasingly being used for more precise diagnostics. Frequency spectrum analysis enables the detection of dominant frequencies, which facilitates the identification of specific system components, such as gears and bearings, which show signs of failure. Wavelet transformation, as a modern technique, provides additional insight into short-term changes that often go unnoticed in traditional frequency analyses, further enhancing the precision of problem detection. Finally, time-domain signal analysis through parameters such as RMS values and peak values enables the direct detection of system performance changes, thereby simplifying the identification of irregularities (Aherwar, 2012; De Silva, 2007; Goyal & Pabla, 2016; Rai & Upadhyay, 2016; Singh & Sehgal, 2022; Vishwakarma et al., 2017).

The thermography method enables visualization of temperature distribution on the surface of machine components and the identification of zones with elevated temperatures, which may indicate potential issues such as friction, inadequate lubrication, wear, or localized mechanical stresses. The use of thermography aids in detecting these anomalies at early stages, allowing for preventive interventions before more serious failures or machine downtime occur. Thermography finds wide applications across fields, from the construction industry to the process and gas industries, and even aerospace, as illustrated in studies (Jakubek et al., 2022; Ristić et al., 2013).

As opposed to vibration diagnostics, which focuses on analyzing vibration patterns to identify mechanical irregularities, thermography provides a different set of insights by relying on temperature variations caused by increased mechanical load or friction. Thermographic analysis is often useful in cases where vibration signals cannot fully reveal the problem, such as issues related to thermal overheating of bearings or electrical components in motors. Integrating these methods offers a comprehensive view of equipment condition, which is especially valuable in critical industrial processes where high machine reliability is essential. In this way, a diagnostic approach that combines thermal and vibration analyses is becoming increasingly important in modern industrial applications to extend the service life of rotating equipment and minimize the risk of unexpected failures (Gawde et al., 2023; Shaalan et al., 2024; Thomas et al., 2001; Watban Khalid Fahmi et al., 2022).

Material and methods

In the pursuit of diagnosing faults in planetary gear reducers, researchers increasingly employ advanced techniques such as vibrodiagnostics and thermography. Vibrodiagnostic methodology involves data acquisition on the vibrations of the reducer through the placement of accelerometers at the key points within the system. Frequency analysis of these vibrations facilitates the identification of characteristic patterns associated with potential malfunctions such as imbalance or gear damage. The sensitivity to changes in the reducer's condition over time allows for an early detection of potential issues. Conversely, thermography relies on infrared cameras to measure temperatures on the surface of the reducer. Through the analysis of thermal profiles, researchers can identify regions with abnormal temperatures, indicative of problems such as friction or inadequate lubrication. The amalgamation of vibrodiagnostics and thermography provides a comprehensive assessment of the planetary gear reducer's condition, enabling precise diagnostics and efficient maintenance of the system. In this case, thermography is utilized for the analysis of temperature elevation on the bearings of a planetary gearbox within an industrial mixer system with a power rating of 1.5 MW, undergoing a speed reduction from 990 rpm to 49 rpm. Based on the presented formulas, it is possible to determine the frequencies at which failures occur in specific bearing components within the system, such as the inner ring, the outer ring, the rolling elements, and the train. The Ball Pass Frequency Outer Ring is represented by Equation (1):

$$BPFO = RPM\frac{n}{2}(1-\frac{d}{D_p}\cos\beta) \quad (1)$$

The Ball Pass Frequency Inner Ring is represented by Equation (2):

$$BPFI = RPM\frac{n}{2}(1+\frac{d}{D_p}\cos\beta) \quad (2)$$

The Fundamental Train Frequency is represented by Equation (3):

$$FTF = \frac{RPM}{2}(1-\frac{d}{D_p}\cos\beta) \quad (3)$$

The Ball Spin Frequency is represented by Equation (4):

$$BSF = RPM\frac{D_p}{d}\left[1-(\frac{d}{D_p}\cos\beta)^2\right] \quad (4)$$

Analysis of vibration and thermal heating in an industrial mixer and a planetary gearbox system

A comprehensive assessment of the condition of a planetary gearbox installed in an industrial mixer system, as well as the issue of heating in specific components of both the gearbox and the mixer, can be achieved by fully integrating both methods for evaluating the condition of individual elements within the gearbox and the mixer. Vibration analysis is used to evaluate the condition of a gearbox by examining dynamic loads that occur during the operation of individual components, such as the gear meshing points and tooth contacts, the condition of ball bearings within the gears, and the alignment of the drive and the driven gear shafts. This method provides insight into mechanical wear, alignment issues, and potential imbalances that may affect gearbox performance and longevity. On the other hand, infrared thermography offers a complete overview that can detect current or potential issues leading to elevated temperatures within the gearbox. Thermal imaging can reveal temperature anomalies often associated with friction, lubrication issues, or excessive loads. By visualizing the thermal distribution, especially in the lubricating fluid and other critical parts of the gearbox and the industrial mixer system, infrared thermography allows for early detection of issues that may not be immediately apparent through vibration analysis alone. This dual-method approach ensures a thorough examination of both the mechanical and thermal conditions, enhancing predictive maintenance and overall system reliability.

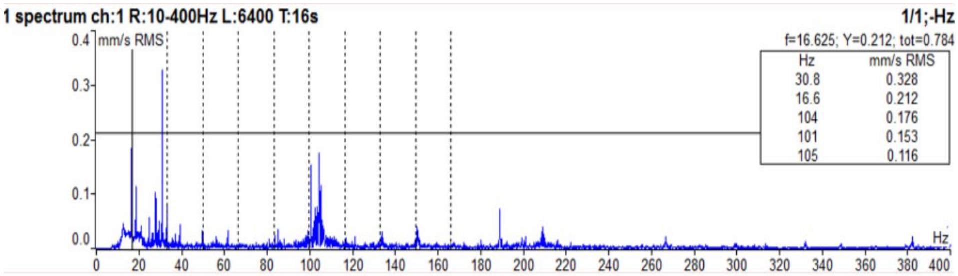

Figure 1 – Spectrum of vibrations at the measurement point of the gearbox input

In Figure 2, the demodulated acceleration spectrum (in g RMS) is shown, aiding in the identification of high-frequency vibrations often associated with bearing defects. Through demodulation, peaks are observed at very low frequencies around 0.75 Hz, 16.5 Hz, and 0.375 Hz. Although the values are relatively low (up to 0.005 g RMS), the presence of pronounced peaks at these frequencies may indicate early signs of wear or faults in the bearings.

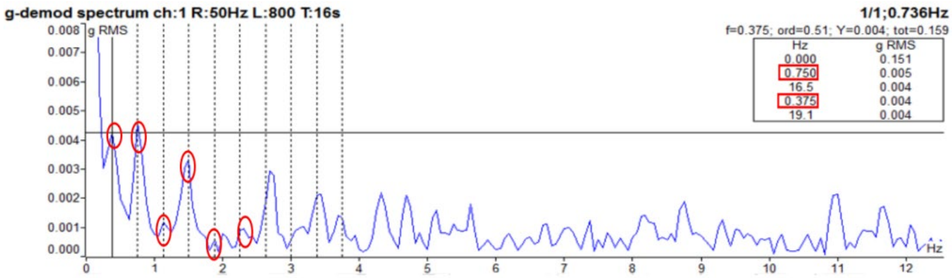

Figure 2 – Demodulated spectrum of vibrations at the reducer outlet - bearing

Based on the FFT analysis of the gearbox, slight looseness was detected in the bearing at the gearbox output. Given the very low vibration levels at the gearbox output, it is recommended to monitor the bearing condition and respond promptly if necessary. Obtain data on the bearings in the gearbox for further analysis.

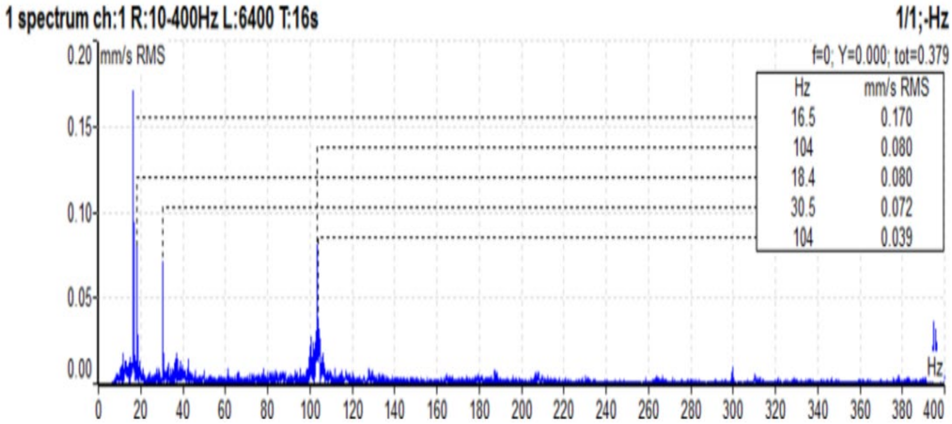

Figure 3 – Spectrum of vibrations at the measurement point of the mixer input

Figure 4 shows the demodulated vibration spectrum at the mixer inlet.

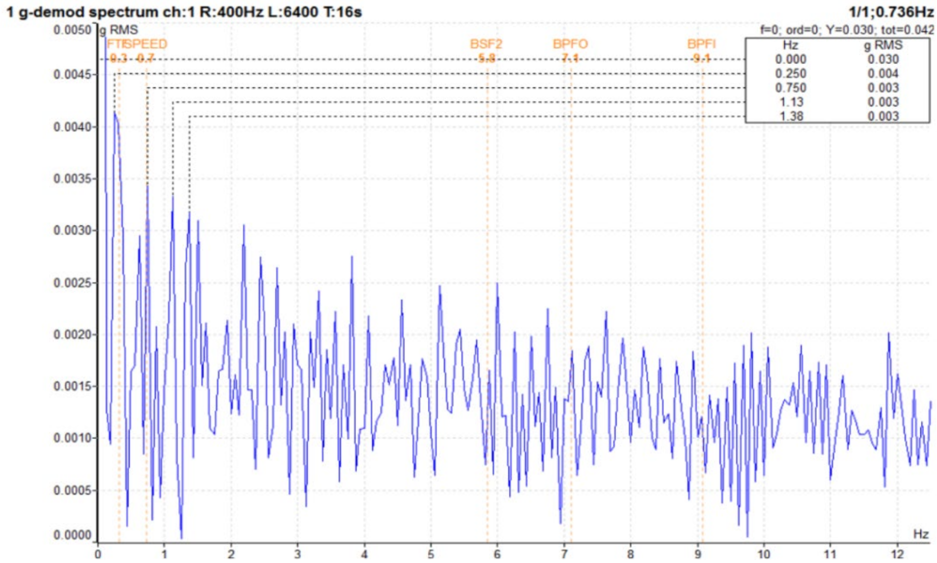

Figure 4 – Demodulated spectrum of vibrations at the mixer input

Based on the vibration spectra shown in Figures 3 and 4, it can be concluded that there are no elevated vibrations beyond acceptable limits, nor any detected irregularities in the mixer's operation at the bearing measurement point at the inlet.

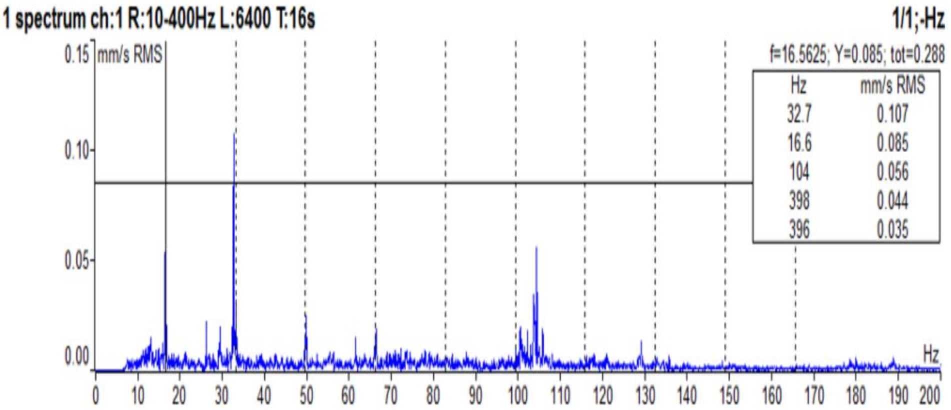

Figure 5 – Spectral analysis of vibrations at the mixer outlet

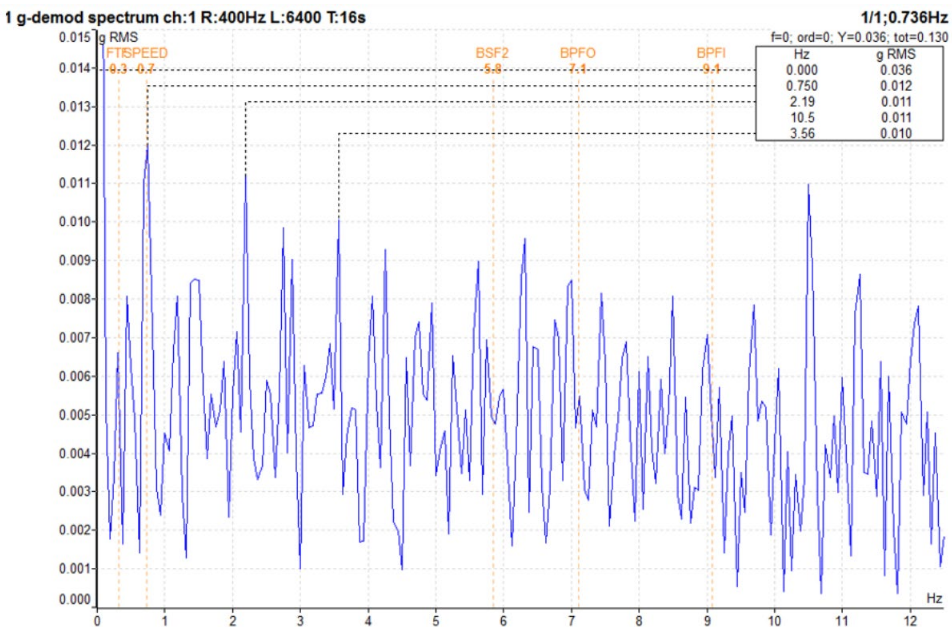

Figure 6 – Demodulated vibration spectrum at the mixer inlet

Given the visually identified potential malfunction of the bearing at the mixer outlet, along with increased lubricant leakage, an additional time-domain vibration acceleration analysis was conducted.

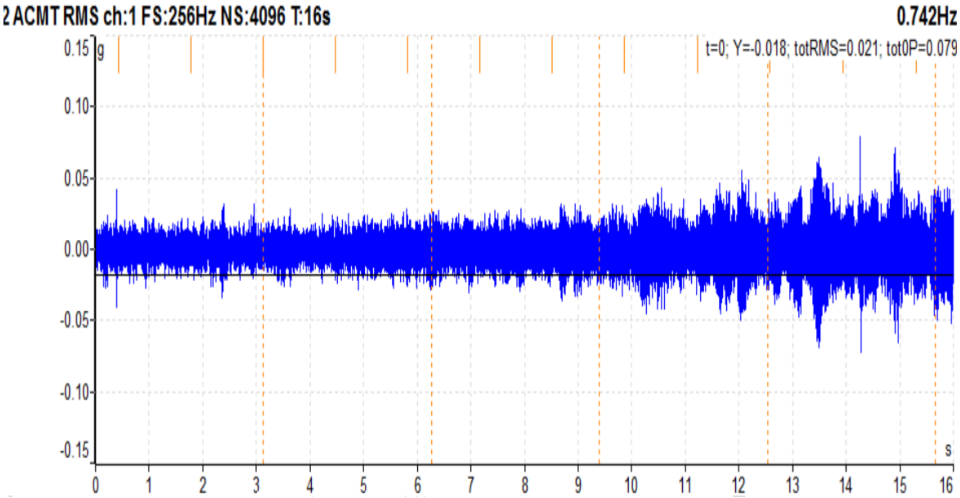

Figure 7 – Time spectrum of vibrations at the mixer outlet

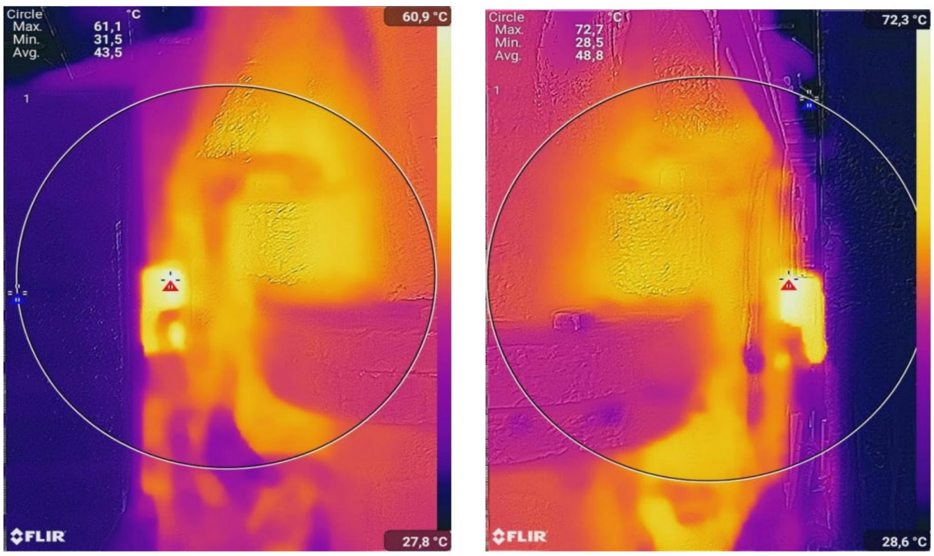

Figure 8 – Thermal image of the gearbox at the inlet

The spectral analysis shows that vibrations are generally stable and low-intensity, with RMS values close to zero for most of the measurement duration. However, certain peaks (more pronounced increases in vibration) occur at specific times, particularly after the 12th second, where the vibration level rises. The overall RMS value measured during this period is 0.021 g, indicating a relatively low level of vibration, though periodic peaks may suggest occasional impacts or asymmetric loads within the system.

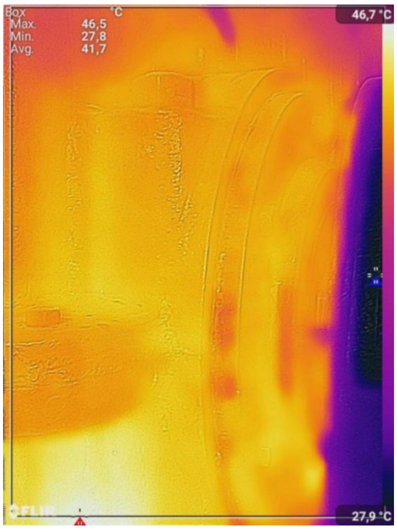

Figure 9 – Thermal image at the gearbox output

Since the vibration analysis did not reveal any specific faults in the operation of the gearbox and the mixer, a thermographic inspection method was applied to the gearbox and the mixer to obtain a comprehensive view and identify any potential system malfunctions.

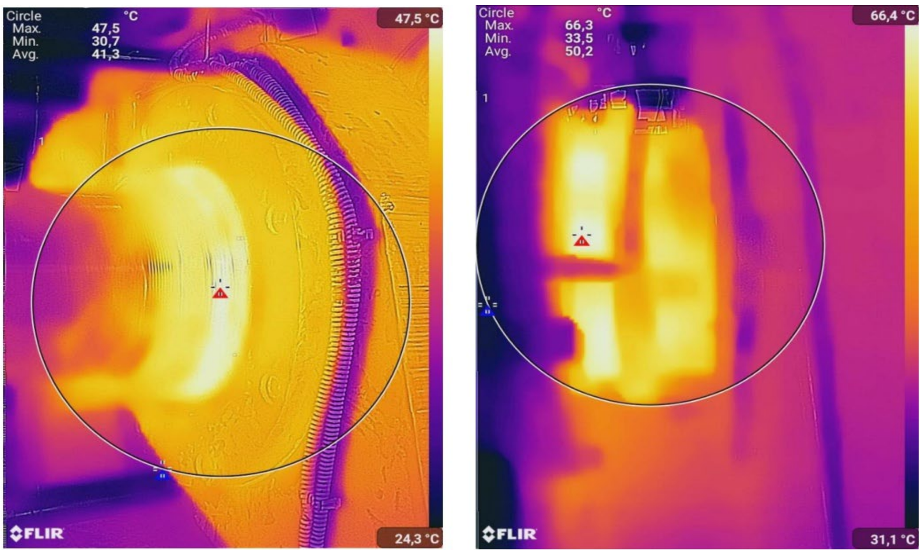

Figure 10 – Thermal image at the mixer inlet

According to Figure 8 and the operational parameters of the gearbox, the recorded temperatures and the heating levels captured by the camera fall within the allowable temperature range, indicating no operational anomalies at the gearbox input.

Additionally, the temperatures at the gearbox output are considered within the tolerance range for optimal operation of both the gearbox and the output bearings.

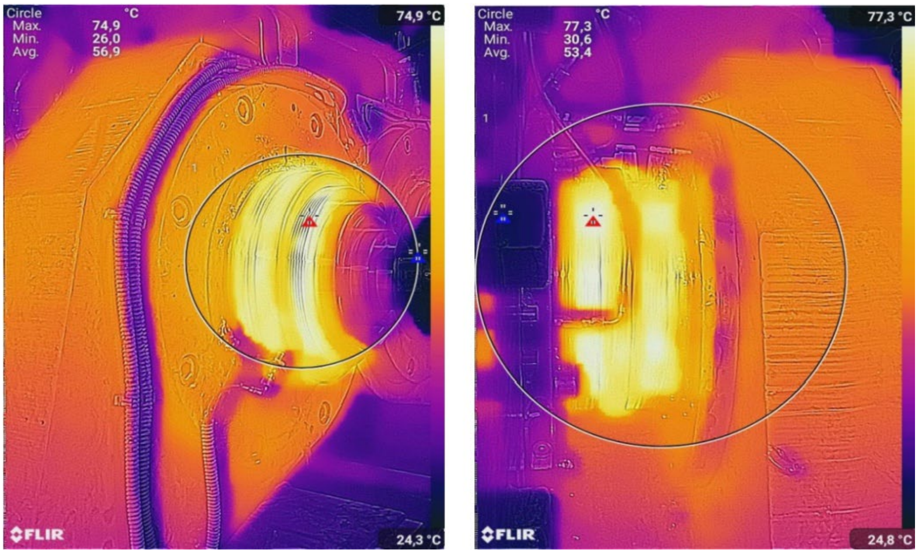

Figure 11 – Thermal image at the mixer outlet

Based on the thermal image of the mixer, it is possible to analyze the presence of high temperatures in specific areas, which may indicate lubrication issues. In particular, the maximum temperature values are relatively high, reaching 74.9°C and 77.3°C, which suggests intense friction in certain zones of the mixer. These temperature peaks may be associated with lubricant leakage problems, often manifesting through specific thermal patterns. Lubricant leakage can lead to a loss of the necessary amount of lubricant at friction points, resulting in increased friction and higher temperatures, as shown in the image.

If leakage occurs, the lack of lubricant at critical points causes overheating because there is insufficient lubricant to form a protective film between contacting surfaces. In the images, we can observe concentrated zones of high temperature, potentially indicating that certain parts of the mixer are inadequately lubricated due to possible lubricant loss. When lubricant leaks or is excessively lost from the system, heat tends to concentrate in specific areas, while other parts may remain cooler. This uneven temperature distribution may point to potential leakage points.

Based on the FFT analysis of the mixer shaft at the output, a minor axial clearance in the bearing at position 1 was detected, attributed to improper bearing installation during assembly. Visual inspection revealed an incorrectly positioned seal on bearing 1, showing signs of wear. Consequently, lubricant leakage from the bearing and the ingress of contaminants into its interior occur, which explains the temperature difference compared to other bearings, given that the seal does not function adequately.

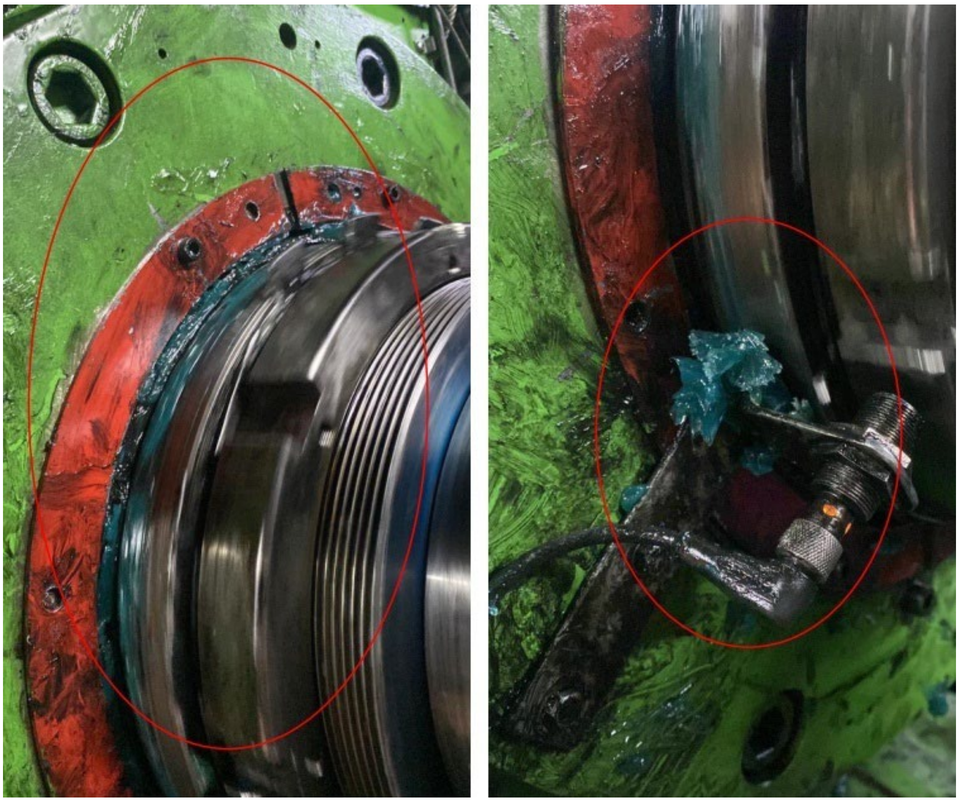

Figure 12 – Point of the mixer outlet

From Figure 12, it is clearly seen that there is leakage at the mixer outlet, causing an excessive concentration of heat on the bearing located at the output section of the shaft. Given that lubricant leakage has been identified in the mixer outlet area, a more detailed lubrication analysis of

VOJNOTEHNIČKI GLASNIK / MILITARY TECHNICAL COURIER, 2025, Vol. 73, Issue 3

the bearing at the mixer outlet is necessary. Figure 13 illustrates the lubrication spectrum at the mixer outlet.

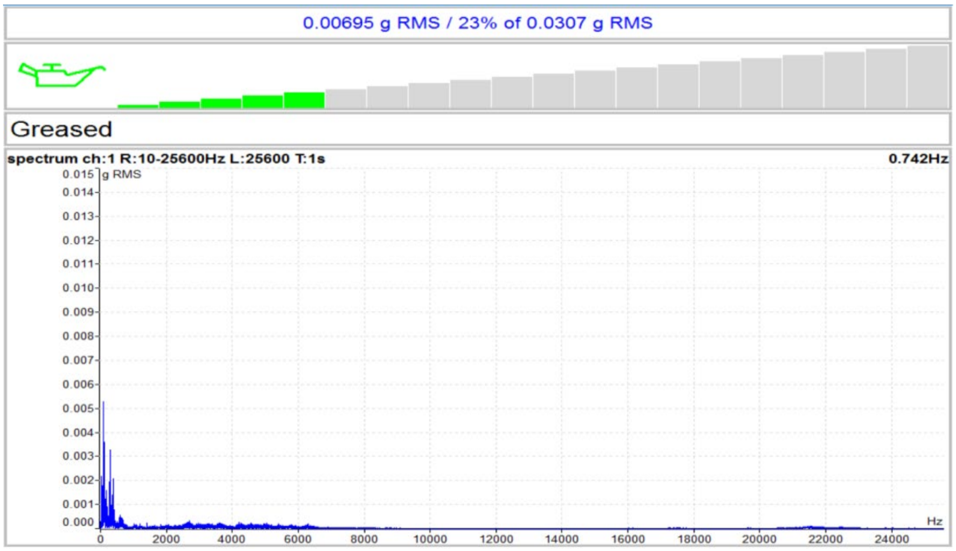

Figure 13 – Lubrication at the mixer outlet

A detailed lubrication analysis of the mixer outlet bearing was conducted using Lubri Mode. According to the data from the obtained spectrum, the lubrication condition of the bearing at the time of inspection is satisfactory, likely due to recent lubricant application to the bearings. However, given that the visual inspection revealed leakage, there is a tendency for peak values on the diagram to increase, potentially placing the lubrication level in the red zone, which necessitates re-lubrication of the examined bearing.

Results and discussion

Based on all applied diagnostics, including vibration analysis, thermography, and additional tools for bearing lubrication assessment, it can be concluded that current testing does not always provide a fully accurate picture of the condition. However, the diagnostic methods performed enable a predictive assessment of the examined component's condition, allowing for timely implementation of appropriate maintenance procedures to prevent extended and unplanned downtimes.

Vibrations, as a parameter, indicate potential damage to both the planetary reducer bearings and the mixer itself. According to the measured values, no critical values were identified per the ISO standard (ISO 20816-

3:2022), and the measured vibration values for the reducer's measuring points are shown in Table 1.

Table 1 – Vibration on the gearbox

Point	1V	1H	2V	2H	3V	3H	3A
Velocity (mm/s)	0,912	0,328	1,030	0,816	0,421	0,637	0,192
Acceleration (g)RMS	0,252	0,380	0,377	0,316	0,229	0,092	0,146

The measurement results indicate that the RMS values of the vibration velocity range from 0.192 mm/s to 1.030 mm/s, with the highest value recorded at the measurement point 2V (1.030 mm/s) and the lowest at the point 3A (0.192 mm/s). All velocity values are below the reference threshold of 2.8 mm/s, indicating a low level of vibration consistent with the standards for rotating machinery. Regarding the RMS values of vibration acceleration, the range is from 0.092 g to 0.380 g, with the maximum value observed at the point 1H (0.380 g) and the minimum value at the point 3V (0.092 g). All acceleration values are below the 0.5 g threshold, indicating the absence of impact vibrations that could compromise the structural integrity of the bearings. Collectively, these data suggest a stable dynamic condition of the system, with no elevated or critical vibrations that would require corrective action.

Table 2 – Vibration on the mixer

Point	**1V**	**1H**	**1A**	**2V**	**2H**	**2A**
Velocity (mm/s)	0,281	0,170	0,116	0,357	0,164	0,150
Acceleration (g)RMS	0,021	0,047	0,036	0,045	0,072	0,021
Point	**3V**	**3H**	**3A**	**4V**	**4H**	**4A**
Velocity (mm/s)	0,240	0,113	0,107	0,377	0,091	0,119
Acceleration (g)RMS	0,013	0,037	0,054	0,045	0,012	0,038

The vibration analysis on the industrial mixer indicates that the RMS values of the vibration velocity at the inlet points range from 0.116 mm/s to 0.357 mm/s, while at the outlet points, they range from 0.091 mm/s to 0.377 mm/s. The highest velocity values were recorded at the points 2V and 4V, yet all values are significantly below the threshold of 2.8 mm/s, indicating a low level of vibration throughout the system. Regarding vibration acceleration, the inlet points show the values between 0.021 g and 0.072 g, while the outlet points range from 0.012 g to 0.054 g, with the highest values at the points 2H and 3A. All acceleration values are below the reference threshold of 0.5 g, indicating the absence of impact vibrations that could compromise the system's integrity. Overall, the results indicate a stable dynamic condition of the mixer, with no elevated vibrations requiring corrective action.

Conclusion

In this study, advanced vibration diagnostics and thermography methods were applied and their results analyzed for an early detection of defects in industrial systems such as gearboxes and mixers. Given that these systems operate under substantial load, monitoring both vibrational and thermal stresses is essential for the timely identification of irregularities that could shorten service life and elevate maintenance costs.

Vibration diagnostics was employed to assess vibration levels accurately during system operation, facilitating the identification of potential issues in bearings, gears, and other moving components. By measuring the RMS values of the vibrations at different bearing measurement points, oscillations were detected that, while within permissible limits according to ISO standard 20816-3, may indicate gradual wear or the onset of damage. The vibration levels at critical points also revealed frequent peaks at specific frequencies, potentially linked to minor axial clearances due to improper bearing installation. These findings underscore the importance of continuous vibration monitoring to reduce the risk of more severe failures.

Thermographic analysis further contributed by identifying key thermal anomalies on bearings and critical gear contact points, which may signal lubrication issues. The elevated temperatures recorded in specific bearing zones exceeded optimal operational thresholds, suggesting intensified friction resulting from either a deficiency in lubricant or inadequate lubrication application. This thermal concentration likely stems from lubricant leakage or uneven distribution, leading to overheating that would not be detectable through vibration analysis alone.

The thermographic measurements enabled the visualization and quantification of thermal peaks, with the highest temperatures observed at the mixer and gearbox output bearings. The analysis of these thermal deviations pointed to uneven lubrication and pronounced thermal zones, which may represent potential hotspots for wear. This thermal data allows for more precise control over lubrication quality, facilitating preventive corrective actions, such as timely lubricant replenishment or replacement, and thus mitigating the risk of further thermal damage to the system.

References

Aherwar, A. 2012. An investigation on gearbox fault detection using vibration analysis techniques: A review. Australian Journal of Mechanical Engineering, 10(2), 169–183. Available at: https://doi.org/10.7158/M11-830.2012.10.2

Batinic, V.J. 2013. Planetary gear dynamic response to mesh. *Vojnotehnički Glasnik*, *61*(1), 58–68. Available at: https://doi.org/10.5937/vojtehg61-2006

Chatterjee, J. & Dethlefs, N. 2021. Scientometric review of artificial intelligence for operations & maintenance of wind turbines: The past, present and future. *Renewable and Sustainable Energy Reviews*, *144*, 111051. Available at: https://doi.org/10.1016/j.rser.2021.111051

Cheng, Z., Hu, N. & Zhang, X. 2012. Crack level estimation approach for planetary gearbox based on simulation signal and GRA. *Journal of Sound and Vibration*, *331*(26), 5853–5863. Available at: https://doi.org/10.1016/j.jsv.2012.07.035

De Silva, C. W. 2007. *Vibration monitoring, testing, and instrumentation*. CRC Press. Available at: https://doi.org/10.1201/9781420053203

Gawde, S., Patil, S., Kumar, S. & Kotecha, K. 2023. A scoping review on multi-fault diagnosis of industrial rotating machines using multi-sensor data fusion. *Artificial Intelligence Review*, *56*(5), 4711–4764. Available at: https://doi.org/10.1007/s10462-022-10243-z

Goyal, D. & Pabla, B. 2016. The vibration monitoring methods and signal processing techniques for structural health monitoring: A review. *Archives of Computational Methods in Engineering*, *23*, 585–594. Available at: https://doi.org/10.1007/s11831-015-9145-0

Guo, Y. & Parker, R. G. 2011. Analytical determination of mesh phase relations in general compound planetary gears. *Mechanism and Machine Theory*, *46*(12), 1869–1887. Available at: https://doi.org/10.1016/j.mechmachtheory.2011.07.010

Jakubek, B., Grochalski, K., Rukat, W. & Sokol, H. 2022. Thermovision measurements of rolling bearings. *Measurement*, *189*, 110512. Available at: https://doi.org/10.1016/j.measurement.2021.110512

Lei, Y., Han, D., Lin, J. & He, Z. 2013. Planetary gearbox fault diagnosis using an adaptive stochastic resonance method. *Mechanical Systems and Signal Processing*, *38*(1), 113–124. Available at: https://doi.org/10.1016/j.ymssp.2012.06.021

Lei, Y., Zuo, M.J., He, Z. & Zi, Y. 2010. A multidimensional hybrid intelligent method for gear fault diagnosis. *Expert Systems with Applications*, *37*(2), 1419–1430. Available at: https://doi.org/10.1016/j.eswa.2009.06.060

Lu, W., Zhang, Y., Cheng, H., Zhou, Y. & Lv, H. 2020. Research on dynamic behavior of multistage gears-bearings and box coupling system. *Measurement*, *150*, 107096. Available at: https://doi.org/10.1016/j.measurement.2019.107096

McNames, J. 2002. *Fourier series analysis of epicyclic gearbox vibration*. Available at: https://doi.org/10.1115/1.1403735

Rai, A., & Upadhyay, S. H. 2016. A review on signal processing techniques utilized in the fault diagnosis of rolling element bearings. *Tribology International*, *96*, 289–306. Available at: https://doi.org/10.1016/j.triboint.2015.12.037

Ristić, S. S., Jegdić, B.V. & Polić-Radovanović, S. R. 2013. Investigation of the energy efficiency of the military museum building by infrared thermography. *Vojnotehnički Glasnik*, *61*(2), 182–199. Available at: https://doi.org/10.5937/vojtehg61-2901

Shaalan, A. A., Mefteh, W. & Frihida, A. M. 2024. Review on deep learning classifiers for faults diagnosis of rotating industrial machinery. *Service Oriented Computing and Applications*, *18*(4), 361–379. Available at: https://doi.org/10.1007/s11761-024-00418-7

Singh, T. & Sehgal, S. 2022. Damage identification using vibration monitoring techniques. *Materials Today: Proceedings*, *69*, 133–141. Available at: https://doi.org/10.1016/j.matpr.2022.08.204

Thomas, R., Jones, N. & Donne, K. 2001. Infrared thermography in industrial diagnostics. *Measurement and Control*, *34*(4), 110–112. Available at: https://doi.org/10.1177/002029400103400407

Vishwakarma, M., Purohit, R., Harshlata, V. & Rajput, P. 2017. Vibration analysis & condition monitoring for rotating machines: A review. *Materials Today: Proceedings*, *4*(2), 2659–2664. Available at: https://doi.org/10.1016/j.matpr.2017.02.140

Watban Khalid Fahmi, A.-T., Reza Kashyzadeh, K. & Ghorbani, S. 2022. A comprehensive review on mechanical failures cause vibration in the gas turbine of combined cycle power plants. *Engineering Failure Analysis*, *134*, 106094. Available at: https://doi.org/10.1016/j.engfailanal.2022.106094

Zhang, S. 2013. Green tribology: Fundamentals and future development. *Friction*, *1*(2), 186–194. Available at: https://doi.org/10.1007/s40544-013-0012-4

Análisis de la aplicación de métodos de diagnóstico de vibraciones y termografía para la detección temprana de defectos en un sistema mezclador-caja de cambios industrial: un caso de estudio

Borivoj Z. Novaković[a], *Luka* Djordjević[a], **autor de correspondencia,** *Damir* Jerković[b], *Mihalj* Bakator[a]

[a] Universidad de Novi Sad, Facultad Técnica “Mihajlo Pupin”, Zrenjanin, República de Serbia

[b] Universidad de Defensa, Academia Militar, Belgrado, República de Serbia

CAMPO: Ingeniería mecánica
TIPO DEL ARTÍCULO: Artículo científico original

Resumen:

Introducción/objetivo: *Los rodamientos constituyen componentes esenciales sin los cuales el funcionamiento de sistemas sometidos a cargas significativas sería inconcebible. El proceso de instalación de los rodamientos en sistemas rotacionales influye considerablemente en su* *longevidad, fiabilidad y eficiencia. Una instalación precisa y meticulosa de los rodamientos es fundamental para garantizar un rendimiento operativo óptimo de los sistemas rotacionales. Un montaje correcto de los rodamientos facilita la distribución uniforme de las cargas, reduce la fricción y minimiza el desgaste. Además, un montaje correcto de los rodamientos reduce el riesgo de vibraciones, ruido y posibles fallos del sistema. Por lo tanto, la instalación de los rodamientos es un paso crucial para mantener el funcionamiento fiable y eficiente de los sistemas rotacionales, prolongando así su vida útil y reduciendo la necesidad de reparaciones.*

Métodos: La metodología empleada en este estudio combina el análisis vibrodiagnóstico de un mezclador industrial equipado con una caja de cambios planetaria y la aplicación simultánea de técnicas termográficas. Este enfoque integrado proporciona una comprensión completa del estado del sistema y ayuda a identificar posibles fuentes de calentamiento tanto en la caja de cambios como en el mezclador. Los exámenes vibrodiagnósticos abarcaron el análisis de las vibraciones generadas por la caja de cambios planetaria durante su funcionamiento, junto con el análisis interpretativo de los resultados para detectar posibles desequilibrios, daños o irregularidades en el sistema mecánico. Por otro lado, la aplicación de la termografía contribuyó a generar una representación visual de las distribuciones de temperatura en puntos críticos de la caja de cambios, facilitando la identificación de anomalías térmicas. La integración de estos métodos permite un enfoque científico holístico para el análisis del sistema de caja de cambios planetaria, lo que permite un diagnóstico detallado y la comprensión de las causas raíz de los posibles problemas operativos en la caja de cambios.

Resultados: La meticulosa interpretación de los datos adquiridos facilitó la identificación de las posibles causas de la carga térmica en el caja de cambios planetaria, proporcionando una visión completa de los aspectos mecánicos y térmicos de todo el sistema. La integración de métodos de vibrodiagnóstico y termografía constituye un componente fundamental de un enfoque analítico holístico, crucial para una comprensión exhaustiva del rendimiento y el estado general de la caja de cambios planetaria y del mezclador industrial. Los resultados obtenidos sirven de base para el desarrollo de procedimientos de diagnóstico precisos, sentando las bases para la implementación de mejoras o estrategias de mantenimiento pertinentes en el sistema. Esto, a su vez, tiene el potencial de optimizar el rendimiento operativo de la caja de cambios planetaria y prolongar su vida útil.

Conclusión: La metodología aplicada, basada en análisis vibrodiagnósticos y técnicas termográficas, ha proporcionado una visión completa del estado tanto de la caja de cambios planetaria como del mezclador industrial que lo contiene. Todos los análisis descritos en el texto se realizaron en cada componente del sistema mezclador. La

interpretación detallada de los datos ha permitido identificar las posibles causas del calentamiento de la caja de cambios, lo que proporciona una comprensión más profunda de los aspectos mecánicos y térmicos del sistema. De esta manera, se puede mejorar la eficiencia del mantenimiento del sistema examinado.

Palabras claves: caja de cambios planetaria, mezclador industrial, vibrodiagnóstico, termografía, análisis, rodamiento, confiabilidad, mantenimiento.

Анализ применения методов вибродиагностики и термографии с целью выявления дефектов на ранней стадии в промышленной системе смеситель-редуктор – тематическое исследование

Боривой З. Новакович[а], *Лука* Джорджевич[а], **корреспондент,** *Дамир* Јеркович[б], *Михаль* Бакатор[а]

[а] Новисадский университет, технологический факультет им. Михайла Пупина, г. Зренянин, Республика Сербия
[б] Университет обороны в Белграде, Военная академия, г. Белград, Республика Сербия

РУБРИКА ГРНТИ: 30.19.00 Механика деформируемого твердого тела,
30.15.35 Теория механизмов и машин,
55.43.00 Автомобилестроение,
ВИД СТАТЬИ: оригинальная научная статья

Резюме:

Ведение/цель: *Подшипники являются важнейшими компонентами, без которых невозможно представить функционирование механических систем, подверженных серьезным нагрузкам. Процесс установки подшипников в роторных системах существенно влияет на срок их службы, надежность и эффективность. Точная и правильная установка подшипников имеет важнейшее значение для обеспечения оптимальных эксплуатационных характеристик роторных систем. Правильный подшипниковый узел способствует равномерному распределению нагрузок, снижению трения и минимизации износа. Кроме того, правильно установленные подшипники уменьшают вибрации, шум и снижают риск от возможных отказов системы. Таким образом, процесс установки подшипников является важным этапом в обеспечении надежной и эффективной работы роторных систем, что позволяет продлить срок их службы и снизить потребность в ремонте.*

Методы: Методология, использованная в данном исследовании, сочетает в себе вибродиагностический анализ промышленного смесителя, оснащенного планетарным редуктором, и одновременное применение термографических методов. Такой

комплексный подход обеспечивает всестороннее понимание состояния системы и помогает выявить потенциальные источники возможных дисбалансов, повреждений или неровностей в механической системе. Помимо того, применение термографии позволило получить визуальное представление о распределении температуры в критических точках коробки передач, что облегчило идентификацию тепловых аномалий. Интеграция этих методов обеспечивает целостный научный подход к анализу системы планетарной коробки передач, позволяющий проводить детальную диагностику и понимать первопричины потенциальных проблем в работе коробки передач.

Результаты: Тщательная интерпретация полученных данных помогла выявить потенциальные причины тепловой нагрузки в планетарной коробке передач, на основании чего складывается полное представление о механических и тепловых аспектах всей системы. Интеграция методов вибродиагностики и термографии является ключевым компонентом целостного аналитического подхода, который имеет решающее значение для полного понимания характеристик и общего состояния планетарного редуктора и промышленного смесителя. Полученные результаты являются основой для разработки точных диагностических процедур, закладывая фундамент для внедрения соответствующих усовершенствований или стратегий технического обслуживания системы. А это, в свою очередь, позволит оптимизировать эксплуатационные характеристики планетарной коробки передач и продлить срок ее службы.

Выводы: Примененная методология, основанная на вибродиагностическом анализе и термографических методах, позволила получить всестороннее представление о состоянии как планетарного редуктора, так и промышленного смесителя. Причем все анализы, описанные в статье, были проведены по каждому компоненту системы смесителя. Подробная интерпретация данных способствовала выявлению возможных причин перегрева коробки передач, что позволило глубже понять механические и тепловые аспекты системы. Руководствуясь результатами данного исследования, можно повысить эффективность обслуживания тестированной системы.

Ключевые слова: планетарная коробка передач, промышленный смеситель, вибродиагностика, термография, анализ, подшипник, надежность, техническое обслуживание.

Анализа примене метода вибродијагностике и термовизије у циљу откривања ране фазе дефеката на индустријском систему мешач-редуктор – студија случаја

Боривој З. Новаковић[a], *Лука* Ђорђевић[б], **аутор за преписку,** *Дамир* Јерковић[a], *Михаљ* Бакатор[a]

[a]Универзитет у Новом Саду, Технички факултет „Михајло Пупин”, Зрењанин, Република Србија

[б]Универзитет одбране у Београду, Војна академија, Београд, Република Србија

ОБЛАСТ: машинство
КАТЕГОРИЈА (ТИП) ЧЛАНКА: оригинални научни рад

Сажетак:

Увод/циљ: Лежајеви представљају кључне компоненте без којих би функционисање система изложених знатним оптерећењима било незамисливо. Процес уградње лежајева у ротационе системе значајно утиче на њихов век трајања, поузданост и ефикасност. Тачна и прецизна монтажа лежајева је од суштинског значаја за постизање оптималних радних перформанси ротационих система. Правилна уградња лежајева доприноси равномерној расподели оптерећења, смањењу трења и минимизацији хабања. Поред тога, адекватно монтирани лежајеви смањују ризик од вибрација, буке и потенцијалних отказа система. Стога, процес уградње лежајева представља кључни корак у одржавању поузданог и ефикасног рада ротационих система, чиме се продужава њихов радни век и смањује потреба за поправкама.

Методе: Методологија примењена у овом истраживању комбинује вибродијагностичку анализу индустријског мешача опремљеног планетарним мењачем и истовремену примену термографских техника. Овај интегрисани приступ омогућава свеобухватни увид у стање система и помаже у идентификацији потенцијалних извора загревања, како у мењачу, тако и у мешачу. Вибродијагностичка испитивања обухватила су анализу вибрација које генерише планетарни мењач током рада, уз интерпретацију резултата ради откривања могућих неуравнотежености, оштећења или неправилности у механичком систему. С друге стране, примена термографије допринела је стварању визуелног приказа дистрибуције температуре на критичним тачкама мењача, олакшавајући идентификацију термичких аномалија. Интеграција ових метода омогућава холистички научни приступ анализи система планетарног мењача, што омогућава детаљну дијагностику и спознавање основних узрока потенцијалних оперативних проблема у мењачу.

Резултати: Пажљива интерпретација прикупљених података омогућила је идентификацију потенцијалних узрока термичког оптерећења у планетарном мењачу, пружајући свеобухватан увид у механичке и термичке аспекте целокупног система. Интеграција вибродијагностичких и термографских метода представља кључну компоненту холистичког аналитичког приступа, који је неопходан за потпуни увид у перформансе и укупно стање планетарног мењача и индустријског мешача. Добијени резултати служе као основа за развој прецизних дијагностичких процедура, постављајући темељ за имплементацију одговарајућих побољшања или стратегија одржавања у систему. То може довести до оптимизације радних перформанси планетарног мењача и продужетка његовог радног века.

Закључак: Примењена методологија, заснована на вибродијагностичким анализама и термографским техникама, пружила је свеобухватан увид у стање како планетарног мењача, тако и индустријског мешача у којем се он налази, при чему су све описане анализе спроведене на свакој компоненти унутар система мешача. Детаљна интерпретација података омогућила је идентификацију потенцијалних узрока загревања мењача, што доприноси бољем разумевању механичких и термичких аспеката система. На овај начин може се унапредити ефикасност одржавања испитиваног система.

Кључне речи: планетарни мењач, индустријски мешач, вибродијагностика, термографија, анализа, лежај, поузданост, одржавање.

Paper received on: 04.01.2025.
Manuscript corrections submitted on:23.02.2025.
Paper accepted for publishing on: 25.02.2025.

Kinematic modeling and workspace analysis of a multi-dual cross-module cable-driven continuum robot

Djedili Amel[a], *Amouri* Ammar[b]

[a] University Frères Mentouri Constantine 1, Department of Mechanical Engineering, Laboratory of Mechanics, Algeria
e-mail: amel.djedili@doc.umc.edu.dz, **corresponding author**,
ORCID iD: https://orcid.org/0009-0001-6213-6400

[b] University Frères Mentouri Constantine 1, Department of Mechanical Engineering, Laboratory of Mechanics, Algeria
e-mail: ammar_amouri@yahoo.fr,
ORCID iD: https://orcid.org/0000-0001-8735-6808

https://doi.org/10.5937/vojtehg73-56975

FIELD: mechanical engineering
ARTICLE TYPE:original scientific paper

Abstract:

The flexibility and capability of continuum robots to navigate complex and constrained environments make them highly suitable for diverse applications, including minimally invasive surgery, industrial manipulation, and exploratory operations in hazardous or confined spaces. Despite these advantages, accurately modeling their kinematics and conducting comprehensive workspace analysis, particularly for multi-section cable-driven continuum robots with dual cross-module configurations, remain significantly challenging. This study begins by presenting a design of a three-section dual-cross cable-driven continuum robot. The forward kinematics model is analytically derived based on the constant curvature assumption, while the inverse kinematics model is formulated as an optimization problem. To support trajectory generation, the robot's workspace is analyzed using MATLAB and SOLIDWORKS software. The simulation example illustrates the robot's trajectory-tracking performance.

Key words: continuum robot, cable-driven continuum robot, kinematics modeling, workspace analysis, trajectory tracking

Introduction

Continuum robots have attracted significant attention in recent years due to their exceptional shape-morphing capabilities, expansive workspaces, and adaptability to navigate complex environments. Inspired by biological organisms (Hannan & Walker, 2003; McMahan et al, 2004), these robots feature continuous, flexible movement, enabling safe operation in obstacle-rich settings. Their capacity to adopt diverse configurations makes them highly versatile, with notable applications in minimally invasive surgery (Burgner-Kahrs et al, 2015) and industrial manipulation within confined spaces (Liu et al, 2016).

According to the literature, there are several types of continuum robots, including flexible and rigid ones. This paper focuses on a rigid type known as cable-driven continuum robots. These robots use cables for actuation instead of traditional rigid components (Hemami, 1985; Murphy et al, 2013). This approach offers advantages such as reduced weight, increased flexibility, and a more compact form factor, which are particularly valuable for tasks that require high adaptability in constrained environments. Additionally, cable-driven robots can provide enhanced safety in delicate applications due to their soft, non-colliding nature. However, while these benefits enhance the robot's capabilities, they also present challenges related to precise control and accurate prediction of the robot's movement, due to the nonlinear mathematical expressions that govern its kinematic and dynamic behavior and the associated modeling complexities.

Kinematic modeling of CDCRs is essential for describing and analyzing their movements without considering the forces that cause them, with the aim of predicting the position, velocity, and orientation of the robot's components. This is crucial for ensuring precise kinematic control, workspace generation, and trajectory planning, especially in complex environments where precision and adaptability are essential. However, one of the primary challenges is modeling the robot's deformation during its motion. This challenge is often simplified using various methods, such as those proposed by Linn (2016), Mahl (2014), Amouri (2019), and Webster & Jones (2010). In Linn (2016) and Mahl (2014), the authors treat the robot's backbone as a one-dimensional elastic rod with bending and twisting characteristics. Nevertheless, the constant curvature assumption (Amouri, 2019; Webster & Jones, 2010) offers the simplest approach. This assumption allows each section of the robot to be represented as a curve with a constant radius, thereby simplifying the complex behavior of a flexible, multi-sectional system into a more manageable form. While this approach provides an effective approximation for many applications, it may not fully capture the intricacies of the robot's deformation in highly dynamic or constrained environments. Further refinements and models may be required for more accurate predictions in such cases.

In the same context, focusing on a specific type of cable-driven continuum robot known as the Dual Cross-Module Cable-Driven Continuum Robot, only a few kinematic studies have been proposed in the literature (Zhou et al, 2022; Amouri et al, 2023). In Zhou et al. (2022) and Amouri et al. (2023), the authors introduced a bio-inspired novel dual cross-module section cable-driven continuum robot that combines the flexibility of continuum robots with the stability of rigid robots. These papers presented the design and kinematics of the manipulator. However, Zhou et al. (2022) did not address several important aspects such as generalizing the inverse kinematic model and calculating the robot's workspace. In contrast, Amouri et al. (2023) focused on a robot with two sections. However, a robot with fewer than three sections faces significant limitations, as it lacks the necessary Degrees of Freedom (DoFs) to independently adjust both position and orientation. Consequently, such a robot is constrained to a limited set of feasible trajectories and cannot achieve the same level of versatility in motion. In this study, we explore the design and kinematic modeling of a dual cross-module cable-driven continuum robot with three sections. This approach aims to address the limitations associated with fewer sections and provide a more versatile solution for complex tasks.

This paper begins by presenting an overview of the robot's design and structural components. Next, kinematic models are developed under the constant kinematic assumption. The forward kinematic models are derived analytically, while the inverse kinematic model for the entire robot is formulated as an optimization problem and solved using Knowledge-Based Particle Swarm Optimization. Additionally, the workspaces of a module and a section are generated and analyzed. Subsequently, a simulation example is presented to illustrate line-shaped trajectory tracking with a fixed end-tip orientation of the robot. Lastly, the main conclusions and future perspectives are summarized in the final section.

Design of a dual-cross module continuum robot

Similar to the work of Amouri et al. (2023), the robot developed in this study is a fish-like, bio-inspired continuum robot designed to balance rigidity and flexibility, allowing it to seamlessly adapt to diverse environments and effectively perform a wide range of tasks. By mimicking the structural adaptability found in biological organisms, this robot can navigate complex or constrained spaces, providing both the strength necessary for stability and the flexibility required for maneuverability. Its unique design enables smooth, continuous movements, making it ideal for a wide range of applications.

The robot consists of two main parts: rigid components and flexible backbones. The rigid components provide stability and contain the actuation cables, while the flexible backbones enable a wider workspace and greater range of motion. The backbone is made of rectangular elastic sheets, each measuring 90 mm in length, 26 mm in width, and 3.4 mm in thickness, and is constructed from ASTM X36 steel which provides the necessary flexibility for the robot’s operation. The rigid components, in the form of cross-shaped sheets, are made from a lightweight 3D-printed ABS material, chosen for its low weight and suitability for constrained environments. The advantage of using this cross-shaped design, rather than the traditional disk shape, is that it conserves material, reduces weight, and makes the robot better suited for navigating tight spaces. For more details on the design development and illustrations, refer to (Amouri et al, 2023). In summary, a rectangular elastic sheet and 15 cross-shaped sheets, with uniform spacing between them, form a module that enables 2D motion. Subsequently, two successively mounted modules create a section enabling 3D motion. The entire robot under consideration is composed of three sections.

Typically, common designs use three or four cables per module, arranged symmetrically around the backbone. However, in this design, each module is actuated by only two cables, reducing the complexity of actuation and control while requiring fewer motors. The guiding holes in the cross-shaped sheets ensure that the cables form an arc-like shape within the designated bending module. In theory, as the number of cross-shaped sheets increases, the bending shape of the cables will become more circular.

Kinematic modeling

Description of a dual-cross module continuum robot

The systematic development of kinematic models requires, first and foremost, an appropriate method for describing the morphology of the robot. Various methods and notations have been proposed in the literature for the kinematic description of continuum robots (Webster & Jones, 2010; Jones & Walker, 2006). In this context, the constant curvature assumption is employed, wherein the central axis of the structure is considered inextensible. This approach simplifies several modeling challenges and enables a more efficient representation of the robot's kinematics, as illustrated in Figure 1 (for further details on the development, refer to (Amouri, 2017).

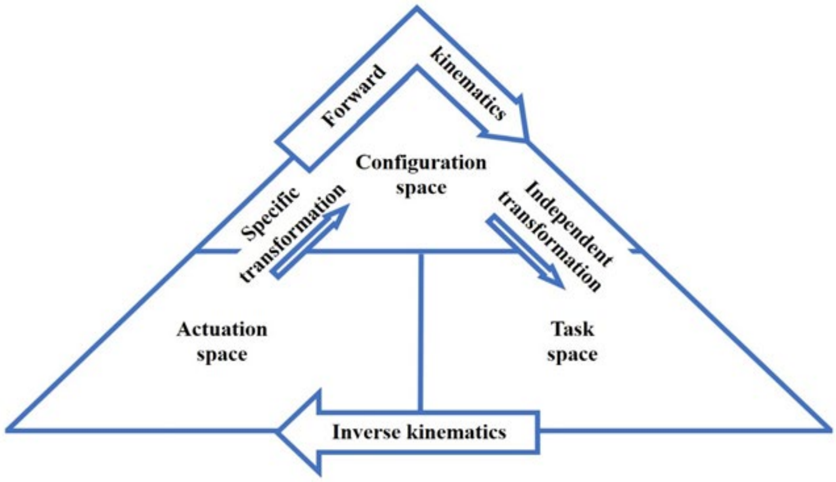

Figure 1 – Overview of the kinematic mapping of a continuum robot using the constant curvature assumption

However, this assumption holds only under specific conditions: (i) the gravitational influence on the robot is disregarded; (ii) only the controlling forces from the cables are considered, while all other external forces are neglected; (iii) the frictional interaction between the cables and the routing holes is ignored; (iv) the elastic sheet backbone is assumed to undergo pure bending without any expansion, contraction, or torsion; and (v) the cable is treated as inextensible, meaning it cannot stretch or extend.

To define the quantities involved in the kinematic description of the robot under consideration, four primary reference frames are established. The first is the absolute frame $\Re_w$. Next, the frames $\Re_k$, with $k = 1,2,3$, are assigned to the upper cross-shaped sheet of each section k, while the frame $\Re_0$ is fixed at the base of the first section (Figure 2a). Additionally, three intermediate frames $\Re_{int,k}$ designated for the first module of each section, provide a localized reference for kinematic calculations (Figure 2b).

As previously mentioned, each module is modeled as an inextensible circular arc lying in a plane, as illustrated in Figure 2 (Amouri et al, 2023). This arc is characterized by its length $\ell_{j,k}$ and its bending angle $\theta_{j,k}$. In this configuration, the orientation angle $\varphi_{j,k}$ of each module, with $j = 1, 2$, is equal to 0 and $\pi/2$, respectively.

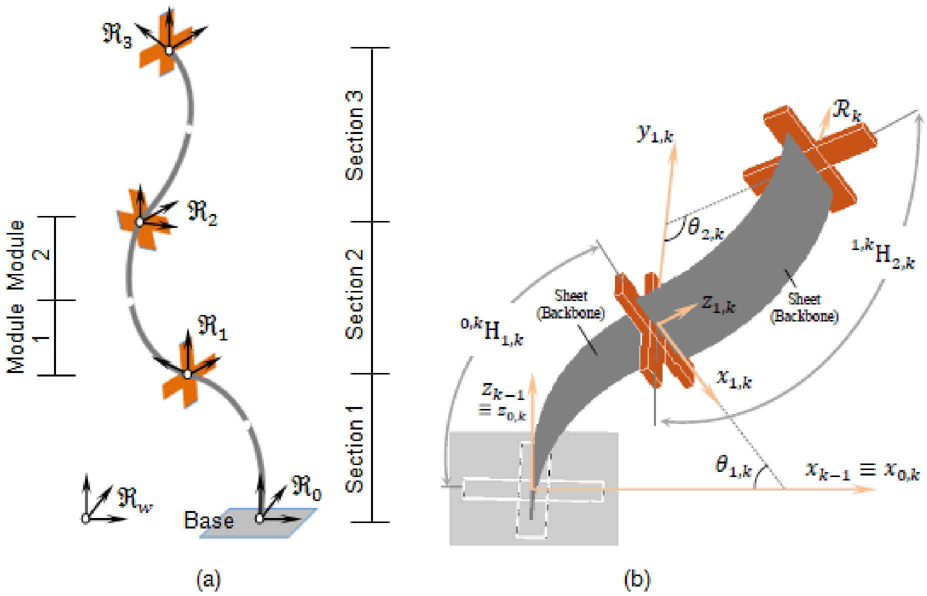

Figure 2 – Depiction of the reference frames defined for the three-section dual-cross cable-driven continuum robot: (a) global reference frames, and (b) intermediate frames

Forward kinematics of the module

Typically, the forward kinematic model of such a robot serves as the foundational step in the modeling process. This subsection aims to establish a relationship that predicts the position and orientation of the module's end-tip based on the varying lengths of the actuation cables. This relationship is described by the following homogeneous transformation matrix:

$$\mathbf{H}_{j,k} = \begin{bmatrix} \mathbf{R}_{j,k} & \mathbf{P}_{j,k} \\ 0_{1\times 3} & 1 \end{bmatrix} \tag{1}$$

where $\mathbf{R}_{j,k}$ represents the 3×3 rotation matrix $\mathbf{R}_{j,k}$, and $\mathbf{P}_{j,k}$ denotes the 3×1 vector position. These components are determined using the following equations:

$$\mathbf{R}_{j,k} = \mathbf{rot}(u, \theta_{j,k}) \tag{2}$$

$$\boldsymbol{P}_{j,k} = \begin{cases} x_{j,k} = \dfrac{\ell_{j,k}}{\theta_{j,k}}\left(1 - cos(\theta_{j,k})\right) cos(\varphi_{j,k}) \\ y_{j,k} = \dfrac{\ell_{j,k}}{\theta_{j,k}}\left(1 - cos(\theta_{j,k})\right) sin(\varphi_{j,k}) \\ z_{j,k} = \dfrac{\ell_{j,k}}{\theta_{j,k}} sin(\theta_{j,k}) \end{cases} \tag{3}$$

where u represents the axis of rotation, which aligns with the $y-$axis for the first module and the $x-$axis for the second module, respectively.

On the other hand, the relationship between the cable lengths $l_{i,j,k}$ and the bending angle $\theta_{j,k}$ can be expressed by the following equation:

$$\theta_{j,k} = \frac{\ell_{j,k} - \Delta l_{i,j,k}}{r} \quad (4)$$

where $\Delta l_{k,i,j}$ represents the value of the change in cable length due to bending, and r denotes the radial distance between the cables and the neutral $z-$axis of the backbone.

Forward kinematics of the section

The forward kinematic model of the section k describes the relationships that express the expression of the position and orientation of the upper cross-shaped sheet as a function of the cable lengths. As previously mentioned, the section k consists of two modules connected in series. This model can be obtained by successively multiplying the transformation matrices of each module (j, k), treating them as a simple open-chain system. This model is represented by the following transformation matrix:

$$\mathbf{H}_k = \prod_{j=1}^{2} \mathbf{H}_{j,k} \quad (5)$$

Forward kinematics of the entire robot

The forward kinematic model of the multi-sectional robot is obtained by successively multiplying the transformation matrices of each section k along with the transformation matrix of the static reference frame. The resulting matrix is expressed by the following equation:

$$\mathbf{H}_3 = \mathbf{H}_0 \prod_{k=1}^{3} \mathbf{H}_k = \begin{bmatrix} \mathbf{R}_3 & \mathbf{P}_3 \\ \mathbf{0} & 1 \end{bmatrix} \quad (6)$$

where $\mathbf{H}_0$ represents the transformation matrix that defines the robot's base frame $\Re_0$ with respect to the global reference frame $\Re_w$.

Workspace analysis

The determination of the workspace is a crucial aspect in the design of a robot, as it defines its range of motion and determines the set of points that can be reached during its operation. This section focuses on determining and analyzing the workspace of the module, the section, and the entire robot, respectively.

Figure 3 illustrates the workspace of the modules within a section as they bend independently, forming a set of points that trace a curve. These curves are plotted for bending angles in the range $[-\pi/2, \pi/2]$ which represents the maximum values that prevent overlap between adjacent cross-shaped sheets.

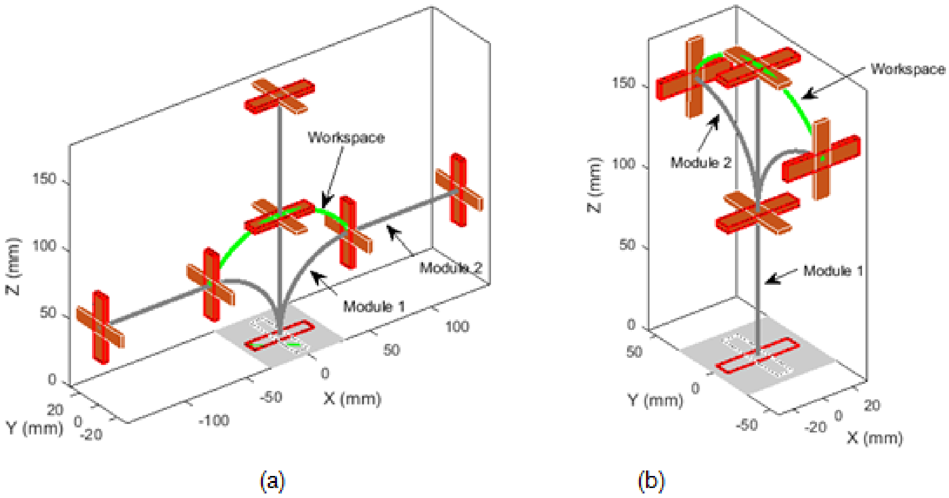

Figure 3 – Workspace of a single module within a section as it bends independently: (a) workspace of the first module during bending, and (b) workspace of the second module during bending. For clarity, the intermediate cross-shaped sheets and the rectangular backbones are not shown

For such a section, this results in an enveloping surface, as shown in Figure 4. The figure also includes the workspace of a section with a cylindrical backbone. These workspaces were computed using Solidworks software.

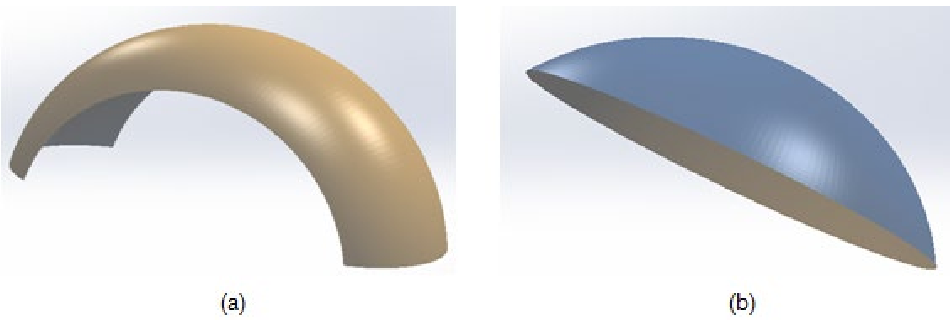

Figure 4 – Workspace of a single section: (a) workspace of the section for the considered robot, and (b) workspace of a section for a robot with a cylindrical backbone

Despite the differences in their shapes, the areas of the workspaces are equivalent, as demonstrated in Figure 5. This difference in workspace shape is advantageous for the robot when adapting to tasks requiring diverse movement patterns or navigating through constrained environments, as it provides greater flexibility and operational versatility.

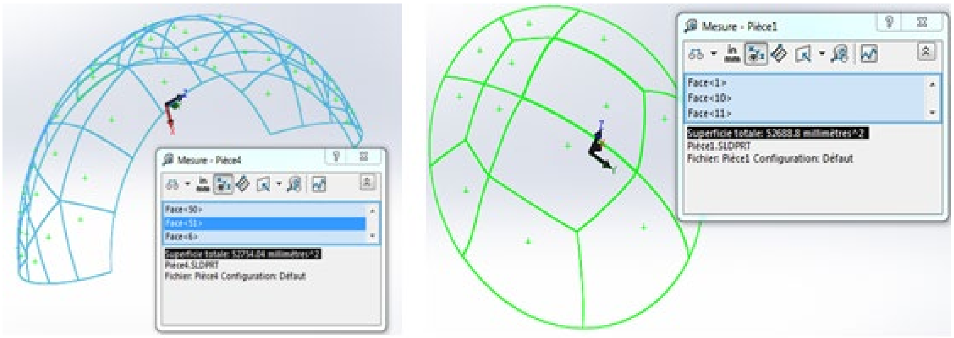

(a) (b)

Figure 5 – Meshing process for calculating the area of a single section: (a) section of the considered robot, and (b) section of a robot with a cylindrical backbone

However, for a three-section dual-cross cable-driven continuum robot or any robot with more than two sections, the workspace extends from a curve or surface to a three-dimensional volume. This volumetric workspace encompasses all possible positions and orientations that the robot's end-tip can achieve within its physical constraints. The complexity of this workspace increases with the number of sections, making its representation challenging to comprehend.

Inverse kinematics of the entire robot: optimized problem formulation

The hyper-redundancy of the robot enables the inverse kinematics problem to be addressed using an optimization algorithm that minimizes a quadratic criterion (Iqbal et al, 2009). While previous studies considered only the Cartesian position in the cost function (Amouri et al, 2023), this work incorporates both the Cartesian position and the orientation of the robot's end-tip. Accordingly, the cost function to be optimized, which determines the necessary adjustments in the actuation cables for the robot's end-tip to accurately follow the desired trajectory, is formulated as:

$$\begin{cases} F(\theta_{j,k}) = \lambda\|\mathbf{P}_{\text{trajet}} - \mathbf{P}_3\|^2 + (1-\lambda)\|\overline{\mathbf{P}}_{\text{trajet}} - \overline{\mathbf{P}}_3\|^2 \\ \text{s.t.} \\ |\theta_{j,k}| \le \theta_{\max} \end{cases} \tag{7}$$

where $\mathbf{P}_{\text{trajet}}$ and $\overline{\mathbf{P}}_{\text{trajet}}$ are the 3×1 vectors representing the desired Cartesian position and the orientation of the robot's end-tip, respectively. Similarly, $\mathbf{P}_3$ and $\overline{\mathbf{P}}_3$ denote the actual position and orientation of the robot's end-tip. The parameter λ is set to 0.5 to balance the position and orientation objectives. The components of the vector $\mathbf{P}_3$ correspond to the fourth column of the matrix $\mathbf{H}_3$, as defined in Equation (6), while $\overline{\mathbf{P}}_3$ can be computed based on the rotation matrix $\mathbf{R}_3$ using the following equation:

$$\overline{\mathbf{P}}_3 = \begin{cases} \mathrm{a} = \tan^{-1}\left(\frac{\mathrm{r}_{21}}{\mathrm{r}_{11}}\right) \\ \mathrm{b} = \tan^{-1}\left(\frac{-\mathrm{r}_{31}}{\mathrm{r}_{11}\mathrm{c}\alpha + \mathrm{r}_{21}\mathrm{s}\alpha}\right) \\ \mathrm{c} = \tan^{-1}\left(\frac{\mathrm{r}_{13}\mathrm{s}\alpha - \mathrm{r}_{23}\mathrm{c}\alpha}{-\mathrm{r}_{12}\mathrm{s}\alpha + \mathrm{r}_{22}\mathrm{c}\alpha}\right) \end{cases} \tag{8}$$

where r_{nm} is the (n, m) element of the direction cosine matrix $\mathbf{R}_3$.

To solve this optimization problem, various algorithms can be employed. As demonstrated in, the Knowledge-based Particle Swarm Optimization (Kb-PSO) algorithm, originally proposed by (Kennedy & Eberhart, 1995), is utilized due to its simplicity and fast convergence properties. The algorithm ensures efficient computation and reliable results, making it well-suited for the inverse kinematics problem of hyper-redundant robots.

Simulation results

This section presents the application of the solution to the inverse kinematics problem of a three-section dual-cross cable-driven continuum robot, formulated as an optimization problem and addressed through numerical simulation. The reference trajectory is defined as follows:

$$\mathbf{P}_{\text{trajet}} = \begin{cases} x = 10t \\ y = 10t \\ z = 540 - 10t \end{cases}, \text{and } \overline{\mathbf{P}}_{\text{trajet}} = \begin{cases} \mathrm{a} = 0 \\ \mathrm{b} = 0 \\ \mathrm{c} = 0 \end{cases} \tag{9}$$

The simulation results, which illustrate the required bending angles, execution time, and combined error for tracking a line-shaped trajectory while maintaining a fixed end-tip orientation, are presented in Figures 6, 7, and 8, respectively.

VOJNOTEHNIČKI GLASNIK / MILITARY TECHNICAL COURIER, 2025, Vol. 73, Issue 3

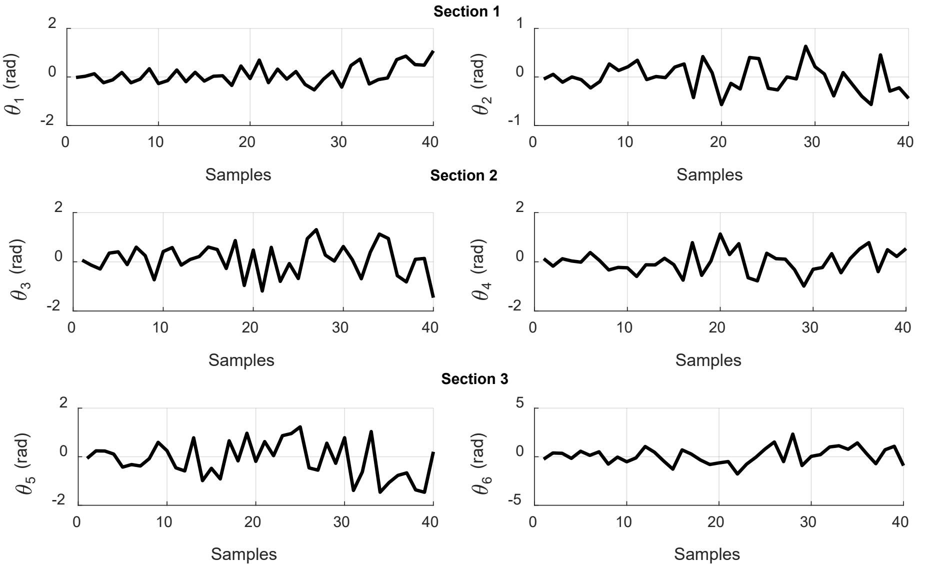

Figure 6 – Required bending angles to track the line-shaped trajectory in a fixed robot's end tip orientation

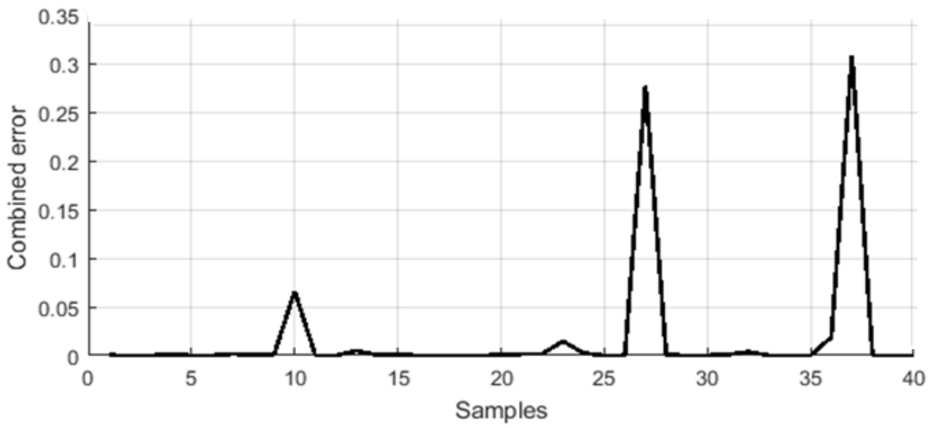

Figure 7 – Combined error for tracking the line-shaped trajectory with a fixed robot end-tip orientation

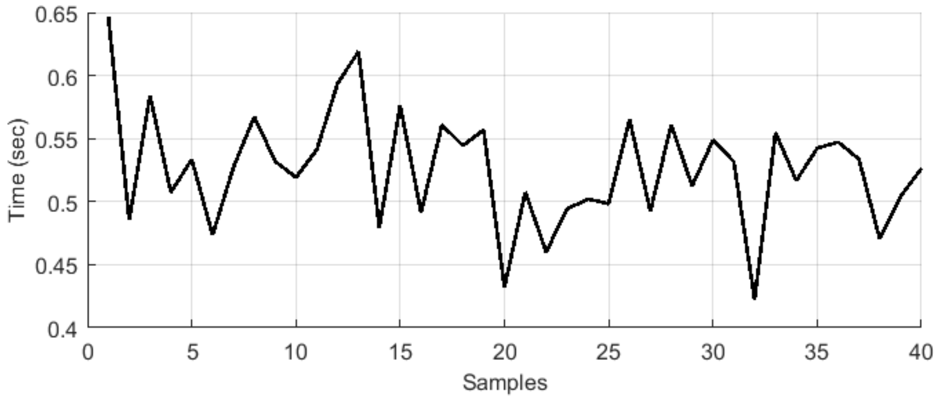

Figure 8 – Execution time for tracking the line-shaped trajectory with a fixed robot end-tip orientation

The combined error, shown in Figure 7, quantifies the deviation between the desired and actual end-tip configuration. Specifically, it represents the weighted sum of the mean squared errors in both position and orientation. The position error is measured as the squared Euclidean distance in the three-dimensional space, while the orientation error is computed as the squared deviation in a three-dimensional representation of orientation. Thus, the combined error accounts for discrepancies across six dimensions: three for position and three for orientation.

Conclusion

This paper introduces the design, kinematic modeling, and workspace analysis of a novel Multi-Dual Cross-Module Cable-Driven Continuum Robot. The proposed robot consists of three sections, each incorporating two planar bending modules. Unlike previous designs in the literature, this configuration enhances adaptability to diverse environments and expands the range of possible tasks. Additionally, it offers several advantages, including a lightweight structure, smooth deformation, enhanced rigidity, lower energy consumption, and a non-uniform workspace.

First, the principal components and materials of the proposed design are discussed in detail. Second, the forward kinematic model is developed using the constant curvature assumption, and the workspaces of the robot, as well as those of the section and module individually, are generated and analyzed using MATLAB and SOLIDWORKS. Given the complexity and highly nonlinear nature of the forward kinematic model, the inverse kinematics problem is formulated as an optimization task with a quadratic cost function that accounts for both the position and orientation of the robot's end-tip. This optimization problem is solved using the Knowledge-based Particle Swarm Optimization (Kb-PSO) algorithm. Finally, to demonstrate the effectiveness of the Kb-PSO algorithm in solving the inverse kinematics problem, a numerical example of point-to-point tracking along a line-shaped trajectory is presented.

As a future perspective, the dynamic model of the robot will be developed, and both classical and advanced control strategies will be implemented to further enhance its capabilities.

References

Amouri, A. 2019. Investigation of the constant curvature kinematic assumption of a 2-DOFs cable-driven continuum robot. UPB *Scientific Bulletin, Series D: Mechanical Engineering*, 81(3), pp.27–38. ISSN 1454-2358.

Amouri, A. 2017. Contribution à la modélisation dynamique d'un robot flexible bionique, Ph.D. dissertation, University of Constantine 1, Algeria.

Amouri, A., Cherfia, A., Belkhiri, A. & Merabti, H. 2023. Bio-inspired a novel dual-cross-module sections cable-driven continuum robot: design, kinematics modeling and workspace analysis. *Journal of the Brazilian Society of Mechanical Sciences and Engineering*, 45(5), p.265. Available at: https://doi.org/10.1007/s40430-023-04197-8

Burgner-Kahrs, J., Rucker, D.C. & Choset, H. 2015. Continuum robots for medical applications: a survey. *IEEE Transactions on Robotics*, 31(6), pp.1261-1280. Available at: https://doi.org/10.1109/tro.2015.2489500

Hannan, M.W. & Walker, I.D. 2003. Kinematics and the implementation of an elephant's trunk manipulator and other continuum-style robots. *Journal of Robotic Systems*, 20(2), pp.45-63. Available at: https://doi.org/10.1002/rob.10070

Hemami, A. 1985. Studies on a light-weight and flexible robot manipulator. *Robotics*, 1(1), pp.27-36. Available at: https://doi.org/10.1016/s0167-8493(85)90306-7

Iqbal, S., Mohammed, S. & Amirat, Y. 2009. A guaranteed approach for kinematic analysis of continuum robot-based catheter. In: *Proceedings of IEEE International Conference on Robotics and Biomimetics*, December 19-23, pp.1573-1578. Available at: https://doi.org/10.1109/robio.2009.5420395

Jones, B.A. & Walker, I.D. 2006. Kinematics for multisection continuum robots. *IEEE Transactions on Robotics*, 22(1), pp.43-55. Available at: https://doi.org/10.1109/tro.2005.861458

Linn, J. 2016. Discrete kinematics of Cosserat rods based on the difference geometry of framed curves. In: *The 4th Joint International Conference on Multibody System Dynamics*, Montreal, Canada. Berlin: [s.n.].

Liu, S., Yang, Z., Zhu, Z., Han, L., Zhu, X. & Xu, K. 2016. Development of a dexterous continuum manipulator for exploration and inspection in confined spaces. *Industrial Robot: An International Journal*, 43(3), pp.284-295. Available at: https://doi.org/10.1108/ir-07-2015-0142

Mahl, T., Hildebrandt, A. & Sawodny, O. 2014. A variable curvature continuum kinematics for kinematic control of the Bionic Handling Assistant. *IEEE Transactions on Robotics*, 30(4), pp.935-949. Available at: https://doi.org/10.1109/tro.2014.2314777

McMahan, W., Jones, B.A., Walker, I., Chitrakaran, V., Seshadri, A. & Dawson, D. 2004. Robotic manipulators inspired by cephalopod limbs. In: *Proceedings of the Canadian Engineering Education Association (CEEA)*, pp.1-10. Available at: https://doi.org/10.24908/pceea.v0i0.3994

Murphy, R.J., Kutzer, M.D., Segreti, S.M., Lucas, B.C. & Armand, M. 2014. Design and kinematic characterization of a surgical manipulator with a focus on treating osteolysis. *Robotica*, 32(6), pp.835-850. Available at: https://doi.org/10.1017/s0263574713001082

Kennedy, J. & Eberhart, R.C. 1995. Particle swarm optimization. In: *Proceedings of IEEE International Conference on Neural Networks IV*, pp.1942-1948. Available at: https://doi.org/10.1109/icnn.1995.488968

Webster, R.J. & Jones, B.A. 2010. Design and kinematic modeling of constant curvature continuum robots: a review. *The International Journal of Robotics Research*, 29(13), pp.1661-1683. Available at: https://doi.org/10.1177/0278364910368147

Zhou, P., Yao, J., Zhang, S., Wei, C., Zhang, H. & Qi, S. 2022. A bioinspired fish-bone continuum robot with rigid-flexible-soft coupling structure. *Bioinspiration&Biomimetics*, *17*(6), p.066012. Available at: https://doi.org/10.1088/1748-3190/ac8c10

Modelado cinemático y análisis del espacio de trabajo de un robot continuo accionado por cable con módulos cruzados multidual

Djedili Amel, **autor de correspondencia**, *Amouri* Ammar

Universidad Frères Mentouri Constantine 1, Departamento de Ingeniería Mecánica, Laboratorio de Mecánica, Argelia

CAMPO: Ingeniería Mecánica.
TIPO DE ARTÍCULO: Artículo científico original.

Resumen:

La flexibilidad y capacidad de los robots continuos para navegar en entornos complejos y restringidos los hacen muy adecuados para diversas aplicaciones, como cirugía mínimamente invasiva, manipulación industrial y operaciones exploratorias en espacios peligrosos o confinados. A pesar de estas ventajas, modelar con precisión su cinemática y realizar un análisis exhaustivo del espacio de trabajo, en particular para robots continuos multisección accionados por cable con configuraciones de doble módulo cruzado, sigue siendo un desafío considerable. Este estudio comienza presentando el diseño de un robot continuo de tres secciones *accionado por cable de doble módulo cruzado. El modelo de cinemática directa se deriva analíticamente con base en el supuesto de curvatura constante, mientras que el modelo de cinemática inversa se formula como un problema de optimización. Para facilitar la generación de trayectorias, el espacio de trabajo del robot se analiza mediante MATLAB y SOLIDWORKS. El ejemplo de simulación ilustra el rendimiento de seguimiento de trayectoria del robot.*

Palabras clave: robot continuo, robot continuo accionado por cable, modelado cinemático, análisis del espacio de trabajo, seguimiento de trayectoria

---

Кинематическое моделирование и анализ рабочего пространства многодуального кросс-модульного кабельного робота непрерывного действия

Дедили Амель,**корреспондент,** *Амури* Аммар

Университет братьев Ментоури Константин, 1, машиностроительный факультет, лаборатория механики, Алжирская Народная Демократическая Республика

РУБРИКА ГРНТИ: 81.09.00 Материаловедение
ВИД СТАТЬИ: оригинальная научная статья

Резюме:

Гибкость и способность роботов непрерывного действия ориентироваться в сложных и стесненных условиях делают их удобными для применения в различных сферах, включая малоинвазивную хирургию, промышленные манипуляции и поисковые работы во взрывоопасных или замкнутых пространствах. Несмотря на эти преимущества, точное моделирование их кинематики и проведение всестороннего анализа рабочего пространства, особенно для многосекционных роботов непрерывного действия с тросовым приводом и двухмодульной конфигурацией, все еще остается сложной задачей. В первой части статьи представлена конструкция трехсецционного параллельного робота непрерывного действия с тросовым приводом. Модель прямой кинематики разработана аналитически на основе предположения о постоянной кривизне, в то время как модель обратной кинематики формулируется как задача по оптимизации. Для генерации траектории рабочее пространство робота анализируется с использованием программных пакетов MATLAB и SOLIDWORKS. Пример моделирования показывает эффективность отслеживания траектории робота.

Ключевые слова: робот непрерывного действия, *робот непрерывного действия* с тросовым приводом, кинематическое

моделирование, анализ рабочего пространства, отслеживание траектории.

Кинематичко моделовање и анализа радног простора вишеструко дуалног унакрсно-модуларног кабловски вођеног континуалног робота

Ђедили Амел*,* **аутор за преписку,** *Амури* Амар

Универзитет браће Ментури Константин 1, Катедра за машинство, Лабораторија за механику, Алжир

ОБЛАСТ: машинство
КАТЕГОРИЈА (ТИП) ЧЛАНКА: оригинални научни рад

Сажетак:
Флексибилност и способност континуалних робота да се сналазе у сложеним и ограниченим окружењима чини их веома погодним за разноврсне примене у областима као што су минимално инванзивна хирургија, индустријско руковање и истраживачке операције у опасним или скученим просторима. И поред оваквих предности, прецизно моделовање њихове кинематике и спровођење свеобухватне анализе радног простора (нарочито када је реч о вишеделном кабловски вођеном континуалном роботу са двоструким унакрсно-модуларним конфигурацијама) представљају значајан изазов. раду је представљен пројекат троделног двострукоунакрсног кабловски вођеног континуалног робота. Модел директне кинематике изведен је аналитичким путем на основу претпоставке о константној закривљености, док је модел инверзне кинематике формулисан као проблем оптимизације. Ради генерисања путање, радни простор робота анализиран је уз помоћ софтверских пакета MATLAB и SOLIDWORKS. Пример симулације илуструје перформансе праћења путање робота.
Кључне речи: континуални робот, кабловски вођен континуални робот, моделовање кинематике, анализа радног простора, праћење путање

Paper received on:22.02.2025.
Manuscript corrections submitted on:28.03.2025.
Paper accepted for publishing on:09.04.2025.

Predictive analysis of brick powder-enhanced self-compacting mortar using artificial neural networks

Zine El Abidine Laidani[a], *Mohamed* Sahraoui[b], *Younes* Ouldkhaoua[c], *Benchaa* Benabed[d], *Mohamed El Ghazali* Belgacem[e]

[a] Blida1 University, Civil Engineering Department, Blida, People's Democratic Republic of Algeria,
e-mail: laidani_z@univ-blida.dz, **corresponding author**,
ORCID iD: https://orcid.org/0000-0002-8502-9819

[b] Blida1 University, Institute of Architecture and Urbanism, Blida, People's Democratic Republic of Algeria,
e-mail: sahraoui_mohamed@univ-blida.dz,
ORCID iD: https://orcid.org/ 0000-0003-4670-9755

[c] University of Science and Technology – Houari Boumediene, Faculty of Civil Engineering, Building in Environment Laboratory, Algiers, People's Democratic Republic of Algeria,
e-mail: younes.ouldkhaoua@usthb.edu.dz,
ORCID iD: https://orcid.org/ 0009-0001-8334-812X

[d] University of Amar Telidji, Department of Civil Engineering, Civil Engineering Research Laboratory, Laghouat, People's Democratic Republic of Algeria,
e-mail: b_benchaa@yahoo.fr,
ORCID iD: https://orcid.org/ 0000-0002-3352-1588

[e] University of Science and Technology – Houari Boumediene, Faculty of Civil Engineering, Building in Environment Laboratory, Algiers, People's Democratic Republic of Algeria,
e-mail: ghazali2017@gmail.com,
ORCID iD: https://orcid.org/ 0000-0001-8515-8568

doi https://doi.org/10.5937/vojtehg73-55812

FIELD: civil engineering, materials, deep learning
ARTICLE TYPE: original scientific paper

Abstract:

Introduction/purpose: Self-compacting mortars possess very good flowability which enables them to consolidate only through the force of their self-weight, not demanding any mechanical vibration. This type of mortars has a significant value in complicated construction and repair works. In this paper, research will be conducted on using brick powder as replacement for cement in SCM with a detailed study of effects on workability, compressive strength, and all other performance.

Methods: The proposed research models the relationships of different parameters, brick powder content and fineness, with the resultant properties of mortar using artificial neural networks (ANN) models.

Results : The results showed that the addition of brick powder up to 10% of cement as replacement improves mortar workability, giving the slump flow ranging from 306 to 309 mm and the funnel flow time between 4.8 and 5.4 s, while its compressive strength was ranging from 45 to 60 MPa at 28 days. However, at replacement levels higher than 20%, the slump flow was reduced to 285 mm, the time to funnel flow increased to 9 s, and the compressive strength decreased to 35 MPa.

Conclusion: The study illustrates brick powder as a promising recycled material for SCM applications not only to reduce environmental impacts but also to improve performance, although optimization of its replacement levels should be taken carefully to balance workability and strength.

Key words: brick powder, self-compacting mortar, cement, workability, artificial neural networks, slump flow, funnel flow time, compressive strength.

Introduction

Self-compacting mortar (SCM) is a type of mortar that can flow and consolidate under its own weight without any added mechanical vibration. This property adds value to SCM while building applications particularly in complex shapes and dense steel reinforced structures where common mortar struggles to fill voids. SCM's ability to achieve uniform placement enhances product quality and durability while improving efficiency and reducing labor costs. These benefits have contributed to the extensive use of SCM in contemporary constructions, especially in precast elements and rehabilitation activities.

The design and selection of self-compacting mortar (SCM) qualities and compositions in practical applications are dependent on various aspects, including workability, strength requirements, and material availability. Workability, characterized by measures such as slump flow, V-funnel flow time, and viscosity, is essential for achieving enough consolidation without external vibration, rendering SCM especially advantageous in highly reinforced structures and complex formwork geometries (Nepomuceno et al., 2012).

The mixture design of SCM generally follows the established approaches such as the EFNARC (European Federation of National Associations Representing Concrete) guidelines, which recommend, for the optimal ratios of cement, supplementary cementitious materials SCMs, fine aggregates, superplasticizers, and viscosity-modifying agents (Ashish and Verma, 2019) (concrete, 2005). A high-flowability supplementary cementitious material (SCM) designed for narrow-section precast elements might require a higher quantity of superplasticizer and a reduced water-to-binder ratio to sustain fluidity and prevent agglomeration (Ghafari et al., 2016). Conversely, a supplementary cementitious material (SCM) designed for structural restoration applications may integrate pozzolanic substances such as fly ash, silica fume, or brick powder to improve durability and long-term strength.

Given the emergence of global urbanization trends, the construction sector is plagued with challenges of sustainability with a keen need for sustainable alternatives. Cement is, however, the third-highest source of CO_2 emissions globally, accounting for nearly 5% of worldwide emissions (Benhelal et al., 2021). Also, extraction of natural aggregates causes many harmful effects on the environment (Pacheco-Torgal et al., 2012).

The search for sustainable alternatives has led to the exploration of waste materials such as brick powder (BP) made from recycled bricks, which minimizes landfill trash and requirements for new raw materials Silva et al., 2016). Typically, BP contains natural silica (SiO_2), alumina (Al_2O_3), and iron oxides that are essential to the pozzolanic activity which enhances strength and durability, making it an attractive choice for SCM (Mansoor et al., 2024).

The use of brick powder waste as supplementary cementitious materials in SCM has been treated in detail by Bouleghebar et al. (2023). The authors proposed substituting cement by weight with 4, 8, 12, 16, and 20% BP, having three levels of Blaine fineness (F1=3300 cm²/g, F2=4400 cm²/g, and F3=6000 cm²/g). The study reported the improvement of the mechanical properties and reduced porosity of mortars in this format, giving them potential in sustainable construction practices and resources conservation.

The study of Si-Ahmed and Kenai (2020) evaluated the effect of utilizing waste BP as a partial replacement for cement in SCMs. It was reported that replacements levels up to 15% of cement had a limited effect on rheology and positively affected long-term compressive strength. However, beyond that percentage, workability was diminished by the increase in water absorption of BP. A slight increase in water absorption by capillarity was reported in this work; this shows a compromise between strength and permeability. This confirms the possibility of using waste BP in SCMs towards sustainability.

Another study carried out by Boukhelkhal and Benabed (2019) assessed the effect of waste brick powder (WBP) as a filler material in self-compacting repair mortar (SCRM) by partially replacing Ordinary Portland Cement (OPC) at substitution levels of 5, 15, and 25%. They found that the incorporation of 5% WBP improved the flowability and stability of mixtures in a fresh state, while at a level of substitution up to 25%, the replacement caused a significant decrease in slump flow. Moreover, in terms of hardened state, the compressive strength decreased by 10.6% at 15% replacement and by 35.3% at 25% replacement levels, highlighting the potential of WBP to produce a new reduced carbon blended cement, which enables reduced carbon emission while achieving environment-friendly sustainability.

The effect of recycled brick powder (RBP) as a partial cement replacement in SCM was the research topic of Irki et al. (2018), who used varying replacement levels (0, 5, 10, 15 and 20%) and three Blaine fineness values (3900, 4300, and 5200 cm^2/g). The results showed that increasing the RBP content led to a decrease in workability, with a 30% reduction observed at more than 20% replacement. However, compressive and splitting tensile strengths improved with higher Blaine fineness and 5% to 10% RBP substitution, attributed to the pozzolanic activity, indicating significant long-term strength gains.

Karatas et al. (2010) analyzed the influence of Elazig region waste brick powder (WBP) on the strength and viscosity properties of SCM. They found that the compressive strength of SCM mixtures made with 5 and 10% WBP exhibited higher compressive strength at early curing ages compared to mixtures without WBP. Beyond this range, the compressive strength of SCM diminished as WBP content increased. Furthermore, the research highlighted that WBP increased cohesion in mortars but decreased its flowability due to the viscous nature of the admixture.

Despite an increasing interest in alternative materials for SCM, there is limited research that examines the use of Artificial Neural Networks (ANNs) to predict the effectiveness of such materials, in the form of BP, on SCM performance. It has been confirmed that ANNs are successful in modeling, solving and understanding complex relationships, particularly in mortar and concrete, as they are heterogeneous materials which makes it difficult to predict their behaviour, using simple analytical methods. However, the use of ANNs to study how BP affects workability, strength and durability of SCM is lacking. Utilizing AAN systems could improve prediction accuracy and optimization according to changed properties of recycled materials as BP, and improving sustainable practices in construction.

The TanH function was chosen for enabling effective gradient flow during backpropagation and convergence stability enhancement (Yan et al., 2022). This activation function is particularly advantageous in modeling construction material properties, as it handles both positive and negative input data, ensuring the model accurately represents the complex interactions in cementitious systems (Sathiparan et al., 2024).

This study's primary goal is to use artificial neural networks (ANNs) to analyze the effects of using BP as an alternative material in SCM. It aims to model the relationship between the amount of BP added and the resulting properties of SCM such as flowability and compressive strength. The study uses neural networks to optimize the mix design of SCM containing BP, ultimately helping to the development of sustainable construction materials and practices. This approach will aid to better understand the performance of BP in SCM while also demonstrating the efficiency of computational tools in cementitious material science.

Methodology

Data collection and preparation

The dataset used in this study was collected to evaluate the influence of BP on the flowability and compressive strength of self-compacting mortar. The key parameters analyzed are:

- Superplasticizer content (%),
- Cement content (Kg/m³),
- Water-to-binder ratio W/B,
- Brick powder (%),
- Sand content (Kg/m³),
- Fineness of brick powder (cm^2/g),
- Dune sand content (Kg/m³), and
- Si/Al/Fe content in BP (%).

The target variables for this study are :

- Slump flow (mm),
- V-funnel flow time (sec), and
- Compressive strength at 28 days (MPa).

The dataset needed to perform this analysis is detailed in the Appendix (Table 1) along with some basic properties of cement and aggregates (Table 2) to enable full documentation and transparency in the study (i.e., the dataset required contains every single detail of all mixtures). It should also be noted that selecting the data was conducted only with mixtures having comparable properties as the same cement types (CEM I) and a superplasticizer of a single type generation were used. This method improves the dataset reliability and the validity of the analysis.

The dataset included some missing values which were addressed through mean imputation. After imputation, the features were scaled using a standard scaler to standardize them to a mean of 0 and a standard deviation of 1. This preprocessing step was essential for the effective operation of the neural network (Aksu et al., 2019).

Model generation

The ANN models used in this study effectively capture the relationships between the key input parameters and the properties of SCM in both its fresh and hardened states. Figure 1 illustrates the ANN structure for predicting the fresh-state properties, namely slump flow (mm) and V-funnel flow time (sec). The inputs to this model include superplasticizer (Sp) content, BP percentage, and BP fineness (cm²/g), all of which significantly influence workability and flowability. These parameters interact through the ANN's hidden nodes to produce accurate predictions for fresh-state performance.

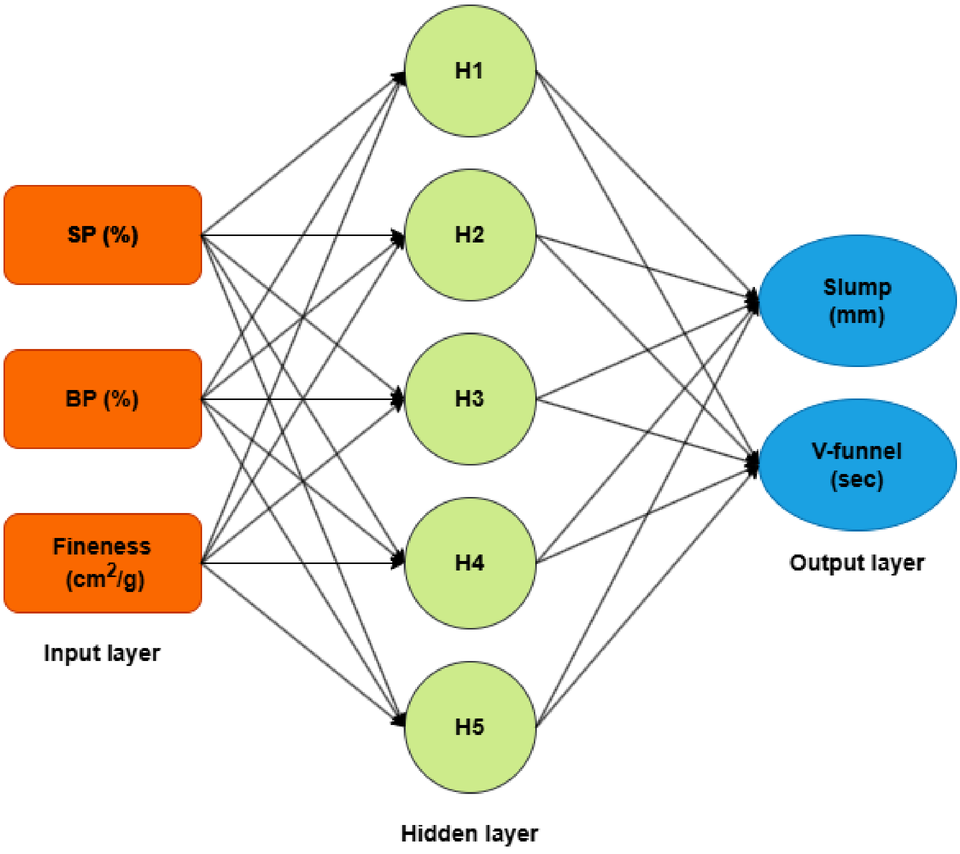

Figure 1 – Schematic diagram of the ANN model for predicting slump flow and V-funnel flow time

On the other hand, the ANN developed for predicting hardened-state properties, specifically compressive strength (MPa), is shown in Figure 2. This model identifies the BP fineness, the Al-Si-Fe composition of brick powder, and the BP percentage as the primary factors affecting strength.

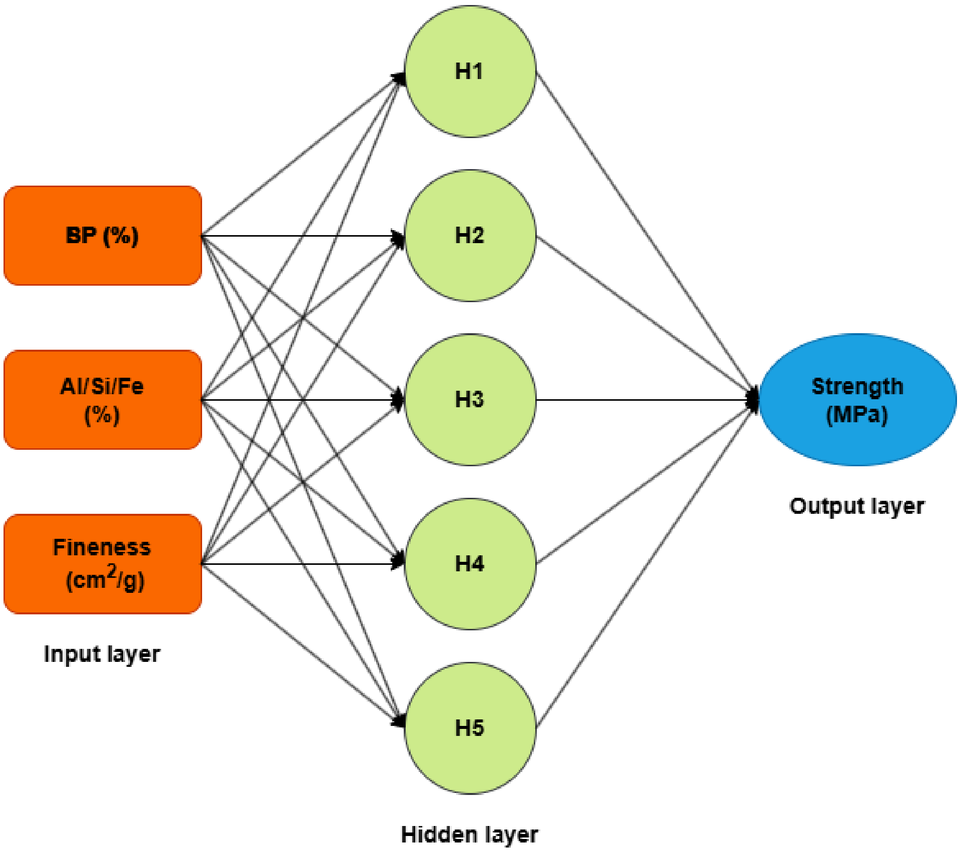

Figure 2 – Schematic diagram of the ANN model for predicting compressive strength

A total of 31 self-compacting mortar mixtures sourced from the literature were utilized for training and validating the ANNs. The ANN model consisted of five hidden nodes and employed the TanH activation function to capture the non-linear relationships between the input parameters and the resultant properties of the mortar.

The dataset was divided into training (80%) and validation (20%) subsets employing a stratified random sampling method to ensure a balanced representation across various BP replacement levels and material characteristics. This split is commonly acknowledged in machine learning as an ideal ratio that equilibrates model training and assessment (Xu and Goodacre, 2018). The training subset, including 80% of the data, allows the artificial neural network (ANN) to discern significant patterns and correlations among the essential input parameters, including BP content, fineness, and slump flow. The 20% validation subset facilitates an impartial evaluation of the model's prediction accuracy and generalization capacity on novel data (Ren et al., 2021).

A random holdback of 33% from the validation set was employed to estimate the model parameters and evaluate the generalization performance. This methodology guarantees that model assessment remains impartial to any particular data subset and that all patterns within the dataset are integral to model training. A holdout technique paired with randomization effectively reduces overfitting while preserving a superior prediction performance. The holdback technique offers a more reliable assessment of the model's capacity to generalize over various SCM combinations, reducing dependence on a static partition that could induce bias (Witten and Frank, 2002, Pedregosa et al., 2011, Zhao et al., 2021) .

Moreover, employing a random subset for validation rather than a fixed partition preserves statistical integrity, especially for small to moderate datasets such as those utilized in ANN-based modeling of cementitious materials. This is especially significant in materials science applications where experimental data is frequently constrained, and the optimization of dataset partitioning is essential for assuring dependable ANN predictions (Zhang et al., 2025, Salama, 2024). Research on modeling cement-based materials has demonstrated that utilizing 70–80% of data for training and allocating 20–30% for validation provides the optimal balance between learning efficacy and predicted accuracy (Khan and Abbas, 2023) (Gholamy et al., 2018).

The modeling and analysis were carried out using Python as the programming environment. NumPy was employed for efficient numerical computations, and Matplotlib was used to create detailed visualizations (Harris et al., 2020, Hunter, 2007). Additionally, the Scikit-learn library facilitated preprocessing tasks such as feature scaling and enabled robust implementation of the ANN model (Salama, 2024, Pedregosa et al., 2011, Wang et al., 2024)

Model performance

The trained ANN model achieved a R^2 score of 0.96 , 0.96 and 0.95 on the training set and 0.99 ,0.98 and 0.84 on the validation set for slum flow ,V-funnel flow time and compressive strength respectively, indicating that the model was able to explain a significant portion of variability in different parameters.

Optimization process and 2D contour plot generation

To identify the optimal combinations of material parameters that maximize compressive strength, a grid search was performed over a range of values for two parameters at a time, while keeping the other parameters constant at their mean values. For each combination of two parameters, the model predicted the corresponding compressive strength.

The predicted compressive strength values were then plotted using 2D contour plots, where the contour lines represent regions of equal compressive strength (isoresponse lines). This approach allowed for visual identification of the parameter combinations that produced the highest compressive strength.

Results and discussion

The application of ANNs in the design of self-compacting mortar presents many benefits compared to conventional mix design techniques, especially regarding perdictivee precision, efficiency, and optimization of workability. Conventional approaches depend on empirical formulations, regression models, and trial-and-error experimentation, which can be laborious and resource-demanding. Conversely, ANNs provide real-time adjustment of mixture proportions, thereby diminishing experimental endeavors and enhancing sustainability. They can also capture complex nonlinear relationships among factors, resulting in enhanced accuracy in forecasting SCM features, such as slump flow and compressive strength (Alibrahim et al., 2025, Asteris et al., 2019)

Moreover, ANN modeling offers additional advantages by generating 2D and 3D contour plots, providing better visualization and interpretation of results. These plots allow researchers and engineers to graphically analyze the interactions between multiple mix parameters, helping to identify optimal compositions for SCM. Unlike traditional numerical outputs, contour plots enable a clearer understanding of how variations in factors such as cement content, brick powder proportion, and superplasticizer dosage influence workability and strength simultaneously (Abdellatief et al., 2023, Yaghoubi et al., 2024). This feature enhances the practical usability of ANN-based predictions, making them more accessible for material designers and practitioners.

Upon completion of training, the ANN model is optimized and fine-tuned by cross-validation and sensitivity analysis to enhance its prediction performance. Ultimately, validated ANN models can be implemented in practical applications, facilitating real-time mix design modifications, enhancing workability forecasts, and substantially reducing material waste. This technique not only optimizes SCM formulation but also improves sustainability by maximizing material utilization (Khan et al., 2023, Meng et al., 2025).

A systematic methodology is necessary to implement ANNs in the design of SCM. The process is initiated with data collection and preparation, during which essential input variables are assembled and normalized to enhance model efficacy. Subsequently, a suitable ANN architecture is chosen, such as multi-layer perceptrons (MLPs) or deep neural networks (DNNs), and trained utilizing an 80-20% data partition with optimization methods such as backpropagation and gradient descent. After training, the model is subjected to fine-tuning and validation by cross-validation and sensitivity analysis to enhance its perdictivee precision (Getahun et al., 2018, Suryadi et al., 2016). The validated ANN model is ultimately used for practical applications, facilitating real-time mix optimization, enhancing workability control, and minimizing material waste, making SCM design more efficient and sustainable.

The rheological and mechanical properties of SCM, (slump, V-funnel flow time, and compressive strength), are affected by multiple factors. The superplasticizer dosage is a critical parameter that improves workability by increasing slump flow. Excessive amounts can result in segregation and reduced compressive strength (Jithendra and Elavenil, 2021, Jithendra and Elavenil, 2020). The water-to-binder ratio is critical, as increased ratios increase flowability but reduce strength, especially in ultra-high-strength concrete (Liu et al., 2022). Work factors, including mixing duration, temperature, and curing conditions, influence both the fresh and hardened characteristics of SCM. Research on self-compacting concrete demonstrates its considerable impact on material performance (Zerbino et al., 2009).

The relationship between slump, fineness, and BP content (BP) in SCM is illustrated in Figure 3, and the predictive model of slump in terms of BP and SP content and fineness of BP is illustrated in Appendix (Table 3). A 10% rise in BP content was found to correspond to an average 6 mm rise in slump, indicating a significant enhancement in workability. Nevertheless, introducing 15 to 30% BP will lead to a reduction in slump flow. Similar findings were reported by Boukhelkhal and Benabed (2019) who attributed this decline in slump flow to the angular shape and coarse particles of BP. Shah et al. (2021) found and declared that the particles of

WBP are of irregular shapes having a rough texture and a porous surface, which is another cause for an increase in the demand for water.

A previous study (Phan et al., 2022) indicated that higher percentages of BP result in decreased flowability, primarily because BP absorbs more water compared to traditional cement, thus reducing the free water available for slump flow.

Karatas et al. (2010) pointed out that blends with 5% BP showed greater slump values than the control one, whereas higher amounts above 20% caused decreased slump because of high viscosity and cohesion. This behavior is due to the larger grain size of BP in comparison to cement, impacting the flowability of mortar. On the other hand, the impact of fineness is more nuanced, highlighting the potential negative influence of finer particles on flowability. Zhao et al. (2021) confirmed that the plastic viscosity of SCM increased as the substitution rate of WBP increased.

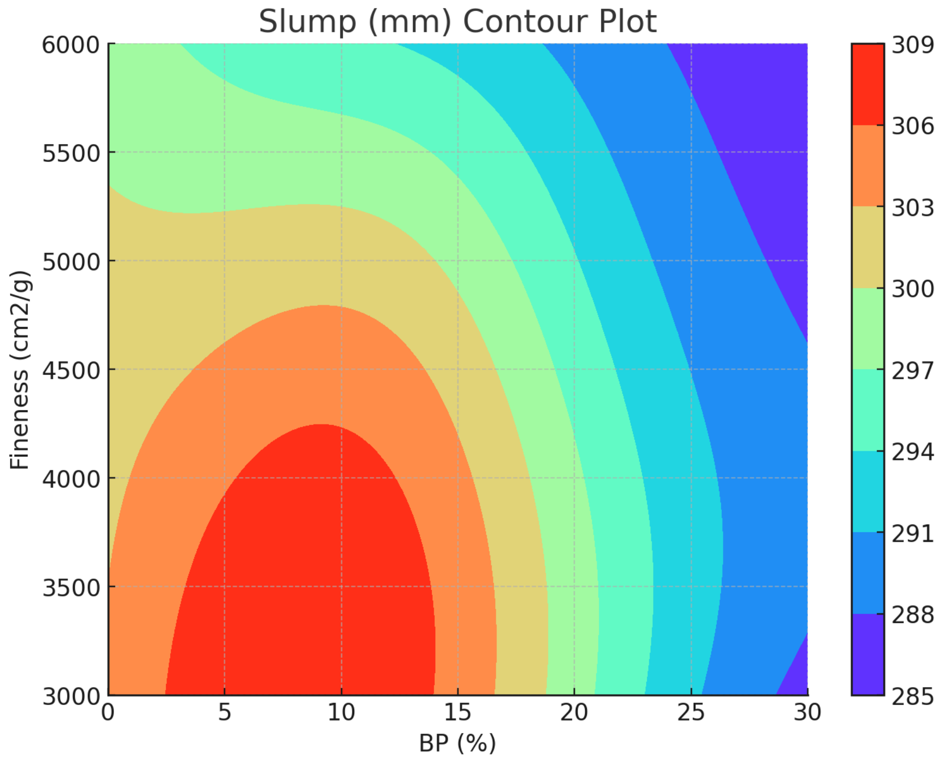

Figure 3 – Effect of fineness and BP content on the slump flow of SCM

Bouleghebar et al. (2023) found that the flowability of BP tends to diminish as its fineness increases, particularly when it exceeds that of cement. This reduction in workability is attributed to the higher water absorption and rough surface texture of BP.

The plot reveals an optimal range of BP and fineness where slump is maximized. The optimal BP content might be between 3% and 14%, while the optimal fineness could range from 3000 to 4200 cm²/g. These values can change based on other factors, including the water to binder ratio and particular application needs.

Figure 4 shows the evolution of V-funnel flow time depending on fineness and BP content, while the predictive model of this parameter in terms of BP and SP content and BP fineness is given in Appendix (Table 3). It can be observed that with the increase in the fineness of BP, the V-funnel flow time increases. For instance, the flow duration varies from 4.2 to 6.0 seconds at a fineness of 3000 cm²/g, but it increases dramatically to 7.8 to 9.0 seconds at 6000 cm²/g. Similarly, the flow time increases with a higher BP content. At 0% BP, the flow time was around 4.2 s; but at 30%, it increases to about 9.0 s. The longest flow times, approximatively 9.0 seconds, are noted when the BP content rises to 30% and the fineness reaches 6000 cm²/g.

In contrast, the flow times are the shortest, approximately 4.2 seconds, when both the fineness and the content of BP were low, for instance, at 3000 cm²/g and between 0-5% of the BP content. This analysis has pointed out that a rise in BP content and fineness results in low flowability, which is manifested by longer flow times when the percentage of BP exceeds 20% and when the degree of fineness is above 5000 cm²/g. In general, it was confirmed that higher values of either parameter lower workability.

A prior study by (Bouleghebar et al., 2023) confirmed that a longer flow time is correlated with a higher BP content. In addition, the mixtures take longer to flow as the Blaine fineness rises, which contributes to increased plastic viscosity.

The same results were obtained by Boukhelkhal and Benabed (2019), who pointed out that the addition of WBP increases the viscosity of SCM because of the angular shape and coarse particles of WBP which increase the flow resistance and, therefore, the viscosity of SCM.

To achieve better flowability, an optimal range is suggested with a BP content between 10% and 15% and a fineness of 3500 cm²/g to 4500 cm²/g. Staying within these parameters keeps the V-funnel flow time relatively low, indicating improved flowability and minimizing flow resistance in the SCM mixture.

Better flowability is indicated in an optimum range where the content of BP varies from 5% to 15% and the fineness in the range of 3500 cm^2/g to 4500 cm^2/g. Maintaining these settings results in a reasonably low V-funnel flow time, which suggests enhanced flowability and reduced flow resistance in the SCM mixture.

Figure 5 shows how the amount of BP with a fineness of 4500 cm^2/g, and its Al-Si-Fe content affects a SCM's compressive strength. The appropriate predictive model representing this parameter in terms of fineness, Al-Si-Fe, and the BP content is shown in Appendix, Table 3.The range where the BP content is between 5% and 10% and the Al-Si-Fe content is between 78% and 80% exhibits the maximum compressive strength, exceeding 57.5 MPa.

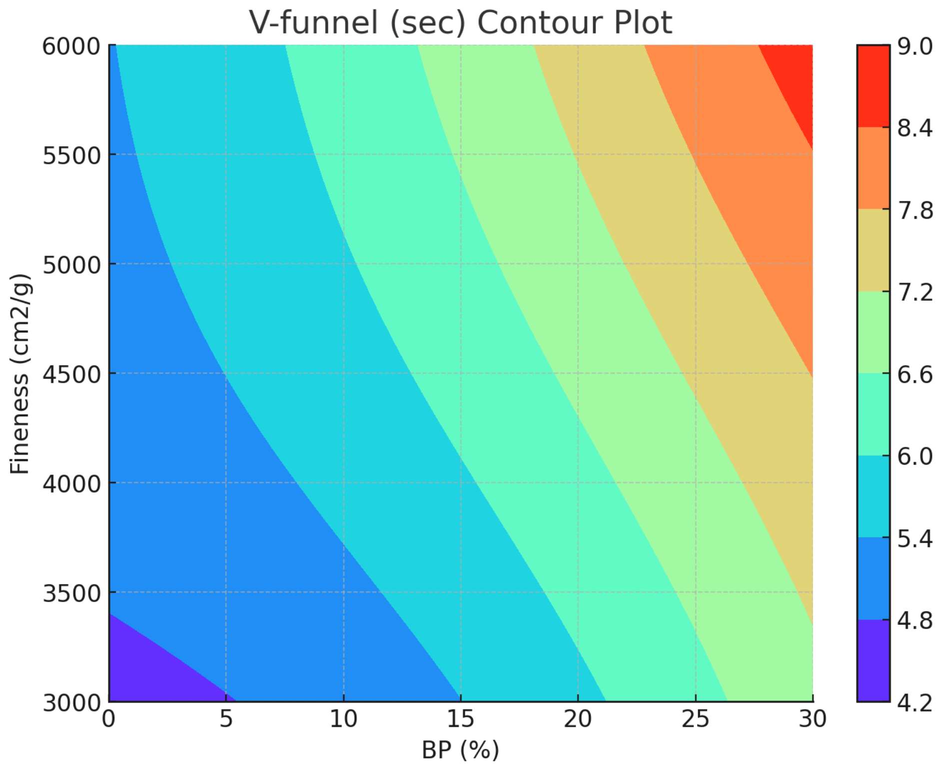

Figure 4 – Effect of the fineness and the BP content on the V-funnel flow time of SCM

Given the minimum requirements established by ASTM C618-15 for pozzolans, where the sum of SiO_2, Al_2O_3, and Fe_2O_3 must be greater than

70%. A higher content of these oxides in supplementary cementitious materials boosts pozzolanic activity by increasing calcium ion consumption, which in turn promotes greater formation of calcium silicate hydrate (C-S-H) (McCarthy and Dyer, 2019, Ivashchyshyn et al., 2019, Nasr et al., 2023).

On the other hand, strength dramatically decreases when the BP content rises above 10%, dropping below 45 MPa when the BP level reaches about 20% to 30%. Furthermore, the Al-Si-Fe composition is important, where its higher levels (78% to 80%) result in increased strength, whereas its lower content (less than 75%) causes a diminution in compressive strength.

According to Bouleghebar et al. (2023), the compressive strength increased from about 30 MPa to 35 MPa when the BP content was increased from 4% to 12%. There are a number of reasons for this improvement. Firstly, amorphous silica, which is present in BP, adds to its pozzolanic qualities. Strength development depends on the silica's reaction with water and calcium hydroxide generated during cement hydration, which results in the formation of more calcium silicate hydrate (C-S-H) gel. Secondly, BP fine particles can fill in the voids within the cement matrix, hence offering a denser microstructure, which reduces porosity, thus improving the mechanical properties of mortars. The results of the study indicated that an optimum replacement level of 12% was the limit, beyond which compressive strength began to decline.

This result is consistent with the findings of Irki et al. (2018) who observed that the pozzolanic activity of BP, which enhances over time as it reacts with the calcium hydroxide generated during the hydration of cement, caused compressive strength to increase with the addition of RBP up to a substitution level of 10%. Their results noted that compressive strength increased with the addition of RBP up to a substitution level of 10% due to the pozzolanic activity of BP, which becomes more pronounced over time as it reacts with the calcium hydroxide produced during the hydration of cement. Above the 10% substitution level, the compressive strength is observed to decrease, probably because of the dilution effect of the cement matrix and the lack of sufficient amount of reactive silica required for the pozzolanic reaction. These findings are confirmed by Nasr et al. (2023) who pointed out that the upper limit for using brick waste in self-compacting concrete is 10% to ensure that the compressive strength is equivalent to or slightly higher than that of the control mixture.

Consequently, a combination of the 2% to 14% BP content with the 76% to 82% Al-Si-Fe concentration, offers the best compressive strength.

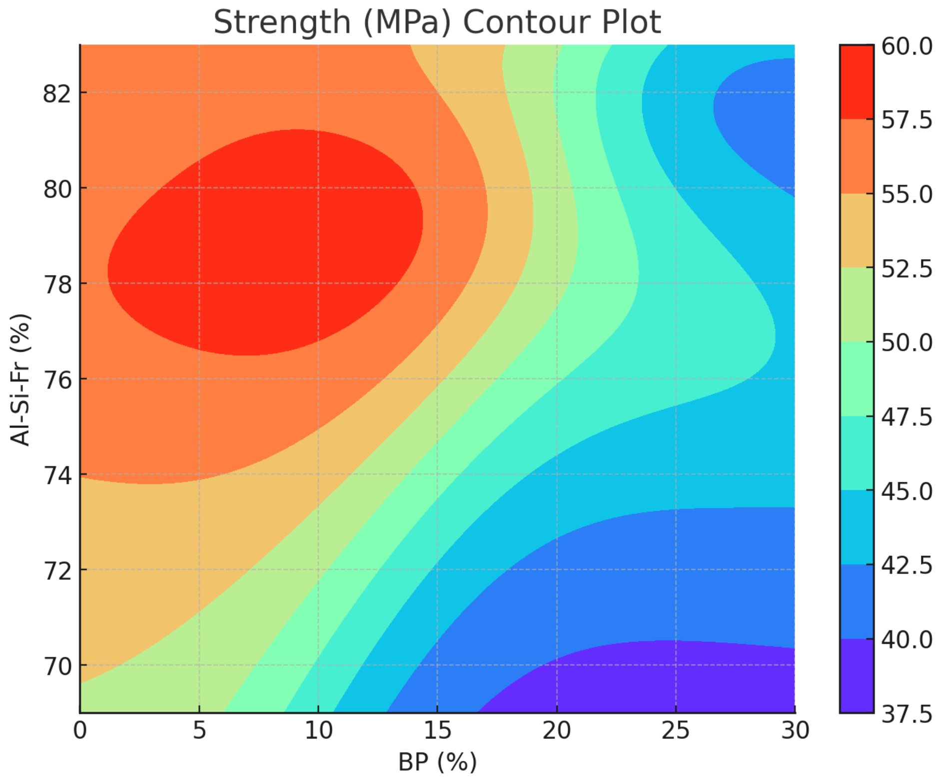

Figure 5– Effect of the Al/Si/Fe content and the BP content with a fineness of 4500 cm²/g on the compressive strength

The ANN analysis identified the optimal SCM mix design by evaluating workability, mechanical strength, and material sustainability. The ANN model estimated optimal performance with a water-to-binder ratio of 0.38, a cement content of 450 kg/m³, a brick powder substitution of 15%, and an optimum Al/Si/Fe value of 0.75. The superplasticizer dosage of 1.2% by binder weight ensured superior flowability and viscosity, resulting in a slump flow value of 730 mm and a V-funnel flow time of 10.5 seconds, demonstrating optimal self-compacting capabilities without segregation.

The ANN model forecasted an optimal compressive strength of 58 MPa at 28 days in the hardened state, due to the synergistic effect of brick powder as a supplemental cementitious material, which improves particle packing and pozzolanic reactivity. The Al/Si/Fr parameter, optimized at 0.75, was important in fine-tuning the mix proportions to attain an optimal equilibrium among workability, strength, and durability. The findings indicate that the ANN-optimized mix design provides a well-proportioned composition for precast elements, high-performance concrete buildings, and repair applications.

Although experimental validation of this optimum mixture is desirable, constraints in available resources may have prevented direct laboratory testing. Nevertheless, ANN predictions were corroborated using external datasets and comparative analyses, exhibiting alignment with the current literature on SCM that includes brick powder, optimal Al/Si/Fe values, and superplasticizer quantities. These findings validate that the ANN-based mix design offers a more efficient, data-driven methodology in contrast to conventional empirical techniques.

Conclusion

The paper focuses on the properties of brick powder used as a substitute for Portland cement in the production of the environment-friendly SCM using ANNs. The following are the major conclusions obtained:

- An optimum range of brick powder content, between 5% and 15%, could be identified where flowability is better; with an increase in the percentage, flowability generally decreases, especially when the replacement is more than 20%, which resulted in longer flowing time and reduced slump.
- There is evidence that an optimal replacement level of brick powder of 2% to 14% enhances the compressive strength; beyond 20%, strength gain started reducing due to a diluted effect.
- Brick powder has pozzolanic properties and tends to react with calcium hydroxide during hydration and forms additional C-S-H, which is responsible for strength development.
- ANNs applied in this work have the capability of modeling mix design efficiently, thus making optimization possible and providing insight into the relationship between material parameters and performance.
- The use of brick powder as a partial replacement for cement provides environmental sustainability due to the use of waste materials, which reduces carbon emissions associated with cement. Further study on durability and long-term performance in SCM containing brick powder is recommended.

References

Abdellatief, M., Elemam, W.E., Alanazi, H. & Tahwia, A.M. 2023. Production and optimization of sustainable cement brick incorporating clay brick wastes using response surface method. *Ceramics International*, 49, pp.9395–9411. Available at: https://doi.org/10.1016/j.ceramint.2022.11.144

Aksu, G., Güzeller, C.O. & Eser, M.T. 2019. The effect of the normalization method used in different sample sizes on the success of artificial neural network model. *International Journal of Assessment Tools in Education*, 6, pp.170–192. Available at: https://doi.org/10.21449/ijate.479404

Alibrahim, B., Habib, A. & Habib, M. 2025. Developing a brain inspired multilobar neural networks architecture for rapidly and accurately estimating concrete compressive strength. *Scientific Reports*, 15, 1989. Available at: https://doi.org/10.1038/s41598-024-84325-z

Asteris, P.G., Apostolopoulou, M., Skentou, A.D. & Moropoulou, A. 2019. Application of artificial neural networks for the prediction of the compressive strength of cement-based mortars. *Computers and Concrete*, 24, pp.329–345. Available at: https://doi.org/10.12989/cac.2019.24.4.329

Benhelal, E., Shamsaei, E. & Rashid, M.I. 2021. Challenges against CO_2 abatement strategies in cement industry: a review. *Journal of Environmental Sciences*, 104, pp.84–101. Available at: https://doi.org/10.1016/j.jes.2020.11.020

Bouleghebar, Y., Bentchikou, M., Boukendakdji, O., El-Hadj, K., Debieb, F. & Maisarah, A. 2023. The effect of brick and glass powder on the mechanical properties and porosity of self-compacting mortar. *Journal of Applied Engineering Sciences*, 13, pp.39–52. Available at: https://doi.org/10.2478/jaes-2023-0006

Boukhelkhal, A. & Benabed, B. 2019. Fresh and hardened properties of self-compacting repair mortar made with a new reduced carbon blended cement. *Építőanyag: Journal of Silicate Based & Composite Materials*, 71. Available at: https://doi.org/10.14382/epitoanyag-jsbcm.2019.19

Getahun, M.A., Shitote, S.M. & Gariy, Z.C.A. 2018. Artificial neural network based modelling approach for strength prediction of concrete incorporating agricultural and construction wastes. *Construction and Building Materials*, 190, pp.517–525. Available at: https://doi.org/10.1016/j.conbuildmat.2018.09.097

Ghafari, E., Ghahari, S.A., Costa, H., Júlio, E., Portugal, A. & Durães, L. 2016. Effect of supplementary cementitious materials on autogenous shrinkage of ultra-high performance concrete. *Construction and Building Materials*, 127, pp.43–48. Available at: https://doi.org/10.1016/j.conbuildmat.2016.09.123

Gholamy, A., Kreinovich, V. & Kosheleva, O. 2018. Why 70/30 or 80/20 relation between training and testing sets: a pedagogical explanation. *International Journal of Intelligent Technologies and Applied Statistics*, 11, pp.105–111. Available at: https://doi.org/10.6148/IJITAS.201806_11(2).0003

Harris, C.R., Millman, K.J., van der Walt, S.J., Gommers, R., Virtanen, P., Cournapeau, D., Wieser, E., Taylor, J., Berg, S. & Smith, N.J. 2020. Array programming with NumPy. *Nature*, 585, pp.357–362. Available at: https://doi.org/10.1038/s41586-020-2649-2

Hunter, J.D. 2007. Matplotlib: a 2D graphics environment. *Computing in Science & Engineering*, 9, pp.90–95. Available at: https://doi.org/10.1109/MCSE.2007.55

Irki, I., Debieb, F., Ouzadid, S., Dilmi, H.L., Settari, C. & Boukhelkhel, D. 2018. Effect of Blaine fineness of recycling brick powder replacing cementitious materials in self-compacting mortar. *Journal of Adhesion Science and Technology*, 32, pp.963–975. Available at: https://doi.org/10.1080/01694243.2017.1393202

Ivashchyshyn, H., Sanytsky, M., Kropyvnytska, T. & Rusyn, B. 2019. Study of low-emission multi-component cements with a high content of supplementary cementitious materials. *Восточно-Европейский журнал передовых технологий*, pp.39–47. (in Russian). Available at: https://doi.org/10.15587/1729-4061.2019.175472

Jithendra, C. & Elavenil, S. 2020. Influences of parameters on slump flow and compressive strength properties of aluminosilicate based flowable geopolymer concrete using Taguchi method. *Silicon*, 12, pp.595–602. Available at: https://doi.org/10.1007/s12633-019-00166-w

Jithendra, C. & Elavenil, S. 2021. Parametric effects on slump and compressive strength properties of geopolymer concrete using Taguchi method. *International Journal of Engineering*, 34(3), 629-635. Available at: https://doi.org/10.5829/ije.2021.34.03c.06

Karatas, M., Turk, K., Acikgenc, M. & Ulucan, Z. 2010. Effect of Elazig region waste brick powder on strength and viscosity properties of self-compacting mortar. *Proceedings of the 9th International Congress on Advances in Civil Engineering*, Trabzon, Turkey, 27–30 September [online]. Available at: https://www.academia.edu/download/71152968/Effect_of_Elazig_Region_Waste_Brick_Powd20211003-16131-1maq0qb.pdf

Khan, A.Q., Awan, H.A., Rasul, M., Siddiqi, Z.A. & Pimanmas, A. 2023. Optimized artificial neural network model for accurate prediction of compressive strength of normal and high strength concrete. *Cleaner Materials*, 10, 100211. Available at: https://doi.org/10.1016/j.clema.2023.100211

Khan, M.I. & Abbas, Y.M. 2023. Intelligent data-driven compressive strength prediction and optimization of reactive powder concrete using multiple ensemble-based machine learning approach. *Construction and Building Materials*, 404, 133148. Available at: https://doi.org/10.1016/j.conbuildmat.2023.133148

Liu, J.-C., Chen, Z., Cai, R. & Ye, H. 2022. Quantitative effects of mixture parameters on alkali-activated binder-based ultra-high strength concrete at ambient and elevated temperatures. *Journal of Advanced Concrete Technology*, 20, pp.1–17. Available at: https://doi.org/10.3151/jact.20.1

Mansoor, S.S., Hama, S.M. & Hamdullah, D.N. 2024. Effectiveness of replacing cement partially with waste brick powder in mortar. *Journal of King Saud University – Engineering Sciences*, 36, pp.524–532. Available at: https://doi.org/10.1016/j.jksues.2022.01.004

McCarthy, M.J. & Dyer, T.D. 2019. Pozzolanas and pozzolanic materials. In: Hewlett, P.C. & Liska, M. eds. *Lea's Chemistry of Cement and Concrete*, 5th ed., pp.363–467. Available at: https://doi.org/10.1016/B978-0-08-100773-0.00009-5

Meng, Q., Xu, H. & He, J. 2025. Using machine learning for sustainable concrete material selection and optimization in building design. *Journal of Computer Technology and Applied Mathematics*, 2, pp.8–14. Available at: https://doi.org/10.70393/6a6374616d.323530

Nasr, M.S., Salman, A.J., Ghayyib, R.J., Shubbar, A., Al-Mamoori, S., Al-Khafaji, Z., Hashim, T.M., Hasan, Z.A. & Sadique, M. 2023. Effect of clay brick waste powder on the fresh and hardened properties of self-compacting concrete: state-of-the-art and life cycle assessment. *Energies*, 16, 4587. Available at: https://doi.org/10.3390/en16124587

Nepomuceno, M., Oliveira, L. & Lopes, S.M.R. 2012. Methodology for mix design of the mortar phase of self-compacting concrete using different mineral additions in binary blends of powders. *Construction and Building Materials*, 26, pp.317–326. Available at: https://doi.org/10.1016/j.conbuildmat.2011.06.027

Pacheco-Torgal, F., Ding, Y., Miraldo, S., Abdollahnejad, Z. & Labrincha, J. 2012. Are geopolymers more suitable than Portland cement to produce high volume recycled aggregates HPC? *Construction and Building Materials*, 36, pp.1048–1052. Available at: https://doi.org/10.1016/j.conbuildmat.2012.07.004

Pedregosa, F., Varoquaux, G., Gramfort, A., Michel, V., Thirion, B., Grisel, O., Blondel, M., Prettenhofer, P., Weiss, R. & Dubourg, V. 2011. Scikit-learn: machine learning in Python. *The Journal of Machine Learning Research*, 12, pp.2825–2830. Available at: https://doi.org/10.48550/arXiv.1201.0490

Phan, N.-L., Vo, D.-H., Ngo, T.-M. & Nguyen, H.-A. 2022. Effect of waste red brick powder on fresh properties and strength development of cement paste. *Proceedings of the 7th National Scientific Conference on Applying New Technology in Green Buildings (ATiGB)*, IEEE, pp.79–82. Available at: https://doi.org/10.1109/ATiGB56486.2022.9984114

Ren, Q., Ding, L., Dai, X., Jiang, Z. & De Schutter, G. 2021. Prediction of compressive strength of concrete with manufactured sand by ensemble classification and regression tree method. *Journal of Materials in Civil Engineering*, 33, 04021135. Available at: https://doi.org/10.1061/(ASCE)MT.1943-5533.0003741

Salama, M. 2024. Optimization of regression models using machine learning: a comprehensive study with Scikit-learn. *IUSRJ*, 5. Available at: https://doi.org/10.59271/s45500.024.0624.16

Sathiparan, N., Jeyananthan, P. & Subramaniam, D.N. 2024. Quantifying the impact of chemical composition on pervious concrete strength: a comparative analysis using full quadratic model and artificial neural network. *International Journal of Pavement Engineering*, 25, 2424381. Available at: https://doi.org/10.1080/10298436.2024.2424381

Shah, M. U., Usman, M., Hanif, M. U., Naseem, I., & Farooq, S. 2021. Utilization of solid waste from brick industry and hydrated lime in self-compacting cement pastes. *Materials*, 14(5), 1109. Available at: https://doi.org/10.3390/ma14051109

Si-Ahmed, M. & Kenai, S. 2020. Behavior of self-compacting mortars based on waste brick powder. *Current Materials Science (Formerly: Recent Patents on Materials Science)*, 13, pp.39–44. Available at: https://doi.org/10.2174/2666145413666200219091459

Silva, R., de Brito, J. & Dhir, R. 2016. Performance of cementitious renderings and masonry mortars containing recycled aggregates from construction and demolition wastes. *Construction and Building Materials*, 105, pp.400–415. Available at: https://doi.org/10.1016/j.conbuildmat.2015.12.171

Suryadi, A., Qomariah, Q. & Sarosa, M. 2016. An artificial neural networks model for compressive strength of self-compacting concrete. *Applied Mechanics and Materials*, 845, pp.226–230. Available at: https://doi.org/10.4028/www.scientific.net/AMM.845.226

Wang, X., Ma, Z., Wang, X., Xue, S., Shen, W., Wu, D., Zhang, X., Han, Z., Sui, S. & Wang, M. 2024. Design of self-compacting ultra-high performance concrete (SCUHPC) towards to the cementitious materials packing optimization. *Cement and Concrete Composites*, 148, 105443. Available at: https://doi.org/10.1016/j.cemconcomp.2024.105443

Witten, I.H. & Frank, E. 2002. Data mining: practical machine learning tools and techniques with Java implementations. *ACM SIGMOD Record*, 31, pp.76–77. Available at: https://doi.org/10.1145/507338.507355

Xu, Y. & Goodacre, R. 2018. On splitting training and validation set: a comparative study of cross-validation, bootstrap and systematic sampling for estimating the generalization performance of supervised learning. *Journal of Analysis and Testing*, 2, pp.249–262. Available at: https://doi.org/10.1007/s41664-018-0068-2

Yaghoubi, E., Khamees, A. & Vakili, A.H. 2024. A systematic review and meta-analysis of artificial neural network, machine learning, deep learning, and ensemble learning approaches in field of geotechnical engineering. *Neural Computing and Applications*, 36, pp.12655–12699. Available at: https://doi.org/10.1007/s00521-024-09893-7

Yan, B., Harp, D.R., Chen, B., Hoteit, H. & Pawar, R.J. 2022. A gradient-based deep neural network model for simulating multiphase flow in porous media. *Journal of Computational Physics*, 463, 111277. Available at: https://doi.org/10.1016/j.jcp.2022.111277

Zerbino, R., Barragán, B., Garcia, T., Agulló, L. & Gettu, R. 2009. Workability tests and rheological parameters in self-compacting concrete. *Materials and Structures*, 42, pp.947–960. Available at: https://doi.org/10.1617/s11527-008-9434-2

Zhang, Y., Cui, S., Yang, B., Wang, X. & Liu, T. 2025. Research on 3D printing concrete mechanical properties prediction model based on machine learning. *Case Studies in Construction Materials*, 22, e04254. Available at: https://doi.org/10.1016/j.cscm.2025.e04254

Zhao, Z., Grellier, A., Bouarroudj, M.E.K., Michel, F., Bulteel, D. & Courard, L. 2021. Substitution of limestone filler by waste brick powder in self-compacting mortars: properties and durability. *Journal of Building Engineering*, 43, 102898. Available at: https://doi.org/10.1016/j.jobe.2021.102898

Análisis predictivo de mortero autocompactante mejorado con polvo de ladrillo mediante redes neuronales artificiales

Zine El Abidine Laidani[a], **autor de correspondencia**, *Mohamed* Sahraoui[b], *Younes* Ouldkhaoua[c], *Benchaa* Benabed[d], *Mohamed El Ghazali* Belgacem[c]

[a] Universidad Blida1, Departamento de Ingeniería Civil, Blida, República Argelina Democrática y Popular,
[b] Universidad Blida1, Instituto de Arquitectura y Urbanismo, Blida, República Argelina Democrática y Popular,
[c] Universidad de Ciencia y Tecnología – Houari Boumediene, Facultad de Ingeniería Civil, Laboratorio de Construcción en Medio Ambiente, Argel, República Argelina Democrática y Popular,
[d] Universidad de Amar Telidji, Departamento de Ingeniería Civil, Laboratorio de Investigación de Ingeniería Civil, Laghouat, República Argelina Democrática y Popular,

CAMPO: ingeniería civil, materiales, aprendizaje profundo
TIPO DE ARTÍCULO: artículo científico original

Resumen:

Introducción/Propósito: Los morteros autocompactantes poseen una excelente fluidez, lo que les permite consolidarse únicamente mediante la fuerza de su propio peso, sin requerir vibración mecánica. Este tipo de morteros es de gran utilidad en obras complejas de construcción y reparación. En este trabajo, se investigará el uso de polvo de ladrillo como sustituto del cemento en SCM, con un estudio detallado de sus efectos sobre la trabajabilidad, la resistencia a la compresión y otras características de rendimiento.
Métodos: La investigación propuesta modela las relaciones de diferentes parámetros, contenido de polvo de ladrillo y finura, con las propiedades resultantes del mortero utilizando modelos de redes neuronales artificiales (ANN).
Resultados: Los resultados mostraron que la adición de polvo de ladrillo hasta un 10% de cemento como reemplazo mejora la trabajabilidad del mortero, alcanzando un caudal de asentamiento de 306 a 309 mm y un tiempo de embudo de 4,8 a 5,4 s, mientras que su resistencia a la compresión se situó entre 45 y 60 MPa a los 28 días. Sin embargo, con niveles de reemplazo superiores al 20%, el caudal de asentamiento se redujo a 285 mm, el tiempo de embudo aumentó a 9 s y la resistencia a la compresión disminuyó a 35 MPa.

Conclusión: El estudio ilustra al polvo de ladrillo como un material reciclado prometedor para aplicaciones de SCM no sólo para reducir los impactos ambientales sino también para mejorar el rendimiento, aunque la optimización de sus niveles de reemplazo debe tomarse con cuidado para equilibrar la trabajabilidad y la resistencia.

Palabras claves: polvo de ladrillo, mortero autocompactante, cemento, trabajabilidad, redes neuronales artificiales, flujo de asentamiento, tiempo de flujo en embudo, resistencia a la compresión.

Прогнозный анализ самоуплотняющегося раствора, укрепленного кирпичным порошком, с использованием искусственных нейронных сетей

Зин Эль Абидин Лайдани[а], **корреспондент**, *Мохамед* Сахрауи[б], *Юнес* Ульдкауа[в], *Бенчаа* Бенабед[г], *Мохамед Эль Газали* Бельгазем[в]

[а] Университет Блида1, кафедра гражданского строительства, Блида, Алжирская Народная Демократическая Республика
[б] Университет Блида1, Институт архитектуры и урбанизма, Блида, Алжирская Народная Демократическая Республика
[в] Университет науки и технологий — Хоари Бумедиен, факультет гражданского строительства, лаборатория строительства в окружающей среде, Алжир, Алжирская Народная Демократическая Республика
[г] Университет Амар Телиджи, кафедра гражданского строительства, лаборатория исследований в области гражданского строительства, Лагуат, Алжирская Народная Демократическая Республика

РУБРИКА ГРНТИ: 67.09.33 Бетоны. Строительные растворы, смеси, составы
ВИД СТАТЬИ: оригинальная статья

Резюме:

Введение/Цель: Самоуплотняющийся раствор — это специальный раствор, который обладает текучестью, достаточной для соединения за счет собственного веса без необходимости в механической вибрации. Благодаря этим свойствам он незаменим в сложных строительных работах и ремонтах. В данной статье проведено исследование использования кирпичного порошка в качестве замены цемента в самоуплотняющихся растворах (SCM). В статье внимательно изучено влияние на обрабатываемость, прочность на сжатие и другие характеристики.

Методы: В данном исследовании моделируется соотношение различных параметров содержания кирпичного порошка и его размельченности с эффективными свойствами раствора. используя модели искусственных нейронных сетей (ANN).

Результаты: Результаты показали, что добавление кирпичного порошка, заменяемого до 10% цемента, улучшает обрабатываемость, обеспечивая оседание (slump flow) в пределах от 306 до 309 мм и время прохода через воронку от 4.8 до 5.4 секунд. Причем прочность на сжатие через 28 дней варьируется от 45 до 60 МПа. Однако при более высоких уровнях замены более 20% оседание снизилось до 285 мм, время прохода через воронку увеличилось до 9 секунд, а прочность на сжатие уменьшилась до 35 МПа.

Выводы: Исследование показало, что кирпичный порошок как переработанный материал в SCM перспективен не только для снижения воздействия на окружающую среду, но и для улучшения характеристик. Однако надо учитывать точную оптимизацию уровня замены с целью достижения баланса между обрабатываемостью и прочностью.

Ключевые слова: Кирпичный порошок, самоуплотняющийся раствор, цемент, обрабатываемость, искусственные нейронные сети, оседание, время прохода через воронку, прочность на сжатие.

Коришћење вештачких неуронских мрежа у предиктивној анализи самозбијајућег малтера ојачаног цигленим прахом

Зин Ел Албидин Лајдани [а], ***аутор за преписку***, *Мухамед* Сахрауи [б], *Јунц* Олдау [в], *Бенча Бенабед* [г], *Мухамед Ел Газали* Белкасем [в]

[а] *Универзитет Блида1, Одељење за грађевинско инжењерство, Блида, Народна Демократска Република Алжир*

[б] *Универзитет Блида1, Институт за архитектуру и урбанизам, Блида, Народна Демократска Република Алжир*

[в] *Универзитет науке и технологије „Хуари Бумедијен”, Факултет за грађевинско инжењерство, Лабораторија заградњу у животној средини, Народна Демократска Република Алжир*

[г] *Универзитет „Амар Телиђи”, Одељење за грађевинско инжењерство, Лабораторија за истраживање грађевинског инжењерства, Лагуат, Народна Демократска Република Алжир*

ОБЛАСТ: грађевинарство, материјали
КАТЕГОРИЈА (ТИП) ЧЛАНКА: оригинални научни рад

Сажетак:

Увод/циљ: Самозбијајући малтери (SCM) поседују веома добру способност течења што им омогућава да се консолидују само под дејством сопствене тежине, без потребе за механичким вибрацијама. Ова врста малтера веома је значајна код сложених структура и радова на репарацији. У овом раду се истражује коришћење прашкастих честица цигле уместо цемента у SCM и детаљно проучавају ефекти на обрадивост, чврстоћу на притисак и све друге перформансе.

Методе: Предложено истраживање моделује однос различитих параметара, садржаја цигленог праха, као и његове финоће, са резултујућим својствима малтера уз помоћ модела вештачких неуронских мрежа.

Резултати: Резултати су показали да је коришћење цигленог праха уместо до 10% цемента побољшало обрадивост тако што је постигнуто слегање распростирањем (slump flow) од 306 до 309 мм и време течења кроз левак (funnel flow time) између 4,8 и 5,4 с, при чему је чврстоћа на притисак била у опсегу од 45 до 60 MPa након 28 дана. Међутим, при заменама већим од 20%, слегање распростирањем се смањило на 285 мм, време течења кроз левак се повећало на 9 с, а чврстоћа на притисак је опала на 35 MPa.

Закључак: Студија указује да циглени прах, као рециклирани материјал, има перспективу у применама SCM не само ради смањивања утицаја на животну средину него и ради побољшавања перформанси, иако је потребно пажљиво вршити оптимизацију нивоа замене како би се постигла равнотежа обрадивости и чврстоће.

Кључне речи: циглени прах, самозбијајући малтер, цемент, обрадивост, вештачке неуронске мреже, слегање распростирањем (slump flow), време протока кроз левак (funnel flow time), чврстоћа на притисак.

Paper received on: 03.01.2025
Manuscript corrections submitted on:01.04.2025.
Paper accepted for publishing on: 04.04.2025.

Removal of basic textile dyes from water by natural and modified Algerian zeolite: kinetic, thermodynamic and equilibrium studies

Nassima Belgaid[a], *Mohamed Redha* Menani[b], *Kamel Eddine* Bouhidel[c]

[a] University of Batna 2, Laboratory of Mobilisation and Water Ressources Management (MGRE), Institute of Earth Sciences and Universe, 53, road of Constantine, Fesdis, Batna 05078, Republic of Algeria.
e-mail: n.belgaid@univ-batna2.dz, **corresponding author**,
ORCiD: https://orcid.org/0009-0008-3508-540X

[b] University of Batna 1, Laboratory of Chemistry and Environmental Chemistry (LCCE), Department of Chemistry, Faculty of Matter Sciences, road of Biskra, Batna 05000, Republic of Algeria
e-mail: redha.menani@univ-batna2.dz
ORCiD: https://orcid.org/0000-0001-7261-9417

[c] University of Batna 1, Laboratory of Chemistry and Environmental Chemistry (LCCE), Department of Chemistry, Faculty of Matter Sciences, road of Biskra, Batna 05000, Republic of Algeria
e-mail: ke.bouhidel@gmail.com
ORCiD: https://orcid.org/0009-0004-1956-7733

doi https://doi.org/10.5937/vojtehg73-56126

FIELD: chemical technologies
ARTICLE TYPE: original scientific paper

Abstract:

Introduction/purpose: Algerian natural zeolite (denoted NZ) was modified using hydrochloric acid (HZ) and sodium hydroxide solution (NaZ). This study investigated the impact of acid and alkaline modifications on the adsorption of two cationic textile dyes (BR_{46} and BY_{13}) from aqueous solutions.

Methods: The XRF analysis confirmed that SiO2 is the predominant mineral in all three zeolites. The XRD results revealed that NZ is primarily composed of mordenite, with chabazite and minor quartz content. The MEB-EDX analysis showed slight variations in the Si and Al content for HZ and NaZ, without significantly altering the zeolite's structure.. The effects of initial dye concentration, contact time and pH were examined in a batch system.

ACKNOWLEDGMENT: We gratefully acknowledge the textile industry (COTITEX Ain Djasser, Batna, Algeria) for kindly providing us with cationic textile dyes (BR_{46} and BY_{13}).

Results: The adsorption on NZ, NaZ and HZ increased with longer contact times, higher initial dye concentrations, and elevated temperatures. Equilibrium was rapidly attained best described using the pseudo-second-order kinetic model. Both the Langmuir and the Freundlich isotherm models fit for the adsorption data.

Conclusion: The highest dye removal efficiency was observed for NaZ, with 97.62% for BR_{46} and 98.97% for BY_{13}. The lowest removal rates occurred at pH= 8 for HZ and pH=10 for NZ and NaZ. Adsorption was spontaneous and endothermic.

Keywords: zeolite, modification, acid, alkaline, adsorption, cationic dyes

Introduction

Dyes used in paper, plastics, food, cosmetics and textile industries are among the most prevalent organic micropollutants in water. Many of these dyes are toxic and have a severe environmental impact, as they block light penetration, inhibit photosynthesis, reduce dissolved oxygen levels, hinder plant growth, enter the food chain, and bioaccumulate (Lellis et al, 2019, Aarden, 2001). Additionally, many dyes are carcinogenic. Their high solubility, chemical stability, and resistance to light and heat make their removal through conventional methods challenging. Various physical and chemical techniques are used to remove dyes from industrial effluents, including coagulation (Li et al, 2016), biological treatments (Aravindhan et al, 2023), flotation, oxidation, and adsorption. Among these, adsorption is the most widely used due to its high efficiency, low material cost, simple design and operation, and the abundance and non-toxicity of materials like: activated carbon (Kumar et al, 2023), silica gel, bentonite (Selim et al, 2014), kaolinite (Ighnih et al, 2023), and zeolite (Senguttuvan et al, 2022) .

Zeolites are microporous hydrated aluminosilicates with a three-dimensional framework that carries a negative charge balanced by exchangeable cations, primarily Na^+, Ca^{2+} and K^+. Naturally occuring in zeolitic-rich rocks, zeolites exist in various forms, including clinoptilolite, heulandite, faujasite, mordenite, chabazite, analcime, etc. They can also be synthesized in laboratories into other forms such as zeolite A, zeolite Y, and zeolite P (Reeve and Fallowfield, 2018). Although synthetic zeolites are valued for their high purity, large surface area, and considerable porosity, their production requires expensive raw marterials, complex synthesis processes, and time-consuming steps. Consequently, recent research has focused on enhancing the properties of natural zeolites such as exchange capacity, and a specific surface area through various modificaton methods, including acid activation (Pastukhov et al, 2023), alkaline activation (Ates and Akgül, 2016), iron oxide modification and organic modification (Wang et al, 2023), and surfactant modification (Ebsa, 2023). The effectiveness of modifications depends not only on the target pollutant but also on the desired properties, environmental impact (toxicity), and cost considerations (expenses and duration). Therefore, a comprehensive understanding of the caracteristics, structure, morphology, and interractions of zeolites is essential, providing valuable insights for future studies.

Zeolites have a broad range of applications, from agriculture and wastewater treatment to petroleum refining, where they serve as adsorbents, molecular sieves, and ion–exchange agents (Visa, 2016).

Mordenite, first discovered in 1864 in Nova Scotia, Canada, and named after the small community of Morden, is a zeolite mineral with the molecular formula (Na^{+}_{8}) $[(AlO_2)_8(SiO_2)_{40}].24H_2O$. The Si/Al ratio in natural mordenite samples varries from 4 to 6, with higher ratios correlating to greater thermal and chemical stability (Nakamoto et al, 2017, Mamo et al, 2015). In Algeria, mordenite-type zeolite is particulary predominant in the northeast region (Mehdi et al, 2022). While its primary application has been in cement activities, only a few studies have explored its potential for removing heavy metals (Mehdi et al, 2022) and dyes (Imessaoudene et al, 2024) from water. The modification of natural zeolites using acid and alkaline solutions significantly impact their composition, morphology and porosity. These treatments facilitate the removal of silicon and aluminum from the zeolite framework, altering the SiO_2/Al_2O_3 ratio and influencing their adsorption properties, leading to the modification of external and internal surface properties (Garcia-Basabe et al, 2010).

In this work, our main objective is to improve properties of natural mordenite such as exchange capacity, specific surface and porosity via treatment with HCl and NaOH solutions without altering the main structure. This is verified by studying the adsorption capacity of two cationic textile dyes by natural and modified mordenite. The effects of contact time, initial dye concentration, pH, and temperature were aslo studied.

Materials and methods

Natural zeolite was obtained from a Tuf deposit in Tinedbar, located in Bejaia, northeast of Algeria. The bulk sample was crushed into smaller particles of varying sizes and subsequently sieved using a column sieve to obtain clay particles with a diameter of<63µm. The processed zeolite was stored in a polyethylene container for further use and designated as NZ.

The following chemicals were used in the study: sodium hydroxide (NaOH,40g/mol, 99%), sulphuric acid (H_2SO_4, 98.08g/mol, 95-97%, d=1.83), hydrochloride acid (HCl,36.5g/mol, 37%, d= 1.18), sodium chloride (NaCl, 58.44 g/mol, 99.5%), and nitric acid (HNO_3, 63.01 g/mol, 69%, d=1.410). All reagents were obtained from Sigma-Aldrish, VWR Prolabo Chemicals, and Fluka Chemicals. Distilled water was used to prepare all solutions.

The textile dye Basic Red 56 (BR_{56} , $C_{18}H_{21}BrN_6$, 401.3 g.mol^{-1}) and Basic Yellow 13 (BY_{13}, $C_{20}H_{23}ClN_2O$, 342.86 g.mol^{-1}, pK_a =10.35) (Figure 1) were supplied from a textile industry plant located in Ain Djasser, Batna, in the eastern region of Algeria. Both dyes are cationic, water-soluble, and commonly used for dyeing acrylic fibers and textile printing.

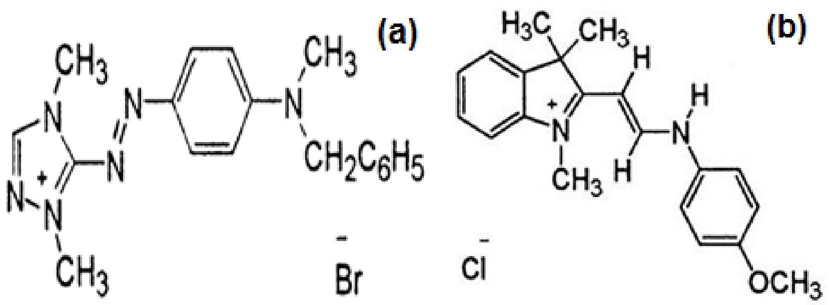

Figure1 – Structure of cationic dyes:(a) Red dye (BR56), and (b)Yellow dye (BY13)

Preparation of adsorbents

A bulk sample of natural zeolite was ground into small particles using an industrial crusher. The crushed material was then passed through a series of sieves with diameters ranging from 1 mm to 63 µm (from 15 to 236 mesh). Zeolite particles with a diameter of <73 µm were collected, stored in bottles, and designated as NZ.

Alkaline modification:

The activation of natural zeolite using an alkaline treatment was conducted as follows:

A measured mass of natural zeolite was mixed with a specific volume of sodium hydroxide solution (500 mol/m^3) at a 2:1 volume-to-mass ratio. The mixture was stirred continuously for six hours while maintaining a temperature of 343 K. The resulting slurry was then washed several times with deionized water, filtred, dried, and sieved to 63 µm before being stored in bottles and labeled as NaZ.

Acid Activation:

The acid activation of zeolite was carried out using the following procedure:

A 5×10^{-4} m^3 reactor equipped with a reflux condenser, a magnetic stirrer, and a thermometer was used. A specified amount of natural zeolite was mixed with a hydrocloridric acid solution (500 mol/m^3) and added to the reactor. The mixture was heated under reflux at 90 °C and agitated for two hours, maintaining a constant temperature throughout the process. The clay was then filtered and repeatedly washed with deionized water until no residual acid was detected (i.e., no white precipitate appeared after the addition of barium chloride). The clay was dried at 110 °C, crushed, sieved to 63 µm, and stored in a bottle, labeled as HZ.

Results and discussion

Characterisation of adsorbents

The chemical composion of the samples was determined using X ray fluorescence (XRF). The X-ray diffraction patterns were rfomed on a diffractometer (Rigaku Miniflex II desktopX-ray diffractometer) with Cu(K_α) radiation, operated at a voltage of 40 kV and a current of 40 mA. The samples were scanned over a 2θ range from 2° to 60° at a scanning rate of 5 deg/min.The morphology of both natural and modified zeolites was analyzed using a scanning electron microscope (SEM, JEOL, JSM-6400). Additionally, FTIR spectra were recorded within the wavenumber range of 500-4000 cm^{-1} using a JASCO spectrophotometer.

Point of zero charge (PZC)

The point of zero charge (PZC) for the three zeolites (NZ, NaZ, and HZ) was determined by mixing a series of 5×10^{-5} m^3 NaCl solutions (5 mol/m^3) with the initial pH values ranging from 3 to 10 by adding 100 mol/m^3 of HNO_3 or NaOH before adding 0.05 g of zeolite. The mixture was stired for 48 hours, after which the final pH was measured. The pH variation ($\Delta pH = pH_f - pH_i$) was plotted against the initial pH.

The PCZ was identified as the intersection point of the curve where $\Delta pH=0$. According to the plot shown in Figure 2, the PZC values for NZ, NaZ, and HZ were determined to be 9.292, 9.71 and 7.25, respectively.

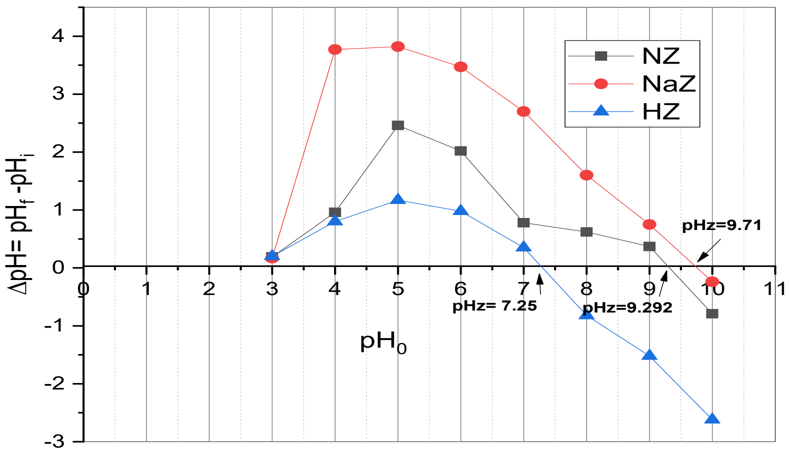

Figure 2 – Zero point of charge value for natural (NZ) and activated zeolites (NaZ and HZ)

X-ray fluoerescence (XRF)

Table 1 shows that SiO_2 is the predominant mineral in all zeolites, followed by Al_2O_3, Fe_2O_3, CaO, K_2O, and other oxides. The Si/Al ratio of NZ indicates that it belongs to the mordenite type (3 < Si/Al < 5). For the two modified zeolites (NaZ and HZ), a slight change in the ratio is observed, although the mordenite structure remains unchanged. The decrease in the silica content for NaZ is attributed to its removal by sodium hydroxide, whereas the decrease in the aluminum content for HZ is due to its removal by hydrochloric acid.

Table 1 – Chemical composition of natural zeolite (NZ), modified zeolites with 100 mol/m³ of NaOH (NaZ) and 100 mol/m³ of HCl (HZ)

	SiO_2	Al_2O_3	Fe_2O_3	CaO	MgO	Na_2O	K_2O	Cl	SO_3
NZ	60.43	16.01	6.57	4.42	0.88	2.41	3.55	0.015	0.025
NaZ	55.94	17.31	6.11	2.96	0.66	6.78	6.38	/	/
HZ	58.17	13.62	6.03	5.58	0.79	2.31	3.05	/	/

X-ray diffraction (XRD)

The X-ray spectra of natural zeolite and treated zeolites (NaZ and HZ) (Figure 3) indicate that mordenite is the major component of NZ, followed by chabazite and minor amounts of quartz.

A comparison of the three diffractograms reveals a shift in the peaks and a reduction in the intensity of some peaks corresponding to impurities. Additionally, an increase in the intensity of the peaks related to mordenite and chabazite was observed, demonstrating the effectiveness of acid and alkali treatments.

Furthermore, a decrease in the intensity of quartz peaks was observed for NaZ, which is attributed to the removal of Si from the framework by acid. Based on the previous studies, NZ mainly contains mordenite ($(Ca, Na_2, K_2)Al_2Si_{10}O_{24}\cdot 7H_2O$), chabazite ($Ca_2Al_2Si_4O_{12}. 6H_2O$), and quartz ($SiO_2$).

The reduction in the HZ peak intensities was mainly caused by the decrease in crystalinity and/or the crystal size of the mordenite framework. This explains why the mordenite structure remained intact and protected after the treatment process.

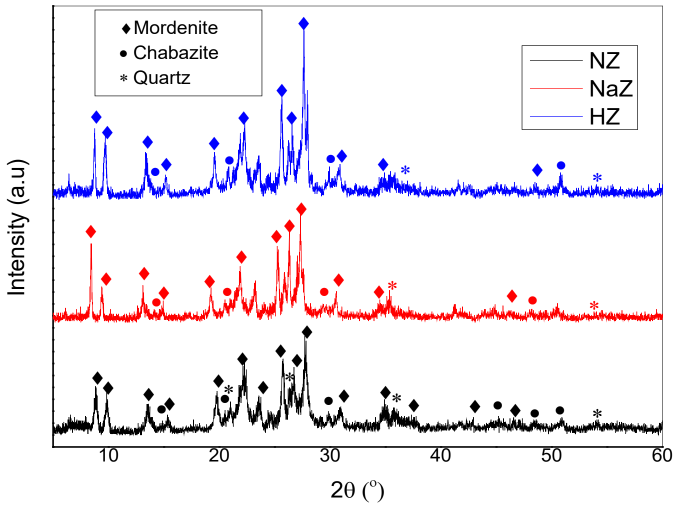

Figure 3 – XRD patterns for NZ,NaZ and HZ

Scanning electron microscopy (SEM/EDX)

The SEM images are presented in Figures 4a, 4c, and 4e. Figure 4c reveals that NaZ exhibits a slightly rougher surface and particle irregularity, mainly due to severe crystal de-agglomeration of the zeolite. In contrast, Figure 4e of HZ particles shows the presence of ultrafine/nanoscale entities surrounding larger particles.

The EDX results presented in Figure 4b, 4d, and 4f indicate changes in the chemical composition of NaZ and HZ compared to that of NZ. A slight decrease in Si and Al percentage and an increase in Na and Ca percentage are observed for NaZ and HZ. Additionally, a significant decrease in the K content was noted in NaZ compared to NZ and HZ, probably due to ion exchange of K ions with Na ions.

The Si/Al ratio in HZ increases due to aluminum removal, while it decreases for NaZ due to the removal of Si. The oxygen content in all three zeolites is higher, probably because either all cations are present in their oxide form or part of the oxygen comes from water molecules and hydronium ions adsorbed on the surface. These findings are consistent with previous results reported by Lycourghiotis et al.(Lycourghiotis et al, 2018).

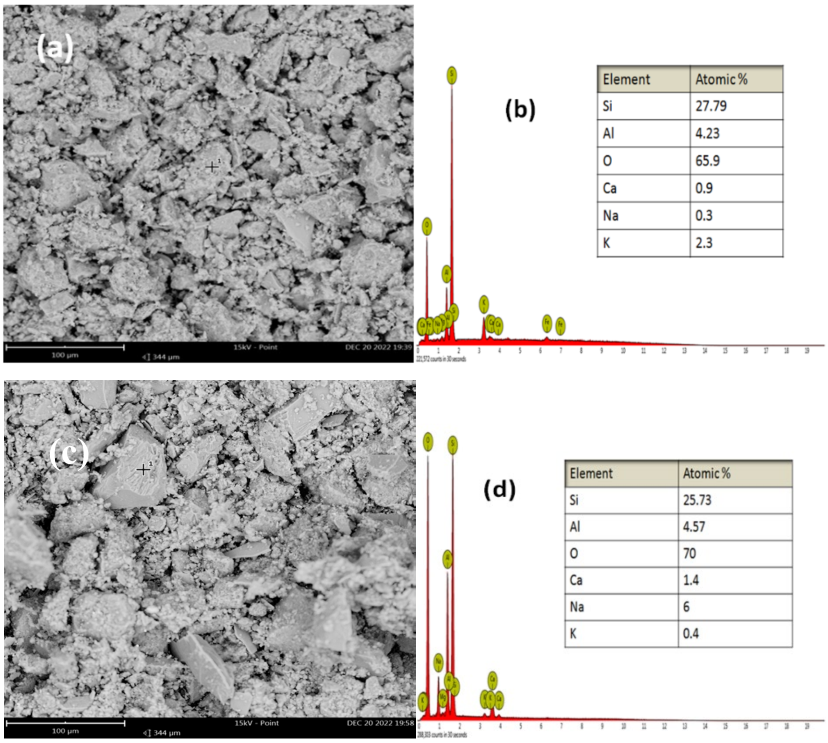

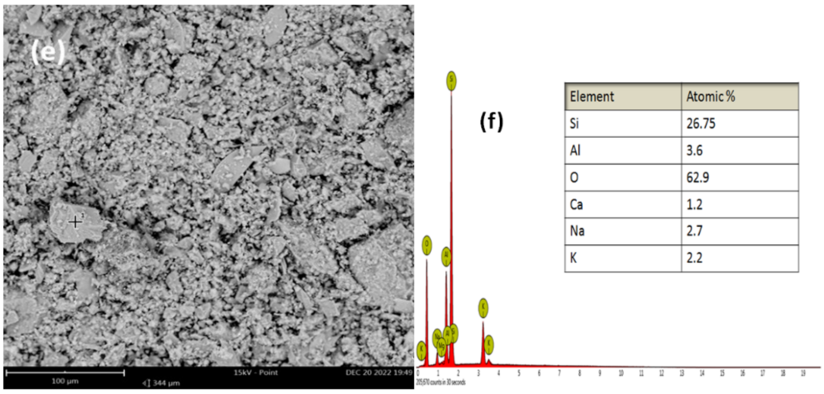

Figure 4 – SEM images and the EDX spectra of NZ (a.b), NaZ (c,d) and HZ (e,f)

Fourrier transform infra red spectroscopy (FTIR)

FTIR spectras are used to detect functional groups. Figure 5 presents the IR spectra of NZ, NaZ, and HZ. For natural zeolite (NZ), the absorption bands at 3639-3442 cm^{-1} correspond to the stretching vibrations of isolated silanol groups (Si-O-H) and H_2O molecules adsorbed on the surface. The band at 710 cm^{-1} is characteristic of the tetrahedral units of SiO_4 and AlO_4.

During the acid treatment, a shift in the main peak from 1075 cm^{-1} to 1032 cm^{-1} was observed, which can be explained by the removal of cations (mainly sodium) from the pores, affecting the vibration frequencies. At 1745 cm^{-1}, an increase in the peak intensity indicates a higher concentration of H_2O/H_3O^+ replacing cations within the framework pores, leading to an increase in microporosity and smaller mesopore volume.

Additionally, the increase in the peak size at 3607 cm^{-1} was caused by the replacement of cations by water molecules and hydronium ions (H_3O^+) on the outer surface.

For the zeolite treated with sodium hydroxide, the intensity of the peak signal at 1543 cm^{-1}, which corresponds to Al sites on the zeolite surface, shows an increase of intensity due to the removal of Si. Additionally, the intensity of the peaks in the range of 600-800 cm^{-1}, associated with exchangeable cations, decreases due to the loss of cations and silica.

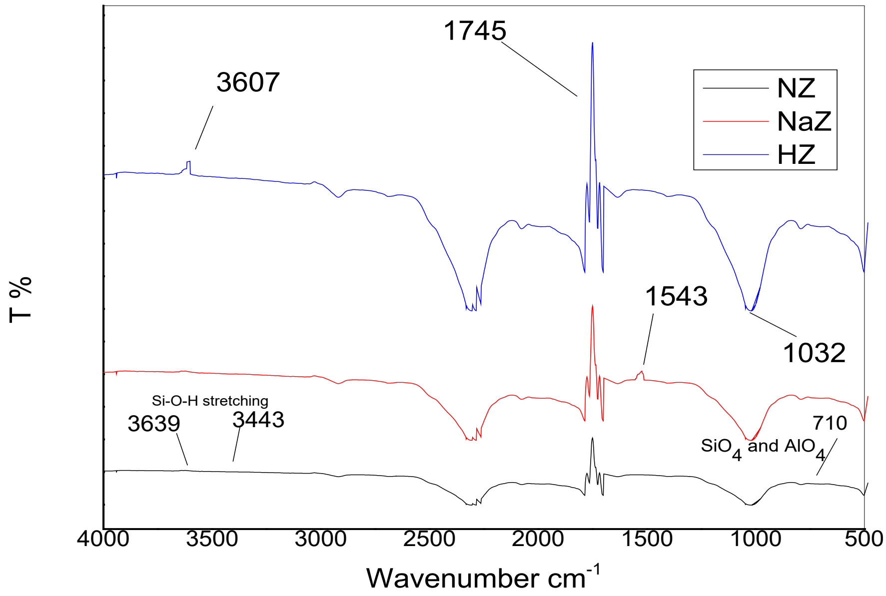

Figure 5 – FTIR spcetra of natural and modified zeolites

Adsorption isotherms modeling

The adsorption experiments were conducted in 100 cm^3 Erlenmeyer flasks by mixing 4 g/l of the adsorbent with 50 cm^3 of an aqueous dye solution. The mixture was agitated at 250 rpm for a specified period, followed by centrifugation at 2000 rpm for 10min.

The dye absorbance was measured using a SHIMADZU UV-Visible spectrophotmeter at the maximum wavelength specific to each dye: 411 nm for BY_{13}, and 532 nm for BR_{56}. The percentage of dye removal was calculated using the following equation :

$$R\% = \frac{(C_0 - C_e)}{C_0} \times 100 \quad (1)$$

The amount of adsorbed dye was calculated as follows:

$$q_e = \frac{(C_0 - C_e) \times V}{m} \quad (2)$$

where C_0 and C_e represent the initial and equilibrium concentrations of the dye in the solution (mg/l). V is the volume of the solution (L), and m is the mass of the adsorbent (g).

The equilibrium adsorption of BR_{56} and BY_{13} onto NZ, NaZ and HZ was analyzed using the Langmuir and Freundlich isotherm models. These adsorption isotherms reflect the relationship between the amount of dye adsorbed onto adsorbents (q_{ads}) and the dye concentration at equilibrium (C_e).

Langmuir isotherm

The Langmuir isotherm describes a simple model for monolayer adsorption on surfaces with identical adsorption sites. The general equation is as follows:

$$q_e = \frac{1 + K_L \cdot C_e}{1 + a_L \cdot C_e} \qquad (3)$$

After linearization, Equation (3) becomes:

$$\frac{C_e}{q_e} = \frac{1}{K_L} + \frac{a_L \cdot C_e}{K_L} \qquad (4)$$

where K_L and a_L are the equilibrium constants, q_e and C_e are the adsorption capacity and the concentration at equilibrium, respectively. The lineair Langmuir plot is obtained by plotting C_e/q_e versus C_e.

Freundlish isotherm

The Freundlish isotherm describes non-ideal and multilayer adsorption on a heterogenous surface. The model is given as follows:

$$q_e = K_F \cdot C_e^{\frac{1}{n}} \qquad (5)$$

The linear form of Equation (5) for data fitting is expressed as follows:

$$\log q_e = \log K_F + \frac{1}{n} \log C_e \qquad (6)$$

where K_F and n are the Freundlish constants, representing adsorption capacity and intensity, respectively.

Modelisation of adsorption kinetics

For a better analysis of the adsorption process, the kinetic data reported here have been fitted to three commonly kinetic models: the pseudo-first–order model, the pseudo-second-order (Lagergren, 1898), and (Ho and Mckay, 1998), and the intra-particule diffusion model (Weber Jr and Morris, 1964).

The pseudo-first-order equation can be expressed as follows:

$$\frac{dq_t}{dt} = K_1 \cdot (q_e - q_t) \quad (7)$$

where K_1 is the adsorption constant rate (s^{-1}), q_t is the amount of adsorbed adsorbate at the time t ($\mu g.g^{-1}$), and q_e is the amount adsorbed at saturation. The integrated form of Equation (7) becomes (8):

$$\log(q_e - q_t) = \log q_e - K_1 \cdot t \quad (8)$$

The pseudo-second-order equation can be expressed as follows:

$$\frac{dqt}{dt} = K_2\,(q_e - q_t)^2 \quad (9)$$

where K_2 is the adsorption constant rate. The integrated form of Equation (9) becomes (10):

$$\frac{t}{q_t} = \frac{1}{K_2} q_e^2 + \frac{t}{q_e} \quad (10)$$

Several factors can limit the adsorption kinetics, including intra-particle diffusion. The influence of this latter can be interpreted by the following equation:

$$q_t = K_{id} \cdot t^{\frac{1}{2}} + C \quad (11)$$

where K_{id} is the intra-particle diffusion rate constant ($\mu g.\ g^{-1}$ min ^{½}), and C is a constant related to the thickness of the boundary layer.

Thermodynamic study

The thermodynamic parameters ΔG, ΔH and ΔS can be calculated by the following equations:

$$K_c = \frac{q_e}{C_e} \quad (12)$$

$$\Delta G = -RT \ln K_c \quad (13)$$

$$\Delta G = \Delta H - T\Delta S \quad (14)$$

$$\ln K_c = \frac{\Delta S}{R} - \frac{\Delta H}{RT} \quad (15)$$

where K_c is the equilibrium constant, q_e the amount of dye adsorbed per liter of the solution at equilibrium (mg/dm^3), C_e is the equilibrium concentration of the adsorbate in the solution (mg/dm^3), T is the temperature (K), and R is the gas constant and is equal to 8.314 J/(mol K). ΔG, ΔH, and ΔS are standard free energy, standard enthalpy and standard entropy, respectively. ΔH and ΔS are caculated from the slope and the intercept of the linear plot of 1/T versus LnK_C.

Results and discussion

Adsorption study of BR_{56} and BY_{13} on natural and activated zeolites

Kinetic study

The effect of contact time on dyes removal by the zeolites (Figure 6) was studied over a range of contact times from 10 to 360min at 298 K. The initial dye concentration was set at 50mg/l, with an adsorbent dosage of 4 kg/m^3.

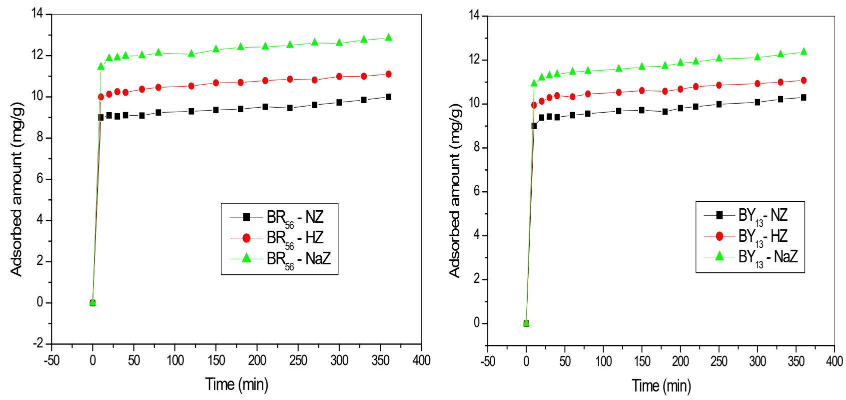

Figure 6 – Effect of the contact time on the adsorption of BR_{46} and BY_{13} on NZ, HZ and NaZ

Figure 6 illustrates that the amount of dye adsorbed increased rapidly during the first 10 min before gradually stabilizing until equilibrium was reached. The optimal time to attain equilibrium was determined to be 60 minutes. The high adsorption efficiency can be attributed to the availability of abundant active sites on the adsorbent surface. This initial rapid uptake is followed by a slower removal rate as the adsorbent reaches a saturation point. It is noteworthy that the highest adsorption capacity was observed for NaZ with both dyes, followed by HZ, whereas NZ exibited the lowest adsorption capacity. This suggests that modifying mordenite with both acid and base enhances adsorption capacity by removing cations from the framework channels, thereby creating mesopres and micropores and increasing the overall porosity of zeolite. Lycourghiotis et al. (**Lycourghiotis et al, 2018**) also demonstrated that acid modification improves the porosity and structure of mordenite. However, in contrast to their study, which employed high-concentration acid, our study utilized low-concentration acid, resulting in only a slight removal of cations without significantly altering the main structure. For alkaline modification, the removal of Si and the incorporation of Na led to an increase in the number of strong acid sites, thereby enhancing the adsorption potential.

The pseudo-second-order model was applied to evaluate the adsorption of cationic dyes onto NZ, NaZ and HZ, as depicted in Figure 7. The pseudo-second-order constants are summarized in Table.2.

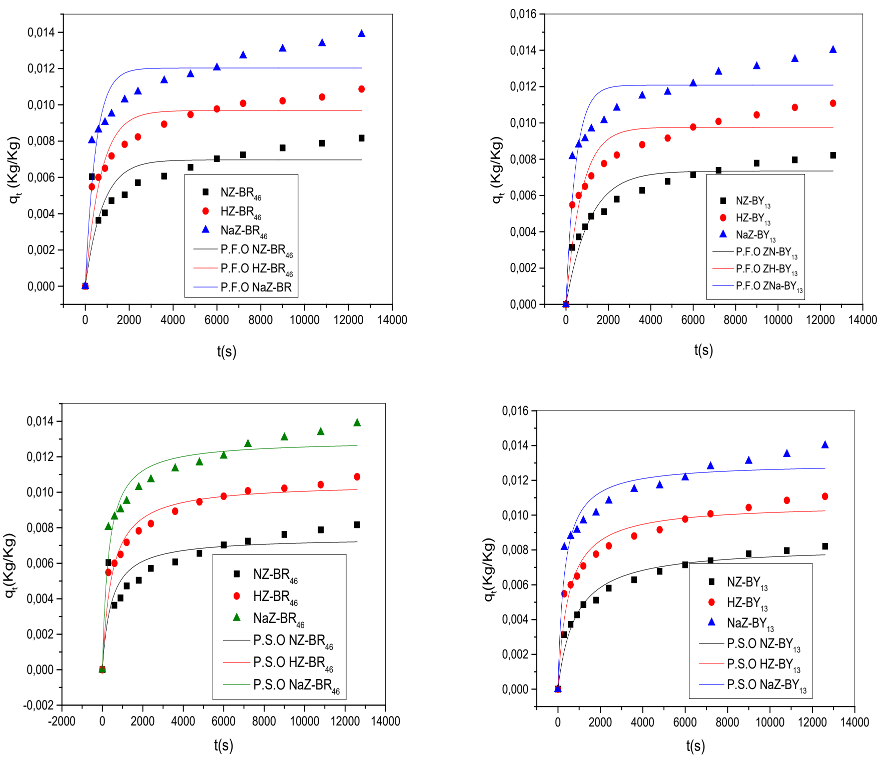

Figure7 – Application of the pseudo-first and –second-order models on the adsorption of BY_{13} and BR_{46} on NZ,NaZ, and HZ

Table 2 – Pseudo-order constants

Pseudo First Order				
	R^2	$χ^2$	q_e	K_1
BR_{46}				
NZ	0.519	$1.808×10^{-6}$	0.0069	0.0012
NaZ	0.588	$9.124×10^{-7}$	0.0096	0.0014
HZ	0.658	$1.717×10^{-6}$	0.012	0.0021
BY_{13}				
NZ	0.605	$4.73×10^{-7}$	0.0073	9*10-4
NaZ	0.670	$1.103×10^{-6}$	0.007	0.0013
HZ	0.754	$1.792×10^{-6}$	0.012	0.00217
Pseudo Second Order				
	R^2	$χ^2$	q_e	K_2
BR_{46}				
NZ	0.941	$1.204×10^{-6}$	0.0074	0.304
NaZ	0.962	$3.09×10^{-7}$	0.010	0.204
HZ	0.944	$6.77×10^{-7}$	0.0129	0.252
BY_{13}				
NZ	0.968	$1.639×10^{-7}$	0.0082	0.149
NaZ	0.950	$4.21×10^{-7}$	0.010	0.189
HZ	0.941	$7.16×10^{-7}$	0.013	0.258

The kinetic data presented in the table compare the pseudo-first-order and pseudo-second-order models in describing the adsorption process. The parameters analyzed include the coefficient of determination (R^2), the chi-square error ($χ^2$), the equilibrium adsorption capacity (q_e), and the rate constant (K).

The accuracy of the kinetic models is primarily assessed using R^2 and $χ^2$. The pseudo-first-order model exhibited relatively low R^2 values, ranging from 0.292 to 0.776, indicating a week to moderate correlation between the experimental and theoretical data. Additionally, the higher $χ^2$ values suggest significant deviations between the predicted and experimental adsorption capacities. Conversely, the pseudo-second-order model demonstrated substantially higher R^2 values (0.951-0.968), indicating a superior fit. The corresponding lower $χ^2$ values confirm a reduced error between theoretical and experimental data, further supporting the suitability of this model.

The equilibrium adsorption capacity (q_e) predicted by the pseudo-second-order model is more consistent with the experimental values compared to the pseudo-first-order model. This stability suggests that the pseudo-second-order model more accurately describes the adsorption process. Furthermore, the rate constant (K) values obtained from this model are lower, which may indicate a slower but more controlled adsorption mechanism. This trend aligns with the previous studies where the pseudo-second-order kinetics have been associated with chemisorption-dominated processes (Amin et al, 2023).

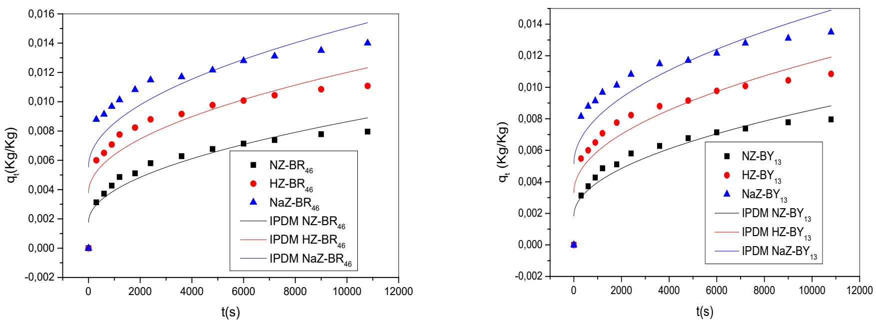

Figure 8 – Application of the intra-particule diffusion model to dye adsorption on NZ, NaZ and HZ

Table 3 – Constants of intra-particle diffusion

Constants of intra-particle diffusion	R^2	K_{id}×10^{-5} (kg/kg s)	C_{id}×10^{-3} (kg/kg)
NZ-BR_{46}	0.892	6.865	1.7
HZ-BR_{46}	0.771	8.22	3.78
NaZ-BR_{46}	0.681	9.483	5.5
NZ-BY_{13}	0.893	6.714	1.8
HZ-BY_{13}	0.813	8.564	3.3
NaZ-BY_{13}	0.709	9.375	5.15

The results indicate that adsorption does not follow to a single linear diffusion model, suggesting the presence of multiple rate-limiting steps. This non-linearity necessitates a more in-depth analysis of the diffusion rate constant (K_{id}), the boundary layer effect (C_{id}), and the correlation coefficient (R^2). The non-zero values of C_{id} (ranging from 2 to 5.465) confirm that adsorption is influenced by boundary layer resistance, implying that film diffusion also plays a significant role in the overall process. The increase in C_{id} values with zeolite modification suggests that surface interactions contribute substantially to adsorption kinetics. The highest C_{id} values, observed for NaZ-BR_{46} (5.5) and NaZ-BY_{13} (5.15), indicate that surface adsorption effects are more pronounced in these materials, further supporting the hypothesis of multi-stage adsorption.

The variation in R^2 values (0.681-0.893) reflects differences in the extent to which intraparticle diffusion governs the adsorption process across different zeolite modifications. The highest R^2 values observed for NZ-BR_{46} (0.829) and NZ-BY_{13} (0.893), suggest a stronger correlation with the intraparticle diffusion model, whereas the lower values for NaZ-BY_{13} (0.703), indicate a more complex adsorption mechanism involving multiple kinetic stages.

Natural zeolite exhibited the lowest K_{id} values (0.485-0.487 mg/g min$^{0.5}$), presumably due to increased pore accessibility and surface acidity, which enhance adsorbates-adsorbent interactions.

The non-linearity observed in the diffusion plots suggests the presence of distinct adsorption phases:

I. External Mass Transfer Phase: Initially, dye molecules migrate from the bulk solution to the zeolite surface. The significant C_{id} values suggest that this phase is not negligible and that film diffusion contributes to the overall rate limitation.

II. Intraparticle Diffusion Phase: Once adsorbates reach the surface, they diffuse into the internal structure of zeolite. The variation in K_{id} values among different zeolites confirms that this phase is influenced by structural and chemical modifications.

III. Equilibrium Phase: At longer contact times, the adsorption rate decreases as active sites become occupied. The lower slopes observed in the latter stages of adsorption support this trend, consistent with diffusion-limited kinetics.

Effect of dye concentration

The effect of dye concentration on the adsorption on natural and activated zeolites (Figure 9) was investigated by varying the initial dye concentration between 10 and 200ppm.

The findings demonstrate that an increase in the initial dye concentration enhances dye removal efficiency. As the concentration increased from 10 to 200 ppm, both the removal percentage and the amount of dye adsorbed exhibited the following trends:

- $NZ\text{-}BR_{46}$: The removal efficiency increased from 44.8% to 70.84% corresponding to an increase in adsorption capacity from 1.1 to 35.5 mg/g.
- $NZ\text{-}BY_{13}$: The removal efficiency increased from 46.7% to 69.25% corresponding to an increase in adsorption capacity from 1.54-34.5 mg/g).
- $HZ\text{-}BR_{46}$: The removal efficiency increased from 55.3% to 76.88% corresponding to an increase in adsorption capacity from 1.38-38.40mg/g.
- $HZ\text{-}BY_{13}$: The removal efficiency increased from 56.7% to 80.43% corresponding to an increase in adsorption capacity from 1.417-40.5mg/g.
- $NaZ\text{-}BR_{46}$: The removal efficiency increased from 85.16% to 97.62% corresponding to an increase in adsorption capacity from 2.12-48.35mg/g.
- $NaZ\text{-}BY_{13}$: The removal efficiency increased from 87% to 98.97% corresponding to an increase in adsorption capacity from 2.175-49.45mg/g.

These findings suggest that dye adsorption is direcly dependent on the initial dye concentration in the solution. The observed variations in the adsorption efficiency among different zeolites highlight the influence of surface properties and activation methods on the adsorption process.

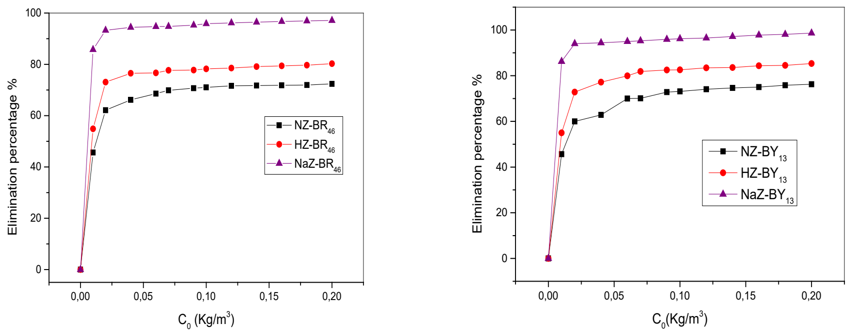

Figure 9 – Effect of the initial concentration on the adsorption of dyes on natural and activated zeolites

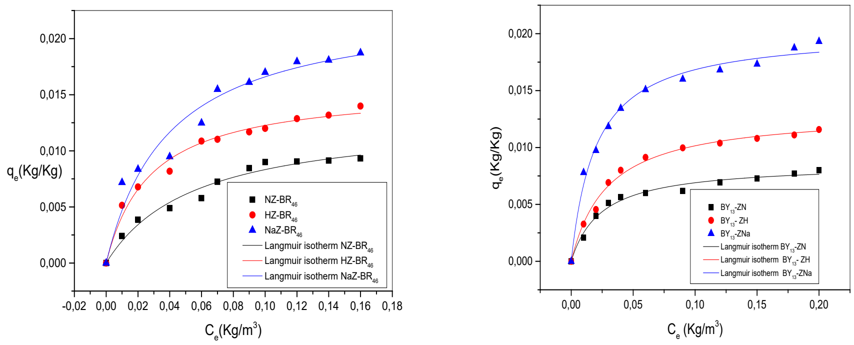

Figure 10 – The non-linear Langmuir adsorption isotherms for BR_{46} (on the left) and BY_{13} (on the right) adsorption on NZ, NaZ, and HZ

Table 4 – Langmuir constants for the adsorption of BR_{46} and BY_{13} on NZ, NaZ, and HZ

	Langmuir isotherm			
	R^2	$\chi^2\times10^{-7}$	q_m	K_L
NZ-BR46	0.974	2.594	0.0130	17.770
NaZ-BR46	0.982	3.138	0.0156	36
HZ-BR46	0.954	0.16	0.0230	25.50
NZ-BY13	0.982	0.108	0.0085	41.301
NaZ-BY13	0.991	0.120	0.0131	34.121
HZ-BY13	0.988	0.374	0.0201	49.885

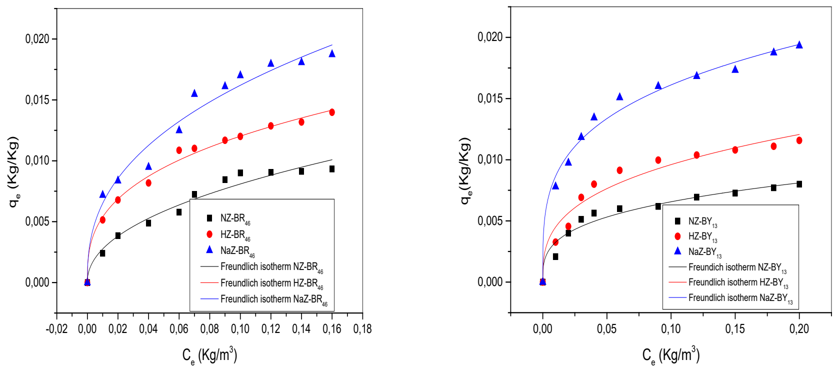

Figure 11 – Non-linear Freundlish adsorption isotherms for BR_{46} and BY_{13}

Table 5 – Freundlish model constants of BR_{46} and BY_{13} removal on NZ, NaZ, and HZ

	R^2	$\chi^2 \times 10^{-7}$	K_f	n
		BR_{46}		
NZ-BR46	0.978	3.23	0.023	2.138
HZ-BR46	0.999	1.493	0.026	2.868
NaZ-BR46	0.978	9.187	0.040	2.533
		BY_{13}		
NZ-BY13	0.978	2.671	0.013	3.282
HZ-BY13	0.987	6.519	0.020	3.033
NaZ-BY13	0.984	4.068	0.03	3.075

By analyzing the correlation coefficient (R^2) presented in Tables 4 and 5, it can be observed that the adsorption of dyes onto natural and activated zeolites follows both the Freundlich and the Langmuir isotherm model. These results imply that both monolayer and multilayer adsorption processes may occur simultaneously, and the zeolites surface exhibit both homogeneous and heterogeneous characteristics (Tian et al, 2016). Moreover, the values of n (Table 5) are greater than 1, suggesting a favorable adsorption process. These findings are consistent with the results reported by **(**Karadag et al, 2007**).**

Effect of pH

The influence of pH on dye adsorption was investigated by variying the initial solution pH (pH_0) from 3 to 10 at 25 °C298 K. Adjustments were made using 100 mol/m^3 HCl or 100 mol/m^3 NaOH, while ensuring that all other experimental conditions remained constant.

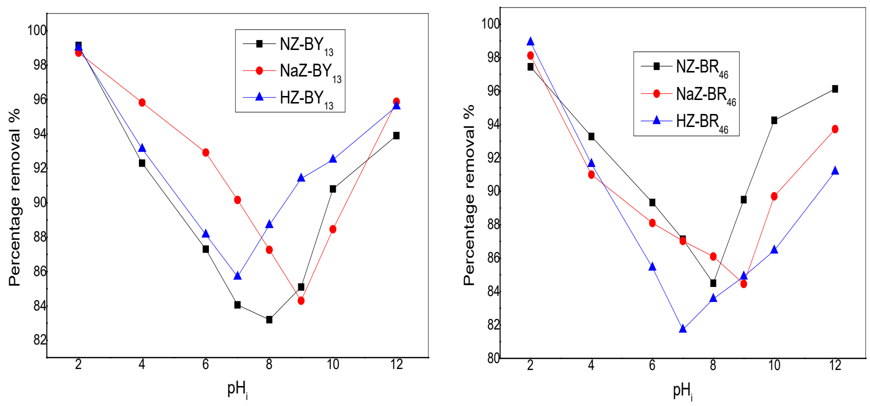

Figure 12 – Effect of pH of the dye solution on the removal of dyes by NZ,HZ, and NaZ

As shown in Figure 12, the dye removal percentage initially decreased with pH up to a certain level for the three zeolites before increasing. The lowest removal percentages were observed at pH 8 for NZ, pH 9 for NaZ, and pH 7 for HZ. This trend can be attributed to the variations in the surface charge of each zeolite and the degree of dye ionization. In the acid medium, the presence of H^+ creates competition with the dyes. At neutral pH, protons and hydroxides are in equilibrium, while at higher pH, OH^- dominates. The observed fluctuations in the removal efficiency can be effectively explained by the point of zero charge (PHZ).

Comparing the pH_i and the PHZ values of NZ, NaZ, and HZ, it was found that at the pH levels below the PHZ, the zeolite surfaces became positively charged, favoring anion adsorption over cations. However, at the pH levels above the PHZ, negative charges on the zeolites dominated, leading to a preference for cation adsorption.

Thermodynamics of adsorption

Table 6 presents the thermodynamic parameters ΔG, ΔH, and ΔS for the adsorption of BR_{46} and BY_{13} on NZ, HZ, and NaZ. The negative values of ΔG at all temperatures indicate that the adsorption process is both spontaneous and thermodynamically favorable. Furthermorer, as the temperature increases, ΔG values decrease, suggesting that higher temperatures enhance the favorability of adsorption. The positive values of ΔH confirm that the adsorption process is endothermic. Additionally, the positive values of ΔS indicate an increase in randomness at the solid-liquid interface during adsorption, for both natural and activated zeolites. These findings are consistent with the previous studies conducted by Karadag et al. **(**Karadag et al, 2007**).**

Table 6 – Thermodynamic parameters of BR_{46} and BY_{13} adsorption on NZ, HZ, and NaZ

	BY_{13}					**BR_{46}**				
	ΔG° (kJ/mol K)			ΔH° (kJ/mol)	ΔS° (J/mol)	ΔG°			ΔH° kJ/mol K	ΔS° J/mol K
	298K	**313K**	**323K**			**298K**	**313K**	**323K**		
NZ	-6.055	-24.55	-33.80	264.97 0.925		-13.87	-26.77	-35.37	242.41 0.86	
NaZ	-8.29	-21.04	-29.54	245.01	0.85	-16.48	-28.53	-36.56	222.81	0.803
HZ	-11.36	-25.83	-35.48	276.21	0.965	-14.85	-27.17	-35.38	229.8	0.821

Conclusion

This study investigated the effect of modifying natural mordenite zeolite with low concentrations of acid and alkaline solutions on the removal of cationic textile dyes from aqueous solutions, comparing their adsorption affinities. XRF and SEM-EDX analyses revealed that the HCl treatment removed Al, while the NaOH treatment removed Si from the zeolite surface, reducing their external framework content while preserving the primary structure. FTIR spectroscopy indicated shifts, disappearance of bands, and decreases in certain peaks for NaZ and HZ, attributed to cation replacement by hydronium inons or the removal of aluminium and silicon. These structural changes also influenced the PHZ of both natural and modified zeolites. The results showed that NaZ exhibited the highest removal efficiency compared to NZ and HZ for cationic dyes in aqueous solutions. Equilibrium was reached gradually, stabilizing due to the high number of active sites on the zeolite surface. The adsorption of BR_{46} and BY_{13} on NZ, NaZ, and HZ was described by both the Langmuir and the Freundlich models, while the pseudo-second-order model accurately represented the adsorption process. The adsorption onto zeolites is governed by a combination of film diffusion and intraparticle diffusion, with zeolite modification significantly influencing diffusion kinetics. Thermodynamic analysis indicated that dye adsorption was spontaneous, random and endothermic.

References:

Aarden, F.B. 2001. *Adsorption onto heterogeneous porous materials: equilibria and kinetics*, Technische Universiteit Eindhoven. ISBN: 90-386-2822-6

Amin, G., Konstantinovic, S., Jordanov, I. & Djordjevic, D. 2023. Adsorption study of textile dye Basic Red 46 on clinoptilolite. *Iran J Chem Chem Eng.,* 5428. Available at: http://doi.org/10.30492/ijcce.2023.557165.5428

Aravindhan, S., Kumar, G.B., Saravanan, M. & Arumugam, A. 2023. Delonix regia biomass as an eco-friendly biosorbent for effective Alizarin Red S textile dye removal: Characterization, kinetics, and isotherm studies. *Bioresource Technology Reports*, 101721. Available at: https://doi.org/10.1016/j.biteb.2023.101721

Ates, A. & Akgül, G. 2016. Modification of natural zeolite with NaOH for removal of manganese in drinking water. *Powder technology,* 287, 285-291. Available at: http://doi.org/10.1016/j.powtec.2015.10.021

Ebsa, D.G. 2023. Defluoridation of drinking water by modified natural zeolite with Cationic surfactant, in the case of Ziway town, Ethiopia. *Cleaner Engineering and Technology,* 12, 100596. Available at: http://doi.org/10.1016/j.clet.2023.100596

Garcia-Basabe, Y., Rodriguez-Iznaga, I., De Menorval, L.-C., Llewellyn, P., Maurin, G., Lewis, D.W., Binions, R., Autie, M. & Ruiz-Salvador, A.R. 2010. Step-wise dealumination of natural clinoptilolite: Structural and physicochemical characterization. *Microporous and Mesoporous Materials,* 135, 187-196. Available at: http://doi.org/10.1016/j.micromeso.2010.07.008

Ho, Y. & Mckay, G. 1998. A comparison of chemisorption kinetic models applied to pollutant removal on various sorbents. *Process safety and environmental protection,* 76, 332-340. Available at: http://doi.org/10.1205/095758298529696

Ighnih, H., Haounati, R., Ouachtak, H., Regti, A., El Ibrahimi, B., Hafid, N., Jada, A., Taha, M.L. & Addi, A.A. 2023. Efficient Removal of Hazardous Dye from Aqueous Solutions Using Magnetic Kaolinite Nanocomposite: Experimental and Monte Carlo Simulation Studies. *Inorganic Chemistry Communications*, 110886. Available at: http://doi.org/10.1016/j.inoche.2023.110886

Imessaoudene, A., Mechraoui, O., Aberkane, B., Benabbas, A., Manseri, A., Moussaoui, Y., Bollinger, J.-C., Amrane, A., Zoukel, A. & Mouni, L. 2024. Synthesis of a TiO2/zeolite composite: Evaluation of adsorption-photodegradation synergy for the removal of Malachite Green. *Nano-Structures & Nano-Objects,* 38, 101191. Available at: http://doi.org/10.1016/j.nanoso.2024.101191

Karadag, D., Akgul, E., Tok, S., Erturk, F., Kaya, M.A. & Turan, M. 2007. Basic and reactive dye removal using natural and modified zeolites. *Journal of Chemical & Engineering Data,* 52, 2436-2441. Available at: http://doi.org/10.1021/je7003726

Kumar, N., Pandey, A. & Sharma, Y.C. 2023. A review on sustainable mesoporous activated carbon as adsorbent for efficient removal of hazardous dyes from industrial wastewater. *Journal of Water Process Engineering,* 54, 104054. Available at: http://doi.org/10.1016/j.jwpe.2023.104054

Lagergren, S. 1898. *About the theory of so-called adsorption of solution substances* [Online]. Available: https://sid.ir/paper/563615/en [Accessed].

Lellis, B., Fávaro-Polonio, C.Z., Pamphile, J.A. & Polonio, J.C. 2019. Effects of textile dyes on health and the environment and bioremediation potential of living organisms. *Biotechnology Research and Innovation,* 3, 275-290. Available at: http://doi.org/10.1016/j.biori.2019.09.001

Li, H., Liu, S., Zhao, J. & Feng, N. 2016. Removal of reactive dyes from wastewater assisted with kaolin clay by magnesium hydroxide coagulation process. *Colloids and Surfaces A: Physicochemical and Engineering Aspects,* 494, 222-227. Available at: http://doi.org/10.1016/j.colsurfa.2016.01.048

Lycourghiotis, S., Makarouni, D., Kordouli, E., Bourikas, K., Kordulis, C. & Dourtoglou, V. 2018. Activation of natural mordenite by various acids: Characterization and evaluation in the transformation of limonene into p-cymene. *Molecular Catalysis,* 450, 95-103. Available at: http://doi.org/10.1016/j.mcat.2018.03.013

Mamo, W., Awoke, Y., Chebude, Y. & Diaz, I. 2015. Mild modification method for the generation of mesoporosity in synthetic and natural mordenite. *Bulletin of* *the Chemical Society of Ethiopia,* 29**,** 95-103. Available at: http://doi.org/10.4314/bcse.v29i1.8

Mehdi, B., Belkacemi, H., Brahmi-Ingrachen, D., Braham, L.A. & Muhr, L. 2022. Study of nickel adsorption on NaCl-modified natural zeolite using response surface methodology and kinetics modeling. *Groundwater for Sustainable Development,* 17**,** 100757. Available at: http://doi.org/10.1016/j.gsd.2022.100757

Nakamoto, K., Ohshiro, M. & Kobayashi, T. 2017. Mordenite zeolite—Polyethersulfone composite fibers developed for decontamination of heavy metal ions. *Journal of Environmental Chemical Engineering,* 5**,** 513-525. Available at: http://doi.org/10.1016/j.jece.2016.12.031

Pastukhov, A.V., Ilyin, M.M. & Chkanikov, N.D. 2023. Acid-activated natural zeolite and montmorillonite as adsorbents decomposing metsulfuron-methyl herbicide. *Inorganic Chemistry Communications,* 158**,** 111615. Available at: http://doi.org/10.1016/j.inoche.2023.111615

Reeve, P.J. & Fallowfield, H.J. 2018. Natural and surfactant modified zeolites: A review of their applications for water remediation with a focus on surfactant desorption and toxicity towards microorganisms. *Journal of environmental management,* 205**,** 253-261. Available at: http://doi.org/10.1016/j.jenvman.2017.09.077

Selim, K., Youssef, M., Abd El-Rahiem, F. & Hassan, M. 2014. Dye removal using some surface modified silicate minerals. *International Journal of Mining Science and Technology,* 24**,** 183-189. Available at: http://doi.org/10.1016/j.ijmst.2014.01.007

Senguttuvan, S., Janaki, V., Senthilkumar, P. & Kamala-Kannan, S. 2022. Polypyrrole/zeolite composite–A nanoadsorbent for reactive dyes removal from synthetic solution. *Chemosphere,* 287**,** 132164. Available at: http://doi.org/10.1016/j.chemosphere.2021.132164

Tian, J., Guan, J., Gao, H., Wen, Y. & Ren, Z. 2016. The adsorption and mass-transfer process of cationic red X-GRL dye on natural zeolite. *Water Science and Technology,* 73**,** 2119-2131. Available at: http://doi.org/10.2166/wst.2016.055

Visa, M. 2016. Synthesis and characterization of new zeolite materials obtained from fly ash for heavy metals removal in advanced wastewater treatment. *Powder Technology,* 294**,** 338-347. Available at: http://doi.org/10.1016/j.powtec.2016.02.019

Wang, C., Wang, L., Du, F., Yu, Q. & Liang, X. 2023. A two-step organic modification strategy for improving surface hydrophobicity of zeolites. *Advanced Powder Technology,* 34**,** 104228. Available at: http://doi.org/10.1016/j.apt.2023.104228

Weber Jr, W.J. & Morris, J.C. 1964. Equilibria and capacities for adsorption on carbon. *Journal of the Sanitary Engineering Division,* 90**,** 79-108. Available at: http://doi.org/10.1061/JSEDAI.0000496

Eliminación de colorantes textiles básicos del agua mediante zeolita argelina natural y modificada: estudios cinéticos, termodinámicos y de equilibrio

Nassima Belgaid[a], **autor de correspondencia,** *Mohamed Redha* Menani[b], *Kamel Eddine* Bouhidel[b]

[a] Universidad de Batna 2, Laboratorio de Movilización y Gestión de Recursos Hídricos (MGRE), Instituto de Ciencias de la Tierra y del Universo, 53, carretera de Constantina, Fesdis, Batna 05078, República de Argelia.

[b] Universidad de Batna 1, Laboratorio de Química y Química Ambiental (LCCE), Departamento de Química, Facultad de Ciencias de la Materia, Carretera de Biskra, Batna 05000, República de Argelia

CAMPO: Tecnologías químicas
CATEGORÍA (TIPO) DEL ARTÍCULO: original de la investigación científica,

Resumen:

Introducción/objetivo: La zeolita natural argelina (denominada NZ) se modificó mediante ácido clorhídrico (HZ) y solución de hidróxido de sodio (Na2). Este estudio investigó el efecto de las modificaciones ácidas y alcalinas en la adsorción de dos colorantes textiles catiónicos (BR46 y BY13) en soluciones acuosas.

Métodos: : El análisis XRF confirmó que el SiO_2 es el mineral predominante en las tres zeolitas. Los resultados de XRD revelaron que la NZ está compuesta principalmente de mordenita, con chabasita y un contenido menor de cuarzo. El análisis MEB-EDX mostró ligeras variaciones en el contenido de Si y Al para HZ y NaZ, sin alterar significativamente la estructura de la zeolita. Se examinaron los efectos de la concentración inicial del tinte, el tiempo de contacto y el pH en un sistema por lotes.

Resultados: La adsorción en NZ, NaZ y HZ aumentó con tiempos de contacto más largos, mayores concentraciones iniciales de colorante y temperaturas elevadas. El equilibrio se alcanzó rápidamente, lo cual se describe mejor mediante el modelo cinético de pseudo-segundo orden. Los modelos de isotermas de Langmuir y Freundlich son compatibles con los datos de adsorción.

Conclusión: La mayor eficiencia de eliminación de colorante se observó para NaZ, con un 97,62 % para BR_{46} y un 98,97 % para BY_{13}. Las tasas de eliminación más bajas se obtuvieron a pH = 8 para HZ y pH = 10 para NZ y NaZ. La adsorción fue espontánea y endotérmica.

Palabras claves: zeolita, modificación, ácido, alcalino, adsorción, colorantes catiónicos

Удаление основных текстильных красителей из воды природным и модифицированным алжирским цеолитом: исследования кинетического, термодинамического и равновесного состояний

Нассима Белгайд[а], **корреспондент,** *Мохамед Редха* Менани[б], *Камель Эддин* Бухидель[б]

[а] Университет Батны, 2, лаборатория мобилизации и управлением водными ресурсами (MGR), Научный иститут о Земле и космосе, дорога Константина 53, Фесдис, Батна 05078, Алжирская Народная Демократическая Республика Алжир.

[б] Университет Батны 1, лаборатория химии и охраны окружающей среды химический институт, факультет материаловедения, дорога Бискра, Батна, 05000, Алжирская Народная Демократическая Республика

РУБРИКА ГРНТИ: 61.13.21 Химические процессы
ВИД СТАТЬИ: оригинальная научная статья

Резюме:

Введение/цель: Алжирский природный цеолит (обозначаемый как NZ) был модифицирован с помощью соляной кислоты (HZ) и раствора гидроксида натрия (NaZ). В данном исследовании изучено влияние кислотных и щелочных модификаций на адсорбцию двух катионных текстильных красителей (BR46 и BY13) из водных растворов.

Методы: Рентгенофазовый анализ подтвердил, что SiO2 является преобладающим минералом во всех трех цеолитах. Результаты рентгенофазового анализа показали, что NZ в основном состоит из морденита с небольшим содержанием шабазита и кварца. Анализ MEB-EDX показал незначительные изменения в содержании Si и Al в HZ и NaZ без существенного изменения структуры цеолита. Влияние начальной концентрации красителя, времени контакта и pH было исследовано по сериям.

Результаты: Адсорбция NZ, NaZ и HZ увеличивалась при более продолжительном времени контакта, увеличении начальной концентрации красителя и повышении температуры. Баланс был быстро установлен, что лучше всего описывается с помощью кинетической модели псевдо-второго порядка. Для получения данных об адсорбции подходят как модели изотерм Ленгмюра, так и Фрейндлиха.

Выводы: Самая высокая эффективность удаления красителя наблюдалась у NaZ − 97,62% для BR_{46} и 98,97% для BY_{13}. Наименьшая скорость удаления наблюдалась при pH = 8 у HZ и pH=10 у NZ и NaZ. Адсорбция была спонтанной и эндотермической.

Ключевые слова: цеолит, модификация, кислота, щелочь, адсорбция, катионные красители.

Уклањање основних текстилних боја из воде помоћу природног и модификованог алжирског зеолита: студије из кинетике, термодинамике и равнотежних стања

Насима Белгаид[a], **аутор за преписку,** *Мохамед Редха* Менани[б], *Камел Един* Бухидел[б]

[a] Универзитет у Батни 2, Лабораторија за мобилизацију и управљање водним ресурсима, Институт за земљане науке и универзум, Фесдис, Батна, Република Алжир

[б] Универзитет у Батни 1, Лабораторија хемије и еколошке хемије, Одсек за хемију, Факултет за науку о материјалу, Батна, Република Алжир

ОБЛАСТ: хемијска технологија
КАТЕГОРИЈА (ТИП) ЧЛАНКА: оригинални научни рад

Сажетак:

Увод/циљ: Природни зеолит (NZ) из Алжира модификован је помоћу хлороводоничне киселине (HZ) и раствора натријум-хидроксида (NaZ). Ова студија испитује утицај модификација киселином и базом на адсорпцију две катјонске боје за текстил (BR_{46} и BY_{13}) из водених раствора

Методе: Анализа XRF је потврдила да минерал SiO2 преовлађује у сва три зеолита. Резултати анализе XRD указују да се NZ превасходно састоји од морденита, уз хабазит и мањи садржај кварца. Анализа MEB-EDX је показала мање варијације у садржају Si и Al код HZ и NaZ, без значајне промене у структури зеолита. Утицаји почетне концентрације боје, времена контакта и pH вредности испитани су по серијама.

Резултати: Адсорпција NZ, NaZ и HZ повећала се са дужим временима контакта, вишим почетним концентрацијама боје и повишеним температурама. Равнотежа је брзо била постигнута, што је најбоље описано кинетичким моделом псеудодругог реда. Изотермни модели и по Лангмиру и по Фројндлиху одговарају адсорпционим подацима.

Закључак: Најефикасније уклањање боје уочено је код NaZ (97,62% за BR_{46} и 98,97% за BY_{13}). Најниже брзине уклањања биле су за pH= 8 код HZ и за pH=10 код NZ и NaZ. Адсорпција је била спонтана и ендотермна.

Кључне речи: зеолит, модификација, киселост, алкалност, адсорпција, катјонске боје

Paper received on: 18.01.2025.
Manuscript corrections submitted on:12.02.2025
Paper accepted for publishing on: 25.02.2025.

Effect of variations in parameters on the crystallization of mordenite zeolite

Ikram Yssaad[a], *Fatiha* Hamidi[b], *Denis* Luart[c]

[a] Mohamed Boudiaf University of Science and Technology, Faculty of Chemistry, Laboratory of Functional and Nanostructured Ecomaterials, Oran, Algeria.
e-mail: ikram.yssaad@univ-usto.dz,**corresponding author**,
ORCID iD: https://orcid.org/0009-0008-1257-741X

[b] Mohamed Boudiaf University of Science and Technology, Faculty of Chemistry, Laboratory of Functional and Nanostructured Ecomaterials, Oran, Algeria.
e-mail: fatiha.hamidi@univ-usto.dz
ORCID iD: https://orcid.org/0009-0000-2216-8195

[c] Université de Technologie de Compiègne, ESCOM, Alliance Sorbonne Université, TIMR, Compiègne, France.
e-mail: d.luart@escom.fr
ORCID iD: https://orcid.org/0000-0003-3136-9815

doi https://doi.org/10.5937/vojtehg73-56746

FIELD: materials, chemical technology
ARTICLE TYPE: original scientific paper

Abstract:

Introduction/purpose: This study highlights the importance of synthesis parameters in the crystallization of mordenite zeolite. Precise control of the SiO_2/Al_2O_3 ratio, alkalinity and crystallization time results in mordenite crystals with high crystallinity and optimum purity, while avoiding the formation of secondary or amorphous phases.

Methods: The materials were prepared by the hydrothermal method, using silica gel and sodium aluminate as sources of silicon and aluminum, respectively. Several synthesis parameters were varied, including SiO_2/Al_2O_3 molar ratio, alkalinity (OH^-/Si), as well as crystallization time, in order to assess their effect on mordenite crystal formation. Experiments were carried out at a constant temperature of 170°C and 190°C.

Results: The results show that the SiO_2/Al_2O_3 ratio plays a crucial role in crystal formation. A low ratio, such as 15, combined with high alkalinity, favors the formation of analcime crystals. On the other hand, a high ratio, such as 30, leads to the formation of mordenite crystals with high crystallinity and purity. However, when this ratio reaches 60 and is combined with low alkalinity, crystalline nucleation is impeded, leading to the formation of an amorphous material.

Concerning alkalinity (OH^-/Si), the values of 0.39 and 0.49 result in pure, well-crystallized mordenite crystals, while higher values, such as 0.59, lead to the formation of secondary phases. With regard to crystallization time, *the periods of 48 and 72 hours at 170°C produced pure, well-crystallized mordenite crystals.*

Conclusion: This study highlights the importance of synthesis parameters in the crystallization of mordenite zeolite. Precise control of the SiO_2/Al_2O_3 ratio, alkalinity and crystallization time results in mordenite crystals with high crystallinity and optimum purity, while avoiding the formation of secondary or amorphous phases.

Key words: mordenite, alkalinity, Si/Al ratio, crystallization, zeolite.

Introduction

Zeolites are crystalline microporous alumina-silicate materials used in a wide range of practical applications. They belong to the silicate group, the tectosilicate subgroup (M. B. Z. Gili and Conato, 2019; Pérez-Botella et al, 2022), and show remarkable properties and performance in domestic, medical, and industrial fields such as catalysis, separation, adsorption, and ion exchange (Jia et al, 2019; Zhang et al, 2011). These characteristics encourage scientific inquiry into the cost-effective production of zeolites.

The shape and size of crystals strongly influence the properties of zeolites. It is therefore crucial to study the influence of synthesis parameters on zeolitic morphology in order to optimize their use in various applications. Controlling the size and morphology of mordenite crystals is currently the focus of much research (Bolshakov et al, 2019; Gili and Conato, 2018; Khalil and Muraza, 2016; Mohamed et al, 2005). Various sources, such as silica gel, rice ball ash, and smoked silica, are used in some works to prepare mordenite-type zeolites, while metakaolin or faujasite zeolite are used as sources of aluminium (Narayanan et al, 2021). Other studies have focused on the optimization of the mordenite synthesis parameters by microwave heating (Khalil and Muraza, 2016; Li et al, 2011), and the use of mono-quaternary ammonium to synthesize hierarchical mordanite monotiges (Bolshakov et al, 2019).

Zeolites have important characteristics such as high cationic exchange capacity. Mordenite is one of a few zeolitic structures that is useful in industry, especially in petrochemistry where it is used as a catalyst for breaking down hydrocarbons, alkylating benzene, reforming, and deparaffinating (Bajpai, 1986). It is also used as an isomerization catalyst for naphta C5/C6 to increase their bonding and improve the octane index of gasoline. Mordenite also plays a significant role in the adsorption of various pollutants, including heavy metals and radioactive materials (Gili and Conato, 2018), and it serves as a selective adsorbent in the production of oxygen enriched air. It offers better nitrogen adsorption than oxygen because of a quadripolar interaction between the nitrogen molecule and the surface of the polar zeolite (Golden and Jenkins, 1981). Additionally, mordenite has shown potential in the catalytic conversion of methane to methanol under mild conditions, leveraging its unique acidic and structural properties to facilitate this transformation, which is a critical step toward utilizing methane as a sustainable chemical feedstock (Brezicki et al, 2021; Le et al, 2017).

Mordenite has an orthorhombic structure with a unit cell a = 18.121 Å, b = 20.517 Å, and c = 7.544 Å belonging to the spatial group Cmcm (M. B. Z. Gili and Conato, 2019). The mordenite structure consists of parallel rings with 12 limbs (MR) (6.5 * 7.0 Å) and 8-MR (2.6 * 5.7 Å) along the c axis (Mohamed et al, 2006), interconnected by 8-MR channels (3.4 * 4.8 Å) across the b axis (Nasser et al, 2016; Zhang et al, 2011).

While natural mordenite exists, some applications prefer synthetic mordenite because of its purity and controlled porous structure (Kordala and Wyszkowski, 2024). Natural mordenite crystals typically appear in the form of needles with an elongation in c (Borissenko, n.d.; Hamidi et al, n.d.), and sometimes are thin in the direction [010] (Hamidi et al, n.d.). Synthesis conditions and post-synthesis treatments have a significant impact on mordenite morphology, size, and structural defects (Borissenko, n.d.). Gels with a SiO_2/Al_2O_3 ratio of 8 to 12 and a Na/Al ratio lower than 3 yield to acicular crystals, whereas increasing gel alkalinity and reducing the amount of aluminum yields prism crystals (Borissenko, n.d.). Hamidi et *al*. discovered that dissolving silica gel before mixing it with other reagents can yield short stick-shaped mordenite crystals (60 nm to 240 nm).

Mordenites obtained by direct hydrothermal synthesis typically have a SiO_2/Al_2O_3 ratio between 10 and 20. One can use an organic template to achieve a higher ratio, but this method is costly and carries risks of contamination and pollution. Direct hydrothermal synthesis therefore remains the best option for controlling the ratio of mordenite-type zeolites (Gili and Conato, 2018; Li et al, 2023; Lima et al, 2023). We observe a notable correlation between the alkalinity of the synthetic solution and the composition of zeolite, where a higher alkalinity facilitates the incorporation of aluminium (Zhang et al, 2011).

In this study, we synthesized mordenite-type zeolites with various parameters using the hydrothermal method, without the use of organic dimensions. We have evaluated the synthetic products in terms of composition, crystallinity, morphology, and grain size using various characterization techniques.

Experimental

Materials

The reagents used in this study are silica gel, sodium aluminate (Haen Riedel), sodium hydroxide (>98%, Prolabo) and demineralized water. A gel was prepared following a precise sequence: 55 cm³ demineralized water, sodium hydroxide, 1.034 g sodium aluminate, and silica added progressively. The resulting gel was aged under magnetic stirring at 600 rpm for 120 minutes, then transferred to a stainless steel autoclave for hydrothermal treatment. The temperature was raised to 170°C /190°C, then maintained at this level for varying lengths of time. The solid material was then rapidly cooled, filtered, washed to a pH of 9.00 or less, and dried at 80°C. Several parameters were investigated to improve crystallinity and reduce the mordenite crystal size, including the impact of the Na_2O/SiO_2 ratio, the SiO_2/Al_2O_3 ratios, and the crystallization time.

Effect of the Na_2O/SiO_2 ratio

The variation in relative proportions (x) of Na_2O was explored while keeping the quantities of the other components constant. We modified the mixture's composition using the following formula:

xNa_2O; Al_2O_3; $ySiO_2$; $560H_2O$

The molar x/y ratios were adjusted between 0.23 and 0.33, or the OH-/Si ratios between 0.39 and 0.59, respectively. We carried out the crystallization at 190 °C for a duration of 24 hours.

Effect of the SiO_2/Al_2O3 ratio

Variations in the SiO2/Al2O3 molar ratio were analyzed by adjusting the ratios according to:

$$7Na_2O;\ yAl_2O_3;\ xSiO_2;\ 560H_2O$$

with $15 \leq x/y \leq 60$.

The crystallization was carried out at 190 °C for a duration of 24 hours.

Effect of the crystallization time

The effect of the crystallization time was evaluated by varying the synthesis time of mordenite between 48 and 72 hours, while maintaining a constant temperature of 170 °C during batch sample preparation.

Characterizations

To find out what kinds of crystals were in the samples, we used X-ray diffraction (XRD) on a Malvern Panalytical diffractometer with Cu Kα (40 kV, 15 mA). Analyses were carried out at a scan speed of 5°/min, over a range from 4 to 50°, at a wavelength of 1.54 Å and a step size of 0.02°. The surface morphology was observed using a scanning electron microscope (SEM) in conjunction with a focused ion beam (Scios 2 Dual Beam). The infrared spectra of zeolites were obtained using Fourier transform infrared spectroscopy (FTIR) and an INVENIO spectrometer.

Results and discussion

Effect of alkalinity

Structure and crystallinity

Alkalinity, defined as the concentration of hydroxide ions (OH-) in the gel solution, plays a decisive role in zeolite purity, morphology and crystallinity. The results of the X-ray diffraction (XRD) analyses shown in Figure 1 illustrate the effects of variations in the OH-/Si ratio (between 0.39 and 0.59) on the crystalline phase obtained. An OH-/Si ratio of 0.39 (S1) favors the formation of pure, well-crystallized mordenite. However, as this ratio increases to 0.49 (S2), a slight decrease in peak intensity is observed. An even higher ratio (0.59) (S3) leads to the formation of another thermodynamically more stable zeolitic phase, identified as analcime.

Alkalinity control is crucial to the crystallization process. At an alkalinity ratio (OH^-/Si =0.39) (S1), pure, well-crystallized mordenite is obtained and crystal growth conditions are optimal.

However, when alkalinity exceeds certain thresholds (OH-/Si =0.49), an increase in nucleation rate is observed, generating a large number of small nuclei. The latter, competing for Si and Al nutrients, limit individual crystal growth, resulting in the reduction in the crystal size (see Table 1).

High alkalinity (OH^-/Si =0.59) also affects the stability of nuclei over a prolonged period and favours the appearance of secondary phases (Hamidi et al, 2011). In addition, it influences the formation of hydroxyl groups on the mordenite surface, thus modifying its reactive and catalytic properties (Limousy et al, 2013). Crystallization kinetics as well as the final phase obtained are strongly influenced by the key parameters such as the OH^-/Si and H_2O/SiO_2 ratios (Larlus and Valtchev, 2004; Zhang et al, 2018)

Table 1 – Effect of varying parameters on the crystal size, the grain size and the crystal phases.

sample	Synthesis condition					Product characterization					
	Composition (molar ratio)			Crystallization time (h)	Crystallization temperature (°C)	Crystal phase (a)	SiO_2/Al_2O_3 (molar ratio)	Crystallite size (b) (nm)	Grain length a(μm)(c)	Grain width b(μm)(c)	Grain height c(μm)(c)
	OH^-/Si	SiO_2/Al_2O_3	H_2O/SiO_2								
1	0.39	30	18.66	24	190	MOR	10.6	43.11	11	5.57	13.07
2	0.49	30	18.66	24	190	MOR	7.8	38.45	8.86	5.21	13.93
3	0.59	30	18.66	24	190	ANA/ MOR	21.2	37.03	-	-	-
4	0.93	15	37.33	24	190	ANA	4.8	41.49	-	-	-
5	0.19	60	9.33	24	190	Amorph	-	-	-	-	-
6	0.39	30	18.66	48	170	MOR	10.48	28.81	1.4	0.73	0.67
7	0.39	30	18.66	72	170	MOR	9.62	30.48	1.35	0.71	0.48

XRD patterns are used to identify the crystal phases (a); MOR, ANA, and Amorph stand for mordenite, analcime, and amorphism, respectively. (b)Shows the crystal size for each sample, calculated using the Scherrer equation. (c)Average dimensions of thirty grains selected from the SEM image, classified according to length, width and height.

Vibrational groups

Figure 2 presents the Fourier Transform Infrared Spectroscopy (FTIR) results of the synthetic products at different alkalinity ratios. For OH^{-}/Si (0.39), the significant bands are as follows. Large bands at 3339.52 and 3240.43 cm^{-1} are due to the asymmetrical stretching vibration of isolated silanol groups (Si-OH) and the stretching of the absorbed water molecules onto the solid surface (Hincapie et al, 2004). A narrow band of low intensity is centered at 1645.03 cm^{-1} which is attributed to the flexion vibration of residual water molecules (H-O-H) in the zeolite voids (Aloulou et al, 2017; Gili and Conato, 2018). The absorption band at 1185.45 cm^{-1} represents the external asymmetrical stretch vibration between the zeolitic SiO_4 and AlO_4 tetrahedra (De Macedo et al, 2004; Gili and Conato, 2018). The band at 1001.50 cm^{-1} corresponds to the asymmetrical stretch vibration of the tetrahedric bonds (TO), while the low intensity bands at 807.65 cm^{-1} and 767.07 cm^{-1} refer to the symmetric stretch of the internal tetrahedral. The thin bands at 700.62 and 629.60 cm^{-1} represent the symmetrical stretching vibration of the external bonds (Aloulou et al, 2017). A centered band at 552.40 cm^{-1} corresponds to the vibration of the five-chain rings of the tetrahedral (V. Rahbari et al, 2017). The results confirm the presence of zeolitic and/or aluminosilicate materials.

On the other hand, the FTIR spectra associated with the alkalinity OH^{-}/Si (0.49) appear to show a strong analogy with those for OH^{-}/Si (0.39), except that the absorption bands for the hydroxyl group (-OH) and the bending vibrations of water molecules (H-O-H) show lower intensities, suggesting a reduction in moisture content (M. Gili and Conato, 2019). The band at 1000.17 cm^{-1} corresponds to the asymmetric stretching vibration of tetrahedral bonds (TO) and becomes more pronounced with increasing alkalinity. This feature is specific to amorphous aluminosilicates, where the tetrahedra have the freedom to vibrate without a specific constraint, unlike crystalline zeolites, which feature a regular structure, thus limiting certain tetrahedra vibrations due to their confinement within a fixed lattice or framework (Gili and Conato, 2018).

Seen from another angle, the FTIR spectra of OH^{-}/Si (0.59) appear closely similar to those of OH^{-}/Si (0.39), with the exception of the intensification of all absorption bands, suggesting the presence of a different type of zeolite to that observed for OH^{-}/Si (0.39) and OH^{-}/Si (0.49). However, the band at 1027.61 cm^{-1}, corresponding to the asymmetric stretching vibration of the tetrahedral (TO) bonds, remains unchanged, indicating the persistence of a regular structure.

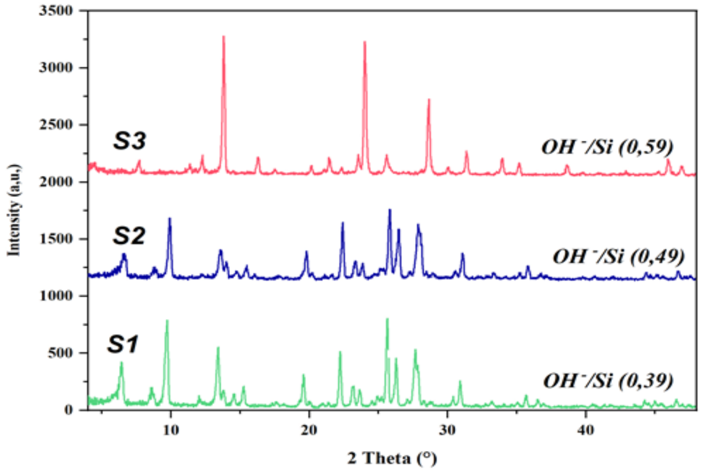

Figure 1 – XRD models of the synthesized MOR samples with various alkalinity ratios

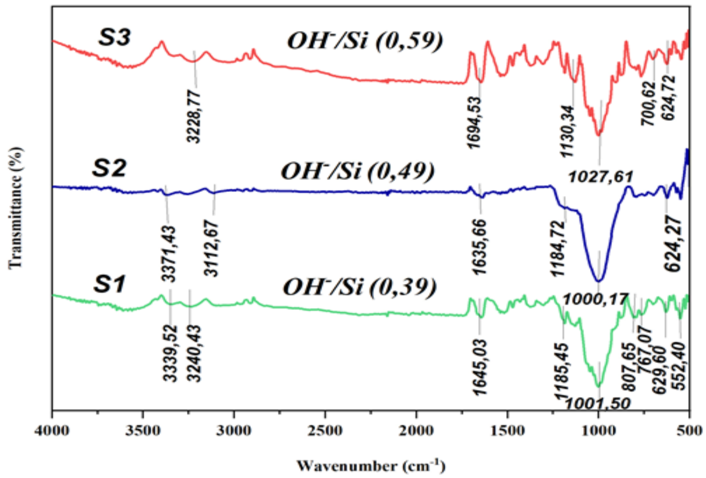

Figure 2 – FTIR spectra of the MOR samples synthesized with different alkalinity ratios

Morphology

Figures 3a to 3c show the SEM images of the synthetic powder products with different alkalinity ratios.

The synthesized sample with an OH^-/Si ratio of 0.39 (Figure 3a) consists of grains with clearly defined linear edges. A significant proportion of these grains have a hexagonal shape, although most are irregular in size and morphology. Grain crystals measure on average:

Length: 11 μm,

Width: approximately 5.57 μm, and

Height: about 13.07 μm.

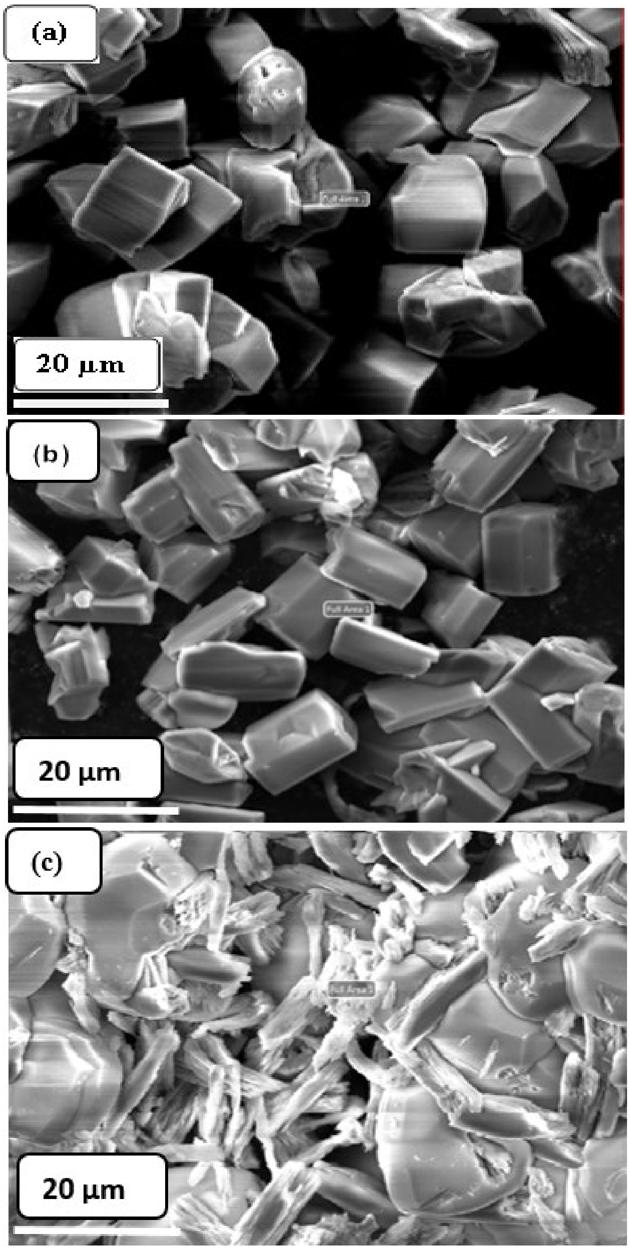

Figure 3 – SEM images of the synthesized MOR samples synthesized with different alkalinity ratios (a) OH^-/Si (0.39), (b) OH^-/Si (0.49), (c) OH^-/Si (0.59).

The synthesized sample with an OH^{-}/Si ratio of 0.49 (Figure 3b) is characterized by grains of irregular shape. The bulk grains show a hexagonal configuration with average dimensions:

Length: 8.857 µm,

Width: about 5.21 µm, and

Height: about 13.93 µm.

The synthetic powder with an OH^{-}/Si ratio of 0.59 (Figure 3c) is composed of spherical-shaped grains, corresponding to the analcime phase. Some grains appear fragmented or damaged due to very high alkalinity, producing amorphous mordenite.

Effect of the SiO_2/Al_2O_3 ratio

Structure and crystallinity

Figure **4** shows diffractograms of the zeolites produced by hydrothermal synthesis at different SiO_2/Al_2O_3 ratios. At a SiO_2/Al_2O_3 ratio of 30 (S1), the resulting product exhibits a high degree of crystallinity. Clearly defined diffraction peaks appear at angles 2θ = 6.43, 9.73, 13.42, 19.59, 22.23, 25.63, 26.26, 27.66, corresponding respectively to the (110), (200), (111), (330), (150), (202), (350), (511) crystal planes of mordenite. These results confirm the formation of the mordenite phase, with a crystallite size measured at 43 nm, testifying to efficient crystallization.

At a lower SiO_2/Al_2O_3 ratio of around 15 (S4), sharp, well-defined peaks were detected at angles 2θ = 15.82, 18.30, 26.01, 30.62, 33.40, 35.93, 37.13, corresponding to the (211), (220), (400), (332), (431), (521), (440) crystal planes characteristic of analcime zeolite (Gili and Conato, 2018; Güngör and Özen, 2021). In addition, further peaks at 2θ = 14.30, 23.45, 27.62 were identified, corresponding to the (021), (002), (511) planes of mordenite, respectively.

The appearance of the analcime phase is generally associated with a low SiO_2/Al_2O_3 ratio or a prolonged crystallization time during mordenite synthesis (Gili and Conato, 2018; Mohamed et al, 2005). This phase is thermodynamically favored under such conditions, as it can incorporate a greater amount of aluminum into its structure. Consequently, analcime appears as a competing product to mordenite when the SiO_2/Al_2O_3 ratio is low and under conditions of high alkalinity.

Conversely, a high SiO_2/Al_2O_3 ratio, such as 60 (S5), alters crystallinity due to alkalinity deficiency. Undissolved silica, which remains unreactive, prevents adequate dissolution of raw materials and hampers the formation of crystalline structures. To achieve even higher SiO_2/Al_2O_3

ratios, up to 100, the use of organic templates is necessary, in line with previous work (Mohamed et al, 2005).

Vibrational group

Figure 5 shows the FTIR spectra of the samples synthesized at different SiO_2/Al_2O_3 ratios. The functional groups detected are characteristic of zeolites and/or aluminosilicates. The FTIR spectrum of the sample synthesized with a SiO_2/Al_2O_3 ratio of 15 (S1) appears closely similar to that obtained with a ratio of 30 (previously interpreted in Section1), with the exception of the intensification of all absorption bands. This indicates the existence of another variety of zeolite.

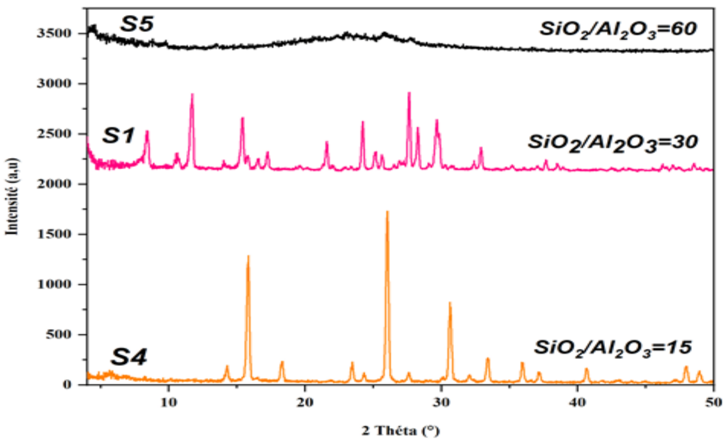

Figure 4 – XRD patterns of the MOR samples synthesized with different SiO_2/Al_2O_3 ratios

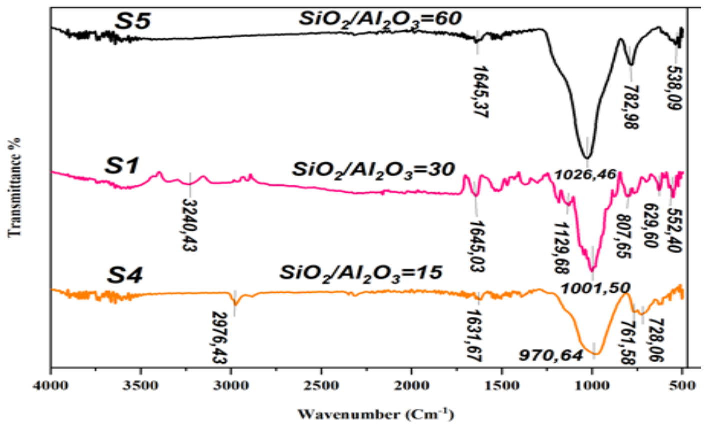

Figure 5 – FTIR spectra of the MOR samples synthesized with different SiO_2/Al_2O_3 ratios

For the sample synthesized with a very high SiO_2/Al_2O_3 ratio, around 60, we observe almost the same vibrational bands as those present in the samples with ratios of 15 and 30. However, the band at 1026.46 cm^{-1}, corresponding to the asymmetric stretching vibration of the tetrahedral (TO) bonds, presents a higher intensity, suggesting a significant amount of amorphous phases, which is in line with the results obtained by X-ray diffraction.

Morphology

Scanning electron microscopy (SEM) images of the synthesized products are shown in Figure 6.

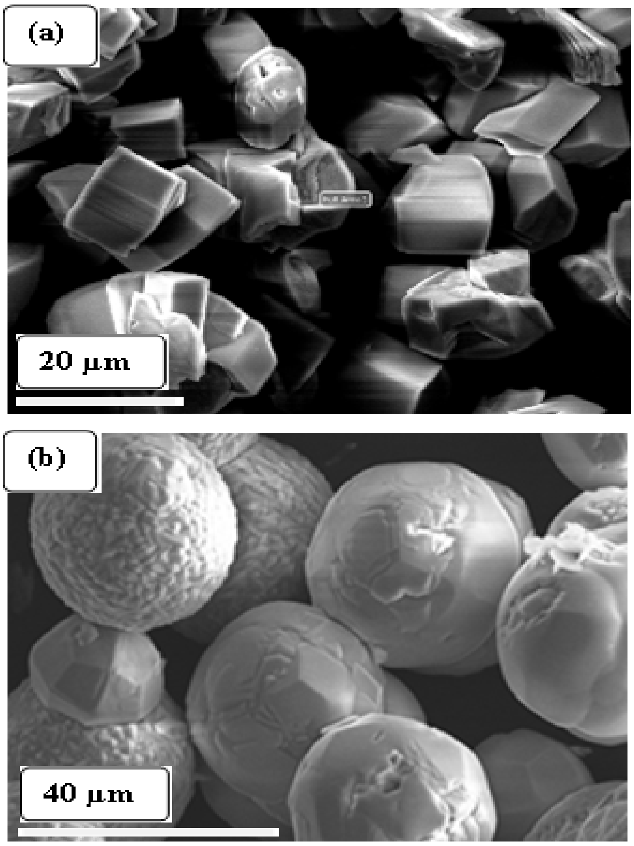

Figure 6 – SEM images of the MOR samples synthesized with different SiO2/Al2O3 ratios (a) SiO2/Al2O3=30, (b) SiO2/Al2O3=15

The sample prepared with an SiO_2/Al_2O_3 ratio of 30 is shown in Figure 6a. It consists of particles with well-defined contours although most of them display an irregular shape. A significant proportion of these particles adopt a hexagonal shape. For the sample synthesized with a SiO_2/Al_2O_3 ratio of 15, spherical analcime single crystals with an irregular surface were obtained, as shown in Figure 6b. Spheres with jagged contours can be observed, while others have a dodecahedron-like appearance, which is characteristic of analcime as it is commonly encountered (Chen et al, 2017).

Effect of the crystallization time

Structure and crystallinity

Figure 7 shows the XRD patterns for mordenite (MOR) synthesized at a constant temperature of 170°C with variable crystallization times. These patterns reveal a high degree of crystallinity in the two samples analyzed (S6) (S7). The XRD spectrum of the sample crystallized for 48 hours is comparable to that obtained after 72 hours, indicating that the structural stability of mordenite is maintained even after prolonged crystallization, without the appearance of undesirable secondary phases.

However, very short crystallization times lead to the formation of amorphous phases, as reported in Gili's study (M. Gili and Conato, 2019). Conversely, excessively long crystallization times can lead to the coexistence of several crystalline phases. The analysis also shows that longer crystallization times favour an increase in crystallite size. This is explained by the longer time available for crystallite growth before the system reaches the thermodynamic equilibrium.

The work of Zhu et *al* (Nazir et al, 2020; Zhu et al, 2014), confirms the significant influence of crystallization time on crystallite growth and dehydration performance of mordenite membranes. This research indicates that longer crystallization times enable increased crystal growth, which improves material performance. In addition, further studies (Zhu et al, 2016) show that longer crystallization times promote better organization of crystalline structures, leading to larger, more homogeneous crystallites.

Vibrational group

Figure 8 shows the FTIR spectra of the synthesized samples at different crystallization times. Both samples show the same profile in the IR spectra. Thus, the samples reveal vibrational bands typical of mordenite (Klunk et al, 2020). The FTIR spectra of mordenite show two vibrational bands of 3336.02 cm^{-1} and 3232.15 cm^{-1} for the sample synthesized at 170 °C for 48 hours and 3334.21 cm^{-1} for the sample synthesized at 170 °C for 72 hours associated with silanol end groups (Si-O-H and Si-OH-Al). In addition, the H-OH bending bands were observed at 1694.14 cm^{-1} and

1645.46 cm^{-1}, while the absorption bands at 1130.23 cm^{-1} and 1130.04 cm^{-1} represent the external asymmetric stretching vibration between the SiO_4 and AlO_4 tetrahedra of zeolite. Vibrational stretching was found at 1027.51 cm^{-1} and 1001.11 cm^{-1}, linked to the TO group. The wavelengths of (808.20 cm^{-1} - 794.38 cm^{-1}), (626.53 cm^{-1} - 605.34 cm^{-1}) and (574.41 cm^{-1} - 549.62 cm^{-1}) for both spectra are related to Al-O-Al, Si-O-Si vibrations, and internal asymmetric stretching of Al-O and Si-O (Klunk et al, 2020).

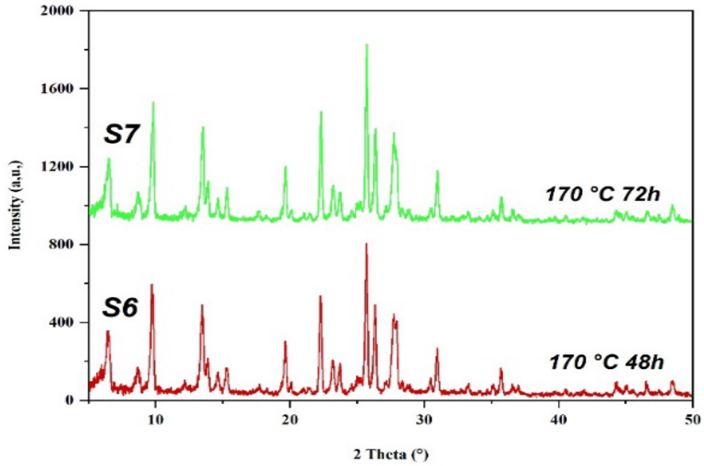

Figure 7– XRD patterns of the MOR samples synthesized with different crystallization times (48 hours and 72 hours)

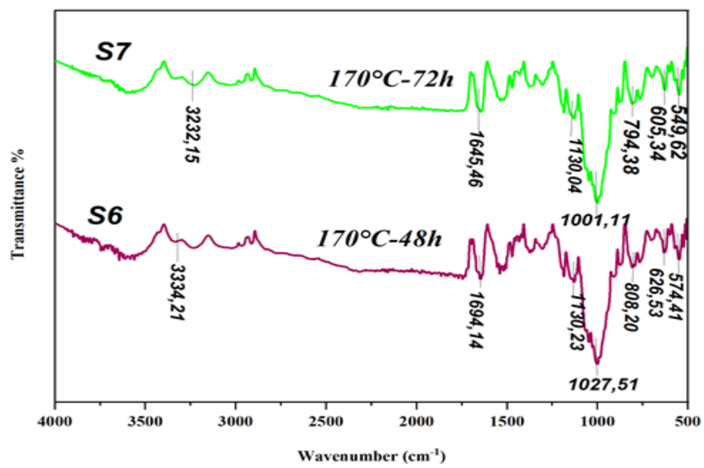

Figure 8 – FTIR spectra of the MOR samples synthesized with different crystallization times (48 and 72 hours)

Morphology

Figures 9a and 9b show the SEM images of the powder products synthesized at varying crystallization times. The sample crystallized for 48 hours is composed of hexagonal-shaped particles with surprisingly linear, well-defined edges, while the other grains are irregular in size and shape. The grain crystals have an average size of a = 1.4 μm, b = 0.73 μm, and c = 0.67 μm. In parallel, the sample crystallized over 72 hours is composed of particles of various sizes and irregular shapes, while the bulk particles have rounded edges. The grain crystals have a length of a = 1.35 μm, a width of b = 0.71 μm, and a height of c = 0.48 μm. The results demonstrate that crystallization time has an impact on particle size and morphology.

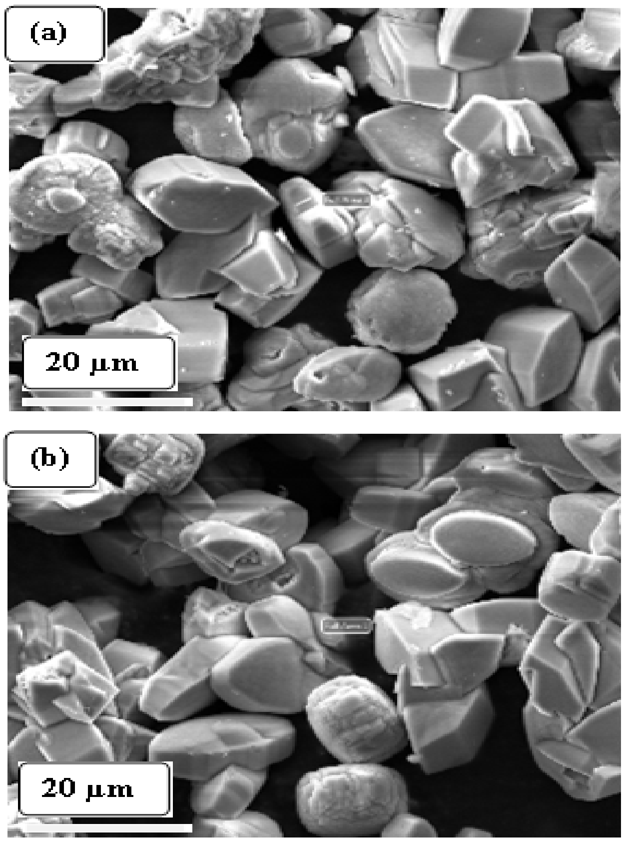

Figure 9 – SEM micrographs of the MOR samples synthesized with different crystallization times (a) 48 hours and (b) 72 hours

Conclusions

This study underscores the critical importance of controlling synthesis parameters to achieve the desired zeolite phase, particularly mordenite. Among these parameters, the OH^-/Si and SiO_2/Al_2O_3 ratios are pivotal in optimizing the crystallinity and purity of the resulting phase. A well-calibrated OH^-/Si ratio promotes the formation of pure, crystalline mordenite, whereas deviations from the optimal value can lead to the emergence of impure or undesirable phases. Similarly, a balanced SiO_2/Al_2O_3 ratio of 30 has been shown to favor the formation of crystalline mordenite. Deviations from this ratio can result in alternative phases, such as analcime or amorphous materials, highlighting the SiO_2/Al_2O_3 ratio as a key determinant of the crystalline phases formed and their degree of crystallinity.

In addition to chemical composition, crystallization time plays a decisive role. A duration of 48 hours is sufficient to produce well-crystallized mordenite, while longer crystallization periods enhance structural stability but may lead to morphological irregularities. Crystallization time is therefore a critical parameter in mordenite synthesis, influencing not only the crystal structure but also the material's functional properties. Striking the right balance is essential to optimize crystal growth while minimizing the formation of amorphous or secondary phases.

These findings provide valuable insights for the design and optimization of zeolite materials. By carefully controlling synthesis parameters, it is possible to develop zeolites with tailored properties for a wide range of applications, paving the way for advancements in material science and industrial applications.

References

Aloulou, H., Bouhamed, H., Ghorbel, A., Ben Amar, R., Khemakhem, S., 2017. Elaboration and characterization of ceramic microfiltration membranes from natural zeolite: application to the treatment of cuttlefish effluents. *Desalination and Water Treatment* 95, pp.9–17. Available at: https://doi.org/10.5004/dwt.2017.21348

Bajpai, P.K., 1986. Synthesis of mordenite type zeolite. *Zeolites* 6(1), pp.2–8. Available at: https://doi.org/10.1016/0144-2449(86)90002-3

Bolshakov, A., Romero Hidalgo, D.E., van Hoof, A.J.F., Kosinov, N., Hensen, E.J.M., 2019. Mordenite Nanorods Prepared by an Inexpensive Pyrrolidine-based Mesoporogen for Alkane Hydroisomerization. *ChemCatChem* 11(12), pp.2803–2811. Available at: https://doi.org/10.1002/cctc.201900298

Borissenko, E., n.d. 2008. *Étude structurale par diffraction, absorption des rayons X et simulations Monte-Carlo de matériaux zéolithiques*. PhD thesis. Laboratory of Crystallography and Modeling of Mineral and Biological Materials. (In Frensh) Available at: https://theses.fr/2008NAN10074

Brezicki, G., Zheng, J., Paolucci, C., Schlögl, R., Davis, R.J., 2021. Effect of the Co-cation on Cu Speciation in Cu-Exchanged Mordenite and ZSM-5 Catalysts for the Oxidation of Methane to Methanol. *ACS Catalysis*. 11(9), pp.4973–4987. Available at: https://doi.org/10.1021/acscatal.1c00543

Chen, J., Ma, H., Liu, C., Yuan, J., 2017. Synthesis of Analcime Crystals and Simultaneous Potassium Extraction from Natrolite Syenite. *Advances in Materials Science and Engineering* 2017(1), pp.1–9. Available at: https://doi.org/10.1155/2017/2617597

De Macedo, J.L., Dias, S.C.L., Dias, J.A., 2004. Multiple adsorption process description of zeolite mordenite acidity. *Microporous and Mesoporous Materials* 72(1-3),pp.119–125.Availableat:https://doi.org/10.1016/j.micromeso.2004.04.009

Gili, M., Conato, M., 2019. Synthesis and characterization of mordenite-type zeolites via hydrothermal method using silica gel and sodium aluminate as Si and Al sources at varying temperature. In : *Banten 2018 : International Symposium on Frontier of Applied Physics,* Indonesia. November 1-2. Journal of Physics.: Conf. Ser. 1191, 012038. Available at: https://doi.org/10.1088/1742-6596/1191/1/012038

Gili, M.B.Z., Conato, M.T., 2019. Adsorption uptake of mordenite-type zeolites with varying Si/Al ratio on Zn 2+ ions in aqueous solution. *Materials Research Express* 6(4), 045508. Available at: https://doi.org/10.1088/2053-1591/aafc08

Gili, M.B.Z., Conato, M.T., 2018. Synthesis and characterization of mordenite-type zeolites with varying Si/Al ratio. *Materials Research Express* 6(3), 015515. Available at: https://doi.org/10.1088/2053-1591/aae8db

Golden, T.C., Jenkins, R.G., 1981. Ion exchange in mordenite. Verification of the triangle rule. *Journal of Chemical and Engineering Data* 26(4), pp.366–367. Available at: https://doi.org/10.1021/je00026a005

Güngör, D., Özen, S., 2021. Development and characterization of clinoptilolite-, mordenite-, and analcime-based geopolymers: A comparative study. *Case Studies in Construction Materials* 15, e00576. Available at: https://doi.org/10.1016/j.cscm.2021.e00576

Hamidi, F., Bengueddach, A., Renzo, F.D., Fajula, F., n.d. Control of Crystal Size and Morphology of Mordenite. *Catalysis Letters* 87, pp.149-152. Available at: http://doi.org/10.1023/A:1023439121921

Hamidi, F., Petitto, C., Signorile, C., Delahay, G., Bengueddach, A., 2011. Selective catalytic reduction of nitric oxide with ammonia over Fe-MOR catalysts prepared from Fe(acac)3 precursor. *Reaction Kinetics, Mechanisms and Catalysis* 104, pp.429–436. Available at: https://doi.org/10.1007/s11144-011-0359-3

Hincapie, B.O., Garces, L.J., Zhang, Q., Sacco, A., Suib, S.L., 2004. Synthesis of mordenite nanocrystals. *Microporous and Mesoporous Materials* 67(1), pp.19–26. Available at: https://doi.org/10.1016/j.micromeso.2003.09.026

Jia, X., Khan, W., Wu, Z., Choi, J., Yip, A.C.K., 2019. Modern synthesis strategies for hierarchical zeolites: Bottom-up versus top-down strategies. *Advanced Powder Technology* 30(3), pp.467–484. Available at: https://doi.org/10.1016/j.apt.2018.12.014

Khalil, U., Muraza, O., 2016. Microwave-assisted hydrothermal synthesis of mordenite zeolite: Optimization of synthesis parameters. *Microporous and Mesoporous Materials* 232, pp.211–217. Available at: https://doi.org/10.1016/j.micromeso.2016.06.016

Klunk, M.A., Schröpfer, S.B., Dasgupta, S., Das, M., Caetano, N.R., Impiombato, A.N., Wander, P.R., Moraes, C.A.M., 2020. Synthesis and characterization of mordenite zeolite from metakaolin and rice husk ash as a source of aluminium and silicon. *Chemical Papers*. 74, pp.2481–2489. Available at: https://doi.org/10.1007/s11696-020-01095-4

Kordala, N., Wyszkowski, M., 2024. Zeolite Properties, Methods of Synthesis, and Selected Applications. *Molecules* 29(5), 1069. Available at: https://doi.org/10.3390/molecules29051069

Larlus, O., Valtchev, V.P., 2004. Crystal Morphology Control of LTL-Type Zeolite Crystals. *Chemistry of Materials*. 16(17), pp.3381–3389. Available at: https://doi.org/10.1021/cm0498741

Le, H.V., Parishan, S., Sagaltchik, A., Göbel, C., Schlesiger, C., Malzer, W., Trunschke, A., Schomäcker, R., Thomas, A., 2017. Solid-State Ion-Exchanged Cu/Mordenite Catalysts for the Direct Conversion of Methane to Methanol. *ACS Catalysis*. 7(2), pp.1403–1412. Available at: https://doi.org/10.1021/acscatal.6b02372

Li, G., Hou, H., Lin, R., 2011. Rapid synthesis of mordenite crystals by microwave heating. *Solid State Sciences* 13(3), pp.662–664. Available at: https://doi.org/10.1016/j.solidstatesciences.2010.12.040

Li, J., Gao, M., Yan, W., Yu, J., 2023. Regulation of the Si/Al ratios and Al distributions of zeolites and their impact on properties. *Chemical Science*. 14(8), pp.1935–1959. Available at: https://doi.org/10.1039/D2SC06010H

Lima, E.G., Medeiros Nascimento Silva, F., Lins Almeida Barbosa, T., Freire Rodrigues, M.G., 2023. Organic Structure-Directing Agent Free Synthesis of Mordenite with Seeds, Used as A Support for Mo Catalysts in the Transesterification of Soybean Oil. *Catalysis Research* 03(2), pp.1–19. Available at: https://doi.org/10.21926/cr.2302015

Limousy, L., Dutournié, P., Chevereau-Landais, E., 2013. Description of the preferential transport of monovalent salts through Na–mordenite membrane: Physico-chemical aspects. *Microporous and Mesoporous Materials* 167, pp.133–136. Available at: https://doi.org/10.1016/j.micromeso.2012.01.025

Mohamed, M.M., Nohman, A.K.H., Zaki, M.I., 2006. Development of Catalytic Properties of Mordenite Zeolite via Chemical Modification. *ChemInform* 37(38), pp.79–99. Available at: https://doi.org/10.1002/chin.200638241

Mohamed, M.M., Salama, T.M., Othman, I., Ellah, I.A., 2005. Synthesis of high silica mordenite nanocrystals using o-phenylenediamine template. *Microporous and Mesoporous Materials* 84(1-3), pp.84–96. Available at: https://doi.org/10.1016/j.micromeso.2005.05.017

Narayanan, S., Tamizhdurai, P., Mangesh, V.L., Ragupathi, C., Santhana Krishnan, P., Ramesh, A., 2021. Recent advances in the synthesis and applications of mordenite zeolite – review. *RSC Advances*. 11(1), pp.250–267. Available at: https://doi.org/10.1039/D0RA09434J

Nasser, G.A., Kurniawan, T., Tago, T., Bakare, I.A., Taniguchi, T., Nakasaka, Y., Masuda, T., Muraza, O., 2016. Cracking of n-hexane over hierarchical MOR zeolites derived from natural minerals. *Journal of the Taiwan Institute of Chemical Engineers* 61, pp.20–25. Available at: https://doi.org/10.1016/j.jtice.2015.11.025

Nazir, L.S.M., Yeong, Y.F., Chew, T.L., 2020. Methods and synthesis parameters affecting the formation of FAU type zeolite membrane and its separation performance: a review. *Journal of Asian Ceramic Societies* 8(3), pp.553–571. Available at: https://doi.org/10.1080/21870764.2020.1769816

Pérez-Botella, E., Valencia, S., Rey, F., 2022. Zeolites in Adsorption Processes: State of the Art and Future Prospects. *Chemical Reviews*. 122(24), pp.17647–17695. Available at: https://doi.org/10.1021/acs.chemrev.2c00140

V. Rahbari, Z., Khosravan, M., N. Kharat, A., 2017. Dealumination of mordenite zeolite and its catalytic performance evaluation in m-xylene isomerization reaction. *Bulletin of the Chemical Society of Ethiopia*. 31(2), pp.281-289. Available at: https://doi.org/10.4314/bcse.v31i2.9

Zhang, L., Xie, S., Xin, W., Li, X., Liu, S., Xu, L., 2011. Crystallization and morphology of mordenite zeolite influenced by various parameters in organic-free synthesis. *Materials Research Bulletin* 46(6), pp.894–900. Available at: https://doi.org/10.1016/j.materresbull.2011.02.018

Zhang, Q., Chen, G., Wang, Y., Chen, M., Guo, G., Shi, J., Luo, J., Yu, J., 2018. High-Quality Single-Crystalline MFI-Type Nanozeolites: A Facile Synthetic Strategy and MTP Catalytic Studies. *Chemistry of Materials*. 30(8), pp.2750–2758. Available at: https://doi.org/10.1021/acs.chemmater.8b00527

Zhu, M.-H., Hua, X.-M., Liu, Y.-S., Hu, H., Li, Y., Hu, N., Kumakiri, I., Chen, X.-S., Kita, H., 2016. Influences of Synthesis Parameters on Preparation of Acid-Stable and Reproducible Mordenite Membrane. *Industrial & Engineering Chemistry Research* 55(47), pp.12268–12275. Available at: https://doi.org/10.1021/acs.iecr.6b02125

Zhu, M.-H., Xia, S.-L., Hua, X.-M., Feng, Z.-J., Hu, N., Zhang, F., Kumakiri, I., Lu, Z.-H., Chen, X.-S., Kita, H., 2014. Rapid Preparation of Acid-Stable and High Dehydration Performance Mordenite Membranes. *Industrial & Engineering Chemistry Research* 53(49), pp.19168–19174. Available at: https://doi.org/10.1021/ie501248y

Efecto de las variaciones de parámetros sobre la cristalización de la zeolita mordenita

Ikram Yssaad[a], **autor de correspondencia**, *Fatiha* Hamidi[a], *Denis* Luart[b]

[a] Universidad de Ciencias y Tecnología Mohamed Boudiaf, Facultad de Química, Laboratorio de Ecomateriales Funcionales y Nanoestructurados, Orán, Argelia.

[b] Universidad Tecnológica de Compiègne, ESCOM, Alliance+ Universidad de la Sorbona, TIMR, Compiègne, Francia.

CAMPO: materiales, tecnología química
TIPO DE ARTÍCULO: artículo científico original

Resumen:

Introducción/objetivo: Este estudio destaca la importancia de los parámetros de síntesis en la cristalización de la zeolita mordenita. El control preciso de la relación SiO_2/Al_2O_3, la alcalinidad y el tiempo de cristalización da como resultado cristales de mordenita con alta cristalinidad y pureza óptima, evitando a la vez la formación de fases secundarias o amorfas.

Métodos: Los materiales se prepararon mediante el método hidrotérmico, utilizando gel de sílice y aluminato de sodio como fuentes de silicio y aluminio, respectivamente. Se modificaron diversos parámetros de síntesis, como la relación molar SiO_2/Al_2O_3, la alcalinidad (OH_2/Si) y el tiempo de cristalización, para evaluar su efecto en la formación de cristales de mordenita. Los experimentos se realizaron a temperatura constante de 170 °C y 190 °C.

Resultados: Los resultados muestran que la relación SiO_2/Al_2O_3 desempeña un papel crucial en la formación de cristales. Una relación baja, como 15, combinada con una alcalinidad alta, favorece la formación de cristales de analcima. Por otro lado, una relación alta, como 30, conduce a la formación de cristales de mordenita con alta cristalinidad y pureza. Sin embargo, cuando esta relación alcanza 60 y se combina con una alcalinidad baja, se impide la nucleación cristalina, dando lugar a la formación de un material amorfo.

En cuanto a la alcalinidad (OH_2/Si), los valores de 0,39 y 0,49 dan lugar a cristales de mordenita puros y bien cristalizados, mientras que valores superiores, como 0,59, conducen a la formación de fases secundarias. En cuanto al tiempo de cristalización, los periodos de 48 y 72 horas a 170 °C produjeron cristales de mordenita puros y bien cristalizados.

Conclusión: Este estudio destaca la importancia de los parámetros de síntesis en la cristalización de la zeolita mordenita. El control preciso de la relación SiO_2/Al_2O_3, la alcalinidad y el tiempo de cristalización da como resultado cristales de mordenita con alta cristalinidad y pureza óptima, evitando a la vez la formación de fases secundarias o amorfas.

Palabras claves: Palabras clave: mordenita, alcalinidad, relación Si/Al, cristalización, zeolita.

Влияние изменений параметров на кристаллизацию цеолита морденита

Икрам ИССААД[а], **корреспондент**, Фатиха ХАМИДИ[а], Денис ЛУАРТ[б]

[а] Научно-технический университет/Университет науки и технологии имени

Мохамеда Будиафа, Химический факультет, лаборатория функциональных и наноструктурированных экоматериалов, Оран, Алжир.
[б] Компьенский технологический университет, ESCOM, Альянс университетов Сорбонны, TIMR, Компьень, Франция

РУБРИКА ГРНТИ: 61.13.21 Химические процессы,
ВИД СТАТЬИ: оригинальная научная статья

Резюме:

Введение/цель: Данное исследование подчеркивает важность параметров синтеза при кристаллизации цеолита морденита. Точный контроль соотношения SiO_2/Al_2O_3, щелочности и времени кристаллизации позволяет получить кристаллы морденита с высокой кристалличностью и оптимальной чистотой, избегая при этом образования вторичных или аморфных фаз.
Методы: Материалы были получены гидротермальным методом с использованием силикагеля и алюмината натрия в качестве источников кремния и алюминия. Были изменены некоторые параметры синтеза, включая молярное соотношение SiO_2/Al_2O_3, щелочность (OH^-/Si), а также время кристаллизации для того, чтобы оценить их влияние на формирование кристаллов морденита. Эксперименты проводились при постоянной температуре: 170°C и 190°C.
Результаты: Результаты показывают, что соотношение SiO_2/Al_2O_3 играет решающую роль в образовании кристаллов. Низкое соотношение, например, 15 в сочетании с высокой щелочностью способствует образованию кристаллов анальцима. С другой стороны, высокое соотношение, например, 30 приводит к образованию кристаллов морденита с высокой степенью кристалличности и чистоты. Однако когда это соотношение достигает 60 и сочетается с низкой щелочностью, усложняется зарождение кристаллов, что приводит к образованию аморфного материала.
Что касается щелочности (OH-Si), то значения 0, 39 и 0, 49 приводят к образованию чистых, хорошо кристаллизованных кристаллов морденита, а более высокие значения, такие как 0, 59, приводят к образованию вторичных фаз. По времени процесс кристаллизации в течение 48 и 72 часа при 170С привел к образованию чистых, хорошо кристаллизованных кристаллов морденита.
Выводы: Данное исследование подчеркивает важность параметров синтеза при кристаллизации цеолита морденита. Точный контроль соотношения SiO_2/Al_2O_3, щелочности и времени кристаллизации способствует образованию кристаллов морденита с высокой кристалличностью и оптимальной

чистотой, избегая при этом образования вторичных или аморфных фаз.

Ключевые слова: Морденит, щелочность, соотношение Si/Al, кристаллизация, цеолит.

Утицај варијација параметара на кристализацију зеолита морденита

Икрам Исад[а], **аутор за преписку**, Фатиха Хамиди[а]б, Денис Луарт[б]

[а] Универзитет науке и технологије „Мохамед Будијаф”, Хемијски факултет, Лабораторија за функционалне и наноструктуриране екоматеријале, Оран, Алжир.

[б] Универзитет технологије у Компјењу, ESCOM, Савез универзитета Сорбоне, TIMR, Компјењ, Француска.

ОБЛАСТ: материјали, хемијске технологије
КАТЕГОРИЈА (ТИП) ЧЛАНКА: оригинални научни рад

Сажетак:

Увод/циљ: У овом истраживању наглашава се значај параметара синтезе у кристализацији зеолита морденита. Прецизна контрола односа SiO_2/Al_2O_3, алкалности и времена кристализације резултира кристалима морденита високе кристалности и оптималне чистоће, уз избегавање формирања секундарних или аморфних фаза.

Методе: Материјали су припремљени хидротермалном методом, коришћењем силика гела и натријум алумината као извора силицијума, односно алуминијума. Неколико параметара синтезе је варирано, укључујући моларни однос SiO_2/Al_2O_3, алкалност (OH^-/Si), као и време кристализације, како би се проценио њихов утицај на формирање кристала морденита. Експерименти су изведени на константној температури од 170°C и 190°C.

Резултати: Резултати показују да однос SiO_2/Al_2O_3 има кључну улогу у формирању кристала. Низак однос, као што је 15, у комбинацији са високом алкалношћу, фаворизује формирање кристала аналкима. С друге стране, висок однос, као што је 30, доводи до формирања кристала морденита високе кристалности и чистоће. Међутим, када овај однос достигне 60 и комбинује се са ниским алкалитетом, кристална нуклеација је ометана, што доводи до формирања аморфног материјала.

Што се тиче алкалности (OH^-/Si), вредности од 0,39 и 0,49 резултирају чистим, добро кристализованим кристалима морденита, док веће вредности, као што је 0,59, доводе до формирања секундарних фаза. Када се посматра време *кристализације, периоди од 48 и 72 сата на 170°C дали су чисте, добро кристализоване кристале морденита.*

Закључак: Ово истраживање наглашава значај параметара синтезе у кристализацији морденита као врсте зеолита. Прецизна контрола односа SiO_2/Al_2O_3, алкалности и времена кристализације резултира кристалима морденита високе кристалности и оптималне чистоће, уз избегавање формирања секундарних или аморфних фаза.

Кључне речи: морденит, алкалитет, Si/Al однос, кристализација, зеолит.

Paper received on: 13.02.2025.
Manuscript corrections submitted on: 08.03.2025.
Paper accepted for publishing on: 01.04.2025.

REVIEW PAPERS

b-metric like spaces: a survey of concepts and applications

Abdelhamid Moussaoui [1*], *Stojan Radenović* [2]

[1] Faculty of Sciences and Techniques,
Laboratory of Applied Mathematics & Scientific Computing,
Sultan Moulay Slimane University, Beni Mellal, Morocco;
e-mail: a.moussaoui@usms.ma,
ORCID iD: https://orcid.org/0000-0003-4897-1132

[2] Faculty of Mechanical Engineering, University of Belgrade,
Kraljice Marije 16, 11120, Beograd 35, Serbia,
e-mail: sradenovic@mas.bg.ac.rs,
ORCID iD: https://orcid.org/0000-0001-8254-6688

doi https://doi.org/10.5937/vojtehg73-56769

FIELD: Mathematics
ARTICLE TYPE: Review paper

Abstract:

Introduction/Purpose: This paper presents a comprehensive survey of fixed-point results in metric-like spaces, with a particular emphasis on b-metric-like spaces. The purpose of the study was to explore the generalization of several important concepts in fixed point theory, including partial metric spaces, metric-like spaces, and b-metric spaces. This research aimed to contribute to the advancement of fixed-point theory in these generalized settings.

Methods: The study involved reviewing foundational and recent research on fixed-point results in b-metric-like spaces. It focused on summarizing key contributions from the early stages of the field to the present, providing an extensive compilation of results. Additionally, the paper addressed open problems arising from the best proximity results in orthogonal 0-complete b-metric-like spaces.

Results: The results highlighted significant contributions to the theory of fixed points in metric-like spaces, particularly in the context of b-metric-like spaces. The study offered affirmative answers to some open problems concerning the best proximity results in orthogonal 0-complete b-metric-like spaces, further enriching the theoretical framework.

Conclusions: This paper is concluded by advancing the understanding of fixed point theory in generalized metric-like spaces. It provides re-

searchers with valuable insights and references, which could facilitate further exploration and development in this field.

Key words: fixed point theory, b-metric-like spaces, metric-like spaces, partial metric spaces, metric spaces, best proximity results, orthogonal 0-complete spaces, generalizations.

Introduction and preliminaries

Let (X, d) be a metric space, and let $\mathcal{G} : X \to X$ be a mapping. The function $\mathcal{G}$ is defined as a contraction on X if there exists a constant k such that $0 \leq k < 1$ and for all $x, y \in X$, the following inequality holds:

$$d(\mathcal{G}(x), \mathcal{G}(y)) \leq k\, d(x, y).$$

This definition essentially means that $\mathcal{G}$ brings points closer together, with the constant k providing a bound on how much closer. The celebrated Banach Fixed-Point Theorem, established by Stefan Banach in 1922, asserts that any contraction mapping on a complete metric space has a unique fixed point. This powerful result has become a cornerstone of modern analysis and has inspired numerous extensions and generalizations, see (Abkar & Gabeleh, 2013; Chen et al., 2015; Ćirić, 1974; Czerwik, 1993; Gregori & Sapena, 2002; Karapinar, 2014; Kirk, 2003; Mattews, 1994; Mihet, 2008; Mirkov et al., 1994; Moussaoui et al., 2022, 2024; Păcurar & Rus, 2010; Petrusel, 2005; Radenović, 2016a; Suzuki, 2008, 2009; Yang et al., 2020).

Researchers have sought to broaden Banach's theorem by considering more general classes of spaces and mappings. The generalizations primarily follow two avenues: either modifying the underlying metric space or replacing the traditional contraction condition with a more flexible form. Specifically, instead of using a constant k, the contraction condition can be expressed in terms of a function φ that maps $(0, +\infty)$ to itself, i.e., by replacing $kd(x, y)$ with $\varphi(d(x, y))$. These extensions have led to the introduction of new types of generalized metric spaces, such as partial metric spaces, metric-like spaces, b-metric spaces, partial b-metric spaces, and b-metric-like spaces. Each of these spaces provides a different framework for studying contraction mappings, which may hold under conditions that relax or modify traditional distance properties. Berinde and Păcurar Berinde & Păcurar (2022) provided a concise overview of the foundational progress in fixed point theory on b-metric spaces, compiled a collection of key references, and analyzed recent advancements in the field. In 2012, Amini-Harandi Amini-Harandi (2012) developed the concept of metric-like spaces as a broadening of partial metric spaces and established foundational fixed point results that unify and extend previous work. Aleksić et al. Aleksić et al. (2020) simplified proofs for key results in b-metric spaces, showing that contractive conditions ensure b-Cauchyness of Picard sequences, improving the existing results. Monika in Monika (2019) compiles a comprehensive overview of fixed point results in metric-like spaces. The study includes significant findings from their inception to recent advancements. In 2013, Alghamdi et al. Alghamdi et al. (2013) defined b-metric-like spaces, proved fixed point theorems, and applied their results to integral equations. Chunfang Chen et al. Chen et al. (2015) explore fixed point theorems in b-metric-like spaces, generalizing the existing results and applying them to an integral equation. Kastriot Zoto et al. Zoto et al. (2018) introduced (s, p, α)-quasi-contractions and (s, p)-weak contractions, establishing fixed point results in b-metric-like spaces.

These generalized structures have proven useful in various areas of mathematics, particularly in fixed-point theory, where they provide more flexible settings for studying existence and uniqueness theorems. They also find applications in the areas such as computer science, optimization, and dynamical systems. The interplay between these important and diverse generalizations is presented as follows:

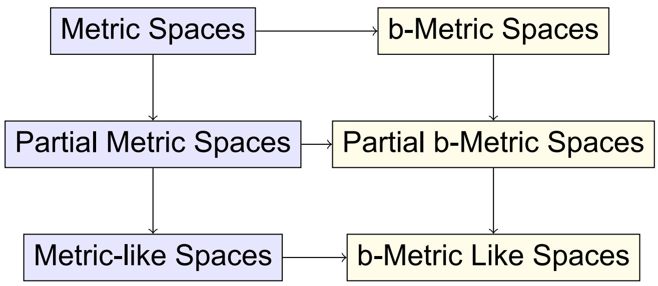

Let us now review the definitions of the six distinct classes of spaces, which encompass the classic metric space and five extended classes of generalized metric spaces.

The concept of a **metric space** was introduced by **Maurice Fréchet** Fréchet (1906) in 1906 during his doctoral work, titled *Sur quelques points du calcul fonctionnel*. This idea marked the beginning of the formal study of abstract spaces equipped with a distance function, forming a foundational aspect of modern analysis and topology.

DEFINITION 1. *Fréchet (1906) Let X be a nonempty set. A mapping $d : X \times X \to \mathbb{R}^+$ is said to be a metric on X if the following conditions holds for all $x, y, z \in X$:*

($\mathcal{M}$1) $d(x,y) = 0$ *if and only if* $x = y$*,*

($\mathcal{M}$2) $d(x,y) = d(y,x)$*, and*

($\mathcal{M}$3) $d(x,z) \leq d(y,x) + d(y,z)$

A pair (X,d) satisfying the above assumptions is a metric space.

The concept of a partial metric space was first introduced by Matthews Mattews (1994), as defined below.

DEFINITION 2. *A mapping $p : X \times X \to \mathbb{R}^+$, where X is a nonempty set, is called a partial metric on X if, for any $x, y, z \in X$, the following conditions hold:*
$(\mathcal{P}1)$ $x = y$ *if and only if* $p(x,x) = p(y,y) = p(x,y)$*,*
$(\mathcal{P}2)$ $p(x,x) \leq p(x,y)$*,*
$(\mathcal{P}3)$ $p(x,y) = p(y,x)$*, and*
$(\mathcal{P}4)$ $p(x,z) \leq p(x,y) + p(y,z) - p(y,y)$.
The pair (X,p) is then referred to as a partial metric space.

Recently, Amini-Harandi (Amini-Harandi, 2012) see also (Amini, 2012) proposed the concept of a metric-like space, which serves as a notable generalization of both partial metric spaces and dislocated metric spaces Aage & Salunke (2008); Sarma & Kumari (2012); Zoto & Hoxha (2012). This new framework extends the traditional notions of distance between elements in a space by relaxing some of the standard conditions of metric spaces. In particular, metric-like spaces allow for the possibility of non-zero values of $\sigma(x,x)$, unlike standard metric spaces where $\sigma(x,x)$ is always zero. This flexibility makes metric-like spaces a powerful tool for studying various types of convergence and continuity in more generalized settings.

DEFINITION 3. *A function $\sigma : X \times X \to \mathbb{R}^+$, where X is a nonempty set, is called a **metric-like function** on X if it satisfies the following conditions for all $x, y, z \in X$:*

(σ_1) $\sigma(x, y) = 0$ implies $x = y$,

(σ_2) $\sigma(x, y) = \sigma(y, x)$ (symmetry), and

(σ_3) $\sigma(x, z) \leq \sigma(x, y) + \sigma(y, z)$ (triangle inequality).

*The pair (X, σ) is referred to as a **metric-like space**. A metric-like on X fulfills all the standard properties of a metric, with the exception that $\sigma(x, x)$ can take a positive value for $x \in X$. Every metric-like function σ on X defines a topology τ_σ on X, with the base given by the family of open σ-balls:*

$$B_\sigma(x, \varepsilon) = \{y \in X : |\sigma(x, y) - \sigma(x, x)| < \varepsilon\}, \quad \text{for all } x \in X \text{ and } \varepsilon > 0.$$

A sequence $\{x_n\}$ in the metric-like space (X, σ) converges to $x \in X$ if and only if $\lim_{n\to+\infty} \sigma(x_n, x) = \sigma(x, x)$.

Let (X, σ) and (Y, τ) be metric-like spaces, and let $\mathcal{G} : X \to Y$ be a continuous mapping. Then,

$$\lim_{n\to+\infty} x_n = x \text{ implies } \lim_{n\to+\infty} \mathcal{G}(x_n) = \mathcal{G}(x).$$

A sequence $\{x_n\}_{n=0}^{+}\infty \subseteq X$ is called σ-Cauchy if the limit $\lim_{m,n\to+\infty} \sigma(x_m, x_n)$ exists and is finite. The metric-like space (X, σ) is complete if every σ-Cauchy sequence $\{x_n\}_{n=0}^{+}\infty$ converges to some $x \in X$ such that

$$\lim_{n\to+\infty} \sigma(x_n, x) = \sigma(x, x) = \lim_{m,n\to+\infty} \sigma(x_m, x_n).$$

It is worth noting that every partial metric space is an example of a metric-like space.

EXAMPLE 1. Consider the set $X = \{0, 1\}$, and let the function $\sigma : X \times X \to \mathbb{R}^+$ be defined as:

$$\sigma(x, y) = \begin{cases} 2 & \text{if } x = y = 0, \\ 1 & \text{if } x \neq y. \end{cases}$$

In this case, the pair (X, σ) forms a metric-like space. However, since $\sigma(0, 0) \nleq \sigma(0, 1)$, we conclude that (X, σ) is not a partial metric space.

The notion of b-metric space was first introduced by Czerwik in his seminal work Czerwik (1993). This concept generalizes the traditional idea of a metric space by relaxing the triangle inequality. Specifically, in a b-metric space, the standard triangle inequality is modified by a constant factor $s \geq 1$.

DEFINITION 4. *A b-metric on a nonempty set X is a function $b : X \times X \to [0, +\infty)$ such that for all $x, y, z \in X$ and a constant $K \geq 1$, the following three conditions hold true:*

(b1) $b(x, y) = 0$ *if and only if* $x = y$*,*

(b2) $b(x, y) = b(y, x)$*, and*

(b3) $b(x, y) \leq s(b(x, z) + b(z, y))$*.*

The pair (X, b) is referred to as a ***b-metric space****.*

DEFINITION 5. *Alghamdi et al. (2013) A b-metric-like on a nonempty set X is a function $\mathcal{D} : X \times X \to [0, +\infty)$ such that for all $x, y, z \in X$ and a constant $s \geq 1$, the following three conditions hold true:*

$(\mathcal{D}1)$ $\mathcal{D}(x, y) = 0$ *implies* $x = y$*,*

$(\mathcal{D}2)$ $\mathcal{D}(x, y) = \mathcal{D}(y, x)$*, and*

$(\mathcal{D}3)$ $\mathcal{D}(x, y) \leq s(\mathcal{D}(x, z) + D(z, y))$*.*

The pair $(X, \mathcal{D})$ is referred to as a ***b-metric-like space****.*

EXAMPLE 2. Alghamdi et al. (2013); Chen et al. (2015)

1) Consider the set $X = [0, +\infty)$ and define a function $\mathcal{D} : X \times X \to [0, +\infty)$ by $\mathcal{D}(x, y) = (x + y)^2$. The pair $(X, \mathcal{D})$ forms a b-metric-like space with a constant $s = 2$. However, $(X, \mathcal{D})$ is neither a b-metric space nor a metric-like space. To verify, for any $x, y, z \in X$, we observe:

$$\mathcal{D}(x, y) = (x+y)^2 \leq (x+z+z+y)^2 = (x+z)^2+(z+y)^2+2(x+z)(z+y),$$

and since

$$(x + z)^2 + (z + y)^2 + 2(x + z)(z + y) \leq 2\big[(x + z)^2 + (z + y)^2\big],$$

it follows that

$$\mathcal{D}(x, y) \leq 2\big(\mathcal{D}(x, z) + \mathcal{D}(z, y)\big),$$

thus satisfying condition $(\mathcal{D}3)$. Additionally, conditions $(\mathcal{D}1)$ and $(\mathcal{D}2)$ are also satisfied.

A. Moussaoui and S. Radenović, b-Metric Like Spaces: A Survey of Concepts and Applications, pp.1068–1097

2) Let $X = [0, +\infty)$, and define the function $\mathcal{D} : X \times X \to [0, +\infty)$ by $\mathcal{D}(x, y) = \left[\max\{x, y\}\right]^2$. In this case, the pair $(X, \mathcal{D})$ forms a b-metric-like space with the constant $s = 2$. However, it is evident that $(X, \mathcal{D})$ does not qualify as either a b-metric space or a metric-like space.

3) Consider the set $X = \{0, 1, 2\}$ and define the function $\mathcal{D} : X \times X \to [0, +\infty)$ by:

$$\mathcal{D}(x, y) = \begin{cases} 2, & \text{if } x = y = 0, \\ \frac{1}{2}, & \text{otherwise.} \end{cases}$$

The pair $(X, \mathcal{D})$ forms a b-metric-like space with the constant $s = 2$.

4) Let $C_b(X) = \{\mathcal{G} : X \to \mathbb{R} : \sup_{x \in X} |\mathcal{G}(x)| < +\infty\}$. Define the function $\mathcal{D} : X \times X \to \mathbb{R}^+$ by:

$$\mathcal{D}(\mathcal{G}, \mathcal{H}) = \sqrt[3]{\sup_{x \in X} (|\mathcal{G}(x)| + |\mathcal{H}(x)|)^3}, \quad \text{for all } \mathcal{G}, \mathcal{H} \in C_b(X).$$

The function $\mathcal{D}$ satisfies the properties of a b-metric-like with the constant $s = \sqrt[3]{4}$, making $(X, \mathcal{D}, \sqrt[3]{4})$ a b-metric-like space.

To verify this, observe that for any two nonnegative real numbers e and c, the following inequalities hold:

$$(e + c)^3 \leq 4(e^3 + c^3) \quad \text{and} \quad \sqrt[3]{e + c} \leq \sqrt[3]{e} + \sqrt[3]{c}.$$

As a result, it can be deduced that:

$$\mathcal{D}(\mathcal{G}, \mathcal{H}) \leq \sqrt[3]{4} \cdot (\mathcal{D}(\mathcal{G}, \mathcal{L}) + D(\mathcal{L}, \mathcal{H})) \quad \text{for all } \mathcal{G}, \mathcal{H}, \mathcal{L} \in C_b(X).$$

Definition 6. *Alghamdi et al. (2013)Let $(X, \mathcal{D})$ be a b-metric-like space, $x \in X$ and $r > 0$. The set*

$$B(x, r) = \{y \in X : |\mathcal{D}(x, y) - \mathcal{D}(x, x)| < r\}$$

is referred to as an open ball in the b-metric-like space $(X, \mathcal{D}, s)$, where x is the center and $r > 0$ represents the radius. Let $\{x_n\}$ be a sequence of points in X. The sequence $\{x_n\}$ is said to converge to a point $x \in X$ if and only if $\lim_{n \to +\infty} \mathcal{D}(x, x_n) = \mathcal{D}(x, x)$, and in this case, we denote this as $x_n \to x$ as $n \to +\infty$. A sequence $\{x_n\}$ is called Cauchy if and only if $\lim_{m,n \to +\infty} \mathcal{D}(x_n, x_m)$ exists and is finite. Furthermore, the b-metric-like *space $(X, \mathcal{D})$ is said to be complete if and only if every Cauchy sequence $\{x_n\}$ in X converges to some $x \in X$, satisfying:*

$$\lim_{m,n\to+\infty} \mathcal{D}(x_n, x_m) = \mathcal{D}(x, x) = \lim_{n\to+\infty} \mathcal{D}(x_n, x).$$

In 1962, Edelstein Edelstein (1962) introduced a notable modification of the Banach contraction principle. Subsequently, in 2009, Suzuki Suzuki (2009) expanded and refined the contributions of Banach and Edelstein, as highlighted in related works Salimi & karapinar (2013); Suzuki (2008). In recent years, the study of cyclic contractions and cyclic contractive mappings has gained significant traction in various mathematical investigations (Păcurar & Rus, 2010; Sintunavarat & Kumam, 2012; Petrusel, 2005; Radenović, 2016a,b). Building on these advancements, Alghamdi et al. Alghamdi et al. (2013) established fixed point theorems for cyclic Edelstein-Suzuki contractions, thereby generalizing the results of Edelstein Edelstein (1962), Suzuki Suzuki (2009), and Kirk et al. Fréchet (1906) within the framework of b-metric-like spaces.

THEOREM 1. *Alghamdi et al. (2013) Let $(X, \mathcal{D}, s)$ be a complete b-metric-like space, and let $\{A_j\}_{j=1}^m$ denote a family of nonempty closed subsets of X, where $Y = \bigcup_{j=1}^m A_j$. Suppose $\mathcal{G} : Y \to Y$ is a mapping that satisfies the condition*

$$\mathcal{G}(A_j) \subseteq A_{j+1}, \quad j = 1, 2, \ldots, m, \text{ with } A_{m+1} = A_1.$$

Furthermore, assume that for all $x \in A_i$ and $y \in A_{i+1}$, the following inequality holds:

$$\begin{aligned}
&\frac{1}{2s}\mathcal{D}(x, \mathcal{G}x) \leq \mathcal{D}(x, y) \text{ implies} \\
&\mathcal{D}(\mathcal{G}x, \mathcal{G}y) \leq \alpha\frac{(s+1)}{s}\mathcal{D}(x, y) + \beta\big[\mathcal{D}(x, \mathcal{G}x) + \mathcal{D}(y, \mathcal{G}y)\big] + \\
&\qquad\qquad \gamma\left[\frac{\mathcal{D}(x, \mathcal{G}y) + \mathcal{D}(y, \mathcal{G}x)}{3s}\right] + \delta\left[\frac{\mathcal{D}(x, x) + \mathcal{D}(y, y)}{4s}\right]
\end{aligned}$$

where $\alpha, \beta, \gamma, \delta \geq 0$ and $\alpha + \beta + \gamma + \delta < \frac{1}{s+1}$. Under these conditions, the mapping $\mathcal{G}$ has a fixed point in $\bigcap_{j=1}^m A_j$.

Taking $\frac{\alpha(s+1)}{s} = \beta = \frac{\gamma}{3s} = \frac{\delta}{4s} = R$, in Theorem 1 leads to the derivation of the following corollary.

COROLLARY 1. *Alghamdi et al. (2013) Let $(X, \mathcal{D}, s)$ be a complete b-metric-like space, and let $\{A_j\}_{j=1}^m$ be a family of nonempty closed subsets of X with $Y = \bigcup_{j=1}^m A_j$. Let $\mathcal{G} : Y \to Y$ be a map satisfying $\mathcal{G}(A_j) \subseteq A_{j+1}$, $j = 1, 2, \ldots, m$, where $A_{m+1} = A_1$. Assume that*

$$\frac{1}{2s}\mathcal{D}(x, \mathcal{G}x) \le \mathcal{D}(x, y)$$
$$\text{implies } \mathcal{D}(\mathcal{G}x, \mathcal{G}y) \le R\big[\mathcal{D}(x, y) + \mathcal{D}(x, \mathcal{G}x) + \mathcal{D}(y, \mathcal{G}y) + \mathcal{D}(x, \mathcal{G}y) + \mathcal{D}(y, \mathcal{G}x) + \mathcal{D}(x, x) + \mathcal{D}(y, y)\big],$$

for all $x \in A_i$ and $y \in A_{i+1}$, where $0 \le R < \frac{1}{(s+1)(7s+1)+s}$. Then $\mathcal{G}$ has a fixed point in $\bigcap_{j=1}^m A_j$.

In their work Chen et al. (2015), a set Φ is defined as the collection of functions $\phi : [0, +\infty) \to [0, +\infty)$ that satisfy two conditions: continuity and non-decreasing nature, along with $\phi(t) = 0$ if and only if $t = 0$. They then proceed to present the main results of the study.

THEOREM 2. *[Chen et al. Chen et al. (2015)] Consider $(X, \mathcal{D})$ as a complete b-metric-like space with a constant $s \ge 1$, and let $\mathcal{G} : X \to X$ be a map that satisfies the inequality*

$$\mathcal{D}(\mathcal{G}x, \mathcal{G}y) \le \frac{\mathcal{D}(x, y)}{s} - \varphi(\mathcal{D}(x, y))$$

for all $x, y \in X$, where $\varphi \in \Phi$. Then, $\mathcal{G}$ has a unique fixed point.

In Theorem 2, they showed that by choosing $\varphi(t) = \frac{t}{s} - \lambda t$ with $0 < \lambda < \frac{1}{s}$, the following corollary can be derived.

COROLLARY 2. *Chen et al. (2015) Let $(X, \mathcal{D})$ be a complete b-metric-like space with constant $s \ge 1$, and let $\mathcal{G} : X \to X$ be a mapping such that for all $x, y \in X$, the inequality*

$$\mathcal{D}(\mathcal{G}x, \mathcal{G}y) \le \lambda \mathcal{D}(x, y) \quad \text{where} \quad 0 < \lambda < \frac{1}{s}$$

holds. Then, $\mathcal{G}$ has a unique fixed point in X.

They pointed out that by choosing $s = 1$ in Theorem 2, one can derive Theorem 2.7 from Amini-Harandi (2012). As an application of their result, the authors studied the existence of a solution to the integral equation

$$x(t) = \int_0^T K(t, r, x(r))\, dr, \tag{1}$$

where $K : [0, T] \times [0, T] \times \mathbb{R} \to \mathbb{R}$. They proved the existence of a solution by considering $X = C[0, T]$, the space of continuous real functions on $[0, T]$, equipped with a b-metric-like structure defined by $\mathcal{D}(u, v) = \max_{t\in[0,T]} (|u(t)| + |v(t)|)^p$, with $p > 1$. The authors show that $(X, \mathcal{D})$ is a complete b-metric-like space with $s = 2^{p-1}$, and the existence of a fixed point for the mapping $f(x(t)) = \int_0^T K(t, r, x(r))\, dr$ ensures the existence of a solution to the equation.

THEOREM 3. *Chen et al. (2015) Let $K : [0, T]\times[0, T]\times\mathbb{R} \to \mathbb{R}$ be continuous. Assume there exists a continuous $\xi : [0, T] \times [0, T] \to \mathbb{R}$ such that for all $t, r \in [0, T]$:*

$$|K(t, r, x(r))| + |K(t, r, y(r))| \leq \lambda^{\frac{1}{p}} \xi(t, r) \left(|x(r)| + |y(r)|\right),$$

with $0 < \lambda < \frac{1}{s}$, and

$$\sup_{t\in[0,T]} \int_0^T \xi(t, r)\, dr \leq 1.$$

Then the integral equation (1) has a unique solution $x \in X$.

In order to present a new contractive condition, Jain et al. Jain & Kaur (2021) introduced the following new class of functions Ξ_m for any $m \in \mathbb{N}$ as the set of functions $\xi : [0, +\infty)^m \to [0, +\infty)$ that satisfy the conditions:

- $(\xi 1)$ $\xi(t_1, t_2, \ldots, t_m) < \max\{t_1, t_2, \ldots, t_m\}$ if $(t_1, t_2, \ldots, t_m) \neq (0, 0, \ldots, 0)$;
- $(\xi 2)$ If $\{t_i^{(n)}\}_{n\in\mathbb{N}}$, for $1 \leq i \leq m$, are sequences in $[0, +\infty)$ such that $\limsup_{n\to+\infty} t_i^{(n)} = t_i < +\infty$ for all $i = 1, \ldots, m$, then

$$\liminf_{n\to+\infty} \xi(t_1^{(n)}, t_2^{(n)}, \ldots, t_m^{(n)}) \leq \xi(t_1, t_2, \ldots, t_m).$$

Jain et al. Jain & Kaur (2021) proved the following result in a b-metric-like space.

THEOREM 4. *Let $(X, \mathcal{D}, s \geq 1)$ be a complete b-metric-like space, and let $\mathcal{G} : X \to X$ be a mapping such that there exists $\xi \in \Xi_4$ and*

$$\mathcal{D}(\mathcal{G}x, \mathcal{G}y) \leq \frac{1}{s}\xi\left(\mathcal{D}(x,y), \mathcal{D}(x,\mathcal{G}x), \mathcal{D}(y,\mathcal{G}y), \frac{\mathcal{D}(x,\mathcal{G}y)+\mathcal{D}(\mathcal{G}x,y)-\mathcal{D}(y,y)}{2s}\right)$$

for all $x, y \in X$ with $\mathcal{D}(x,\mathcal{G}y) + \mathcal{D}(\mathcal{G}x, y) \geq \mathcal{D}(y, y)$. Then, $\mathcal{G}$ has a unique fixed point.

Nawab et al. Hussain et al. (2014) extended the fixed point theory to partially ordered b-metric-like spaces. Let $(X, \preceq)$ be a partially ordered set, and $(X, \mathcal{D})$ a b-metric-like space, which we refer to as a partially ordered b-metric-like space.

THEOREM 5 (Nawab et al. Hussain et al. (2014)). *Consider a nondecreasing map $\mathcal{G} : X \to X$ such that for all $x, y \in X$ with $x \preceq y$,*

$$\mathcal{D}(\mathcal{G}(x), \mathcal{G}(y)) \leq \alpha M(x, y),$$

where $\alpha \in [0, \frac{1}{2s^2})$ and

$$M(x,y) = \max\left\{\mathcal{D}(x,y), \mathcal{D}(x,\mathcal{G}(x)), \mathcal{D}(y,\mathcal{G}(y)), \mathcal{D}(x,\mathcal{G}(y)), \mathcal{D}(y,\mathcal{G}(x))\right\}.$$

Under these conditions, the fixed point set $F(\mathcal{G})$ is nonempty if there exists $x_0 \in (LF)_\mathcal{G}$, where $(LF)_\mathcal{G} = \{x \in X : x \preceq \mathcal{G}(x)\}$, and one of the following holds: (a) $\mathcal{G}$ is continuous, or (b) $(X, \preceq, \mathcal{D})$ satisfies the sequential limit comparison property. Additionally, $\mathcal{G}$ has a unique fixed point if and only if every pair of fixed points is comparable.

Nawab et al. Hussain et al. (2014) studied fixed point results for nondecreasing mappings in the framework of partially ordered b-metric-like spaces. Prior to presenting their main theorem, they introduced the concept of the *sequential limit comparison property*:

An ordered b-metric-like space $(X, \preceq, \mathcal{D})$ is said to satisfy the sequential limit comparison property if, for any nondecreasing (or nonincreasing) sequence $\{x_n\}_{n\in\mathbb{N}}$ in X, the convergence $x_n \to x$ implies $x_n \preceq x$ (or $x \preceq x_n$) for all $n \in \mathbb{N}$.

Their main result is stated as follows:

THEOREM 6. *Hussain et al. (2014) Let $(X, \preceq, \mathcal{D})$ be a partially ordered complete b-metric-like space with a coefficient $s > 1$. If a nondecreasing map*

$\mathcal{G} : X \to X$ satisfies

$$s\mathcal{D}(\mathcal{G}(x), \mathcal{G}(y)) \leq \mathcal{M}(x, y) - \varphi(m(x, y)), \tag{2}$$

for all $x, y \in X$ with $x \preceq y$, where

$$\mathcal{M}(x, y) = \frac{\mathcal{D}(x, \mathcal{G}(y)) + \mathcal{D}(y, \mathcal{G}(x))}{4s},$$

$$m(x, y) = \min\left\{\mathcal{D}(x, \mathcal{G}(y)), \mathcal{D}(y, \mathcal{G}(x))\right\},$$

and $\varphi : [0, +\infty) \to [0, +\infty)$ is a continuous and nondecreasing function such that $\varphi(t) > 0$ for all $t > 0$ and $\varphi(0) = 0$, then the fixed point set $F(\mathcal{G})$ is nonempty, provided there exists $x_0 \in (LF)_{\mathcal{G}}$ and one of the following conditions holds:

(i) *$\mathcal{G}$ is continuous.*

(ii) *$(X, \preceq, \mathcal{D})$ satisfies the sequential limit comparison property.*

Furthermore, $\mathcal{G}$ has a unique fixed point if and only if the fixed points of $\mathcal{G}$ are comparable.

In their work, Zoto et al. Zoto et al. (2018) introduced the concept of generalized (s, p, α)-contractions and obtained fixed point theorems for this class of contractions in the framework of b-metric-like spaces. Specifically, they define a self-mapping $\mathcal{G} : X \to X$ on a complete b-metric-like space $(X, \mathcal{D})$ with parameter $s \geq 1$ as an (s, α)-Banach contraction if it satisfies the condition

$$s\mathcal{D}(\mathcal{G}x, \mathcal{G}y) \leq \alpha\mathcal{D}(x, y)$$

for some $\alpha \in [0, 1)$ and all $x, y \in X$.

Based on Círic's quasi-contractions, Zoto et al. Zoto et al. (2018) introduced the concept of generalized (ψ, s, p, α)-contractions in b-metric-like spaces. Let Ψ and Φ denote the families of altering distance functions satisfying the following conditions, respectively:

Ψ : $[0, +\infty) \to [0, +\infty)$ is an increasing and continuous function, and $\Psi(t) = 0$ if and only if $t = 0$.

$\Phi : [0, +\infty) \to [0, +\infty)$ is a lower semicontinuous function, and $\Phi(t) = 0$ if and only if $t = 0$.

Using these families, they defined (ψ, s, p, α)-$\acute{C}$irić-type quasi-contractions as follows:

DEFINITION 7. *Zoto et al. (2018) Let $(X, \mathcal{D})$ be a b-metric-like space with the parameter $s \geq 1$. Consider $\psi \in \Psi$, and let α and p be constants such that $0 \leq \alpha < 1$ and $p \geq 2$. A mapping $\mathcal{G} : X \to X$ is called a (ψ, s, p, α)-Ćirić-type quasi-contraction if, for all $x, y \in X$, the following inequality holds:*

$$\psi^{2sp}(\mathcal{D}(\mathcal{G}x, \mathcal{G}y)) \leq \alpha\psi\Big(\max\Big\{\mathcal{D}(x, y), \mathcal{D}(x, \mathcal{G}x), \mathcal{D}(y, \mathcal{G}y), \mathcal{D}(x, \mathcal{G}y), \mathcal{D}(y, \mathcal{G}x)\Big\}\Big).$$

REMARK 1. The authors also illustrated that these generalized contractions extend and unify several well-known results in the fixed point theory of metric-like spaces.

1. By taking $\psi(t) = \frac{1}{2}t$ (or the identity mapping $\psi(t) = t$), the notion of a (ψ, s, p, α)-$\acute{C}$irić-type quasi-contraction reduces to an (s, p, α)-quasi-contraction.

2. For $\psi(t) = \frac{1}{2}t$ and $p = 2$, the definition simplifies to the (s, α)-quasi-contraction presented in Ćirić (1974).

3. Setting $s = 1$ corresponds to the special case of metric-like spaces.

THEOREM 7. *[Kastriot Zoto al. Zoto et al. (2018)] Let $(X, \mathcal{D})$ be a complete b-metric-like space with the parameter $s \geq 1$, and let $f : X \to X$ be a given self-mapping. If f is a (ψ, s, p, α)-quasicontraction, then f has a unique fixed point.*

The following corollary, derived by Zoto et al. Zoto et al. (2018), provides a version of the Hardy-Rogers result in Gordji & Rogers (1973).

COROLLARY 3. *Let $(X, \mathcal{D})$ be a complete b-metric-like space with the parameter $s \geq 1$. If $\mathcal{G} : X \to X$ is a self-mapping and there exist $p \geq 2$ and constants $a_i \geq 0$, $i = 1, \ldots, 5$, such that $a_1 + a_2 + a_3 + a_4 + a_5 < 1$ and*

$$s^p\mathcal{D}(\mathcal{G}x, \mathcal{G}y) \leq \alpha_1\mathcal{D}(x, y)+\alpha_2\mathcal{D}(x, \mathcal{G}x)+\alpha_3\mathcal{D}(y, \mathcal{G}y)+\alpha_4\mathcal{D}(x, \mathcal{G}y)+\alpha_5\mathcal{D}(y, \mathcal{G}x),$$

for all $x, y \in X$, then $\mathcal{G}$ has a unique fixed point in X.

In addition to the results already discussed, Zoto et al. also derived several corollaries as immediate consequences of Theorem 7. These corollaries deal with self-maps that satisfy contractive conditions expressed through rational expressions, utilizing the functions $\psi \in \Psi$ and $\phi \in \Phi$.

COROLLARY 4. *Let $(X, \mathcal{D})$ be a complete b-metric-like space with parameter $s \geq 1$, and let $\mathcal{G} : X \to X$ be a self-map. If there exist $\psi \in \Psi$, $0 \leq \alpha < \frac{1}{2}$, and $p \geq 2$, such that the condition*

$$\psi\left(2sp\,\mathcal{D}(\mathcal{G}x, \mathcal{G}y)\right) \leq \alpha \frac{\psi(M(x,y))}{1+\psi(M(x,y))}$$

is satisfied for all $x, y \in X$, where $M(x,y)$ is defined as in (2), then $\mathcal{G}$ has a unique fixed point in X.

Fabiano et al. Fabiano et al. (2020) studied cyclic (s,q)-Dass-Gupta-Jaggi type contractions in b-metric-like spaces, proving that a Picard sequence is Cauchy in this setting, thus extending and refining the existing results. They further established the equivalence between the cyclic results of Kirk et al. and the standard fixed point results for such contractions.

Before stating the main result, let us recall the notions of η-admissibility and η-continuity. A mapping $\mathcal{G} : X \to X$ is called η-admissible if $\eta(x,y) \geq 1$ implies $\eta(\mathcal{G}(x), \mathcal{G}(y)) \geq 1$ for all $x, y \in X$. Moreover, $\mathcal{G}$ is said to be η-continuous on a b-metric-like space $(X, \mathcal{D})$ if, for any sequence $\{z_n\}$ in X satisfying $\lim\limits_{n\to+\infty} z_n = z$ and $\eta(z_n, z_{n+1}) \geq 1$ for all n, it follows that $\lim\limits_{n\to+\infty} \mathcal{G}(z_n) = \mathcal{G}(z)$.

THEOREM 8. *Fabiano et al. (2020) Let $(X, \mathcal{D})$ be a $\mathcal{D}$-complete b-metric-like space, and let $\eta : X \times X \to [0, +\infty)$ and $\mathcal{G} : X \to X$ be the given mappings. Suppose that for all $x, y \in X$ with $\eta(x, \mathcal{G}x)\eta(y, \mathcal{G}y) \geq 1$ implies*

$$2s^q \mathcal{D}(\mathcal{G}x, \mathcal{G}y) \leq \phi(N(x,y))$$

where $q > 1$, $\phi : [0, +\infty) \to [0, +\infty)$ is a is non-decreasing and continuous function satisfying $\lim_{n\to+\infty} \phi^n(t) = 0$, and

$$N(x,y) = \max\left\{\mathcal{D}(x,y), \mathcal{D}(y,\mathcal{G}x), \frac{\mathcal{D}(x,y)\mathcal{D}(y,\mathcal{G}y)}{1+\mathcal{D}(x,\mathcal{G}x)}, \frac{\mathcal{D}(y,\mathcal{G}y)[1+\mathcal{D}(x,\mathcal{G}x)]}{1+\mathcal{D}(x,y)}, \frac{\mathcal{D}(x,\mathcal{G}y)+\mathcal{D}(y,\mathcal{G}x)}{4s}\right\}.$$

Assume that the mapping $\mathcal{G} : X \to X$ satisfies the following conditions:

1. *$\mathcal{G}$ is η-admissible.*
2. *There exists $z_0 \in X$ such that $\eta(z_0, \mathcal{G}(z_0)) \geq 1$.*
3. *Either $\mathcal{G}$ is η-continuous, or for any sequence $\{z_n\}$ in X such that for all $n \geq 0$, $\eta(z_n, z_{n+1}) \geq 1$ and $\lim_{n\to+\infty} z_n = z$, we have $\eta(z, \mathcal{G}(z)) \geq 1$.*

Then $\mathcal{G}$ has a fixed point $z \in X$. Furthermore, if:

4. *For all $z \in F(\mathcal{G}) = \{a \in X : \mathcal{G}(a) = a\}$, we have $\eta(z, z) \geq 1$,*

then $\mathcal{G}$ has a unique fixed point in X.

An example is given below to support Theorem 8.

EXAMPLE 3. Fabiano et al. (2020) Consider $X = [0, 1]$ equipped with the b-metric-like function $\mathcal{D}(x, y) = (x + y)^2$ for all $x, y \in X$, with the parameters $s = 2$ and $q > 1$. Let $\mathcal{G} : X \to X$ and $\eta : X \times X \to [0, +\infty)$ be defined as follows:

$$\mathcal{G}x = \frac{x}{6}\ ,\ \eta(x, y) = \begin{cases} 1, & \text{if } x = y = 0, \\ 0, & \text{otherwise.} \end{cases}$$

Additionally, let $\phi : [0, +\infty) \to [0, +\infty)$ be given by $\phi(t) = t^2$. For the pair $(x, y) = (0, 0)$, we observe that $\eta(x, \mathcal{G}x)\eta(y, \mathcal{G}y) \geq 1$ holds only when $x = y = 0$. Now, for this specific pair, we calculate $2s^q\mathcal{D}(\mathcal{G}(0), \mathcal{G}(0)) = 0$, while the expression for φ yields

$$\begin{aligned}
&\phi\Bigg(\max\Bigg\{\mathcal{D}(0,0), \mathcal{D}(0,\mathcal{G}0), \frac{\mathcal{D}(0,0)\cdot\mathcal{D}(0,\mathcal{G}0)}{1+\mathcal{D}(0,\mathcal{G}0)}, \\
&\frac{\mathcal{D}(0,\mathcal{G}0)[1+\mathcal{D}(0,\mathcal{G}0)]}{1+\mathcal{D}(0,0)}, \frac{\mathcal{D}(0,\mathcal{G}0)+\mathcal{D}(0,\mathcal{G}0)}{4\cdot 2}\Bigg\}\Bigg) \\
&= \frac{1}{2}\max\Bigg\{\mathcal{D}(0,0), \mathcal{D}(0,\mathcal{G}0), \frac{\mathcal{D}(0,0)\cdot\mathcal{D}(0,\mathcal{G}0)}{1+\mathcal{D}(0,\mathcal{G}0)}, \\
&\frac{\mathcal{D}(0,\mathcal{G}0)[1+\mathcal{D}(0,\mathcal{G}0)]}{1+\mathcal{D}(0,0)}, \frac{\mathcal{D}(0,\mathcal{G}0)+\mathcal{D}(0,\mathcal{G}0)}{8}\Bigg\} \\
&= \frac{1}{2}\max\left\{0, 0, \frac{0\cdot 0}{1+0}, \frac{0\cdot(1+0)}{1+0}, \frac{0+0}{8}\right\} \\
&= \frac{1}{2}\times 0 = 0.
\end{aligned}$$

Thus, this example demonstrates the applicability of Theorem 8; in particular, it confirms that $z = 0$ is the unique fixed point of $\mathcal{G}$.

Mirkov et al. Mirkov et al. (1994) proposed a simplified and concise proof of Banach's contraction principle using Palais's method within the generalized framework of b-metric-like spaces. Their result extends existing findings in the literature by demonstrating that the Lipschitz constant in Banach's contraction principle can belong to the entire interval $[0,1)$ across six types of spaces: metric spaces, b-metric spaces, partial metric spaces, partial b-metric spaces, metric-like spaces, and the broader b-metric-like spaces.

First, using Palais's method, they obtained the following result.

Lemma 1 (Mirkov et al. Mirkov et al. (1994)). *Let $(X,\mathcal{D})$ be a b-metric-like space with $s \geq 1$ and $\{x_n\}$ be a sequence in X such that*

$$\mathcal{D}(x_m, x_n) \leq k\mathcal{D}(x_{m-1}, x_{n-1}),$$

for all $m, n \in \mathbb{N}$, where $k \in [0,1)$. Then the following inequality holds:

$$\mathcal{D}(x_m, x_n) \leq s\left(k^m + k^n\right)\mathcal{D}(x_0, x_{n_0})\big/\left(1 - k^{n_0}s\right),$$

where $n_0 \in \mathbb{N}$ such that $k^{n_0}s < 1$.

Theorem 9. *Mirkov et al. (1994) Consider a complete b-metric-like space $(X,\mathcal{D})$ with $s \geq 1$. If a mapping $\mathcal{G} : X \to X$ satisfies the condition*

$$\mathcal{D}(\mathcal{G}(x), \mathcal{G}(y)) \leq k\mathcal{D}(x, y),$$

for all $x, y \in X$, where $k \in [0,1)$, then $\mathcal{G}$ admits a unique fixed point in X.

In recent years, extensive research has been conducted on the generalization of Geraghty contractions Karapinar (2014, et al.); Aydi et al. (2017). In 2017, Fulga et al. Fluga & Proca (2017) introduced the notion of φ_E-Geraghty contractions and established a corresponding fixed point theorem in complete metric spaces. Subsequently, this concept was explored in metric-like spaces Aydi et al. (2017), leading to the following result:

Theorem 10. *Aydi et al. (2017) Let (X,σ) be a complete metric-like space, and let $\mathcal{G} : X \to X$ be a self-mapping. Suppose there exists $\beta \in \mathbb{B}$ such* *that*

$$\sigma(\mathcal{G}x, \mathcal{G}y) \leq \beta(F(x,y))F(x,y), \quad \forall x, y \in X,$$

where

$$F(x,y) = \sigma(x,y) + |\sigma(x, \mathcal{G}x) - \sigma(y, \mathcal{G}y)|.$$

Then, $\mathcal{G}$ has a unique fixed point.

Note that; $\mathbb{B}$ consists of all functions $\beta : [0, +\infty) \to [0, 1)$ such that:

$$\lim_{n \to +\infty} \beta(t_n) = 1 \quad \text{implies} \quad \lim_{n \to +\infty} t_n = 0.$$

Dakun Yu et al. Yu et al. (2018) initiated the concept of $(T, g)_F$-contractions of Geraghty type and studied common fixed point theorems for these contractions in b-metric-like spaces. We recall that, according to Abbas et al. Abbas & Jungck (2008), the following definition is given: Let X be a nonempty set, and let f and g be self-mappings on X. The set of common points of f and g is defined as $C(f, g) = \{x \in X : fx = gx\}$. The pair (f, g) is said to be weakly compatible if $fgx = gfx$ for all $x \in C(f, g)$. Moreover, if there exists $x \in X$ such that $fx = gx = w$, then x is called a coincidence point of f and g, and w is referred to as a ***point of coincidence*** of f and g.

Definition 8. *Yu et al. (2018) Let $(X, \mathcal{D})$ be a b-metric-like space with the coefficient $s \geq 1$, and let $T, g : X \to X$ be two mappings. The pair (T, g) is said to be a $(T, g)_F$-contraction of Geraghty type if there exists $\beta \in \mathbb{B}$ such that*

$$\mathcal{D}(Tx, Ty) \leq \beta(F_g(x,y))F_g(x,y)$$

for all $x, y \in X$, where $F_g(x,y) = \frac{1}{s^2}\left[\mathcal{D}(gx, gy) + |\mathcal{D}(gx, Tx) - \mathcal{D}(gy, Ty)|\right]$.

Theorem 11. *Yu et al. (2018) Let $(X, \mathcal{D})$ be a b-metric-like space with the coefficient $s \geq 1$, and let $T, g : X \times X \to X$ be two mappings such that $T(X) \subseteq g(X)$ and $g(X)$ is complete. If the pair (T, g) is a $(T, g)_F$-contraction of Geraghty type, then T and g have a unique point of coincidence. Furthermore, if T and g are weakly compatible, then they have a unique common fixed point.*

By specializing Theorem 11 to the case $g = I_X$ (the identity mapping), they obtained the following result.

Corollary 5. *Yu et al. (2018) Let $(X, \mathcal{D})$ be a complete b-metric-like space with the coefficient $s \geq 1$, and let $T : X \to X$ be a mapping. If there exists $\beta \in \mathbb{B}$ such that*

$$\mathcal{D}(Tx, Ty) \leq \beta(F(x, y))F(x, y)$$

for all $x, y \in X$, where $F(x, y) = \frac{1}{s^2}\left[\mathcal{D}(x, y) + |\mathcal{D}(x, Tx) - \mathcal{D}(y, Ty)|\right]$, then T has a unique fixed point.

As an application of the previous corollary, Dakun Yu et al. Yu et al. (2018) investigated the integral equation $(E) : x(t) = \int_0^1 K(t, r, x(r))\, dr$, where $K : [0, 1] \times [0, 1] \times \mathbb{R} \to \mathbb{R}$. They considered the function space $X = C[0, 1]$ with the b-metric-like: $\mathcal{D}(u, v) = \max_{t\in[0,1]}(|u(t)| + |v(t)|)^p, \quad p \geq 1$, which forms a complete b-metric-like space with $s = 2^{p-1}$. By defining $f(x)(t) = \int_0^1 K(t, r, x(r))\, dr$, they established the existence of a solution as a direct consequence of the corollary.

Theorem 12. *Yu et al. (2018) Let $K : [0, 1] \times [0, 1] \times \mathbb{R} \to \mathbb{R}$ be continuous. Suppose there exists a continuous function $\xi : [0, 1] \times [0, 1] \to [0, +\infty)$ such that*

$$|K(t, r, x(r))| \leq \xi(t, r)|x(r)|.$$

If there exists $\beta \in \mathbb{B}$ satisfying

$$\sup_{t\in[0,1]} \int_0^1 \xi(t, r)dr \leq \sqrt[p]{\frac{1}{2^{2p-2}}\beta\left(\frac{1}{2^{2p-2}}(\|x - y\|_\infty + |\|x - fx\|_\infty - \|y - fy\|_\infty|)\right)}$$

then (E) has a unique solution $x \in X$.

Best proximity theory provides a framework for approximating solutions in situations where exact fixed points do not exist. Suppose U and V are two closed, nonempty subsets of a space X such that $U \cap V = \emptyset$, and let $\mathcal{G} : U \to V$ be a mapping. Since the equation $\mathcal{G}(x) = x$ has no solution, one instead seeks a point $x \in U$ that is closest to $\mathcal{G}(x) \in V$. This point is known as a *best proximity point* of $\mathcal{G}$.

The study of best proximity points initially focused on classical metric spaces before being extended to more generalized settings (see, for instance, Gardašević et al. (2023); Fallahi & Eivani (2022); Abkar & Gabeleh (2013); Aydi et al. (2020); Choudhury et al. (2015); Mongkolkeha et al. (2013)). A notable development in this area was introduced by Gordji et al. Gordji & Habibi (2017); Gordji et al. (2017), who explored the role of orthogonal sets and introduced essential concepts such as O-sequences, O-Cauchy sequences, O-continuity, O-contractions, O-preserving properties, and the P-property. Their work established best proximity point results under more generalized contractive conditions. Subsequent research has built upon these ideas, particularly in the context of orthogonality Fallahi & Eivani (2022); Mongkolkeha et al. (2013); Sawangsup & Sintunavara (2020); Garakoti et al. (2014); Yang et al. (2020), leading to significant progress in this field.

Milanka et al. Gardašević et al. (in press) addressed the open question raised in Gardašević et al. (2023) by introducing the assumption that the set X is $\perp$-transitive. Before delving into their result, we will first recall some definitions pertinent to the context of orthogonal metrics and best proximity theorems.

DEFINITION 9. *Gordji et al. (2017) Let X be a nonempty set and $\perp \subset X \times X$ be a binary relation. If there exists an element $x_0 \in X$ such that for all $y \in X$, either $y \perp x_0$ or $x_0 \perp y$, then the pair $(X, \perp)$ is called an orthogonal set (or O-set), and x_0 is referred to as the orthogonal element.*

If X is equipped with a metric d, then the pair $(X, \perp, d)$ is referred to as an orthogonal metric space. Orthogonal partial metric spaces, orthogonal b-metric spaces, and other generalized orthogonal spaces are similarly defined. For additional examples of these concepts, refer to Fallahi & Eivani (2022); Gardašević et al. (2023); Gordji & Habibi (2017); Gordji et al. (2017); Javed (et al.); Yamaod & Sintunavarat (2018).

The next example provides insight into the practical use of an orthogonal set.

EXAMPLE 4. Gordji et al. (2017) Let X be the set of all people in the world. We define $x \perp y$ if x can give blood to y. According to the following table, if x_0 is a person with blood type O$^-$, then there exists $x_0 \perp y$ for all $y \in X$.

This means that $(X, \perp)$ is an O^{-}-set, and x_0 is not unique.

Blood type	**Can donate to**	**Can receive from**
$A+$	$A+\quad AB+$	$A+\quad A-\quad O+\quad O-$
$O+$	$O+\quad A+\quad B+\quad AB+$	$O+\quad O-$
$B+$	$B+\quad AB+$	$B+\quad B-\quad O+\quad O-$
$AB+$	$AB+$	$everyone$
$A-$	$A+\quad A-\quad AB+\quad AB-$	$A-\quad O-$
$O-$	$everyone$	$O-$
$B-$	$B+\quad B-\quad AB+\quad AB-$	$B-\quad O-$
$AB-$	$AB+\quad AB-$	$AB-\quad B-\quad O-\quad A-$

Definition 10. *Gordji et al. (2017) A sequence $\{x_n\}_{n\in\mathbb{N}}$ is called an orthogonal sequence (or O-sequence) if for all $n \in \mathbb{N}$, the following condition holds: $x_n \perp x_{n+1}$* or *$x_{n+1} \perp x_n$.*

Definition 11. Gordji & Habibi (2017) *A function $\mathcal{G} : X \to X$ is said to be orthogonal-preserving (or $\perp$-preserving) if for all $x, y \in X$ such that $x \perp y$, it follows that $\mathcal{G}x \perp \mathcal{G}y$.*

Definition 12. *Gardašević et al. (in press) An orthogonal set X is said to be $\perp$-transitive if the following condition holds: for all $x, y, z \in X$, if $(y \perp x$ or $x \perp y)$ and $(y \perp z$ or $z \perp y)$, then it follows that $(x \perp z$ or $z \perp x)$.*

Definition 13. *Gordji & Habibi (2017)* Let *$(X, \perp, d)$ be an orthogonal metric space, which means $(X, \perp)$ is an O-set and (X, d) is a metric space. A function $\mathcal{G} : X \to X$ is called orthogonal continuous (or $\perp$-continuous) at a point $x \in X$ if, for every O-sequence $\{x_n\}_{n\in\mathbb{N}}$ in X satisfying $x_n \to x$* as *$n \to +\infty$, it follows that $\mathcal{G}(x_n) \to \mathcal{G}(x)$* as *$n \to +\infty$.*

Note that, every continuous mapping is a $\perp$-continuous mapping; however, the converse does not necessarily hold. An example illustrating this can be found in Gordji & Habibi (2017).

Definition 14. *Gordji et al. (2017)* Let *$(X, \perp, \mathcal{D})$ be an orthogonal metric space, and let $\lambda \in [0, 1)$. A function $\mathcal{G} : X \to X$ is called an orthogonal contraction (or $\perp$-contraction) with the Lipschitz constant λ if, for all $x, y \in X$ satisfying $x \perp y$, the following inequality holds:*

$$\mathcal{D}(\mathcal{G}x, \mathcal{G}y) \le \lambda \mathcal{D}(x, y).$$

REMARK 2. Gordji et al. (2017) Every contraction mapping is a $\perp$-contraction mapping, but the converse is not true. For an example, see Gordji et al. (2017).

Let (X, d) be a metric space, and let $U, V \subset X$ be two nonempty subsets. The distance between U and V is defined as

$$D(U, V) = \inf\{d(u, v) \mid u \in U, v \in V\}.$$

A point $u \in U$ is called a best proximity point of a non-self mapping $\mathcal{G} : U \to V$ if it satisfies

$$d(u, \mathcal{G}u) = D(U, V).$$

For arbitrary sets $U, V \subset X$ such that $U, V \neq \emptyset$, we define

$$U_0 = \{u \in U \mid d(u, v) = D(U, V) \text{ for some } v \in V\},$$

$$V_0 = \{v \in V \mid d(u, v) = D(U, V) \text{ for some } u \in U\}.$$

Let (X, d) be a metric space, and let $U, V \subset X$ be nonempty subsets such that $U_0 \neq \emptyset$. The pair (U, V) is said to have the P-property if and only if

$$\begin{cases} d(u_1, v_1) = D(U, V) \\ d(u_2, v_2) = D(U, V) \end{cases} \text{ implies } d(u_1, u_2) = d(v_1, v_2),$$

for all $u_1, u_2 \in U_0$ and $v_1, v_2 \in V_0$.

Considering that $d(x, \mathcal{G}x) \geq D(U, V)$ for all $x \in U$, it follows that the global minimum of the function $x \mapsto d(x, \mathcal{G}x)$ is attained at a best proximity point. Furthermore, it is straightforward to observe that a best proximity point coincides with a fixed point when the mapping $\mathcal{G}$ is a self-mapping.

THEOREM 13. *Gardašević et al. (in press) Let $(X, \perp, \mathcal{D}, s)$ be an orthogonal 0-$\mathcal{D}$-complete b-metric-like space, and let (U, V) be a pair of two non-empty closed subsets of X with an empty intersection, satisfying the P-property. Assume that X is $\perp$-transitive. Let $\mathcal{G} : U \to V$ be a $\perp$-continuous, $\perp$-preserving, and $\perp$-contractive mapping with the Lipschitz constant $k \in (0, 1)$. Suppose that $\mathcal{G}$ satisfies the following conditions:*

(i) *$\mathcal{G}(U_0) \subset V_0$;*

(ii) *There exist $x_0, x_1 \in U_0$ such that $x_0 \perp x_1$ and $\mathcal{D}(x_1, \mathcal{G}x_0) = D(U, V)$, where $D(U, V) = \inf\{\mathcal{D}(x, y) \mid x \in U, y \in V\}$.*

Then $\mathcal{G}$ has a unique best proximity point $x' \in U$, i.e., $\mathcal{D}(x', \mathcal{G}x') = D(U, V)$.

In papers [36] and [37], the issues of best proximity results in orthogonal 0-complete b-metric-like spaces were considered. For proving the results in these works, a sequence $\{x_n\}$, where $n = 0, 1, 2, \ldots$, is constructed such that the following relation holds:

$$\mathcal{D}(x_n, x_{n+1}) \leq \lambda \mathcal{D}(x_{n-1}, x_n) \quad \text{for} \quad n = 1, 2, \ldots$$

where λ belongs to the interval $[0, 1/s)$ with $s \geq 1$. Based on this relation, it is routinely proved that the constructed sequence $\{x_n\}$ is Cauchy. The open problem raised in these papers was whether the obtained results are still valid if λ belongs to the interval $[0, 1)$.

By utilizing the following result, we provide an affirmative answer to the question posed in the paper. Gardašević et al. (in press, 2023).

LEMMA 2. *Let $(X, D, s > 1)$ be a b-metric-like space, and let $\{x_n\}$ be a sequence in X satisfying the following condition: There exists $\lambda \in [0, 1)$ such that*

$$\mathcal{D}(x_n, x_{n+1}) \leq \lambda \mathcal{D}(x_{n-1}, x_n), \quad \text{for all } n \in \mathbb{N}.$$

Then, the sequence $\{x_n\}$ is Cauchy.

Proof. If $x_n = x_{n-1}$ for some $n \in \mathbb{N}$, the proof is complete. Otherwise, assume that $x_n \neq x_{n-1}$ for all $n \in \mathbb{N}$. We consider two cases:

Case 1: $\lambda \in \left[0, \frac{1}{s}\right)$.

Case 2: $\lambda \in \left[\frac{1}{s}, 1\right)$.

The proof for the first case follows similarly to the arguments presented in Gardašević et al. (in press, 2023). Now, consider the second case. Since $\lambda^n \to 0$ as $n \to +\infty$, there exists $k \in \mathbb{N}$ such that $\lambda^k < \frac{1}{s}$. Define the mapping $\mathcal{G}$ on the sequence $\{x_n\}, n \in \mathbb{N}$, by

$$\mathcal{G}(x_n) = x_{n+1}, \quad \text{for all } n = 0, 1, 2, \ldots$$

It follows that $\mathcal{G}^k(x_n) = x_{k+n}$ for all $n \in \mathbb{N}$ and

$$\mathcal{D}(\mathcal{G}^k x_{n-1}, \mathcal{G}^k x_n) \leq \lambda^k \mathcal{D}(x_{n-1}, x_n).$$

Proceeding analogously as in Gardašević et al. (in press, 2023) for the first case, we establish that the sequence $\{x_{k+n}\}$ is Cauchy. Specifically, if

$n < m$, it is shown that

$$\mathcal{D}(x_{k+n}, x_{k+m}) \to 0 \quad \text{as } n, m \to +\infty.$$

Since $\{x_n\} = \{x_0, x_1, \ldots, x_{k-1}\} \cup \{x_k, x_{k+1}, \ldots, x_{k+n}, \ldots\}$, it follows that the sequence $\{x_n\}$, $n = 0, 1, 2, \ldots$, is Cauchy. $\square$

References

Abbas, M. and Jungck, J., 2008. Common fixed point results for noncommuting mappings without continuity in cone metric spaces. *Journal of Mathematical Analysis and Applications*, 341(1), pp. 416–420. Available at: https://doi.org/10.1016/j.jmaa.2007.09.070.

Abkar, A. and Gabeleh, M., 2013. A note on some best proximity point theorems proved under P-property. *Abstract and Applied Analysis*, Vol. 2013, Article ID 189567. Available at: https://doi.org/10.1155/2013/189567.

Aleksić, S., Mitrović, Z.D. and Radenović, S., 2020. Picard sequences in b-metric spaces. *Fixed Point Theory*, 21(1), pp. 35-46. Available at: https://doi.org/10.24193/fpt-ro.2020.1.03.

Alghamdi, M.A., Hussain, N., Salimi, P., 2013. Fixed point and coupled fixed point theorems on b-metric-like spaces. *Journal of Inequalities and Applications*, 2013, Article 402. Available at: https://doi.org/10.1186/1029-242X-2013-402.

Amini-Harandi, A., 2012. Fixed point theorems for monotone operators in partially ordered metric-like spaces and application to integral equations. *Journal of Nonlinear and Convex Analysis*. Available at: https://content.iospress.com/articles/journal-of-nonlinear-and-convex-analysis/jnca180.

Amini-Harandi, A., 2012. Metric-like spaces, partial metric spaces and fixed points. *Fixed Point Theory and Applications*, 2012. Available at: https://doi.org/10.1186/1687-1812-2012-204.

Aage, C.T., Salunke, J.N., 2008. The results on fixed points in dislocated and dislocated quasi-metric space. *Applied Mathematical Sciences*, 2(59), pp. 2941-2948. Available at: https://www.m-hikari.com/ams/ams-2008/ams-59-2008/ageams59-2941-2948.pdf.

Aydi, H., Felhi, A. and Afshari, H., 2017. New Geraghty type contractions on metric-like spaces. *Journal of Nonlinear Science and Applications*, 10, pp. 780–788. Available at: http://dx.doi.org/10.22436/jnsa.010.02.38.

Aydi, H., Lakzian, H., Mitrovic, Z.D. and Radenović, S., 2020. Best proximity points of MT-cyclic contractions with property UC. *Numerical Functional Analysis and Optimization*, 41, pp. 871–882. Available at: https://doi.org/10.1080/01630563.2020.1796959.

Berinde, V. and Păcurar, M., 2022. The early developments in fixed point theory on b-metric spaces: a brief survey and some important related aspects. *Carpathian Journal of Mathematics*, 38(3), pp. 523–538. Available at: https://doi.org/10.37193/CJM.2022.03.01.

Chen, C., Dong, J. and Zhu, C., 2015. Some fixed point theorems in b-metric-like spaces. *Fixed Point Theory and Applications*, 2015, Article ID 122. Available at: https://doi.org/10.1186/s13663-015-0369-3.

Choudhury, B., Metiya, N., Postolache, M. and Konar, P., 2015. A discussion on best proximity point and coupled best proximity point in partially ordered metric spaces. *Fixed Point Theory and Applications*, 2015, Article 170. Available at: https://doi.org/10.1186/s13663-015-0397-3.

Ćirić, L.B., 1974. A generalization of Banach's contraction principle. *Proceedings of the American Mathematical Society*, 45(2), pp. 267–273. Available at: https://doi.org/10.1090/S0002-9939-1974-0356011-2.

Czerwik, S., 1993. Contraction mappings in b-metric spaces. *Acta Mathematica et Informatica Universitatis Ostraviensis*, 1(1), pp. 5–11. Available at: https://doi.org/10.5817/AMUO1993-1-1.

Edelstein, M., 1962. On fixed and periodic points under contractive mappings. *Journal of the London Mathematical Society*, 37, pp. 74-79. Available at: https://doi.org/10.1112/JLMS/S1-37.1.74.

Fabiano, N., Dosenović, T., Rakić, D., Radenović, S., 2020. Some new results on (s,q)-Dass-Gupta-Jaggi type contractive mappings in b-metric-like spaces. *Filomat*, 34(12), pp. 4015-4026. Available at: https://doi.org/10.2298/FIL2012015F.

Fallahi, K. and Eivani, Sh., 2022. Orthogonal b-metric spaces and best proximity points. *Journal of Mathematical Extension*, 16(6), pp. 1–17. Available at: https://doi.org/10.30495/JME.2022.2000.

Fréchet, M., 1906. Sur quelques points du calcul fonctionnel. *Rendiconti del Circolo Matematico di Palermo*, 22, pp. 1–74. Available at: https://doi.org/10.1007/BF03018603.

Fulga, A. and Proca, A.M., 2017. Fixed point for φ_a-Geraghty contraction. *Journal of Nonlinear Science and Applications*, 10, pp. 5125–5131. Available at: https://doi.org/10.22436/jnsa.010.09.5699.

Garakoti, N., Joshi, M.C. and Kumar, R., 2014. Fixed point for $F_{\perp}$-weakly commuting mappings. *Nonlinear Analysis*, 97, pp. 62–71. Available at: https://doi.org/10.1016/j.na.2013.09.002.

Gardašević-Filipović, M., Kukić, K., Gardašević, D. and Mitrović, Z.D., 2023. Some best proximity point results in the orthogonal 0-complete b-metric-like spaces. *Journal of Contemporary Mathematical Analysis*, 58(2), pp. 105–115. Available at: https://doi.org/10.3103/S1068362323020036.

Gardasevic-Filipovic, M., Mitrovic, Z.D., Gardasevic, D. and Radenovic, S., In press. Some best proximity point results in the orthogonal 0-complete b-metric-like spaces and rectangular b-metric-like spaces. *TWMS Journal of Pure and Applied Mathematics*.

Gordji, M.E. and Habibi, H., 2017. Fixed point theory in generalized orthogonal metric space. *Journal of Linear Topology and Algebra*, 6(3), pp. 251-260. Available at: https://doi.org/10.1234/jlta.2017.00603.

Gordji, M.E., Rameani, M., De La Sen, M. and Cho, Y.J., 2017. On orthogonal sets and Banach fixed point theorem. *Fixed Point Theory*, 18(2), pp. 569–578. Available at: https://doi.org/10.24193/fpt-ro.2017.2.45.

Gregori, V.; Sapena, A., 2002. On fixed-point theorems in fuzzy metric spaces. *Fuzzy Sets and Systems*, 125, pp. 245–252. Available at: https://doi.org/10.1016/S0165-0114(01)00282-1.

Hardy, G.E. and Rogers, T.D., 1973. A generalization of a fixed point theorem of Reich. *Canadian Mathematical Bulletin*, 16(2), pp. 201–206. Available at: https://doi.org/10.4153/CMB-1973-036-0.

Hussain, N., Rezaei, J.R., Parvaneh, V. and Kadelburg, Z., 2014. Fixed points of contractive mappings in b-metric-like spaces. *The Scientific World Journal*, 2014, Article ID 471827. Available at: https://doi.org/10.1155/2014/471827.

Jain, K., Kaur, J., 2021. Some fixed point results in b-metric spaces and b-metric-like spaces with new contractive mappings. *Axioms*, 10, 55. Available at: https://doi.org/10.3390/axioms10020055.

Javed, K., Aydi, H., Uddin, F., Arshad, M., 2021. On orthogonal partial b-metric spaces with an application. *J. Math.*, 1-7.

Karapinar, E., 2014. α-ψ-Geraghty contraction type mappings and some related fixed point results. *Filomat*, 28(1), pp. 37–48. Available at: https://doi.org/10.2298/FIL1401037K.

Karapinar, E., Alsulami, H. and Noorwali, M., 2015. Some extensions for Geraghty type contractive mappings. *Journal of Inequalities and Applications*, 2015, Article ID 303. Available at: https://doi.org/10.1186/s13660-015-0830-1.

Kirk, W.A., Srinivas, P.S. and Veeramani, P., 2003. Fixed points for mappings satisfying cyclical contractive conditions. *Fixed Point Theory*, 4(1), pp. 79-89. Available at: http://www.mathjournals.org/.

Matthews, S.G., 1994. Partial metric topology. In: Proceedings of the 8th Summer Conference on General Topology and Applications. *Annals of the New York Academy of Sciences*, 728, pp. 183–197. Available at: https://doi.org/10.1111/j.1749-6632.1994.tb44144.x.

Miheţ, D., 2008. Fuzzy ψ-contractive mappings in non-archimedean fuzzy metric spaces. *Fuzzy Sets and Systems*, 159(6), pp. 739-744. Available at: https://doi.org/10.1016/j.fss.2007.07.017.

Mirkov, N., Mitrovic, Z.D., Younis, M., Radenović, S., 2021. On Palais method in b-metric-like spaces. *Math. Anal. Contemp. Appl.*, 3(3), pp. 33-38. Available at: https://doi.org/10.30495/maca.2021.1932449.1015.

Mongkolkeha, C., Cho, Y.J. and Kumam, P., 2013. Best proximity points for generalized proximal C-contraction mappings in metric spaces with partial orders. *Journal of Inequalities and Applications*, 2013, Article 94. Available at: https://doi.org/10.1186/1029-242X-2013-94.

Monika, 2019. On Metric-Like Spaces: A Survey. *International Journal of Applied Engineering Research*, 14(6), pp. 1390-1395. Available at: https://www.ripublication.com/ijaer19/ijaerv14n6_19.pdf.

Moussaoui, A., Hussain, N., Melliani, S., Hayel, N. and Imdad, M., 2022. Fixed point results via extended $\mathcal{FZ}$-simulation functions in fuzzy metric spaces. *Journal of Inequalities and Applications*, 2022, Paper No. 69. Available at: https://doi.org/10.1186/s13660-022-03027-4.

Moussaoui, A., Radenović, S., and Melliani, S., 2024. A generalization of parametric metric spaces via $\mathcal{B}$-actions. *Filomat*, 38:15, pp. 5475–5485. Available at: https://doi.org/10.2298/FIL2415475M.

Păcurar, M. and Rus, I.A., 2010. Fixed point theory for cyclic φ-contractions. *Nonlinear Analysis*, 72(3–4), pp. 1181–1187. Available at: https://doi.org/10.1016/j.na.2009.08.002.

Petrusel, G., 2005. Cyclic representations and periodic points. *Studia Universitatis Babes-Bolyai, Mathematica*, 50, pp. 107-112. Available at: http://www.studiauniversitatis.ro/.

Radenović, S., 2016. Classical fixed point results in 0-complete partial metric spaces via cyclic-type extension. *Bulletin of the Allahabad Mathematical Society*, 31(1), pp. 39–55. Available at: https://doi.org/10.1007/s13370-015-0339-2.

Radenović, S., 2016. Some remarks on mappings satisfying cyclical contractive conditions. *Afrika Matematika*, 27(1), pp. 291–295. Available at: https://doi.org/10.1007/s13370-015-0339-2.

Salimi, P. and Karapinar, E., 2013. Suzuki-Edelstein type contractions via auxiliary functions. *Mathematical Problems in Engineering*, 2013, Article ID 648528. Available at: https://doi.org/10.1155/2013/648528.

Sarma, I.R., Kumari, P.S., 2012. On dislocated metric spaces. *International Journal of Mathematical Archive*, 3(1), pp. 72-77. Available at: https://www.ijma.info/.

Sawangsup, K., Sintunavarat, W. and Cho, Y.J., 2020. Fixed point theorems for orthogonal F-contraction mappings on O-complete metric spaces. *Journal of Fixed Point Theory and Applications*, 22(10). Available at: https://doi.org/10.1007/s11784-020-00785-9.

Sintunavarat, W. and Kumam, P., 2012. Common fixed point theorem for cyclic generalized multi-valued contraction mappings. *Applied Mathematics Letters*, 25(11), pp. 1849-1855. Available at: https://doi.org/10.1016/j.aml.2012.02.045.

Suzuki, T., 2008. A Generalized Banach Contraction Principle That Characterizes Metric Completeness. *Proceedings of the American Mathematical Society*, 136(5), 1861–1869. Available at: http://www.jstor.org/stable/20535364.

Suzuki, T., 2009. A new type of fixed point theorem in metric spaces. *Nonlinear Analysis*, 71(11), pp. 5313-5317. Available at: https://doi.org/10.1016/j.na.2009.04.017.

Yang, Q. and Bai, C., 2020. Fixed point theorem for orthogonal contraction of Hardy-Rogers type mapping on O-complete metric space. *AIMS Mathematics*, 5(6), pp. 5734–5742. Available at: https://doi.org/10.3934/math.2020.6.5734.

Yamaod, O., Sintunavarat, W., 2018. On new orthogonal contractions in b-metric spaces. *International Journal of Pure and Applied Mathematics*, 5(4), pp. 37-40. Available at: https://doi.org/10.12732/ijpam.v5i4.6.

Yu, D., Chen, C., Wang, H., 2018. Common fixed point theorems for $(T, g)_F$-contraction in b-metric-like spaces. *Journal of Inequalities and Applications*, 2018, Article 222. Available at: https://doi.org/10.1186/s13660-018-1802-z.

Zoto, K., Radenović, S. and Ansari, A.H., 2018. On some fixed point results for (s, p, α)-contractive mappings in b-metric-like spaces and applications to integral equations. *Open Mathematics*, 16, pp. 235-249. Available at: https://doi.org/10.1515/math-2018-0024.

Zoto, K., Hoxha, E., 2012. Fixed point theorems in dislocated and dislocated quasi-metric spaces. *Journal of Advanced Studies in Topology*, 3(4), pp. 119-124. Available at: https://www.sdiarticle2.in/prh/JAST/2012/.

Espacios b-métricos: Una revisión de conceptos y aplicaciones

Abdelhamid Moussaoui[1], *Stojan* Radenovic[2]

[1] Facultad de Ciencias y Técnicas, Laboratorio de Matemáticas Aplicadas y Computación Científica, Universidad Sultan Moulay Slimane, Beni Mellal, Marruecos; **autor de correspondencia**

[b] Faculty of Mechanical Engineering, University of Belgrade, Kraljice Marije 16, 11120, Beograd 35, Serbia, e-mail: sradenovic@mas.bg.ac.rs,

CAMPO: matemáticas
TIPO DE ARTÍCULO: artículo de revisión

Este artículo ofrece una revisión exhaustiva de los resultados de puntos fijos en espacios métricos-like, con un enfoque particular en los espacios b-métrico-like. La noción de espacios b-métrico-like generaliza varios conceptos importantes, incluidos los espacios métricos parciales, los espacios métricos-like y los espacios b-métricos. El artículo destaca contribuciones significativas desde las primeras etapas de la investigación hasta el presente, ofreciendo una compilación extensa de resultados fundamentales y recientes. Finalmente, proporcionamos respuestas afirmativas a algunos problemas abiertos derivados de los resultados de proximidad óptima en espacios b-métrico-like ortogonales 0-completos, avanzando aún más en la comprensión de la teoría de puntos fijos en estos entornos generalizados. Esta revisión tiene como objetivo proporcionar a los investigadores valiosas ideas y referencias, facilitando la exploración y el desarrollo futuros en el estudio de los espacios métricos-like y sus generalizaciones.

Espacios b-métrico-like, Espacios métricos, Espacios métricos parciales, Espacios b-métricos, Espacios métricos-like, Teoría de puntos fijos.

Обзор концепций и приложений пространств b-метрик

Abdelhamid Moussaoui[1], *Stojan* Radenovic[б]

[1] Факультет наук и технологий, Лаборатория прикладной математики и научных вычислений, Университет Султана Мулай Слимана, Бени-Меллал, Марокко; электронная почта: a.moussaoui@usms.ma,

[2] Факультет машиностроения, Белградский университет, Краљице Марије 16, 11120, Белград 35, Сербия, электронная почта: sradenovic@mas.bg.ac.rs,

РУБРИКА ГРНТИ: 36.00.00 ГЕОДЕЗИЯ. КАРТОГРАФИЯ;
36.29.00 Топография. Фототопография
36.29.33 Топографические и специализированные карты и планы. Цифровые модели местности.

ВИД СТАТЬИ: обзорная статья

В этой статье представлен подробный обзор результатов существования фиксированных точек в пространствах, подобных метрическим, с особым акцентом на b-метрические пространства. Понятие b-метрических пространств обобщает несколько важных концепций, включая частичные метрические пространства, метрические пространства и b-метрические пространства. Статья освещает значительные достижения в этой области, начиная с ранних исследований и до настоящего времени, предлагая обширную компиляцию фундаментальных и современных результатов. Кроме того, в статье даются положительные ответы на некоторые открытые вопросы, связанные с лучшими результатами близости в ортогональных 0-замкнутых b-метрических пространствах, что способствует дальнейшему развитию теории фиксированных точек в этих обобщенных структурах. Цель этого обзора — предоставить исследователям ценные идеи и ссылки, способствуя дальнейшему изучению и развитию теории пространств, подобных метрическим, и их обобщений.

Ключевые слова: b-метрические пространства, метрические пространства, частичные метрические пространства, b-метрические пространства, пространства, подобные метрическим, теория фиксированных точек.

---

b-Metrijski Prostori: Pregled Koncepata i Primena

Abdelhamid Moussaoui [1], ***Stojan Radenović*** [2]

[1] Fakultet za nauke i tehnike, Laboratorija primenjenih matematika i naučno računanje, Univerzitet Sultan Moulay Slimane, Beni Mellal, Maroko; e-mail: a.moussaoui@usms.ma, ORCID iD: https://orcid.org/0000-0003-4897-1132

[2] Fakultet za mehaničko inženjerstvo, Univerzitet u Beogradu, Kraljice Marije 16, 11120, Beograd 35, Srbija, e-mail: sradenovic@mas.bg.ac.rs, ORCID iD: https://orcid.org/0000-0001-8254-6688

ОБЛАСТ: математика
КАТЕГОРИЈА (ТИП) ЧЛАНКА: прегледни рад

У овом раду представљен је свеобухватан преглед резултата фиксних тачака у просторима сличним метричким, са посебним акцентом на b-метричке просторе. Појам b-

метричких простора обухвата неколико важних концепата, укључујући парцијалне метричке просторе, метричке просторе и b-метричке просторе. Рад истиче значајне доприносе од раних истраживања до данас, нудећи обимну компилацију фундаменталних и савремених резултата. Коначно, дајемо позитивне одговоре на неке отворене проблеме који произилазе из најбољих резултата близине у ортогоналним 0-комплетним b-метричким просторима, чиме даље унапређујемо разумевање теорије фиксних тачака у овим генерализованим окружењима. Овај преглед има за циљ да истраживачима пружи драгоцене увиде и референце, олакшавајући даље истраживање и развој у проучавању простора сличних метричким и њиховим генерализацијама.

Кључне речи: b-метрички простори, метрички простори, парцијални метрички простори, b-метрички простори, простори слични метричким, теорија фиксних тачака.

Paper received on: 14.02.2025.
Manuscript corrections submitted on: 01.04.2025.
Paper accepted for publishing on: 17.04.2025.

VOJNOTEHNIČKI GLASNIK / MILITARY TECHNICAL COURIER, 2025, Vol. 73, Issue 3

A comprehensive review of control and guidance strategies for unmanned ground vehicles in lane tracking and leader-follower applications

Amokrane B. Salem-Bilal[a], *Momir* R. Stanković[b], *Stojadin* M. Manojlović[c], *Ahmed Taki-Eddine* A. Benyahia[d]

[a] University of Defence in Belgrade, Military Academy, Department of Military Electronic Engineering, Belgrade, Republic of Serbia, e-mail: amokranesalembilal@gmail.com, **corresponding author**, ORCID iD: https://orcid.org/0009-0009-7588-5708

[b] University of Defence in Belgrade, Military Academy, Department of Military Electronic Engineering, Belgrade, Republic of Serbia, e-mail:momir_stankovic@yahoo.com , ORCID iD: https://orcid.org/0000-0001-8371-9341

[c] University of Defence in Belgrade, Military Academy, Department of Military Electronic Engineering, Belgrade, Republic of Serbia, e-mail:colemanojle@yahoo.com , ORCID iD: https://orcid.org/0000-0003-1268-5310

[d] University of Defence in Belgrade, Military Academy, Department of Military Electronic Engineering, Belgrade, Republic of Serbia, e-mail: benyahia.taki@gmail.com, ORCID iD: https://orcid.org/0009-0006-6025-6915

doi https://doi.org/10.5937/vojtehg73-59271

FIELD: robotics, autonomous systems, control engineering, mechanical engineering, computer science
ARTICLE TYPE: review paper

Abstract:

Introduction/purpose: *Unmanned Ground Vehicles (UGVs) offer significant advantages for various operations; yet their autonomous control and guidance present substantial difficulties, especially for diverse locomotion types (e.g., tracked, wheeled) in challenging terrains due to complex dynamics, nonholonomic constraints, and environmental interactions. This paper provides a comprehensive review of control and guidance strategies for UGVs, with a specific focus on leader-follower and lane tracking with obstacle avoidance applications. It aims to synthesize the state of the art, identify key challenges generic to UGV autonomy*

ACKNOWLEDGMENT: This research has been a part of Project No. VA/TT/1/25-27 supported by the Ministry of Defence, Republic of Serbia.

in these tasks, and discuss promising guidance and control methodologies.

Methods: *An extensive literature review was conducted, analyzing existing research on UGV, autonomy levels, system architectures, control methodologies (including classical, adaptive, robust, and intelligent approaches), guidance approaches, and specific application domains. Methodologies for guidance and control relevant to UGVs in leader-follower and lane tracking tasks were critically examined.*

Results: *The review identifies dominant trends, including the increasing use of deep learning for guidance perception and growing interest in robust control techniques capable of handling UGV operational challenges. Significant challenges persist in perception for unstructured environments, accurate dynamic modeling for diverse UGV platforms, seamless integration of perception with robust control and guidance systems, and extensive real-world validation.*

Conclusions: *Achieving robust autonomy for UGVs in complex real-world scenarios require integrated solutions addressing guidance and control. Advanced robust control methods emerge as strong candidates for UGV control, but their full potential necessitates further research into their integration with advanced guidance systems.*

Key words: *unmanned ground vehicles (UGVs), control systems, guidance systems, leader-follower, lane tracking, obstacle avoidance, autonomous navigation.*

Introduction

The field of robotics and autonomous systems has witnessed exponential growth, leading to the development and deployment of sophisticated Unmanned Ground Vehicles (UGVs) across a multitude of domains (Sethi, 2024; Fareh et al., 2021). UGVs, capable of operating autonomously or semi-autonomously without direct human piloting, offer transformative potential in areas deemed too dangerous or complex for human operators. Applications span military operations (reconnaissance, logistics, explosive ordnance disposal), agriculture (precision farming, harvesting), search and rescue, logistics (warehouse automation, last-mile delivery), and infrastructure inspection (Ni et al., 2021; Shafaei & Mousazadeh, 2023; Gadekar et al., 2023; Durst et al., 2018).

Among diverse UGV platforms, various locomotion types exist, each with unique advantages and control complexities. For instance, tracked vehicles offer superior traction in unstructured terrains but introduce challenges like skid-steering dynamics and track slippage (Sebastian & Ben-Tzvi, 2019b; Zou et al., 2018). Wheeled vehicles are efficient on structured surfaces but are limited in off-road mobility. Achieving reliable autonomous operation for any UGV type introduces significant complexities in their control and guidance, including inherent nonlinearities, platform-specific dynamics (e.g., skid-steering in tracked vehicles, Ackermann steering in some wheeled vehicles), sensitivity to terrain variations, and susceptibility to external disturbances (Al-Jarrah et al., 2019; BaniHani et al., 2021; Zou et al., 2018; Artuñedo et al., 2024).

This review paper focuses on the critical aspects of control and guidance for UGVs, specifically addressing two demanding autonomous tasks: leader-follower control and lane tracking with obstacle avoidance. Leader-follower systems, where a UGV autonomously follows a human or vehicular leader, are essential for applications like convoying, collaborative robotics, and human assistance (Ramírez-Neria et al., 2023a; Wang, 2024). Lane tracking with obstacle avoidance is fundamental for UGV navigation in semi-structured environments, such as agricultural fields, mining sites, or pathways, requiring the UGV to adhere to lane boundaries while safely avoiding obstacles (Cao et al., 2020; Zhang et al., 2023). Both tasks demand high levels of robustness, adaptability, and real-time responsiveness from UGVs operating in dynamic and often unpredictable environments.

Traditional control methods, such as Proportional-Integral-Derivative (PID) controllers, often struggle to provide the required performance and robustness for diverse dynamics encountered in UGVs, especially when dealing with strong nonlinearities, time-varying parameters, and unmodeled dynamics (Kayacan et al., 2015; Rizk et al., 2023). While advanced techniques like Model Predictive Control (MPC) or adaptive control offer potential benefits, they often rely on accurate system models or complex tuning procedures, which can be impractical for UGVs operating in diverse conditions (Zuo et al., 2021; Fareh et al., 2021).

More recent approaches, such as observer-based robust control methods, aim to address these limitations by actively estimating and compensating for disturbances and model uncertainties, often reducing the dependence on precise mathematical models and offering inherent robustness. These characteristics make them well-suited for complex and often poorly modeled dynamics found across various UGV platforms (Fareh et al., 2021; Sebastian & Ben-Tzvi, 2019a).

This paper is structured as follows: the section “Overview of unmanned ground vehicles (UGVs)” provides an overview of UGVs, covering their history, levels of autonomy, and types of locomotion. The section “System architecture for autonomous navigation in UGVs” details the system architecture for UGV autonomous navigation, focusing on the guidance system and the control system. The sections “Lane tracking task in UGVs” and “Leader-follower task in UGVs” delve into the overview for lane tracking/obstacle avoidance and leader-follower control for UGVs, respectively. The section “Synthesis of findings and dominant trends” discusses the findings and the section “Conclusion and future research directions” concludes the review and suggests future research directions applicable to UGVs.

Overview of unmanned ground vehicles (UGVs)

Unmanned Vehicles (UVs) are frequently engineered as autonomous systems, capable of environmental perception, trajectory planning, and autonomous control without human intervention (Sethi, 2024). This broad category encompasses aerial, underwater, and ground-based systems. Unmanned Ground Vehicles (UGVs), the focus here, have seen significant development driven by technological advancements and diverse application demands (Fareh et al., 2021).

To provide a comprehensive foundational framework necessary for effective control and guidance, this section will detail the various levels of autonomy in UGVs, explore their diverse types based on locomotion, and outline the inherent challenges associated with their autonomous operation.

Levels of autonomy in UGVs

UGV capabilities are often defined by levels of autonomy, indicating the degree of independent operation. The Society of Automotive Engineers (SAE) provides a standard six-level classification for driving automation (Sethi, 2024; van der Sande & Nijmeijer, 2017), illustrated in Figure 1. This ranges from **Level 0** (no automation), where humans perform all driving tasks. The next, **Level 1** (assisted driving automation), offers either steering or speed control with full human supervision, while **Level 2** (partial automation) provides both steering and speed control, requiring constant driver readiness for intervention. In **Level 3** (conditional automation) the

Amokrane, salem-bilal. et al., Review of Control and Guidance for UGVs in Lane Tracking and Leader-Follower Applications, pp.1098–1140

system performs all driving tasks under specific conditions, prompting the driver for control when needed, and **Level 4** (high automation) allows the system to handle all driving tasks and fallback within a defined operational domain, even without driver's response. Finally, **Level 5** (full automation) signifies the system's ability to perform all driving tasks under all conditions, requiring no human intervention.

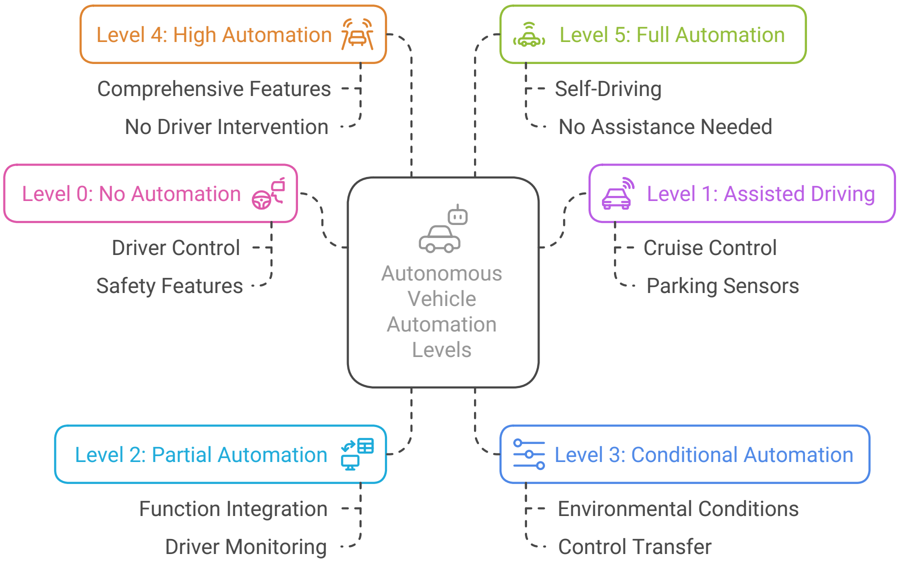

Figure 1 – Autonomy levels in UGV systems

Types of UGVs based on locomotion

UGVs have evolved into a diverse range of platforms, each with unique locomotion mechanisms and capabilities. These differences stem from the need to adapt to various operational environments and tasks. The primary locomotion strategies employed in UGVs can be categorized into four main types: wheeled, tracked, legged, and hybrid systems.

- **Wheeled UGVs**: utilize the rotational motion of wheels for movement, common for their simplicity and efficiency on structured surfaces. Various steering architectures (e.g., differential, Ackermann, omnidirectional) provide varying degrees of maneuverability and stability (Ahluwalia et al., 2022; Rubio et al., 2019; Tagliavini et al., 2022).

- **Tracked UGVs**: employ continuous tracks for a large ground contact area, enhancing traction and stability on complex, uneven terrains. Skid-steering is typically used by varying track speeds. This structural design facilitates maneuverability and robust locomotion in complex and rough environments, such as military operations and agriculture (Sebastian & Ben-Tzvi, 2019b; Zou et al., 2018; Shafaei & Mousazadeh, 2023).
- **Legged UGVs**: mimic living things (e.g., animal, human) locomotion using actuated limbs for movement in discrete steps, enabling traversal of highly unstructured terrains and obstacles (Ahluwalia et al., 2022; Zhao et al., 2023).
- **Hybrid UGVs**: combine multiple locomotion types to leverage their respective advantages and enhance adaptability across diverse conditions, leading to a more complex and flexible system (Ahluwalia et al., 2022; Teji et al., 2023).

Table 1 summarizes the advantages and disadvantages of each type.

System architecture for autonomous navigation in UGVs

Autonomous UGV operation typically relies on a hierarchical system architecture to manage the complexity from sensing to actuation. This review adopts a common conceptualization involving distinct but interconnected systems: a guidance system (encompassing perception and decision-making) and a control system (responsible for motion execution) (Ni et al., 2018; Samak et al., 2021; Yao et al., 2020; Zhang et al., 2023). Figure 2 illustrates this general architecture. The following subsections will provide the details of these two core systems, exploring their functionalities and key components in UGV autonomous navigation.

Guidance system

The guidance system acts as the ”brain” of the UGV, responsible for interpreting the environment, making intelligent decisions, and planning the vehicle’s motion (Wang, 2024; Horri et al., 2024; Zheng & Gao, 2010). It forms the cornerstone of the architecture, supplying essential environmental awareness that supports higher-level decision-making and control processes (Gao et al., 2001; Durst et al., 2018; Samak et al., 2021).

UGV Type	Advantages	Disadvantages	References
Wheeled	High energy efficiency, low cost, simple control, high speed on flat terrain, suited for structured environments.	Limited off-road capability, prone to slipping/skidding on loose surfaces, poor mobility on rough terrains.	Man et al. (2018); Thrun et al. (2006); Ahluwalia et al. (2022); Rubio et al. (2019); Tagliavini et al. (2022); Teji et al. (2023)
Tracked	Superior traction/stability on challenging terrains (sand, mud, slopes, rocks), high load capacity, large ground contact.	High energy consumption, complex mechanics, less maneuverable than wheeled, complex turning dynamics, prone to slippage.	Sebastian & Ben-Tzvi (2019b); Zou et al. (2018); Shafaei & Mousazadeh (2023); Ahluwalia et al. (2022); Li et al. (2021); Alexa et al. (2023); Wang et al. (2024b); Al-Jarrah et al. (2019); BaniHani et al. (2021); Liu et al. (2024)
Legged	High maneuverability in complex/cluttered terrains, stair climbing, high adaptability/obstacle negotiation.	High system complexity, high energy/computational load, less efficient over long distances, difficult control design.	Ahluwalia et al. (2022); Tian et al. (2021); Zhao et al. (2023)
Hybrid	High versatility across terrains due to multiple locomotion mechanisms, adaptable for complex tasks, enhanced performance.	Complex control implementation, high cost/design complexity, increased hardware/computational needs.	Ahluwalia et al. (2022); Teji et al. (2023)

Table 1 – Comparison of UGV locomotion types

Types of autonomous navigation and decision making

The guidance system plans the UGV motion based on the perceived environment and mission goals. Autonomous navigation tasks for UGVs can be categorized into three fundamental types:

- **Point-to-Point navigation**: the UGV moves from a start to a goal location without a predefined path, primarily focusing on reaching the destination while avoiding obstacles, regardless of the specific path geometry or velocity profiles (Ruslan et al., 2023; Stanković et al., 2024).

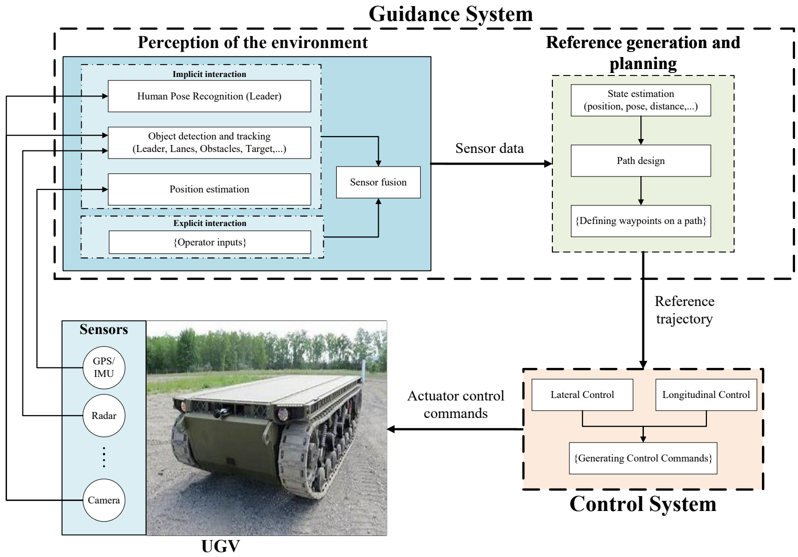

Figure 2 – Typical system architecture for autonomous UGV navigation

- **Path following**: the UGV converges to and follows a predefined geometric path (e.g., lane centerline) without strict temporal constraints. The objective is spatial convergence (minimizing cross-track error), allowing velocity flexibility along the path. The UGV's forward speed follows a predefined speed profile, while the control system primarily regulates the vehicle's orientation to ensure convergence to the desired path (Hung et al., 2023; Ruslan et al., 2023; Sarcinelli-Filho & Carelli, 2023). This typically involves regulating orientation for path convergence, often resulting in smoother control than trajectory tracking (Aguiar & Hespanha, 2007; Stanković et al., 2024).
- **Trajectory tracking**: the UGV must follow a time-parameterized trajectory specifying both position and velocity at each instant. This requires simultaneous spatial and temporal convergence, making it more complex than path following (Sarcinelli-Filho & Carelli, 2023). It is crucial for applications like leader-follower systems where precise motion (speed and orientation) replication is needed (Ruslan et al., 2023; Hung et al., 2023; Stanković et al., 2024).

In essence, Point-to-Point navigation only specifies a destination. Path following focuses on spatial adherence to a geometric path, whereas the velocity of the vehicle is defined by the designer. Trajectory tracking requires traversing the specified path while the velocity of the vehicle, in terms of both magnitude and direction, is defined by the trajectory being tracked.

Sensing and scene understanding for guidance

This sub-system acts as the system's senses, responsible for gathering and fusing information about the vehicle's internal state and its external environment to create a meaningful representation for decision making (Balasubramaniam & Pasricha, 2022). Key components include:

- **Exteroceptive sensors:** provide information about the external surroundings (Liu et al., 2021c). Common types include:
  - **Cameras (monocular, stereo, omnidirectional):** capture visual data (color, texture) for tasks like lane/object detection, leader tracking, and obstacle avoidance (Burke & Brink, 2010; Schulte et al., 2022; Liu et al., 2021c). Images are often processed by machine learning (ML) and deep learning (DL) models for real time and adaptability to various lighting conditions. Vision is critical for this review's focus on leader following and lane tracking with obstacle avoidance.
  - **LiDAR (Light Detection and Ranging):** emits laser pulses to measure distances, generating 3D point clouds for environmental mapping, obstacle avoidance, and path planning (Gadekar et al., 2023; Balestrieri et al., 2021).
  - **Radar:** uses radio waves to detect objects, measuring their distance, speed, and direction. Effective in diverse weather and at long ranges, complementing optical sensors (Balestrieri et al., 2021).
- **Proprioceptive sensors:** measure the UGV internal state (Liu et al., 2021c). Common types include:
  - **GNSS (Global Navigation Satellite System):** e.g., GPS - determines absolute vehicle position for global navigation and trajectory tracking.
  - **IMU (Inertial Measurement Unit):** provides acceleration and angular velocity data for precise state estimation and motion control, especially in GPS-denied environments.

- **Sensor fusion algorithms:** integrate data from diverse sensors to yield a more comprehensive and robust environmental understanding than possible with individual sensors (Hu et al., 2020). For instance, fusing LiDAR and camera data can enhance 3D mapping and object detection accuracy, improving overall perception reliability by combining complementary information and filtering noise.
- **Detection and recognition algorithms:** process sensor data to identify relevant entities.
  - *Object detection/tracking:* involves identifying and tracking entities like pedestrians, vehicles, obstacles, or specific leaders. Deep learning, particularly convolutional neural networks (CNNs) like YOLO and its variants (e.g., YOLOv8), are prominent for their real-time speed and accuracy (Redmon et al., 2016; Terven et al., 2023; Vijayakumar & Vairavasundaram, 2024). The name YOLO stands for "You Only Look Once", referring to the fact that it was able to accomplish the detection task with a single pass of the network (Redmon et al., 2016). YOLO models, known for efficiency with monocular cameras, have evolved to offer high performance in autonomous navigation and robotics (Terven et al., 2023; Hussain, 2024).
  - *Lane detection:* focuses on identifying lane markings or road boundaries. While traditional methods used edge detection and Hough transforms (Aly, 2008), modern approaches heavily rely on DL, often using semantic segmentation (e.g., encoder-decoder architectures) (Ni et al., 2020; Sun et al., 2019). Multi-task learning models like YOLOP advance this by simultaneously performing lane detection, drivable area segmentation, and object detection for improved efficiency and contextual awareness (Wu et al., 2022; Sridevi & Harish, 2024; Zhan et al., 2024). YOLOP architectures leverage shared backbones for panoptic perception, enhancing robustness and overall model efficiency (Li & Xu, 2024). YOLOPv2 (Sridevi & Harish, 2024) preserves the core design concepts of YOLOP and HybridNets while employing a more robust network structure and an efficient training strategy, achieving state-of-the-art (SOTA) performance in both accuracy and speed (Zhan et al., 2024).

– *Human pose estimation (HPE):* localizes human joints or landmarks in images/videos, crucial for UGV applications like gesture-based control from a leader operator. Deep learning has largely superseded classical HPE methods due to better accuracy and generalization (Kulkarni et al., 2023; Zheng et al., 2023). Frameworks like MediaPipe Pose (MPP), an open-source cross-platform framework developed by Google, provide real-time 2D/3D landmark extraction (e.g., 33 body landmarks with BlazePose), offering valuable geometric and motion data for human-robot interaction and leader following (Google, 2023).

Vision sensors are increasingly vital in UVs, complementing or replacing GPS-based navigation due to their small size, low weight, low cost, and ability to extract rich data for target/obstacle identification when paired with the appropriate image processing software (Li, 2013). As passive sensors, they operate non-invasively, reducing inter-sensor interference, and are often the most reliable option in GPS-denied or cluttered environments.

Vision-based guidance leverages camera data for critical tasks like lane tracking, leader recognition, and obstacle detection, enabling UGVs to navigate complex environments and enhancing their autonomy and human-vehicle interaction (Liu et al., 2021c; Zhang et al., 2023; Chen, 2016).

- **Leader following and pose recognition:** vision is crucial for detecting, tracking, and interpreting a human leader's intent. DL algorithms analyze real time imagery to determine leader position, orientation, and infer movement or commands via pose estimation (Burke & Brink, 2010; Schulte et al., 2022). This allows the UGV to anticipate actions and improve decision making, with CNNs often used to identify leader features and actions.
- **Lane detection and obstacle avoidance:** vision-based guidance identifies lane markings and obstacles from camera data. DL algorithms detect lane boundaries for accurate UGV trajectory generation, requiring robustness to dynamic conditions (e.g., lighting, road quality) (Artuñedo et al., 2024; Andrade et al., 2019). Similarly, DL models detect and track obstacles, enabling collision-free path planning and proactive avoidance by predicting dynamic object movements.

This layer's processing of sensory data guides the control system by providing necessary information, which ultimately enables safe, accurate, and efficient operations in complex and uncertain environments. The guidance system provides the intelligence for autonomous UGV operation, making high-level decisions and generating navigation commands. The information provided by the guidance system defines the desired behavior for the control system to execute. This crucial control system will be discussed in the following section.

Control system

The control system executes trajectories or commands from the guidance system, calculating actuator commands (e.g., track motor torques/speeds) for accurate and stable motion despite disturbances and uncertainties (Samak et al., 2021; Wang et al., 2024a; Al-Jarrah et al., 2019; Zou et al., 2018; Gao et al., 2025; Rizk et al., 2023; Xia et al., 2016; Wang et al., 2021; Azam et al., 2020). It typically involves:

- **Longitudinal control:** manages the UGV's speed and acceleration (via throttle/brakes) to maintain desired velocity, ensure safety, and optimize efficiency. It must handle varying dynamics (e.g., engine torque, road grade, resistance) and adapt to changing conditions for smooth, stable motion.
- **Lateral control:** manages UGV steering to follow the intended trajectory and maintain orientation (e.g., relative to a lane or a leader) by minimizing cross-track and heading errors. It must reject side disturbances and account for platform-specific steering dynamics (e.g., track slip in tracked vehicles, tire-road interaction in wheeled vehicles), terrain variations, and nonholonomic constraints to generate smooth, stable steering commands.

The design of longitudinal and lateral controllers can be approached in two ways (Sabiha et al., 2022; Wang et al., 2024a; Al-Jarrah et al., 2019; Samak et al., 2021):

- **Decoupled control:** longitudinal and lateral control are designed and implemented independently, neglecting the coupling effects between them. This simplifies control design but may compromise performance in highly dynamic maneuvers where coupling effects are significant.
- **Coupled control:** design explicitly considers longitudinal-lateral dynamic coupling for more coordinated and robust control, especially in challenging conditions allowing the controllers to compensate for the

effects of each other. This enhances stability and performance but increases design complexity.

The choice between decoupled and coupled control depends on system characteristics, performance needs, and design complexity, requiring a balance between implementation simplicity and potential performance gains.

Control strategies for UGVs

Selecting an appropriate control strategy is crucial for achieving desired UGV performance (accuracy, stability, robustness) in the face of evolving environmental and dynamic challenges. Strategies are broadly categorized as classical control, adaptive control, robust control, advanced control techniques (including MPC and observer-based control like ADRC), and intelligent control (e.g., neural networks NN, fuzzy logic control FLC, reinforcement learning RL). Each category encompasses various methods with distinct principles, advantages, and limitations. For a detailed comparison, Table 2 summarizes these primary control strategies.

The control strategies can also be classified by their reliance on a system model:

- **Model-based control:** these methods rely on the use of a mathematical representation to design the control law, optimizing for specific objectives while considering the system's dynamics and operational constraints. Classical control techniques such as PID and geometric controllers, along with advanced methods such as MPC, fall under this category (Kebbati et al., 2023; Samak et al., 2021; Santoso et al., 2020). While these methods have a solid theoretical base and well-known design principles, their main drawback is the dependence on a precise mathematical model, which might be difficult to achieve for complex, nonlinear, and uncertain systems.
- **Model-free control:** these control strategies, such as those implemented through artificial intelligence techniques (e.g., neural networks, fuzzy logic, and reinforcement learning), do not rely on a specific mathematical representation of the system (Kebbati et al., 2023; Rizk et al., 2023). Instead, they operate by directly interacting with the environment and updating their control laws based on operational feedback. The advantages of model-free approaches lie in their ability to operate in highly complex and uncertain environments and to learn from data (Samak et al., 2021). However, their limitations in-

Control strategy	Main idea	Advantages	Limitations
Classical control	Using simplified system models to generate control actions.	Simple and easy to implement in linear systems.	Limited in nonlinear systems with uncertainties and disturbances.
Adaptive control	Dynamically adjusts control parameters based on the system's changes and operating conditions.	Improves performance in time-varying environments.	Complex implementation and may be highly dependent on the system model.
Robust control	Designs controllers to maintain stability despite the presence of uncertainties.	Guarantees performance over a range of uncertainties.	Requires detailed mathematical models with uncertainty descriptions; sensitive to modeling errors.
MPC	Predicts the system behavior over a future horizon and finds the optimal control actions.	Handles constraints and is suitable for nonlinear systems.	Computationally intensive and dependent on model accuracy.
Observer-based control (e.g. ADRC)	Uses observers to estimate the system state and/or disturbances.	Provides state/disturbance estimation; robustness to unmodeled dynamics and external disturbances with reduced model dependency.	Tuning of observer and controller parameters can be challenging; performance relies on observer accuracy.
Intelligent control	Uses AI techniques to generate robust and adaptive control systems.	Flexible; can learn complex nonlinear relationships and adapt to changing environments.	Requires high computational power, large datasets for training, and complex parameter tuning.

Table 2 – Summary of the control strategies in UGVs

clude a significant computational load during real-time execution and the requirement for large datasets for training.

- **Hybrid control:** combines model-based and model-free aspects. A prominent example within this category is Active Disturbance Rejection Control (ADRC). ADRC's core philosophy involves treating all uncertainties (internal dynamics, parameter variations, external disturbances) as a single "total disturbance" and actively estimating and compensating for it in real time using an Extended State Observer

(ESO) (Han, 2009; Gao, 2006). This approach significantly reduces the dependence on an accurate mathematical model and offers inherent robustness against uncertainties and disturbances, making it well-suited for the complex and often poorly modeled dynamics of UGVs across various platforms. Its key advantages include robustness to uncertainties/disturbances, reduced model dependency, relative simplicity in implementation/tuning, effectiveness for nonlinear systems without explicit linearization, real-time disturbance rejection, adaptability to changing conditions (terrain, payload, environmental variations), and proven success in diverse applications (Fareh et al., 2021; Han, 2009; Sebastian & Ben-Tzvi, 2019a; Gao, 2006; Zheng & Gao, 2016; Guo & Zhao, 2015; Benyahia et al., 2025; Stanković et al., 2019; Madonski et al., 2019).

ADRC's capabilities are particularly relevant for the UGV applications discussed in this review, such as leader-following, where its real-time disturbance rejection is crucial for compensating for unpredictable leader motion and vehicle slip (Amokrane et al., 2024; Fareh et al., 2021), and lane tracking with obstacle avoidance, where its ability to handle unmodeled dynamics aids tracking on uneven terrains and can mitigate sensing errors (Teji et al., 2023; Zhang et al., 2023; Ramírez-Neria et al., 2023a). ADRC has been successfully applied across various vehicle control domains, including longitudinal velocity tracking (Gao et al., 2025; Jin et al., 2023), integrated motion control considering longitudinal-lateral coupling (Wang et al., 2024a), and lateral path following (Xia et al., 2016; Kang et al., 2022; Sang & Chen, 2020; Wang et al., 2022). Specific studies on tracked vehicles, for instance, have leveraged ADRC to address challenges like slip compensation (Sebastian & Ben-Tzvi, 2019a), robust trajectory tracking (Stanković et al., 2024), and handling disturbances in demanding environments such as mining (Liu et al., 2024).

While existing literature offers valuable insights into UGV control, the specific challenges of leader-follower and lane tracking control, particularly under uncertain conditions and with complex terrain interaction, demand careful selection and adaptation of control strategies. The following sections will present how different papers address these tasks, their perception sensors and algorithms, and their chosen control approaches.

Lane tracking task in UGVs

Lane tracking is a critical capability for UGVs, enabling them to navigate along predefined or perceived lanes in structured or semi-structured environments. This task primarily involves detecting lane boundaries and controlling the vehicle to follow them accurately. For certain UGV types, like tracked vehicles, effective lane tracking is particularly challenging due to their skid-steering dynamics, with lanes potentially poorly defined, exhibiting sharp curvatures, or being partially obscured.

A crucial aspect often considered essential for practical lane tracking is **obstacle avoidance**. While maintaining adherence to the lane, the UGV must also possess the ability to detect and safely maneuver around any obstacles encountered in its path. Therefore, robust guidance systems must encompass both lane interpretation and obstacle detection, and control systems must execute maneuvers that ensure both accurate path adherence and collision avoidance, maintaining stability against disturbances such as slippage or uneven terrain.

Categorized as **path following** (see the section "Types of autonomous navigation and decision making"), the primary objective is to maintain spatial alignment with the lane's geometric centerline, managing speed for safety rather than adhering to strict temporal constraints. Real-time sensing, utilizing sensors such as cameras, LiDAR, and Radar to identify lane boundaries and obstacles, is foundational. This section reviews literature pertinent to UGVs performing lane tracking, including the associated challenge of obstacle avoidance, which is crucial for navigating semi-structured environments.

Given that general control systems for UGVs were comprehensively addressed previously in the section "System architecture for autonomous navigation in UGVs", the subsequent discussion in this section will primarily focus on the design aspects of the guidance system specific to lane tracking, including sensing and detection modules. Following this, an overview of the existing solutions will be presented, covering approaches which integrate both guidance and control for this specific autonomous task.

Guidance system design in the lane tracking task

Effective guidance system design for lane tracking in UGVs relies on robust environmental interpretation. This typically involves two critical mod-

Amokrane, salem-bilal. et al., Review of Control and Guidance for UGVs in Lane Tracking and Leader-Follower Applications, pp.1098–1140

ules: a lane detection module to identify the lane boundaries, and an obstacle detection module to perceive obstacles in the environment and ensure safe navigation, both of which are detailed in the following subsections.

Lane detection module design

Lane detection methods have evolved from traditional geometric approaches to advanced ML and DL techniques, adapting to the complexities of real-world driving environments with varying lighting, road types, and occlusions (Xing et al., 2018).

Cameras are the most widely utilized sensors for lane detection (Chetan et al., 2020; Zakaria et al., 2023; Yang, 2024). A literature review from 2018 to 2021 reveals that over 53 articles focused on camera-based lane detection, while only about three published articles explored the use of other sensors, often in combination with cameras (Zakaria et al., 2023). This preference stems from vision-based imaging aligning with human driver perception (as lane markings are visual cues) and the cost-effectiveness and robustness of camera technology, supported by significant advancements in machine vision (Bar Hillel et al., 2014).

Despite its advantages, vision-based lane detection faces challenges including lighting variations (shadows, glare, low light), adverse weather (rain, snow, fog), occlusions from vehicles/objects, and misdetections from road artifacts (skid marks, cracks), necessitating advanced algorithms for robust performance (Yang, 2024; Sultana et al., 2023).

Lane detection techniques can be broadly categorized:

1. **Model-based methods:** these methods typically involve a multi-stage pipeline: image preprocessing (noise reduction, ROI isolation), feature extraction (edge detection, thresholding, color filtering), lane model fitting (Hough Transform, least-squares, polynomial/hyperbolic curves), and tracking (Kalman filters) (Zhang et al., 2021b; Munir et al., 2022; Ghanem et al., 2023; Lee & Moon, 2018; Aly, 2008). While simple and efficient, they require manual parameter adjustment and struggle to adapt to diverse conditions.
2. **Intelligent-based methods:** in contrast, intelligent-based methods leverage ML and DL to learn features and patterns directly from data, enabling them to handle variability in road scenes.
   - *Machine learning methods* integrate traditional feature extraction (e.g., adaptive thresholding, morphological operations) with

classifiers (e.g., Bayesian, SVM, ANN) trained on labeled data (Dhanakshirur et al., 2019; Feng et al., 2019; Fakhfakh et al., 2020). Their performance remains dependent on the quality of manually extracted features.

- *Deep learning methods* are state of the art due to their ability to automatically learn hierarchical features from raw images. CNNs are common, often used in encoder-decoder networks for semantic segmentation. Some methods use recurrent layers (e.g., convLSTM) for temporal dependency or attention mechanisms for challenging conditions. DL's adaptability makes it widely used (Sun et al., 2019; Philion, 2019; Dewangan et al., 2021; Dawam & Feng, 2020; Wu et al., 2021; Zhang et al., 2021a; Liu et al., 2021a; Baek et al., 2022; Oğuz et al., 2022). DL-based lane detection is broadly categorized into two groups (Ni et al., 2020): (1) *One-Stage methods* directly predict lane parameters (e.g., curvature, position) from the network, offering greater speed and efficiency while (2) *Two-Stage methods* first perform semantic segmentation before curve-fitting to obtain parametric representations, typically achieving higher accuracy at greater computational cost. The choice depends on application needs (real-time performance vs. precision), with both demonstrating success in addressing the challenges of lane detection in complex and dynamic environments (Ni et al., 2020).

Obstacle detection module design

Obstacle detection is critical for UGVs, especially in unpredictable off-road environments. Dima et al. (Dima et al., 2004) defined obstacles as "a region that cannot or should not be traversed by the vehicle", including pedestrians, vehicles, or terrain features. Effective systems integrate real time perception, decision making, and control to avoid collisions and maintain mission objectives (Zhang et al., 2019). System efficacy depends on sensor choice, algorithmic robustness, and environmental adaptability.

Generally, sensors for obstacle detection can be categorized as (Hu et al., 2020; Islam et al., 2022; Yu & Marinov, 2020):

1. **Range-based sensors:** include LiDAR (for high-resolution 3D point clouds) and Radar (robust in diverse weather for range, speed, and angle, but with lower resolution).

2. **Image-based sensors:** comprise monocular cameras (cost-effective, provide rich semantic data but lack inherent depth), stereo cameras (for depth via triangulation), and infrared cameras (effective for night vision).
3. **Hybrid sensors:** combine multiple data sources (e.g., RGB-D cameras capturing color and depth) for comprehensive environmental understanding, typically with limited range.

While LiDAR and radar offer valuable detection capabilities, visual cameras, both monocular and stereo, serve as essential components of obstacle detection systems. These systems employ both traditional image processing techniques and modern deep learning methods to interpret visual data, aiding in object classification (Hu et al., 2020; Islam et al., 2022).

Monocular cameras are particularly advantageous for UGV obstacle avoidance due to cost-effectiveness, versatility in extracting rich semantic information, favorable performance-to-resource balance (ideal for limited payload/power), adaptability to diverse lighting, and scalability (supporting multiple perception tasks). The synergy of monocular cameras with DL (e.g., CNNs for real-time semantic segmentation, depth estimation, obstacle classification) has significantly advanced their capabilities, making them an efficient sensing modality for resource-constrained UGVs.

Several important approaches exist for vision-based obstacle detection, including:

- **Traditional computer vision methods:** focus on extracting and tracking feature descriptors (e.g., SIFT, SURF, HOG) from images to infer obstacle presence or motion. These are often paired with classifiers like SVM or KNN (Parmar et al., 2019). Motion-based techniques analyze optical flow (Vera-Yanez et al., 2024), while appearance-based methods segment traversable regions based on learned patterns (Badrloo et al., 2022). These approaches are generally slow for real-time applications.
- **Modern deep learning methods:** leverage DL architectures, particularly CNNs, to automatically learn hierarchical features, significantly improving speed and robustness. Object detection CNNs can locate and classify pre-trained objects, outputting bounding boxes, pixel-level segmentations, or key points (Parmar et al., 2019; Badrloo et al., 2022). One-stage networks like YOLO and SSD are favored for their real-time performance and accuracy over older two-stage methods

like R-CNN variants (Terven et al., 2023; Hussain, 2024; Vijayakumar & Vairavasundaram, 2024).

Overview of the existing UGV lane tracking solutions

The control system is responsible for translating the planned path, generated by the guidance system, into specific commands for the vehicle's actuators, effectively executing the desired trajectory. Reviewing the existing literature on lane tracking for UGVs reveals that there are numerous different areas being actively explored by researchers in this field.

Some studies place a strong emphasis on the **control aspect**, developing sophisticated algorithms to ensure precise lane adherence and stability, often assuming well-defined perceptual input. For example, (Marino et al., 2009) proposed a nested PID steering control for vision-based lane tracking, where an inner PI loop controlled yaw rate error for disturbance rejection, and an outer PID loop managed lateral offset, validated via CarSim simulations. (Chen et al., 2014) developed an Adaptive Model Predictive Control (AMPC) system for lane tracking, using a linear time-variant (LTV) prediction model with real-time online tire stiffness estimation, demonstrating superior performance in simulations compared to conventional MPC. (Chu et al., 2018b) combined ADRC with Quantitative Feedback Theory (QFT) for lane tracking, with QFT tuning the ADRC controller for robustness against uncertainties; simulations and scale vehicle experiments confirmed effective lane tracking. Subsequently, (Chu et al., 2018a) further explored ADRC for autonomous vehicle lane tracking, showing its real-time compensation capabilities for internal uncertainties and external disturbances, with stability confirmed by Lyapunov analysis and improved performance over PID in simulations and experiments.

In contrast, other research studies focus more on the **guidance and perception challenges**, aiming to robustly detect lanes and obstacles, particularly in complex or unstructured environments, sometimes with simpler control strategies. (Singhal et al., 2019) introduced a real-time lane detection, fitting, and navigation approach for unstructured environments, integrating 2D LiDAR and camera data to detect lanes and obstacles and generate waypoints. The methodology was validated experimentally for robustness against illumination changes and occlusions. (Amaradi et al., 2016) detailed a real-time lane following and obstacle detection system for autonomous vehicles using a fish-eye camera and LiDAR, employing

Hough Transform for lane detection and LiDAR for obstacle identification, demonstrating real-time performance experimentally.

Finally, other solutions adopt an integrated approach, that tightly couple advanced guidance with robust control. (Liu et al., 2021b) developed an autonomous lane tracking system that integrates deep learning (LaneFC-Net for real-time detection) with tracking and control. Experimental results showed robustness across various road conditions and lane structures. (Al-Zaher et al., 2012) presented an integrated UGV mechatronics system for lane tracking and obstacle avoidance using a single camera (enhanced Hough Transform for lanes, cone detection for obstacles) and PID control; its feasibility was shown through simulations and small scale vehicle field tests.

A comprehensive comparison of these studies, categorized by their primary focus, sensor utilization, and validation methods, is provided in Table 3.

Table 3 – Summary of the state of the art methods for lane detection and obstacle avoidance

Work	Vehicle type	Lane tracking	Obstacle avoidance	Focus	Sensors used	Validation
Control-focused approaches						
Marino et al. (2009)	Standard car model	Yes	No	Control (Nested PID)	Vision system, Gyroscope	Simulation
Chen et al. (2014)	Standard car model	Yes	No	Control (AMPC)	Not specified	Simulation
Chu et al. (2018b)	Scaled vehicle	Yes	No	Control (ADRC-QFT)	Camera	Simulation & Experiment
Chu et al. (2018a)	Scaled vehicle	Yes	No	Control (ADRC)	Camera	Simulation & Experiment
Vision-focused approaches						
Singhal et al. (2019)	Three-wheeled differential drive	Yes	Yes	Vision	2D LiDAR, Camera	Experiment
Amaradi et al. (2016)	Mobile vehicle	Yes	Yes	Vision	Fish-eye camera, LiDAR	Experiment
Integrated approaches (vision and control)						
Liu et al. (2021b)	Wheeled vehicle	Yes	No	Vision & Control (MPC)	Camera	Experiment
Al-Zaher et al. (2012)	Small-scale UGV	Yes	Yes	Vision & Control (PID)	Single camera	Simulation & Experiment

Leader-follower task in UGVs

Leader-follower control enables UGVs to track and maintain formation with a designated leader (human or vehicle). This capability is vital for collaborative tasks, convoying, and human-robot interaction (Durst et al., 2018; Islam et al., 2019). This section will first detail the key aspects of guidance system design pertinent to the leader-follower task. Subsequently, building upon the general control strategies discussed in the section "System architecture for autonomous navigation in UGVs", an overview of the existing leader-follower solutions will be presented, highlighting perception-focused, control-focused, and integrated system approaches specific to this task.

Categorization of the leader-follower systems

Leader-follower systems can be categorized based on:

- **Sensors used:** common choices include Vision (monocular/stereo cameras for detection, tracking, pose estimation (Chen, 2018; Burke & Brink, 2010)), LiDAR/LRF (for accurate distance/relative position (Chung et al., 2012)), Radar (robust to weather, good for range/velocity (Kumar et al., 2020)), RGB-D Sensors (color and depth, effective indoors (Chen, 2018)), GPS/GNSS (for absolute positioning), and Tags (UWB, RFID). Sensor fusion (e.g., Camera + LiDAR) is often employed to overcome individual sensor limitations (Fan et al., 2024).
- **Interaction mode:**
  - *Explicit:* leader provides direct commands (e.g., wireless, markers). Simpler perception but requires leader cooperation.
  - *Implicit:* follower autonomously detects and tracks the leader using onboard sensors, offering more flexibility but demanding sophisticated perception and guidance (Islam et al., 2019).
- **Follower autonomy level:** adapted from the SAE framework (Islam et al., 2019), follower autonomy ranges from Low (Teleoperated, SAE 0-1) to Partial (automates basic tasks, human supervises, SAE 2), Conditional (operates autonomously in defined conditions, human supervises/intervenes, SAE 3-4), and High (fully independent, SAE 5).

Amokrane, salem-bilal. et al., Review of Control and Guidance for UGVs in Lane Tracking and Leader-Follower Applications, pp.1098–1140

Overview of the existing UGV leader-follower solutions

Research in leader-follower systems for UGVs similarly spans various areas of emphasis. Many contributions concentrate on the **perception challenges** inherent in robustly detecting, identifying, and tracking a designated leader, which can be a human or another vehicle. For instance, (Cao et al., 2021) enhanced UGV visual tracking for person following by introducing a Scene Analysis Module (SAM) to distinguish targets from distractors, validated on custom and public datasets, showing improved robustness in challenging scenarios. (Burke & Brink, 2010) improved human following by extracting upper body orientation using monocular vision and SURF feature matching to infer travel direction, which was then used by a simple controller. (Chung et al., 2012) presented a method for detecting human legs using LRFs, employing a leg geometry-based data approach for robust and accurate object identification in various environments.

Other research studies emphasize the design and robustness of control strategies for leader-follower tasks to accurately maintain a desired formation or distance relative to the leader, often under dynamic conditions. (Ramírez-Neria et al., 2023a) proposed an ADRC-based leader-follower strategy for omnidirectional mobile robots, integrating distance-based formation control with real-time disturbance estimation via a General Proportional Integral Observer (GPIO). (Chen, 2016) presented a 3DOF path trajectory tracking controller with closed-loop guidance for UGV vehicle-to-vehicle following, using Trajectory Linearization Control (TLC) and validated its effectiveness via MATLAB/SIMULINK. (Fan et al., 2024) addressed Unmanned Tracked Vehicle (UTV) leader following by proposing a decoupled speed and curvature control using Model Reference Adaptive Control (MRAC), reporting significant improvements over PID in following distance and braking.

Furthermore, extensive studies examine **integrated approaches** that combine advanced perception techniques with sophisticated control laws to create complete and robust leader-follower systems. (Sira-Ramírez et al., 2014) proposed a robust dynamic feedback control for non-holonomic car formations, using kinematic models with a generalized proportional integral (GPI) observer for disturbance and tracking error estimation, demonstrated experimentally on Pioneer 3-DX robots. (Ramírez-Neria et al., 2023b) introduced an ADRC strategy for omnidirectional mobile robots in leader-follower formations, minimizing reliance on time derivatives by using measurable robot positions and a special error-based ESO for disturbance rejection. (Chen, 2018) introduced "FOLO," a vision-based human-following robot using a 2D-appearance tracking method with adaptive background segmentation and a two-layer PID control for robust, real-time human following with an RGB-D camera. (Amokrane et al., 2024) presented an ADRC-based strategy for leader-follower control for UTV, highlighting its capability in compensating for unpredictable leader motion, vehicle slip and noise measurements, validated through a comprehensive experimental setup utilizing camera and laser sensors for error signals and human pose recognition.

Table 4 summarizes these representative works, detailing their vehicle type, perception system, control approach, and validation.

Reference	**Vehicle type**	**Perception system**	**Control approach**	**Experiments**
Cao et al. (2021)	Not applied	Monocular vision with Scene Analysis Module	Not applied	Simulation
Burke & Brink (2010)	Not defined	Monocular vision with SURF	Basic controller	Experiment
Ramírez-Neria et al. (2023a)	Omnidirectional mobile robots	Multi-camera, marker-based motion capture system	ADRC + GPIO	Simulation + Experiment
Chen (2016)	UGV	Target seeker (camera + laser range finder)	TLC + PPG	Simulation
Fan et al. (2024)	UTV	Cameras, Lidar, and inertial navigation	MRAC	Simulation + Experiment
Sira-Ramírez et al. (2014)	Non-holonomic mobile robot	Range-finding sonar	ADRC+ GPI	Experiment
Ramírez-Neria et al. (2023b)	Omnidirectional mobile robots	Infrared cameras	ADRC + special ESO	Experiment
Chung et al. (2012)	Omnidirectional mobile robots	Single laser range finder	Not mentioned	Simulation + Experiment
Chen (2018)	Mobile robots	RGB-D camera	Two-layer PID	Experiment
Amokrane et al. (2024)	UTV	Monocular camera, Lidar	ADRC (lateral and longitudinal)	Simulation + Experiment

Table 4 – Summary of the current approaches in the leader-follower task

Synthesis of findings and dominant trends

The reviewed literature demonstrates significant progress in UGV control and guidance, while simultaneously highlighting critical gaps and challenges for autonomous UGV operation in complex tasks like leader following and lane tracking with obstacle avoidance. Several key trends emerge:

- **Increasing autonomy sophistication:** a clear progression from simple teleoperation towards systems capable of handling complex scenarios with minimal human intervention.
- **Deep learning dominance in perception:** DL methods (e.g., CNNs, YOLO, YOLOP, MPP) have largely superseded traditional techniques for tasks like object/lane detection and pose estimation, offering superior robustness to environmental variations by learning features directly from data (Ni et al., 2020; Terven et al., 2023).
- **Growing interest in robust control:** recognizing classical PID limitations, advanced control strategies are increasingly explored. While MPC is popular for constraints and optimization (Zuo et al., 2021), its computational cost and model dependency are drawbacks. Robust control techniques, particularly observer-based methods like ADRC that offer disturbance estimation and rejection with reduced model dependency, are gaining traction for UGV applications (Fareh et al., 2021; Sebastian & Ben-Tzvi, 2019a; Stanković et al., 2024; Han, 2009).
- **Shift towards integrated systems:** there is a growing understanding that robust autonomy necessitates integration between guidance and control (Liu et al., 2021b). However, achieving seamless, real-time integration under uncertainty remains a challenge.
- **Importance of platform-specific considerations:** the unique characteristics of UGV platforms (wheeled, tracked, legged) significantly impact design, with platform-specific challenges (e.g., skid-steering and track-slip in tracked vehicles, tire-road interaction in wheeled vehicles) being increasingly investigated, highlighting the need for tailored solutions.

Conclusion and future research directions

This review has synthesized the state of the art in control and guidance for UGVs, focusing on leader-follower and lane tracking with obstacle avoidance applications. Despite significant advancements, particularly in DL-based sensing, robust autonomous operation of UGVs in complex, unstructured environments remains challenging. Advanced robust control methodologies, including observer-based techniques like ADRC, emerge as promising strategies for UGVs. These are well-suited to handle inherent nonlinearities, uncertainties, and disturbances, often with reduced model dependency and real-time compensation capabilities (Han, 2009; Gao, 2006). Further research and validation of such robust methods in integrated UGV systems are key for future progress in critical civilian and military operations.

The following directions are recommended for future research:

1. **UGV environment specific perception:** develop DL perception models trained on diverse UGV operational data, emphasizing robustness to clutter and adverse off-road conditions.
2. **Advanced robust and adaptive control for UGVs:** investigate and enhance robust control strategies (e.g., adaptive versions of ADRC, sliding mode control, MPC with uncertainty handling) for UGVs, including online parameter tuning for varying terrain, slip, and mission requirements, with experimental validation on real systems.
3. **Optimized sensor fusion:** investigate optimal sensor fusion strategies (e.g., vision, LiDAR, Radar, IMU) to provide robust state, terrain, and disturbance information, crucial for effective performance of advanced control systems.
4. **Real-World UGV validation:** conduct thorough experimental validation of the proposed UGV systems on full-scale platforms in challenging real-world environments, establishing metrics for objective performance comparison.

Addressing these directions is crucial for advancing UGV autonomy and enabling their reliable deployment in demanding applications.

References

Aguiar, A.P. & Hespanha, J.P. 2007. Trajectory-Tracking and Path-Following of Underactuated Autonomous Vehicles With Parametric Modeling Uncertainty. *IEEE Transactions on Automatic Control*, 52(8), pp. 1362–1379. Available at: https://doi.org/10.1109/TAC.2007.902731

Ahluwalia, V., Arents, J., Oraby, A. & Greitans, M. 2022. Construction and benchmark of an autonomous tracked mobile robot system. *Robotic Systems and*

Applications, 2(1), pp. 15–28. Available at: https://doi.org/10.21595/rsa.2022.22336

Al-Jarrah, A., Salah, M. & Almomani, F. 2019. Controlling a Skid-Steered Tracked Mobile Robot with Slippage Using Various Control Schemes. In: *2019 20th International Conference on Research and Education in Mechatronics (REM)*. IEEE, pp. 1–7. Available at: https://doi.org/10.1109/REM.2019.8744123.

Al-Zaher, T.S.A., Bayoumy, A.M., Sharaf, A.H.M. & El-din, Y.H.H. 2012. Lane tracking and obstacle avoidance for Autonomous Ground Vehicles. In: *2012 9th France-Japan & 7th Europe-Asia Congress on Mechatronics (MECATRONICS) / 13th Int'l Workshop on Research and Education in Mechatronics (REM)*. pp. 264–271. Available at: https://doi.org/10.1109/MECATRONICS.2012.6451019.

Alexa, O., Ciobotaru, T., Grigore, L.Ş., Grigorie, T.L., Ștefan, A., Oncioiu, I., Priescu, I. & Vlădescu, C. 2023. A Review of Mathematical Models Used to Estimate Wheeled and Tracked Unmanned Ground Vehicle Kinematics and Dynamics. *Mathematics*, 11(17), p. 3735. Available at: https://doi.org/10.3390/math11173735

Aly, M. 2008. Real time detection of lane markers in urban streets. In: *2008 IEEE Intelligent Vehicles Symposium*. pp. 7–12. Available at: https://doi.org/10.1109/IVS.2008.4621152.

Amaradi, P., Sriramoju, N., Dang, L., Tewolde, G.S. & Kwon, J. 2016. Lane following and obstacle detection techniques in autonomous driving vehicles. In: *2016 IEEE International Conference on Electro Information Technology (EIT)*. pp. 0674–0679. Available at: https://doi.org/10.1109/EIT.2016.7535320.

Amokrane, S.B., Laidouni, M.Z., Adli, T., Madonski, R. & Stanković, M. 2024. Active disturbance rejection control for unmanned tracked vehicles in leader–follower scenarios: Discrete-time implementation and field test validation. *Mechatronics*, 97, p. 103114. Available at: https://doi.org/10.1016/j.mechatronics.2023.103114

Andrade, D.C., Bueno, F., Franco, F.R., Silva, R.A., Neme, J.H.Z., Margraf, E., Omoto, W.T., Farinelli, F.A., Tusset, A.M., Okida, S., Santos, M.M.D., Ventura, A., Carvalho, S. & Amaral, R.d.S. 2019. A Novel Strategy for Road Lane Detection and Tracking Based on a Vehicle's Forward Monocular Camera. *IEEE Transactions on Intelligent Transportation Systems*, 20(4), pp. 1497–1507. Available at: https://doi.org/10.1109/TITS.2018.2856361

Artuñedo, A., Moreno-Gonzalez, M. & Villagra, J. 2024. Lateral control for autonomous vehicles: A comparative evaluation. *Annual Reviews in Control*, 57, p. 100910. Available at: https://doi.org/10.1016/j.arcontrol.2023.100910

Azam, S., Munir, F. & Jeon, M. 2020. Dynamic Control System Design for Autonomous Car. In: *Proceedings of the 6th International Conference on Vehicle Technology and Intelligent Transport Systems - VEHITS*. pp. 456–463. Available at: https://doi.org/10.5220/0009392904560463.

Badrloo, S., Varshosaz, M., Pirasteh, S. & Li, J. 2022. Image-Based Obstacle Detection Methods for the Safe Navigation of Unmanned Vehicles: A Review. *Remote Sensing*, 14(15), p. 3824. Available at: https://doi.org/10.3390/rs14153824

Baek, S.W., Kim, M.J., Suddamalla, U., Wong, A., Lee, B.H. & Kim, J.H. 2022. Real-Time Lane Detection Based on Deep Learning. *Journal of Electrical Engineering & Technology*, 17(1), pp. 655–664. Available at: https://doi.org/10.1007/s42835-021-00902-6

Balasubramaniam, A. & Pasricha, S. 2022. Object Detection in Autonomous Vehicles: Status and Open Challenges. *arXiv preprint*. Available at: https://doi.org/10.48550/arXiv.2201.07706

Balestrieri, E., Daponte, P., De Vito, L. & Lamonaca, F. 2021. Sensors and Measurements for Unmanned Systems: An Overview. *Sensors*, 21(4), p. 1518. Available at: https://doi.org/10.3390/s21041518

BaniHani, S., Hayajneh, M.R.M., Al-Jarrah, A. & Mutawe, S. 2021. New Control Approaches for Trajectory Tracking and Motion Planning of Unmanned Tracked Robot. *Advances in Electrical and Electronic Engineering*, 19(1), pp. 42–56. Available at: https://doi.org/10.15598/aeee.v19i1.4006

Bar Hillel, A., Lerner, R., Levi, D. & Raz, G. 2014. Recent progress in road and lane detection: a survey. *Machine Vision and Applications*, 25(3), pp. 727–745. Available at: https://doi.org/10.1007/s00138-011-0404-2

Benyahia, A.T.E., Stanković, M., Madonski, R., Babayomi, O. & Manojlović, S.M. 2025. Improving Control Performance by Cascading Observers: Case of ADRC With Cascade ESO. *IEEE/CAA Journal of Automatica Sinica*, 12(8), pp. 1702–1712. Available at: https://doi.org/10.1109/JAS.2024.124995

Burke, M. & Brink, W. 2010. Estimating target orientation with a single camera for use in a human-following robot. In: *21st Annual Symposium of the Pattern Recognition Association of South Africa (PRASA)*. [online]. Available at: https://api.semanticscholar.org/CorpusID:129396257 [Accessed: 09 July 2025].

Cao, J., Song, C., Peng, S., Song, S., Zhang, X. & Xiao, F. 2020. Trajectory Tracking Control Algorithm for Autonomous Vehicle Considering Cornering Characteristics. *IEEE Access*, 8, pp. 59470–59484. Available at: https://doi.org/10.1109/ACCESS.2020.2982963

Cao, M., Wang, J. & Ming, L. 2021. Multi-Templates Based Robust Tracking for Robot Person-Following Tasks. *Applied Sciences*, 11(18), p. 8698. Available at: https://doi.org/10.3390/app11188698

Chen, B.C., Luan, B.C. & Lee, K. 2014. Design of lane keeping system using adaptive model predictive control. In: *2014 IEEE International Conference on Automation Science and Engineering (CASE)*. pp. 922–926. Available at: https://doi.org/10.1109/CoASE.2014.6899436.

Chen, E. 2018. “FOLO”: A vision-based human-following robot. In: *2018 3rd International Conference on Automation, Mechanical Control and Computational*

Engineering (AMCCE 2018). Atlantis Press, pp. 224–232. Available at: https://doi.org/10.2991/amcce-18.2018.39.

Chen, Y. 2016. *Autonomous Unmanned Ground Vehicle (UGV) Follower Design*. Master's thesis, Ohio University. [online]. Available at: https://docslib.org/doc/8343660/autonomous-unmanned-ground-vehicle-ugv-follower-design [Accessed: 11 June 2025].

Chetan, N.B., Gong, J., Zhou, H., Bi, D., Lan, J. & Qie, L. 2020. An Overview of Recent Progress of Lane Detection for Autonomous Driving. In: *2019 6th International Conference on Dependable Systems and Their Applications (DSA)*. pp. 341–346. Available at: https://doi.org/10.1109/DSA.2019.00052.

Chu, Z., Sun, Y., Wu, C. & Sepehri, N. 2018a. Active disturbance rejection control applied to automated steering for lane keeping in autonomous vehicles. *Control Engineering Practice*, 74, pp. 13–21. Available at: https://doi.org/10.1016/j.conengprac.2018.02.002

Chu, Z., Wu, C. & Sepehri, N. 2018b. Automated steering controller design for vehicle lane keeping combining linear active disturbance rejection control and quantitative feedback theory. *Proceedings of the Institution of Mechanical Engineers, Part I: Journal of Systems and Control Engineering*, 232(7), pp. 937–948. Available at: https://doi.org/10.1177/0959651818770344

Chung, W., Kim, H., Yoo, Y., Moon, C.B. & Park, J. 2012. The Detection and Following of Human Legs Through Inductive Approaches for a Mobile Robot With a Single Laser Range Finder. *IEEE Transactions on Industrial Electronics*, 59(8), pp. 3156–3166. Available at: https://doi.org/10.1109/TIE.2011.2170389

Dawam, E.S. & Feng, X. 2020. Smart City Lane Detection for Autonomous Vehicle. In: *2020 IEEE Intl Conf on Dependable, Autonomic and Secure Computing, Intl Conf on Pervasive Intelligence and Computing, Intl Conf on Cloud and Big Data Computing, Intl Conf on Cyber Science and Technology Congress (DASC/PiCom/CBDCom/CyberSciTech)*. pp. 334–338. Available at: https://doi.org/10.1109/DASC-PICom-CBDCom-CyberSciTech49142.2020.00065.

Dewangan, D.K., Sahu, S.P., Sairam, B. & Agrawal, A. 2021. VLDNet: Vision-based lane region detection network for intelligent vehicle system using semantic segmentation. *Computing*, 103(12), pp. 2867–2892. Available at: https://doi.org/10.1007/s00607-021-00974-2

Dhanakshirur, R.R., Pillai, P., Tabib, R.A., Patil, U. & Mudenagudi, U. 2019. A Framework for Lane Prediction on Unstructured Roads. In: *Advances in Signal Processing and Intelligent Recognition Systems*. pp. 178–189. Available at: https://doi.org/10.1007/978-981-13-5758-9_16.

Dima, C., Vandapel, N. & Hebert, M. 2004. Classifier fusion for outdoor obstacle detection. In: *IEEE International Conference on Robotics and Automation, 2004. Proceedings. ICRA '04. 2004*, vol. 1. pp. 665–671. Available at: https://doi.org/10.1109/ROBOT.2004.1307225.

Durst, P.J., Monroe, G., Bethel, C.L., Anderson, D.T. & Carruth, D.W. 2018. A history and overview of mobility modeling for autonomous unmanned ground vehicles. In: *Autonomous Systems: Sensors, Vehicles, Security, and the Internet of Everything*, vol. 10643. SPIE, pp. 103–113. Available at: https://doi.org/10.1117/12.2309570.

Fakhfakh, M., Chaari, L. & Fakhfakh, N. 2020. Bayesian curved lane estimation for autonomous driving. *Journal of Ambient Intelligence and Humanized Computing*, 11(10), pp. 4133–4143. Available at: https://doi.org/10.1007/s12652-020-01688-7

Fan, J., Yan, P., Li, R., Liu, Y., Wang, F., Liu, Y. & Chen, C. 2024. Decoupled Adaptive Motion Control for Unmanned Tracked Vehicles in the Leader-Following Task. *World Electric Vehicle Journal*, 15(6). Available at: https://doi.org/10.3390/wevj15060239

Fareh, R., Khadraoui, S., Abdallah, M.Y., Baziyad, M. & Bettayeb, M. 2021. Active disturbance rejection control for robotic systems: A review. *Mechatronics*, 80, p. 102671. Available at: https://doi.org/10.1016/j.mechatronics.2021.102671

Feng, Z., Zhang, S., Kunert, M. & Wiesbeck, W. 2019. Applying Neural Networks with a High-Resolution Automotive Radar for Lane Detection. In: *AmE 2019 - Automotive meets Electronics; 10th GMM-Symposium*. pp. 1–6. Available at: https://ieeexplore.ieee.org/document/8727838.

Gadekar, A., Fulsundar, S., Deshmukh, P., Aher, J., Kataria, K., Patel, V. & Barve, S. 2023. Rakshak: A modular unmanned ground vehicle for surveillance and logistics operations. *Cognitive Robotics*, 3, pp. 23–33. Available at: https://doi.org/10.1016/j.cogr.2023.02.001

Gao, H., Yang, H., Zhang, X., Ren, X., Liang, F., Yan, R., Liu, Q., Hu, M., Zhang, F., Gao, J., Bao, S., Li, K., Li, D. & Wang, D. 2025. Longitudinal velocity control of autonomous driving based on extended state observer. *CAAI Transactions on Intelligence Technology*, 10(1), pp. 36–46. Available at: https://doi.org/10.1049/cit2.12397

Gao, Z. 2006. Active disturbance rejection control: a paradigm shift in feedback control system design. In: *2006 American Control Conference*. pp. 7 pp.–. Available at: https://doi.org/10.1109/ACC.2006.1656579.

Gao, Z., Hu, S. & Jiang, F. 2001. A novel motion control design approach based on active disturbance rejection. In: *Proceedings of the 40th IEEE Conference on Decision and Control (Cat. No.01CH37228)*, vol. 5. IEEE, pp. 4877–4882. Available at: https://doi.org/10.1109/CDC.2001.980980.

Ghanem, S., Kanungo, P., Panda, G., Satapathy, S.C. & Sharma, R. 2023. Lane detection under artificial colored light in tunnels and on highways: an IoT-based framework for smart city infrastructure. *Complex & Intelligent Systems*, 9(4), pp. 3601–3612. Available at: https://doi.org/10.1007/s40747-021-00381-2

MediaPipe. [online]. Available at: https://developers.google.com/mediapipe/solutions/vision/pose_landmarker/ [Accessed: 09 July 2025].

Guo, B.Z. & Zhao, Z.L. 2015. Active disturbance rejection control: Theoretical perspectives. *Communications in Information and Systems*, 15(3), pp. 361–421. Available at: https://doi.org/10.4310/CIS.2015.v15.n3.a3

Han, J. 2009. From PID to Active Disturbance Rejection Control. *IEEE Transactions on Industrial Electronics*, 56(3), pp. 900–906. Available at: https://doi.org/10.1109/TIE.2008.2011621

Horri, N., Holderbaum, W. & Giulietti, F. 2024. Challenges in the Guidance, Navigation and Control of Autonomous and Transport Vehicles. *Applied Sciences*, 14(15). Available at: https://doi.org/10.3390/app14156635

Hu, J.w., Zheng, B.y., Wang, C., Zhao, C.h., Hou, X.l., Pan, Q. & Xu, Z. 2020. A survey on multi-sensor fusion based obstacle detection for intelligent ground vehicles in off-road environments. *Frontiers of Information Technology & Electronic Engineering*, 21(5), pp. 675–692. Available at: https://doi.org/10.1631/FITEE.1900518

Hung, N., Rego, F., Quintas, J., Cruz, J., Jacinto, M., Souto, D., Potes, A., Sebastiao, L. & Pascoal, A. 2023. A review of path following control strategies for autonomous robotic vehicles: Theory, simulations, and experiments. *Journal of Field Robotics*, 40(3), pp. 747–779. Available at: https://doi.org/10.1002/rob.22142

Hussain, M. 2024. YOLOv1 to v8: Unveiling Each Variant–A Comprehensive Review of YOLO. *IEEE Access*, 12, pp. 42816–42833. Available at: https://doi.org/10.1109/ACCESS.2024.3378568

Islam, F., Nabi, M. & Ball, J.E. 2022. Off-Road Detection Analysis for Autonomous Ground Vehicles: A Review. *Sensors*, 22(21), p. 8463. Available at: https://doi.org/10.3390/s22218463

Islam, M.J., Hong, J. & Sattar, J. 2019. Person-following by autonomous robots: A categorical overview. *The International Journal of Robotics Research*, 38(14), pp. 1581–1618. Available at: https://doi.org/10.1177/0278364919881683

Jin, X., Lv, H., He, Z., Li, Z., Wang, Z. & Ikiela, N.V.O. 2023. Design of Active Disturbance Rejection Controller for Trajectory-Following of Autonomous Ground Electric Vehicles. *Symmetry*, 15(9), p. 1786. Available at: https://doi.org/10.3390/sym15091786

Kang, N., Han, Y., Guan, T. & Wang, S. 2022. Improved ADRC-Based Autonomous Vehicle Path-Tracking Control Study Considering Lateral Stability. *Applied Sciences*, 12(9). Available at: https://doi.org/10.3390/app12094660

Kayacan, E., Ramon, H. & Saeys, W. 2015. Robust Trajectory Tracking Error Model-Based Predictive Control for Unmanned Ground Vehicles. *IEEE/ASME Transactions on Mechatronics*, 21(2), pp. 806–814. Available at: https://doi.org/10.1109/TMECH.2015.2492984

Kebbati, Y., Ait-Oufroukh, N., Ichalal, D. & Vigneron, V. 2023. Lateral control for autonomous wheeled vehicles: A technical review. *Asian Journal of Control*, 25(4), pp. 2539–2563. Available at: https://doi.org/10.1002/asjc.2980

Kulkarni, S., Deshmukh, S., Fernandes, F., Patil, A. & Jabade, V. 2023. PoseAnalyser: A Survey on Human Pose Estimation. *SN Computer Science*, 4(2), p. 136. Available at: https://doi.org/10.1007/s42979-022-01567-2

Kumar, G.A., Lee, J.H., Hwang, J., Park, J., Youn, S.H. & Kwon, S. 2020. LiDAR and Camera Fusion Approach for Object Distance Estimation in Self-Driving Vehicles. *Symmetry*, 12(2), p. 324. Available at: https://doi.org/10.3390/sym12020324

Lee, C. & Moon, J.H. 2018. Robust Lane Detection and Tracking for Real-Time Applications. *IEEE Transactions on Intelligent Transportation Systems*, 19(12), pp. 4043–4048. Available at: https://doi.org/10.1109/TITS.2018.2791572

Li, D., Wu, S., Zhao, Y., Li, Z. & Gong, J. 2021. A Hierarchical Path Tracking Method for High-speed Unmanned Tracked Vehicle. In: *2021 IEEE International Intelligent Transportation Systems Conference (ITSC)*. IEEE, pp. 38–43. Available at: https://doi.org/10.1109/ITSC48978.2021.9564774.

Li, Y. & Xu, L. 2024. Panoptic Perception for Autonomous Driving: A Survey. *arXiv preprint*, abs/2408.15388. Available at: https://doi.org/10.48550/arXiv.2408.15388

Li, Z. 2013. Guidance, control and estimation of autonomous vehicle systems. *University of Illinois at Urbana-Champaign*. [online]. Available at: https://www.ideals.illinois.edu/items/46890 [Accessed: 15 June 2025].

Liu, L., Chen, X., Zhu, S. & Tan, P. 2021a. CondLaneNet: a Top-to-down Lane Detection Framework Based on Conditional Convolution. In: *2021 IEEE/CVF International Conference on Computer Vision (ICCV)*. pp. 3753–3762. Available at: https://doi.org/10.1109/ICCV48922.2021.00375.

Liu, M., Deng, X., Lei, Z., Jiang, C. & Piao, C. 2021b. Autonomous Lane Keeping System: Lane Detection, Tracking and Control on Embedded System. *Journal of Electrical Engineering & Technology*, 16(1), pp. 569–578. Available at: https://doi.org/10.1007/s42835-020-00570-y

Liu, M., Xu, Y., Lin, X., Tan, Y., Pu, Y., Li, W. & Oetomo, D. 2024. On Active Disturbance Rejection Control for Unmanned Tracked Ground Vehicles with Non-smooth Disturbances. *Unmanned Systems*, 12(06), pp. 1023–1037. Available at: https://doi.org/10.1142/S2301385024500353

Liu, Q., Li, Z., Yuan, S., Zhu, Y. & Li, X. 2021c. Review on Vehicle Detection Technology for Unmanned Ground Vehicles. *Sensors*, 21(4), p. 1354. Available at: https://doi.org/10.3390/s21041354

Madonski, R., Ramirez-Neria, M., Stanković, M., Yang, J. & Li, S. 2019. On vibration suppression and trajectory tracking in largely uncertain torsional system: An error-based ADRC approach. *Mechanical Systems and Signal Processing*, 134, p. 106300. Available at: https://doi.org/10.1016/j.ymssp.2019.106300

Man, C.K.Y.L.L., Koonjul, Y. & Nagowah, L. 2018. A low cost autonomous unmanned ground vehicle. *Future Computing and Informatics Journal*, 3(2), pp. 304–320. Available at: https://doi.org/10.1016/j.fcij.2018.10.001

Marino, R., Scalzi, S., Orlando, G. & Netto, M. 2009. A nested PID steering control for lane keeping in vision based autonomous vehicles. In: *2009 American Control Conference*. pp. 2885–2890. Available at: https://doi.org/10.1109/ACC.2009.5160343.

Munir, F., Azam, S., Jeon, M., Lee, B.G. & Pedrycz, W. 2022. LDNet: End-to-End Lane Marking Detection Approach Using a Dynamic Vision Sensor. *IEEE Transactions on Intelligent Transportation Systems*, 23(7), pp. 9318–9334. Available at: https://doi.org/10.1109/TITS.2021.3102479

Ni, J., Chen, Y., Chen, Y., Zhu, J., Ali, D. & Cao, W. 2020. A Survey on Theories and Applications for Self-Driving Cars Based on Deep Learning Methods. *Applied Sciences*, 10(8), p. 2749. Available at: https://doi.org/10.3390/app10082749

Ni, J., Hu, J. & Xiang, C. 2018. Unmanned Ground Vehicles: An Introduction. In: *Design and Advanced Robust Chassis Dynamics Control for X-by-Wire Unmanned Ground Vehicle*. Springer, pp. 1–19. Available at: https://doi.org/10.1007/978-3-031-01496-3_1.

Ni, J., Hu, J. & Xiang, C. 2021. A review for design and dynamics control of unmanned ground vehicle. *Proceedings of the Institution of Mechanical Engineers, Part D: Journal of Automobile Engineering*, 235(4), pp. 1084–1100. Available at: https://doi.org/10.1177/0954407020912097

Oğuz, E., Küçükmanisa, A., Duvar, R. & Urhan, O. 2022. A deep learning based fast lane detection approach. *Chaos, Solitons & Fractals*, 155, p. 111722. Available at: https://doi.org/10.1016/j.chaos.2021.111722

Parmar, Y., Natarajan, S. & Sobha, G. 2019. Deeprange: deep-learning-based object detection and ranging in autonomous driving. *IET Intelligent Transport Systems*, 13(8), pp. 1256–1264. Available at: https://doi.org/10.1049/iet-its.2018.5144

Philion, J. 2019. FastDraw: Addressing the Long Tail of Lane Detection by Adapting a Sequential Prediction Network. In: *2019 IEEE/CVF Conference on Computer Vision and Pattern Recognition (CVPR)*. pp. 11574–11583. Available at: https://doi.org/10.1109/CVPR.2019.01185.

Ramírez-Neria, M., González-Sierra, J., Madonski, R., Ramírez-Juárez, R., Hernandez-Martinez, E. & Fernández-Anaya, G. 2023a. Leader–Follower Formation and Disturbance Rejection Control for Omnidirectional Mobile Robots. *Robotics*, 12(5), p. 122. Available at: https://doi.org/10.3390/robotics12050122

Ramírez-Neria, M., Luviano-Juárez, A., Madonski, R., Ramírez-Juárez, R., Lozada-Castillo, N. & Gao, Z. 2023b. Leader-Follower ADRC Strategy for Omnidirectional Mobile Robots without Time-Derivatives in the Tracking Controller. In: *2023 American Control Conference (ACC)*. IEEE, pp. 405–410. Available at: https://doi.org/10.23919/ACC55779.2023.10156648.

Redmon, J., Divvala, S., Girshick, R. & Farhadi, A. 2016. You Only Look Once: Unified, Real-Time Object Detection. In: *Proceedings of the IEEE Conference* *on Computer Vision and Pattern Recognition (CVPR)*. pp. 779–788. Available at: https://doi.org/10.1109/CVPR.2016.91.

Rizk, H., Chaibet, A. & Kribèche, A. 2023. Model-Based Control and Model-Free Control Techniques for Autonomous Vehicles: A Technical Survey. *Applied Sciences*, 13(11), p. 6700. Available at: https://doi.org/10.3390/app13116700

Rubio, F., Valero, F. & Llopis-Albert, C. 2019. A review of mobile robots: Concepts, methods, theoretical framework, and applications. *International Journal of Advanced Robotic Systems*, 16(2), p. 1729881419839596. Available at: https://doi.org/10.1177/1729881419839596

Ruslan, N.A.I., Amer, N.H., Hudha, K., Kadir, Z.A., Ishak, S.A.F.M. & Dardin, S.M.F.S. 2023. Modelling and control strategies in path tracking control for autonomous tracked vehicles: A review of state of the art and challenges. *Journal of Terramechanics*, 105, pp. 67–79. Available at: https://doi.org/10.1016/j.jterra.2022.10.003

Sabiha, A.D., Kamel, M.A., Said, E. & Hussein, W.M. 2022. ROS-based trajectory tracking control for autonomous tracked vehicle using optimized backstepping and sliding mode control. *Robotics and Autonomous Systems*, 152, p. 104058. Available at: https://doi.org/10.1016/j.robot.2022.104058

Samak, C.V., Samak, T.V. & Kandhasamy, S. 2021. Control strategies for autonomous vehicles. In: *Autonomous Driving and Advanced Driver-Assistance Systems (ADAS)*. CRC Press, pp. 37–86. Available at: https://doi.org/10.1201/9781003048381-2.

Sang, N. & Chen, L. 2020. Design of an active front steering system for a vehicle using an active disturbance rejection control method. *Science Progress*, 103(1), p. 0036850419883565. Available at: https://doi.org/10.1177/0036850419883565

Santoso, F., Garratt, M.A. & Anavatti, S.G. 2020. State-of-the-Art Integrated Guidance and Control Systems in Unmanned Vehicles: A Review. *IEEE Systems Journal*, 15(3), pp. 3312–3323. Available at: https://doi.org/10.1109/JSYST.2020.3007428

Sarcinelli-Filho, M. & Carelli, R. 2023. Control of Ground and Aerial Robots. *Springer*. Available at: https://doi.org/10.1007/978-3-031-23088-2.

Schulte, J., Kocherovsky, M., Paul, N., Pleune, M. & Chung, C.J. 2022. Autonomous Human-Vehicle Leader-Follower Control Using Deep-Learning-Driven Gesture Recognition. *Vehicles*, 4(1), pp. 243–258. Available at: https://doi.org/10.3390/vehicles4010016

Sebastian, B. & Ben-Tzvi, P. 2019a. Active Disturbance Rejection Control for Handling Slip in Tracked Vehicle Locomotion. *Journal of Mechanisms and Robotics*, 11(2), p. 021003. Available at: https://doi.org/10.1115/1.4042347

Sebastian, B. & Ben-Tzvi, P. 2019b. Physics Based Path Planning for Autonomous Tracked Vehicle in Challenging Terrain. *Journal of Intelligent & Robotic*

Systems, 95, pp. 511–526. Available at: https://doi.org/10.1007/s10846-018-0851-3

Sethi, I.K. 2024. Autonomous Vehicles and Systems: A Technological and Societal Perspective. *CRC Press*. Available at: https://doi.org/10.1201/9781032629537.

Shafaei, S. & Mousazadeh, H. 2023. On the power characteristics of an unmanned tracked vehicle for autonomous transportation of agricultural payloads. *Journal of Terramechanics*, 109, pp. 21–36. Available at: https://doi.org/10.1016/j.jterra.2023.05.006

Singhal, A., Mohta, V., Jha, A., Khandelwal, Y., Agrawal, D., Kowshik, S., Agarwal, S., Shrivastava, S., Lodhi, V. & Chakravarty, D. 2019. Real-time lane detection, fitting and navigation for unstructured environments. In: *2019 International Conference on Image and Video Processing, and Artificial Intelligence*, vol. 11321. SPIE, pp. 146–151. Available at: https://doi.org/10.1117/12.2547333.

Sira-Ramírez, H., Castro-Linares, R. & Puriel-Gil, G. 2014. An Active Disturbance Rejection Approach to Leader-Follower Controlled Formation. *Asian Journal of Control*, 16(2), pp. 382–395. Available at: https://doi.org/10.1002/asjc.714

Sridevi, M. & Harish, M. 2024. Computer Vision based Panoptic Driving Perception under Various Weather Conditions. *Procedia Computer Science*, 237, pp. 803–810. Available at: https://doi.org/10.1016/j.procs.2024.05.168

Stanković, M., Madonski, R. & Manojlović, S. 2024. Systematic design of ADRC-based unmanned tracked vehicle trajectory tracking with FPGA-in-the-loop validation. *Military Technical Courier*, 72(4), pp. 1700–1725. Available at: https://doi.org/10.5937/vojtehg72-49983

Stanković, M.R., Rapaić, M.R., Manojlović, S.M., Mitrović, S.T., Simić, S.M. & Naumović, M.B. 2019. Optimised active disturbance rejection motion control with resonant extended state observer. *International Journal of Control*, 92(8), pp. 1815–1826. Available at: https://doi.org/10.1080/00207179.2017.1414308

Sultana, S., Ahmed, B., Paul, M., Islam, M.R. & Ahmad, S. 2023. Vision-Based Robust Lane Detection and Tracking in Challenging Conditions. *IEEE Access*, 11, pp. 67938–67955. Available at: https://doi.org/10.1109/ACCESS.2023.3292128

Sun, Y., Wang, L., Chen, Y. & Liu, M. 2019. Accurate Lane Detection with Atrous Convolution and Spatial Pyramid Pooling for Autonomous Driving. In: *2019 IEEE International Conference on Robotics and Biomimetics (ROBIO)*. pp. 642–647. Available at: https://doi.org/10.1109/ROBIO49542.2019.8961705.

Tagliavini, L., Colucci, G., Botta, A., Cavallone, P., Baglieri, L. & Quaglia, G. 2022. Wheeled Mobile Robots: State of the Art Overview and Kinematic Comparison Among Three Omnidirectional Locomotion Strategies. *Journal of Intelligent & Robotic Systems*, 106(3), p. 57. Available at: https://doi.org/10.1007/s10846-022-01745-7

Teji, M.D., Zou, T. & Zeleke, D.S. 2023. A Survey of Off-Road Mobile Robots: Slippage Estimation, Robot Control, and Sensing Technology. *Journal of Intelligent & Robotic Systems*, 109(2), p. 38. Available at: https://doi.org/10.1007/s10846-023-01968-2

Terven, J., Córdova-Esparza, D. & Romero-González, J. 2023. A Comprehensive Review of YOLO Architectures in Computer Vision: From YOLOv1 to YOLOv8 and YOLO-NAS. *Machine Learning and Knowledge Extraction*, 5(4), pp. 1680–1716. Available at: https://doi.org/10.3390/make5040083

Thrun, S., Montemerlo, M., Dahlkamp, H., Stavens, D., Aron, A., Diebel, J., Fong, P., Gale, J., Halpenny, M., Hoffmann, G., Lau, K., Oakley, C., Palatucci, M., Pratt, V., Stang, P., Strohband, S., Dupont, C., Jendrossek, L.E., Koelen, C., Markey, C., Rummel, C., van Niekerk, J., Jensen, E., Alessandrini, P., Bradski, G., Davies, B., Ettinger, S., Kaehler, A., Nefian, A. & Mahoney, P. 2006. Stanley: The robot that won the DARPA Grand Challenge. *Journal of Field Robotics*, 23(9), pp. 661–692. Available at: https://doi.org/10.1002/rob.20147

Tian, D., Gao, J., Liu, C. & Shi, X. 2021. Simulation of Upward Jump Control for One-Legged Robot Based on QP Optimization. *Sensors*, 21(5), p. 1893. Available at: https://doi.org/10.3390/s21051893

van der Sande, T. & Nijmeijer, H. 2017. From Cooperative to Autonomous Vehicles. In: *Sensing and Control for Autonomous Vehicles: Applications to Land, Water and Air Vehicles*. Springer, pp. 435–452. Available at: https://doi.org/10.1007/978-3-319-55372-6_20.

Vera-Yanez, D., Pereira, A., Rodrigues, N., Molina, J.P., García, A.S. & Fernández-Caballero, A. 2024. Optical Flow-Based Obstacle Detection for Mid-Air Collision Avoidance. *Sensors*, 24(10), p. 3016. Available at: https://doi.org/10.3390/s24103016

Vijayakumar, A. & Vairavasundaram, S. 2024. YOLO-based Object Detection Models: A Review and its Applications. *Multimedia Tools and Applications*, 83(35), pp. 83535–83574. Available at: https://doi.org/10.1007/s11042-024-18872-y

Wang, H., Zuo, Z., Wang, Y., Yang, H. & Chang, S. 2021. Composite nonlinear extended state observer and its application to unmanned ground vehicles. *Control Engineering Practice*, 109, p. 104731. Available at: https://doi.org/10.1016/j.conengprac.2021.104731

Wang, H., Zuo, Z., Wang, Y., Yang, H. & Hu, C. 2022. Estimator-Based Turning Control for Unmanned Ground Vehicles: An Anti-Peak Extended State Observer Approach. *IEEE Transactions on Vehicular Technology*, 71(12), pp. 12489–12498. Available at: https://doi.org/10.1109/TVT.2022.3195637

Wang, H., Zuo, Z., Xue, W., Wang, Y. & Yang, H. 2024a. Switching Longitudinal and Lateral Semi-decoupled Active Disturbance Rejection Control for Unmanned Ground Vehicles. *IEEE Transactions on Industrial Electronics*, 71(3), pp. 3034–3043. Available at: https://doi.org/10.1109/TIE.2023.3265048

Wang, X., Wang, Y., Sun, Q., Chen, Y. & Al-Zahran, A. 2024b. Adaptive robust control of unmanned tracked vehicles for trajectory tracking based on constraint modeling and analysis. *Nonlinear Dynamics*, 112(11), pp. 9117–9135. Available at: https://doi.org/10.1007/s11071-024-09514-x

Wang, Z. 2024. A survey on convex optimization for guidance and control of vehicular systems. *Annual Reviews in Control*, 57, p. 100957. Available at: https://doi.org/10.1016/j.arcontrol.2024.100957

Wu, D., Liao, M.W., Zhang, W.T., Wang, X.G., Bai, X., Cheng, W.Q. & Liu, W.Y. 2022. YOLOP: You Only Look Once for Panoptic Driving Perception. *Machine Intelligence Research*, 19(6), pp. 550–562. Available at: https://doi.org/10.1007/s11633-022-1339-y

Wu, Z., Qiu, K., Yuan, T. & Chen, H. 2021. A method to keep autonomous vehicles steadily drive based on lane detection. *International Journal of Advanced Robotic Systems*, 18(2). Available at: https://doi.org/10.1177/17298814211002974

Xia, Y., Pu, F., Li, S. & Gao, Y. 2016. Lateral Path Tracking Control of Autonomous Land Vehicle Based on ADRC and Differential Flatness. *IEEE Transactions on Industrial Electronics*, 63(5), pp. 3091–3099. Available at: https://doi.org/10.1109/TIE.2016.2531021

Xing, Y., Lv, C., Chen, L., Wang, H., Wang, H., Cao, D., Velenis, E. & Wang, F.Y. 2018. Advances in Vision-Based Lane Detection: Algorithms, Integration, Assessment, and Perspectives on ACP-Based Parallel Vision. *IEEE/CAA Journal of Automatica Sinica*, 5(3), pp. 645–661. Available at: https://doi.org/10.1109/JAS.2018.7511063

Yang, Y. 2024. A Review of Lane Detection in Autonomous Vehicles. *Journal of Advances in Engineering and Technology*, 1(4), pp. 30–36. Available at: https://doi.org/10.62177/jaet.v1i4.130

Yao, Q., Tian, Y., Wang, Q. & Wang, S. 2020. Control Strategies on Path Tracking for Autonomous Vehicle: State of the Art and Future Challenges. *IEEE Access*, 8, pp. 211–222. Available at: https://doi.org/10.1109/ACCESS.2020.3020075

Yu, X. & Marinov, M. 2020. A Study on Recent Developments and Issues with Obstacle Detection Systems for Automated Vehicles. *Sustainability*, 12(8), p. 3281. Available at: https://doi.org/10.3390/su12083281

Zakaria, N.J., Shapiai, M.I., Ghani, R.A., Yassin, M.N.M., Ibrahim, M.Z. & Wahid, N. 2023. Lane Detection in Autonomous Vehicles: A Systematic Review. *IEEE Access*, 11, pp. 3729–3765. Available at: https://doi.org/10.1109/ACCESS.2023.3234442

Zhan, J., Luo, Y., Guo, C., Wu, Y., Meng, J. & Liu, J. 2024. YOLOPX: Anchor-free multi-task learning network for panoptic driving perception. *Pattern Recognition*, 148, p. 110152. Available at: https://doi.org/10.1016/j.patcog.2023.110152

Zhang, J., Yang, X., Wang, W., Guan, J., Ding, L. & Lee, V.C. 2023. Automated guided vehicles and autonomous mobile robots for recognition and tracking in civil engineering. *Automation in Construction*, 146, p. 104699. Available at: https://doi.org/10.1016/j.autcon.2022.104699

Zhang, L., Jiang, F., Kong, B., Yang, J. & Wang, C. 2021a. Real-Time Lane Detection by Using Biologically Inspired Attention Mechanism to Learn Contextual Information. *Cognitive Computation*, 13, pp. 1333–1344. Available at: https://doi.org/10.1007/s12559-021-09935-5

Zhang, R., Wu, Y., Gou, W. & Chen, J. 2021b. RS-Lane: A Robust Lane Detection Method Based on ResNeSt and Self-Attention Distillation for Challenging Traffic Situations. *Journal of Advanced Transportation*, 2021(1), p. 7544355. Available at: https://doi.org/10.1155/2021/7544355

Zhang, X., Zhou, M., Qiu, P., Huang, Y. & Li, J. 2019. Radar and vision fusion for the real-time obstacle detection and identification. *Industrial Robot-an International Journal*, 46(3), pp. 391–395. Available at: https://doi.org/10.1108/IR-06-2018-0113

Zhao, Y., Wang, J., Cao, G., Yuan, Y., Yao, X. & Qi, L. 2023. Intelligent Control of Multilegged Robot Smooth Motion: A Review. *IEEE Access*, 11, pp. 86645–86685. Available at: https://doi.org/10.1109/ACCESS.2023.3304992

Zheng, C., Wu, W., Chen, C., Yang, T., Zhu, S., Shen, J., Kehtarnavaz, N. & Shah, M. 2023. Deep Learning-based Human Pose Estimation: A Survey. *ACM Computing Surveys*, 56(1), pp. 1–37. Available at: https://doi.org/10.1145/3603618

Zheng, Q. & Gao, Z. 2010. On practical applications of active disturbance rejection control. In: *Proceedings of the 29th Chinese Control Conference*. IEEE, pp. 6095–6100. Available at: https://ieeexplore.ieee.org/abstract/document/5572922.

Zheng, Q. & Gao, Z. 2016. Active disturbance rejection control: between the formulation in time and the understanding in frequency. *Control Theory and Technology*, 14, pp. 250–259. Available at: https://doi.org/10.1007/s11768-016-6059-9

Zou, T., Angeles, J. & Hassani, F. 2018. Dynamic modeling and trajectory tracking control of unmanned tracked vehicles. *Robotics and Autonomous Systems*, 110, pp. 102–111. Available at: https://doi.org/10.1016/j.robot.2018.09.008

Zuo, Z., Yang, M., Wang, H., Wang, Y., Wang, L. & Luo, X. 2021. A lateral control strategy for unmanned ground vehicles with model predictive control and active disturbance rejection control. *Transactions of the Institute of Measurement and Control*, 43(15), pp. 3473–3482. Available at: https://doi.org/10.1177/01423312211025337

Una revisión exhaustiva de las estrategias de control y guía para vehículos terrestres no tripulados en aplicaciones de seguimiento de carril y líder-seguidor.

Amokrane B. Salem-bilal[a], *Stanković* R. Momir[b], *Manojlović* M. Stojadin[c], *Benyahia* A. Taki-eddine Ahmed [d]

[a] Universidad de Defensa en Belgrado – Academia Militar, Departamento de Ingeniería Electrónica Militar, Belgrado, Serbia. **autor de correspondencia**

[b] Universidad de Defensa en Belgrado – Academia Militar, Departamento de Ingeniería Electrónica Militar, Belgrado, Serbia.

[c] Universidad de Defensa en Belgrado – Academia Militar, Departamento de Ingeniería Electrónica Militar, Belgrado, Serbia..

[d] Universidad de Defensa en Belgrado – Academia Militar, Departamento de Ingeniería Electrónica Militar, Belgrado, Serbia..

CAMPO: robótica, sistemas autónomos, control y regulación, ingeniería mecánica, ciencias de la computación;
TIPO DE ARTÍCULO: artículo de revisión

Introducción/objetivo: *Los Vehículos Terrestres No Tripulados (UGVs) ofrecen ventajas significativas para diversas operaciones pero su control y guiado autónomos presentan importantes dificultades, especialmente para diferentes tipos de locomoción (por ejemplo, de orugas o ruedas) en terrenos desafiantes, debido a la dinámicas complejas, restricciones no holonómicas e interacciones con el ambiente. Este artículo proporciona una revisión exhaustiva de las estrategias de control y guiado para UGVs, con un enfoque específico en aplicaciones de seguimiento de carril y líder-seguidor con evasión de obstáculos. El objetivo es sintetizar el estado actual, identificar los principales desafíos genéricos para la autonomía de los UGVs en estas tareas, y discutir metodologías prometedoras de orientación y control.*

Métodos: *Se realizó una revisión extensa de la literatura, analizando investigaciones existentes sobre UGVs, niveles de autonomía, arquitecturas de sistemas, metodologías de control (incluyendo enfoques clásicos, adaptativos, robustos e inteligentes), enfoques de guiado y dominios de aplicación específicos. Se examinaron críticamente las metodologías de guiado y control relevantes para UGV en tareas de líder-seguidor y seguimiento de carril.*

Resultados: *La revisión identifica tendencias dominantes, incluyendo el uso creciente del aprendizaje profundo para la per-*

cepción de guiado y un interés creciente en técnicas de control robusto capaces de enfrentar los desafíos operativos de los UGVs. Persisten desafíos importantes en la percepción en entornos no estructurados, el modelado dinámico preciso para diversas plataformas UGV, la integración perfecta de la percepción con sistemas robustos de guía y control, y la validación extensa en condiciones reales.

Conclusión: *Lograr una autonomía robusta para los UGVs en escenarios reales complejos requiere soluciones integradas que aborden tanto el guiado como el control. Los métodos avanzados de control robusto surgen como candidatos fuertes para el control de UGVs, pero su máximo potencial requiere más investigación en su integración con sistemas de guiado avanzado.*

Palabras clave: *Vehículos Terrestres No Tripulados (UGVs), Sistemas de control, Sistemas de guiado, Seguimiento de líder, Seguimiento de carril, Evasión de obstáculos, Navegación autónoma.*

Всесторонний обзор стратегий управления и навигации наземных беспилотных транспортных средств при выполнении задач автономного движения по полосе и следования за лидером

Амокране В. Салем-билал[а], *Станкович* Р. Момир[б], *Манойлович* М. Стоядин[в],*Беньяхия* А. Таки-эддин Ахмед [д]

[а] Университет обороны в Белграде – Военная академия, Кафедра военноэлектронного инженерства, Белград, Сербия, **корреспондент**

[б] Университет обороны в Белграде – Военная академия, Кафедра военноэлектронного инженерства, Белград, Сербия

[в] Университет обороны в Белграде – Военная академия, Кафедра военноэлектронного инженерства, Белград, Сербия

[д] Университет обороны в Белграде – Военная академия, Кафедра военноэлектронного инженерства, Белград, Сербия

РУБРИКА ГРНТИ: робототехника, автономные системы, управление и регулирование, машиностроение, вычислительные науки;

ВИД СТАТЬИ: обзорная статья

Введение/цель: *Несмотря на то что наземные беспилотные транспортные средства (НБТС) пользуются значительными преимуществами в различных операциях, их* *автономное управление и навигация сопряжены с серьёзными трудностями, собенно когда речь идет о различных типах передвижения (например, гусеничных или колёсных) по труднопроходимой местности из-за сложной динамики, неголономных ограничений и взаимодействия с окружающей средой. Данная статья представляет собой всесторонний обзор стратегий управления и навигации НБТС, делая особый акцент на взаимодействие лидера и последователя и отслеживание полосы движения с помощью приложений для объезда препятствий. Цель статьи — представить современное состояние данной области, выявить ключевые проблемы, общие для автономии НБТС, и рассмотреть перспективные методологии управления и навигации.*

Методы: *В ходе исследования проведен обширный обзор литературы, на основании которого были проанализированы существующие исследования по НБТС, уровням автономии, системным архитектурам, методологиям управления (включая классический, адаптивный, надежный и интеллектуальный подходы), подходам к навигации и конкретным областям применения. Были тщательно изучены методы, применимые к задачам «лидер-последователь» и «отслеживание полосы движения».*

Результаты: *Обзор выявил доминирующие тенденции, включая растущее использование методов глубокого обучения для восприятия и возросший интерес к робастным методам управления, способным справляться с операционными вызовами НБТС. Были выявлены серьёзные проблемы в области восприятия в неструктурированных средах, точного динамического моделирования для различных платформ НБТС, интеграции восприятия с робастными системами управления и навигации, а также необходимость общей валидации в реальных условиях.*

Заключение: *Для достижения робастной автономии НБТС в сложных реальных сценариях требуются интегрированные решения, охватывающие как навигацию, так и управление. Продвинутые робастные методы управления представляются многообещающими в управлении НБТС, однако для полного раскрытия их потенциала необходимо продолжать исследование их интеграции с современными системами навигации.*

Ключевые слова: *наземные беспилотные транспортные средства (НБТС), системы управления, системы навигации, следование за лидером, движение по полосе, объезд препятствий, автономная навигация.*

свеобухватни преглед стратегија управљања и вођења беспосадних возила у задацима аутономног праћења возне траке и праћења вође

Амокране Б. Салем-билал[а], *Станковић* Р. Момир[б], *Манојловић* М. Стојадин[в],*Бенјахија* А. Такi-еддин Ахмед [д]

[а] Универзитет одбране у Београду - Војна академија, Катедра војноелектронског инжењерства, Београд, Србија, **аутор за преписку**

[б] Универзитет одбране у Београду - Војна академија, Катедра војноелектронског инжењерства, Београд, Србија,

[в] Универзитет одбране у Београду - Војна академија, Катедра војноелектронског инжењерства, Београд, Србија,

[д] Универзитет одбране у Београду - Војна академија, Катедра војноелектронског инжењерства, Београд, Србија,

ОБЛАСТ: роботика, аутономни системи, регулација и управљање, машинство, рачунарске науке
КАТЕГОРИЈА (ТИП) ЧЛАНКА: прегледни рад

Увод/циљ: *Беспилотна земаљска возила (БЗВ) пружају значајне предности за различите операције, али при њиховом аутономном управљању и вођењу долази до знатних потешкоћа, које се посебно односе на различите типове локомоције (нпр. гусеничне, точкашке) на изазовним теренима, услед сложене динамике, нехолономних ограничења и интеракција са окружењем. У раду је представљен свеобухватан преглед стратегија управљања и вођења за БЗВ, са посебним фокусом на примене праћења вође и праћења траке са избегавањем препрека. Циљ је да се синтетише тренутно стање технике, идентификују кључни изазови генерички за аутономију БЗВ у овим задацима, и размотре обећавајуће методологије управљања.*

Методе: *При опсежном прегледу литературе, анализирана су постојећа истраживања о историји БЗВ, нивоима аутономије, системским архитектурама, методологијама управљања (укључујући класичне, адаптивне, робустне и интелигентне приступе), као и специфичним доменима* *примене. Критички су испитане методологије за вођење и управљање релевантне за БГВ у задацима праћења вође и праћења траке.*

Резултати: *Идентификовани су доминантни трендови, укључујући све чешћу употребу дубоког учења за перцепцију и растуће интересовање за робусне технике управљања способне да одговоре на оперативне изазове БЗВ-а. Значајни изазови и даље постоје у перцепцији за неструктурирана окружења, тачном динамичком моделирању за различите платформе БЗВ-а, беспрекорној интеграцији перцепције са робустним управљањем и опсежној валидацији у реалним условима. Стратегије управљања засноване на осматрачима, као што је активно потискивање поремећаја (ADRC), показују значајан потенцијал у управљању нелинеарностима, несигурностима и поремећајима БЗВ-а са смањеном зависношћу од модела.*

Закључак: *Постизање робустне аутономије за БЗВ у сложеним реалним сценаријима захтева интегрисана решења која обухватају вођење и управљање. Напредне робустне методе управљања, укључујући ADRC, појављују се као снажни кандидати за управљање БЗВ-има, али њихов пуни потенцијал захтева даља истраживања њихове интеграције са напредним сензорским системима и темељну експерименталну валидацију у циљаним оперативним доменима БЗВ-а.*

Кључне речи: *беспилотна земаљска возила (БЗВ), системи управљања, системи вођења, праћење вође, праћење траке, избегавање препрека, аутономна навигација.*

Paper received on: 03.06.2025.
Manuscript corrections submitted on: 16.07.2025.
Paper accepted for publishing on: 18.07.2025.

Valorization of glass waste into glass powder in the manufacture of concrete

Slimane Merdaci[a], *Noursaid* Ikhlef[b], *Adda* Hadj Mostefa[c]

[a] University of Sidi Bel Abbes, Department of Civil Engineering and Public Works,Structures and Advanced Materials in Civil Engineering and Public Works Laboratory, Sidi Bel Abbes, People's Democratic Republic of Algeria,
e-mail: slimanem2016@gmail.com, **corresponding author,**
ORCID iD: https://orcid.org/0000-0001-8221-3760

[b] University of Sidi Bel Abbes, Department of Civil Engineering and Public Works, Civil Engineering and Environmental Laboratory, Sidi Bel Abbes, People's Democratic Republic of Algeria,
e-mail: ikhlefsaidnour@gmail.com,
ORCID iD: https://orcid.org/0009-0000-3908-0026

[c] University of Relizane, Department of Civil Engineering and Public Works, Innovative Materials and Renewable Energies Laboratory, Relizane, People's Democratic Republic of Algeria,
e-mail: addahadjmostefa@yahoo.fr,
ORCID iD: https://orcid.org/0009-0004-0086-9280

doi https://doi.org/10.5937/vojtehg73-56839

FIELD: materials, civil engineering
ARTICLE TYPE: brief report

Abstract:

Introduction/purpose: The valorization of waste in civil engineering is an essential practice due to its environmental and economic benefits. In many countries, various waste materials are incorporated into construction, particularly in cement and concrete, in the form of powders, fibers, or aggregates. This study focuses on reusing glass waste, a material that poses a significant environmental challenge. The primary objective is to evaluate the feasibility of partially replacing sand with glass waste in concrete production and analyzing its impact on the material's properties.

Method: Different types of glass waste are added to concrete as a partial replacement for sand, using varying percentages. The resulting concrete

samples undergo testing and are compared to conventional (control) concrete to assess their physical and mechanical properties.
Results: The analysis indicates that incorporating recycled glass into concrete is feasible, although the material's properties vary depending on the type and amount of glass used. In some cases, certain characteristics of the concrete improve, while in others, challenges related to strength and durability may arise.
Conclusion: Using glass waste in concrete is a sustainable alternative that helps reduce waste and conserve natural resources. Despite some limitations, this technique represents a promising solution for the construction sector, promoting sustainable development and a circular economy.

Key words: valorization, glass powder, concrete, substitution, mechanical properties.

Introduction

Concrete is the most widely used construction material worldwide due to its availability, relatively low cost, and ease of use. It is employed in a wide range of applications, from residential buildings to infrastructure projects such as bridges and roads. Its standard composition generally includes cement, sand, gravel, and water, although numerous variations exist depending on specific requirements for mechanical strength, durability, and workability.

In the context of sustainable development and responsible resource management, the construction industry faces several environmental challenges. Cement production is particularly energy-intensive and significantly contributes to CO2 emissions. Furthermore, the massive extraction of sand and gravel causes severe ecological disturbances, including habitat destruction, air and water pollution, and increased greenhouse gas emissions.

Recycling waste materials presents a promising solution to mitigate the environmental impact of the construction sector. Among recyclable materials, waste glass is an underutilized resource despite its abundance and potential in various applications, including concrete production. Recycled glass can be ground into fine powder and used as a partial sand replacement in concrete mixtures, thereby reducing landfill waste and conserving natural resources.

This study aims to evaluate the impact of incorporated glass powder on the mechanical properties of concrete. To achieve this, we used the Dreux-Gorisse mix design method to formulate a control concrete and six modified concrete mixes containing different proportions of glass powder

(5%, 10%, 15%, 20%, 25%, and 30%) as a partial replacement for sand. The main focus is to assess how this substitution affects the mechanical behavior of concrete, particularly in terms of its strength and durability over time.

The incorporation of recycled glass in concrete has been extensively studied due to its unique properties, including its silica-rich composition and potential pozzolanic reactivity when finely ground. A review of previous research helps to contextualize this study within the scientific framework and identify current advancements and limitations in this field. Glass can be classified into various categories based on its application and chemical composition, including container glass, lamp glass, and cathode ray tube (CRT) glass (Topcu et al, 2004). Specialized glass types, such as borosilicate glass, are known for their chemical resistance and high softening points, making them suitable for cookware and laboratory equipment (Samtur, 1974). However, impurities and contaminants in mixed-color glass waste can affect the properties of recycled glass and, consequently, the performance of glass-containing concrete (Isa, 2008). The cement industry is one of the most energy-intensive industries, with energy costs representing up to 40% of variable production expenses and even 50–60% in some countries (Jani, 2014). The valorization of glass waste in construction materials, including concrete, presents a promising approach to reducing these costs while enhancing sustainability. A comprehensive review of glass recycling methods in building materials, including concrete, has been provided in (Lu et al, 2019). Several studies have investigated the performance of concrete containing recycled glass in various forms. An in-depth analysis of the use of recycled glass powder in concrete has been presented in (Mallum et al, 2022), highlighting its influence on mechanical strength and durability. Other studies have examined the advantages and limitations of glass powder as a supplementary cementitious material (Federico et al, 2009) or as a fine aggregate substitute (Ismail et al, 2009; Harrison et al, 2020). Research indicates that glass powder, due to its fine particle size and silica content, can exhibit a pozzolanic reaction, improving the long-term strength of concrete. The shortage of natural sand and the environmental consequences of its extraction have led to the search for sustainable alternatives. The use of crushed glass powder as a partial sand substitute in concrete is a viable solution that reduces natural aggregate consumption while repurposing industrial waste. Studies have demonstrated that glass powder effectively fills voids between larger aggregates, enhancing the compactness and mechanical performance of concrete.

While numerous studies have explored the incorporation of glass powder in concrete, several questions remain open, particularly regarding optimal dosage and its effects on mechanical performance. The unique contribution of this study includes:

- Rigorous application of the Dreux-Gorisse method to develop an optimized concrete mix with varying proportions of glass powder, ensuring precise formulation;
- Systematic experimental comparison between a control concrete and six modified mixes containing 5% to 30% glass powder as a sand replacement;
- Comprehensive mechanical evaluation, focusing on the evolution of tensile and compressive strength over time; and
- Identification of the optimal glass powder dosage that improves concrete performance while maintaining an economically and environmentally viable formulation.

This research enhances the understanding of how recycled glass affects concrete properties, providing valuable insights for sustainable construction practices.

This study aligns with sustainable development objectives by reducing the environmental impact of concrete production while improving its performance. Using glass powder as a sand substitute not only recycles an abundant waste material but also optimizes concrete formulation in terms of compactness and strength. The experimental findings will contribute to advancing knowledge on recycled glass in construction materials and guide future research on optimizing concrete mixtures for sustainability.

Materials and methods

Concrete is a building material made from a mixture of cement, gravel, sand, water, and various additives that alter its properties. The components must be appropriate to produce concrete that satisfies the necessary specifications.

The aggregates subject to this study are located in the Sidi Bel Abbes region in Algeria, and their source is as follows:

Cement

CEM II/A-L 42.5N cement is a Portland limestone cement, composed mainly of clinker (80 to 94%) and pure limestone (6 to 20%), with the addition of gypsum (0 to 5%) as a setting regulator.

The cement used in producing different types of concrete complies with standards NF P15-301(Yaragal et al, 2017) and NF EN196-1. It is Portland cement of class CEM II 42.5N, produced at the ZAHANA cement plant. Its strength at 28 days is (≥42.5 MPa).

Sand

The sand utilized in our study is quarry sand sourced from Hasnaoui Sidi Ali Ben Youb. Its cleanliness was evaluated through the sand equivalent test and the sand grain size analysis is presented in Figure 1. According to the results of the sand equivalent test, our sand is clean sand.

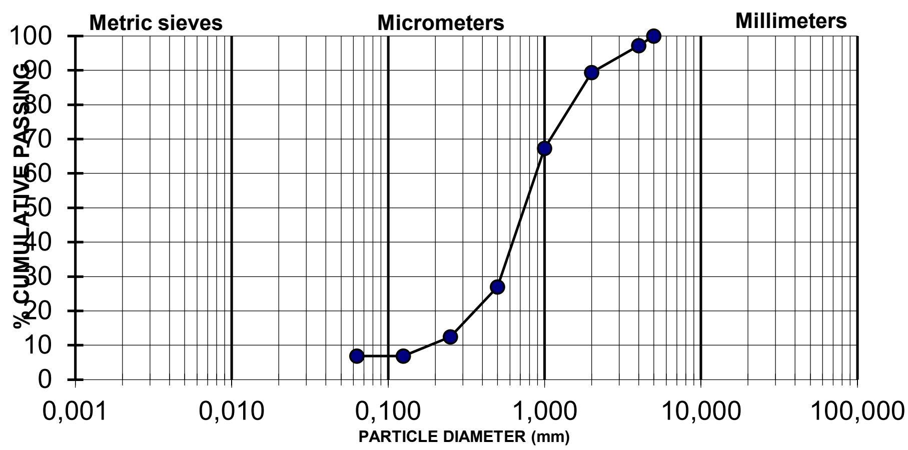

Figure 1 – Grain size analysis curve of the used sand

Gravel

The aggregates utilized in this study are sourced from the Hasnaoui Sidi Ali Ben Youb quarry situated in the Sidi Bel Abbes province of Algeria.

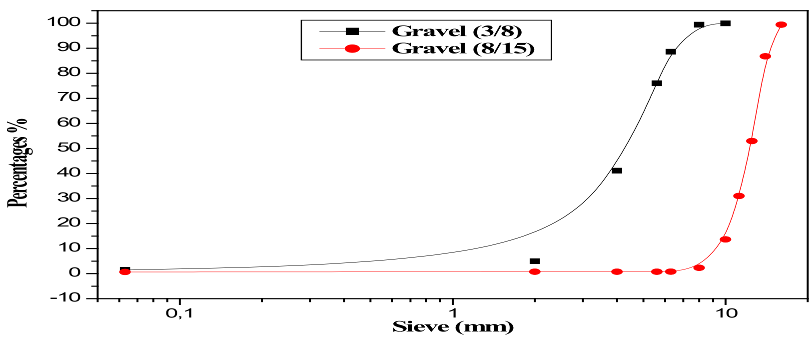

Figure 2 – Grain size analysis curve of the aggregates

These aggregates are available in two size ranges: 3/8 and 8/15 (Figure 2). The concrete is prepared using a mixer with a capacity of 500 liters.

Water

Water plays a crucial role in concrete, as it directly contributes to the chemical reaction with cement (Federico et al, 2009). The quantity of water used should be enough to ensure both the hydration process and the workability of concrete. Potable water is typically used for this purpose.

Glass powder

The glass powder used in our concrete is a finely ground material obtained from recycled glass. The LOS ANGELES machine used for our tests grinds this glass into powder with a diameter of (D ≤ 0/3) (Figure 3).

Figure 3 – Glass powder (0/3) sample

Methodology

To guarantee clarity and precision in our study, we decided to use a reference concrete (RC) as a standard for comparison in our tests. We use the Dreux-Gorisse method to optimize the filling of voids for denser and more resistant concrete and to control workability and durability. Our concrete was designed using the Dreux-Gorisse method, based on a 1 m³ formulation, providing a continuous granular skeleton with a target strength of 40 MPa and a slump of 12 cm. We adopted different compositions of concrete without and with the addition of glass powder at different percentages in all that follows (Table 1).

In this paper, we present the characteristics of the materials and the formulation of the concretes to be studied. We conducted several experimental tests on these concretes (Table 2). The crushing of the cubic specimens (15*15*15 cm³) is presented in Figure 4.

Figure 4 – Concrete made in 15x15x15 cm³ cubic test specimens

Table 1 – Concrete conventions with and without glass powder

Concrete type	Composition
BT	Control concrete with 0% glass powder
BV01	Concrete with 5% glass powder
BV02	Concrete with 10% glass powder
BV03	Concrete with 15% glass powder
BV04	Concrete with 20% glass powder
BV05	Concrete with 25% glass powder
BV06	Concrete with 30% glass powder

Table 2 – Formulation and composition of concrete based on glass powder

Types	Cement (Kg/m^3)	Sand (Kg/m^3)	Gravel (Kg/m^3)	Gravel (Kg/m^3)	Water (L/m^3)	Glass powder (Kg/m^3)
			3/8	**8/15**		
BT	350	**445.00**	356	534	175	**0**
BV01	350	**422.75**	356	534	175	**22.25**
BV02	350	**400.00**	356	534	175	**45.00**
BV03	350	**378.25**	356	534	175	**66.75**
BV04	350	**356.00**	356	534	175	**89.00**
BV05	350	**333.75**	356	534	175	**111.25**
BV06	350	**311.50**	356	534	175	**133.50**

Results and discussions

This section presents the outcomes of the experimental tests conducted on these concrete samples, specifically focusing on compressive and tensile strength assessments.

As stated in (Ismail et al, 2009), the average compressive strengths of various concrete mixtures were measured at intervals of 7, 14, and 28 days using a compression machine.

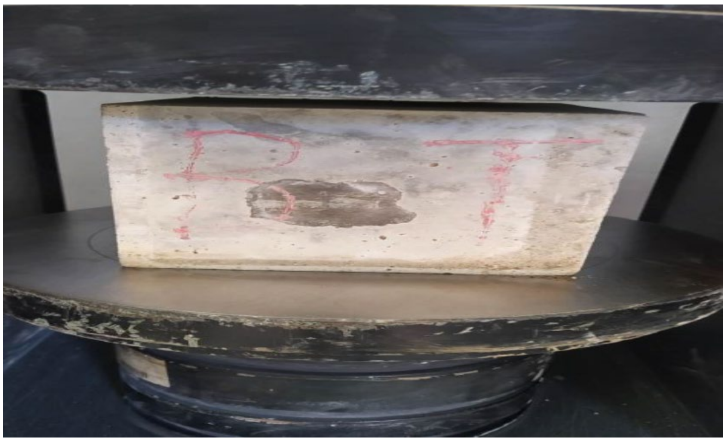

Figure 5 – Crushing of a cubic specimen of witness concrete

Based on the compression tests conducted in the RAH laboratory, the results are as follows:

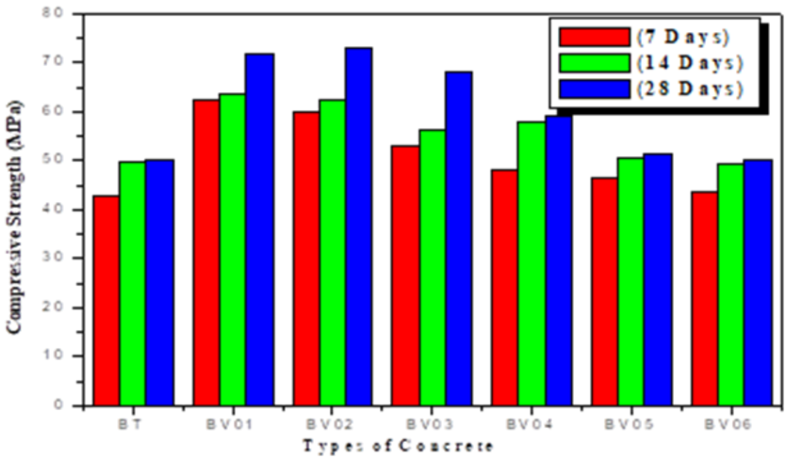

Figure 6 – Results of the compressive strength test

Figure 6 presents the results of the compression tests conducted on the standard concrete (BT) and the concrete containing varying volumetric fractions of glass powder at 5%, 10%, 15%, 20%, 25%, and 30%. The compressive strength was assessed at 7, 14, and 28 day intervals, based on the percentage of glass powder relative to the conventional concrete mix. The compressive strength of the cubic specimens measuring 15 cm x 15 cm x 15 cm, incorporating 5% glass powder, showed a 42.52% increase compared to the standard concrete after 28 days. In contrast, the specimens containing 10% glass powder exhibited a 44.95% increase in compressive strength. However, for the specimens with 15%, 20%, 25%, and 30% glass powder, there was a decline in their compressive strength, with reductions of approximately 35.88%, 17.62%, and 2.07%, ultimately reaching 0%. The findings indicate that incorporating just 10% glass powder (BV02) enhances the concrete strength to 72.88 MPa. This suggests a strong bond between sand and a binder, reflecting the effective integration of glass powder within the matrix. However, increasing the glass powder content to 15%, 20%, 25%, and 30% results in a decline in concrete strength. This decrease is attributed to inadequate implementation and management, resulting in the creation of voids that contribute to the lower strength relative to the standard concrete. Substituting 10% of sand with glass powder is considered a viable option.

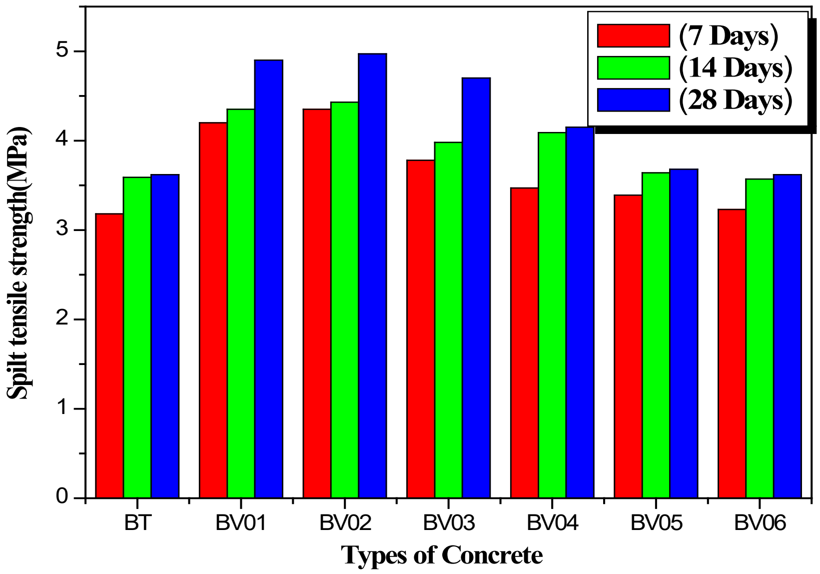

Figure 7 – Tensile strength of the concrete used

Spilt tensile strength was tested in the compressive testing machine. Cylinder specimens of 300mm*150mm were used. The split tensile strength of the cylinder is calculated using:

L = 30cm, length of the cylinder, and

D = 15cm, diameter of the cylinder.

As illustrated in Figure 7, the inclusion of glass powder can significantly improve the tensile strength of concrete. The data indicates that concrete mixed with glass powder exhibits a tensile strength increase ranging from 5% to 30% compared to that of conventional concrete across all ages. Specifically, at 28 days, the tensile strength of concrete containing glass powder shows increments of 35.47% and 37.49% for 5% and 10% glass powder content, respectively. In contrast, for the 15%, 20%, 25%, and 30% glass powder mix, the tensile strength increases by 29.93%, 14.70%, 39.83%, and remains unchanged at 0%.

Conclusions

This research presents findings on the mechanical properties of glass powder in relation to the compressive and tensile strength of concrete, including a comparison with conventional concrete. The key conclusions are as follows:

- The compressive strength of concrete increases with the inclusion of 5% and 10% glass powder (samples BV01 and BV02) compared to standard concrete.
- Concrete mixtures containing 15%, 20%, 25%, and 30% glass powder demonstrate lower compressive strength than the 10% glass powder concrete (BV02).
- The incorporation of glass powder positively influences the strength of concrete, indicating that glass powder concrete fulfills construction requirements and serves as a viable option for the industry.
- While resistant glass powder is valued for enhancing the strength and ductility of concrete, excessive amounts may lead to segregation issues and an overall decrease in concrete strength.
- High concentrations of glass powder can also pose workability challenges due to their increased surface area. However, the performance of glass powder in locally produced concrete shows marked improvements in overall strength and toughness compared to traditional concrete.
- Glass powder is used in various fields, such as coatings manufacturing, construction materials, abrasives, ceramics, etc.

- Glass powder is an environmentally friendly material. Its manufacturing and infinite recyclability make it a sustainable choice for the environment.
- The glass powder is an innovative material. New technologies enable the development of glass powders with increasingly higher performance properties.

This research expands knowledge on alternative materials in concrete, promoting innovation for more eco-friendly, durable, and high-performance concrete.

References

Comité Européen de normalisation: Norme européenne EN197-1 Ciment – partie I: composition, spécifications et critères de conformité des ciments courants. CEN. [online]. Available at: https://www.infociments.fr/ciments/norme-ciment-nf-en-197-1-presentation-generale [Accessed: 21 July 2024].

Federico, L.M. & Chidiac, S.E. 2009. Waste glass as a supplementary cementitious material in concrete – Criticalreview of treatment methods. *Cement & Concrete Composites*, 31, pp.606–610. Available at: https://doi.org/10.1016/j.cemconcomp.2009.02.001

Harrison, E., Berenjian, A. & Seifan, M. 2020. Recycling of waste glass as aggregate in cement-based materials. *Environmental Science and Ecotechnology,* 4,100064. Available at: https://doi.org/10.1016/j.ese.2020.100064

Isa, H. 2008. The need for waste management in the glass industries: a review, *Scientific Research and Essay*, 3(7), pp.276-279. ISSN 1992-2248. [online]. Available at: https://academicjournals.org/journal/SRE/article-full-text-pdf/82276DE14318 [Accessed: 21 July 2024].

Ismail, Z.Z. & AL-Hashmi, E.A. 2009. Recycling of waste glass as a partial replacement for fine aggregate in concrete. *Waste Management*, 29(2), pp.655-659. Available at: https://doi.org/10.1016/j.wasman.2008.08.012

Jani, Y. & Hogland, W. 2014. Waste glass in the production of cement and concrete. *Journal of Environmental Chemical Engineering*, 2, pp.1767-1775. Available at: https://doi.org/10.1016/j.jece.2014.03.016

Lu, J-X. & Poon, CS. 2019. Recycling of waste glass in construction materials. *New Trends in Eco-efficient and Recycled Concrete*, pp.153-167. Available at: https://doi.org/10.1016/B978-0-08-102480-5.00006-3

Mallum, I., Mohd.Sam, A.R., Lim, N.H.A.S., Omolayo, N. 2022. Sustainable Utilization of Waste Glass in Concrete: a Review. *Silicon 14*, pp.3199–3214. Available at: https://doi.org/10.1007/s12633-021-01152-x

NF EN196-1 : méthode d'essais des ciments – détermination des résistances mécaniques (indice de classement P15-471-1). [online]. Available at:

https://www.boutique.afnor.org/fr-fr/norme/nf-en-1961/methodes-dessais-des-ciments-partie-1-determination-des-resistances [Accessed: 21 July 2024].

NF EN 12390-3 : Essais pour béton durci - Partie 3 : résistance à la compression des éprouvettes. [online]. Available at: https://www.scribd.com/document/737423308/EN-12390-3-2019-F [Accessed: 21 July 2024].

Samtur, H. 1974. Glass recycling and reuse. University of Wisconsin, National Science Foundation, NTIS PB239674. [online]. Available at: https://ui.adsabs.harvard.edu/abs/1974STIN...7528536S/abstract [Accessed: 21 July 2024].

Topcu, I.B. & Canbaz, M. 2004. Properties of concrete containing waste glass. *Cement and Concrete Research*, 34, pp.267–274. Available at: https://doi.org/10.1016/j.cemconres.2003.07.003

Yaragal, S.C. & Roshan, M.A.K. 2017. Usage potential of recycled aggregates in mortar and concrete. *Advances in Concrete Construction*, 5(3), pp.201-219 Available at: https://doi.org/10.12989/acc.2017.5.3.201

Valorización de residuos de vidrio en polvo de vidrio en la fabricación de hormigón

Slimane Merdaci[a] , **autor de correspondencia,** *Noursaid* Ikhlef[b], *Adda* Hadj Mostefa[c]

[a] Universidad de Sidi Bel Abbes, Departamento de Ingeniería Civil y Obras Públicas, Laboratorio de Estructuras y Materiales Avanzados en Ingeniería Civil y Obras Públicas, Sidi Bel Abbes, República Argelina Democrática y Popular.

[b] Universidad de Sidi Bel Abbes, Departamento de Ingeniería Civil y Obras Públicas, Laboratorio de Ingeniería Civil y Medio Ambiente, Sidi Bel Abbes, República Argelina Democrática y Popular,

[c] Universidad de Relizane, Departamento de Ingeniería Civil y Obras Públicas, Laboratorio de Materiales Innovadores y Energías Renovables, Relizane, República Argelina Democrática y Popular,

CAMPO: materiales, ingeniería civil
TIPO DE ARTÍCULO: breve anuncio

Resumen:

Introducción/objetivo: La valorización de residuos en la ingeniería civil es una práctica esencial debido a sus beneficios ambientales y económicos. En muchos países, diversos materiales de desecho se incorporan a la construcción, especialmente en cemento y hormigón, en forma de polvos, fibras o agregados. Este estudio se centra en la reutilización de residuos de vidrio, un material que representa un importante reto ambiental. El objetivo principal es evaluar la viabilidad de sustituir parcialmente la arena *por residuos de vidrio en la producción de hormigón y analizar su impacto en las propiedades del material.*

Métodos: Se añaden al hormigón diferentes tipos de residuos de vidrio como sustituto parcial de la arena, en porcentajes variables. Las muestras de hormigón resultantes se someten a pruebas y se comparan con el hormigón convencional (de control) para evaluar sus propiedades físicas y mecánicas.

Resultados: El análisis indica que la incorporación de vidrio reciclado al hormigón es viable, aunque las propiedades del material varían según el tipo y la cantidad de vidrio utilizado. En algunos casos, ciertas características del hormigón mejoran, mientras que en otros pueden surgir desafíos relacionados con la resistencia y la durabilidad.

Conclusión: El uso de residuos de vidrio en el hormigón es una alternativa sostenible que ayuda a reducir los residuos y a conservar los recursos naturales. A pesar de algunas limitaciones, esta técnica representa una solución prometedora para el sector de la construcción, promoviendo el desarrollo sostenible y la economía circular.

Palabras claves:. valorización, polvo de vidrio, hormigón, sustitución, propiedades mecánicas.

Переработка стеклоотходов в стеклянный порошок и его использование в производстве бетона

Слимейн Мердачи[а], **корреспондент,** *Нурсад* Иклеф[б], *Ада* Хадж Мустафа[в]

[а] Университет Сиди-Бель-Аббес, кафедра гражданского строительства и общественных работ, лаборатория конструкций и современных материалов в гражданском строительстве и общественных работах, Сиди-Бель-Аббес, Алжирская Народная Демократическая Республика

[б] Университет Сиди-Бель-Аббес, кафедра гражданского строительства и общественных работ, лаборатория гражданского строительства и охраны окружающей среды, Сиди-Бель-Аббес, Алжирская Народная Демократическая Республика

[в] Университет в Релизане, кафедра гражданского строительства и общественных работ, лаборатория инновационных материалов и возобновляемых источников энергии, Релизан, Алжирская Народная Демократическая Республика

РУБРИКА ГРНТИ: 81.09.00 Материаловедение
ВИД СТАТЬИ: краткое заявление

Резюме:

Введение/цель: Валоризация отходов в гражданском строительстве является важной практикой из-за экологических и экономических преимуществ. Во многих странах различные *отходы используются в строительстве, особенно в цементе и бетоне, в виде порошков, волокон или заполнителей. Данное исследование посвящено вторичному использованию стеклянных отходов − материала, представляющего серьезную угрозу для окружающей среды. Основная цель статьи заключается в оценке возможности частичной замены песка стеклянными отходами при производстве бетона и анализе его влияния на свойства материала.*

Методы: В ходе исследования различные виды стеклоотходов были добавлены в бетон в качестве частичной замены песка в разных процентных соотношениях. Затем полученные образцы бетона были испытаны и сравнены с обычным (контрольным) бетоном для оценки их физических и механических свойств.

Результаты: Анализ показал, что добавление переработанного стекла в состав бетона возможно. Однако свойства полученного материала различаются в зависимости от типа и количества используемого стекла. В некоторых случаях характеристики бетона улучшаются, в то время как в других случаях могут возникнуть проблемы с прочностью и долговечностью.

Выводы: Добавление стеклоотходов в бетоне является экологичной альтернативой, которая помогает сократить количество отходов и сохранить природные ресурсы. Несмотря на некоторые ограничения, этот метод представляет собой многообещающее решение в строительной отрасли, способствующее устойчивому развитию и экономике замкнутого цикла.

Ключевые слова: валоризация, стеклянный порошок, бетон, замещение, механические свойства.

Валоризација стакленог отпада у стаклени прах у производњи бетона

Слимејн Мердачи[а], **аутор за преписку,** *Нурсад* Иклеф [б], *Ада* Хаџ Мустафа [в]

[а] Универзитет Сиди Бел Абес, Катедра за грађевинарство и јавне радове, Лабораторија за конструкције и напредне материјале у грађевинарству и јавним радовима, Сиди Бел Абес, Народна Демократска Република Алжир,

[б] Универзитет Сиди Бел Абес, Катедра за грађевинарство и јавне радове, Лабораторија за грађевинарство и животну средину, Сиди Бел Абес, Народна Демократска Република Алжир,

[в] Универзитет у Релизану, Катедра за грађевинарство и јавне радове, Лабораторија за иновативне материјале и обновљиве енергије, Релизан, Народна Демократска Република Алжир

ОБЛАСТ: материјали, грађевинарство
КАТЕГОРИЈА (ТИП) ЧЛАНКА: кратко саопштење

Сажетак:

Увод/циљ: Валоризација отпада у грађевинарству представља суштински важну праксу због користи како за *економију, тако и за животну средину., Различити отпадни материјали употребљавају се у многим земљама као додатак грађевинским материјалима, нарочито цементу и бетону, у облику праха, влакана или агрегата. Стога се у овом раду разматра поновно коришћење стакленог отпада, материјала који представља значајан еколошки изазов. Основни циљ јесте да се процени изводљивост делимичне замене песка стакленим отпадом у производњи бетона, као и да се анализира утицај који таква замена има на својства материјала.*

Методе: Бетону су додаване различите врсте стакленог отпада као делимичне замене за песак, у различитим процентима. Узорци тако добијеног бетона тестирани су и упоређени са стандардним (контролним) бетоном ради оцене њихових физичких и механичких својстава.

Резултати: Анализа показује да је изводљиво уградити рециклирано стакло у бетон, иако својства тако добијеног материјала варирају зависно од врсте и количине коришћеног стакла. У неким случајевима одређене карактеристике бетона се побољшавају, док се у другим могу јавити проблеми у вези с чврстоћом и трајношћу.

Закључак: Коришћење стакленог отпада у бетону представља одрживу алтернативу којом се смањује отпад и чувају природни ресурси. Упркос неким ограничењима, ова техника може да буде једно од решења у грађевинском сектору којим се промовише одрживи развој и циркуларна економија.

Кључне речи: валоризација, стаклени прах, бетон, супституција, механичка својства

Paper received on: 12.02.2025.
Manuscript corrections submitted on: 27.02.2025.
Paper accepted for publishing on: 10.03.2025.

САВРЕМЕНО НАОРУЖАЊЕ И ВОЈНА ОПРЕМА

СОВРЕМЕННОЕ ВООРУЖЕНИЕ И ВОЕННОЕ ОБОРУДОВАНИЕ

MODERN WEAPONS AND MILITARY EQUIPMENT

Противракетни систем „Тамни орао”:

У време када претња од балистичких ракета и других далекометних оружја постаје све софистициранија, развој противракетних одбрамбених система је од пресудног значаја. Међу водећим системима који су се појавили у области одбране од ракета налази се противракетни систем „Тамни орао”, најсавременија технологија дизајнирана да пресреће и неутралише долазне претње пре него што стигну до својих циљева. У чланку се разматрају концепт, дизајн, могућности, оперативни значај и будући изгледи овог противракетног система.

Лансер ракета система „Тамни рао”

1. Увод

„Тамни орао” је систем за одбрану од ракета нове генерације који је развијен да би се супротставио различитим ракетним претњама, од краткорочних до интерконтиненталних балистичких ракета (intercontinental ballistic missiles — ICBMs).Његова основна сврха је да пресреће и уништи непријатељске ракете у различитим фазама лета: при подизању, у средњој и терминалној фази. Ради се о хиперсоничном оружју дугог домета (Long-Range Hypersonic Weapon — LRHW).Оружни систем се састоји од ракетног бустера који носи хиперсонично клизно возило (Hypersonic Glide Body — C-HGB). Када ракетни бустер достигне одговарајућу висину и брзину, ослобађа хиперсонично клизно возило C-HGB, које клизи хиперсоничним брзинама док се спушта ка свом циљу.

Развијен као део ширег напора неколико земаља да побољшају своје капацитете за одбрану од ракета, „Тамни орао" је пројектован да се супротставља растућим претњама које представљају ракете и софистицирани непријатељи који стално унапређују своје оружане системе. Циљ је да се државама обезбеди способност да бране кључну инфраструктуру, војне објекте и цивилну популацију од ракетних напада.

2. Еволуција противракетних одбрамбених система

Успон ракетне технологије током 20. века довео је до драматичне промене у војним стратегијама, јер је способност лансирања ракета дугог домета које могу носити нуклеарне, хемијске или конвенционалне бојеве главе представљала значајне изазове за глобалну безбедност. Као одговор на то, западна алијанса почела је да развија системе за пресретање и неутралисање ракетних претњи, укључујући познати систем *патриот* за одбрану од ракета, *гвоздену куполу*, као и напредније системе као што су THAAD (Terminal High Altitude Area Defense) и противбалистичка одбрана Aegis, док је руска војна индустрија развијале противавионске и противракетне системе S-300, S-400 и S-500.

„Тамни орао", међутим, представља значајан напредак у погледу брзине, прецизности и поузданости. Он интегрише најновије напредне технологије радарских система, вештачке интелигенције (ВИ) и дизајна ракета за пресретање. Са способношћу да прати, идентификује и уништи различите врсте долазних претњи, он није само одбрамбени систем, већ и стратешки алат за обезбеђивање глобалне стабилности.

3. Технологија система „Тамни орао"

„Тамни орао" користи комбинацију најсавременијих технологија како би постигао своју изузетну ефикасност у пресретању балистичких и крстарећих ракета. Систем је дизајниран да ради аутономно уз минималну људску интервенцију, ослањајући се углавном на своје напредне сензорске мреже и алгоритме вештачке интелигенције за идентификацију и пресретање циљева.

3.1 Радар и праћење система

У основи система „Тамни орао" налази се софистицирана радарска мрежа која омогућава свеобухватно 360-степенско праћење ваздушног простора око одбрамбеног периметра. Ови радарски системи користе више фреквенција како би пратили како обичне, тако и тајне ракетне претње са високом прецизношћу. Способност система да детектује лансирање ракета и прати циљеве на великим раздаљинама је једна од кључних особина која га издваја од старијих генерација система за одбрану од ракета.

„Тамни орао” такође интегрише технологију фузије више сензора, која комбинује податке са различитих радара, инфрацрвених и оптичких сензора како би створила прецизну слику ваздушног простора у реалном времену. Ова фузија података омогућава систему да ефикасно прати више циљева истовремено, чак и у високо загушеним окружењима или у присуству контрамера као што су ометање или мамци.

3.2 Ракете за пресретање

Након што се претња идентификује, систем „Тамни орао” лансира ракете за пресретање које су дизајниране да униште долазећу ракету током лета. Оне су опремљене врло напредним системима за навођење и ракетним главама које обезбеђују висок проценат поготка. У зависности од врсте ракете, „Тамни орао” може распоредити различите врсте ракета за пресретање, као што су кинетички пројектили који се физички сударају са долазном ракетом или експлозивне бојеве главе пројектоване да униште циљ помоћу експлозије.

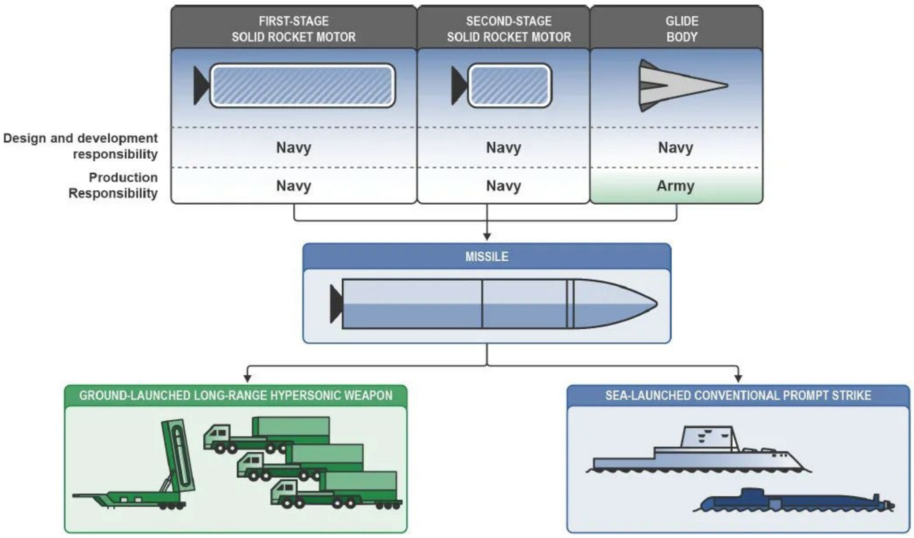

Врсте ракета пресретача система „Тамни орао” у зависности од лансирних платформи

Ракете за пресретање дизајниране су с циљем да пресрећу ракете у различитим фазама њихове трајекторије, од почетне фазе лансирања до терминалне фазе непосредно пре удара. Способност система да гађа ракете током фазе лансирања је посебно корисна јер омогућава пресретање ракете док је још близу места лансирања, чиме се повећава шанса да се претња неутралише пре него што достигне свој циљ. Домет хиперсоничних ракета система „Тамни орао” износи око 2780 км.

VOJNOTEHNIČKI GLASNIK / MILITARY TECHNICAL COURIER, 2022, Vol. 70, Issue 4

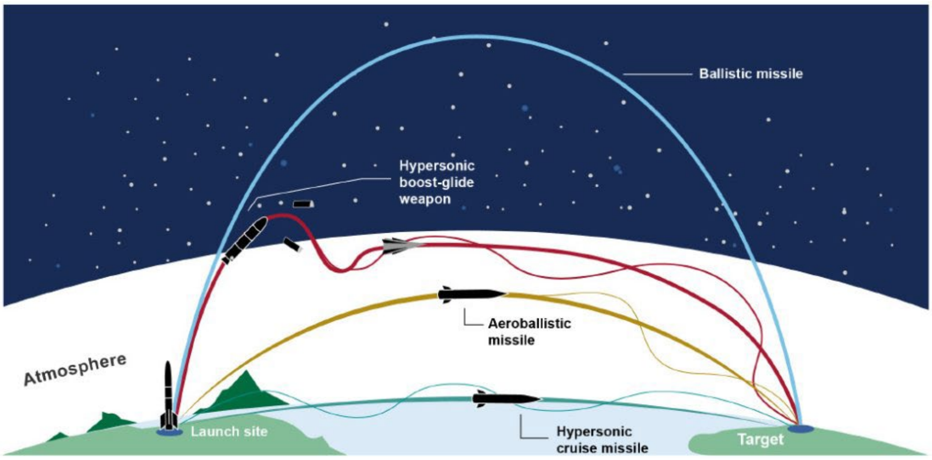

Различите трајекторије балистичких и хиперсоничних ракета

3.3 Вештачка интелигенција (ВИ) и доношење одлука

Интеграција вештачке интелигенције у систем „Тамни орао” представља значајан напредак у области одбране од ракета. Она функционише као „мозак” система, који је у стању да анализира огромне количине података са сензора у реалном времену како би идентификовао, класификовао и пратио више циљева. Такође, ВИ процењује вероватноћу да ће ракета погодити циљ и брзо одлучује која ракета треба да се лансира и када.

Системи засновани на ВИ могу доносити одлуке у делићу секунде, осигуравајући да се одговарајућа ракета лансира према правом циљу на најефикаснији начин. Штавише, систем стално учи из претходних дејстава, побољшавајући своје способности доношења одлука током времена.

4. Оперативне способности система „Тамни орао”

„Тамни орао” је пројектован с циљем да буде веома флексибилан и способан да се адаптира на различите сценарије мисије, било да је у питању одбрана војне базе, велике урбане области или морнарице. Његове оперативне способности обухватају:

4.1 Вишеструко препознавање претњи

„Тамни орао” може истовремено да се бори са више претњи, што га чини идеалним за одбрану од великог броја ракетних напада. Без обзира на то да ли претња подразумева ракетни бараж кратког домета или софистицирани напад интерконтиненталним ракетама, може да приоритетно пресреће претње на основу процењене опасности и трајекторије.

4.2 Свестраност и мобилност
Модуларни дизајн система „Тамни орао" обезбеђује му могућност распоређивања у различита окружења, укључујући земаљске, поморске па чак и ваздухопловне платформе. Предвиђена је инсталација система на копнене, морске и подморске лансере (на ратне бродове класе *Zumwalt,* , подморницу класе *Virginia Block V)*. Систем може бити брзо распоређен и пресељен како би бранио кључне локације, а његове мобилне јединице могу се транспортовати различитим војним возилима или авионима.

4.3 Отпорност на контрамере и електронско ратовање
Један од кључних изазова са којима се суочавају системи за одбрану од ракета јесте способност да се супротставе софистицираним контрамерама које користе непријатељи. „Тамни орао" је пројектован да превазиђе ометање, мамце и друге контрамере које би иначе учиниле традиционалне системе одбране од ракета неефикасним. Уз помоћ адаптивних алгоритама и фузије сензора, овај систем је у стању да разликује стварне претње од мамаца или других ометања, осигуравајући њену ефикасност и у изазовним окружењима.

5. Стратешки значај система „Тамни Орао"
Распоређивање противракетног система „Тамни орао" нуди више стратешких предности, како у погледу националне безбедности, тако и у међународним односима, што обухвата:

5.1 Одвраћање
Присуство система Тамни Орао делује као моћно средство одвраћања за непријатеље који разматрају ракете као могућност напада. Сазнање да држава има капацитет за неутралисање ракетних претњи са високим степеном поузданости може одвратити потенцијалне агресоре од покретања ракетних напада, чиме се доприноси регионалној и глобалној стабилности.

5.2 Заштита кључне инфраструктуре
Способност система „Тамни орао" да штити виталну инфраструктуру, као што су војне базе, електране и владине зграде, од пресудног је значаја за одржавање националне безбедности. Обезбеђујући заштиту од ракетних напада, она гарантује да кључни објекти остану оперативни и током периода појачаних тензија или сукоба.

5.3 Глобални одбрамбени савези
„Тамни орао" није само значајан за појединачне земље, већ доприноси и глобалним одбрамбеним партнерствима. Интероперабилност система са другим системима за одбрану од ракета (као што су Aegis систем за противбалистичку одбрану или систем THAAD) омогућава координиране одбрамбене напоре у случају великог ракетног напада.

6. Будући изгледи и надоградње

Како ракетна технологија наставља да се развија, тако ће се развијати и способности система као што је „Тамни орао”. Будуће надоградње могу укључити побољшања радарских система за праћење, развој ракета за пресретање хиперсоничних ракета и побољшање способности ВИ која ће омогућити још брже и прецизније доношење одлука. Такође, истраживање усмерених енергетских оружја, као што су ласери, могло би имати одговарајућу улогу у следећој генерацији ракета за пресретање система „Тамни орао”, обезбеђујући економичан и високо ефикасан метод за неутралисање долазних претњи.

Штавише, како сајбер претње постају све учесталије, потребно је ојачати сајбер одбрану овог система како би остао оперативан у условима електронског ратовања.

7. Закључак

Иако је извршено неколико пробних лансирања, од којих је последње реализовано децембра 2024. године, Пентагон сејош увек не изјашњава по питању да ли је систем спреман за увођење у оперативну употребу.
Упркос томе, противракетни систем „Тамни орао” налази се на челу савремених технологија одбране од ракета и представља кључни алат у заштити земаља од растућих претњи ракетних напада. Својим напредним радарским системима, интелигентним одлучивањем и свестраношћу у разликовању различитих врста ракета, претпоставља се да ће имати кључну улогу у глобалној одбрани у наредним деценијама. Како непријатељи настављају да усавршавају своје ракетне технологије, нарочито по питању хиперсоничних ракета и пројектила, систем „Тамни орао” ће се сигурно развијати, адаптирајући се на нове изазове и обезбеђујући снажан одговор на једну од најозбиљнијих претњи савремене безбедности.

Током будућих иновација и надоградњи, „Тамни орао” ће вероватно остати темељ националних и међународних одбрамбених стратегија, обезбеђујући како одвраћање, тако и заштиту у све сложенијем и нестабилнијем свету.

Драган М. Вучковић (*Dragan* M. Vučković),
e-mail: draganvuckovic64@gmail.com,
ORCID iD: https://orcid.org/0000-0003-1620-5601

Поређење америчког ловца F-22 и руског Su-57

Амерички ловац F-22 *Raptor* и руски Su-57 (T-50) само су два од најсавременијих стелт ловца који представљају технологију будућности у авијацији. F-22 је врхунски стелт ловац пете генерације, док је Su-57 руски одговор на захтеве савремених и будућих ратних окружења. Иако оба авиона припадају истој категорији, они се значајно разликују по својој конструкцији, могућностима и стратегијама употребе.

1. Опште информације и развој
2.

F-22 Raptor
Произвођач: Lockheed Martin
Први лет: 1997. година
Оперативно: око 180 примерака
Држава: Сједињене Америчке Државе
Класа: ловац 5. генерације, стелт,
развијен као ловачки авион домена ваздушне супериорности и спада у део шире стратегија САД за одржавање превласти у ваздушном простору. Током свог развоја F-22 је прошао кроз опсежне тестове како би постао најефикаснији стелт ловачки авион на свету. Његова конструкција и напредна електроника чине га веома способним у ваздушним борбама, посебно против напредних противничких авиона.

Su-57 Felon:

Произвођач: Сухој
Први лет: 2010. година
Оперативно: од 32 до 50 комада,и даље је у производњи
Држава: Русија
Класа: ловац 5. генерације, стелт, мултифункционални ловацбомбардер
Први руски ловац бомбардер Su-57 развијен је као одговор на западне авионе као што је F-22 и касније F-35. Иако није тако рано уведен у службу као F-22, Su-57 има сличан циљ – доминацију у ваздушном простору и способност да се носи са различитим претњама, од ракетних система до других авиона. Такође, развијен је не само за постизање ваздушне супериорности, већ и за напад на копнене циљеве.

2. Дизајн и стелт технологија
F-22 Raptor:

Стелт способности: F-22 поседује развијену стелт технологију, што му омогућава да буде тешко детектован радарима. Сматра се да му је радарски одраз свега 0,0001m. Његов дизајн карактеришу глатки и агресивни углови, као и напредни материјали који апсорбују радарске таласе. Стелт својства су му изузетно ефикасна у области авиона који се користе за ваздушну супериорност, посебно против других ловаца.

Vučković, D., SAVREMENO NAORUŽANJE I VOJNA OPREMA / MODERN WEAPONS AND MILITARY EQUIPMENT, pp.1156-1178

Su-57:

Стелт способности: Su-57 такође користи напредне стелт технологије, али је његов дизајн нешто другачији. Иако има стелт својства, као што су равне и глатке површине, и неке специфичне углове који смањују радарску видљивост, Su-57 није толико „невидљив” као F-22; сматра се да је његов радарски одраз од 0,1 до 1 m. Руси су усмерили напоре ка постизању стелт способности, али са тежиштем на многострукој намени, што значи да је стелт технологија више компромисна- Међутим, наводно је Su-57 много окретнији у ваздушним маневрима.

3. Перформансе и маневрабилност

F-22 *Raptor*:

Максимална брзина: 2,25 маха (2.414 км/ч)
Доминантне способности: F-22 је познат по својој изузетној маневрабилности. Са своје две турбине и напредном контролом лета, овај авион може да маневрише великим брзинама, што му омогућава да изводи веома сложене маневре. То је посебно корисно у борбама у ваздушном простору где је маневрисање кључно. Ловац је опремљен са по два мотора F119-PW-100 који му омогућују суперкстарење брзином од 1,8 маха. Сваки мотор развија потисак од 15,875кг ,односно 32.000 кг укупно.

Su-57:

Максимална брзина: 2 маха (2.120 км/ч)
Доминантне способности: Su-57 је такође веома маневрабилан и може да изводи сложене маневре. Има напредни систем управљања лета, али се сматра да није тако супериоран у домену маневрабилности као F-22. Ускоро ће бити опремљен новим моторима izdeliye 30, односно AL-51F-1, са потиском од по 14.500 кг,односно скоро 29. 000 кг потиска укупно.

4. Електроника и оружје

F-22 *Raptor*:

Електронски системи: F-22 је опремљен напредним радаром AN/APG-77 који користи фазну антену за детекцију и праћење циљева на великом растојању. Поред тога, има висококвалитетне инфрацрвене и електронске сензоре који омогућавају детекцију циљева у пасивном режиму.

Оружје: F-22 је наоружан различитим типовима ракета кратког и дугог домета, укључујући AIM-120 AMRAAM (ракету за пресретање) и AIM-9M/X

Sidewinder. Такође, има унутрашњи контејнер оружја који је важан за очување стелт својстава.

Su-57:

Електронски системи: Su-57 је опремљен напредним радаром Н036 „Белка” који има више фаза, а који је у стању да открије и прати велики број циљева истовремено, иако се сматра да је нешто мање напредан од АН/APG-77 који користи F-22. Авион је опремљен системом за електронске противмере L402. На кратким раздаљинама користи електрооптички систем 101KS Atoll који обухвата инфрацрвени систем за претрагу и праћење који помаже пилоту при нападу ракетама са инфрацрвеним вођењем.

Оружје: Su-57 поседује широк спектар наоружања, укључујући ракете великог домета за напад на ваздушне циљеве, као што су R-77M и R-74M са дометом до 160 км и ракете за ваздушне и земаљске нападе. Такође, може да користи и нуклеарно оружје, што му даје додатне стратешке могућности.

5. Цена и производња

F-22 *Raptor*:

Цена: Процењује се да је цена једног F-22 око 150 милиона долара , али је увелико повећана због ограничене производње и сложене технологије. Ловац је развијен у условима постојања хладног рата између САД и СССР-а и средином деведесетих година прошлог века постојале су пројекције да би производња могла да обезбеди и 750 авиона чија цена не била већа од 50 до 70 милиона долара. Међутим, након распада СССР-а дошло је до обуставе производње, тако да је сада у оперативној употреби само 183 авиона чија се цена процењује на око 150 милиона долара.

Su-57:

Цена: Su-57 је процењен на око 50 до 70 милиона долара, што је знатно јефтиније у поређењу са F-22, пре свега због руске способности да користи јефтиније производне методе и материјале, али и због прецењености производа америчке војне индустрије.

6. Извоз

Ловац F-22 је један од ретких америчких авиона који није нигде извезен, чак ни у Израел, због тога што су употребљена, тада, најновија техничка достигнућа која представљају војну тајну. Тренутно не постоји серијска производња ових ловаца, а ради се на продужењу ресурса авиона, уграђивању нових сензорских система, као и модификације пилотске кациге према данашњим стандардима.

Ловац Su-57 серијски је произвођен доста касно с обзиром на то да је први пут летео још 2010. године. Након неколико година употребе авиона у борбеним условима постоји неколико земаља које су заинтересоване за куповину, као што је Алжир који је, по неким информацијама, поручио до 24 летелице. У Индији се, по непровереним информацијама, размишља о производњи ових авиона по лиценци.

7. Закључак

Иако F-22 и Su-57 припадају истој категорији ловачких авиона пете генерације, постоје значајне разлике у њиховим могућностима и намени. F-22 је вероватно најнапреднија стелт платформа на свету када је реч о ваздушној супериорности, са изузетним перформансама, маневрабилношћу и електронским системима. С друге стране, Su-57 је вишенаменски авион који комбинује стелт способности са мулти-функционалним способностима, али не достиже исти ниво стелт технологије као F-22.

У контексту геополитике, и САД и Русија настављају да развијају своје авионе и модернизују војне капацитете, али свака од ових платформи има свој приступ у зависности од стратешких и оперативних потреба.

Драган М. Вучковић (*Dragan* M. Vučković),
e-mail: draganvuckovic64@gmail.com,
ORCID iD: https://orcid.org/0000-0003-1620-5601

.

Нарастање кинеске нуклеарне подморничке флоте подморницама типа 093B [1]

Седмог фебруара 2025. појавила се фотографија снимљена 4. фебруара 2025, на којој је приказано бродоградилиште нуклеарних подморница *Huludao*. На њој се види нападна подморница типа 093B на нуклеарни погон (SSN/SSGN) са отвореним коморама вертикалног лансирног система (ВЛС), који је открио повећан број лансирних силоса на 12, што значи да је моћ подморнице знатно повећана. Најмање четири подморнице типа 093 су примећене у бродоградилишту, мада је нејасно да ли су све новоизграђене или су у току одржавања, односно модернизације.

[1] Naval News Navy 2025, 10 Feb, 2025

Нападна подморница на нуклеарни погон типа 093B са отвореним отворима система за вертикално лансирање (ВЛС) открива већи број лансирних цеви, што указује на знатно повећање ватрене моћи за ову класу нападних подморница

Чини се да је Кина покренула програм брзог ширења подморничке флоте, посебно серије Тип 093B. Према извештајима неколико аналитичара, између седам и осам подморница типа 093B изграђено је само у последње три године, што је стопа производње која премашује број јуришних подморница које је Кина израдила у последње три деценије. Када се укључе конвенционалне подморнице, као што је нови Тип 039C, укупан број лансираних подморница у последње три године премашује 15. Кина стално повећава своју флоту подморница на нуклеарни погон, а ускоро се очекује увођење следеће генерације нападних подморница типа 095.

До тада ће Тип 093B вероватно заменити застарела пловила, а ради се на постизању значајног квалитативног скока у подводним способностима. Усвајање погона у облику млазне пумпе у типу 093B сугерише настојање да се смање акустичне карактеристике и побољшају подводне перформансе. Пумпно-млазне пропулзоре углавном имају подморнице које су пројектоване за веће брзине и умањену звучну слику. Почетне процене сугерисале су почетну серију од шест јединица. Тренутни извештаји показују да је производња типа 093B у току и да се ради на замени старијих подморница и повећање укупне величине флоте нуклеарних нападних подморница.

Кинески развој подморница на нуклеарни погон почео је седамдесетих година нападном подморницом класе тип 091 (класа Хан), која је касније замењена нападном подморницом на нуклеарни погон Тип 093 (класа Шанг) како би се побољшале подводне способности Ратне морнарице

Народне ослободилачке војске (ПЛАН). Подморница је пројектована уз помоћ Русије. Њен развој имао је за циљ да отклони ограничења подморнице типа 091, што се посебно односило на смањење буке и борбену ефикасност. Први Тип 093 ушао је у употребу почетком 2000-их, са побољшаном хидродинамиком, тишим радом и већом издржљивошћу. Касније варијанте, као што су Тип 093А и 093В, укључивале су системе за вертикално лансирање (ВЛС) за неколико типова крстарећих пројектила, што је први пут да је таква способност приказана на кинеској нападној подморници. Верује се да Тип 093В, који има издужен труп и напредне сензоре, служи као прелаз ка следећој генерацији подморнице типа 095, такође означеној као 09-В.

Тип 093В има аеродинамичан труп дизајниран да смањи акустичне потписе. Користи систем пумпно-млазног погона уместо конвенционалног пропелера, што је промена у складу са недавним трендовима у дизајну нападних подморница. Овај погонски систем побољшава ефикасност и смањује буку при већим брзинама. Кључна карактеристика типа 093В је интеграција система за вертикално лансирање (ВЛС), што је први познати пример кинеске нападне подморнице опремљене вертикалним лансером, омогућавајући му да лансира низ типова пројектила. Уочена конфигурација која, судећи по фотографији, укључује између 12 и 24 ВЛС ћелије сугерише да подморница може бити наоружана противбродским крстарећим ракетама (*anti-ship cruise missiles — ASCM*), крстарећим ракетама за копнени напад (*land-attack cruise missiles LACM)* и потенцијално балистичким ракетама које се лансирају са подморница (*submarine-launched ballistic missiles SLBM*).

Сателитски снимци са почетка 2023. године показали су да је Кина поринула своју осму подморницу класе 093 у бродоградилишту *Huludao,* од којих су две потврђене као варијанте типа 093В. Стопа производње сугерише степен њене стандардизације. Током 70. годишњице кинеских подморничких снага, у јуну 2024. године, кинески државни медији истакли су све већу улогу нападних подморница на нуклеарни погон у поморским операцијама. Извештаји сугеришу да би подморница Тип 093В могла бити способна да носи варијанту хиперсоничне ракете YJ-21 која се лансира испод мора. Таквим ракетама наоружан је и нови кинески разарач типа 055. Ако буде распоређена са подморница, ова ракета би проширила кинеске ударне способности.

Повећана стопа производње Типа 093В такође поставља питања о будућем саставу кинеске подводне флоте, посебно у погледу односа SSN и подморница на конвенционални погон (SSK) као што је Тип 039С. Усвајање пумпно-млазног погона указује на то да би нове нуклеарне нападне подморнице SSN могле бити агресивније распоређене од претходних. Поред тога, осим типа 093В, Кина наставља да развија своју стратешку нуклеарну подморничку флоту са подморницама типа 094 које се користе за стратешке патроле одвраћања, иако неки аналитичари сугеришу да кинеска нуклеарна тријада још није у потпуности оперативна. Постоје извештаји да би Кина могла да модификује неке стратешке подморнице SSBN типа 094 у подморнице са вођеним ракетама SSGN, као што је америчка морнарица урадила са својим старијим стратешким подморницама класе Ohio, потенцијално повећавајући њихове ракетне способности. То ће повећати способност кинеске ратне морнарице за операције у дубоким водама, проширити њен оперативни домет и ојачати њене способности против приступа/ускраћивања подручја (A2/AD). Конвенционалне подморнице ће вероватно остати део флоте за регионалну одбрану и приморске операције, док ће растућа флота нападних подморница имати задатак да спроводи патроле дугог домета, прати групе носача и доприноси стратешком одвраћању у Пацифику и околним водама.

Истовремено, Кина активно унапређује ракетне способности својих главних бродова. Разарач Тип 055, на пример, опремљен је са 112 ћелија вертикалног лансирног система (ВЛС), способних за размештање различитих пројектила, укључујући противбродску крстарећу ракету YJ-18 и крстарећу ракету за копнени напад CJ-10. Ракета YJ-18 има подзвучни режим крстарења и надзвучни терминални напад, са процењеним дометом од 220 до 540 километара, док је CJ-10 крстарећа ракета за копнени напад са дометом већим од 1.500 км. Поред тога, Кина је представила YJ-21, хиперсоничну противбродску балистичку ракету са процењеним дометом од приближно 1.500 км и брзинама између 6 и 10 маха. Недавно је уведена у оперативну употребу и фрегата типа 054B која такође има модерне ракетне системе, доприносећи растућој поморској ватреној моћи Кине, о чему извештава Међународни институт за стратешке студије (IISS). По том институту, до 2024. године. кинеска морнарица достигла је више од 50% ватрене моћи америчке морнарице по броју вертикалних ракетних лансера.

Драган М. Вучковић (*Dragan* M. Vučković),
e-mail: draganvuckovic64@gmail.com,
ORCID iD: https://orcid.org/0000-0003-1620-5601

„Electromagnetic Warfare: Are Railguns the Next Big Leap? “

For years, the railgun has been a symbol of futuristic warfare—a sleek, silent weapon capable of launching metal slugs at hypersonic speeds, striking targets with pinpoint precision and overwhelming force. Once confined to the pages of science fiction and defense white papers, this electromagnetic marvel is now edging closer to deployment. And if it reaches the battlefield, it won't just be a new weapon—it will be a revolution.

Imagine a weapon that doesn't need explosives to destroy its target. No gunpowder. No propellant. Just a pulse of electricity, two metal rails, and a projectile accelerated to speeds so fast, it tears through the air like a thunderbolt. A railgun's strike isn't just fast—it's nearly impossible to intercept, and its impact is purely kinetic, reducing collateral damage and changing how we think about destructive power.

Behind closed doors and in highly controlled test environments, that future is being forged today. Defense labs in the U.S., China, and elsewhere are racing to solve the last few technical barriers—managing extreme heat, refining barrel durability, and generating the vast power needed to fire at full capacity. Each breakthrough brings the railgun one step closer to changing the balance of power.

Imagine a weapon capable of striking its target before the sound of its launch even arrives—delivering such immense kinetic energy that it destroys through velocity alone, without the need for explosives. This is not speculative fiction. This is the railgun: a cutting-edge electromagnetic weapon system that has the potential to render traditional munitions—bullets, missiles, and conventional artillery—strategically outdated.

A brief history of the railgun

While railguns sound like very modern pieces of kit, they actually have a long and exciting history.
French inventor André Louis Octave Fauchon-Villeplée first introduced the concept of an electromagnetic railgun to the world with a functional, small-scale prototype of an electric cannon in 1918, and several weapons engineers worldwide took notice.

They began work on their futuristic railguns.

It wasn't until World War 2 that we saw plans for a fully functional, combat-ready railgun laid out. German engineer Joachim Hänsler proposed creating what was essentially a railgun – an electromagnetically powered anti-air gun placement.

This was to be an iteration of Villeplée's design decades earlier, a 'cannon' that utilized a charged current to propel its projectiles forward.

But that's all Hänsler's idea ended up being: a design.

Since 1993 the British and American governments have collaborated on a railgun project at the Dundrennan Weapons Testing Centre that culminated in the 2010 test where BAE Systems fired a 3.2 kg (7 pound) projectile at 18.4-megajoules [3,390 m/s (7,600 mph; 12,200 km/h; 11,100 ft/s)] In 1994, India's DRDO's Armament Research and Development Establishment developed a railgun with a 240 kJ, low inductance capacitor bank operating at 5 kV power able to launch projectiles of 3–3.5 g weight to a velocity of more than 2,000 m/s (4,500 mph; 7,200 km/h; 6,600 ft/s).[29] In 1995, the Center for Electromagnetics at the University of Texas at Austin designed and developed a rapid-fire railgun launcher called the Cannon-Caliber Electromagnetic Gun. The launcher prototype was later tested at the U.S. Army Research Laboratory, where it demonstrated a breech efficiency over 50 percent.

In 2010, the United States Navy tested a BAE Systems-designed compact-sized railgun for ship emplacement that accelerated a 3.2 kg (7 pound) projectile to hypersonic velocities of approximately 3,390 m/s (7,600 mph; 12,200 km/h; 11,100 ft/s), or about Mach 10, with 18.4 MJ of kinetic energy. It was the first time in history that such levels of performance were reached.

The Speed of War Just Got Rewritten

The rules of the battlefield are changing—and fast. Traditional weapons are starting to show their age in the face of a new technological leap. The railgun isn't just faster; it's fundamentally redefining what's possible in modern warfare.

Bullets? Too Slow.

A standard 5.56mm rifle round clocks in at around Mach 2.7 (~2,100 mph). That's fast—until you compare it to a railgun. These electromagnetic projectiles can reach speeds exceeding Mach 6 (4,500+ mph), making them faster than any non-hypersonic weapon in active service.

Missiles? Too Predictable.

Cruise missiles typically cruise at Mach 0.8, while even today's hypersonic weapons struggle to push beyond Mach 10. A railgun round reaches Mach 6+ within seconds, delivering impact before most missile defense systems can even lock on.

Artillery? Too Limited.

Conventional howitzers cap out at about 25 miles of range. Railguns? They can reach targets over 100 miles away with precision accuracy—no arc, no delay, just raw speed and power.

The Basic Principle Behind Railguns

At their core, railguns operate on a simple but powerful concept: using electromagnetic force to launch a projectile at extreme velocity. Instead of relying on chemical reactions or combustion, railguns harness electricity to generate force—clean, controlled, and incredibly fast.

The system involves two parallel conductive rails and a sliding armature between them. When a high-voltage current is applied, a magnetic field is created, and the resulting force pushes the armature—and the projectile—forward at tremendous speeds. It's not an explosion, it's a controlled burst of energy translating directly into motion.

What makes railguns stand out is not just their speed, but the efficiency of their destructive power. Because they don't rely on explosive warheads, the impact is purely kinetic. All the energy is focused on velocity and precision. The result? Devastating force delivered in a straight line with minimal collateral damage and no risk of onboard detonation.

Additionally, the lack of propellants or chemical fuel simplifies logistics and reduces storage risks. The power source is internal, and reloading is streamlined. This makes railguns highly scalable—ideal for integration into modern platforms that demand both power and flexibility.

In short, railguns represent a clean, efficient, and high-impact alternative to conventional weapons, opening the door to a new era of precision warfare powered by physics—not fire.

Cheaper, Faster, Deadlier

Railguns aren't just about speed—they're about redefining combat economics and efficiency. In an era where cost, rate of fire, and survivability matter as much as raw firepower, railguns offer a compelling advantage across the board.

Cost per Shot

Modern precision-guided munitions come with a high price tag. A single Tomahawk cruise missile costs approximately $2 million per launch. In contrast, a railgun projectile—essentially a solid metal slug accelerated by electricity—can be manufactured for just $25,000 to $50,000. That's a fraction of the cost for a weapon that can deliver equivalent, if not greater, destructive capability.

Rate of Fire

Traditional artillery systems like howitzers manage 2 to 4 rounds per minute, limited by mechanical reload times and heat buildup. Railguns, on the other hand, have the potential to fire 10 or more rounds per minute, depending on advancements in power delivery and thermal regulation. This higher rate of fire translates directly to increased battlefield effectiveness, especially in high-intensity engagements.

Interception? Nearly Impossible

Current missile defense systems are challenged by hypersonic threats—targets traveling at Mach 5 or faster. Railgun projectiles not only exceed these speeds, but their smaller size, lack of a thermal signature, and non-ballistic trajectory make them exponentially harder to detect, track, or intercept. Once fired, there is virtually no time to respond.

In terms of raw battlefield value, railguns promise more than just innovation—they offer a strategic edge that could dramatically shift the economics and tactics of modern warfare.

The Catch: Why Aren't Railguns Everywhere Yet?

Despite their promise, railguns remain largely experimental—and for good reason. Behind the impressive stats lies a set of formidable engineering and logistical challenges that have so far kept them from widespread deployment.

Power Demands

Firing a single round requires an extraordinary surge of energy—25 megawatts or more per shot. That's enough to power a small town. Currently, only the most advanced naval vessels, such as the USS *Zumwalt*, possess the onboard power generation systems capable of supporting a railgun. Integrating this level of energy requirement into land-based or mobile platforms remains a major hurdle.

Barrel Wear and Rail Erosion

The intense electromagnetic forces and extreme speeds involved in each launch inflict significant damage on the gun itself. Rails can melt, warp, or erode after just a few shots, severely limiting operational longevity. Without breakthroughs in materials science and barrel design, sustained fire remains impractical.

Thermal Management

Railguns generate massive heat—not just in the projectile path, but throughout the entire system. Rapid, repeated firing can turn the weapon into a molten, inoperable system without advanced, compact cooling technologies. Solving this problem is essential for transitioning from test-firing to combat readiness.

Countries Developing Railguns

Several countries are pouring resources into railgun research, driven by the potential to revolutionize warfare with a new class of weapons. Here's a breakdown of the nations making strides in this field:

1. United States

The United States has been a pioneer in railgun development, with research dating back to the early 2000s. Through various defense agencies, including the Office of Naval Research (ONR), the U.S. military has conducted extensive testing of railgun prototypes. The most notable efforts have focused on integrating railguns into naval platforms, particularly destroyers and future warships like the USS Zumwalt, which have the necessary power generation systems to support these high-energy weapons.

Navy considers railgun for a Zumwalt-class destroyer

While the U.S. military has scaled back its plans for immediate deployment in favor of hypersonic missile development, the railgun remains part of long-term strategies for naval warfare. Research is ongoing, particularly into enhancing power storage, cooling systems, and barrel durability. The U.S. has maintained its position as one of the front-runners in railgun technology, although full-scale operational deployment is still a few years away.

2. China

China is aggressively pursuing railgun technology as part of its broader strategy to modernize its military and assert itself as a global leader in emerging technologies. Reports suggest that China has successfully tested a working naval railgun, with trials conducted in 2018. The Chinese military has been focusing on integrating this technology into its naval forces, with the possibility of deploying railguns on advanced ships like the Type 055 destroyers.

Chinese landing ship armed with what could be a prototype railgun

The images now circulating online show the People's Liberation Army Navy's (PLAN) *Haiyang Shan*, a Type 072III-class landing ship with the pennant number 936, sitting in *Wuchang Shipyard* in *Hubei* province with a new, massive gun turret fitted on its bow. The mount appears to be fully enclosed and features a large diameter gun barrel. The other vessels in the class have a significantly smaller twin 37mm cannon in that position.
The gun aboard *Haiyang Shan* could also just be a large conventional cannon or a hybrid system of some type that combines a railgun's inert, hypervelocity projectile design with a traditional chemical propelling charge.

China's efforts in railgun development are not just about power; they're about gaining a strategic edge in both regional and global military power. The rapid pace of their research and testing places them in a strong position to potentially deploy railguns on a wide scale, particularly as the technology matures and power generation systems improve. China's focus on military modernization and technological innovation means that railguns are expected to play a significant role in their future naval and defense capabilities.

3. Russia

Russia has expressed interest in railgun technology, though its progress has been slower compared to the U.S. and China. While Russia is known for its emphasis on advanced weaponry, including hypersonic missiles and direct-energy weapons, railgun development faces challenges, particularly in terms of funding and technological infrastructure. Despite these hurdles, Russia is still exploring the possibility of railgun integration into its naval fleets and land-based artillery systems

Reports from Russian defense sources indicate that railgun prototypes have been under development for years, but due to limited resources and technological barriers, Russia has not yet produced a fully operational model. Still, the potential remains for rapid advancements if Russia can overcome these challenges, making it a country to watch in the race for electromagnetic weapons.

4. Japan

Japan, traditionally focused on missile defense and advanced naval systems, has also entered the railgun race in recent years. Japan's Japan Self-Defense Forces (JSDF) have explored electromagnetic weapons as part of their technological modernization efforts. While Japan's focus has mainly been on non-lethal electromagnetic railguns for defensive applications—such as countering drones or missiles—there is speculation that they may eventually develop more offensive variants.

Turret-mounted electromagnetic railgun now installed on the test ship JS Asuka

In 2023, ATLA (Acquisition, Technology & Logistics Agency) said that it had successfully conducted test firings of a prototype railgun at sea from an unspecified platform, which the organization claimed at the time was a first-of-its-kind achievement for any country. Imagery ATLA released from that testing showed the weapon installed on a test mount rather than the full naval turret now installed on JS *Asuka*.

ATLA has reportedly been able to demonstrate the ability to fire rounds at a velocity of around 4,988 miles per hour (2,230 meters per second; Mach 6.5) while using five megajoules (MJ), or 5 million joules (J), of charge energy in previous tests. Being able to achieve a muzzle velocity of at least 4,473 miles-per-hour (2,000 meters-per-second) and a barrel life of 120 rounds are among previous testing goals.

In addition, railguns have typically been very physically bulky due to the need for large energy storage batteries and cooling systems. The railgun now on JS *Asuka* is notably fixed to the ship's rear flight deck where there is ample open space. Integrating the weapon onto an operational warship in a more traditional arrangement would require finding space for the other components inside the hull.

Japan's significant investments in electromagnetic technologies, coupled with its position as a leading technological power in Asia, could allow it to develop railgun capabilities that complement its existing defense systems, especially for protecting its maritime borders in an increasingly volatile region.

5. Europe (Various Nations)

While no European country has yet demonstrated the same level of commitment to railgun development as the U.S. or China, certain nations within the European Union have been exploring electromagnetic weapons as part of defense innovation programs. Countries such as France, Germany, and the United Kingdom are investing in directed-energy weapons and electromagnetic railguns for potential applications in both naval and land-based defense systems.

Given Europe's collective focus on strategic defense initiatives and advanced research in military technologies, it's likely that railguns will eventually be integrated into European defense platforms, particularly as power systems evolve and demand for energy-efficient weapons grows.

Conclusion: As nations work to overcome technical hurdles, railguns have the potential to reshape modern warfare. While the U.S. and China are leading, other countries are not far behind in the race for this game-changing technology.

Драган М. Вучковић (*Dragan* M. Vučković),
e-mail: draganvuckovic64@gmail.com,
ORCID iD: https://orcid.org/0000-0003-1620-5601

VOJNOTEHNIČKI GLASNIK / MILITARY TECHNICAL COURIER, 2022, Vol. 70, Issue 4

ИЗЈАВА О ЕТИЧКОМ ПОСТУПАЊУ

ЭТИЧЕСКИЙ КОДЕКС

PUBLICATION ETHICS STATEMENT

ИЗЈАВА *ВОЈНОТЕХНИЧКОГ ГЛАСНИКА* О ЕТИЧКОМ ПОСТУПАЊУ

НАПОМЕНА: Уређивачка политика Војнотехничког гласника заснива се на препорукама Одбора за етичност у издаваштву (COPE Core Practices) и заједничким принципима транспарентности и најбоље праксе у издаваштву COPE, DOAJ, OASPA и WAME, као и на најбољим прихваћеним праксама у научном издаваштву. Војнотехнички гласник је члан COPE (Committee on Publication Ethics) од 2. маја 2018. године и члан OASPA (Open Access Scholarly Publishers Association) од од 27. новембра 2015. године. Уредништво примењује Контролну листу за издаваче отвореног приступа о спровођењу Препоруке УНЕСКО-а о отвореној науци. Овај документ је део Унесковог комплета алата за отворену науку, осмишљеног да подржи имплементацију Препоруке Унеска о отвореној науци. Произведен је у партнерству са OASPA.

Основна делатност научног часописа *Војнотехнички гласник* је објављивање чланака након стручне рецензије. У процесу уређивања, који има за циљ објављивање научних чланака, неопходно је постићи сагласност о етичким начелима у поступцима свих учесника (редакције, тј. уредника, чланова Уређивачког одбора и рецензената часописа, као и самих аутора). Поменута начела и поступци дефинисани су овом Изјавом Војнотехничког гласника о етичком поступању.

Мере, радње, одговорности и обавезе Редакције Војнотехничког гласника

Уредништво Војнотехничког гласника не тражи од аутора, нити од трећих страна, плаћање накнаде за аплицирање чланка за објављивање. Читав поступак уређивања и објављивања чланка за ауторе је потпуно бесплатан, како услуге пријављивања рукописа и њихове обраде, тако и услуге публиковања чланака. Не постоје било какви скривени трошкови.

Уредништво Војнотехничког гласника доноси коначну одлуку о томе који ће се рукописи објавити. Одлуке се доносе искључиво на основу вредности рукописа. Морају бити ослобођене расних, полних/родних, верских, етничких или политичких предрасуда. Приликом доношења одлуке о објављивању уредништво се руководи уређивачком политиком, водећи рачуна о законским прописима који се односе на клевету, кршења ауторских права и плагирање.

Рукописи се чувају као поверљив материјал. Информације и идеје садржане у рукописима не смеју се користити у личне сврхе без изричите писане дозволе аутора.

У свом раду, према препоруци Центра за евалуацију у образовању и науци (ЦЕОН), Редакција користи електронски систем уређивања часописа СЦИндекс (Српски цитатни индекс) АСИСТЕНТ (развијен на бази платформе OJS), који омогућава транспарентност и јавност рада, подразумевајући пуну одговорност за прихватање и објављивање чланка.

Процес уређивања чланка у Војнотехничком гласнику подразумева следеће обавезе Редакције:

1. Након пријема чланка, Редакција од аутора прибавља Изјаву о ауторству у којој аутори: наводе свој појединачни допринос у изради чланка; потврђују да су упознати са политком часописа у вези са повлачењем већ објављених радова; потврђују да послати рукопис представља оригиналан рад који су написали и потписали наведени аутори и који није објављен раније на неком другом месту, те да

се рукопис не разматра за објављивање на другом месту и није истовремено послат на рецензију у друге часописе; потврђују да чланак и додатни материјали не садрже тврдње које би се могле сматрати клеветом или било какве незаконите тврдње и не садрже материјал који на било који начин угрожава лична или власничка права физичких или правних лица; потврђују да немају сукоб интереса који би могао да доведе у питање интегритет и веродостојност резултата који су објављени у чланку, као и да су добили сагласност од носилаца ауторских права за коришћење свих извода из дела заштићених ауторским правима и других материјала заштићених ауторским правима који су коришћени у рукопису и да су навели изворе у рукопису и додатним материјалима.

2. Пре доделе рукописа уреднику Редакција проверава да ли је садржај рукописа плагијат, ради провере оригиналности приспелих радова и спречавања публиковања плагијата и дупликата. Војнотехнички гласник не објављује плагиране радове. Уредништво полази од става да је плагирање, односно преузимање туђих идеја, речи или других облика креативног доприноса и њихово представљање као сопствених, грубо кршење научне и издавачке етике. Плагирање може да укључује и кршење ауторских права, што је законом кажњиво.

Плагирање обухвата:

– дословно (реч по реч) или готово дословно преузимање или смишљено, ради прикривања извора, парафразирање делова текстова других аутора без јасног назначавања извора;

– копирање једначина, података или табела из других докумената без правилног назначавања извора и/или без дозволе изворног аутора или носиоца ауторског права.

Рукопис у којем се утврде јасне индиције да је плагиран биће аутоматски одбијен. У случају да се плагијаризам открије у већ објављеном раду, чланак ће бити опозван (повучен) у складу са процедуром описаном у тачки 6.

Ради спречавања плагијата у часопису рукописи се подвргавају провери уз помоћ система iThenticate/CrossRef у оквиру сервиса СЦИндекс АСИСТЕНТ. Резултате добијене провером верификује уредништво часописа у складу са смерницама и препорукама Комитета за етику публиковања (COPE).

Војнотехнички гласник не дозвољава употребу генеративне вештачке интелигенције (енгл. generative AI), као ни технологија подржаних вештачком интелигенцијом (енгл. AI-assisted), као што су велики језички модели (енгл. Large Language Models), за писање рада. Употреба ових технологија дозвољена је једино за унапређење језика и читљивости рада, али уз строгу контролу аутора. Редакција Војнотехничког гласника може користити форензичке алате и специјалне софтвере за идентификацију нерегуларног писања рада помоћу генеративне вештачке интелигенције и технологија подржаних вештачком интелигенцијом. Радови код којих се утврди нерегуларно коришћење ових технологија биће одбијени у процесу уређивања и рецензије или накнадно опозвани ако се ови недостаци утврде у већ објављеним чланцима.

3. Након провере на плагијаризам Редакција додељује приспели рукопис уреднику који ће надаље водити уређивачки процес и одабрати рецензенте. Уредништво и уредник којем је додељен приспели чланак не смеју бити у сукобу интереса у вези са рукописом који разматрају.

Ако такав сукоб интереса постоји, о избору рецензената и судбини рукописа одлучује Уређивачки одбор. Чланови Уређивачког одбора за које се претпостави да би могли бити у сукобу интереса такође не учествују у поступку одлучивања о одређеном рукопису.

4. Рукописи се упућују на рецензију тек након иницијалне оцене да ли су, с обзиром на форму и тематски делокруг, подобни за објављивање у Војнотехничком гласнику. Посебна се води рачуна да иницијална оцена не траје дуже него што је неопходно.

Војнотехнички гласник примењује поступак „двоструког анонимног рецензирања свих радова”.

Главни уредник и чланови уредништва дужни су да предузму одговарајуће мере да аутори и рецензенти остану међусобно анонимни током и након процеса рецензије, у складу са двоструким слепим процесом рецензије. Поред тога, уредништво Војнотехничког гласника може пружити информацију о пристиглом рукопису само аутору, рецензентима или потенцијалним рецензентима, уколико је то потребно.

Сваки рукопис рецензирају бар два рецензента, независно један од другог, а њихов идентитет је међусобно непознат. Рецензенти се бирају искључиво према томе да ли располажу релевантним знањима за оцену рукописа. Не смеју бити из исте институције као аутори рукописа, нити бити њихови коаутори у скоријој прошлости. Евентуални предлози аутора рукописа да се ангажују одређени рецензенти не уважавају се.

Циљ рецензије јесте да уредништву помогне у доношењу одлуке да ли рад треба прихватити или одбити, као и да се у процесу комуникације с уредником, ауторима и другим рецензентима побољша квалитет рукописа.

Током поступка рецензије главни уредник може да захтева од аутора да доставе додатне информације, укључујући и примарне податке, ако су оне неопходне за доношење суда о рукопису. Уредник и рецензенти морају да чувају такве информације као поверљиве и не смеју их употребити у друге сврхе.

У редовним околностима поступак рецензирања траје највише четири недеље, а само изузетно до три месеца. Период од пријема рада до његовог објављивања траје, у просеку, 90 дана.

У случају да аутори имају озбиљне и основане замерке на рецензију, уредништво проверава да ли је она објективна и да ли задовољава академске стандарде. Ако се посумња у објективност или квалитет рецензије, уредник ангажује додатне рецензенте.

Додатни рецензенти се ангажују и у случају када су одлуке постојећа два рецензента међусобно опречне (одбити/прихватити) или на други начин непомирљиве.

Коначну одлуку о прихватању рукописа за објављивање доноси искључиво уредништво.

5. У изузетним случајевима, а посебно у оним околностима када је избор часописа ограничен због специфичне тематике чланка, чланови уредништва часописа Војнотехнички гласник могу бити и аутори његових научних радова. Ипак, у овом случају уредништво спроводи додатно транспарентнији и ригорознији двоструко слепи процес рецензије. То подразумева да ће Редакција часописа уложити напор да одржи интегритет рецензије и необјективност сведе на најмању могућу меру, тако што ће други уредник сарадник водити процедуру рецензије независно од уредника аутора, при чему ће тај процес бити апсолутно транспарентан. Уредништво ће посебно водити рачуна да рецензент не препозна ко је написао рад. Као додатну меру предострожности, ако и када се такав чланак објави, уредништво може објавити пропратни коментар који показује колико је процес уређивања и рецензије био транспарентан.

6. У случају кршења права Војнотехничког гласника, носилаца ауторских права или самих аутора, објављивања истог рукописа у више часописа, лажног ауторства, плагијата, манипулације подацима ради преваре или било које друге злоупотребе, објављени рад се мора опозвати.

Чланак се може опозвати и зато да би се исправиле озбиљне и бројне омашке које није могуће обухватити објављивањем исправке. Опозив објављује уредништво, аутор(и) или обе стране споразумно.

Опозив има облик засебног рада који се приказује у садржају свеске и уреднички класификује као Опозив или Ретракција.

Опозиви се публикују према захтевима COPE које је разрадио CEON, као издавач базе у којој се Војнотехнички гласник примарно индексира, односно издавач националног цитатног индекса где се метаподаци опозива и опозваних радова морају означити одговарајућим упозорењима и међусобно повезати унакрсним линковима:

У електронској верзији изворног чланка (оног који се повлачи) успоставља се веза (HTML линк) са обавештењем о повлачењу. Повучени чланак се чува у изворној форми, али са воденим жигом на PDF документу, на свакој страници, који указује да је чланак повучен (RETRACTED).

7. Редакција је отворена за академску, научно засновану, колегијалну и подстицајну размену мишљења и критику, односно за изношење евентуалних неслагања у вези са резултатима објављеним у чланцима Војнотехничког гласника, тиме што ће пружити могућност учесницима да њихови предметни дописи или полемике буду објављени у рубрици часописа „Писма уреднику”.

Мере, радње, одговорности и обавезе рецензената Војнотехничког гласника

Рецензенти су дужни да квалификовано и у задатим роковима доставе уреднику оцену научне, односно стручне вредности рукописа. Рецензент води посебну бригу о стварном доприносу и оригиналности рукописа. Рецензија мора бити сасвим објективна, а суд рецензента јасан и поткрепљен аргументима.

Рецензенти оцењују рукописе у односу на усклађеност садржаја с профилом Војнотехничког гласника, значај и корисност садржаја, адекватност примењених метода, научну вредност садржаних информација, стил излагања и опремљеност текста. Рецензија има стандардни формат који обухвата оцене појединих димензија рада, општу оцену и закључну препоруку. Неприхватљива је лична критика аутора.

Рецензент не сме бити у сукобу интереса са ауторима или финансијером истраживања. Уколико такав сукоб постоји, рецензент је дужан да о томе правовремено обавести уредника. Рецензент не прихвата на рецензију радове изван области за коју се сматра потпуно компетентним.

Рецензенти треба да упозоре главног уредника ако основано сумњају или имају сазнање о повредама етичких стандарда од стране аутора рукописа. Дужност рецензента јесте да скрене пажњу уреднику на значајна подударања или сличност рукописа са већ објављеним радом, уколико о томе има лична сазнања. Такође, треба да препозна релевантне изворе који у раду нису узети у обзир. Може да препоручи цитирање одређених референци, али не сме да захтева цитирање радова објављених у часопису Војнотехнички гласник или својих радова, ако за то не постоји оправдање.

Од рецензената се очекује да својим сугестијама унапреде квалитет рукописа. Ако оцене да рад заслужује објављивање уз корекције, дужни су да прецизирају начин на који то може да се оствари.

Рукописи који су послати рецензенту морају се сматрати поверљивим документима. Рецензенти не смеју да користе материјал из рукописа за своја истраживања без изричите писане дозволе аутора.

Редакција Војнотехничког гласника подстиче рецензенте да рецензије верификују на својим персонализованим страницама на платформи Web of Science (WoS). Када рецензент уради рецензију чланка за Војнотехнички гласник биће питан да ли жели да прати, потврди и добије признање за свој рад на платформи WoS. Рецензент затим може користити своју верификовану рецензију као доказ о својим доприносима научној заједници у апликацијама за промоцију, финансирање и сл.

Рецензентска политика часописа:

– омогућава јавно приказивање рецензије (**искључиво након објављивања чланка**),

– рецензентима приказује наслове рецензираног чланка (**искључиво након објављивања чланка**).

Мере, радње, одговорности и обавезе аутора који пишу чланке за Војнотехнички гласник

Аутори гарантују да рукопис представља њихов оригиналан допринос, да није објављен раније и да се не разматра за објављивање на другом месту. Истовремено предавање истог рукописа у више часописа представља кршење етичких стандарда, што га искључује из даљег разматрања за објављивање у Војнотехничком гласнику. Рад који је већ објављен на неком другом месту не може бити прештампан у часопису Војнотехнички гласник.

Аутори сносе сву одговорност за целокупни садржај рукописа. Рукопис не сме да садржи неосноване или незаконите тврдње, нити да крши права других лица.

Приликом писања рада, аутори не смеју користити генеративне вештачке интелигенције (енгл. generative AI), као ни технологије подржане вештачком интелигенцијом (енгл. AI-assisted), као што су велики језички модели (енгл. Large Language Models). Ове технологије се не могу користити за реализацију кључног задатка аутора, а то је извођење закључака и препорука који су научно засновани. Алати вештачке интелигенције се могу користити у процесу истраживања за анализу и извођење закључака из података.

Аутори су дужни да обезбеде да њихов ауторски тим наведен у рукопису обухвати само она лица која су значајно допринела садржају рукописа. Ако су у битним аспектима истраживачког пројекта и припреме рада учествовала и друга лица, њихов допринос треба навести у фусноти или посебној напомени (Захвалница, Acknowledgements).

Обавеза је аутора да у напомени наведу назив и кодну ознаку научноистраживачког пројекта у оквиру којег је рад настао, као и пун назив финансирајуће институције. У случају да је рад под истим или сличним насловом био изложен на неком скупу у виду усменог саопштења, детаљи о томе треба да буду наведени на истом месту.

Аутори су дужни да потпуно и правилно цитирају изворе који су значајно утицали на садржај истраживања и рукописа. Делови рукописа, укључујући текст, једначине, слике или табеле, који су дословно преузети из других радова, морају бити јасно означени посебном напоменом, нпр. знацима навода са прецизном ознаком места преузимања (броја странице) или, ако су обимнији, наведени у засебном параграфу.

Пуне референце свих навода у тексту (цитата) морају бити наведене у засебном одељку (Литература) и то на једнообразан начин, у складу са цитатним стилом који Војнотехнички гласник користи (Harvard Style Manuel). У одељку Литература наводе се само цитирани, а не и остали извори коришћени приликом припреме рукописа.

У случају да аутори открију важну грешку у свом раду након његовог објављивања, дужни су да одмах о томе обавесте главног уредника (или Редакцију Војнотехничког гласника) и да сарађују у процесу повлачења или исправљања рада.

Обавеза је аутора да у рукопису наведу да ли су у финансијском или било ком другом битном сукобу интереса који би могао да утиче на њихове резултате или интерпретацију резултата.

Ако се у ауторовом истраживању појављују хемијска једињења, поступци или опрема који су опасни по здравље људи или животиња, то мора бити јасно назначено у рукопису.

Предавањем рукописа аутори се обавезују на поштовање уређивачке политике часописа Војнотехнички гласник, што потврђују достављањем Изјаве о ауторству.

Разрешавање спорних ситуација

Сваки појединац или институција могу уреднику и/или уредништву пријавити сазнања о кршењу етичких стандарда и другим неправилностима и о томе доставити веродостојне информације/доказе ради покретања истраге. Поступак провере изнетих доказа одвија се на следећи начин:

– главни уредник доноси одлуку о покретању истраге;

– током тог поступка сви докази се сматрају поверљивим материјалом и предочавају само оним лицима која су директно обухваћена случајем;

– осумњиченим лицима пружа се прилика да одговоре на изнете оптужбе;

– ако се утврди да је заиста дошло до неправилности, оцењује се да ли је реч о мањем прекршају или грубом кршењу етичких стандарда.

Мањи прекршаји, без последица по интегритет рада и Војнотехничког гласника, на пример када је реч о неразумевању или погрешној примени публицистичких стандарда, разрешавају се у директној комуникацији с ауторима и рецензентима, без укључивања трећих лица, на неки од следећих начина:

– ауторима и/или рецензентима упућује се писмо упозорења;

– објављује се исправка рада, на пример у случају када се са списка референци изоставе извори који су у самом тексту цитирани на прописан начин;

– објављује се ератум, на примеруколико се испостави да је грешка настала омашком уредништва.

У случају грубог кршења етичких стандарда, уредништво може да предузме различите мере:

– објављује саопштење или уводник у којем се случај описује;

– службено обавештава афилијативну организацију аутора/рецензента;

– повлачи објављени рада;

– изриче забрану објављивања у часопису на одређени период;

– предочава случај надлежним организацијама и регулаторним телима ради предузимања мера из њихове надлежности.

Ове мере могу се примењивати појединачно или истовремено. У процесу разрешавања случаја по потреби се консултују релевантне експертске организације, тела или појединци.

Приликом разрешавања етички спорних поступака уредништво се руководи смерницама Комитета за етику публиковања (COPE).

Одрицање одговорности

Изнесени ставови у објављеним радовима не изражавају ставове уредника, чланова Редакције и Уређивачког одбора часописа Војнотехнички гласник. Аутори преузимају правну и моралну одговорност за идеје изнесене у својим радовима.

Изнесени ставови у објављеним радовима не изражавају ставове уредника, чланова Редакције и Уређивачког одбора часописа Војнотехнички гласник. Аутори преузимају правну и моралну одговорност за идеје изнесене у својим радовима. Издавач неће сносити никакву одговорност у случају испостављања било каквих захтева за накнаду штете.

Сукоб интереса

Војнотехнички гласник се придржава политике сукоба интереса коју препоручују COPE и/или друга међународна регулаторна тела (ICMJE, EASE). Од аутора се тражи да се изјасне о свом сукобу интереса у Изјави о сукобу интереса. У Изјави су аутори дужни да наведу: 1) изјаву о свим потенцијалним сукобима интереса за сваког именованог аутора релевантну за садржај чланка или изјаву да немају такве сукобе; 2) тврдња о начину на који је чланак финансиран, конкретно о финансирању, делимично или потпуно, од стране неке компаније или, алтернативно, тврдња да није било тог учешћа и 3) свеобухватно објашњење улоге спонзора у припреми чланка ако је чланак спонзорисан, било у целини или делимично.

Рекламирање

Није дозвољено рекламирање у Војнотехничком гласнику.

Детаљи о етичком поступању Војнотехничког гласника доступни су и на страницама часописа: ***Уређивачка политика, Управљање квалитетом часописа, Подршка квалитету радова*** *у Српском цитатном индексу – издавачу базе у којој се Војнотехнички гласник примарно индексира, односно издавачу националног цитатног индекса.*

КОДЕКС ПРОФЕССИОНАЛЬНОЙ ЭТИКИ ЖУРНАЛА «*ВОЕННО-ТЕХНИЧЕСКИЙ ВЕСТНИК*» ЗАЯВЛЕНИЕ

ПРИМЕЧАНИЕ: Редакционная политика журнала «Военно-технический вестник» основана на рекомендациях Комитета по этике научных публикаций (COPE Core Practices), общих принципах прозрачности и лучшей практике издательской деятельности COPE, DOAJ, OASPA и WAME, а также на лучшей практике научно-издательской деятельности. Журнал «Военно-технический вестник» является членом COPE (Комитет по этике научных публикаций) со 2 мая 2018 года и членом OASPA (Ассоциация научных издателей открытого доступа) с 27 ноября 2015 года. Редакция применяет Контрольный перечень по выполнению Рекомендации ЮНЕСКО об открытой науке для издателей с открытым доступом. Данный документ является частью инструментария ЮНЕСКО по открытой науке, разработанного с целью поддержки внедрения Рекомендации ЮНЕСКО по открытой науке. Документ составлен при содействии с OASPA.

Публикация статей после их профессиональной рецензии является основной деятельностью научного журнала «Военно-технический вестник». В редакционно-издательском процессе в первую очередь необходимо достичь договоренности об этических нормах и принципах, применяемых ко всем участникам, начиная с автора, редакционной коллегии, профессиональных рецензентов до самого издателя. Вышеперечисленные принципы и процедуры утверждены настоящим Заявлением и Кодексом профессиональной этики журнала «Военно-технический вестник».

Меры, деятельность, права и обязанности редакции журнала «Военно-технический вестник»

Редакция журнала «Военно-технический вестник» не взимает плату за подачу и публикацию статей ни с их авторов, ни с третьих лиц. Все процедуры редактирования и публикации абсолютно бесплатны для авторов, включая подачу, прием, редактуру, корректуру, обработку и публикацию статьи. Нет никаких скрытых затрат.

Окончательное решение по выбору статей к публикации принимается редколлегией журнала «Военно-технический вестник». Решение принимается исключительно на основании научной ценности статьи. Не допускается дискриминация по признаку расы, пола, религии, этнического происхождения или политических убеждений. При принятии решений редакция руководствуется редакционной политикой, соблюдая положения законодательства, касающихся клеветы, нарушения авторских прав или плагиата.

Рукописи являются конфиденциальным материалом и хранятся соответствующим образом. Пользоваться информацией и идеями из рукописей в личных целях без письменного согласия авторов недопустимо.

По рекомендациям Центра поддержки оценки в образовании и науке (ЦЕОН) редакция журнала в своей работе пользуется электронной системой редактирования SCIndex (Сербский индекс цитирования) ASSISTANT (разработанной на основе платформы OJS), обеспечивающей прозрачность и доступность информации о текущем состоянии рукописи. Редакция несет полную ответственность за принятие решения о её публикации.

Процедура редактирования статьи в журнале «Военно-технический вестник» включает следующие обязанности редакции:

1. После приема статьи редакции необходимо получить от автора Авторское заявление, в котором авторы: должны указать свой индивидуальный вклад в создание статьи; подтвердить, что ознакомлены с политикой журнала в отношении отзыва уже опубликованных статей; подтвердить, что представленная рукопись является оригинальной работой, написанной и подписанной указанными авторами, что ранее она не публиковалась, а также, что рукопись не рассматривается другими изданиями для публикации и не проходит рецензирование в других журналах; подтвердить, что статья и дополнительные материалы не содержат никаких ложных высказываний, которые могли бы рассматриваться как клевета, не содержат никаких противоречащих закону утверждений или материалов, которые каким-либо образом могут поставить под угрозу личные или имущественные права физических или юридических лиц; подтвердить, что у них нет конфликта интересов, который мог бы поставить под сомнение целостность и достоверность результатов, представленных в статье, и что авторы получили согласие от правообладателей на использование всех выдержек из трудов и других материалов, защищенных авторским правом, которые использовались в рукописи, а также подтвердить, что они указали цитируемые источники в рукописи и дополнительных материалах.

2. Прежде чем редактор ознакомится с рукописью, редколлегия проверяет содержание рукописи на предмет плагиата, для того чтобы удостовериться в оригинальности представленных статей и предотвратить публикацию плагиата и дублирования. Журнал «Военно-технический вестник» не публикует статьи, содержащие плагиат. Редакция придерживается мнения, что плагиат, то есть использование чужих идей, слов или других творческих способов внесения вклада в науку без намеренного указания источника и их представление как своих собственных, является серьезным нарушением исследовательской и публикационной этики. Плагиат является нарушением авторских прав, и он уголовно наказуем.

Под плагиатом понимается:

- Дословное или приблизительное заимствование, а также намеренное перефразирование частей текстов других авторов без четкого указания источника, с целью скрыть источник;
- Копирование уравнений, данных или таблиц из чужих документов без четкого указания источника и/или без согласия автора или правообладателя;

Рукописи с явными признаками плагиата будут автоматически отклонены. Если плагиат выявлен в уже опубликованной статье, то она будет отозвана в порядке, описанном в пункте 6.

В целях предотвращения публикации плагиата в журнале рукописи проверяются с помощью системы iThenticate/CrossRef в рамках платформы SCIndex ASSISTANT. Результаты проверки перепроверяются редакционной коллегией журнала в соответствии с принципами и рекомендациями Комитета по этике научных публикаций (COPE).

Журнал «Военно-технический вестник» запрещает использование генеративных инструментов искусственного интеллекта (ИИ) (engl. AI-assisted), таких как большие языковые модели (engl. Large Language Models) при написании статьи. Использование этих технологий разрешено исключительно для улучшения языка и удобочитаемости статей, но только под строгим наблюдением авторов. Редакция журнала «Военно-технический вестник» может использовать форензические инструменты и специальное программное обеспечение для выявления неэтичного написания статей с помощью генеративного искусственного интеллекта и технологий, поддерживаемых ИИ. Статьи, в которых было обнаружено неэтичное использование этих технологий, будут отклонены в процессе редактирования и рецензирования. Если такого рода нарушения будут выявлены в ранее опубликованных статьях, то они будут отозваны.

3. После проверки на плагиат редколлегия передает рукопись редактору, который в дальнейшем будет вести редакционный процесс и выбирать рецензентов. Редколлегия и редактор, которым направлена представленная статья, не должны иметь конфликта интересов в отношении рассматриваемой ими рукописи.

При наличии такого конфликта интересов о выборе рецензентов и судьбе рукописи решение принимает редакционный совет. Члены редакционного совета, у которых тоже может быть конфликт интересов, также не участвуют в процессе принятия решения по конкретной рукописи.

4. Рукописи представляются на рецензирование только после первичной оценки с учетом соответствия оформления и тематики статьи для публикации в журнале «Военно-технический вестник». Особое внимание уделяется продолжительности оценки, которая длится ровно столько, сколько это необходимо.

Редакция журнала «Военно-технический вестник» проводит конфиденциальное рецензирование всех статей, применяя «двойной слепой метод».

Главный редактор и члены редколлегии обязаны принять соответствующие меры для того, чтобы авторы и рецензенты оставались анонимными друг для друга во время и после процесса рецензирования, проведенного методом двойного слепого рецензирования. Редакция журнала «Военно-технический вестник» при необходимости может предоставить информацию о представленной рукописи только автору, рецензентам или потенциальным рецензентам.

Все рукописи рецензируются как минимум двумя анонимными рецензентами, которые рецензируют рукопись независимо друг от друга. Рецензенты выбираются исключительно на основании их компетенции в области исследования рукописи. Рецензенты не могут быть коллегами авторов, то есть работать в том же учреждении, где работает автор, и они не должны иметь с авторами совместных работ, опубликованных в ближайшем прошлом. Возможные пожелания и предложения авторов о привлечении конкретных рецензентов не принимаются.

Рецензирование проводится с целью оказания помощи редколлегии при принятии решений о публикации статей или отказе авторам, а также улучшения качества статьи путем коммуникации рецензента с редактором, авторами и другими рецензентами.

В процессе рецензирования главный редактор вправе потребовать от автора дополнительную информацию, включая исходные данные, если это необходимо для оценки рукописи. Редактор и рецензенты должны хранить данную информацию в конфиденциальности и не вправе использовать ее в иных целях.

Процесс рецензирования обычно занимает максимум четыре недели и только в исключительных случаях он может длиться до трех месяцев. Период времени от подачи рукописи до ее публикации составляет примерно 90 дней.

Если авторы предъявляют серьезные и обоснованные претензии на рецензию, редколлегия должна проверить являются ли рассматриваемые рецензии объективными и соответствуют ли они академическим стандартам. Если объективность или качество этих рецензий вызывает сомнения, редактор привлекает дополнительных рецензентов.

Дополнительные рецензенты также привлекаются, в случае если решения выбранных рецензентов полностью расходятся (принять/отклонить) или противоречат друг другу по другим признакам.

Окончательное решение о принятии рукописи к публикации принимается исключительно редакционной коллегией.

5. В исключительных случаях, особенно когда выбор журнала ограничен из-за специфической темы статьи, членам редколлегии журнала «Военно-технический вестник» допускается публиковаться в нем. В таком случае редколлегия гарантирует, что процесс двойного слепого рецензирования будет еще более прозрачным и строгим. Это означает, что редакция приложит все усилия для того, чтобы сохранить целостность рецензии и свести к минимуму любую предвзятость. Заместитель редактора проведет абсолютно прозрачную процедуру рецензирования независимо от редактора-автора. Редакционная коллегия позаботится о том, чтобы рецензент не узнал кто является автором статьи. В качестве дополнительной меры предосторожности, если и когда такая статья будет опубликована, редколлегия к статье добавит примечание, содержащее информацию о высоком уровне прозрачности, проведенных процессов редактирования и рецензирования.

6. В случае нарушения прав журнала «Военно-технический вестник», авторских прав или самих авторов, а также в случае повторной публикации одной и той же статьи в различных изданиях, присвоения авторства, плагиата, манипулирования данными или другого вида нарушения этических норм, опубликованная статья будет отозвана.

Статья также может быть отозваны с целью исправления многочисленных и/или фундаментальных недостатков, которые не могут быть устранены исправлениями после публикации. Отзыв статьи производится редакцией, автором (авторами) или обеими сторонами по взаимному согласию.

Уведомление об отзыве имеет форму отдельного документа, указанного в содержании выпуска под названием «Отзыв» или «Ретракция».

Отзывы публикуются в соответствии с требованиями COPE, разработанными CEON в его базе данных, где «Военно-технический вестник» индексируется в первую очередь, при этом метаданные отозванных и снятых с публикации статей должны быть обозначены соответствующим предупреждением и связаны между собой ссылками.

За статьей (утвержденной к отзыву) в электронном формате закрепляют HTML ссылку с уведомлением о её снятии с публикации. Изъятая статья хранится в исходном виде, но каждая страница ПДФ формата визируется водяным знаком, свидетельствующим об изъятии статьи с публикации (RETRACTED).

7. Редакция открыта для академического, научно обоснованного, коллегиального и продуктивного обмена мнениями и критикой, а также для выражения возможных разногласий относительно результатов в статьях, опубликованных в журнале «Военно-технический вестник», предоставляя возможность участникам дискуссии публиковать свои письма по предмету полемики в рубрике: «Письма редактору».

Меры, деятельность, права и обязанности рецензентов журнала «Военно-технический вестник»

Рецензенты должны профессионально и объективно аргументировать свою позицию и в указанный срок предоставлять редактору оценку научной ценности и оригинальности рукописи.

Рецензенты, рассматривая работы оценивают соответствие содержания статьи с профилем журнала «Военно-технический вестник», релевантность исследуемой области и примененных методов, оригинальность и научную значимость результатов, представленных в рукописи, стиль научного изложения, а также использование в тексте научного аппарата. Рецензия должна быть выполнена в стандартном формате, включающем оценки отдельных аспектов работы, общую оценку и заключительную рекомендацию. Личная критика автора недопустима.

У рецензента не должно быть конфликта интересов с авторами или организацией, финансирующей исследование. При наличии такого конфликта рецензент обязан своевременно сообщить об этом редактору. Рецензент может выполнять оценку только тех рукописей, которые соответствуют его области научных и профессиональных интересов, в которой он считается экспертом.

Рецензенты обязаны уведомлять главного редактора в случае, если они обоснованно подозревают или, если они выявили нарушения этических норм в рукописи.

Рецензенты обязаны идентифицировать релевантные существующие работы, которые автор не цитировал. По любому общему сведению или аргументу приведенным в работе должны быть указаны соответствующие источники цитирования. Рецензент обязан обратить внимание редактора на значимые сходства работы с другими опубликованными работами, в случае если такое будет обнаружено. Также рецензенты должны рекомендовать релевантные источники для цитирования, которые не были учтены в работе. Однако они не вправе необоснованно требовать от авторов цитирования работ, опубликованных в журнале «Военно-технический вестник» или своих собственных работ.

Рецензенты оказывают содействие в улучшении качества рукописи своими предложениями и рекомендациями. Если они считают, что работу можно публиковать только после внесения определенных исправлений, то они обязаны указать каким именно образом это лучше сделать.

Рукописи, представленные рецензенту, считаются конфиденциальным документом. Рецензенты не вправе использовать материалы рукописей в своих собственных исследованиях без письменного согласия автора.

Редакция журнала «Военно-технический вестник» призывает рецензентов подтверждать свои рецензии на своей личной странице на платформе Web of Science (WoS). По завершении рецензии статьи, предложенной к публикации в журнале «Военно-технический вестник» рецензенты получат вопрос о том, желают ли они чтобы их рецензия была оценена и признана системой WoS. Таким образом, подтверждённую рецензию рецензент сможете использовать в качестве подтверждения научной деятельности, что поможет при подаче заявок на получение научных грантов, их финансирование и т.д.

Политика журнала относительно рецензий:

- обеспечивает публичный доступ к рецензии (**но только после публикации статьи**),
- позволяет рецензентам отображать заголовок рецензируемой статьи (**но только после публикации статьи**).

Меры, деятельность, права и обязанности авторов, публикующихся в журнале «Военно-технический вестник»

При подаче рукописи в журнал «Военно-технический вестник» автор гарантирует, что рукопись является оригинальной работой, которая не была опубликована ранее и не рассматривается к публикации в других издательствах. Дублирование одной и той же статьи является нарушением этического кодекса, соответственно при обнаружении дублирования автору будет отказано в ее публикации.

Авторы несут ответственность за полное содержание своей рукописи. Рукопись не должна содержать необоснованных или противоречащих закону высказываний, а также не должна нарушать права других лиц.

При написании статьи авторам запрещено пользоваться генеративным искусственным интеллектом (engl. generative AI), а также технологиями, поддерживаемыми искусственным интеллектом (engl. AI-assisted), такими как большие языковые модели (engl. Large Language Models). Этими технологиями нельзя пользоваться в осуществлении ключевой авторской задачи, которая заключается в научных выводах и рекомендациях автора. Инструменты искусственного интеллекта могут использоваться в процессе исследования для анализа и выводов на основании данных.

Авторы должны указать имена, отчества, фамилии всех соавторов, действительно участвующих в процессе исследования и внесших вклад в содержание рукописи. Если в важных аспектах исследовательского проекта и подготовке работы участвовали и другие лица необходимо описать их вклад в сноске или в отдельном примечании (Благодарность, Acknowledgements).

В примечании также должны быть указаны название и кодовый номер научно-исследовательского проекта, в рамках которого была написана статья, а также полное название учреждения/организации, оказавшей финансовую поддержку в осуществлении исследования. В случае, если данное исследование ранее уже было представлено в устной форме, например, на конференции, в примечании необходимо указать название конференции и прочие данные.

Авторы обязаны правильно и полностью цитировать источники, которые оказали значительное влияние на содержание исследования и рукописи. Фрагменты рукописи, включая текст, уравнения, рисунки, графики и таблицы, непосредственно взятые из работ других авторов, должны быть наглядно выделены, например, кавычками с точной ссылкой на первоисточник (номер страницы). Если предмет цитирования длинный, то его следует оформить отдельным абзацем.

Подробная информация о ссылках в тексте (цитирование) должна быть указана в отдельном разделе (Литература) в соответствии со стилем цитирования, используемым журналом «Военно-технический вестник» (Harvard Style Manuel). В разделе «Литература» следует указывать не все источники, использованные при подготовке рукописи, а только цитируемые.

Авторы обязаны незамедлительно уведомить главного редактора (или редакцию журнала «Военно-технический вестник») и содействовать редакции в процессе отзыва или исправления ошибок, в случае если после публикации статьи ими была обнаружена грубая ошибка в ее содержании.

Авторы обязаны указать в рукописи, если существует финансовый или любой другой конфликт интересов, который может повлиять на результаты или интерпретацию результатов исследования.

Если исследование связано с химическими веществами, видами деятельности или оборудованием, представляющими угрозу здоровью людей или животных, это должно быть четко указано в рукописи.

При подаче рукописи авторы соглашаются соблюдать редакционную политику журнала «Военно-технический вестник», подтвердив свое согласие с условиями редакционной политики журнала предоставлением Авторского заявления.

Разрешение спорных ситуаций

Любое лицо либо учреждение вправе в любой момент предъявить претензию редактору или редколлегии в связи с нарушением этических стандартов, подкрепив ее достоверными доказательствами. По получении претензии, подкрепленной доказательствами, редакционная комиссия проведет расследование в соответствии со следующими принципами:

- главный редактор принимает решение о проведении расследования;
- в процессе проверки доказательств все материалы считаются конфиденциальными и будут предоставлены только тем лицам, которые непосредственно причастны к процессу проверки;
- подозреваемым лицам в нарушении этических норм будет предоставлена возможность ответить на выдвинутое против них обвинение;
- если установлено, что нарушение действительно произошло, оценивается степень тяжести нарушения этических норм.

В случае негрубого нарушения (без угрозы репутации журнала „Военно-технический вестник"), например, в случае неправильного толкования или применения публикационных стандартов, редакция напрямую без содействия третьих лиц, обращается к нарушителю следующим образом:

- автору/рецензенту, допустившему ошибку/нарушение направляется письменное предупреждение;
- публикуется уведомление об исправлении, например, если источник, цитируемый в тексте статьи не внесен в список литературы;
- публикуется исправление ошибки, в случае если ошибка произошла по вине редакции.

В случае грубого нарушения этических норм редакция принимает решение о дальнейших мерах:

- публикуется отдельная заметка или статья редактора с описанием случая нарушения этических стандартов;
- направляет официальное уведомление руководителям учреждения, в котором работает автор/рецензент;
- редакция производит отзыв опубликованной статьи;
- редакция объявляет запрет к публикации автора/рецензента на определенный срок;
- информирует соответствующие профессиональные организации и компетентные учреждения о случае, в целях привлечения нарушителя к ответственности.

Редакция вправе предпринимать меры одновременно или поочередно по отдельности. В процессе разрешения дела по мере необходимости проводятся консультации с соответствующими экспертными организациями, органами или лицами.

При разрешении спорных ситуаций редакция журнала руководствуется предписаниями и инструкциями Комитета по этике научных публикаций (COPE).

Отказ от ответственности

Выносимые положения в опубликованных статьях не отражают точку зрения редактора, редколлегии и редакционного совета журнала «Военно-технический вестник». Авторы несут юридическую и моральную ответственность за представленные в своих работах идеи. Редакция не несет никакой ответственности в случае возникновения требований по возмещению материального ущерба и взысканию компенсации морального вреда.

Конфликт интересов

Журнал «Военно-технический вестник» придерживается политики конфликта интересов, рекомендованной COPE и/или другими международными органами, регулирующими публикации научных исследований (ICMJE, EASE). Авторы должны заявить о своем конфликте интересов в Заявлении о конфликте интересов (CoIS). В CoIS каждый названный автор статьи обязан предоставить: (1) Заявление о любых потенциальных конфликтах интересов, имеющих отношение к содержанию, или заявление об отсутствии таких конфликтов. (2) Раскрытие информации о том, как финансируется статья, включая конкретное раскрытие любого и всего финансирования компании (частичного или полного) или заявление об отсутствии такого участия (если применимо). (3) Подробное объяснение роли спонсоров в подготовке статьи, если статья спонсируется частично или полностью.

Реклама

Реклама в журнале «Военно-технический вестник» не допускается.

Более подробно с информацией об Этическом кодексе журнала «Военно-технический вестник» можно ознакомиться на интернет-страницах журнала: ***Редакционная политика, Управление качеством журнала, Поддержка качеству работ*** *на сайте Сербского индекса научного цитирования, в базе которой журнал «Военно-технический вестник» первично индексируется.*

STATEMENT OF THE *MILITARY TECHNICAL COURIER* ON ETHICAL CONDUCT

NOTE: The editorial policy of the Military Technical Courier is based on the COPE Core Practices, common COPE, DOAJ, OASPA and WAME Principles of Transparency and Best Practice in Scholarly Publishing as well as on the best accepted practices in scientific publishing. The Military Technical Courier has been a COPE (Committee on Publication Ethics) member since 2nd May 2018 and a member of OASPA (Open Access Scholarly Publishers Association) since 27th November 2015. The editorial office applies Checklist for open access publishers on implementing the UNESCO Recommendation on Open Science. This document is part of the UNESCO Open Science Toolkit, designed to support implementation of the UNESCO Recommendation on Open Science. It has been produced in partnership with OASPA.

The main scope of the Military Technical Courier scientific journal is publishing scientific articles after peer reviewing. In the editing process leading to publishing scientific articles, it is necessary to reach an agreement on ethical principles in the behavior of all parties involved (Editorial Office i.e. Editor, members of the Editorial Board, reviewers, and authors alike). The aforementioned principles and practices are defined by this Statement of the Military Technical Courier on Ethical Conduct.

Measures, activities, responsibilities, and duties of the Military Technical Courier Editorial Office

The Editorial Office of the Military Technical Courier does not charge for submitting manuscripts from their authors nor from third parties. The whole process of processing and publishing is completely free of charge for authors – from the manuscript submission services through processing to the article publishing services. There are no hidden costs whatsoever.

The Editorial Office decides finally which manuscripts are to be published. Decisions are based only on manuscript values. In making decisions, there is no discrimination on the basis of race, sex/gender, religion, ethnic origin or political beliefs. In making decisions, the Editorial Office is guided by the Journal's policy, complying with legal regulations dealing with libel, copyright infringement and plagiarism.

Manuscripts are kept as confidential material. No information and/or ideas from manuscripts are to be used for private purposes without authors' explicit consent in writing.

In its work, following the recommendations of the Centre for Evaluation in Education and Science (CEON/CEES), the Editorial Office uses the Serbian Citation Index (SCIndeks) ASSISTANT electronic editing system which provides full transparency of the publishing process (developed on the basis of the OJS platform) while being fully responsible for accepting and publishing articles.

The editing process in the Military Technical Courier consists of the following steps of the Editorial Office:

1. After receiving manuscripts, the Office asks the authors to fill in the Authorship Statement in which they: specify their contribution to the manuscript; confirm that they are familiar with the Journal's policy regarding the retraction of already published articles; confirm that the submitted manuscript is an original paper written and signed by its authors, not previously published, not considered for publication elsewhere and not concurrently sent for review to other journals; confirm that the manuscript and the additional material contain neither any false statements that could be considered defamation, any false claims nor material that in any way endangers personal or property rights of natural or legal persons; confirm that they do not have a conflict of interest that could cast doubt on the

article's integrity and the credibility of the results published in it; confirm that they have obtained permission from copyright holders to use all content from copyright-protected works and other copyright-protected material used in the manuscript; and confirm that they have acknowledged the sources in the manuscript and supplementary material.

2. Before the Editor attends to the manuscript, the Editorial Office checks the manuscript content for plagiarism in order to establish the originality of submitted papers and prevent plagiarism and duplication. The Military Technical Courier does not publish plagiarized papers. The Editorial Office is of the opinion that plagiarism i.e. using another's ideas, words or other creative ways of contributing without acknowledging their source and presenting them as one's own is serious violation of research and publication ethics. Plagiarism may also involve copyright infringement which is violation of law.

Plagiarism involves:

- Verbatim or nearly verbatim copying or paraphrasing parts of other authors' texts without clear citing of the source purposefully, in order to hide the source;

- Copying equations, data or graphical presentations from documents of others without clearly acknowledging the source and/or without the authorization of the original author or copyright holder;

A manuscript showing obvious signs of plagiarism is rejected automatically. In case plagiarism is found in an already published article, the article is revoked (retracted) following the procedure given in point 6.

In order to prevent plagiarism, the Journal uses the iThenticate/CrossRef system within the SCIndeks Assistant service for checking manuscripts. The results obtained by such checking are verified by the Editorial Office in accordance with the COPE guidelines and recommendations.

The Military Technical Courier does not allow the use of generative AI nor AI-assisted technologies such as Large Language Models for writing papers. The use of these technologies is allowed exclusively for improving the language and readability of papers but only under strong supervision of authors. The Editorial Office of the Military Technical Courier may use forensic tools and special software to identify unethical writing of papers with the help of generative artificial intelligence and AI-assisted technologies. Papers found to have used these technologies unethically will be rejected during the editing and review process or they will be subsequently retracted if these malpractices are found in already published articles.

3. After being checked for plagiarism, a manuscript is dealt with by the Editor who continues the publishing process by choosing peer reviewers. Neither the Editorial Team nor the Editor in charge of the particular manuscript are allowed to be in a conflict of interest in the case of the manuscript in question.

If there is a conflict of interest, it is up to the Editorial Board to decide on peer reviewers and further actions regarding the manuscript. The Editorial Board members who might be in a conflict of interest are also excluded from the decision-making process in the case of the manuscript in question.

4. Manuscripts are sent to reviewers only after the initial assessment stating that, based on their form and content scope, they are eligible for publication in the Military Technical Courier. Special care is taken that the initial assessment does not last longer than necessary.

The Military Technical Courier makes use of double-blind peer review of all papers.

It is mandatory for the Editor-in-Chief and the Editorial Team members to take appropriate measures that authors and reviewers remain anonymous to each other during and after the reviewing process, in accordance with the double-blind peer review method.

The Editorial Team of the Military Technical Courier can give information on the submitted manuscript only to the author, reviewers or potential reviewers if necessary.

Every manuscript has to be reviewed by at least two reviewers who are not aware of each other's identity and who review the manuscript independently of each other. Reviewers are chosen solely based on whether they have relevant knowledge for the particular paper review. They must not have the same affiliation as the paper author(s) and they are not allowed to have been co-authors with them in the recent past. Possible suggestions of manuscript authors on engaging particular reviewers are not accepted.

The purpose of a review is to help the Editorial Team make a decision whether the paper should be accepted or rejected and to improve the quality of the manuscript through the process of communication with the Editor, authors and other reviewers. During the reviewing process, the Editor-in-Chief may ask the author to submit additional information, including raw data, if it is necessary for assessing the manuscript. The Editor and the reviewers should treat such information as confidential and should not use it for any other purpose.

The reviewing process usually lasts for four weeks maximum, and only exceptionally up to three months. The period of time from the manuscript submission to its publishing is approximately 90 days.

If authors have some serious and justifiable concern with reviews, the Office checks whether the reviews in question are objective and of academic standard. If the objectivity or quality of these reviews are questionable, the Editor engages additional peer reviewers.

Additional reviewers are also engaged when the decisions of the assigned reviewers are contradictory (accept/reject) or somehow incompatible.

The final decision on the acceptance of a manuscript for publication is made exclusively by the Editorial Team.

5. In extreme cases, especially when the choice of journals is limited due to the paper's narrow subject field, it is acceptable that the members of the Editorial Team of the Military Technical Courier may also be authors of scientific articles published in it. However, in this case, the Editorial Team ensures that the double-blind review process is even more transparent and more rigorous. This means that the Editorial Office will make every effort to maintain the integrity of the review and to minimize any bias by having another associate editor handle the review procedure independently of the editor – author in a completely transparent process. The Editorial Team will take special care that a reviewer does not recognize the author's identity. As an extra precaution, if and when such an article is published, the Editorial Team may accompany the article with a note about a high level of transparency of the editing and reviewing processes in question.

6. In case of the violation of the rights of the Military Technical Courier, copyright holders or authors as well as in case of multiple publication, fake authorship, plagiarism, data manipulation or any other malpractice, the published article must be retracted.

Articles can also be retracted for correcting numerous and/or fundamental flaws which cannot be dealt with by post-publication corrections. Retractions are issued by the Editorial Team, the author(s) or by both parties based on mutual agreement.

A retraction notice has a form of a separate paper listed in the Contents of an issue, classified as “Retraction”.

Retractions are published in accordance with the COPE Guidelines elaborated by the CEON/CEES in its database where the Military Technical Courier is primarily indexed.

The CEON/CEES publishes the national citation index where the metadata of retraction notices and related retracted articles must be clearly and appropriately marked and mutually cross-linked. An electronic version of the original article (the one being retracted) is provided with a HTML link to the retraction notice. Retracted articles are retained in their original form but with a watermark on each page of the PDF document indicating that the article in question is RETRACTED.

7. The Editorial Office is open to academic, scientifically based, collegial and productive exchange of opinions and critiques as well as for expressing possible disagreements regarding the results in articles published in the Military Technical Courier by enabling polemics and reactions to be published in the Journal's section "Letters to the Editor".

Measures, activities, responsibilities, and duties of the Military Technical Courier reviewers

Reviewers are required to assess the scientific and professional values of manuscripts in a qualified and timely manner. They have to focus especially on the genuine contribution and originality of manuscripts. A review should be completely unbiased and the reviewer's assessment unambiguous and backed with arguments.

Reviewers assess manuscripts with regard to the compliance of the content with the Journal's character, importance and effectiveness of the content, convenience of the methods applied, scientific value of the presented information as well as with regard to the style, tone and form of the text. A review has a standard form which comprises assessment of particular elements of a manuscript, general assessment and final recommendation. Personal criticism of the author is unacceptable.

Reviewers must not be in a conflict of interest with authors or research funders. If such a conflict exists, the reviewer is obliged to inform the Editor about it in due time. Reviewers should not accept to review papers out of the scope of their full competence.

They should notify the Editor-in-Chief if they have a reasonable doubt about the author violating ethical standards. A duty of reviewers is to call to the editor's attention any substantial similarity or overlap between the manuscript under consideration and any other published paper of which they have personal knowledge. Also, hey should recognize relevant sources which have not been taken into account in the manuscript. They may recommend citing particular references but must not insist on citing articles published in the Military Technical Courier or their own papers if there is no justification for doing so.

Their suggestions should aim at improving the manuscript's quality. If they conclude the paper deserves to be published but with corrections, they are required to provide detailed instructions.

Manuscripts sent to reviewers must be treated as confidential documents. The material from manuscripts must not be used for reviewers' own research without the author's explicit consent in writing.

The Editorial Office of The Military Technical Courier encourages reviewers to verify their reviews on their personal profile pages on the Web of Science (WoS) platform. When reviewers submit their peer reviews to The Military Technical Courier, they will be asked whether they would like to track, verify and showcase them on the WoS platform. Reviewers can further use their verified peer reviews as evidence of their contribution to the scientific community in applications for promotion, grants, etc.

The reviewing policy of the journal:

- allows visibility of the review in public (**only after the article has been published**),
- shows titles of reviewed articles to reviewers (**only after the article has been published**).

Measures, activities, responsibilities and duties of the Military Technical Courier authors

Authors undertake that the manuscripts are their original contribution, that they have not been published before, and that they are not considered for publication elsewhere.

Parallel submission represents violation of ethical codes which eliminates the manuscript in question from being further considered for publication in the Military Technical Courier. A paper already published elsewhere cannot be published in the Military Technical Courier.

Authors are fully responsible for the complete content of their manuscripts. The manuscript should not contain unfunded or illegal statements nor infringe on the rights of others.

When writing their papers, authors are not allowed to use generative AI nor AI-assisted technologies such as Large Language Models. These technologies are not to be used for the realization of the key authors' task which is to draw scientifically based conclusions and recommendations. Artificial intelligence tools can be used in the process of research to analyze and draw conclusions from data.

Authors are required to make sure that their team mentioned in the manuscript consisits only of individuals whose contribution to the content of the manuscript is significant. If there were other individuals who participated in some other important moments of the research project or in the manuscript preparation, their contribution is to be mentioned in a footnote or in a separate note (Acknowledgement).

The name and the code number of the research project from which the paper originates must be given in a note, as well as the full name of the funding institution. In case the paper has been presented orally elsewhere with the same title or a similar one, the details of such a communication have to be metioned in a note as well.

Authors' duty is to correctly and completely quote the sources which had a significant influence on the content of the research and the manuscript. Fragments of the manuscript, including the text, equations, graphical presentations, figures and tables, directly included from the works of others, must be clearly marked e.g. by quotation marks with a precise reference to the original source (page number) or in a separate paragraph if they are bigger in size.

Full references of all citations in the main text must be given in a separate section (References) in a uniform way, complying with the citation style used in the Military Technical Courier (Harvard Style Manual). The Reference Section contains only the cited sources, not all sources used in the preparation of the manuscript.

In case authors find an error in their article after its publication, they are obliged to promptly notify the Editor-in-Chief (or the Editorial Office) and cooperate in the process of retracting or correcting the article.

Authors are under the obligation to declare in their manuscript whether there is a financial or any other conflict of interest that may influence the results or interpretations of the results.

If the research involves chemicals, activities or equipment posing risk to the health of humans or animals, this must be clearly stated in the manuscript.

When submitting their manuscript, authors agree to comply with the editorial policy of the Military Technical Courier and they confirm such compliance by submitting the Authorship Statement.

Handling allegations of misconduct

Any individual or institution may notify the Editor and/or Editorial Team of ethical malpractice and other misconduct by supplying undisputed information/evidence to start an enquiry. The procedure for investigating the case raised with the supplied evidence is as follows:

- Editor-in-Chief determines to start investigation;
- all evidence is considered confidential during investigation and is available only to those directly involved in the case;
- individuals suspected of ethical breaches are given a chance to respond to the allegations;
- if a misconduct is confirmed, it is further established whether there is a minor or a major violation of publication ethics.

Minor issues not affecting either the integrity of the paper or that of the Journal, e.g. misunderstanding or misapplication of publication standards, are dealt with by directly communicating authors and reviewers, without third parties involved, in one of the following ways:

- authors and/or reviewers are sent a letter of warning;
- a correction notice is published, e.g. when a source, otherwise properly cited within the main text, has been omitted from the Reference List;
- an erratum is published, e.g. when an error is made by the Editorial staff. Serious, major violations of the ethical code may lead to different measures:
- a separate note or a leading article is published, describing the case;
- afilliate institution of the author/reviewer is officially notified;
- the published article is retracted;
- publishing in the Journal is prohibited for a defined period of time;
- relevant organisations and regulatory bodies are informed about the case for taking course of actions within their competence.

These measures may be taken separately or jointly. In the process of handling the case, relevant expert organisations, bodies or individuals are consulted when necessary.

In resolving ethically controversial issues, the Editorial Team follows the guidelines of the Committee on Publication Ethics (COPE).

Disclaimer

The views in the published articles do not represent the views of the Editor, the Editorial Office, the Editorial Team or the Editorial Board of the Military Technical Courier journal. Authors take full legal and moral responsibility for the information and opinions expressed in their articles. The publisher will not be held liable in any way for any claims or damages.

Conflict of interest

The Military Technical Courier adheres to the conflict of interest policy recommended by COPE and/or other international research publishing regulatory authorities (ICMJE, EASE). The authors must declare their conflicts of interest in the Conflict of Interest Statement (CoIS). In the CoIS, each named author of the article is required to provide: (1) A statement of any potential conflicts of interest relevant to the content or a statement that there are no such conflicts. (2) Disclosure of how the article is funded, including specific disclosure of any and all company funding (partial or total), or a statement that there was no such involvement (if applicable). (3) A comprehensive explanation of the role of sponsors in article preparation if the article is sponsored in part or whole.

Advertising

Advertising in the Military Technical Courier is not permitted.

Details on the ethical conduct of the Military Technical Courier are also available on the Journal pages: ***Publication Policy, Journal Quality Management and Article Quality Support*** *via the website of the Serbian Citation Index (SCIndex) – publisher of the national citation index, i.e. publisher of the base in which the Military Technical Courier is primarily indexed.*

ПОЗИВ И УПУТСТВО АУТОРИМА

ПРИГЛАШЕНИЕ И ИНСТРУКЦИЯ ДЛЯ АВТОРОВ РАБОТ

CALL FOR PAPERS AND INSTRUCTIONS FOR AUTHORS

ПОЗИВ И УПУТСТВО АУТОРИМА О НАЧИНУ ПРИПРЕМЕ ЧЛАНКА

Упутство ауторима о начину припреме чланка за објављивање у *Војнотехничком гласнику* урађено је на основу Правилника о категоризацији и рангирању научних часописа Министарства просвете, науке и технолошког развоја Републике Србије ("Службени гласник РС", број 159/20). Примена овог Правилника првенствено служи унапређењу квалитета домаћих часописа и њиховог потпунијег укључивања у међународни систем размене научних информација.

Војнотехнички гласник / Vojnotehnički glasnik / Military Technical Courier (втг.мо.упр.срб, www.vtg.mod.gov.rs, ISSN 0042-8469 – штампано издање, e-ISSN 2217-4753 – online, UDC 623+355/359, DOI: 10.5937/VojnotehnickiGlasnik; https://doi.org/10.5937/VojnotehnickiGlasnik), јесте рецензирани научни часопис.

Власници часописа су Министарство одбране Републике Србије и Војска Србије. Издавач и финансијер часописа је Универзитет одбране у Београду (Војна академија).

Програмска оријентација часописа заснива се на годишњој категоризацији часописа, коју врши надлежно државно министарство у одређеним областима, као и на његовом индексирању у међународним индексним базама.

Часопис обухвата научне, односно стручне области у оквиру образовно-научног поља **природно-математичких наука**, као и у оквиру образовно-научног поља **техничко-технолошких наука**, а нарочито области **одбрамбених наука и технологија**. Објављује теоријска и практична достигнућа која доприносе усавршавању свих припадника српске, регионалне и међународне академске заједнице, а посебно припадника војски и министарстава одбране. Публикује радове са уравнотеженим извештавањем о аналитичким, експерименталним и примењеним истраживањима, као и нумеричким симулацијама, обухватајући различите дисциплине. Објављени материјали су високог квалитета и релевантности, написани на начин који их чини доступним широкој читалачкој публици. Сви радови који извештавају о оригиналним теоријским и/или практично оријентисаним истраживањима или проширеним верзијама већ објављених радова са конференција су добродошли. Радови за објављивање одабиру се двоструко слепим поступком рецензије како би се осигурала оригиналност, релевантност и читљивост. Притом циљ није само да се квалитет објављених радова одржи високим већ и да се обезбеди правовремени, темељни и уравнотежени поступак рецензије.

Уређивачка политика *Војнотехничког гласника* заснива се на препорукама Одбора за етичност у издаваштву (COPE Core Practices) и заједничким принципима транспарентности и најбоље праксе у издаваштву COPE, DOAJ, OASPA и WAME, као и на најбољим прихваћеним праксама у научном издаваштву. *Војнотехнички гласник* је члан COPE (Committee on Publication Ethics) од 2. маја 2018. године и члан OASPA (Open Access Scholarly Publishers Association) од од 27. новембра 2015. године.

Министарство науке, технолошког развоја и иновација Републике Србије утврдило је дана 13. 12. 2024. године категоризацију *Војнотехничког гласника*, за 2024. годину:

– на листи часописа за рачунарске науке:
категорија врхунски часопис националног значаја **(M51)**,

– **на листи часописа за електронику, телекомуникације и информационе технологије:**
категорија врхунски часопис националног значаја **(М51)**,

– **на листи часописа за машинство:**
категорија врхунски часопис националног значаја **(М51)**,

– **на листи часописа за материјале и хемијске технологије:**
категорија национални часопис међународног значаја **(М24)**.

Усвојене листе домаћих часописа за 2024. годину могу се видети на сајту *Војнотехничког гласника*, страница *Категоризација часописа*.

Детаљније информације могу се пронаћи и на сајту Министарства просвете, науке и технолошког развоја Републике Србије.

Подаци о категоризацији могу се пратити и на сајту КОБСОН-а (Конзорцијум библиотека Србије за обједињену набавку).

Категоризација часописа извршена је према Правилнику о категоризацији и рангирању научних часописа Министарства просвете, науке и технолошког развоја Републике Србије ("Службени гласник РС", број 159/20).

Часопис се прати у контексту Српског цитатног индекса – СЦиндекс (база података домаћих научних часописа), Научно-информационог система Redalyc и Руског индекса научног цитирања (РИНЦ). Подвргнут је сталном вредновању (мониторингу) у зависности од утицајности (импакта) у самим базама. Детаљи о индексирању могу се видети на сајту *Војнотехничког гласника*, страница *Индексирање часописа*.

Војнотехнички гласник, у погледу свог садржаја, пружа могућност отвореног приступа (DIAMOND OPEN ACCESS) и примењује Creative Commons (CC BY) одредбе о ауторским правима. Детаљи о ауторским правима могу се видети на сајту часописа, страница *Ауторска права и политика самоархивирања*.

Радови се предају путем онлајн система за електронско уређивање АСИСТЕНТ, који је развио Центар за евалуацију у образовању и науци (ЦЕОН).

Приступ и регистрација за сервис врше се на сајту www.vtg.mod.gov.rs, преко странице *АСИСТЕНТ* или *СЦИНДЕКС*, односно директно на линку aseestant.ceon.rs/index.php/vtg.

Детаљно упутство о регистрацији и пријави за сервис налази се на сајту www.vtg.mod.gov.rs, страница *Упутство за АСИСТЕНТ*.

Потребно је да се сви аутори који подносе рукопис за објављивање у *Војнотехничком гласнику* региструју у регистар ORCID (Open Researcher and Contributor ID), према упутству на страници сајта *Регистрација за добијање ORCID идентификационе шифре*.

Војнотехнички гласник објављује чланке на енглеском језику (arial, величина слова 11 pt, проред Single).

Поступак припреме, писања и уређивања чланка треба да буде у сагласности са *Изјавом о етичком поступању* (http://www.vtg.mod.gov.rs/izjava-o-etickom-postupanju.html).

Чланак треба да садржи сажетак са кључним речима, увод (мотивацију за рад), разраду (адекватан преглед репрезентативности рада у његовој области, јасну изјаву о новини у представљеном истраживању, одговарајућу теоријску позадину, један или више примера за демонстрирање и дискусију о представљеним идејама), закључак и литературу (без нумерације наслова и поднаслова). Обим чланка треба да буде до једног ауторског табака (16 страница формата А4 са проредом Single), а највише 24 странице.

Чланак треба да буде написан на обрасцу за писање чланка, који се у електронској форми може преузети са сајта на страници *Образац за писање чланка*.

Наслов

Наслов треба да одражава тему чланка. У интересу је часописа и аутора да се користе речи прикладне за индексирање и претраживање. Ако таквих речи нема у наслову, пожељно је да се придода и поднаслов.

Текући наслов

Текући наслов се исписује са стране сваке странице чланка ради лакше идентификације, посебно копија чланака у електронском облику. Садржи презиме и иницијал имена аутора (ако аутора има више, преостали се означавају са „et al.“ или „и др.“), наслове рада и часописа и колацију (година, волумен, свеска, почетна и завршна страница). Наслови часописа и чланка могу се дати у скраћеном облику.

Име аутора

Наводи се пуно име и презиме (свих) аутора. Веома је пожељно да се наведу и средња слова аутора. Имена и презимена домаћих аутора увек се исписују у оригиналном облику (са српским дијакритичким знаковима), независно од језика на којем је написан рад.

Назив установе аутора (афилијација)

Наводи се пун (званични) назив и седиште установе у којој је аутор запослен, а евентуално и назив установе у којој је аутор обавио истраживање. У сложеним организацијама наводи се укупна хијерархија (нпр. Универзитет одбране у Београду, Војна академија, Катедра природно-математичких наука). Бар једна организација у хијерархији мора бити правно лице. Ако аутора има више, а неки потичу из исте установе, мора се, посебним ознакама или на други начин, назначити из које од наведених установа потиче сваки од наведених аутора. Афилијација се исписује непосредно након имена аутора. Функција и звање аутора се не наводе.

Контакт подаци

Адреса или е-адреса свих аутора даје се поред имена и презимена аутора.

Категорија (тип) чланка

Категоризација чланака обавеза је уредништва и од посебне је важности. Категорију чланка могу предлагати рецензенти и чланови уредништва, односно уредници рубрика, али одговорност за категоризацију сноси искључиво главни уредник.

Војнотехнички гласник објављује научне чланке.

Научни чланак је:

– оригиналан научни рад (рад у којем се износе претходно необјављени резултати сопствених истраживања научним методом);

– прегледни рад (рад који садржи оригиналан, детаљан и критички приказ истраживачког проблема или подручја у којем је аутор остварио одређени допринос, видљив на основу аутоцитата);

– кратко или претходно саопштење (оригинални научни рад пуног формата, али мањег обима или прелиминарног карактера);

– научна критика, односно полемика (расправа на одређену научну тему, заснована искључиво на научној аргументацији) и осврти.

Изузетно, у неким областима, научни рад у часопису може имати облик монографске студије, као и критичког издања научне грађе (историјско-архивске, лексикографске, библиографске, прегледа података и сл.), дотад непознате или недовољно приступачне за научна истраживања.

Радови класификовани као научни морају имати бар две позитивне рецензије.

Ако се у часопису објављују и прилози ваннаучног карактера, научни чланци треба да буду груписани и јасно издвојени у првом делу свеске.

Пожељно је да обим кратких саопштења буде 4 до 7 страница, научних чланака и студија случаја 10 до 14 страница, док прегледни радови могу бити и дужи. Број страница није строго ограничен и, уз одговарајуће образложење, пријављени чланци такође могу бити дужи или краћи.

Ако су радови који су претходно објављени на конференцији проширени, уредници ће проверити да ли је додато довољно новог материјала који испуњава стандарде часописа и квалификује поднесак за поступак рецензије. Додати материјал не сме бити претходно објављен. Нови резултати нису нужно потребни, али су пожељни. Међутим, поднесак треба да садржи проширене кључне идеје, примере, разраде, итд., који су претходно били садржани у поднеску са конференције.

Језик рада

Језик рада треба да буде енглески.

Текст мора бити језички и стилски дотеран, систематизован, без скраћеница (осим стандардних). Све физичке величине морају бити изражене у Међународном систему мерних јединица – SI. Редослед образаца (формула) означава се редним бројевима, са десне стране у округлим заградама.

Сажетак

Сажетак јесте кратак информативан приказ садржаја чланка који читаоцу омогућава да брзо и тачно оцени његову релевантност. У интересу је уредништава и аутора да сажетак садржи термине који се често користе за индексирање и претрагу чланака. Саставни делови сажетка су увод/циљ истраживања, методи, резултати и закључак. Сажетак треба да има од 100 до 250 речи и треба да се налази између заглавља (наслов, имена аутора и др.) и кључних речи, након којих следи текст чланка.

Кључне речи

Кључне речи су термини или фразе које адекватно представљају садржај чланка за потребе индексирања и претраживања. Треба их додељивати ослањајући се на неки међународни извор (попис, речник или тезаурус) који је најшире прихваћен или унутар дате научне области. За нпр. науку уопште, то је листа кључних речи Web of Science. Број кључних речи не може бити већи од 10, а у интересу је уредништва и аутора да учесталост њихове употребе буде што већа. У чланку се пишу непосредно након сажетка.

Систем АСИСТЕНТ у ту сврху користи специјалну алатку KWASS: аутоматско екстраховање кључних речи из дисциплинарних тезауруса/речника по избору и рутине за њихов одабир, тј. прихватање односно одбацивање од стране аутора и/или уредника.

Датум прихватања чланка

Датум када је уредништво примило чланак, датум када је уредништво коначно прихватило чланак за објављивање, као и датуми када су у међувремену достављене евентуалне исправке рукописа наводе се хронолошким редоследом, на сталном месту, по правилу на крају чланка.

Захвалница

Назив и број пројекта, односно назив програма у оквиру којег је чланак настао, као и назив институције која је финансирала пројекат или програм, наводи се у посебној напомени на сталном месту, по правилу при дну прве стране чланка.

Претходне верзије рада

Ако је чланак у претходној верзији био изложен на скупу у виду усменог саопштења (под истим или сличним насловом), податак о томе треба да буде наведен у посебној напомени, по правилу при дну прве стране чланка. Рад који је већ објављен у неком часопису не може се објавити у *Војнотехничком гласнику* (прештампати), ни под сличним насловом и измењеном облику.

Табеларни и графички прикази

Пожељно је да наслови свих приказа, а по могућству и текстуални садржај, буду дати двојезично, на језику рада и на енглеском језику.

Табеле се пишу на исти начин као и текст, а означавају се редним бројевима са горње стране. Фотографије и цртежи треба да буду јасни, прегледни и погодни за репродукцију. Цртеже треба радити у програму word или corel. Фотографије и цртеже треба поставити на жељено место у тексту.

За слике и графиконе не сме се користити снимак са екрана рачунара програма за прикупљање података. У самом тексту чланка препоручује се употреба слика и графикона непосредно из програма за анализу података (као што су Excel, Matlab, Origin, SigmaPlot и други).

Навођење (цитирање) у тексту

Начин позивања на изворе у оквиру чланка мора бити једнообразан.

Војнотехнички гласник за референцирање (цитирање и навођење литературе) примењује Харвардски систем референци, односно Харвардски приручник за стил (Harvard Referencing System, Harvard Style Manual). У самом тексту, у обичним заградама, на месту на којем се врши позивање, односно цитирање литературе набројане на крају чланка, обавезно у обичној загради написати презиме цитираног аутора, годину издања публикације из које цитирате и, евентуално, број страница. Нпр. (Petrović, 2012, pp.10–12).

Детаљно упутство о начину цитирања, са примерима, дато је на страници сајта *Упутство за Харвардски приручник за стил*. Потребно је да се позивање на литературу у тексту уради у складу са поменутим упутством.

Систем АСИСТЕНТ у сврху контроле навођења (цитирања) у тексту користи специјалну алатку CiteMatcher: откривање изостављених цитата у тексту рада и у попису референци.

Напомене (фусноте)

Напомене се дају при дну стране на којој се налази текст на који се односе. Могу садржати мање важне детаље, допунска објашњења, назнаке о коришћеним изворима (на пример, научној грађи, приручницима), али не могу бити замена за цитирану литературу.

Листа референци (литература)

Цитирана литература обухвата, по правилу, библиографске изворе (чланке, монографије и сл.) и даје се искључиво у засебном одељку чланка, у виду листе референци. Референце се не преводе на језик рада и набрајају се у посебном одељку на крају чланка.

Војнотехнички гласник, као начин исписа литературе, примењује Харвардски систем референци, односно Харвардски приручник за стил (Harvard Referencing System, Harvard Style Manual).

Литература се обавезно пише на латиничном писму и набраја по абецедном редоследу, наводећи најпре презимена аутора, без нумерације.

Детаљно упутство о начину пописа референци, са примерима, дато је на страници сајта *Упутство за Харвардски приручник за стил*. Потребно је да се попис литературе на крају чланка уради у складу са поменутим упутством.

Нестандардно, непотпуно или недоследно навођење литературе у системима вредновања часописа сматра се довољним разлогом за оспоравање научног статуса часописа.

Систем АСИСТЕНТ у сврху контроле правилног исписа листе референци користи специјалну алатку RefFormatter: контрола обликовања референци у складу са Харвардским приручником за стил.

Изјава о ауторству

Поред чланка доставља се *Изјава о ауторству* у којој аутори наводе свој појединачни допринос у изради чланка. Такође, у тој изјави потврђују да су чланак урадили у складу са *Позивом и упутством ауторима* и *Изјавом о етичком поступању часописа*.

Сви радови подлежу стручној рецензији.

Списак рецензената *Војнотехничког гласника* може се видети на страници сајта *Списак рецензената*. Процес рецензирања објашњен је на страници сајта *Рецензентски поступак*.

Уредништво

Адреса редакције:
Војнотехнички гласник
Вељка Лукића Курјака 33
11042 Београд
e-mail: vojnotehnicki.glasnik@mod.gov.rs.
тел: војни 40-260 (011/3603-260), 066/8700-123

ПРИГЛАШЕНИЕ И ИНСТРУКЦИЯ ДЛЯ АВТОРОВ О ПОРЯДКЕ ПОДГОТОВКИ СТАТЬИ

Инструкция для авторов о порядке подготовки статьи к опубликованию в журнале *«Военно-технический вестник»* разработана согласно Регламенту о категоризации и ранжировании научных журналов Министерства образования, науки и технологического развития Республики Сербия («Службени гласник РС», № 159/20). Применение этого Регламента способствует повышению качества отечественных журналов и их более полному вовлечению в международную систему обмена научной информацией.

Военно-технический вестник (**Vojnotehnički glasnik / Military Technical Courier**), втг.мо.упр.срб, www.vtg.mod.gov.rs/index-ru.html, ISSN 0042-8469 – печатное издание, e-ISSN 2217-4753 – online, UDK 623+355/359, DOI: 10.5937/VojnotehnickiGlasnik; https://doi.org/10.5937/VojnotehnickiGlasnik, является рецензируемым научным журналом.

Собственники журнала: Министерство обороны и Вооруженые силы Республики Србия.

Издатель журнала: Университет обороны в г. Белград (Военная академия).

Программная ориентация журнала основана на ежегодной категоризации журнала, которая производится соответствующим отраслевым министерством, в зависимости от области исследований, а также на его индексировании в международных наукометрических базах данных.

Журнал охватывает научные и профессиональные сферы в рамках учебно-научной области **естественно-математических наук**, а также в рамках учебно-научной области **технико-технологических наук**, особенно в области **оборонных наук и технологии**. В журнале публикуются теоретические и практические достижения, которые способствуют повышению квалификации представителей сербского, регионального и международного академического сообщества, особенно служащих Министерств Обороны и Вооружённых сил. В журнале публикуются статьи со соответствующими обзорами об аналитических, экспериментальных и прикладных исследованиях, а также о численном моделировании, охватывая различные дисциплины. Публикуемые материалы отличаются высоким качеством и актуальностью. Они написаны научным, но понятным и доступным для широкого круга читателей языком. Приветствуются все статьи, сообщающие об оригинальных теоретических и/или практических исследованиях и/или расширенные версии ранее опубликованных статей, представленных на конференциях. Статьи для публикации отбираются путем двойного слепого рецензирования, которое гарантирует оригинальность, актуальность и удобочитаемость. Цель состоит не только в поддержании высокого качества публикуемых статей, но и в обеспечении своевременного, тщательного и соответствующего процесса рецензирования.

Редакционная политика журнала *«Военно-технический вестник»* основана на рекомендациях Комитета по этике научных публикаций (COPE Core Practices), общих принципах прозрачности и лучшей практике издательской деятельности COPE, DOAJ, OASPA и WAME, а также на лучшей практике научно-издательской деятельности. Журнал *«Военно-технический вестник»* является членом COPE (Комитет по этике научных публикаций) со 2 мая 2018 года и членом OASPA (Ассоциация научных издателей открытого доступа) с 27 ноября 2015 года.

Министерством науки, технологического развития и инноваций Республики Сербия утверждена 13 декабря 2024 г. категоризация журнала *«Военно-технический вестник»* за 2024 год:

– **Область компьютерные науки:**
ведущий журнал государственного значения **(M51)**,
– **Область электроники, телекоммуникаций и информационных технологий:**
ведущий журнал государственного значения **(M51)**,
– **Область машиностроения:**
ведущий журнал государственного значения **(M51)**,
– **Область материалов и химической технологии:**
национальный журнал международного значения **(M24)**.

С информацией относительно категоризации за 2024 год можно ознакомиться на странице сайта *«Военно-технического вестника» Категоризация Вестника*.

Более подробную информацию можно найти на сайте Министерства образования, науки и технологического развития Республики Сербия.

С информацией о категоризации можно ознакомиться и на сайте КОБСОН (Консорциум библиотек Республики Сербия по вопросам объединения закупок).

Категоризация Вестника проведена согласно Регламенту о категоризации и ранжировании научных журналов Министерства образования, науки и технологического развития Республики Сербия («Службени гласник РС», № 159/20)

Журнал соответствует стандартам Сербского индекса научного цитирования (СЦИндекс/SCIndeks) - наукометрической базы данных научных журналов Республики Сербия, Научно-информационного система Redalyc, а также Российского индекса научного цитирования (РИНЦ). Журнал постоянно подвергается мониторингу и оценивается количественными наукометрическими показателями отражающими его научную ценность.

С информацией об индексировании можно ознакомиться на странице сайта журнала *Индексирование Вестника*.

«Военно-технический вестник» относительно своего содержания предоставляет пользователям возможность открытого доступа (DIAMOND OPEN ACCESS) и положениями об авторских правах, утвержденными Creative Commons (CC BY). С инструкцией об авторских правах можно ознакомиться на странице сайта журнала *Авторские права и политика самоархивирования*.

Рукописи статей направляются в редакцию журнала с использованием online системы ASSISTANT, запущенной Центром поддержи развития образования и науки (ЦПРОН). Регистрация в системе и оформление прав доступа выполняется по адресу http://www.vtg.mod.gov.rs/index-ru.html, через страницу *ASSISTANT* или *СЦИНДЕКС* (aseestant.ceon.rs/index.php/vtg). С инструкцией по регистрации и правам доступа можно ознакомиться по адресу http://www.vtg.mod.gov.rs/index-ru.html, на странице *Инструкция по ASSISTANT*.

Все авторы, предоставляющие свои рукописи для публикации в редакцию журнала *«Военно-технический вестник»* должны пройти предварительную регистрацию в реестре ORCID (Open Researcher and Contributor ID). Эта процедура осуществляется в соответствии с инструкцией, размещенной на странице сайта *Регистрация в реестре ORCID для присвоения идентификационного кода*.

«Военно-технический вестник» публикует статьи на английском языке (Arial, шрифт 11 pt, пробел Single). Процесс подготовки, написания и редактирования статьи должен осуществляться в соответствии с принципами *Этического кодекса*

(http://www.vtg.mod.gov.rs/etichyeskiy-kodyeks.html). Статья должна содержать резюме с ключевыми словами, введение (цель исследования), основную часть (соответствующий обзор представительного исследования в данной области, четкое изложение научной новизны в представленном исследовании, соответствующую теоретическую основу, один или несколько примеров для демонстрирования и обсуждения представленных тезисов), заключение и список литературы (без нумерации заголовков и подзаголовков). Объем статьи не должен превышать один авторский лист (16 страниц формата А4 с одинарным интервалом, максимум до 24 страниц, включая ссылки и приложения). Статья должна быть набрана на компьютере с использованием специально подготовленного редакцией макета, который можно скачать на странице сайта *Правила и образец составления статьи*.

Заголовок

Заголовок должен отражать тему статьи. В интересах журнала и автора необходимо использовать слова и словосочетания, удобные для индексации и поиска. Если такие слова не содержатся в заголовке, то желательно их добавить в подзаголовок.

Текущий заголовок

Текущий заголовок пишется в титуле каждой страницы статьи с целью упрощения процесса идентификации, в первую очередь копий статьей в электронном виде. Заголовок содержит в себе фамилию и инициал имени автора (в случае если авторов несколько, остальные обозначаются с «et al.» или «и др.»), название работы и журнала (год, том, выпуск, начальная и заключительная страница). Заголовок статьи и название журнала могут быть приведены в сокращенном виде.

ФИО автора

Приводятся полная фамилия и полное имя (всех) авторов. Желательно, чтобы были указаны инициалы отчеств авторов. Фамилия и имя авторов из Республики Сербия всегда пишутся в оригинальном виде (с сербскими диакритическими знаками), независимо от языка, на котором написана работа.

Наименование учреждения автора (аффилиация)

Приводится полное (официальное) наименование и местонахождение учреждения, в котором работает автор, а также наименование учреждения, в котором автор провёл исследование. В случае организаций со сложной структурой приводится их иерархическая соподчинённость (напр. Военная академия, кафедра военных электронных систем, г. Белград). По крайней мере, одна из организаций в иерархии должна иметь статус юридического лица. В случае если указано несколько авторов, и если некоторые из них работают в одном учреждении, нужно отдельными обозначениями или каким-либо другим способом указать в каком из приведённых учреждений работает каждый из авторов. Аффилиация пишется непосредственно после ФИО автора. Должность и специальность по диплому не указываются.

Контактные данные

Электронный адрес автора указываются рядом с его именем на первой страницы статьи.

Категория (тип) статьи

Категоризация статьей является обязанностью редакции и имеет особое значение. Категорию статьи могут предлагать рецензенты и члены редакции, т.е. редакторы рубрик, но ответственность за категоризацию несет исключительно главный редактор.

Журнал *«Военно-технический вестник»* публикует научные статьи.

Научные статьи:

– оригинальная научная статья (работа, в которой приводятся ранее неопубликованные результаты собственных исследований, полученных научным методом);

– обзорная статья (работа, содержащая оригинальный, детальный и критический обзор исследуемой проблемы или области, в который автор внёс определённый вклад, видимый на основе автоцитат);

– краткое сообщение (оригинальная научная работа полного формата, но меньшего объёма или имеющая предварительный характер);

– научная критическая статья (дискуссия-полемика на определённую научную тему, основанная исключительно на научной аргументации) и научный комментарий.

Однако, в некоторых областях знаний научная работа в журнале может иметь форму монографического исследования, а также критического обсуждения научного материала (историко-архивного, лексикографического, библиографического, обзора данных и т.п.) – до сих пор неизвестного или недостаточно доступного для научных исследований. Работы, классифицированные в качестве научных, должны иметь, по меньшей мере, две положительные рецензии. В случае если в журнале объявляются и приложения, не имеющие научный характер, научные статьи должны быть сгруппированы и четко выделены в первой части номера.

Объем кратких сообщений составляет 4-7 страниц, исследовательские статьи и тематические исследования с проблемно-ситуационным анализом − 10-14 страниц, однако объем обзорных статей может быть больше. Ограничения по количеству страниц не являются строгими, следовательно при соответствующем обосновании предоставленные работы могут быть длиннее или короче. В случае подачи расширенных версий ранее опубликованных докладов, представленных на конференции, редакция проверит было ли добавлено достаточно новых материалов для того, чтобы статья соответствовала стандартам журнала и условиям рецензирования. Добавленный материал должен быть новым, неопубликованным ранее. Новые результаты приветствуются, но не являются обязательным условием; однако ключевые тезисы, примеры, разработки и пр. должны быть более подробно представлены в статье по сравнению с первичным докладом на конфереции.

Язык работы

Статья должна быть написана на английском языке. Текст должен быть в лингвистическом и стилистическом смысле упорядочен, систематизирован, без сокращений (за исключением стандартных). Все физические величины должны соответствовать Международной системе единиц измерения – СИ. Очередность формул обозначается порядковыми номерами, проставляемыми с правой стороны в круглых скобках.

Резюме

Резюме является кратким информативным обзором содержания статьи, обеспечивающим читателю быстроту и точность оценки её релевантности. В интересах редакции и авторов, чтобы резюме содержало термины, часто используемые для индексирования и поиска статьей. Составными частями резюме являются введение/цель исследования, методы, результаты и выводы. В резюме должно быть от 100 до 250 слов, и оно должно находится между титулами (заголовок, ФИО авторов и др.) и ключевыми словами, за которыми следует текст статьи.

Ключевые слова

Ключевыми словами являются термины или фразы, адекватно представляющие содержание статьи, необходимые для индексирования и поиска. Ключевые слова необходимо выбирать, опираясь при этом на какой-либо международный источник (регистр, словарь, тезаурус), наиболее используемый внутри данной научной области. Число ключевых слов не может превышать 10. В интересах редакции и авторов, чтобы частота их встречи в статье была как можно большей. В статье они пишутся непосредственно после резюме.

Программа ASSISTANT предоставляет возможность использования сервиса KWASS, автоматически фиксирующего ключевые слова из источников/словарей по выбору автора/редактора.

Дата получения статьи

Дата, когда редакция получила статью; дата, когда редакция окончательно приняла статью к публикации; а также дата, когда были предоставлены необходимые исправления рукописи, приводятся в хронологическом порядке, как правило, в конце статьи.

Выражение благодарности

Наименование и номер проекта, т.е. название программы благодаря которой статья возникла, совместно с наименованием учреждения, которое финансировало проект или программу, приводятся в отдельном примечании, как правило, внизу первой страницы статьи.

Предыдущие версии работы

В случае если статья в предыдущей версии была изложена устно (под одинаковым или похожим названием, например, в виде доклада на научной конференции), сведения об этом должны быть указаны в отдельном примечании, как правило, внизу первой страницы статьи. Работа, которая уже была опубликована в каком-либо из журналов, не может быть напечатана в *«Военно-техническом вестнике»* ни под похожим названием, ни в изменённом виде.

Нумерация и название таблиц и графиков

Желательно, чтобы нумерация и название таблиц и графиков были исполнены на двух языках (на языке оригинала и на английском). Таблицы подписываются таким же способом как и текст и обозначаются порядковым номером с верхней стороны. Фотографии и рисунки должны быть понятны, наглядны и удобны для репродукции. Рисунки необходимо делать в программах Word или Corel. Фотографии и рисунки надо поставить на желаемое место в тексте. Для создания изображений и графиков использование функции снимка с экрана (скриншота) не допускается. В самом тексте статьи рекомендуется применение изображений и графиков, обработанных такими компьютерными программами, как: Excel, Matlab, Origin, SigmaPlot и др.

Ссылки (цитирование) в тексте

Оформление ссылок на источники в рамках статьи должно быть однообразным. *«Военно-технический вестник»* для оформления ссылок, цитат и списка использованной литературы применяет Гарвардскую систему (Harvard Referencing System, Harvard Style Manual). В тексте в скобках приводится фамилия цитируемого автора (или фамилия первого автора, если авторов несколько), год издания и по необходимости номер страницы. Например: (Petrović, 2010, pp.10-20). Рекомендации о способе цитирования размещены на странице сайта *Инструкция по использованию Гарвардского стиля*. При оформлении ссылок, цитат и списка использованной литературы необходимо придерживаться установленных норм. Программа

ASSISTANT предоставляет при цитировании возможность использования сервиса CiteMatcher, фиксирующего пропущенные цитаты в работе и в списке литературы.

Примечания (сноски)

Примечания (сноски) к тексту указываются внизу страницы, к которой они относятся. Примечания могут содержать менее важные детали, дополнительные объяснения, указания об использованных источниках (напр. научном материале, справочниках), но не могут быть заменой процедуры цитирования литературы.

Литература (референции)

Цитированной литературой охватываются, как правило, такие библиографические источники как статьи, монографии и т.п. Вся используемая литература в виде референций размещается в отдельном разделе статьи. Названия литературных источников не переводятся на язык работы. *«Военно-технический вестник»* для оформления списка использованной литературы применяет Гарвардскую систему (Harvard Style Manual). В списке литературы источники указываются в алфавитном порядке фамилий авторов или редакторов. Рекомендации о способе цитирования размещены на странице сайта *Инструкция по использованию Гарвардского стиля*. При оформлении списка использованной литературы необходимо придерживаться установленных норм. При оформлении списка литературы программа ASSISTANT предоставляет возможность использования сервиса RefFormatter, осуществляющего контроль оформления списка литературы в соответствии со стандартами Гарвардского стиля. Нестандартное, неполное и непоследовательное приведение литературы в системах оценки журнала считается достаточной причиной для оспаривания научного статуса журнала.

Авторское заявление

Авторское заявление предоставляется вместе со статьей, в нем авторы заявляют о своем личном вкладе в написание статьи. В заявлении авторы подтверждают, что статья написана в соответствии с *Приглашением и инструкциями для авторов*, а также с *Кодексом профессиональной этики журнала*.

Все рукописи статей подлежат профессиональному рецензированию.

Список рецензентов журнала *«Военно-технический вестник»* размещён на странице сайта *Список рецензентов*. Процесс рецензирования описан в разделе *Правила рецензирования*.

Редакция

Почтовый адрес редакции:

«Војнотехнички гласник»
ул. Велька Лукича Куряка 33, 11042 Белград, Республика Сербия
e-mail: vojnotehnicki.glasnik@mod.gov.rs,
тел: +381 11 3603 260, +381 66 8700 123

CALL FOR PAPERS AND ARTICLE FORMATTING INSTRUCTIONS

The instructions to authors about the article preparation for publication in the *Military Technical Courier* are based on the Regulations on categorization and ranking of scientific journals of the Ministry of Education, Science and Technological Development of the Republic of Serbia (Official Gazette of the Republic of Serbia, No 159/20). This Regulations aims at improving the quality of national journals and raising the level of their compliance with the international system of scientific information exchange.

The Military Technical Courier / Vojnotehnički glasnik (www.vtg.mod.gov.rs/index-e.html, втг.мо.упр.срб, ISSN 0042-8469 – print issue, e-ISSN 2217-4753 – online, UDC 623+355/359, DOI: 10.5937/VojnotehnickiGlasnik; https://doi.org/10.5937/VojnotehnickiGlasnik), is an peer-reviewed scientific journal.

The owners of the journal are the Ministry of Defence of the Republic of Serbia and the Serbian Armed Forces. The publisher and financier of the *Military Technical Courier* is the University of Defence in Belgrade (Military Academy).

The program of the journal is based on the annual classification of journals performed by a relevant Ministry as well as on its indexing in international indexing databases.

The journal covers scientific and professional fields within the educational-scientific field of **Natural-Mathematical Sciences**, as well as within the educational-scientific field of **Technical-Technological Sciences**, and especially the field of **defense sciences and technologies**. It publishes theoretical and practical achievements leading to professional development of all members of Serbian, regional and international academic communities as well as members of the military and ministries of defence in particular. It publishes papers with balanced coverage of analytical, experimental, and applied research as well as numerical simulations from various disciplines. The material published is of high quality and relevance, written in a manner that makes it accessible to a wider readership. The journal welcomes papers reporting original theoretical and/or practice-oriented research as well as extended versions of already published conference papers. Manuscripts for publication are selected through a double-blind peer-review process to validate their originality, relevance, and readability. This being so, the objective is not only to keep the quality of published papers high but also to provide a timely, thorough, and balanced review process.

The editorial policy of the *Military Technical Courier* is based on the COPE Core Practices, common COPE, DOAJ, OASPA and WAME Principles of Transparency and Best Practice in Scholarly Publishing as well as on the best accepted practices in scientific publishing. The Military Technical Courier has been a COPE (Committee on Publication Ethics) member since 2nd May 2018 and a member of OASPA (Open Access Scholarly Publishers Association) since 27th November 2015.

The Ministry of Science, Technological Development and Innovation of the Republic of Serbia classified the *Military Technical Courier* for the year 2024, on December 13, 2024

– **on the list of periodicals for computer sciences,**
  category: reputed national journal **(M51)**,
– **on the list of periodicals for electronics, telecommunications and IT,**
  category: reputed national journal **(M51)**,
– **on the list of periodicals for mechanical engineering,**
  category: reputed national journal **(M51)**,
– **on the list of periodicals for materials and chemical technology,**
  category: national journal of international importance **(M24)**.

The approved lists of national periodicals for the year 2024 can be viewed on the website of the *Military Technical Courier*, page *Journal categorization*.

More detailed information can be found on the website of the Ministry of Education, Science and Technological Development of the Republic of Serbia.

The information on the categorization can be also found on the website of KOBSON (Consortium of Libraries of Serbia for Unified Acquisition).

The periodical is categorized in compliance with the Regulations on categorization and ranking of scientific journals of the Ministry of Education, Science and Technological Development of the Republic of Serbia (Official Gazette of the Republic of Serbia, No 159/20). More detailed information can be found on the website of the Ministry of Education, Science and Technological Development.

The journal is in the Serbian Citation Index – SCIndex (data base of national scientific journals), in the Scientific Information System Redalyc, and in the Russian Index of Science Citation/Российский индекс научного цитирования (RINC/РИНЦ) and is constantly monitored depending on the impact within the bases themselves. More detailed information can be viewed on the website of the *Military Technical Courier*, page *Journal indexing*.

The *Military Technical Courier*, in terms of its content, offers the possibility of open access (DIAMOND OPEN ACCESS) and applies the Creative Commons Attribution (CC BY) licence on copyright. The copyright details can be found on the *Copyright notice and Self-archiving policy* page of the journal's website.

Manuscripts are submitted online, through the electronic editing system ASSISTANT, developed by the Center for Evaluation in Education and Science – CEON.

The access and the registration are through the *Military Technical Courier* site http://www.vtg.mod.gov.rs/index-e.html, on the page *ASSISTANT* or the page *SCINDEKS* or directly through the link (aseestant.ceon.rs/index.php/vtg).

The detailed instructions about the registration for the service are on the website http://www.vtg.mod.gov.rs/index-e.html, on the page *Instructions for ASSISTANT*.

All authors submitting a manuscript for publishing in the *Military Technical Courier* should register for an ORCID ID following the instructions on the web page *Registration for an ORCID identifier*.

The *Military Technical Courier* publishes articles in English, using Arial and a font size of 11pt with Single Spacing.

The procedures of article preparation, writing and editing should be in accordance with the *Publication ethics statement* (http://www.vtg.mod.gov.rs/publication-ethics-statement.html).

The article should contain an abstract with keywords, introduction (motivation for the work), body (adequate overview of the representative work in the field, a clear statement of the novelty in the presented research, suitable theoretical background, one or more examples to demonstrate and discuss the presented ideas), conclusion, and references (without heading and subheading enumeration). The article length should not normally exceed 16 pages of the A4 paper format with single spacing, up to a maximum of 24 pages with references and supplementary material included.

The article should be formatted following the instructions in the Article Form which can be downloaded from website page *Article form*.

Title

The title should be informative. It is in both Journal’s and author’s best interest to use terms suitable for indexing and word search. If there are no such terms in the title, the author is strongly advised to add a subtitle.

Letterhead title

The letterhead title is given at a top of each page for easier identification of article copies in an electronic form in particular. It contains the author’s surname and first name initial (for multiple authors add “et al”), article title, journal title and collation (year, volume, issue, first and last page). The journal and article titles can be given in a shortened form.

Author’s name

Full name(s) of author(s) should be used. It is advisable to give the middle initial. Names are given in their original form (with diacritic signs if in Serbian).

Author’s affiliation

The full official name and seat of the author’s affiliation is given, possibly with the name of the institution where the research was carried out. For organizations with complex structures, give the whole hierarchy (for example, University of Defence in Belgrade, Military Academy, Department for Military Electronic Systems). At least one organization in the hierarchy must be a legal entity. When some of multiple authors have the same affiliation, it must be clearly stated, by special signs or in other way, which department exactly they are affiliated with. The affiliation follows the author’s name. The function and title are not given.

Contact details

The postal addresses or the e-mail addresses of the authors are given in the first page.

Type of articles

Classification of articles is a duty of the editorial staff and is of special importance. Referees and the members of the editorial staff, or section editors, can propose a category, but the editor-in-chief has the sole responsibility for their classification.

The *Military Technical Courier* publishes scientific articles.

Scientific articles:

– Original scientific papers (giving the previously unpublished results of the author’s own research based on scientific methods);

– Review papers (giving an original, detailed and critical view of a research problem or an area to which the author has made a contribution demonstrated by self-citation);

– Short communications or Preliminary communications (original scientific full papers but shorter or of a preliminary character);

– Scientific commentaries or discussions (discussions on a particular scientific topic, based exclusively on scientific argumentation) and opinion pieces.

Exceptionally, in particular areas, a scientific paper in the Journal can be in a form of a monograph or a critical edition of scientific data (historical, archival, lexicographic, bibliographic, data survey, etc.) which were unknown or hardly accessible for scientific research.

Papers classified as scientific must have at least two positive reviews.

If the journal contains non-scientific contributions as well, the section with scientific papers should be clearly denoted in the first part of the Journal.

Short communications are usually 4-7 pages long, research articles and case studies 10-14 pages, while reviews can be longer. Page number limits are not strict and, with appropriate reasoning, submitted manuscripts can also be longer or shorter. If extended versions of previously published conference papers are submitted, Editors will check if sufficient new material has been added to meet the journal standards and to qualify such manuscripts for the review process. The added material must not have been previously published. New results are desired but not necessarily required; however, submissions should contain expansions of key ideas, examples, elaborations, etc. of conference papers.

Language

The language of the article should be in English. The grammar and style of the article should be of good quality. The systematized text should be without abbreviations (except standard ones). All measurements must be in SI units. The sequence of formulae is denoted in Arabic numerals in parentheses on the right-hand side.

Abstract and summary

An abstract is a concise informative presentation of the article content for fast and accurate evaluation of its relevance. It contains the terms often used for indexing and article search. A 100- to 250-word abstract has the following parts: introduction/purpose of the research, methods, results and conclusion.

Keywords

Keywords are terms or phrases showing adequately the article content for indexing and search purposes. They should be allocated heaving in mind widely accepted international sources (index, dictionary or thesaurus), such as the Web of Science keyword list for science in general. The higher their usage frequency is, the better. Up to 10 keywords immediately follow the abstract and the summary, in respective languages. For this purpose, the ASSISTANT system uses a special tool KWASS for the automatic extraction of key words from disciplinary thesauruses/dictionaries by choice and the routine for their selection, i.e. acceptance or rejection by author and/or editor.

Article acceptance date

The date of the reception of the article, the dates of submitted corrections in the manuscript (optional) and the date when the Editorial Board accepted the article for publication are all given in a chronological order at the end of the article.

Acknowledgements

The name and the number of the project or programme within which the article was realised is given in a separate note at the bottom of the first page together with the name of the institution which financially supported the project or programme.

Article preliminary version

If an article preliminary version has appeared previously at a meeting in a form of an oral presentation (under the same or similar title), this should be stated in a separate note at the bottom of the first page. An article published previously cannot be published in the *Military Technical Courier* even under a similar title or in a changed form.

Tables and illustrations

All the captions should be in the original language as well as in English, together with the texts in illustrations if possible. Tables are typed in the same style as the text and are denoted by Arabic numerals at the top. Photographs and drawings, placed appropriately in the text, should be clear, precise and suitable for reproduction. Drawings should be created in Word or Corel.

For figures and graphs, proper data plot is recommended i.e. using a data analysis program such as Excel, Matlab, Origin, SigmaPlot, etc. It is not recommended to use a screen capture of a data acquisition program as a figure or a graph.

Citation in the text

Citation in the text must be uniform. The *Military Technical Courier* applies the Harvard Referencing System given in the Harvard Style Manual. When citing sources within your paper, i.e. for in-text references of the works listed at the end of the paper, place the year of publication of the work in parentheses and optionally the number of the page(s) after the author's name, e.g. (Petrovic, 2012, pp.10-12). A detailed guide on citing, with examples, can be found on *Military Technical Courier* website on the page *Instructions for Harvard Style Manual*. In-text citations should follow its guidelines. For checking in-text citations, the ASSISTANT system uses a special tool CiteMatcher to find out quotes left out within papers and in reference lists.

Footnotes

Footnotes are given at the bottom of the page with the text they refer to. They can contain less relevant details, additional explanations or used sources (e.g. scientific material, manuals). They cannot replace the cited literature.

Reference list (Literature)

The cited literature encompasses bibliographic sources such as articles and monographs and is given in a separate section in a form of a reference list. References are not translated to the language of the article.

In compiling the reference list and bibliography, the *Military Technical Courier* applies the Harvard System – Harvard Style Manual. All bibliography items should be listed alphabetically by author's name, without numeration. A detailed guide for listing references, with examples, can be found on *Military Technical Courier* website on the page *Instructions for Harvard Style Manual*. Reference lists at the end of papers should follow its guidelines. In journal evaluation systems, non-standard, insufficient or inconsequent citation is considered to be a sufficient cause for denying the scientific status to a journal.

Authorship Statement

The Authorship statement, submitted together with the paper, states authors' individual contributions to the creation of the paper. In this statement, the authors also confirm that they followed the guidelines given in *the Call for papers* and the *Publication ethics and malpractice statement of the journal*.

All articles are peer reviewed.

The list of referees of the *Military Technical Courier* can be viewed at website page *List of referees*. The article review process is described on the *Peer Review Process* page of the website.

Editorial Team

Address of the Editorial Office:
Vojnotehnički glasnik / Military Technical Courier
Veljka Lukića Kurjaka 33
11042 Belgrade, Republic of Serbia
e-mail: vojnotehnicki.glasnik@mod.gov.rs, tel.: +381 11 3603 260, +381 66 8700 123

Ликовно-графички уредник
Марија Марић, e-mail: marija.maric@mod.gov.rs

Лектор
Добрила Милетић, e-mail: miletic.dobrila@gmail.com

Превод на енглески
Јасна Вишњић, e-mail: jasnavisnjic@yahoo.com

Превод на шпански
Јована Јовановић, e-mail: jovana.jov92@gmail.com

Превод на руски
Др *Карина* Авагјан, e-mail: karinka2576@mail.ru

CIP – Каталогизација у публикацији
Народна библиотека Србије, Београд

623+355/359

ВОЈНОТЕХНИЧКИ гласник : научни часопис Министарства одбране
и Војске Србије = Военно-технический вестник : научный журнал
Министерства обороны и Вооружённых сил Республики Сербия =
Military Technical Courier : scientific Journal of the Ministry of Defence and the Serbian
Armed Forces / главни и одговорни уредник Драган Памучар. -
Год. 1, бр. 1 (1. јан. 1953)- . - Београд : Универзитет одбране у Београду,
Војна академија, 1953- (Београд : Војна штампарија). - 23 cm

Тромесечно. - Текст на срп., рус. и енгл. језику. - Друго издање
на другом медијуму: Vojnotehnički glasnik (Online) = ISSN 2217-4753
ISSN 0042-8469 = Војнотехнички гласник
COBISS.SR-ID 4423938

Цена: 600,00 динара

Тираж: 100 примерака

На основу мишљења Министарства за науку, технологију и развој Републике
Србије, број 413-00-1201/2001-01 од 12. 9. 2001. године,
часопис „Војнотехнички гласник“ је публикација од посебног интереса за науку.

УДК: Народна библиотека Србије, Београд

Адреса редакције: Војнотехнички гласник,
Вељка Лукића Курјака 33, 11042 Београд

https://www.scopus.com/sourceid/21101207440
http://www.vtg.mod.gov.rs
http://aseestant.ceon.rs/index.php/vtg/issue/current
http://scindeks.nb.rs/journaldetails.aspx?issn=0042-8469
https://www.redalyc.org/revista.oa?id=6617
http://elibrary.ru/title_about.asp?id=53280
https://doaj.org/toc/2217-4753

Војнотехнички гласник је лиценциран код EBSCO Publishing-а.
Комплетан текст *Војнотехничког гласника* доступан је у базама података EBSCO Publishing-а.

e-mail: vojnotehnicki.glasnik@mod.gov.rs; X: @MilTechCourier

Претплата на штампано издање: e-mail: vojnotehnicki.glasnik@mod.gov.rs; тел. 066/87-00-123.

Часопис излази тромесечно.

Први штампани број *Војнотехничког гласника* објављен је 1. 1. 1953. године.

Прво електронско издање *Војнотехничког гласника* на Интернету објављено је 1. 1. 2011. г.

Штампа: Војна штампарија – Београд, Ресавска 40б, e-mail: vojna.stamparija@mod.gov.rs

Художественный редактор
Мария Марич, e-mail: marija.maric@mod.gov.rs

Корректор
Добрила Милетич, e-mail: miletic.dobrila@gmail.com

Перевод на английский язык
Ясна Вишнич, e-mail: jasnavisnjic@yahoo.com

Перевод на испанский язык
Йована Йованович, e-mail: jovana.jov92@gmail.com

Перевод на русский язык
Д.филол.н. *Карина* Кареновна Авагян, e-mail: karinka2576@mail.ru

CIP – Каталогизация в публикации
Национальная библиотека Сербии, г. Белград

623+355/359

ВОЈНОТЕХНИЧКИ гласник : научни часопис Министарства одбране
и Војске Србије = Военно-технический вестник : научный журнал
Министерства обороны и Вооружённых сил Республики Сербия =
Military Technical Courier : scientific Journal of the Ministry of Defence and the Serbian
Armed Forces / главни и одговорни уредник Драган Памучар. -
Год. 1, бр. 1 (1. јан. 1953)- . - Београд : Универзитет одбране у Београду,
Војна академија, 1953- (Београд : Војна штампарија). - 23 cm

Тромесечно. - Текст на срп., рус. и енгл. језику. - Друго издање
на другом медијуму: Vojnotehnički glasnik (Online) = ISSN 2217-4753
ISSN 0042-8469 = Војнотехнички гласник
COBISS.SR-ID 4423938

Цена: 600,00 динаров

Тираж: 100 экземпляров

На основании решения Министерства науки и технологий Республики Сербия,
№ 413-00-1201/2001-01 от 12. 9. 2001 года, журнал «Военно-технический вестник»
объявлен изданием, имеющим особое значение для науки.

УДК: Национальная библиотека Сербии, г. Белград

Адрес редакции: Војнотехнички гласник,
Ул. Велька Лукича Куряка 33, 11042 Белград, Республика Сербия

https://www.scopus.com/sourceid/21101207440
http://www.vtg.mod.gov.rs
http://aseestant.ceon.rs/index.php/vtg/issue/current
http://scindeks.nb.rs/journaldetails.aspx?issn=0042-8469
https://www.redalyc.org/revista.oa?id=6617
http://elibrary.ru/title_about.asp?id=53280
https://doaj.org/toc/2217-4753

«Военно-технический вестник» включен в систему EBSCO. Полный текст журнала
«Военно-технический вестник» можно найти в базах данных EBSCO Publishing.

e-mail: vojnotehnicki.glasnik@mod.gov.rs, X: @MilTechCourier
Подписка на печатную версию журнала: e-mail: vojnotehnicki.glasnik@mod.gov.rs;
тел. +381 66 87 00 123.

Журнал выпускается ежеквартально.

Первый номер журнала «Военно-технический вестник» выпущен 1.1.1953 года.

Первая электронная версия журнала размещена на интернет странице 1.1.2011 года.

Типография: Војна штампарија – Белград, Ресавска 40б, e-mail: vojna.stamparija@mod.gov.rs

Graphic design editor
Marija Marić, e-mail: marija.maric@mod.gov.rs

Proofreader
Dobrila Miletić, e-mail: miletic.dobrila@gmail.com

English translation and polishing
Jasna Višnjić, e-mail: jasnavisnjic@yahoo.com

Spanish translation and polishing
Jovana Jovanović, e-mail: jovana.jov92@gmail.com

Russian translation and polishing
Dr. *Karina* Avagyan, e-mail: karinka2576@mail.ru

CIP – Catalogisation in the publication
National Library of Serbia, Belgrade

623+355/359

ВОЈНОТЕХНИЧКИ гласник : научни часопис Министарства одбране
и Војске Србије = Военно-технический вестник : научный журнал
Министерства обороны и Вооружённых сил Республики Сербия =
Military Technical Courier : scientific Journal of the Ministry of Defence and the Serbian
Armed Forces / главни и одговорни уредник Драган Памучар. -
Год. 1, бр. 1 (1. јан. 1953)- . - Београд : Универзитет одбране у Београду,
Војна академија, 1953- (Београд : Војна штампарија). - 23 cm

Тромесечно. - Текст на срп., рус. и енгл. језику. - Друго издање
на другом медијуму: Vojnotehnički glasnik (Online) = ISSN 2217-4753
ISSN 0042-8469 = Војнотехнички гласник
COBISS.SR-ID 4423938

Price: 600.00 RSD

Printed in 100 copies

According to the Opinion of the Ministry of Science and Technological Development No 413-00-1201/2001-01 of 12th September 2001, the *Military Technical Courier* is a publication of special interest for science.

UDC: National Library of Serbia, Belgrade

Address: Vojnotehnički glasnik/Military Technical Courier,
Veljka Lukića Kurjaka 33, 11042 Belgrade, Republic of Serbia

https://www.scopus.com/sourceid/21101207440
http://www.vtg.mod.gov.rs/index-e.html
http://aseestant.ceon.rs/index.php/vtg/issue/current
http://scindeks.nb.rs/journaldetails.aspx?issn=0042-8469
https://www.redalyc.org/revista.oa?id=6617
http://elibrary.ru/title_about.asp?id=53280
https://doaj.org/toc/2217-4753

Military Technical Courier has entered into an electronic licensing relationship with EBSCO Publishing. The full text of *Military Technical Courier* can be found on EBSCO Publishing's databases.

e-mail: vojnotehnicki.glasnik@mod.gov.rs, X: @MilTechCourier
Subscription to print edition: e-mail: vojnotehnicki.glasnik@mod.gov.rs; Tel. +381 66 87 00 123.

The journal is published quarterly.

The first printed issue of the *Military Technical Courier* appeared on 1st January 1953.

The first electronic edition of the *Military Technical Courier* on the Internet appeared on 1st January 2011.

Printed by Vojna štamparija – Belgrade, Resavska 40b, e-mail: vojna.stamparija@mod.gov.rs

73 ГОДИНА
ОД 1953.
ВТГ

73 GODINA
OD 1953.
VTG

73 ЛЕТ
С 1953 г.
ВТГ

73 YEARS
SINCE 1953
MTG